Discovery of Epigenetic Probes Against the Bromodomain Family of Proteins

A thesis submitted in partial fulfilment of the requirement for the degree of Doctor of Philosophy (D. Phil.)

Peter George Keith Clark

Supervisor: Prof. Darren J. Dixon
Magdalen College, University of Oxford, Trinity 2015

Abstract

Discovery of Epigenetic Probes Against the Bromodomain Family of Proteins
Peter George Keith Clark; Magdalen College, Oxford; D. Phil.; Trinity Term 2015.

Chemical probes are necessary for elucidating the biochemical roles of proteins. Bromodomains are protein-interaction modules found in a family of proteins implicated in the epigenetic regulation of transcription; however, the individual roles remain unknown for many bromodomain proteins, without potent and selective ligands available to assist in their study. From lead compounds, a structure-based drug discovery program was to be explored with the use of biophysical assays and appropriate chemical methods to expediate development of probes against a number of these proteins. A fragment lead against BRD4 was developed into PNZ5, a potent (K_D 5 nM) BRD4 probe with a high ligand efficiency. Although enantioselective syntheses and the use of an alternative synthetic route were unsuccessful, PNZ5 showed cytotoxic activity against gastric cancer cell lines that had proved resilient to existing anticancer agents. Optimisation of a lead compound against BRD9 resulted in the development of LP99, the first reported BRD7/9 probe, that was potent (BRD9 K_D 99 nM, BRD7 K_D 909 nM), selective amongst bromodomain proteins and active in cells. An enantioselective synthesis was performed using chiral organocatalyts and LP99 was used to identify a previously unknown role of BRD7/9 in the regulation of inflammatory processes. Research is ongoing to assess further biochemical roles of these proteins with LP99. Arising from a more potent lead against BRD9, a series of structurally related compounds were synthesised to explore SAR around this ligand, however no improvement on the affinity of the lead was realised. Finally, based on disclosed lead structures against PCAF, a series of compounds were synthesised to replicate their activity. A number of important binding interactions were assessed and a lead structure was identified (K_D 1 μM). Development is ongoing to progress this lead into the first reported PCAF probe.

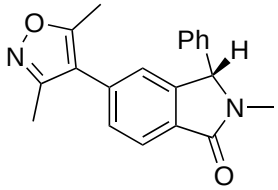

PNZ5

K_D 5 nM vs BRD4(1)

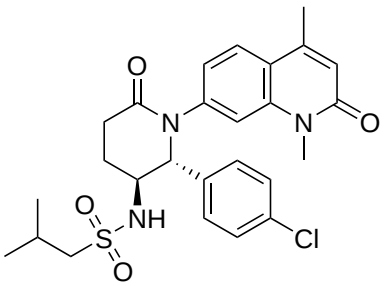

LP99

K_D 99 nM vs BRD9
K_D 909 nM vs BRD7

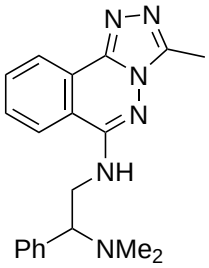

PCAF lead

K_D 1 μM vs PCAF

Declarations and copyright

I declare that this thesis has been written by me, that it is the record of work carried out by me and that it has not been submitted in any previous application for a higher degree at this or any other university or institute of learning. Any work done in collaboration with a research colleague has been fully acknowledged and referenced within the text, which includes: preliminary synthetic research performed by L. Vieira on BRD9; preliminary synthetic research performed by S. Consalvi on BRD9; further synthetic research performed by L. Trulli on PCAF; BROMO*scan* assays performed by DiscoveRx Corporation; NanoBRET assays performed by Promega corporation; NCI60 panel performed by the National Cancer Institute; with all remaining biological experiments and x-ray crystallography performed by the SGC. All compounds in the experimental chapter were synthesised and characterised by myself. I was admitted as a probationary research student in October 2011 and as a candidate for the degree of Doctor of Philosophy in October 2012; the higher study for which this is a record was carried out in the University of Oxford between 2011 and 2015.

Peter George Keith Clark

Date:

Acknowledgements

- Brendan, BAB˙ – For setting me on my way.
- Darren and Paul – My carrot and my whip. Thank you, both, for teaching me so very much. A little knowledge can go a long way: lets see what I can do with it.
- DJD Group – Thanks for the camaraderie, the help, and the near-death experiences.
- Lucas, Sara and Laura – This research, 'our' research, could not have been possible without you. I thank you for this, and for the eternal joke that I was in charge.
- Katherine, Thilina, Fleur, Tegwen, Daniel, Chris, Aubrey and Ina – For being there for all the good times, and for being there for all the bad times.
- Mum and Dad (and Tony) – Nothing, *nothing*, I have achieved could have been possible without you there, always encouraging me, inspiring me, and, when necessary, pushing me. Mum, I know that you now have no grounds on which to refer to me as "your little Rhodes scholar" anymore, but hopefully "your little Dr from Oxford" will suffice to replace it.
- Nick, Rob, Alan, Owen and Steve of the Magdalen College Porters Lodge – For forever keeping me grounded amongst the dreaming spires.
- Oxford – Thanks for the good times, the bizarre stories and the rejection letter (I'm having it framed).
- Steed – For showing me how a great man should live. You are missed, but never forgotten.
- The Woolf Fisher Trust – You sent me here on the attributes I had – Oxford has added inspiration and determination to that list – and on the promise of tomorrow. Rest assured: the cheque's in the mail.

Table of Contents

List of Figures

List of Schemes

List of Tables

Glossary

AlphaScreen	Amplified Luminescent Proximity Homogeneous Assay
aq.	aqueous
BAF	BRG1-associated factor
BEMP	2-*tert*butylimino-2-diethylamino-1,3-dimethylperhydro-1,3,2-diazaphosphorine
BET	bromodomain and extra-terminal domain
Boc	*tert*-butyloxycarbonyl
BRD4	bromodomain-containing protein 4
BRD4(1)	first bromodomain of bromodomain-containing protein 4
BRD7	bromodomain-containing protein 7
BRD9	bromodomain-containing protein 9
BRET	bioluminescence resonance energy transfer
CAN	cerium ammonium nitrate
DBU	1,8-diazabicyclo[5.4.0]undec-7-ene
DMAc	*N,N*-dimethylacetamide
DMF	*N,N*-dimethylformamide
DMPU	1,3-dimethyl-3,4,5,6-tetrahydro-2(1*H*)-pyrimidinone
DPP	diphenylphosphoric acid
dr	diastereomeric ratio
ee	enantiomeric excess
ET	extra-terminal domain
FCC	flash column chromatography
FRET	fluorescence resonance energy transfer
GFP	green fluorescent protein
H-bond	hydrogen-bond
HAT	histone acetyl transferase
HPLC	high performance liquid chromatography
HIV	human immunodeficiency virus
HR-ESI-MS	high resolution electrospray ionisation mass spectrometry
HTS	high-throughput screening
IC_{50}	half maximal inhibitory constant
IL-6	interleukin-6
IL-9	interleukin-9
IR	infrared
IUPAC	International Union of Pure and Applied Chemistry
K_D	dissociation constant

LDA	lithium diisopropylamide
LP99	BRD7/9 probe developed
LPS	lipopolysaccharide
LR-ESI-MS	low resolution electrospray ionisation mass spectrometry
MCR	multicomponent reaction
miR	microRNA
Mpt	melting point
MS	molecular sieves
mTOR	mammalian target of rapamycin protein
NanoBRET	Nanoluc luciferase bioluminescence resonance energy transfer
NCI60	US National Cancer Institute 60 human tumour cell line anticancer drug screen
NF-κB	nuclear factor-κB
NMP	*N*-methylpyrrolidone
NMR	nuclear magnetic resonance
NUT	nuclear protein in Testis
P-TEFb	positive transcription elongation factor b
PBAF	Polybromo-associated BRG1-associated factor
PCAF	p300/CBP-associated factor
PE	petroleum ether
*Pf*BDP3	*Plasmodium falciparum* bromodomain protein 3
PMP	*para*-methoxyphenyl
PNZ5	BRD4 probe developed
PTC	phase-transfer catalyst
PTM	post-translational modification
RNAII	RNA polymerase II
rt	room (ambient) temperature
SAHA	Suberoylanilide hydroxamic acid
SAR	structure-activity relationship
sat.	saturated
siRNA	small interfering RNA
soln	solution
TBAB	tetrabutylammonium bromide
TBAI	tetrabutylammonium iodide
TBHP	*tert*-butyl hydroperoxide
TBME	*tert*-butyl methyl ether
ΔT_m	Change in melting point of a protein
TFA	trifluoroacetic acid
THF	tetrahydrofuran
TOF	time of flight
TLC	thin layer chromatography
UV	ultraviolet
Xantphos	4,5-bis(diphenylphosphino)-9,9-dimethylxanthene

Chapter 1

Introduction

Small molecule ligands are necessary in the pursuit of deciphering biochemical pathways. To allow for cells to respond to many different stimuli simultaneously, discrete biological pathways are heavily interlinked, with many levels of redundancy and points of control to allow for a full range of responses. As such, identifying the role or, more commonly, the roles of one protein is difficult. Small molecule probes allow the rapid and reversible modulation of an individual function of a protein to assist in this identification.[1] Use of chemical probes has some advantages over protein knockdown/out experiments, which affect all the roles of the protein simultaneously.[2] This has been exemplified in the case of the natural product rapamycin and the aptly named mammalian target of rapamycin (mTOR) protein: rapamycin inhibits the activity of the mTOR-raptor complex[3] but not the mTOR-rictor complex,[4] whereas gene deletion or use of interference RNA against mTOR affects both simultaneously. Developing small-molecule modulators to be used in conjunction with genetic approaches allows the best chance for biochemical pathways to be understood. It is important to note here though that the probes developed must be potent, selective and have a proven mechanism of action, as the use of sub-par probes to date has greatly hampered biological understanding.[5]

1.1 Bromodomains

The bromodomain is a protein interaction module involved in epigenetic regulation of transcription. Acetylation of histone lysine residues is an important post-translation modification (PTM)

that is involved in transcriptional regulation: modifications to histones can directly affect binding with DNA or can recruit transcriptional complexes that control gene expression.[6,7] In addition to protein families that add ("writers") and remove ("erasers") PTMs, "reader" proteins recognise and bind to PTMs. The bromodomain, named for the *Drosophilia* gene *brahma* from which it was first identified,[8,9] is a protein module that recognises and binds acetylated lysine residues.[10] Bromodomains are comprised of approximately 110 amino acids that form a characteristic antiparallel four-helix bundle [Figure 1.1]. Acetylated lysine residues bind in a pocket at one end of the bundle, with recognition mediated by hydrogen-bonds (H-bonds) between the carbonyl oxygen atom of the acetyl group and both the NH_2 of a conserved asparagine residue and the hydroxyl of a conserved tyrosine residue, the latter of which is mediated by one of four structured water molecules in the binding pocket.[11]

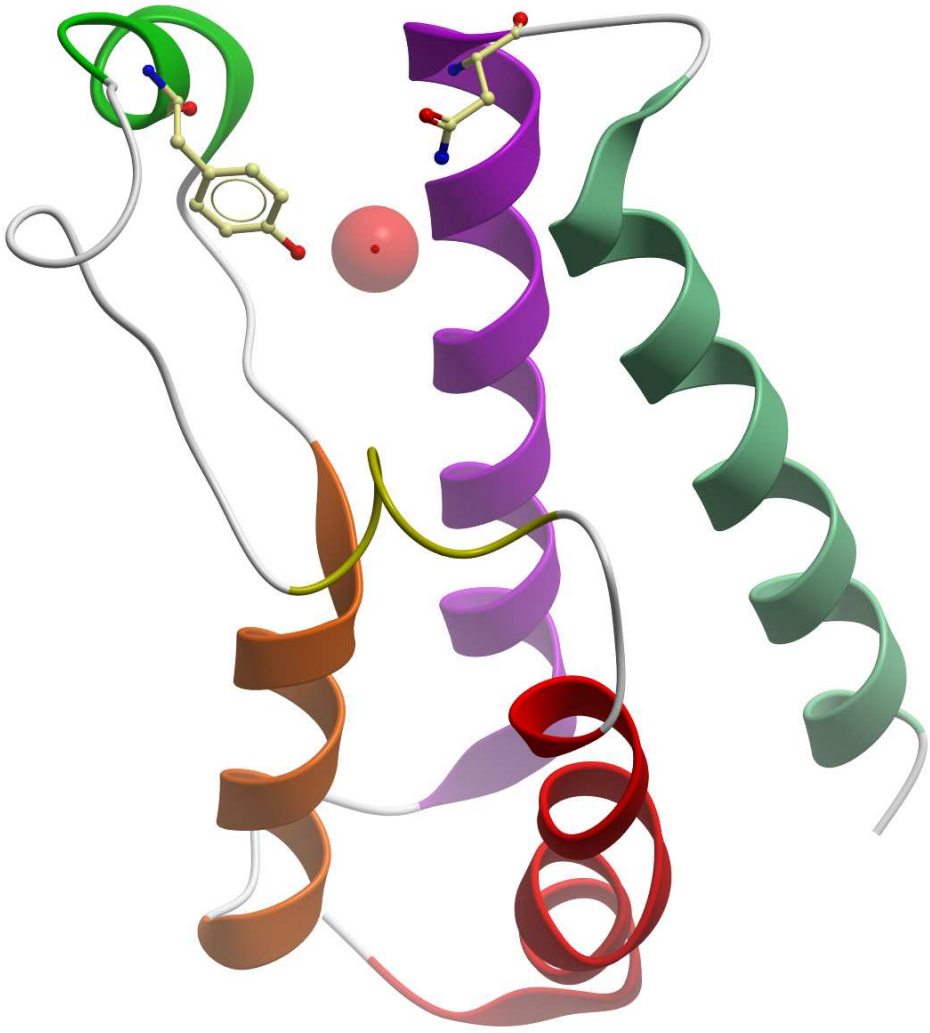

Figure 1.1 General structure of a bromodomain module, as exemplified by BRD4(1) of the BRD4 protein, with the conserved asparagine and tyrosine residues of acetyl lysine recognition (ball and stick) displayed, in addition to the structured water molecule (red ball and sphere) that mediates binding to the tyrosine. [PDB ID:3MUK].

Structural differences in the bromodomain pocket allow different protein binding partners to be discriminated.[12] 61 Human bromodomains have been identified in 46 proteins, some of which contain multiple bromodomain modules. Bromodomains have been classed into eight subfamilies from a structure-based alignment [Figure 1.2]. These proteins act to convey the signal of histone acetylation, with actions mediated: through other domains, such as acetyltransferase, helicase or methyltransferase domains, of the bromodomain protein; or through anchoring other proteins, such as chromatin-remodelling complexes, transcriptional cofactors, transcriptional mediators, or nuclear-scaffolding proteins, to chromatin through protein-protein interactions.[13] In many cases, however, the exact biological role of many of these epigenetic proteins is still unknown, with the structural similarities between the proteins and their important roles in gene expression impairing discovery of their individual actions.

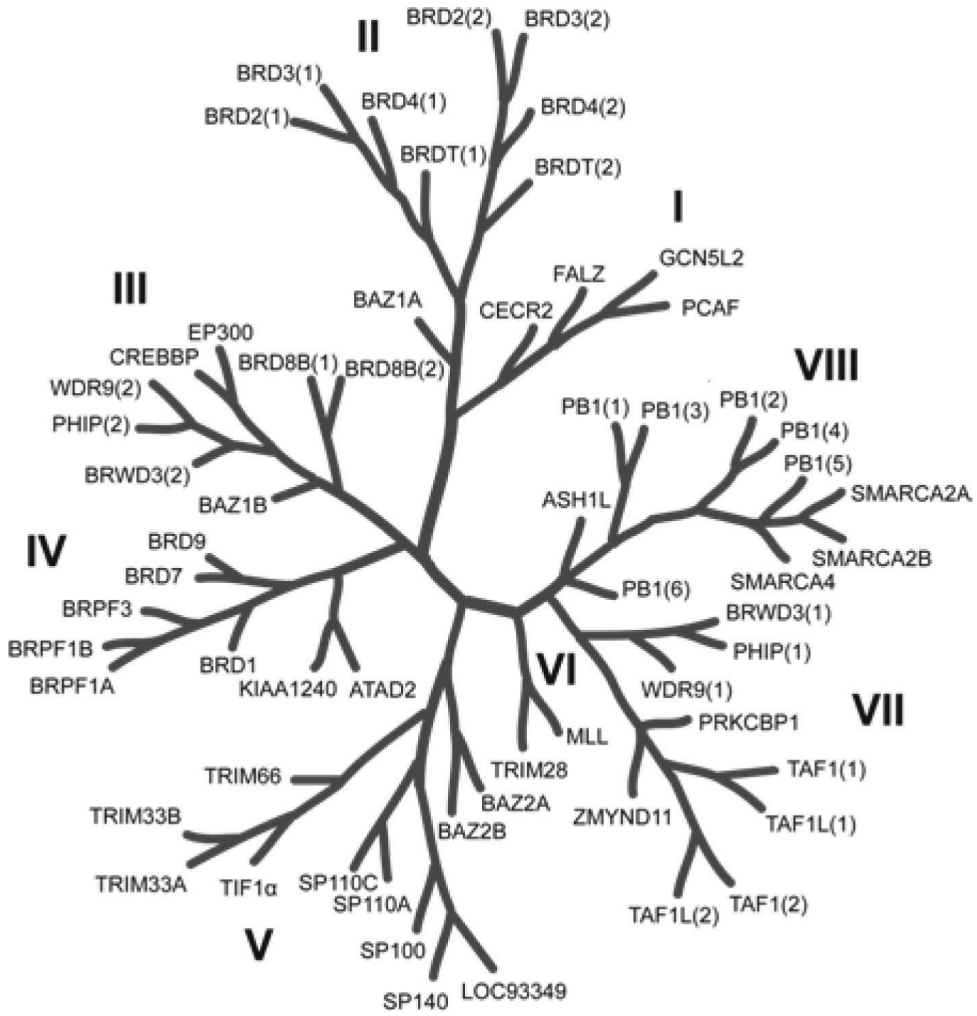

Figure 1.2 Structure-based phlyogenetic tree of bromodomains with subfamilies denoted by roman numerals. Reprinted with permission from *J. Med. Chem.* 2012, **55**, 9393–9413. Copyright 2012 American Chemical Society.[14]

1.1.1 Bromodomain-containing protein 4, BRD4

Bromodomain-containing protein 4 (BRD4) has important roles in the control of transcription. BRD4 is a member of the bromodomain and extra-terminal domain (BET) family of proteins (subfamily II), and contains two bromodomains and an extra-terminal (ET) domain;[15] the ET domain has been identified as a protein-protein interaction motif,[16] but also as an atypical serine kinase.[17] The effect of BRD4 on transcriptional activation is mediated through the positive transcription elongation factor b (P-TEFb), which phosphorylates RNA polymerase II (RNAII) to stimulate transcription: BRD4 both recruits P-TEFb to promoters[18] and displaces the negative regulators HEXIM1 and 7sksnRNA.[19] Increased expression of BRD4 was found to increase transcription, whereas reduction of BRD4 through small interfering RNA (siRNA) reduced gene expression.[20] Independent of P-TEFb, BRD4 has also been demonstrated to directly phosphorylate RNAII through the atypical kinase ET domain.[21] Specifically, BRD4 is important for transcriptional regulation across cell division. Although many transcription factors dissociate from chromatin during mitosis, BRD4 remains bound during the M-G_1 transition, recruiting P-TEFb to promote G_1 gene expression and cell cycle progression;[22] consequently, knockdown of BRD4 results in G_1 arrest and apoptosis. Given the importance of BRD4, it is unsurprising that sustained BRD4 suppression with siRNA was found to have a profound detrimental effect in multiple tissues.[23]

The targeting of BRD4, either as the oncogene or as the expressed protein, has shown efficacy in a number of pathologies. BRD4 modulation has been achieved with the use of pan-BET protein inhibitors, including (+)-JQ1[24] and I-BET151[25] [Figure 1.3], and genetic knockdown. The BRD4 protein, through control of transcription, can facilitate the proliferation of cancer; a correlation has been observed between dysregulation of BRD4 and breast cancer progression.[26] As a result, inhibition or reduction of the BRD4 protein has been demonstrated as a therapy in a variety of cancers: the viability of B-cell acute lymphoblastic leukemia has been reduced through treatment with (+)-JQ1;[27] lung adenocarcinoma cell lines were sensitised through both (+)-JQ1 treatment and knockdown of BRD4;[28] a mixed lineage leukaemia-fusion leukaemia has been effectively treated with I-BET151;[29] and treatment with (+)-JQ1 or suppression of BRD4 through short hairpin RNAs has shown a significant effect on acute myeloid leukaemia.[30] Translocation of the nuclear protein in Testis (NUT) gene has led to a number of BRD-NUT

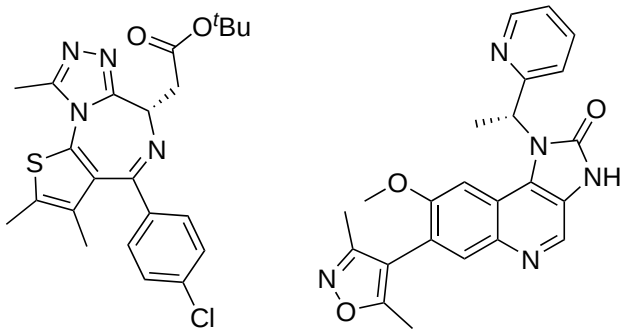

(+)-JQ1 I-BET151

Figure 1.3 pan-BET protein inhibitors.

fusion proteins, including a highly lethal BRD4-NUT fusion oncogene,[31] that have been identified in aggressive NUT midline carcinomas;[32] (+)-JQ1 has been shown to displace this NUT-fusion protein from chromatin and induce antiproliferative effects.[24] Finally, any cancer that is dependent on the Myc transcription factor – the expression of which is in part controlled by BRD4[18] – may be susceptible to BET inhibitors, with (+)-JQ1 inducing cell cycle arrest and apoptosis in models of Burkitt's lymphoma and acute myeloid leukemia.[33]

BRD4 also features prominently in viral pathologies. A range of viruses produce proteins that bind BRD4 to facilitate colocalisation of the viral genomes with mitotic chromosomes: the EBNA1 protein of the Epstein-Barr virus interacts with BRD4 to boost viral transcriptional activation, which could be reduced through BRD4 silencing;[34] the LANA protein of Kaposi's sarcoma-associated herpesvirus binds BRD4 through the ET domain to colocalise the viral genome with mitotic chromosomes;[35] and the E2 protein of papillomaviruses uses BRD4 to recruit P-TEFb to the viral genome for transactivation, with (+)-JQ1 treatment reducing transcription of viral proteins.[36] In comparison, overexpression of BRD4 has been found to disrupt the interaction between the human immunodeficiency virus (HIV) transactivator protein Tat and P-TEFb, interfering with recruitment to the HIV promoter and negatively affecting viral transcription.[37] Although pan-BET inhibitors have been described, selective probes for the individual BET family proteins have not yet been reported, preventing further roles of each member being ascertained.

1.1.2 Bromodomain-containing protein 7, BRD7

The original discovery of bromodomain-containing protein 7 (BRD7) demonstrated a potential role for this protein in regulatory pathways. BRD7, a member of subfamily IV, was simultaneously identified by two research groups.[38,39] Both sets of research corroborated the nuclear localisation of the protein but reported different interacting partners: one identified a protein tyrosine phosphatase;[38] whereas the other identified association with interferon regulatory factor-2 and hyperacetylated chromatin.[39] Following on from this evidence of protein-protein interactions, a subsequent pull-down study identified BRD7 as a member of the Polybromo-associated BRG1-associated factor (PBAF) SWI/SNF nucleosome remodelling complex, which controls the packaging of – and hence accessibility to – DNA.[40,41] BRD7 has also been shown to interact with the nuclear ribonucleoprotein E1B-AP5, through a region of the protein other than the bromodomain module.[42] The interaction of BRD7 with chromatin suggested a further role for this protein in the regulation of gene expression.

The BRD7 gene is a tumour suppressor that acts to limit progression of the cell cycle. BRD7 has been shown to be required for p53 signalling, which is important in both replicative and oncogene-induced senescence.[43,44] G_1-S transition in the cell cycle is chiefly controlled by the Rb/E2F pathway,[45] which extracellular signaling can activate through the ras/MEK/ERK pathway;[46] BRD7 has been shown to downregulate both pathways and suppress cell-cycle progression.[47] The downregulation of the ras/MEK/ERK pathway occurs through inhibition of β-catenin translocation by BRD7,[48] as has been observed in suppression of epithelial ovarian carcinoma.[49] BRD7 has also been shown to translocate the p83α[50] and XBP1[51] proteins to the nucleus, leading to attenuation of the PI3K signalling pathway. Finally, BRD7 has shown involvement with steroid receptors: BRD7 represses androgen receptor signalling, which is of importance in prostate cancer;[52] and BRD7 aids binding and recruitment of the proteins BRCA1 and Oct-1 to regulate the transcription of estrogen receptor α,[53] through which the breast cancer drug fulvestrant operates.[54]

In line with designation as a tumour suppressor, BRD7 has been found to be downregulated or targeted in a number of pathologies. Downregulation of the BRD7 protein has been identified in both colorectal cancer[55] and nasopharyngeal carcinomas.[47] Conversely, upregulation of

microRNA (miR) that targets and inhibits BRD7 expression has been found in a number of cancers: miR-200c in endometrial cancer;[56] miR-300 in osteosarcoma;[57] miR-410 in non-small cell lung cancer;[58] and miR-182 and miR-381 in gliomas.[59] In addition to targeting at the level of mRNA, degradation of the BRD7 protein is triggered in some forms of osteosarcoma.[60] Besides supressing oncogenesis, however, BRD7 is also important to normal cellular development, and BRD7 knockout has been linked to impaired cognitive behaviour.[61] The use of chemical probes to further identify the role of BRD7, and any potential therapies through this, has not been possible because, at the time this research was begun, no potent and specific probes against BRD7 had been reported.

1.1.3 Bromodomain-containing protein 9, BRD9

Only limited information is available about bromodomain-containing protein 9 (BRD9). A member of subfamily IV, it has been identified to have both nuclear and cytoplasmic distribution,[12] with binding to histone H4 demonstrated.[62] Through pull-down studies, BRD9 has been demonstrated to associate with the BRG1-associated factor (BAF) SWI/SNF nucleosome remodelling complex.[40,41] The BRD9 gene has been found to be frequently mutated in lung carcinoma samples,[63] and upregulation of BRD9 has been seen in hepatocellular carcinomas.[64] The protein is also frequently over-expressed due to copy number gains of the short arm of chromosome 5,[65] which is characteristic of both cervical cancer[66] and non-small cell lung cancer.[67] As with translocation of the NUT gene with BRD4, a BRD9-NUTM1 fusion protein has been identified in some cases of infant acute lymphoblastic leukemia.[68] Further exploration of the role of BRD9 in these pathologies has yet to be established, in part due to the absence of available BRD9 probes.

1.1.4 p300/CBP-associated factor, PCAF

The bromodomain protein p300/CBP-associated factor (PCAF) has also been demonstrated to have a role in cellular processes. PCAF, a member of subfamily I, was originally identified by sequence similarity with yeast co-factors involved in cell-signalling pathways[69] and through a

search of bromodomain sequences in protein databases.[70] Binding of PCAF to the p300/CBP proteins was found to influence cell-cycle progression through inhibition of G_1-S progression. PCAF also has a histone acetyl transferase (HAT) domain,[71] which, in conjuction with the presence of a bromodomain module, represents a direct link between transcriptional regulation and chromatin modification:[72] many roles of PCAF in transcriptional regulation and histone acetylation have now been identified.[73,74] More recently, PCAF has additionally been shown to possess ubiquitin ligase activity.[75]

Given this significant role in the regulation of gene expression, PCAF has been implicated in numerous cancers.[76] In lung cancer, PCAF has been found to acetylate and stabilise overexpressed ATP-citrate lyase, which controls lipid synthesis and promotes tumour growth.[77] The Hedgehog signaling pathway has been implicated in several cancers, including medulloblastoma and glioblastoma;[78] PCAF has been demonstrated to act as a coactivator of the genes involved in this pathway.[79,80] PCAF has also been found to compete for the binding site of p300/CBP with E1A, an adenoviral oncoprotein that induces cell cycle progression,[81] highlighting a tumour suppressor function for PCAF.[69] However, PCAF has also been found to stabilise β-catenin, which is involved in a majority of colorectal cancers,[82] and upregulation of PCAF has been correlated with prostate cancer.[83]

PCAF has also been shown to play a role in other pathologies. Nuclear factor-κB (NF-κB)[84] – a key regulator in neuroinflammation[85] – has been linked to a number of neurodegenerative diseases;[86] the HAT activity of PCAF has been demonstrated to acetylate NF-κB,[84] modulating the nuclear localisation and activity of this protein.[87,88] The HIV Tat protein is a transcriptional activator that assembles with an RNA polymerase to promote transcription of the HIV genome;[89] Tat activity has been found to be dependent on PCAF binding for viral replication.[90–92] More recently, PCAF has been found to be involved in regulating antibody production, and hence implicated in inflammatory pathways.[93] Finally, PCAF has been demonstrated to be active in the central nervous system, with PCAF activity correlated with memory formation in mice.[94]

No probes against the bromodomain of PCAF have yet been described. Although the HAT

domain of PCAF has been targeted with a number of broad-activity HAT inhibitors,[95–97] only small progress towards a potent and selective bromodomain inhibitor has been achieved; some selective PCAF inhibitors have been studied towards suppressing viral replication in HIV through bromodomain binding,[98,99] however no ligand with an IC_{50} of <2 μM was identified. Given the number of pathologies that PCAF is involved in, the development of potent and selective inhibitors of PCAF is required to provide new avenues of treatment to these diseases.

1.1.5 Malarial bromodomains

Bromodomains are not limited to eukaryotes, with the domain also appearing in protozoan genomes. Malaria, caused by protozoan parasites of the genus *Plasmodium*, is responsible for between 0.8 and 1.2 million deaths annually.[100] It has been postulated that the complicated life cycle, with rapid transitions between morphological states, is controlled in a large part by epigenetic gene expression; transciptional profiling has revealed distinct RNA profiles for the six different stages of the life cycle.[101] Seven bromodomain proteins have been identified in *P. falciparum*, the most lethal malarial parasite, to date, including: P*f*GCN5, a HAT homologue of yeast transcriptional coactivator GCN5, that has been demonstrated to affect chromatin-remodelling in *P. falciparum*;[102] and *P. falciparum* bromodomain protein 1 (P*f*BDP1), a reader protein that has been shown to control the expression of invasion-related genes, the conditional knock-down of which lead to the significant downregulation of genes vital for invasion.[103] To date, however, no inhibitors of malarial bromodomain proteins have yet been described, significantly curtailing further fundamental research on these proteins and avenues of pharmaceutical treatment for malaria.

1.1.6 Acetyl lysine mimics

To further understand the roles of these bromodomain proteins, each requires a potent and selective chemical probe to be developed that replicates acetyl lysine binding. To develop probes against bromodomain binding sites, acetyl lysine bioisosteres are used to mimic the native ligand. The key elements recognising acetyl lysine are H-bonds from conserved

asparagine and tyrosine residues in the binding site, the latter mediated through a structural water molecule. Through *in silico* and fragment library screening, a number of acetyl lysine mimics have been identified to date [Figure 1.4]. Mimics reported include *N*-phenylacetamides (**1**), *N*-acetyl-2-methyltetrahydroquinolines (**2**), indolizinethanones (**3**),[104] 4-acylpyrroles (**4**),[105] 3,5-dimethylisoxazoles (**5**),[106] methyltriazoles (**6**),[107] triazolophtalazines (**7**),[108–112] thiazolidinone (**8**),[113] chloropyridones (**9**),[114] 3-methyl-3,4-dihydroquinazolinones (**10**),[115] triazolopyrimidines (**11**) and methylquinolines (**12**).[114] By building on these acetyl lysine bioisosteres, to generate new binding interactions for potency and selectivity, chemical probes can be developed to target unique bromodomains.

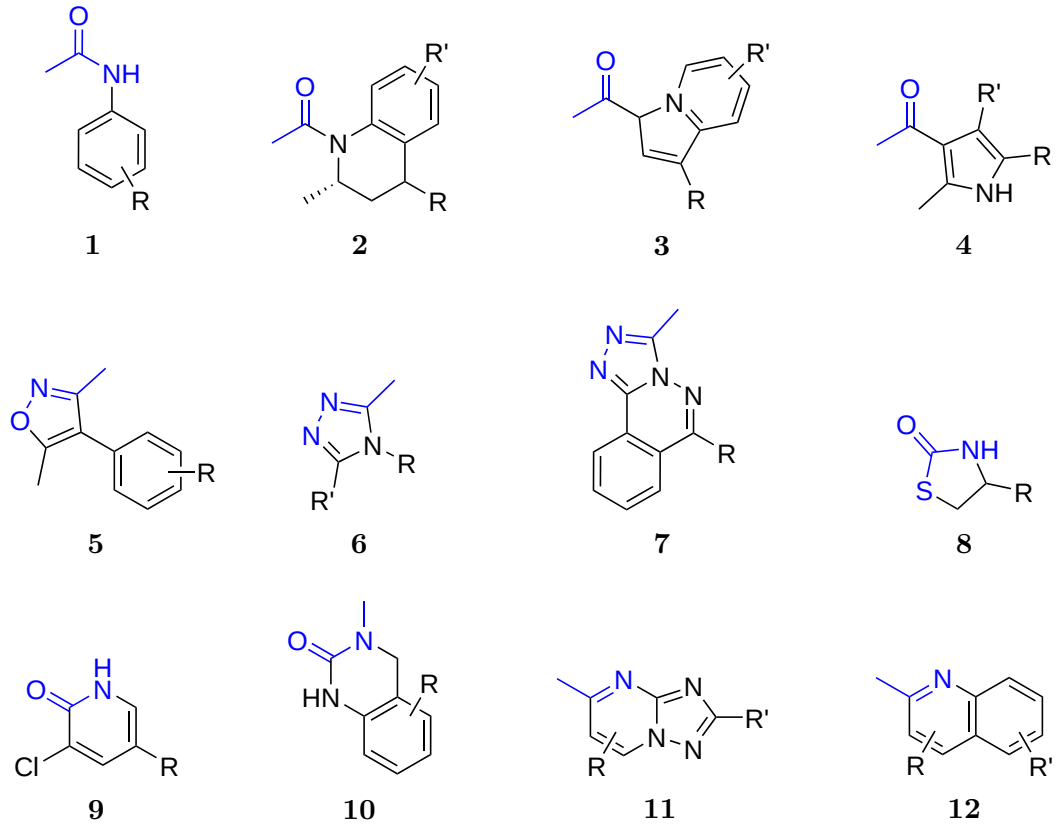

Figure 1.4 Acetyl lysine bioisosteres. The acetyl lysine mimic motif of each structure is highlighted (blue).

1.2 Chemical methods

The role of chemistry in the development of bioactive molecules extends beyond that of just synthesis. When developing new biologically-active probes, it is possible to relegate chemistry as simply a means to obtain the new molecules. However, probe development and chemical

synthesis are not mutually exclusive, and there are many ways in which chemistry facilitates or influences the development of new probes. Given the inherently chiral nature of biological systems, typically only one of a pair of enantiomers is biologically active, or the enantiomers may have different biological activity, as was tragically discovered in the case of thalidomide; through the use of enantioselective methodology, synthesis of only the more potent enantiomer can often be achieved to facilitate the probe discovery process. Meanwhile, multicomponent reactions (MCRs) allow many points of derivatisation to be introduced simultaneously, generating a diverse library of compounds from which structure-activity relationships (SARs) can be readily explored. As such, families of compounds that are amenable to synthesis through MCRs may be preferentially explored over families requiring target-orientated syntheses of each member, highlighting that the methods used may both facilitate and influence the direction of ligand development. Finally, chemical methods can dictate the molecules actually explored as opposed to those targeted. Based on the current organic synthetic toolbox, some targets may be readily obtained while others may be synthetically inaccessible; related compounds, with complimentary but synthetically-achievable substitution, may be made as alternatives. Additionally, some intermediates and byproducts in the synthesis, which were not original synthetic targets, also become available for testing; due to the possession of an acetyl lysine mimic, these allow for the further exploration of the focused chemical space. In this way, importance must be placed on the chemical methods to be used as they influence probe development.

1.2.1 Multicomponent reactions towards exploring SAR

MCRs allow for the rapid attainment of derivatives from which SAR can be assessed. MCRs are chemical transformations in which three or more substrates combine to form a single product derived from all of the components.[116] These represent a powerful tool in the rapid preparation of diverse libraries of compounds for a number of reasons:[117] multiple substitutions can be incorporated in a single step to economically give a large range of compounds; by obtaining compounds with related scaffolds, the libraries obtained allow for SAR to be readily studied; and focused libraries can be quickly generated after lead structures are identified. To date, MCRs have been used in the development of numerous novel bioactive compounds.[118–122]

1.2.1.1 Nitro-Mannich/lactamisation cascade to substituted piperidones

Towards exploring the activity of substituted piperidones, a nitro-Mannich/lactamisation cascade had been previously developed. It was discovered that combining γ-nitrobutyrate **13** with aldehydes in the presence of ammonium acetate afforded *trans*-substituted piperidones upon heating in ethanol.[123,124] This MCR was believed to occur through a nitro-Mannich/lactamisation cascade [Scheme 1.1]. The ammonium acetate both condenses with the aldehyde to give the equivalent imine (**14**) and catalyses formation of a nitronate (**15**) from the nitrobutyrate. This nitronate then reacts with the imine in a nitro-Mannich reaction to give β-nitroamines **16** that can subsequently undergo an intramolecular lactamisation to give substituted piperidones (**17**). This cascade has been further developed by members of the Dixon group,[125] and has been most notably applied in the total synthesis of manzamine A[126] and (–)-nakadomarin A[127–129] [Scheme 1.2].

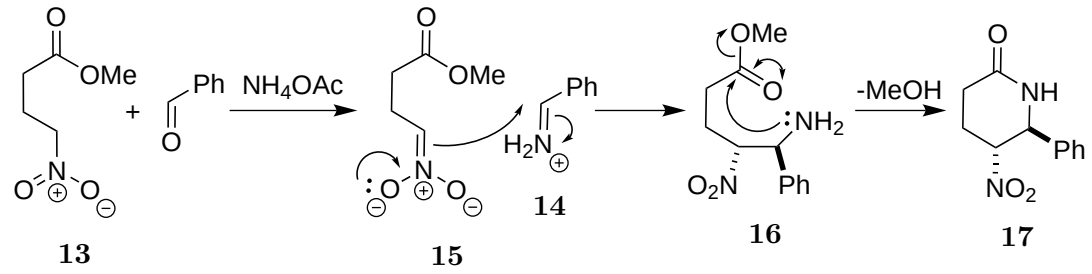

Scheme 1.1 Mechanism of nitro-Mannich/lactamisation cascade to substituted piperidones.

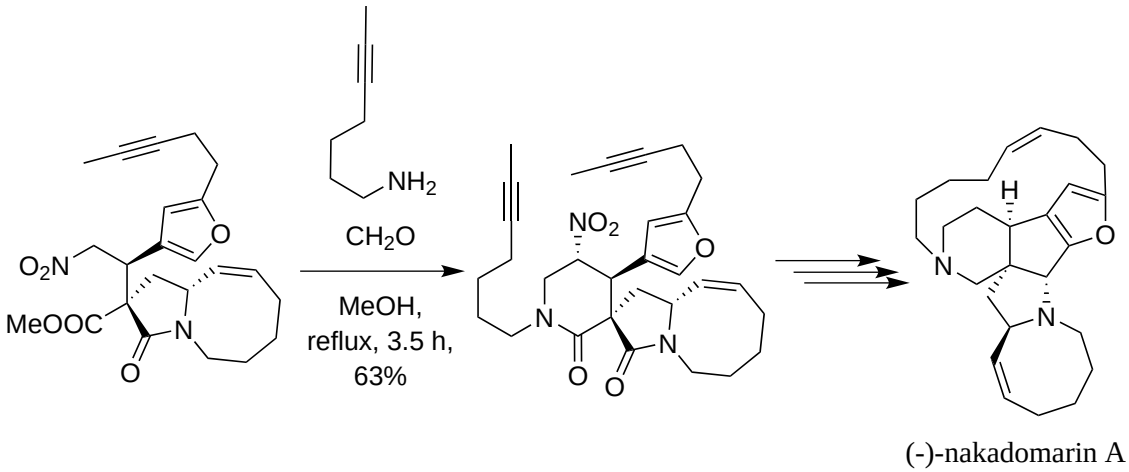

Scheme 1.2 Nitro-Mannich/lactamisation cascade in the synthesis of (–)-nakadomarin A.

This cascade has been used to explore SAR around a biologically active compound. In the development of antagonists of the neuropeptide Substance P, functionalised piperidones were synthesised to perform SAR around the known ligand CP-99,994.[130] A range of heteroaromatic, alicyclic and acyclic aldehydes were used to give substituted piperidone products **18** in 67–98% yields [Scheme 1.3]. Alternatively, the ketones 1-methoxypiperidin-4-one and bicyclo[2.2.1]heptan-2-one could be used to furnish the spirocyclic products **19** and **20** (17% and 24% yields respectively). Substitution of the nitrobutyrate was also explored, with 2-Me and 4-Me groups being well tolerated in the reaction (87% and 90% yields respectively). Using the requisite piperidone product, CP-99,994 was obtained through a number of transformations, validating the use of this MCR in generating piperidones from which SAR could ultimately be explored. The general nature of the cascade, and ability to generate a variety of substituted piperidinones, lends this MCR to exploring SAR around piperidone scaffolds.

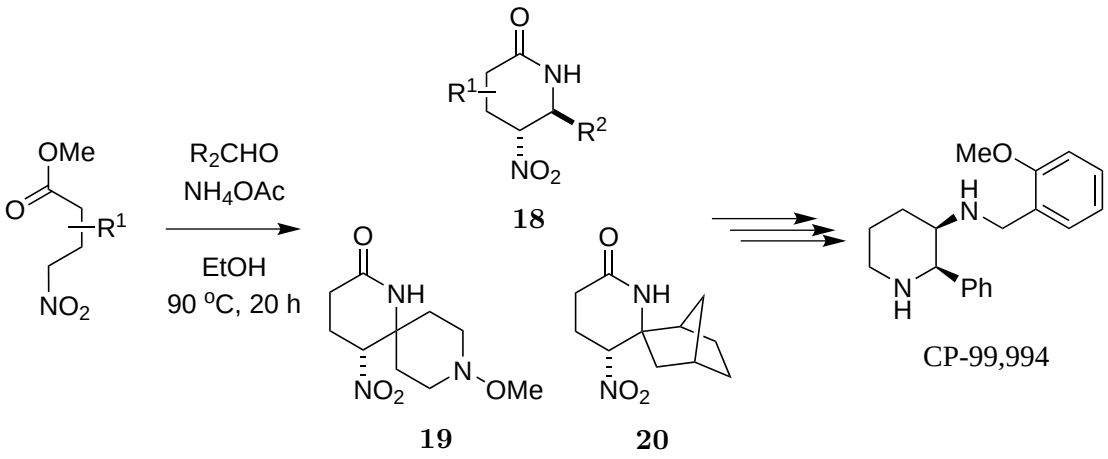

Scheme 1.3 Synthesis of substituted piperidones towards exploring SAR around CP-99,994.

1.2.1.2 Nitro-Mannich/lactamisation cascade to substituted pyrrolidones

A series of related nitro-Mannich/lactamisation cascades were previously developed to afford substituted pyrrolidones. In an analogous method to that used to obtain the substituted piperidones, a range of MCRs using 3-nitropropanoates were developed by Sophie Pelletier of the Dixon group to yield a range of γ-lactams.[131] The methods explored addressed the use of different nitrogen species and the nature of the formation of the imine partner. In the first instance, an MCR was performed with *in situ* generation of an imine, from an aldehyde and

an amine, and a benzoic acid catalyst [Scheme 1.4.1].[132,133] A range of aliphatic and aromatic aldehydes were explored in combination with amines and nitroalkanes bearing aliphatic or benzylic substituents; moderate to excellent diastereoselectivities (diastereomeric ratio (dr) 3:1–30:1) and moderate to good yields (60–85%) were observed, with a *trans* relationship between vicinal substituents preferred. Although the effect of substitution at any one position showed no correlation with diastereoselectivity, increasing the steric bulk at multiple sites simultaneously led to an increase in dr. In a non-MCR modification, preformed *N*-*para*-methoxy-phenyl (PMP)-protected imines (**25**) with aliphatic, aromatic and heteroaromatic side chains were reacted with **13** and chiral phosphoric acid catalysts [Scheme 1.4.2]; compounds of the form **26** were obtained in low yields (15–50%) and a range of enantioselectivities (enantiomeric excess (ee) 0–99% (*sic.*)), but as a single diastereomer. Finally, as a proof of principle, NH_4OAc

1. With *in situ* imine formation

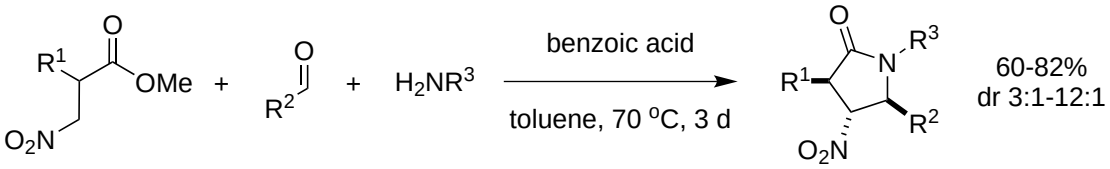

21 **22**

R^1 = Me, Et, *i*Pr, Bn
R^2 = *i*Pr, *n*Pent, Ph, *o*-MeO-C_6H_4, *m*-MeO-C_6H_4, *p*-MeO-C_6H_4, *p*-NO_2-C_6H_4, *p*-Cl-C_6H_4
R^3 = *i*Pr, *n*Bu, Bn

2. With preformed imine

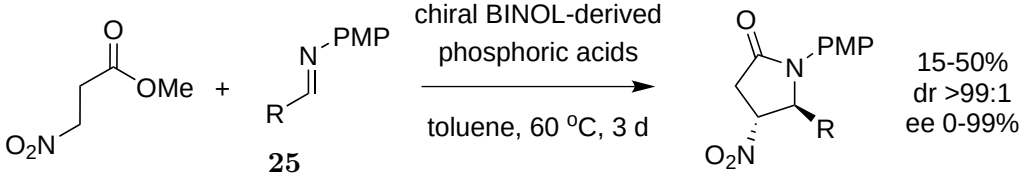

23 **25** **26**

R = cyclohexyl, ethyl carboxylate, PMP, C_6H_5, *p*-CF_3-C_6H_4, *p*-NO_2-C_6H_4, 2,4,6-trifluoro-C_6H_4, pyridin-2-yl, thiophen-2-yl, furan-2-yl

3. Reaction through a primary aldimine

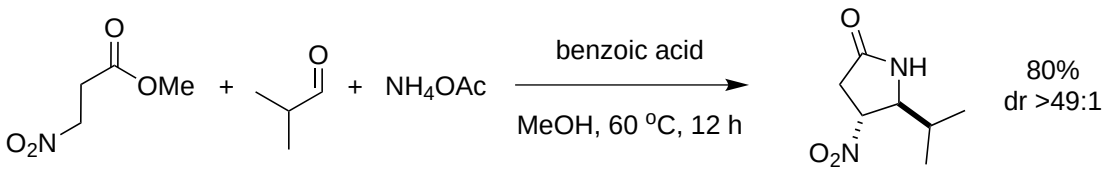

23 **24**

Scheme 1.4 Methods to substituted pyrrolidones developed by S. Pelletier.

was used with **13** and isobutyraldehyde to generate **24** in good yield (80%) and excellent dr (>48:1), demonstrating the reaction can be performed to directly yield *N*-unsubstituted lactams [Scheme 1.4.3]. This collection of methods allows for the ready generation of substituted pyrrolidones, expediating the exploration of SAR around this scaffold.

1.2.2 Enantioselective organocatalysis

An alternative area of chemistry that can be readily adapted to facilitate the development of chemical probes is enantioselective organocatalysis.[134–136] Traditionally, enantioselective catalysis has been performed with metal-based catalysts or enzymes. Although both can give high levels of enantiocontrol, there are inherent disadvantages with each method: metal-based catalysts can be expensive, toxic, and run the risk of contaminating subsequent reactions; whilst typically enzymes have high substrate specificities, stability issues, and pose significant challenges in obtaining enantiomeric pairs. To circumvent many of these issues, there has been an increasing push to replace these through the use of organocatalysts: low molecular weight, single enantiomer organic compounds that have the ability to donate or remove electrons or protons. Many of these catalysts have been inspired by molecules identified from nature, whilst others have been developed *ab initio*, and a range of different functionalities have been incorporated to perform their catalytic function.

Many organocatalyst families are now available for use in chemical synthesis. The body of research documenting families of organocatalysts and their use in enantioselective synthesis is considerable, to the point that a new journal entitled *Current Organocatalysis* has recently been established. Within the Dixon laboratories a number of organocatalysts have been previously developed or used in enantioselective reactions [Figure 1.5], including: BINOL-derived phosphoric acid catalysts, both with (**27**) or without (**28**) reduced backbones;[137] *N*-triflyl phosphoramides (**29**);[138] bifunctional cinchona-derived Brønsted base/H-bond donors (**30**);[139] cinchona-derived phase-transfer catalysts (PTCs) (**31**);[140] cinchona-derived bifunctional PTCs (**32**);[141] chiral arenesulfonic acids (**33**);[142] bifunctional iminophosphoranes (**34**);[143] and chiral thiourea catalysts (**35**).[144] These catalysts have each found application in many different reactions, including use in enantioselective nitro-Mannich reactions and hydride transfers.

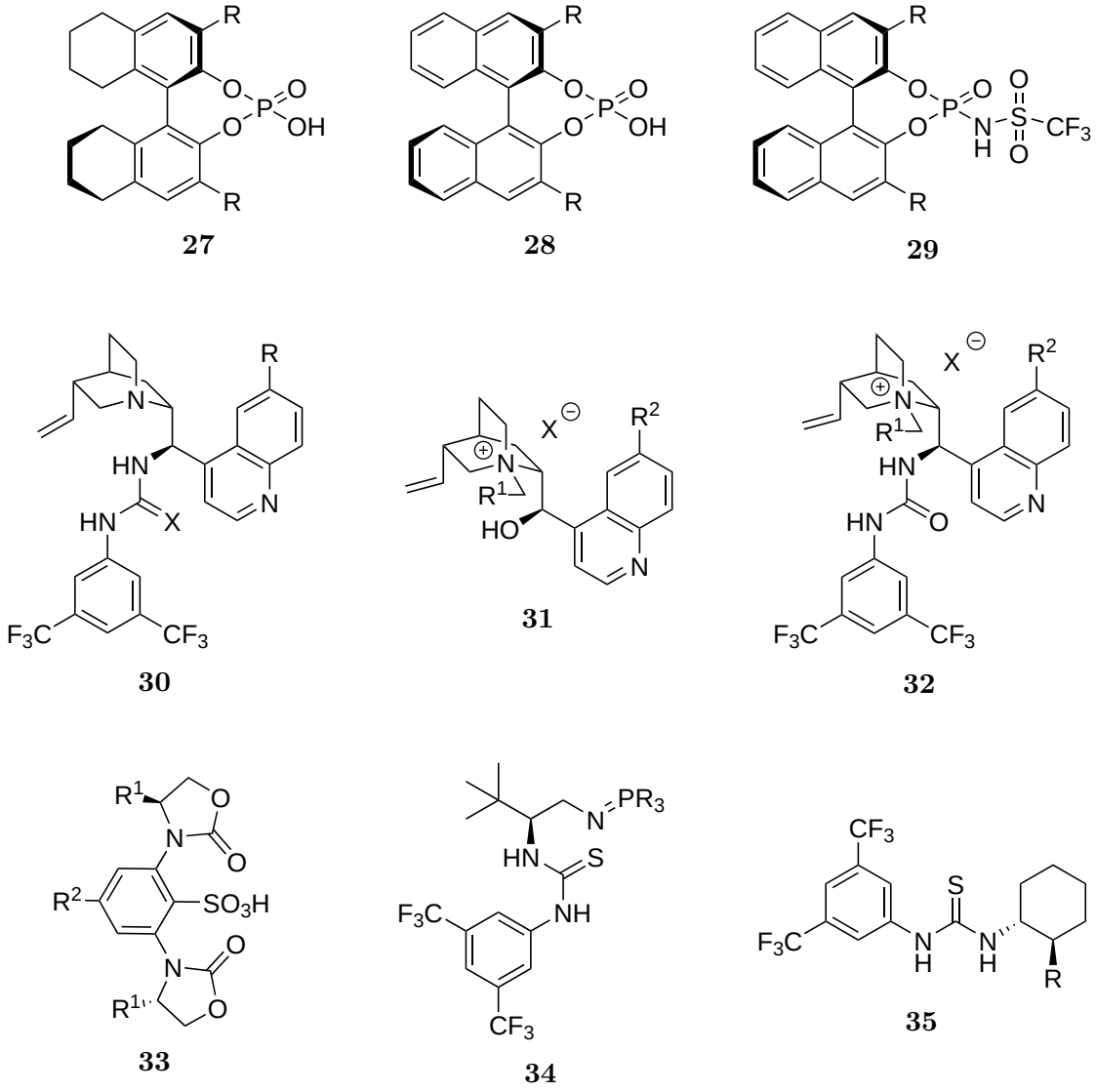

Figure 1.5 Organocatalyst families in the Dixon laboratories: Reduced backbone BINOL-derived phosphoric acid catalysts (**27**); BINOL-derived phosphoric acid catalysts (**28**); *N*-triflyl phosphoramides (**29**); bifunctional cinchona-derived Brønsted base/H-bond donors (**30**); cinchona-derived phase-transfer catalysts (PTCs) (**31**); cinchona-derived bifunctional PTCs (**32**); chiral arenesulfonic acids (**33**); bifunctional iminophosphoranes (**34**);[143] chiral thiourea catalysts (**35**). Only one enantiomer, or pseudo-enantiomer, for each family is shown.

1.2.2.1 Enantioselective nitro-Mannich reaction

The nitro-Mannich reaction is a valuable method for generating enantioenriched nitrogen-containing compounds. The nitro-Mannich, or aza-Henry, reaction yields β-nitroamines with a vicinal nitrogen motif [exemplified in Scheme 1.1]; furthermore, the nitrogens are in different oxidation states that can be selectively manipulated for further derivatisation. The reaction was first documented in 1896,[145] but has shown a resurgence in study through the use of

chiral elements to perform the reaction in an asymmetric fashion.[146,147] Initial research focused on metal-catalysis, but emphasis has since shifted to the use of organocatalysts as chiral controllers. Numerous organocatalysts have now been employed in these reactions, including urea & thiourea catalysts, Brønsted acids, Brønsted bases and PTCs.[148]

1.2.2.2 Bifunctional asymmetric PTCs developed by K. Johnson in an enantioselective nitro-Mannich reaction

Bifunctional asymmetric PTCs developed by Kayli Johnson in the Dixon group have been employed in enantioselective nitro-Mannich reactions. K. Johnson developed a new family of cinchona-derived bifunctional PTCs (**32** and the pseudoenantiomeric series **36**) [Figure 1.6],[141] which acted to combine both Brønsted base/H-bond donor catalysis[139] with phase-transfer catalysis.[140] This fusion allowed the benefits of the privileged cinchona scaffold, preorganisation and activation leading to high levels of enantiocontrol, with those of phase transfer catalysis, higher levels of reactivity through the use of strong external bases. The use of this new catalyst family was first demonstrated through a nitro-Mannich reaction between *N*-Boc-amidosulfones (**37**) and nitroalkanes (**38**) to generate β-nitroamines (**39**) [Scheme 1.5]. Under the basic conditions, **37** eliminates phenyl sulfinate to generate a *N*-Boc-protected imine *in situ* that is attacked by the nucleophilic nitronate of **38** in the presence of the catalyst. The exact interactions through which the catalyst controls the enantioselectivity in this reaction are not known: both the nitronate or the Boc group of the imine are capable of interacting with the urea motif; and the location of the base in the reaction is unconfirmed. Nonetheless, a range of aromatic, polycyclic aromatic, heterocyclic and aliphatic amidosulfones were used with

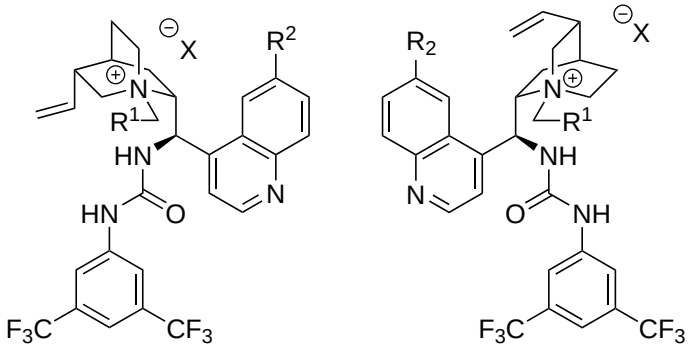

Figure 1.6 Cinchona-derived bifunctional asymmetric PTCs developed by K. Johnson.

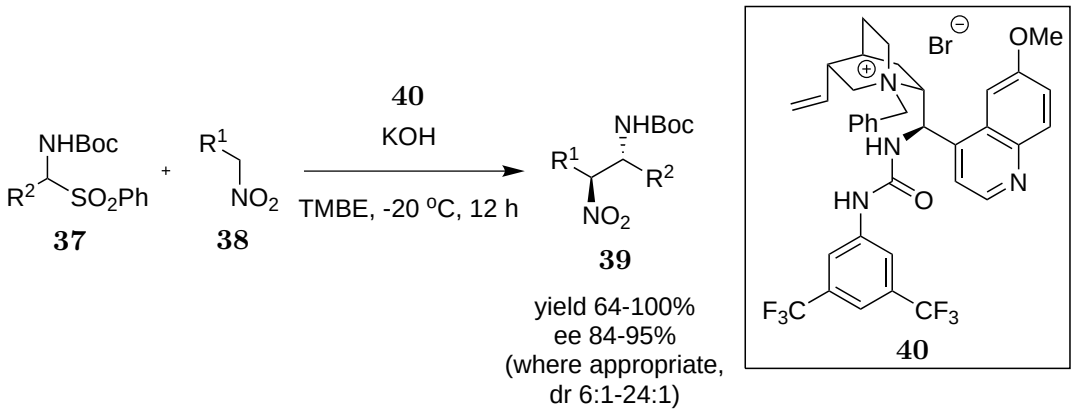

R^1 = H, Me, Et, $CH_2CH{=}CH_2$
R^2 = *i*Bu, *t*Bu, cyclohexyl, *p*-Me-C_6H_4, *p*-OMe-C_6H_4, *p*-F-C_6H_4, *p*-CF_3-C_6H_4, 2-naphthyl, 3-pyridyl

Scheme 1.5 Enantioselective nitro-Mannich reaction with cinchona-derived bifunctional asymmetric PTCs.

substituted nitroalkenes in the presence of **40** to give nitro-Mannich products in moderate to excellent yields (64–100% (*sic.*)), excellent enantioselectivity (ee 84–95%) and good to great diastereoselectivity (dr 6:1–24:1) where the products were diastereomers. Given the high level of control possible, these catalysts can be readily applied to the enantioselective synthesis of biologically active molecules containing β-nitroamines.

1.2.2.3 Enantioselective hydride transfer using Hantzsch esters

Organocatalysts can alternatively be used in enantioselective reductions using Hantzsch esters as a hydride source. In nature, cofactors – such as nicotinamide adenine dinucleotide (NADH) [Figure 1.7] – containing 1,4-dihydropyridine rings are commonly used as a hydride source; in

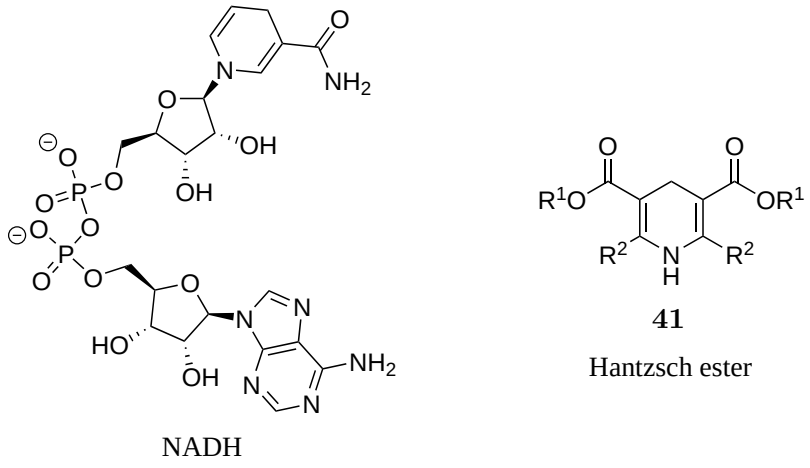

Figure 1.7 1,4-dihydropyridines as hydride sources.

the presence of a suitable redox partner, a nicotinamide system is formed and a hydride ion is produced. Hantzsch esters (**41**), named after Arthur Rudolf Hantzsch who first devised a one-pot synthesis of these,[149] have been used as bio-inspired hydride donors. Under thermal conditions or in the presence of acid or base catalysts, **41** can transfer a hydride to an imine electrophile (**42**), reducing this species to the amine **43** whilst being oxidised in turn to the pyridine **44** [Scheme 1.6]. Use of chiral Brønsted acid catalysts allows enantioselective hydride transfer, and has been exemplified with: *N*-aryl imines, nitrogen heterocycles, α,β-unsaturated aldehydes & ketones, β,β-disubstituted nitroolefins, ketimines, α-imino esters, *N*-acyl enamides, tertiary amides and α-ketoesters.[150–152] The most commonly used organocatalysts in these reactions are BINOL-derived phosphoric acids, **27** and **28**, with high levels of enantiocontrol observed in the reduction of imines.[153] This reaction has been studied computationally: research suggests that both the Hantsch ester and the imine nucleophile H-bond with the phosphate of the catalyst, with the imine orientated so as to minise steric interactions with the BINOL-scaffold [Figure 1.8].[154]

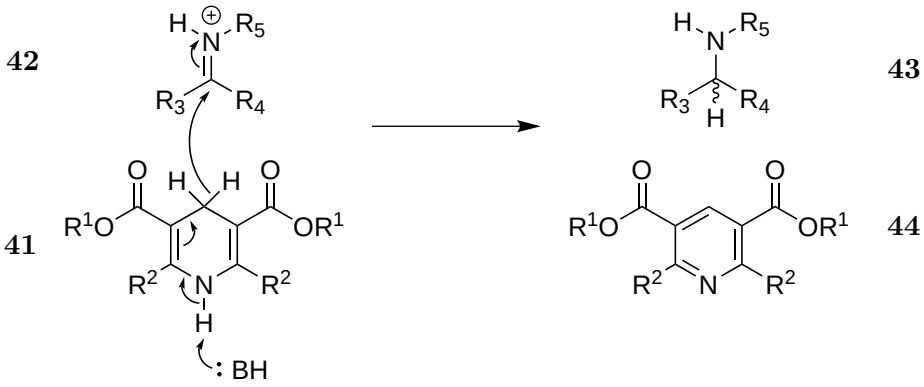

Scheme 1.6 Mechanism for hydride transfer from Hantzsch esters.

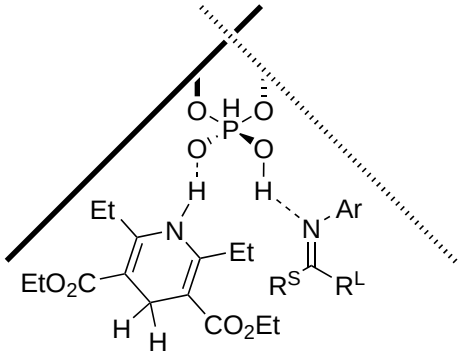

Figure 1.8 Proposed model for enantioselectivity in the Hantzsch reduction of imines. In this example, the imine lies above the plane of the Hantzsch ester.

1.3 Biological methods

To assess the biological activity of the compounds synthesised, a range of bioassays were employed. The choice of assay depends upon the biology of the target protein that is intended to be modulated;[155,156] as bromodomains are involved in protein binding, assays that measure affinity to the binding site give physiologically-significant results. Two rounds of assessment are typically used when screening compounds: a primary assay that allows for a high throughput of samples, allowing the qualitative binding of a large set of molecules to be assessed; followed by a secondary assay that gives quantitative data on a subset of the compounds. With compounds derived from a potent lead structure, a quantitative assay alone may be used, due to the expected activity and the need for accurate data to compare high affinity ligands. Once a lead structure has been identified, biological methods are then used to validate the biological activity of the ligand, which can include: confirming that the activity assayed for is pharmacologically relevant; assessing whether the probe produces an observable biological effect; and the effect of this probe on models of various pathologies. A range of biological experiments were used in this research, all performed on our behalf by collaborators at the Structural Genomics Consortium (SGC), the Promega Corporation, the DiscoveRx Corporation or the National Cancer Institute, which were centered around assessing either protein-ligand interactions or the effect of the ligand on protein-protein interactions.

1.3.1 Differential scanning fluorimetry, DSF

The differential scanning fluorimetry (DSF) assay measures ligand-induced conformational stabilisation of a protein. This assay is based on the principle that binding of a compound to a protein will result in the formation of a more thermally-stable ligand-protein complex.[157–159] Upon heating, intramolecular bonding in a protein is broken and a protein unfolds, described by a thermally-induced melting curve [Figure 1.9]; the point on the curve with the largest gradient is defined as the melting point (T_m) of the protein. To assist in visualisation a fluorescent dye is used, which is quenched by solvent but which fluoresces when binding to non-polar residues exposed by protein unfolding. Upon ligand binding, the resulting complex gains binding elements, such as H-bonds, Van der Waals interactions or ionic forces, that

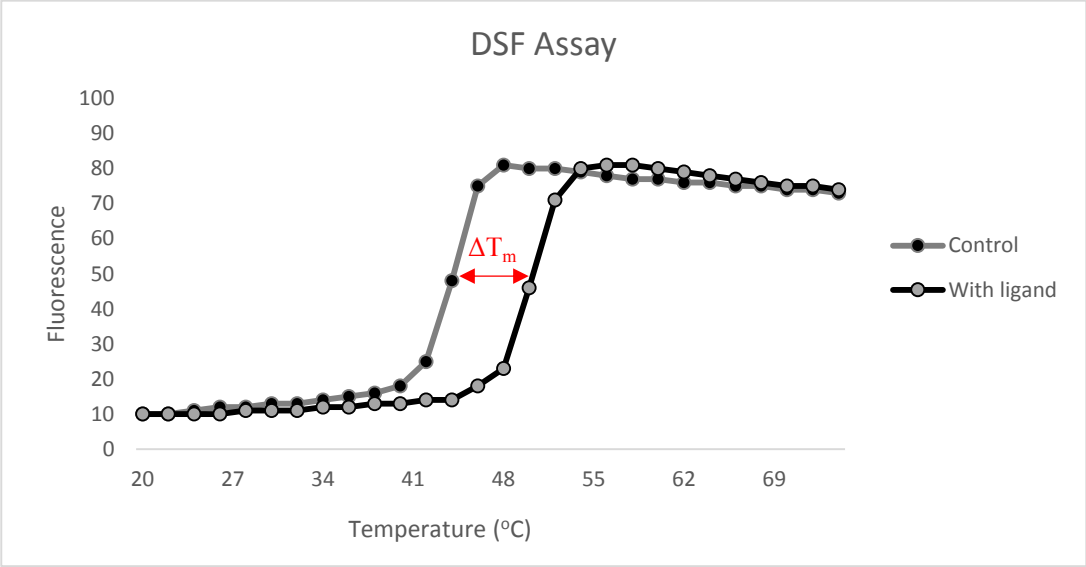

Figure 1.9 Model example of a DSF assay. A thermal shift is visible dependent on the presence of the ligand.

may confer thermal stability to the protein, observed as a displacement of the melting curve with a concomitant shift in melting temperature relative to the uncomplexed protein (ΔT_m). The stabilising effect of compounds upon binding has been shown to be proportional to the concentration and affinity of the ligands;[160–162] however, compounds should not be ranked on ΔT_m alone as this depends on the enthalpy and entropy of binding of a particular ligand, not the affinity of the ligand.[163] That aside, the assay benefits from low protein loadings due to the fluorescent nature of the measurement, no substrate modification is required and it is amenable to high throughput screening (HTS).

1.3.2 Isothermal titration calorimetry, ITC

Isothermal titration calorimetry (ITC) measures both the thermodynamics and affinity of ligand binding to a protein. This assay is based upon heat being generated or absorbed upon binding as a result of changes in the enthalpy and entropy of the species involved.[164] In an ITC experiment, the ligand is titrated into a cell containing the protein, and the power required to maintain a constant temperature between this and a reference cell is measured [Figure 1.10]. From this, binding constants, reaction stoichiometry and the thermodynamic profile of the interaction can be determined. This method has been referred to as the "gold standard" for characterising protein-ligand interactions, due to the accuracy of the data obtained and because the affinity ob-

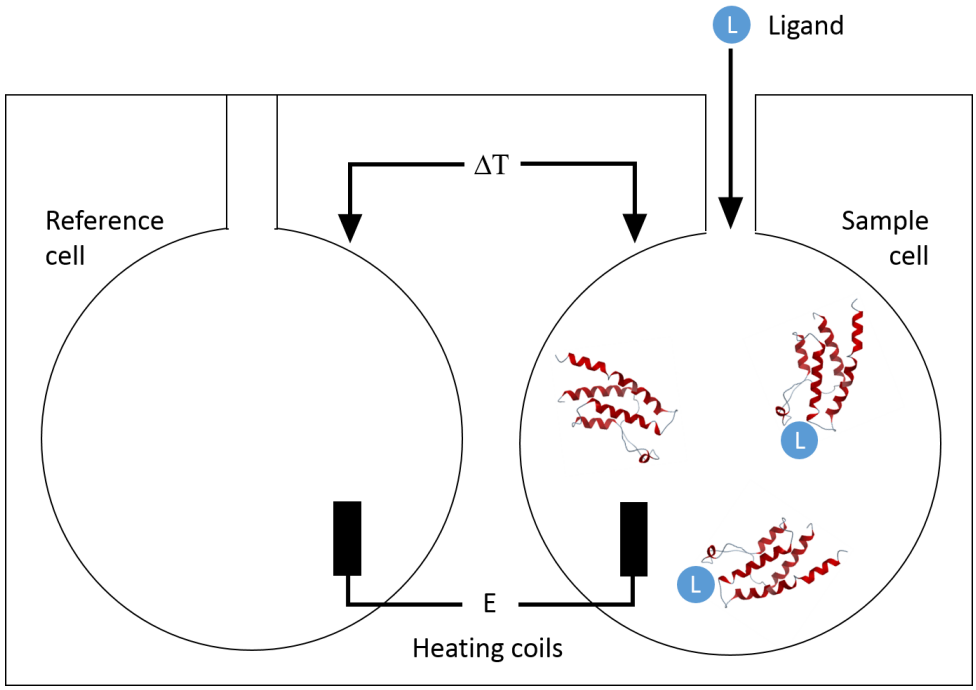

Figure 1.10 Schematic of an ITC experiment. Ligand is titrated into the sample cell, and the difference in temperature due to binding results in energy being expended to equilibrate the temperature of the two cells.

tained (K_D) is a measure solely of ligand binding to the protein.[165,166] Additionally, this assay does not require the introduction of labels to immobilise or tag the substrates; however, the assay requires a high protein loading, especially with low affinity ligands, and is not amenable to HTS.

1.3.3 BROMO*scan* assay

The BROMO*scan* assay, operated by DiscoveRx Corporation, is a competition binding assay for ligands against bromodomains. This is centered around the competition of the compound of interest with an immobilised ligand for a bromodomain.[167,168] In this, a known bromodomain ligand is immobilised on a bead and a solution is added that contains known quantities of bromodomain protein and compound being tested. After equilibration, the liquid phase is decanted and the protein remaining in this phase, which did not bind to the solid support, is quantified by quantitative real-time polymerase chain reaction. Through competition with the immobilised ligand for the binding site, the compound being tested prevents the bromodomain binding to the support and increases the amount of protein remaining in the liquid phase; the quantity of protein in the liquid phase can therefore be correlated with the affinity of the ligand. Through assessing binding across a serial dilution, a dose-response curve is obtained

and the IC_{50} of the compound can be assessed. As this assay measures competitive inhibition, the affinity obtained (IC_{50}) also includes a measure of binding between the solid-supported ligand and the bromodomain, residency times of each ligand in the bromodomain and the reversibility of the binding events. In addition to physical sources of error, including non-specific protein adherence and material loss through the multi-step procedure, the affinity estimates from this assay are liable to be higher than those obtained from assays that directly measure protein-ligand interactions (ITC).

1.3.4 Fluorescence recovery after photobleaching assay, FRAP

The fluorescence recovery after photobleaching (FRAP) assay is used to assess the diffusion of biomolecules. The assay centers around the rate of recovery of fluorescence to a photobleached area giving insight to the diffusion of a biomolecule to which a fluorescent entity is attached.[169–171] The biomolecule of interest is tagged with a fluorophore, commonly the fluorescent dye fluorescein or the fluorescent protein green fluorescent protein (GFP), before a microscopic region of the sample is photobleached with an intense light beam to quench the fluorescence of the fluorophores in this area [Figure 1.11]. Fluorophores from elsewhere in the sample then diffuse into the photobleached area and return fluorescence to the area, the rate of which is correlated to the mobility of the biomolecule. If the biomolecule is unbound, the recovery time is dependent only on diffusion; however, if the entity is binding to a large component of the cell, then diffusion is restricted and the recovery time increases. Through quantitative analysis, expressions for diffusion coefficients and binding kinetics can also be

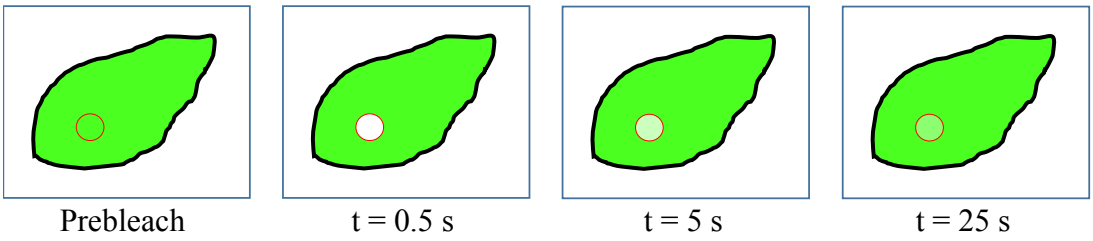

Figure 1.11 Model example of a FRAP assay. The red circle denotes the area that is photobleached. After photobleaching (t = 0 s), the fluorescence recovers towards prebleaching levels with time.

obtained. This assay has the advantage of being non-invasive, however photoswitching – where GFP regains fluorescence over time – and the need to express a modified peptide are weaknesses of this method.

1.3.5 Amplified luminescent proximity homogeneous assay, AlphaScreen

The amplified luminescent proximity homogeneous assay (AlphaScreen) measures the proximity of biological binding partners. This assay relies on the transfer of singlet oxygen between two beads tagged to biomolecules that bind each other.[172,173] To measure bromodomain-histone binding,[174] a histone peptide with a biotin tag is expressed, which is bound by strepavidin-coated donor beads [Figure 1.12]. Meanwhile, the bromodomain is expressed with an *N*-terminal His_6 tag that specifically chelates to Ni^{2+} ions on the surface of the acceptor bead. Upon irradiation at 680 nm, phthalocyanine, a photosensitiser, in the donor bead absorbs this energy and produces many molecules of singlet oxygen, which amplifies the incident signal. Chemiluminescent molecules in the acceptor bead react with the singlet oxygen and undergo transformations that ultimately transfer energy to fluorophores in the bead, which emit light at

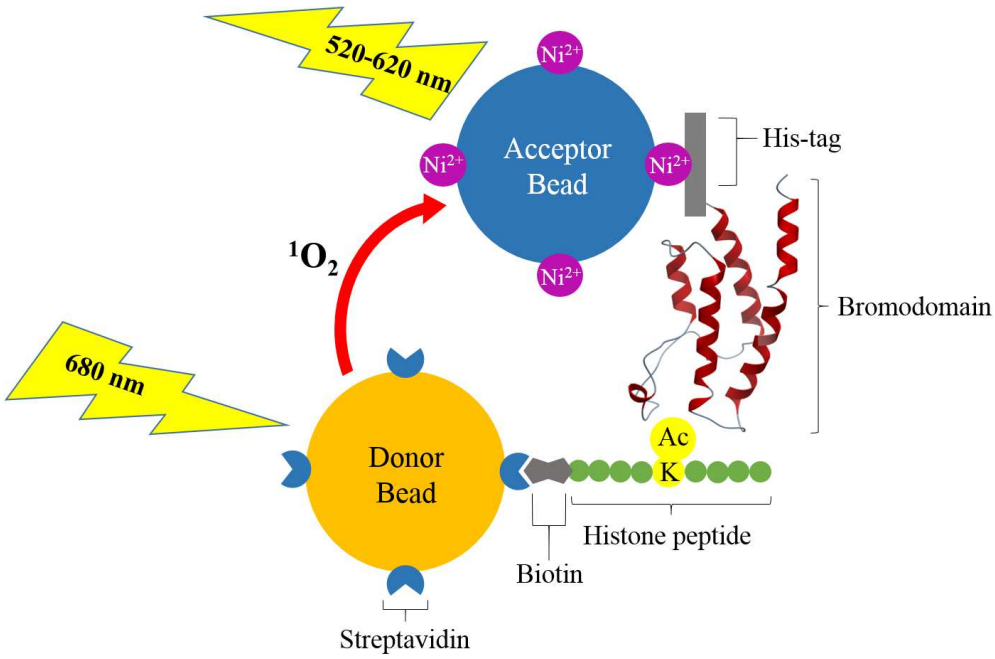

Figure 1.12 Schematic of an AlphaScreen assay. The donor beads contains phthalocyanine, a photosensitizer that generates short-lived singlet oxygen upon excitation, and the acceptor beads contain chemiluminescent molecules that react with the singlet oxygen and transfer energy to fluorophores also in the acceptor beads.

520-620 nm. The use of chemiluminescent intermediaries acts to delay energy transfer, allowing for a delayed detection that negates short-lived background fluorescence to increase sensitivity. Binding of the biomolecules results in the beads being within the 200 nm diffusion distance of singlet oxygen, allowing fluorescence to be observed. Addition of a competitive ligand prevents binding and the biomolecules diffuse apart with a concomitant loss in fluorescence. By analysing emitted fluoresence as a function of ligand concentration, dose-response curves and estimates of IC_{50} can be obtained. The assay requires only a low protein loading due to the amplification, and is amenable to HTS; however, both biomolecules need to be expressed with tags and the incident beam can lead to photobleaching and autofluorescence that can act as sources of error in this assay.

1.3.6 Nanoluc luciferase Bioluminescence Resonance Energy Transfer assay, NanoBRET

The Nanoluc luciferase bioluminescence resonance energy transfer (NanoBRET) assay, operated by Promega Corportation, also measures the proximity of biological binding partners. Whereas the AlphaScreen depended on transfer of singlet oxygen, the NanoBRET assay instead centers upon bioluminescence resonance energy transfer (BRET). A luciferase fusion protein emits bioluminescence when converting furimazine to furimamide [exemplified by Figure 1.13].[175] A fluorophore attached to another biomolecule can absorb this bioluminescence, and in turn emit fluorescence at a different wavelength. Binding of the biomolecules ensures sufficient proximity of the luciferase and the fluorophore for BRET to occur; however, addition of a competitive ligand decreases the interaction and BRET. Analysing fluorescence as a function of ligand concentration allows the affinity (IC_{50}) to be assessed. A standard BRET assay uses a *Renilla* luciferase as the energy donor matched with yellow fluorescent protein,[176] however, there is only a 55 nm separation between the peak fluroscences that affects sensitivity because of experimental noise. The NanoBRET assay instead uses an engineered Nanoluc luciferase, that produces higher intensity fluorescence with a narrower bioluminescence spectrum,[177] matched with an imidazopyrazine dye as the acceptor [Figure 1.13].[178] The 175 nm separation between the emission peaks of the donor and the acceptor improve sensitivity, and the higher intensity of the donor allows interactions to be observed at protein concentrations comparable to physiological levels. This assay avoids the issues of photobleaching and autofluorescence

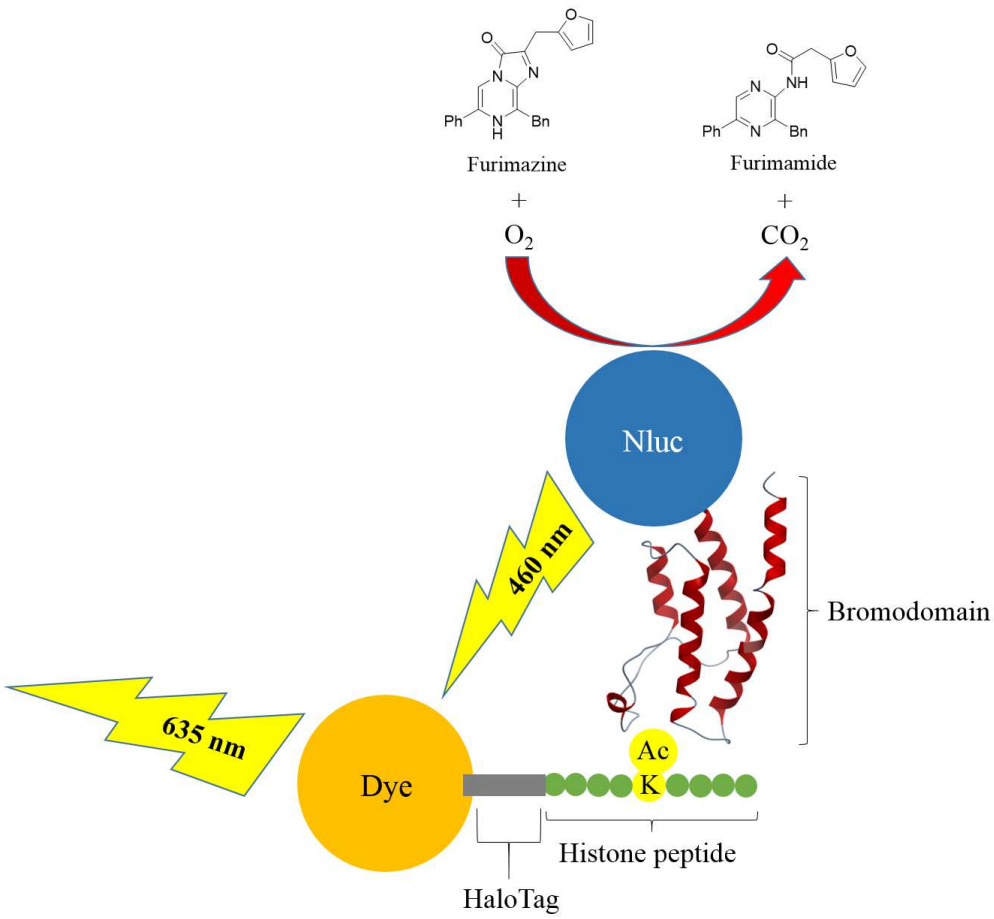

Figure 1.13 Schematic of a NanoBRET assay. The Nanoluc luciferase is expressed as a fusion protein with the bromodomain under investigation, whilst the NCT fluorophore is covalently linked to a HaloTag expressed on the histone peptide.

encountered with direct excitation in the AlphaScreen assay; however, the substrates again need to be expressed with tags and only an IC_{50}, and not a K_D, can be obtained as the measure of ligand affinity.

1.4 General Research Aims

The aim of this research was to develop new probes that could be used as chemical tools in the elucidation of bromodomain protein activity. From fragment hits or lead compounds, in conjunction with crystallographic knowledge of the binding site, a structure-based drug design program was to be pursued against unprobed bromodomain proteins. At each step of structural refinement, biophysical assays were to be used to guide the optimisation process. Any chemical probes – defined by an affinity of <100 nM and a selectivity of >30-fold over related proteins –

that were obtained were then to be used in cellular assays to assess the effect on bromodomain binding to chromatin. Any probes that were successfully validated in this way were then to be used in further biological experiments to decipher the role of the target protein. Where possible, chemical methods that could facilitate the exploration of SAR, such as MCRs, or allow for the enantioenriched synthesis of biologically active molecules, such as enantioselective organocatalysis, were to be used to assist in probe development.

Chapter 2

BRD4

2.1 Project origin

2.1.1 Lead compounds

The 3,5-dimethylisoxazole motif was identified as an effective acetyl lysine mimic for binding to BRD4. As discussed previously [Section 1.1.1], a number of pan-BET benzodiazepine inihibitors have been described that, although potent, lack specificity for BRD4, preventing the individual role of the protein to be elucidated. Towards addressing this deficit, Hewings *et al* discovered that the solvent *N*-methyl pyrrolidone showed a weak affinity for BRD4(1).[106] This prompted a fragment screen of methyl-bearing heterocycles, during which compound **45** was discovered to have a significant affinity for BRD4(1), with an IC_{50} of 7 μM [Figure 2.1]. To confirm the binding mode of the ligand, as both 3,5-dimethylisoxazoles and dihydroquinazolinones are known acetyl-lysine mimics [Section 1.1.6], a co-crystal structure was obtained [Figure 2.2].

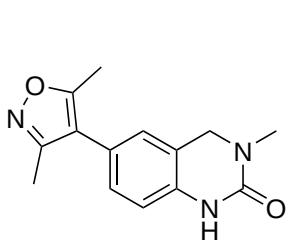

45

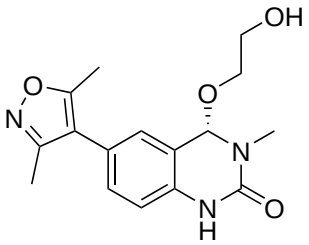

46

Figure 2.1 3,5-dimethylisoxazole compounds identified as leads against BRD4(1).

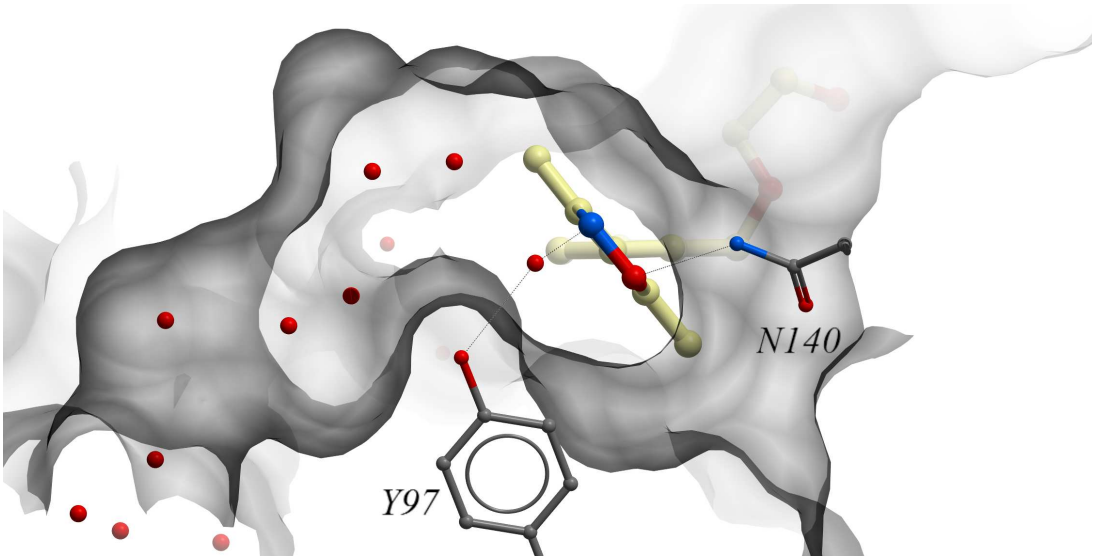

(a) H-bonds were observed between the 3,5-dimethylisoxazole motif and residues N140 and Y97, the latter mediated through the first of a column of water molecules in the binding pocket.

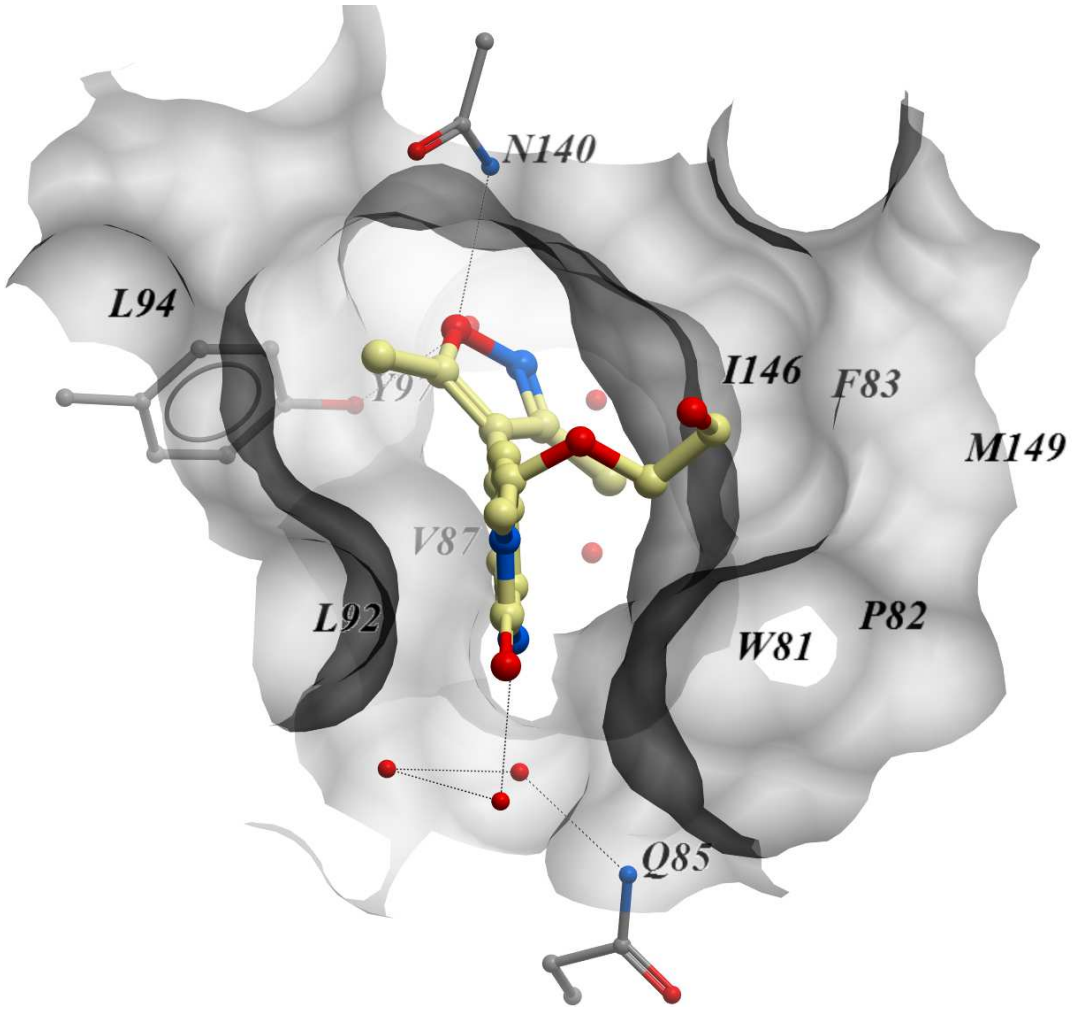

(b) The scaffold of **46** orientating into the ZA channel of BRD4(1), with the ethylene glycol substituent occupying the WPF shelf and a network of water molecules bound around the opening.

Figure 2.2 A co-crystal structure of **46** bound to BRD4(1) with key H-bonds (dotted black lines) and conserved water molecules (red dots) [PDB ID: 3SVF].

When the electron density was solved, the ligand bound was found not to be **45**, but instead an artifact of the assay conditions (**46**). Nonetheless, the key binding elements could be assessed from the co-crystal structure.

The 3,5-dimethylisoxazole motif was found to direct binding. From the co-crystal structure, the oxygen of the isoxazole was found to accept a H-bond from the conserved N140 residue, whilst the nitrogen of the isoxazole H-bonded to the hydroxyl of Y97 via a structured water molecule, the first of a column of water molecules descending through the protein [Figure 2.2a]. On the surface, the dihydroquinazolinone was found to reside in a hydrophobic cleft bound on one side by V87, L92 and L94, and by W81, F83 and I146 on the other, with the ethylene glycol substituent occupying the WPF shelf bound by W81, P82, F83, and M149 [Figure 2.2b]. Finally, the urea moiety of the scaffold was observed to reside in the narrow ZA channel, between W81 and L92, at the opening of which a network of water molecules were observed that mediated interactions between the unsubstituted urea nitrogen and Q85. Having identified key binding elements, an optimisation was performed that resulted in the identification of **47** as a lead fragment against the BET family and CREBBP bromodomains (IC_{50} 1.6–28.1 μM) [Figure 2.3].[106]

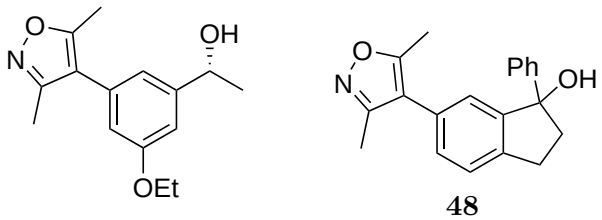

47 **48**

Figure 2.3 Further lead compounds identified against BRD4(1).

Alternative scaffolds were then explored with this bioisostere. As demonstrated by **45** and **46**, bicyclic scaffolds were tolerated in BRD4(1) binding, and it was envisioned that an indene-based system would allow new substitution patterns to be explored. Dihydroindene **48** was found to have an IC_{50} of 1.3 μM against BRD4(1) [Figure 2.3].[179] A co-crystal structure of this with BRD4(1) confirmed similar binding elements as seen with **46** [Figure 2.4]: the isoxazole oxygen exhibited the key H-bond to N140 of acetyl lysine recognition while the nitrogen atom H-bonded to Y97 through an intermediary water molecule; the exocyclic phenyl ring occupied the WPF shelf, bound on the top side by D145; and the saturated cyclopentyl moiety occupied

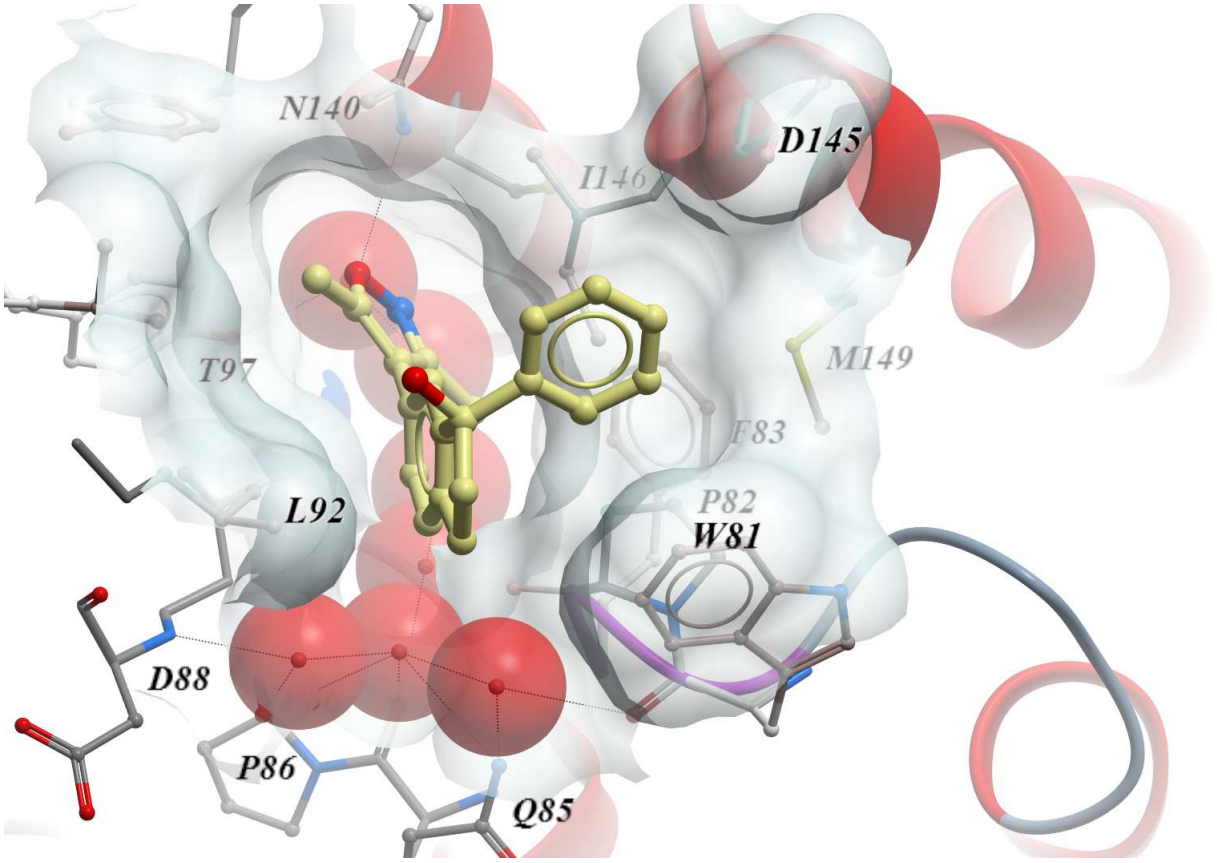

Figure 2.4 Co-crystal structure of **48** bound to BRD4(1) with key H-bonds (dotted black lines) and water molecules (red dots and spheres) [PDB ID: 4GPJ].

the narrow ZA channel between W81 and L92. Although a similar network of water molecules was seen anchored to W81, Q85, P86 and D88 in the base of the pocket, no binding interactions were formed with these due to the lack of H-bonding groups in the ring.

This scaffold was then progressed in two directions. Due to apparent instability of the compounds, optimisation of **48** was initially pursued through a related benzimidazole scaffold.[179] After successive rounds of optimisation, **49** was obtained that showed a higher affinity for BRD4(1) than the structurally-related CREBBP protein (IC_{50} 195 nM vs >100 μM, AlphaScreen) [Figure 2.5]; a further selectivity screen against 9 other bromodomain proteins

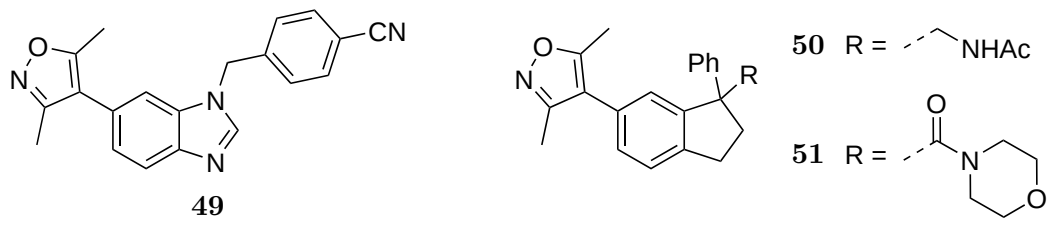

Figure 2.5 Alternative optimisations of **48**.

revealed a significant binding preference for BRD4(1) (ΔT_m 3.2 °C vs -0.4 – 1.1 °C, DSF). An alternative optimisation performed by collaborators at the SGC examined the effect of derivatisation at the tertiary alcohol of **48**. A series of compounds were made with a quaternary carbon bearing different pendant groups, of which **50** and **51** were identified as the most potent leads (IC_{50} 540 nM and 470 nM, ITC). Although limited on scope, this preliminary research demonstrated the tolerance of significant substitution at this position, a good indication that SAR could be explored extensively around this part of the ligand.

2.1.2 Aim

The aim of this research was to combine binding elements of the existing lead compounds into a single, high affinity ligand. Building upon **48**, we intended to retain a 6,5-bicyclic scaffold, but with sp^2-hybridisation in the five-membered ring to minimise unfavourable steric clashes with the narrow ZA channel; this unsaturation was to be realised through the incorporation of a lactam motif, as part of a larger isoindolin-1-one scaffold in the general targets **52** and **53** [Figure 2.6]. This functionality was chosen because the carbonyl group would be orientated towards the network of water molecules found around the opening of the ZA channel, with the intention to replicate the H-bond seen with **46** to increase the strength of binding. Given the tolerance for substituents at C3 as demonstrated by **50** and **51**, extensive derivatisation was to be explored at this position to improve both potency and selectivity. Finally, alternative substitution of the nitrogen of the lactam was to be investigated to assess the effect of this group on binding. Where possible, enantioselective chemical methods were to be used to selectively furnish the more biologically-active enantiomer. It was hoped that exploring derivatives of the general form **52** and **53** would lead to the development of the first probe for BRD4(1).

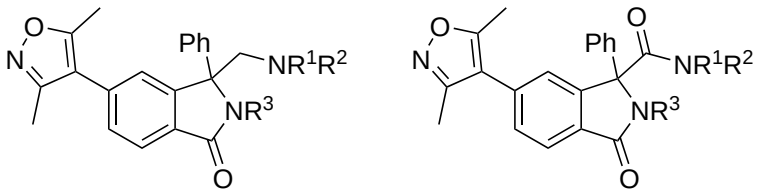

52 **53**

Figure 2.6 General structures for ligands intended against BRD4(1).

2.2 Development of a BRD4(1) probe

2.2.1 Validation of the isoindolinone scaffold

The first stage of probe development was validation of the isoindolinone scaffold. Using a synthetic route comprised of known reactions, a small number of preliminary compouds were to be made for testing to assess the alternative scaffold used. Phthalic anhydride was brominated in the C5 position – for later attachment of the 3,5-dimethylisoxazole moiety – using Br_2 and NaOH, with the diacid intermediate cyclised back to an anhydride using $SOCl_2$ (**54**) [Scheme 2.1].[180] The regioselectivity observed arises from the deactivating effect of the carboxylates on the electrophilic aromatic substitution through induction, which affects the C4 position to a greater degree due to proximity. A Friedel-Crafts acylation using benzene and $AlCl_3$ resulted in a 2:1 mixture of regioisomers (**55**) in favour of phenyl attachment at C3.[181] This preference was expected due to inductive and resonance effects of the bromine atom: through induction, the bromine would decrease electron density at C3 more than C1; and through resonance would increase electron density on the oxygen of C1 more than at C3. Collectively, this would result in preferential binding of $AlCl_3$ to the C1 position, generating an oxonium ion at C3 that could then undergo the Friedel-Crafts acylation.

Chromatographic separation of the regioisomeric acids **55** proved problematic. Separation using conventional flash column chromatography (FCC) was unsuccessful, with minimal resolution observed when using the mobile phases required to elute these highly polar compounds. To mitigate this issue, the crude material isolated from the Friedel-Crafts acylation was converted to an acid chloride using $SOCl_2$ and reacted with methylamine to give the isomeric hydroxylactams **56** and **57**. The preference for these compounds to exist as cyclic hydroxylactam isomers rather than acyclic acylamides has been observed previously under different conditions.[182] In comparison to **55**, these compounds were readily separable by FCC, and obtained pure in poor yields over the three steps (6.5% and 11.7%). An alternative method to aid isolation of the Friedel-Crafts product involved formation of the methyl ester **58**, which was fortuitously found to selectively crystallise from the mixture.[183] Aminolysis with methylamine then selectively gave **57** in reasonable yield over the three steps (30%).[184] The aryl bromides were then directly coupled with 3,5-dimethylisoxazole using a ligand-free Pd-catalysed C-H bond

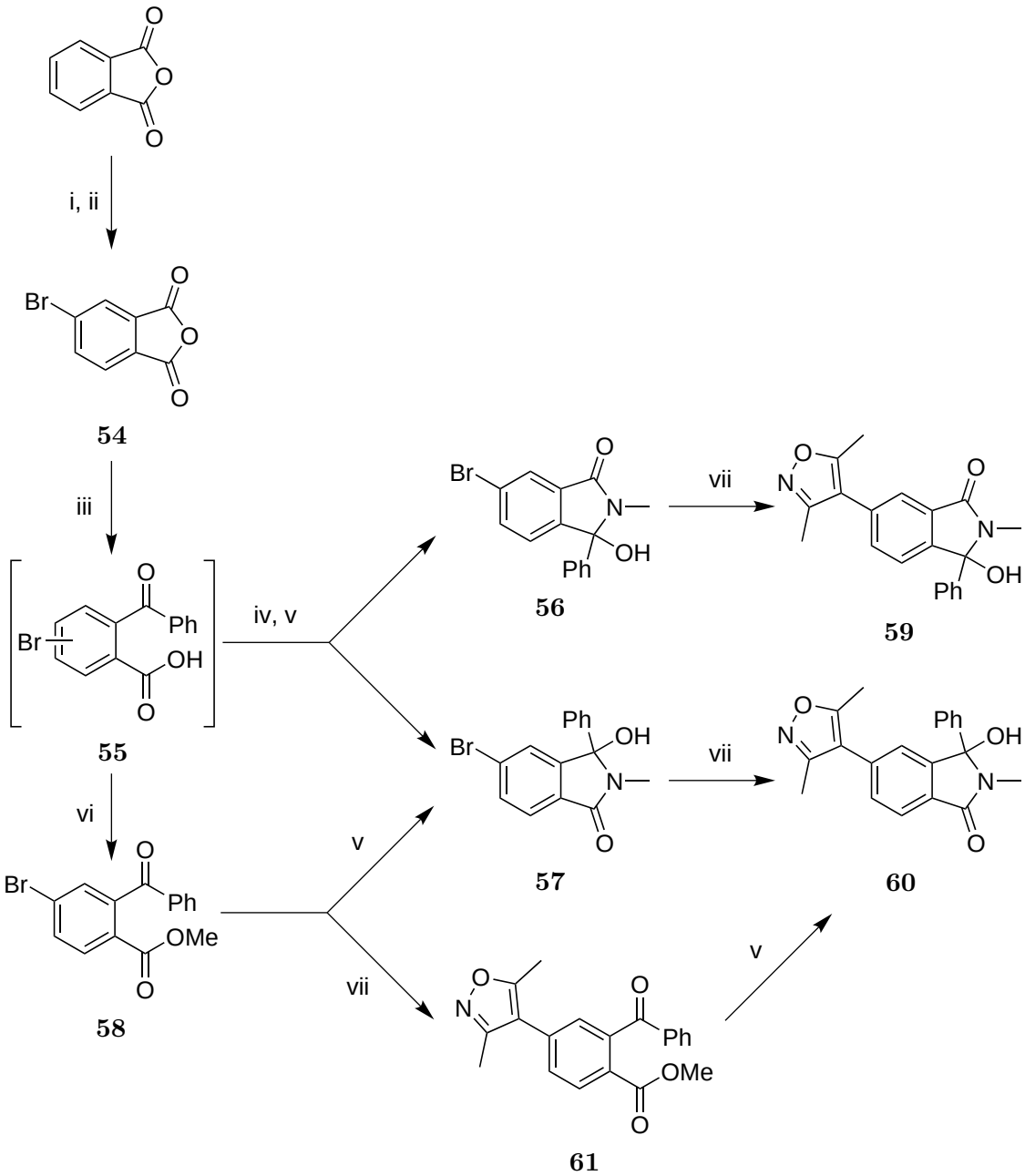

Reagents and Conditions: i. Br_2, NaOH, H_2O, 90 °C, 6 h; ii. $SOCl_2$, reflux, 2.5 h, 48% (2 steps); iii. $AlCl_3$, benzene, rt, 12 h, 4-Br:5-Br 2:1; iv. $SOCl_2$, DMF, rt, 4 h; v. $MeNH_2$, EtOH, rt, 14 h, **56**: 6.5% (3 steps), **57**: 11.7% (from **54**, 3 steps), 68% (from **58**), **60**: 25%; vi. $SOCl_2$, MeOH, rt, 14 h, 44% (2 steps); vii. 3,5-dimethylisoxazole, $PdCl_2$, KOAc, DMAc, 130 °C, 6 h, **59**: 62%, **60**: 87%, **61**: 80%.

Scheme 2.1 Synthesis of preliminary compounds to validate isoindolinone scaffold.

activation to yield **59**, **60** and **61** for testing.[185] The ester **61** could also be reacted with methylamine to obtain **60**, an important manipulation that could allow for late-stage *N*-diversification.

Initial screening revealed the isoindolinone scaffold showed a high affinity for BRD4(1). Compounds **59**–**61** bearing the 3,5-dimethylisoxazole group were screened by DSF and AlphaScreen against BRD4(1) [Table 2.1]. Ester **61** showed only limited binding by both DSF (ΔT_m 2.6

Table 2.1 Screening of preliminary isoindolinone structures against BRD4(1) by DSF and AlphaScreen assays.

Compound Structure	#	ΔT_m (°C)*	IC_{50} (nM)
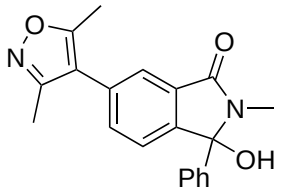	**59**	1.2	
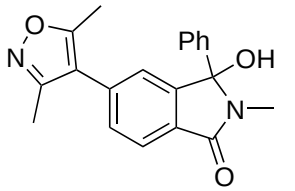	**60**	8.2	13
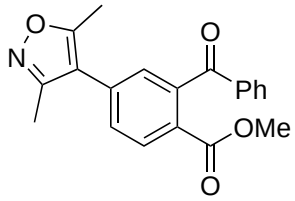	**61**	2.6	1510

*All compounds were tested at 10 μM.
Performed by collaborators at the SGC.

°C) and AlphaScreen (IC_{50} 1.5 μM), which was unsurprising given the narrowness of the ZA channel and the desire for the two carbonyls of **61** to adopt a perpendicular arrangement to minimise clashes. Hemiaminal **59** similarly showed a poor affinity for BRD4(1) (1.2 °C, DSF), which was likely due to, assuming a similar binding mode as for **46** and **48**, the exocyclic phenyl ring being orientated into the protein. This aside, the desired model **60** showed fantastic affinity in both assays: a ΔT_m of 8.2 °C (DSF) was at this time without parallel, and an IC_{50} of 13 nM (AlphaScreen) was an unprecedented affinity amongst known BRD4(1) ligands. This confirmed the applicability of an isoindolinone scaffold, with further optimisation of the ligand to be initially targeted through the C3 position.

2.2.2 Exploration of SAR around the isoindolinone scaffold

2.2.2.1 Derivatisation at C3

Establishing SAR at the C3 position was originally limited to the pendant chain for synthetic reasons. The double substitution of C3 presented two groups around which SAR could be

established. However, given the early installation of this ring and the empirical isolation of **58** through selective crystallisation, the phenyl group was to be unchanged initially. Given the tolerance of the binding pocket for significant pendant groups attached at C3, as demonstrated by the affinities of **50** and **51**, SAR around the second substituent was to be explored instead. Synthetic methods were first trialled on model substrates lacking the 3,5-dimethylisoxazole moiety to validate and establish the chemistry.

Synthetic attempts that allowed for a late stage *N*-derivatisation were largely unsuccessful. The first synthetic approach was centered around having the lactam nitrogen unsubstituted, such that an *N*-alkylation could be performed as the final step to readily obtain a range of derivatives at that position. Phthalimide was reacted with phenylmagnesium bromide to give the hydroxylactam **62** [Scheme 2.2].[186] As bond formation at C3 required the elimination of hydroxide, a methoxide leaving group was installed through treatment of **62** with H_2SO_4 in MeOH to give **63** that would more readily eliminate.[187] This proved unnecessary, as with a diphenyl phosphoric acid (DPP) catalyst **62** readily underwent both a nitro-Mannich reaction with nitromethane to give **64**,[188] and a hydrogenolysis with a Hantzsch ester to give **65**.[189]

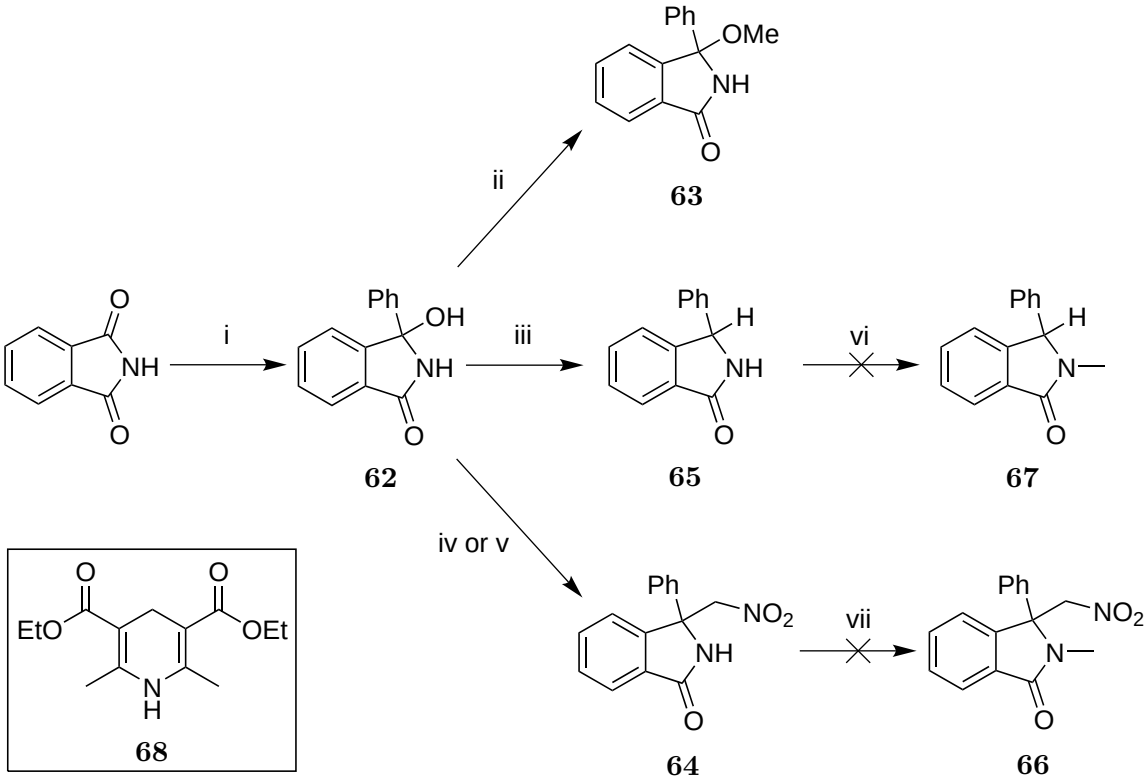

Reagents and Conditions: i. PhMgBr, THF, CH_2Cl_2, rt, 5 h, 78%; ii. H_2SO_4, MeOH, reflux, 24 h, 75%; iii. **68**, DPP, toluene, rt, 20 h, 78%; iv. CH_3NO_2, DPP, reflux, 66 h, 24%; v. CH_3NO_2, BEMP, reflux, 66 h, 11%; vi. MeI, NaH, DMF, rt, 2 h, 0%; vii. MeI, K_2CO_3, DMF, 0 °C, 2 d, 0%.

Scheme 2.2 Derivatisation of model species with a *N*-unsubstituted lactam.

Attempts to *N*-methylate these species with MeI under basic conditions, however, failed to give **66** and **67**;[190,191] rapid elimination of nitromethane occured with **64**, and no reaction was observed with **65**. Although alternative alkylation methods may have been able to furnish **66** and **67**, the synthetic approach was modified instead.

Using *N*-substituted lactams, some C3 derivatised targets were achievable. Akin to the brominated reaction sequence [Scheme 2.1], phthalic anhydride was able to undergo a Friedel-Crafts acylation with benzene and $AlCl_3$ to generate **70**, which could be activated with $SOCl_2$ and subsequently reacted with methylamine to give **71** [Scheme 2.3].[181,182] As before, a nitro-Mannich reaction with nitromethane and DPP rapidly yielded **66**,[188] whilst a Hantzsch reduction gave **67**. All attempts to install a nitrile group – a useful chemical handle which could be readily manipulated for further derivatisation – were unsuccessful. A range of methodologies were trialled, including: the use of both TMSCN and NaCN as the cyanide source; adding TMSCl to activate the substrate; and the addition of TBAB to ensure heterogeneity of the reaction mixture was not preventative.[192,193] In no case was the desired product observed. At this point it was unclear whether cyanide was not sufficiently nucleophilic to attack the iminium

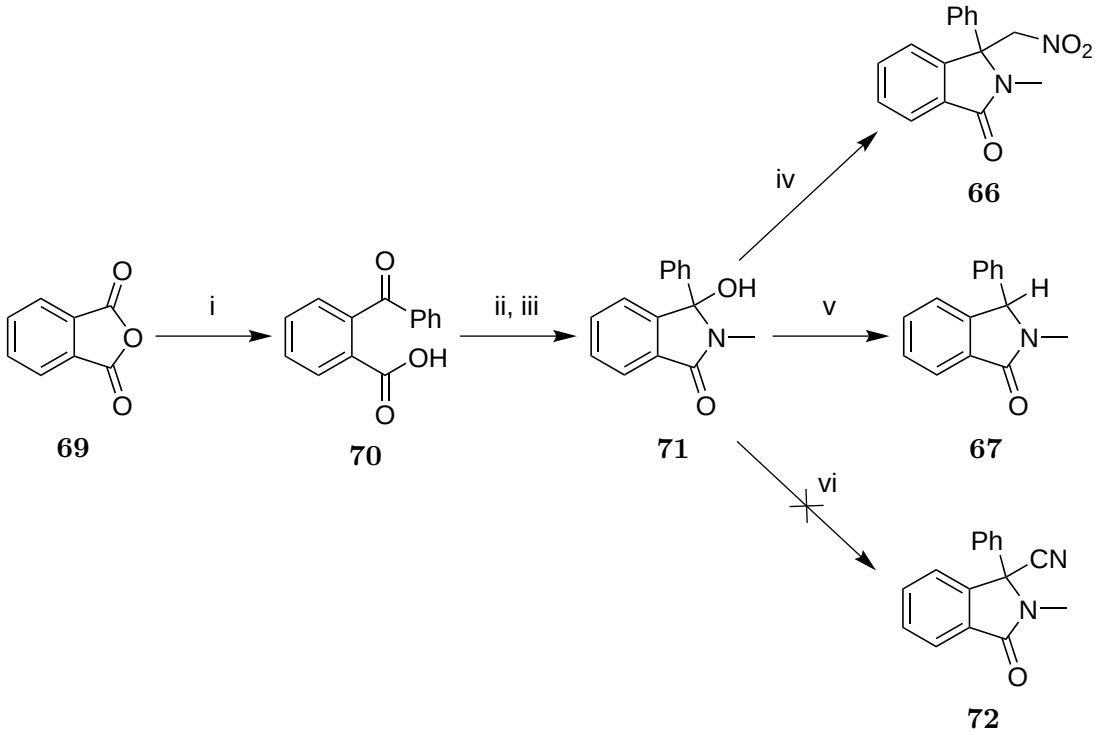

Reagents and Conditions: i. $AlCl_3$, benzene, rt, 14 h, 93%; ii. $SOCl_2$, DMF, rt, 4h; iii. $MeNH_2$, EtOH, rt, 14 h, 72% (2 steps); iv. CH_3NO_2, DPP, reflux, 36 h, 76%; v. **68**, DPP, toluene, rt, 72 h, 98%; vi. TMSCN or NaCN, with or without TMSCl or TBAB, TBME, CH_2Cl_2 or THF, 0%.

Scheme 2.3 Derivatisation of model species with *N*-alkylated lactam.

species resulting from **71** or whether the equilibrium favoured the substrate for this reversible reaction. Further methods to install a C3 nitrile were explored later using the real substrate.

Applying these methods to substrates bearing the 3,5-dimethylisoxazole moiety gave a number of novel compounds. The nitro-Mannich reaction, as performed on the model compounds, was readily achieved with hemiaminal **60** to yield the nitromethyl-adduct **73** [Scheme 2.4].[188] The nitro group could then be reduced with zinc powder in refluxing acetic acid to yield the acetamide **74**.[194] To avoid the concomitant protection, the reaction was repeated, but instead using zinc, ammonium chloride and methanol, to give the primary amine **75**.[195] Subjecting this to Eschweiler-Clarke conditions yielded the dimethylamine derivative **76** for testing.[196] To circumvent the previous issues with cyanation, dehydration of the nitro group was attempted: sequential dehydrations of **73** with benzyl bromide then $SOCl_2$ under basic conditions furnished the desired nitrile **77**.[197] A direct formation of this could also be achieved through the use of *t*BuNC, in which nucleophilic attack of the isocyanide is followed by the loss of isobutene to drive formation of the nitrile.[198] These reactions demonstrated that the previous issues in synthesising this motif were not due to inherent instability of the product.

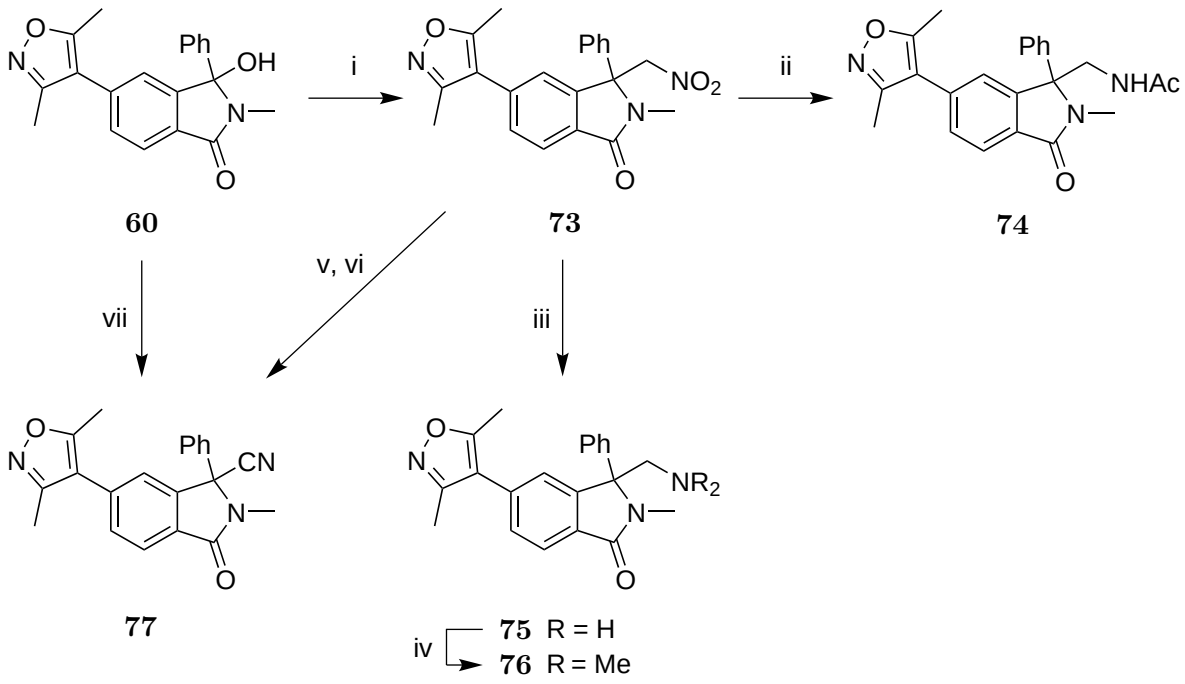

Reagents and Conditions: i. CH_3NO_2, DPP, reflux, 2 d, 89%; ii. Zn, AcOH, reflux, 14 h, 55%; iii. Zn, NH_4Cl, MeOH, 60 °C, 17 h, 85%; iv. formic acid, formaldehyde, H_2O, reflux, 7 h, 92%; v. BnBr, KOH, *n*-Bu_4NI, THF, rt, 3 h; vi. $SOCl_2$, NEt_3, THF, rt, 12 h, 38% (2 steps); vii. *t*-BuNC, pTsOH, THF, 120 °C, 15 h, 75%.

Scheme 2.4 Synthesis of *C3*-derivatives for testing.

The intended derivatisation of this nitrile was hindered by a competing decarboxylation. Although **77** could be converted to the primary amide **78** with sulfuric acid in CH_2Cl_2 [Scheme 2.5],[199] all attempts to convert either of these compounds into the secondary amide **79** or the carboxylic acid **80** were unsuccessful,[200–202] with degradation of the material occuring in most cases. The one exception was treatment of the primary amide **78** with HCl in H_2O and THF, which yielded the decarboxylated species **81**;[203] this product was confirmed through reduction of hemiaminal **60** with both a Hantzsch ester or triethylsilane.[204] This species could ostensibly be formed through spontaneous decarboxylation of **80**, which would be driven by the liberation of CO_2 and acid-catalysed vinylogous enolisation [Scheme 2.6]; the resulting enol **82** could then tautomerise to the observed compound **81**. A related decarboxylation has been observed previously,[205] however without any comment on the occurrence by the researchers. As the other methods trialled involved the formation of **80** as either an intermediate or as the product, the same decarboxylation could be occurring; however, as these methods involved basic conditions, the charge of the resulting anionic species would not be readily stabilised, and further degradation may have then occurred. Although this unexpected decarboxylation decreased the number of targeted compounds attained, a range of *C3*-derivatives were synthesised that could be used to assess SAR at this position.

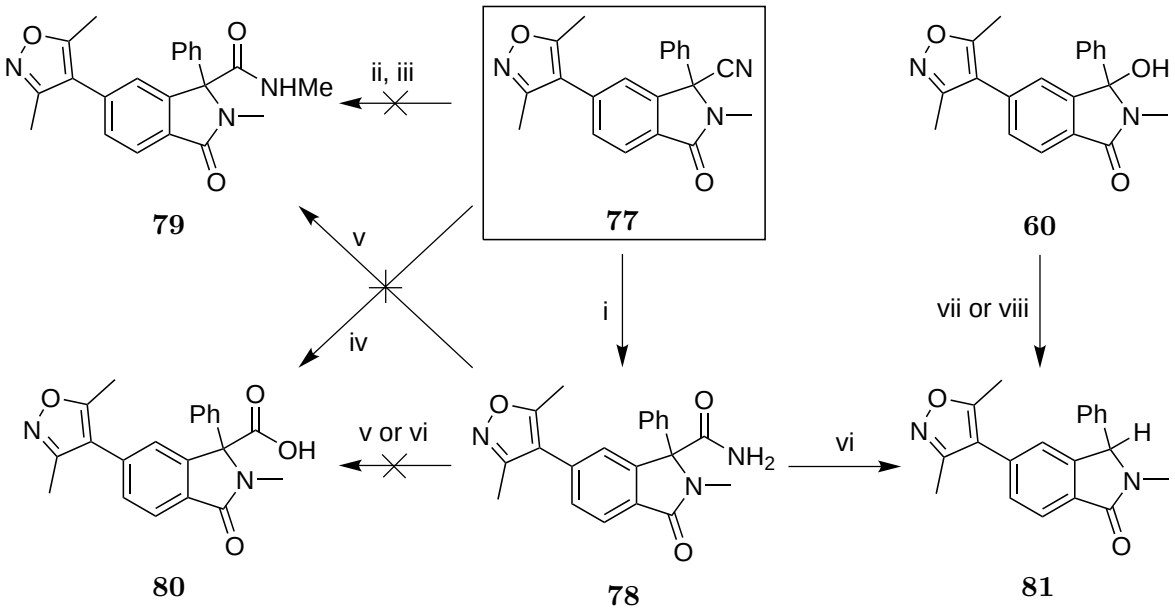

Reagents and Conditions: i. H_2SO_4, CH_2Cl_2, reflux, 16 h, 81%; ii. H_2SO_4, H_2O, reflux, 14 h; iii. $SOCl_2$, $MeNH_2$, EtOH, rt, 16 h, 0% (2 steps); iv. NaH, MeI, THF, DMF, rt, 4 h, 0%; v. NaOH, H_2O, THF, rt, 16 h, 0%; vi. HCl, H_2O, THF, reflux, 20 h, **80**: 0%, **81**: 47%; vii. Et_3SiH, TFA, CH_2Cl_2, rt, 4 h, 34%; viii. **68**, DPP, toluene, rt, 7 d, 98%.

Scheme 2.5 Attempted synthesis of further *C3*-derivatives.

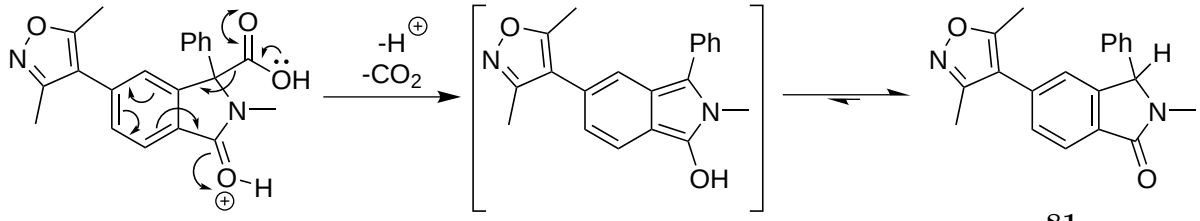

Scheme 2.6 Proposed mechanism of formation of **81**.

2.2.2.2 Derivatisation of the lactam nitrogen

Focus then shifted to the synthesis of *N*-derivatives. The *N*-methyl of **60** was positioned towards the outside of the ZA channel of BRD4(1) [Figure 2.4], and it was envisioned that exploring alternative substitution at this position may lead to the formation of novel binding elements. As demonstrated previously, the ester **61** reacts with amines to directly form acylamides (**I**) that can isomerise to cyclic hydroxylactams (**II**) [Table 2.2].[184] The preference of this equilibrium to favour the cyclic species **II**[182] was readily demonstrated with benzylamine and *N,N*-diethylethylenediamine: hydroxylactams **83** and **84** were observed, with no evidence of their acyclic counterparts. However, reaction with aminoacetaldehyde dimethyl acetal gave a mixture of acyclic (**85**) and cyclic (**86**) products. This amine has increased steric hindrance closer to the ring, and it would be expected that unfavourable steric clashes would raise

Table 2.2 Synthesis of *N*-alkyl derivatives.

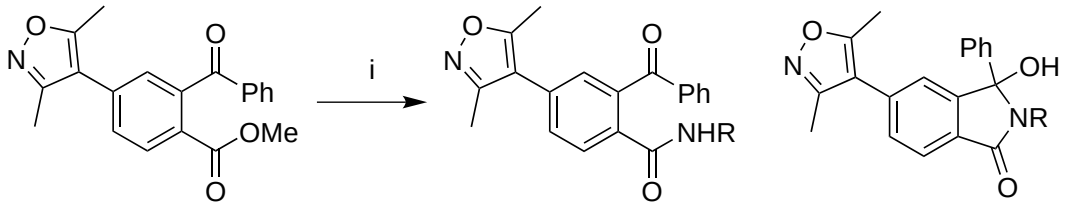

Reagents and Conditions: i. RNH_2, Base (0.1 eq), EtOH, reflux, 2 d.

		I		II	
	Exogenous		Yield		Yield
R	**Base**	#	(%)	#	(%)
Bn			-	**83**	15%
$(CH_2)_2NEt_2$			-	**84**	16%
$CH_2CH(OMe)_2$		**85**	37%	**86**	18%
$(CH_2)_2Cl$*	NEt_3		-		-
CH_2CCH	NEt_3		-		-

*Reaction performed in THF.

the energy of the cyclic species such that equilibrium favoured the acyclic isomer. Despite differences in the position of equilibrium, these amines were successful in aminolysis of the ester; use of 2-chloroethan-1-amine resulted in no product formation, potentially as a result of intramolecular cyclisation to an aziridine;[206] while propargylamine was similarly unsuccessful, potentially as a result of the inductive effects of the alkyne decreasing the basicity of the amine.

The use of 2-hydroxyalkylamines to generate tricyclic scaffolds appeared to be highly substrate-dependent. To assess the possibility of extending the scaffold further to allow the attachment of more substituents, amines featuring a C2-hydroxyl group were trialled to form oxazolidines **III** [Table 2.3]. In the first instance, the linear amine 2-aminoethan-1-ol was used, yielding a mixture of both the bicyclic **87** and tricyclic species **88**. In comparison, use of the branched amine 2-amino-2-methyl-1,3-propanediol yielded only the acyclic species **89**. In conjunction with the preferential formation of **85** over **86** seen previously [Table 2.2], these results suggested that steric concerns can override the equilibrium preference for the cyclic isomer of these species. This observation curtailed further investigation of substituents on the oxazolidine ring, in the absence of an alternative synthetic method being developed.

Table 2.3 Synthesis of tricyclic derivatives.

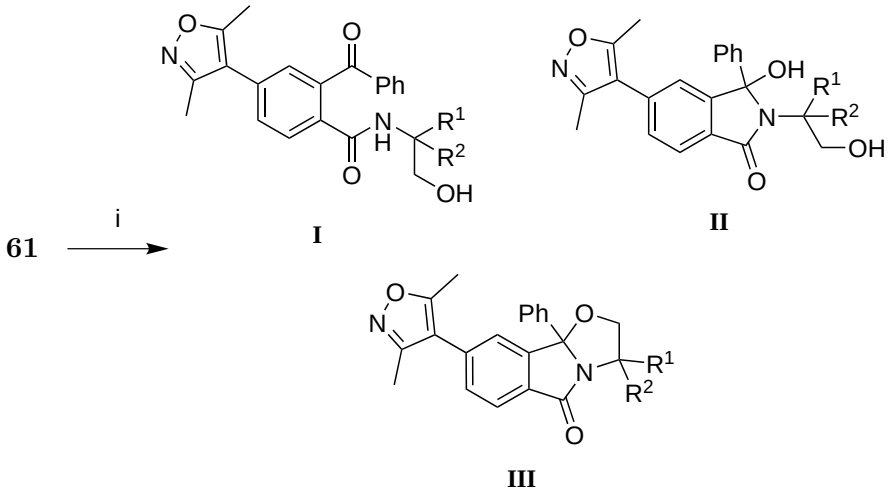

Reagents and Conditions: i. Amine, EtOH, reflux, 2 d.

		I		**II**		**III**	
			Yield		Yield		Yield
$\mathbf{R^1}$	$\mathbf{R^2}$	#	(%)	#	(%)	#	(%)
H	H		-	**87**	14%	**88**	26%
Me	CH_2OH	**89**	42%		-		-

*Reaction performed in THF.

A final attempt to synthesise a novel *N*-derivative resulted in the discovery of another unexpected reduction. When heating ester **61** with allylamine to form **90**, the reduced species **91** was unexpectedly isolated [Scheme 2.7]. The identity of this compound was confirmed through first reacting **61** with ammonium hydroxide to give **92**, which was subsequently reduced with a Hantzsch ester and DPP to give **91**. One putative pathway for the formation of this centered around a [1,5]-hydride shift. Initial formation of **90** could be followed by thermal elimination of hydroxide to give the iminium species **93**. A tautomerisation of the allyl chain would then yield isomeric **94**, which could undergo a [1,5]-hydride shift to the reduced species **95**, with a hydrolytic work-up finally yielding **91**. Although this isomerisation of the allyl chain usually requires the use of strong bases or metal catalysts,[207] the electron withdrawing effect of the iminium may sufficiently increase the acidity of the α-protons to facilitate some formation of **94**; the subsequent irreversible hydride shift would then drive the equilibrium towards the ultimate

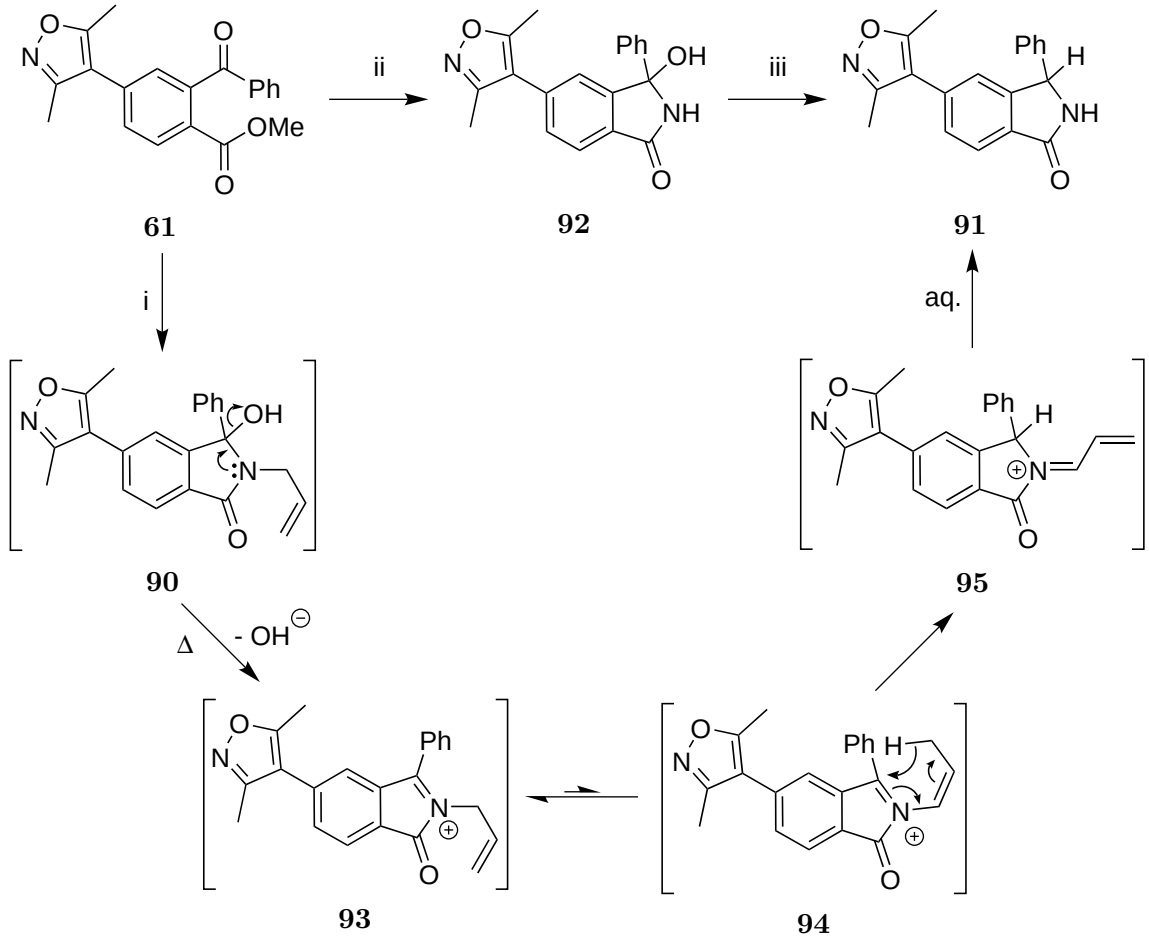

Reagents and Conditions: i. allylamine, EtOH, reflux, 36 h, 29%; ii. NH_4OH, H_2O, 1,4-dioxane, 80 °C, 20 h, 15%; iii. **68**, DPP, CH_2Cl_2, rt, 36 h, 53%.

Scheme 2.7 Putative mechanism for the formation of **91**.

production of **91**. Further research would be required to assess the origin of this occurrence, but despite this a number of compounds had been successfully obtained for biological testing.

2.2.2.3 Biological activity of *C3*- and *N*-derivatives

All compounds synthesised with the 3,5-dimethylisoxazole moiety were screened by DSF and ITC against BRD4(1), with the *N*-derivatives assessed first. A benzyl substituent (**83**) was fairly well tolerated, with only a small drop in ΔT_m (7.2 °C, DSF) and IC_{50} (78 nM, AlphaScreen) compared to the lead **60**, confirming that *N*-substituents could be accommodated in the binding site [Table 2.4]. The more sterically-demanding species **86** and **89**, however, were both poorly tolerated (1.3 °C and 1.7 °C). The tricyclic species **88**, whilst not improving on existing affinity (8.3 °C), demonstrated that an elaborate scaffold could be tolerated, around which further SAR could be assessed. These findings were shortly eclipsed by the affinity of the proto-compound **91**, with a ΔT_m of 11.6 °C measured, suggesting substituents at this position were detrimental to binding. As this compound involved an additional change to the hemiaminal, comparing the results with those of the *C3*-derivatives would first be necessary to confirm these observations.

In a similar trend as seen for the *N*-derivatives, minimal substitution at the C3 position conferred the highest affinities. Compounds **74**–**76** and **78** all showed a decreased affinity for BRD4(1) than the lead compound **60** (ΔT_m 4.5 – 7.2 °C vs 8.2 °C, DSF) [Table 2.5]; this was confirmed for **78** by AlphaScreen (IC_{50} 135 nM vs 13 nM). Compounds bearing smaller *N*-derivatives, the nitrile **77** and the reduced species **81**, showed stronger binding by DSF (8.5 °C and 10.1 °C) than the larger derivatives **74**–**76** and **78**; however, the nitrile **77** was a worse ligand for BRD4(1) than the lead **60**, as assessed by a more accurate AlphaScreen assay (195 nM vs 13 nM). These results suggested that although double substitution of the C3 position is tolerated by the binding pocket, it is in fact detrimental to ligand binding; this might be a result of potential steric interactions with the proximal and flexible sidechain of L92 in the binding pocket. The one exception to this trend was the nitro-compound **73**, which showed an affinity akin to the lead compound **60** (IC_{50} 20 nM, AlphaScreen). Given the similarities of these affinities, and the potential for this product to spontaneously eliminate nitromethane with a subsequent hydration yielding **60**, the question could be raised

Table 2.4 Screening of *N*-derivatives against BRD4(1) by DSF and AlphaScreen assays.

Compound Structure	#	$\Delta\mathbf{T}_m$ (°C)	IC_{50} (nM)
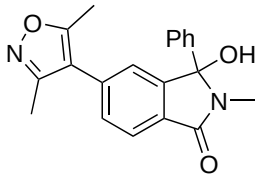	**60**	8.2	13
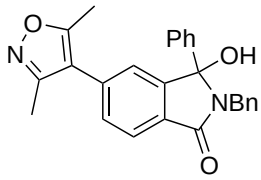	**83**	7.2	78
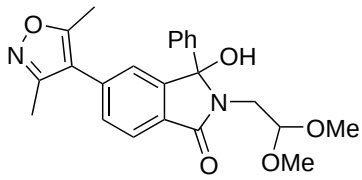	**86**	1.3	
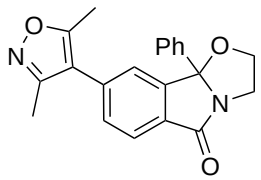	**88**	8.3	
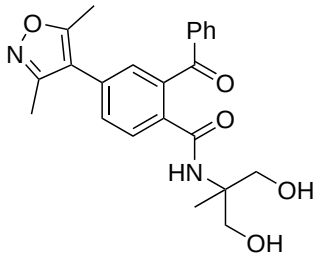	**89**	1.7	
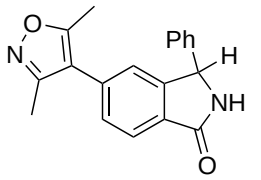	**91**	11.6	

Performed by collaborators at the SGC.

as to the identity of this compound in the assay. Notwithstanding this, it was generally observed that less substitution was favourable for binding to BRD4(1); although this allowed the compounds to achieve a high ligand efficiency, this limited further opportunities for optimisation.

To identify the ligand with the highest affinity, the best compounds were to be resolved into their component enantiomers and assessed. Given the measured affinities for these compounds were approaching the limits of the AlphaScreen assay, a more accurate ITC assay was to be employed to identify the best ligand. For accurate modelling of K_D, the racemic material

Table 2.5 Screening of *C3*-derivatives against BRD4(1) by DSF and AlphaScreen assays.

Compound Structure	#	$\Delta\mathbf{T}_m$ (°C)	IC_{50} (nM)
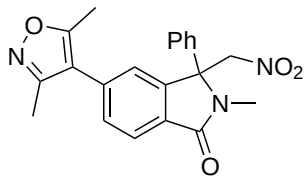	**73**	9.7	20
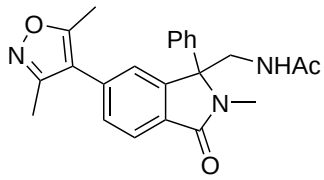	**74**	4.5	
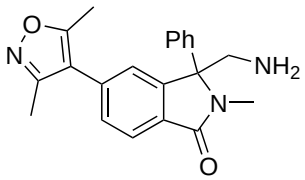	**75**	5.1	
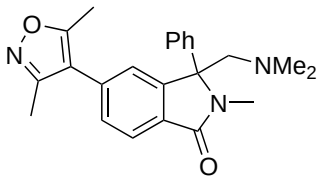	**76**	6.5	
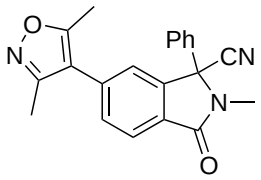	**77**	8.5	195
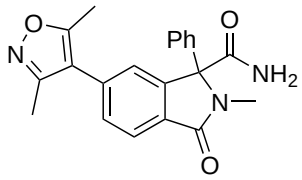	**78**	7.2	135
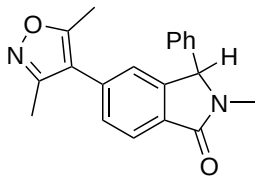	**81**	10.1	

Performed by collaborators at the SGC.

needed to be first separated into the component enantiomers. Resolution of the three best compounds, **73**, **81** and **91**, was attempted with preparative chiral HPLC. Separation of the nitro compound **73** was hampered by the spontaneous degradation of the compound with time and handling, lending further support to the question of the identity of this species in the assays. Although **91** did not suffer from stability issues, resolution could not be achieved with the available equipment. Fortunately, **81** could be readily separated, and the

(–)-enantiomer was identified as the more biologically active enantiomer by DSF (ΔT_m 11.3 °C) [Table 2.6]; further assessment by ITC revealed (–)-**81** to have a K_D of 5 nM, the highest affinity observed to date. This compound, hereafter referred to as PNZ5 (**P**eter **N**ew **Z**ealand **5** nM), was selected for further biological profiling to validate the activity of this probe candidate.

Table 2.6 Biological screening of the enantiomers of **81** by DSF and ITC.

Compound	ΔT_m (°C)	K_D (nM)
(+)-**81**	3.6	
(–)-**81** (PNZ5)	11.3	5

Performed by collaborators at the SGC.

The binding mode of PNZ5 was confirmed by a co-crystal structure with BRD4(1) [Figure 2.7]. Based on the electron density of the co-crystal obtained, the absolute stereochemistry of PNZ5 was found to be *S* at C3 [Figure 2.7a]. In a similar fashion to the lead compound **48** [Figure 2.4], the oxygen of the isoxazole was found to accept a H-bond from N140, whilst the nitrogen H-bonded to Y97 through a structural water molecule. The exocyclic phenyl ring was seen to neatly occupy and share hydrophobic interactions with the largely nonpolar WPF shelf bound by W81, P82 and F83. The introduced lactam moiety resided in the ZA channel bound by W81 and L92, with the planar nature of the ring minimising steric clashes [Figure 2.7b]. Finally, and most pleasingly, it was observed that the carbonyl of the lactam H-bonds to the network of water molecules lining the pocket, mediating interactions with P82, Q85, P86 and D88. Further, a more superficial water molecule could potentially be mediating additional H-bonding between the carbonyl of the lactam and K91, an interaction not previously observed. From this, PNZ5 could be seen to neatly complement the bromodomain of BRD4(1) with a number of key interactions despite the small size of the ligand.

2.2.3 Enantioselective synthesis of the lead compounds.

Given the difference in activity of the enantiomers of **81** against BRD4(1), enantioselective syntheses of the most potent compounds were to be explored. As **73**, **81** and **91** showed similar affinity, enantioselective nitro-Mannich and Hantzsch reductions using chiral organocatalysts were to be developed to selectively obtain the active enantiomer of each compound [Sections

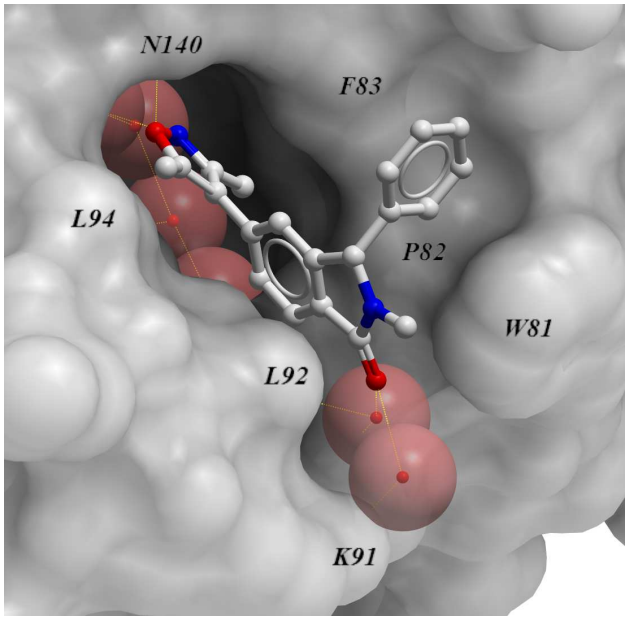

(a) The absolute stereochemistry of PNZ5 was assigned as 3*S*.

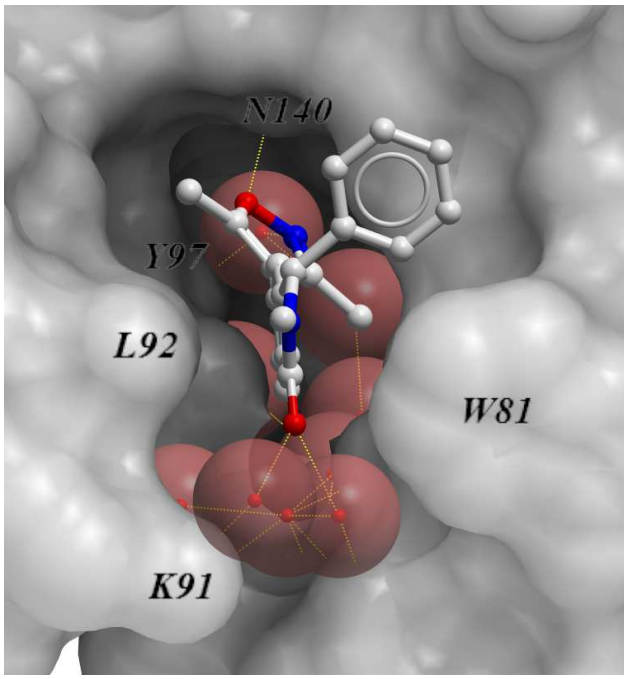

(b) The 3,5-dimethylisoxazole motif H-bonded to N140 and Y97 (via a water molecule) and the carbonyl of the isoindolinone H-bonded to the network of water molecules in the base of the binding pocket. An additional interaction to K91 was mediated through another water molecule.

Figure 2.7 Co-crystal structure of PNZ5 bound to BRD4(1) with key H-bonds (yellow lines) and conserved water molecules (red dots and spheres). Obtained by collaborators at the SGC.

1.2.2, 1.2.2.1 and 1.2.2.3]. Given the research performed by members of the Dixon group in the area of organocatalysis,[141–143] a number of chiral phosphoric acid catalysts (**96**–**109**) and other classes of organocatalysts (**110**–**116**) were available for screening [Table 2.7]. Optimisation studies were to be performed on model compounds in the first instance before being applied to the real system with the 3,5-dimethylisoxazole motif in place.

Table 2.7 Organocatalysts available for screening from the Dixon group in enantioselective reactions.

Scaffold	#	R
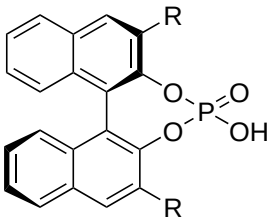	**96**	H
	97	Ph
	98	Bn
	99	2-hydroxyphenyl
	100	2,4,6-triisopropylphenyl
	101	3,5-bis(trifluoromethyl)phenyl
	102	anthracen-9-yl
	103	triethylsilyl
	104	triisopropylsilyl
	105	triphenylsilyl
	106	*tert*-butyldimethylsilyl
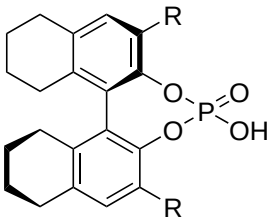	**107**	2,4,6-triisopropylphenyl
	108	3,5-bis(trifluoromethyl)phenyl
	109	triphenylsilyl
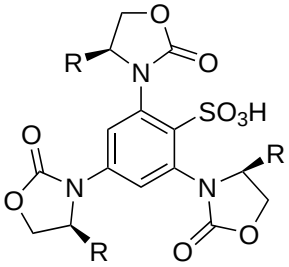	**110**	*n*Pr
	111	*i*Pr
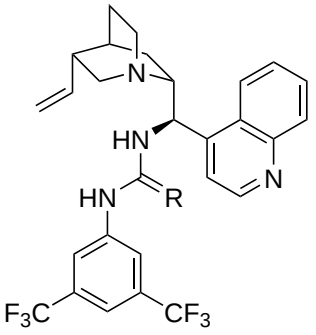	**112**	O
	113	S
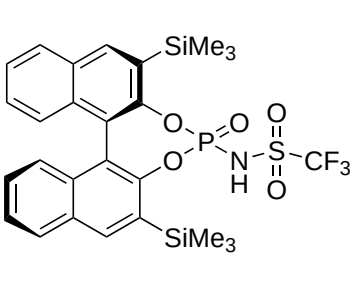	**114**	
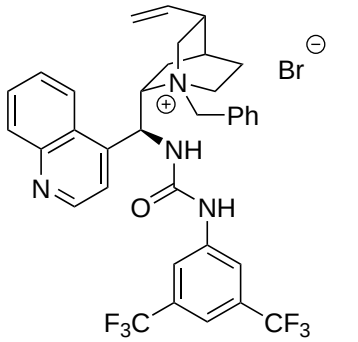	**115**	
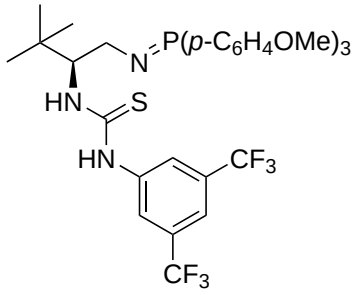	**116**	

2.2.3.1 Nitro-Mannich reaction

As a *C3*-nitromethyl substituent was found to contribute to a high affinity for BRD4(1), an enantioselective nitro-Mannich reaction was explored to install this group. The nitro-Mannich reaction of *N*-methylated compound **71** directly generated the functionality of the lead compound **73**, hence this substrate was assessed first [Table 2.8]. An initial solvent composition of 1:1 toluene:CH_3NO_2 was trialled at reflux, but although reactivity was good, no selectivity was observed. Using pure CH_3NO_2 as the solvent instead, a range of chiral phosphoric acid catalysts, in addition to the chiral sulfonic acid **112** and the *N*-triflylphosphoramide **114**, were screened in the reaction; however, only minimal control was observed (ee 0% – 12%). It was hoped that changing the substrate would allow for a better association with the catalyst,

Table 2.8 Screen for enantioselectivity in the nitro-Mannich reaction.

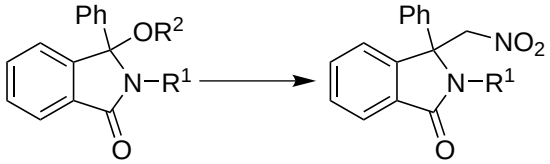

Reagents and Conditions: i. CH_3NO_2, Catalyst (10 mol%), reflux, 64 h.

Substrate		Conditions		ee	Substrate		Conditions		ee
R^1	R^2	Catalyst	MS	(%)	R^1	R^2	Catalyst	MS	(%)
Me	H	**96***		1	H	H	**107**		35
Me	H	**97**		0	H	H	**108**		20
Me	H	**98**		1	H	H	**109**		51
Me	H	**99**		4	H	H	**111**		2
Me	H	**100**		5	H	H	**112**		36
Me	H	**101**		3	H	H	**115**		36
Me	H	**102**		12	H	H	**113**		37
Me	H	**103**		3	H	H	**116**		1
Me	H	**105**		8	H	H	**109**	4 Å	62
Me	H	**106**		4	H	H	**109**	5 Å	60
Me	H	**110**		3	H	H	**109***	4 Å	50
Me	H	**114**		4					
H	Me	**97**		36					
H	Me	**104**		43					
H	Me	**105**		33					
H	Me	**109**		38					
H	Me	**111**		24					
H	Me	**112**		51					

*Toluene co-solvent, toluene:CH_3NO_2 1:1 v:v; MS: molecular sieves.

and therefore control. Trialling the *N*-H model **63**, modest enantioselectivities were observed for a range of catalysts (ee 24% – 51%), with the bifunctional cinchona-alkaloid derived catalyst **112** giving the greatest control. Trialling the hemiaminal model **62** instead, similar enantioselectivities were observed as for **63**, with the chiral phosphoric acid **109** identified as the best catalyst, generating an ee of 51%.

Further optimisation of the enantioselective synthesis of **73** was unsuccessful. The addition of molecular sieves (MS) to the reaction to remove the eliminated water, which may otherwise interfere with the complexation of the catalyst with the substrates, was found to boost selectivity: an ee of 62% was observed when 4 Å MS were employed, the highest enantioselectivity observed to date. In an attempt to decrease the rate of any background reaction that might be affecting the observed enantioselectivity of the reaction, the use of a co-solvent and lower reaction temperatures were assessed: both changes were detrimental to enantiocontrol and yield, and were not pursued further. At this point, the optimal conditions were applied to the enriched synthesis of the nitro compound **73** [Scheme 2.8]. Due to the absence of alkylation methods that did not automatically induce the elimination of nitromethane, *N*-methyl **60** was used in place of **92**. Unfortunately, no product was seen in the nitro-Mannich reaction under these conditions. As reactivity had been demonstrated previously using DPP as the catalyst [Scheme 2.4], it was suggested that steric interactions between the substrate and the BINOL-scaffold of the catalyst were the source of this problem. Research efforts at this point focused instead on the enantioselective reduction of these compounds.

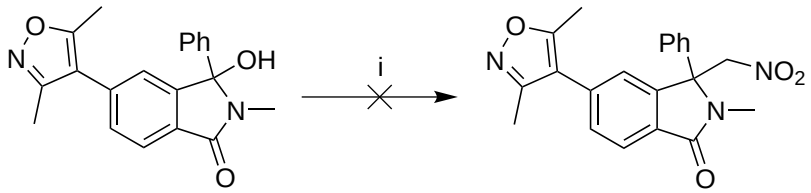

60 **73**

Reagents and Conditions: i. **109** (10 mol%), CH_3NO_2, 4Å MS, reflux, 64 h, 0%.

Scheme 2.8 Optimised enantioselective nitro-Mannich conditions with **60**.

2.2.3.2 Hantzsch reduction

An enantioselective reduction with Hantzsch esters towards PNZ5 was explored next. As for the nitro-Mannich reaction, substitution of achiral DPP with chiral Brønsted acid catalysts was to be explored to allow the reduction to proceed in an enantioselective fashion. In addition to optimisation of the reaction conditions and identity of the catalyst, the Hantzsch esters themselves offer another point of diversity that can be explored. Although **68** is most commonly used, a range of other Hantzsch esters, **117**–**122**, were prepared to assess the effect of the hydride source on the enantioselectivity of the reaction [Table 2.9].[149]

Table 2.9 Hantzsch esters prepared for screening in enantioselective reductions.

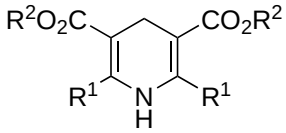

#	$\mathbf{R}^1$	$\mathbf{R}^2$
117	Et	Me
118	Me	Me
68	Me	Et
120	Me	CEt_3
121	Me	Adamantan-1-yl
122	Me	Me/*t*Bu
119	Me	*t*Bu

Optimisation of the reaction conditions offered some progress towards increasing enantioselectivity. To identify the ideal substrate, Hantzsch reductions using Hantzsch ester **68** and a chiral BINOL-derived phosphoric acid (**109**) were trialled with both the *N*-methyl hemiaminal **71** and the *N*-H hemiaminal **62** [Table 2.10]; no selectivity was observed for the *N*-methylated substrate **71** (ee 2%), but the *N*-H substrate **62** showed promise with an initial ee of 9% observed. The effect of temperature on selectivity was assessed: performing the reaction at 0 °C lead to decreased selectivity (ee 6%); whilst no reaction was observed at -20 °C. As with the nitro-Mannich optimisation, the effect of 4 Å MS to absorb the eliminated water was assessed and found to marginally increase the selectivity (ee 10%). The solvent-dependence was more substantial, with no reduction observed in nonhalogenated solvents (such as Et_2O and 1,4-dioxane) but great variation in selectivity amongst halogenated solvents (ee 12% - 32%), with CH_2Cl_2 giving the greatest control. The effect of concentration on the reaction was

Table 2.10 Screen for enantioselectivity in the Hantzsch reduction.

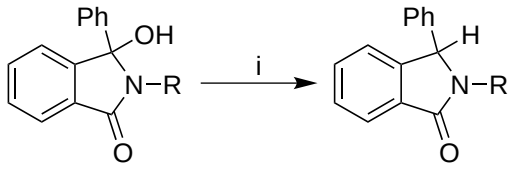

Reagents and Conditions: i. Substrate (1 eq), Hantzsch ester (1.25 eq), Catalyst (5 mol%), 48 h.

Substrates		**Conditions**						
R	Hantzsch ester	Catalyst	Solvent	MS	Conc. (M)	Temp. (°C)	**Yield** (%)	**ee** (%)
Me	**68**	**109**	toluene		0.025	18	74	2
H	**68**	**109**	toluene		0.025	18	81	9
H	**68**	**109**	toluene		0.025	0	51	6
H	**68**	**109**	toluene		0.025	-20	0	-
H	**68**	**109**	toluene	4 Å	0.025	18	67	10
H	**68**	**109**	Et_2O	4 Å	0.025	18	0	-
H	**68**	**109**	1,4-dioxane	4 Å	0.025	18	0	-
H	**68**	**109**	$CHCl_3$	4 Å	0.025	18	61	12
H	**68**	**109**	benzene	4 Å	0.025	18	81	20
H	**68**	**109**	chlorobenzene	4 Å	0.025	18	78	21
H	**68**	**109**	CH_2Cl_2	4 Å	0.025	18	69	32
H	**68**	**109**	CH_2Cl_2	4 Å	0.4	18	67	17
H	**68**	**109**	CH_2Cl_2	4 Å	0.2	18	64	18
H	**68**	**109**	CH_2Cl_2	4 Å	0.1	18	74	23
H	**68**	**109**	CH_2Cl_2	4 Å	0.05	18	70	27
H	**68**	**109**	CH_2Cl_2	4 Å	0.01	18	62	27
H	**68**	**109**	CH_2Cl_2	4 Å	0.005	18	65	27
H	**68**	**97**	CH_2Cl_2	4 Å	0.025	18	70	10
H	**68**	**104**	CH_2Cl_2	4 Å	0.025	18	77	2
H	**68**	**105**	CH_2Cl_2	4 Å	0.025	18	76	13
H	**68**	**107**	CH_2Cl_2	4 Å	0.025	18	68	59
H	**68**	**108**	CH_2Cl_2	4 Å	0.025	18	64	13
H	**117**	**107**	CH_2Cl_2	4 Å	0.025	18	57	16
H	**118**	**107**	CH_2Cl_2	4 Å	0.025	18	69	50
H	**120**	**107**	CH_2Cl_2	4 Å	0.025	18	71	87
H	**121**	**107**	CH_2Cl_2	4 Å	0.025	18	73	86
H	**122**	**107**	CH_2Cl_2	4 Å	0.025	18	77	73
H	**119**	**107**	CH_2Cl_2	4 Å	0.025	18	64	90
Me	**119**	**107**	CH_2Cl_2	4 Å	0.025	18	61	2

assessed last, however it appeared that the highest enantioselectivity was obtained with the concentration already in use (0.025 M).

The catalyst and Hantzsch ester employed had the greatest effect on stereocontrol. Using the optimised conditions, a number of different BINOL-derived phosphoric acid catalysts were screened, with a range of enantioselectivities observed (ee 2% – 59%). Although the sample size was too small to draw conclusions on the importance of saturation of the BINOL-backbone, the reduced-backbone species **107** gave the highest enantioselectivity. Finally, different Hantzsch esters were screened, for which a strong correlation between substituent size and stereocontrol was observed. The dimethyl diesters **117** and **118** gave less control than the benchmark diethyl species **68** (16% and 50% vs 59%), while the mixed diester **122**, bearing both a bulkier *t*Bu group and a smaller Me group, offered improved selectivity (73%). The bulkiest substituents, *t*Bu, CEt_3 and adamantan-1-yl, however, gave high levels of enantioselectivity (86% – 90%), with the di-*t*Bu species **119** the best ester identified. The correlation between substituent size and enantiocontrol is likely due to these esters, which flank the "hydride," increasing steric interactions with the catalyst and leading to greater facial-control of the approach of the hydride source to the electrophile.

Some enantiocontrol was reproduced when using the optimised conditions with the real substrate. Applying the optimised reduction conditions to **92**, **91** was obtained in 24% yield and 79% ee [Scheme 2.9]. Although this enantiocontrol was lower than for the model substrate, this represented an enriched synthesis of the potent compound **91** in which almost 90% of the material featured the correct absolute stereochemistry. To progress this material to complete the enriched synthesis of PNZ5, a methylation with MeI and NaH was trialled; however, a doubly-methylated species was the only product isolated. Although the desired product **81** was not obtained, the evidence of the C-N bond formation suggested that, with exploration of alternative methylation conditions, an enantioselective synthesis of PNZ5 could be achieved.

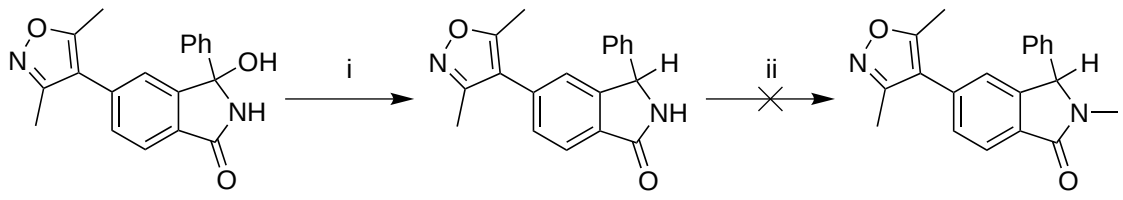

92 **91** **81**

Reagents and Conditions: i. **119** (1.25 eq), **107** (5 mol%), 4 Å MS, CH_2Cl_2 (0.025M), rt, 48 h, 24%, ee 79%; ii. MeI, NaH, THF, rt, 16 h, 0%.

Scheme 2.9 Attempted enantioenriched synthesis of **81** and **91**.

2.2.4 Development of an alternative synthetic route

An alternative synthesis of PNZ5 was targeted to overcome existing synthetic difficulties. The initial synthetic pathway to PNZ5 was far from ideal [Scheme 2.1]: the Friedel-Crafts acylation had only limited regioselectivity for the desired isomer; separation of the regioisomeric products was problematic; and the synthesis was very low yielding, with, depending on the synthetic route, only a 6% or 15% yield over the first 5 steps. A synthesis was envisioned starting from a symmetrical starting material (**123**) that could undergo a directed C-H bond activation to directly yield **124**, from which PNZ5 could be synthesised using the existing endgame [Scheme 2.10]. As the key C-C bond forming step would also be the point of desymmetrisation, the previous issue of regioselectivity would be negated. Further, utilisation of a directing group would allow for activation of the C-H bond without the need for prior functionalisation. In addition to decreasing the step count, this approach would also allow new and powerful C-H bond activation methods to be used, which would collectively allow for a higher yielding entry into the synthesis of PNZ5.

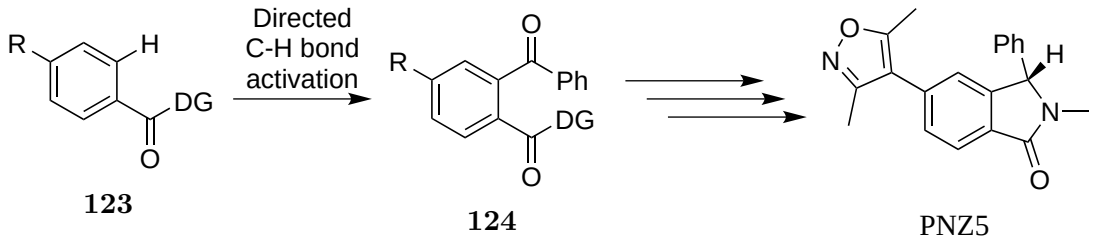

123 **124** PNZ5

Scheme 2.10 Synthesis of PNZ5 through a key *ortho*-directed C-H bond activation.

Many functional groups have been used to direct *ortho*-acylations, a number of which were explored here.[208,209] To allow a large number of methods to be trialled, substrates bearing different functional groups were to be synthesised. Before this, a decision first needed to be made on the substrate to be used: although 3,5-dimethylisoxazole moieties have a number of functionalities that could interfere in C-H bond activations, aryl bromides have been known, on occasion, to react with some of the palladium and lithium reagents that were expected to be employed.[210] As a result, C-H bond activations were to be trialled on substrates with the 3,5-dimethylisoxazole moiety already installed. Towards this, compound **125** was coupled with

3,5-dimethylisoxazole using the Pd-catalysed C-H bond activation method employed previously to give the ester **126** [Scheme 2.11]. This functional group was then interconverted through reaction with methylamine to the secondary amide **127**, and through hydrolysis to yield the carboxylic acid **128**, to give a range of substrates on which *ortho*-acylation reactions could be attempted.

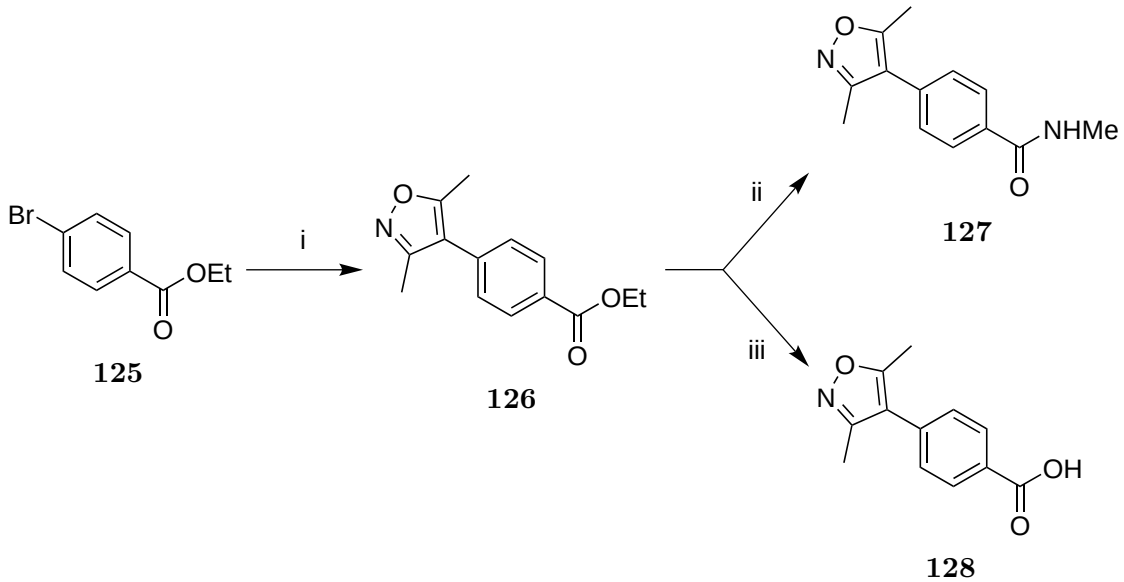

Reagents and Conditions: i. 3,5-dimethylisoxazole, $PdCl_2$, KOAc, DMAc, 130 °C, 16 h, 93%; ii. $MeNH_2$, EtOH, 70 °C, 18 h, 71%; iii. NaOH, EtOH, reflux, 24 h, 94%.

Scheme 2.11 Synthesis of substrates for *ortho*-acylation reactions.

The amide **127** was explored first as a directing group. An *ortho*-lithiation using *n*BuLi and quenching with methyl benzoate as an electrophile was attempted, however neither product nor starting material were returned, and spectroscopic evidence suggested that the methyls of the isoxazoles were being deprotonated [Table 2.11].[211,212] Generating lithiated species using alternative bases (*s*BuLi[213] and *t*BuLi)[214] and reacting these with CD_3OD was intended to identify the site of deprotonation: deuteration of the 3,5-dimethylisoxazole methyl groups was observed. With lithiation methods apparently incompatible with the 3,5-dimethylisoxazole moiety, other metals were screened. A palladium-catalysed aroylation, with a benzoyl radical generated *in situ* from benzaldehyde and *tert*-butyl hydroperoxide (TBHP),[215] could ostensibly be used with a benzamide directing group,[216] however no reaction was observed; use of benzoyl chloride as the electrophilic partner was similarly unsuccessful.[217] A related ruthenium-catalysed coupling was also unsuccessful.[218] Although the 3,5-dimethylisoxazole could potentially complex with the metal and act to sequester this from the desired site of reaction, the ability of secondary amides to act as directing groups was believed to be the more fundamental issue with regards to reactivity in these reactions.

Table 2.11 *ortho*-Derivatisations trialled with a *N*-methyl benzamide directing group.

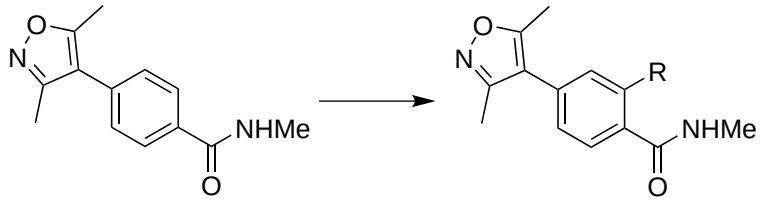

	Method			Conversion
R	R source	Additives	Lit.	(%)
COPh	PhCOOMe	*n*BuLi	[211,212]	0
D	CD_3OD	*s*BuLi, TMEDA	[213]	0
D	CD_3OD	*t*BuLi	[214]	0
COPh	PhCOH	$Pd(OAc)_2$, TBHP	[215,216]	0
COPh	PhCOCl	$Pd(OAc)_2$, KOAc	[217]	0
COPh	PhCOCl	$RuCl_2(PPh_3)_3$, K_2CO_3	[218]	0

A range of *O*-based directing groups were also explored for derivatisations at the *ortho*-position. The ester **126**, which lacks labile protons that may have been inhibiting the previous catalytic systems, was explored first. A Pd-catalysed *ortho*-aroylation was trialled with benzaldehyde and a range of peroxides (TBHP, $(BzO)_2$ and BzO*O*t*Bu*) to generate the aroyl group, but no reactivity was observed, even when exploring an alternative palladium source [Table 2.12]. Similarly, trialling the Ru-catalysed method as before also gave no evidence of reactivity.[218] A final *ortho*-acylation was trialled employing the carboxylic acid **128** and phenylglyoxylic acid in a decarboxylative cross-coupling reaction [Scheme 2.12].[221] A

Table 2.12 *ortho*-Acylations trialled with *O*-based directing groups.

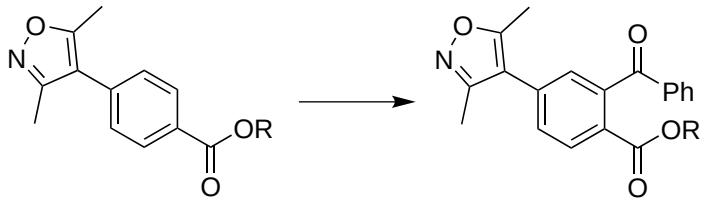

	Method			Conversion
R	Acyl source	Additives	Lit.	(%)
Et	PhCHO	$Pd(OAc)_2$, TBHP	[219]	0
Et	PhCHO	$Pd(OAc)_2$, $(BzO)_2$	[219]	0
Et	PhCHO	$Pd(OAc)_2$, BzOOtBu	[219]	0
Et	PhCHO	$PdCl_2$, TBHP	[219]	0
Et	PhCOCl	$RuCl_2(PPh_3)_3$, K_2CO_3	[218]	0
H	$PhC(O)CO_2H$	$Pd(TFA)_2$, Ag_2CO_3	[220]	0

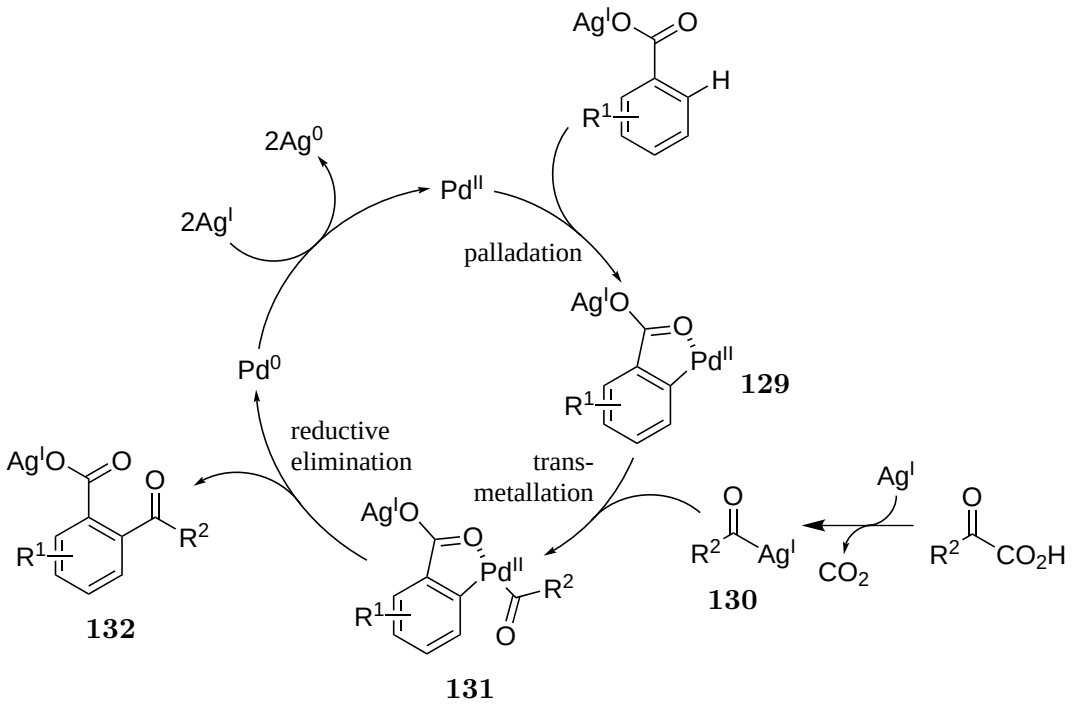

Scheme 2.12 Proposed mechanism for Pd-catalysed decarboxylative *ortho*-acylation.

directed C-H bond palladation would give the palladacycle **129**, whilst phenylglyoxylic acid would undergo a silver-mediated decarboxylation to form the acyl silver compound **130**.[220] A transmetallation between these species would lead to the transfer of the acyl group to the palladium (**131**), with a subsequent reductive elimination furnishing the *ortho*-acylated product **132**. When this method was attempted with the substrate **128**, no reaction was observed. As only the substrate differs from this reported reaction, the isoxazole was directly implicated in these negative results. This may have been as a result of ligation to the metal catalysts, though the possibility also arose that donation of electron density into the phenyl ring would act to decrease the basicity of the *ortho*-protons, and prevent the reaction in this way.

With *ortho*-acylation methods proving unsuccessful, alternative C-H bond functionalisations were explored. It was envisioned that introduction of a halogen at this position, which could subsequently be converted into an acyl group, would prove to be a successful route to the desired compounds. A range of *ortho*-brominations with ester **126** were explored [Table 2.13]: Brominations using Br_2 with acetic acid[222] or tBuNH$_2$[223] were unsuccessful, as was direct bromination with NBS.[224] Pd-catalysed halogenation methods that had been demonstrated to be effective with a range of weak coordinating groups were similarly unsuccessful.[225] Worryingly, evidence of Pd-addition into the C_{aryl}-isoxazole bond was found in the identification of the dimeric species **133** in the crude material from one of the Pd-catalysed reactions.

Table 2.13 *ortho*-Halogenations trialled with *O*-based directing groups.

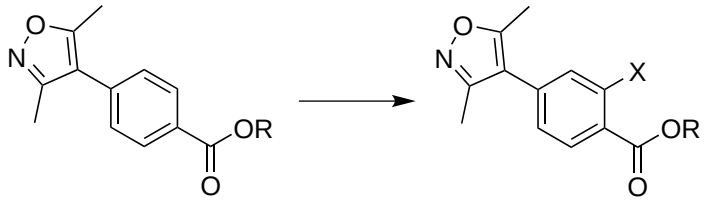

		Method			Conversion
R	**X**	Halogen source	Additives	Lit.	(%)
Et	Br	Br_2	AcOH	[222]	0
Et	Br	Br_2	AcOH, NaOAc	[222]	0
Et	Br	Br_2	tBuNH$_2$	[223]	0
Et	Br	NBS		[224]	0
Et	Br	NBS	$Pd(OAc)_2$, $K_2S_2O_8$, TFA	[225]	0
Et	Br	NBS	$Pd(OAc)_2$, $Na_2S_2O_8$, TfOH	[225]	0*
H	I	TBAI	$Pd(OAc)_2$, I_2, $PhI(OAc)_2$	[226]	0
H	Br	TBAB	$Pd(OAc)_2$, I_2, $PhI(OAc)_2$	[226]	70

*Biaryl species **133** observed.

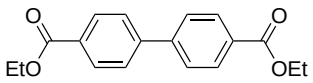

ortho-Bromination was ultimately achieved through the use of a carboxylic acid directing group with palladium catalysis. As methods using amide and ester substrates were exhausted, use of the carboxylic acid **128** was explored in a reported Pd-catalysed *ortho*-halogenation.[226] The proposed mechanism for this reaction involved carboxylate-directed palladation of the *ortho*-position to give a Pd^{II}-palladacycle **134** [Scheme 2.13]. IOAc, generated *in situ* from a reaction between I_2 and $PhI(OAc)_2$, could then undergo an oxidative addition with **134** to give the Pd^{IV} complex **135**. Reductive elimination of this species would then afford the *ortho*-iodinated product **136**. To suppress diiodination, tetrabutylammonium iodide (TBAI) was used to displace the palladium from the product. When investigating this reaction with the substrate **128**, no iodination was observed [Table 2.12]. To assess whether this was due to an absence of reactivity or due to instability of the aryl iodide product, a reported modification to yield the aryl bromide was trialled instead. In this method, tetrabutylammonium bromide (TBAB), used in place of TBAI, reacts with I_2 and $PhI(OAc)_2$ to generate IBr *in situ* [Scheme 2.14]. This reacts with the palladacycle to give the Pd^{IV} complex **137**, which could eliminate to yield a brominated product (**138**). Pleasingly, a 50% conversion to the *ortho*-brominated species **139** was achieved when using this reaction, confirming that the aryl iodide equivalent was likely not

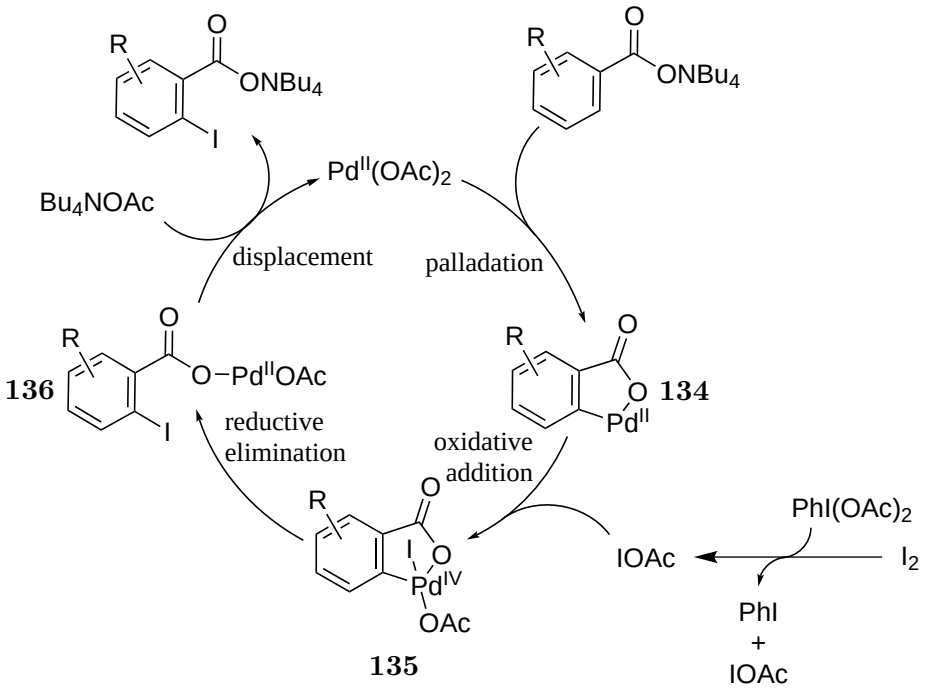

Scheme 2.13 Proposed mechanism for Pd-catalysed *ortho*-iodination.

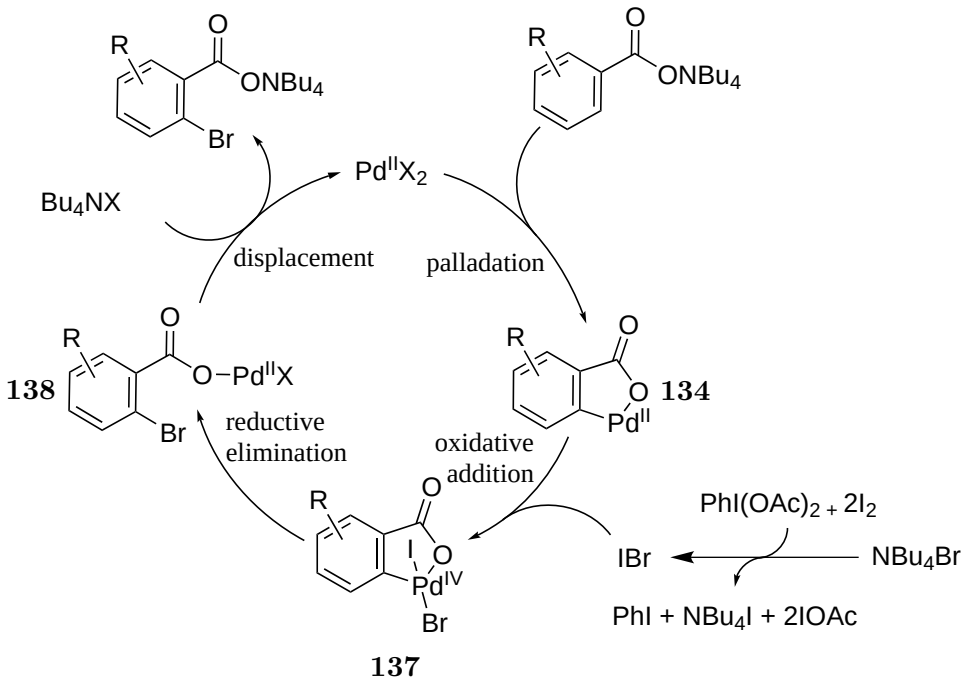

Scheme 2.14 Proposed mechanism for Pd-catalysed *ortho*-bromination.

observed due to instability. Through optimisation of the conditions, the conversion was further increased to 70%. Separation of the starting material **128** and brominated-product **139** was not possible, so the crude brominated product was used in further reactions.

Unfortunately, acylation of the *ortho*-brominated species **139** could not be achieved. Given the difficulties encountered with derivatising the *ortho*-position, direct evidence of manipulation was first desired. Lithiation with *n*BuLi[227] then quenching with a DCl solution resulted in only a 10% incorporation of deuterium (**140**), with the remaining material being the regenerated proto-compound **128** [Scheme 2.15]. This low incorporation, believed to be the result of the instability of the aryl bromide, prompted fast handling of the brominated material. Following the lithiation with addition of benzoyl chloride or benzonitrile gave no evidence of *ortho*-acylated product **142**. To increase the chance of reaction between the lithiated-center

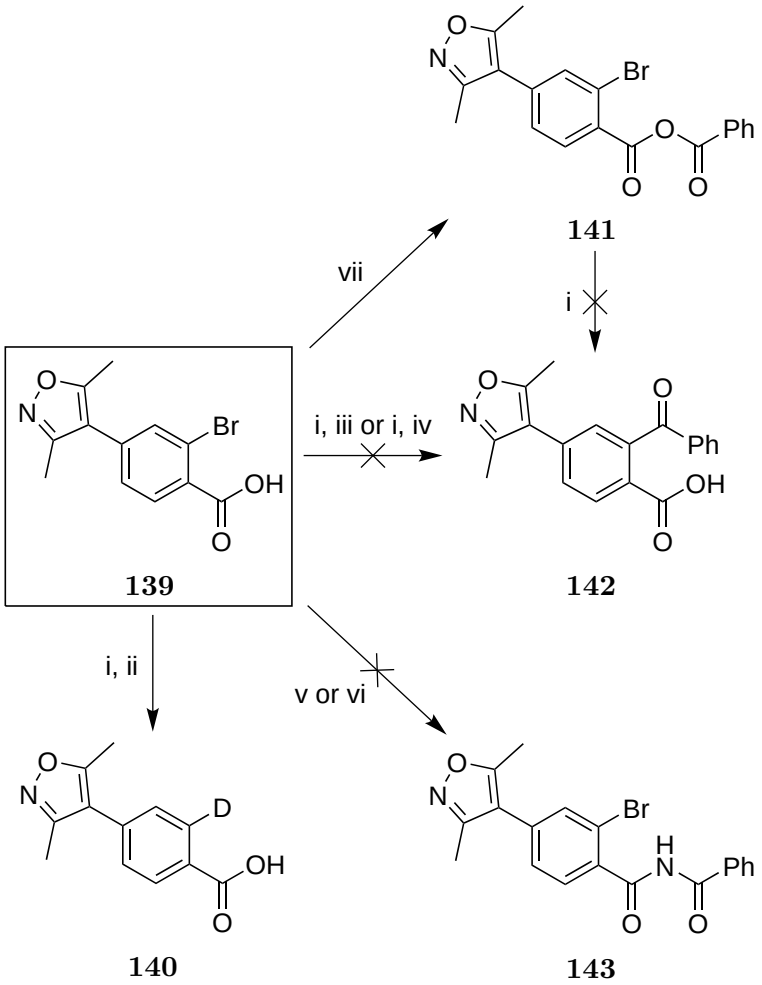

Reagents and Conditions: i. *n*BuLi, THF, -78 °C, 5 min; ii. DCl, D_2O, rt, 5 min, 10% conversion; iii. benzoyl chloride, rt, 5 min, 0%; iv. benzonitrile, -78 °C, 1 h then HCl, rt, 30 min, 0%; v. benzamide, oxalyl chloride, NaH, DMF, CH_2Cl_2, rt, 30 min, 0%; vi. benzamide, $SOCl_2$, K_2CO_3, CH_2Cl_2, rt, 16 h, 0%; vii. benzoyl chloride, NEt_3, CH_2Cl_2, rt, 24 h, 40% conversion.

Scheme 2.15 Attempted *ortho*-acylations of brominated **139**.

and the electrophile, it was decided to tether these to the molecule as an anhydride or imide. Whilst attempts to form the imide **143** using oxalyl chloride[228] or thionyl chloride[229] were unsuccessful, the anhydride **141** was synthesised using benzoyl chloride and NEt_3.[230] Rapidly subjecting this product to the lithiation conditions resulted, disappointingly, in no *ortho*-acylation. The efforts towards development of a new synthetic route was finally brought to a close when an independent discovery of PNZ5 appeared in the patent literature.[231]

2.3 BRD4(1) inhibitors reported during probe development

2.3.1 Dual report of PNZ5 by Engelhardt and co-workers

As an alternative synthetic route and the biological activity of PNZ5 were being assessed, an independent discovery of PNZ5 was reported. Engelhardt and co-workers, from Boehringer Ingelheim, published a patent detailing the design of a family of BRD4(1) inhibitors with a 3,5-dimethylisoxazole acetyl-lysine mimic [Table 2.14].[231] Of the 35 compounds synthesised, two of these (**81** and **88**) were matched compounds to those we had produced. These were screened using an AlphaScreen assay to assess inhibition of binding of BRD4(1) and BRD4(2) with tetraacetylated histone H4 peptides. Of the compounds screened, they also discovered that PNZ5 was the most potent ligand developed, with a measured IC_{50} of 14 nM. Unfortunately, besides potency data against BRD4(1), no other biological activity, in the form of selectivity or application, was reported.

From the isoindolinone compounds screened in the patent, a number of conclusions about SAR around the ligand could be confirmed. Alternative *N*-substituents (**144**–**147**) could be tolerated by the binding site but did not increase affinity relative to PNZ5 (IC_{50} 43–75 nM). SAR around the exocyclic phenyl ring was explored (**148**–**151**), which showed that larger substituents were poorly tolerated (**148**, 1.1 μM) compared to smaller systems (**151**, 43 nM). This was in fitting with the co-crystal structure of PNZ5 and BRD4(1) that showed only limited space around the ring in the WPF shelf to accommodate extended substituents [Figure 2.7]. The difference in measured affinities for PNZ5, K_D 5 nM (ITC) and IC_{50} 14 nM (AlphaScreen), represented the

Table 2.14 Isoindolinone derivatives screened by Engelhardt *et al.*

Compound			IC_{50}
Scaffold	#	R	(nM)
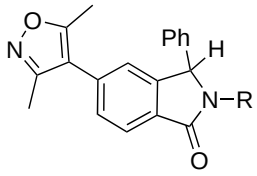	**144**	*i*Pr	75
	145	2-dimethylamino-ethyl	65
	146	1-methyl-piperidin-4-yl	57
	147	3-dimethylamino-propyl	43
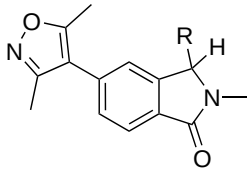	**148**	spiro[3.5]non-7-yl	1094
	149	3-fluoro-5-methoxyphenyl	380
	150	3,5-difluorophenyl	229
	151	cyclohexyl	43
	81	Ph	55
	(*S*)-**81**	Ph	14
	[PNZ5]		
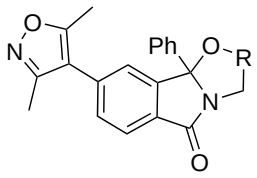	**88**	CH_2	72
	152	$(CH_2)_2$	36
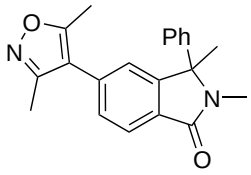	**153**		38
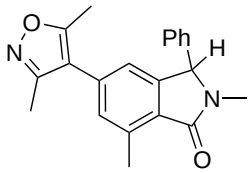	**154**		2486

difference in what was measured in each assay: the first was a measure of only the equilibrium between PNZ5 and BRD4(1), whereas the latter also included a measure of the binding, and competition, of the native peptide ligand. Towards the possibility of a tricyclic scaffold, both **88** and **152** showed good affinity, in line with our findings. Installation of a methyl at C3 (**153**), which would be expected to be well tolerated given the small nature of the group, was found as such with an IC_{50} of 38 nM. Finally, attachment of a methyl group on the underside of the ligand (**154**), which would clash with both the peptide and the network of H-bonding water molecules, was very poorly tolerated (2.5 μM).

Investigating the other reported scaffolds yielded more interesting observations. With the lactone scaffold, it was seen that adding substituents to the top of the ligand (**155** and **156**), which are orientated out of the binding pocket, was detrimental to affinity when compared to the proto-species **157** (1082 nM and 350 nM vs 193 nM), potentially as a result of clashes with the flexible alkyl chain of L94 [Table 2.15]. Futher, **157** is a matched lactone-scaffold compound of PNZ5; the weaker affinity (193 nM vs 55 nM) potentially highlighted the importance of hydrophobic interactions of the *N*-methyl group in the ZA channel. Alternatively, this was a reflection of the importance of the carbonyl as a H-bond acceptor, the binding ability of which is heavily-influenced by the motif of which it is a part. When reviewing the isomeric isoindolinone

Table 2.15 Alternative scaffolds explored by Engelhardt *et al.*

Compound			**IC$_{50}$**
Scaffold	#	R	(nM)
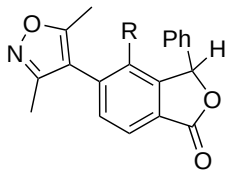	**155**	Me	1082
	156	OMe	350
	157	H	193
	158	tetrahydro-pyran-4-yl	1572
	159	5-methyl-pyridin-3-yl	1037
	160	*o*-tolyl	1060
	161	cyclopentyl	698
	162	benzo[1,3]-dioxol-5-yl	541
	163	pyridin-3-yl	395
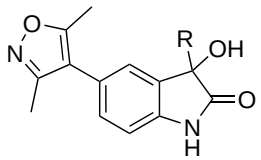	**164**	pyridin-2-yl	332
	165	thiophen-2-yl	320
	166	4-chlorophenyl	295
	167	3,4-difluorophenyl	203
	168	cyclohexyl	196
	169	Ph	259
	(*R*)-**169**	Ph	48
	170	2-morpholin-4-ylmethyl-phenyl	176
	(*R*)-**170**	2-morpholin-4-ylmethyl-phenyl	41
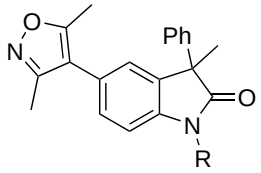	**171**	pyridin-3-yl	242
	172	Me	275
	173	H	54

scaffold (**158**–**173**), a contrasting conclusion about SAR around the exocyclic ring was reached: instead of bulky substituents being detrimental to binding, a large range of substituents were tolerated (**158**–**170**), and indeed the compound with the highest affinity bore an elaborate 2-morpholin-4-ylmethyl-phenyl group ((*R*)-**170**, 41 nM). Given the alternative orientation of the lactam relative to PNZ5, it was possible that the ligand adopts a different binding conformation to maximise H-bonding; this may have had the effect of lifting the exocyclic ring out of the WPF shelf and allowing other substituents to be tolerated. This theory is given substance by the tolerance of *N*-substituents (**171** and **172**) which would be highly detrimental to affinity in the original binding mode. Finally, in comparing the two isomeric lactam species, **153** (38 nM) and **173** (54 nM), which differ only in the orientation of the lactam group, it can be seen that the optimal scaffold was used in the development of PNZ5 in terms of orientation of the lactam motif.

In this patent, an alternative synthesis of PNZ5 was documented that progressed through an aza-Nazarov reaction. With a similar intention, a synthesis from a symmetrical starting material was achieved to overcome any regioselectivity issues. Initially, the imine **178** was condensed with the carboxylic acid **174** [Scheme 2.16], to yield the iminium **176**, which, given the presence of eliminated water, may also exist in a hydrated form. Although usually this condensation is facilitated with an activating group,[232] this method specified a considerable reaction period for these two species prior to the Lewis acid addition, raising the prospect of

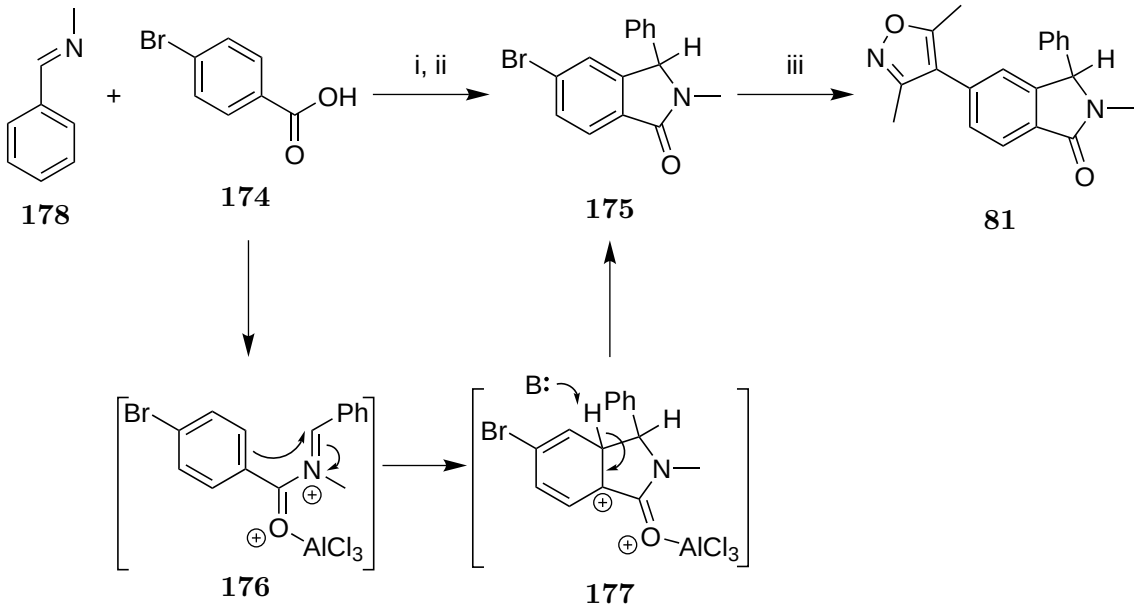

Reagents and Conditions: i. CH_2Cl_2, rt, 16 h; ii. $AlCl_3$, rt, 36 h, 87% (2 steps); iii. 3,5-dimethyl-4-isoxazolylboronic acid, $Pd(PtBu_3)_2$, Cs_2CO_3, THF, 50 °C, 2 h, 57%.

Scheme 2.16 Synthesis of PNZ5 through an aza-Nazarov reaction.

spontaneous C-N bond formation occurring. Regardless of this, addition of $AlCl_3$ would both facilitate the formation of **176** and activate this species to undergo an aza-Nazarov reaction to give the cyclic compound **177**, which, following removal of the proton to regenerate aromaticity, would yield the isoindolinone **175**. Subjecting this to a Suzuki coupling with the boronic ester of 3,5-dimethylisoxazole yielded racemic **81** that could be resolved by preparative chiral HPLC to give PNZ5. This two-pot synthesis with a 25% yield represented a distinct improvement upon the existing synthesis of PNZ5.

2.3.2 Further BRD4(1) ligands reported during the completion of this research

During the completion of the research, two other novel compounds were identified, and fully characterised, as BRD4(1) inhibitors. PFI-1 [Figure 2.8], the result of a fragment-based drug design program against BRD4(1), is a quinazolinone-based ligand developed against the BET family of proteins, with the carbonyl of the quinazolinone acting as the acetyl lysine mimic.[115] PFI-1 has a K_D of 47 nM against BRD4(1) (ITC), however its pan-BET nature is highlighted by affinities of 76 nM – 220 nM against other BET proteins.[233] PFI-1 was found to inhibit binding of BRD4(1) to chromatin by a FRAP assay, to have antiproliferative effects on leukemic cell lines, and to inhibit the cell cycle at G_1-S by downregulating c-Myc. Alongside other BET inhibitors, PFI-1 has seen use in reducing muscular weakness resulting from facioscapulohumeral muscular dystrophy, a muscular degenerative condition for which no treatment currently exists.[234] In comparison, the acylpyrrole **179** was the result of *in silico* screening.[105] A library of 7 million small molecules were screened against the binding site of BRD4(1), from which 22 lead compounds were identified and experimentally verified; seven of these showed significant binding to BRD4(1) (237 nM – 168 μM), with

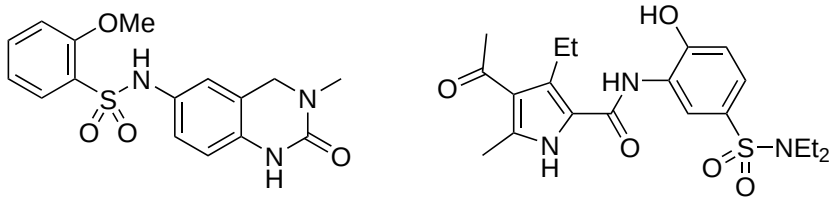

Figure 2.8 Novel and fully characterised BRD4(1) inhibitors reported.

the 4-acyl pyrrole **179** the most potent ligand identified. A co-crystal structure of **179** with BRD4(1) confirmed the 4-acyl group as the acetyl-lysine mimic with a H-bond to N140 observed. A selectivity screen against other bromodomain proteins showed that **179** has a strong affinity for the BET family of proteins (BRD4(1): 160 nM, BRD2(1): 170 nM, BRD3(1): 380 nM, BRD3(2): 490 nM). As for PFI-1, **179** was found to have activity against leukemic cell lines, confirming the potential role of BET inhibition in the treatment of leukaemia.

Additionally during this time, a number of kinase inhibitors were identified as having dual-activity against BRD4(1). Kinase inhibition is an established therapy for many forms of cancer,[235] whereas the targeting of bromodomains is only now emerging as an alternative mode of treatment.[236] To attempt to identify dual-action kinase-bromodomain inhibitors, two studies assessed clinical kinase inhibitors for bromodomain affinity.[237,238] The JAK2 kinase inhibitors TG101209[239] and TG101348[240] were found to have affinities for BRD4(1) (123 nM and 164 nM respectively) and other BET proteins [Figure 2.9]. The PLK1 kinase inhibitors BI-2536[241] and BI-6727[242] are currently in clinical trials,[243] but both were shown to have a high affinity for BRD4(1) (37 nM and 79 nM, respectively) and other BET proteins. BI-2536 has since been

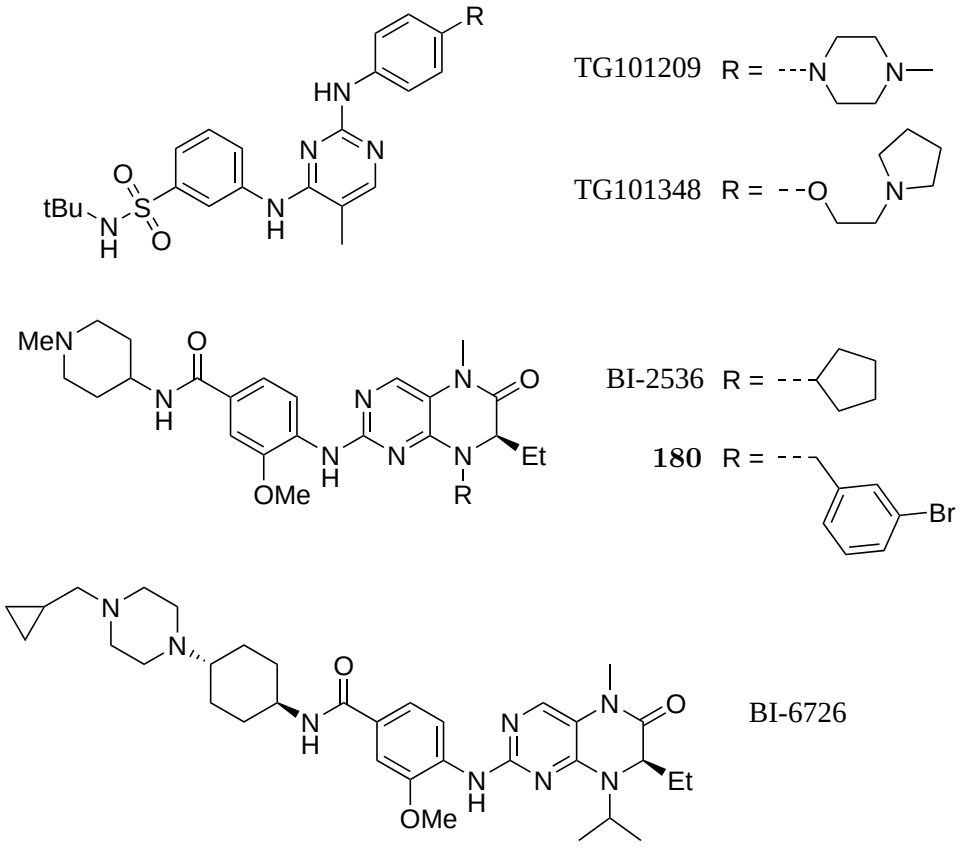

Figure 2.9 Known compounds re-identified as BRD4(1) inhibitors.

used as a lead compound against BRD4(1) in the development of **180**, a highly potent BRD4(1) ligand (K_i of 9 nM).[244] Given the biological activity of some of these compounds and their dual kinase-bromodomain inhibitor identities, the clinical mode of action of these compounds need to be assessed closely.

A number of patents also emerged detailing novel BRD4(1) inhibitors centered around the 3,5-dimethylisoxazole motif. Unfortunately, as is often the case with patents, the compounds listed were generally not characterised beyond their affinity for BRD4(1), so selectivity and biological activity of these compounds remains unknown. This aside, a family of compounds centered around an imidazo[4,5-c]quinoline core (**181**–**186**) were reported with affinities for BRD4(1) between 10-300 nM [Figure 2.10].[245] A structurally similar family with the generic structure **187** were reported with IC_{50} values of less than 200 nM against BRD4(1).[246] A

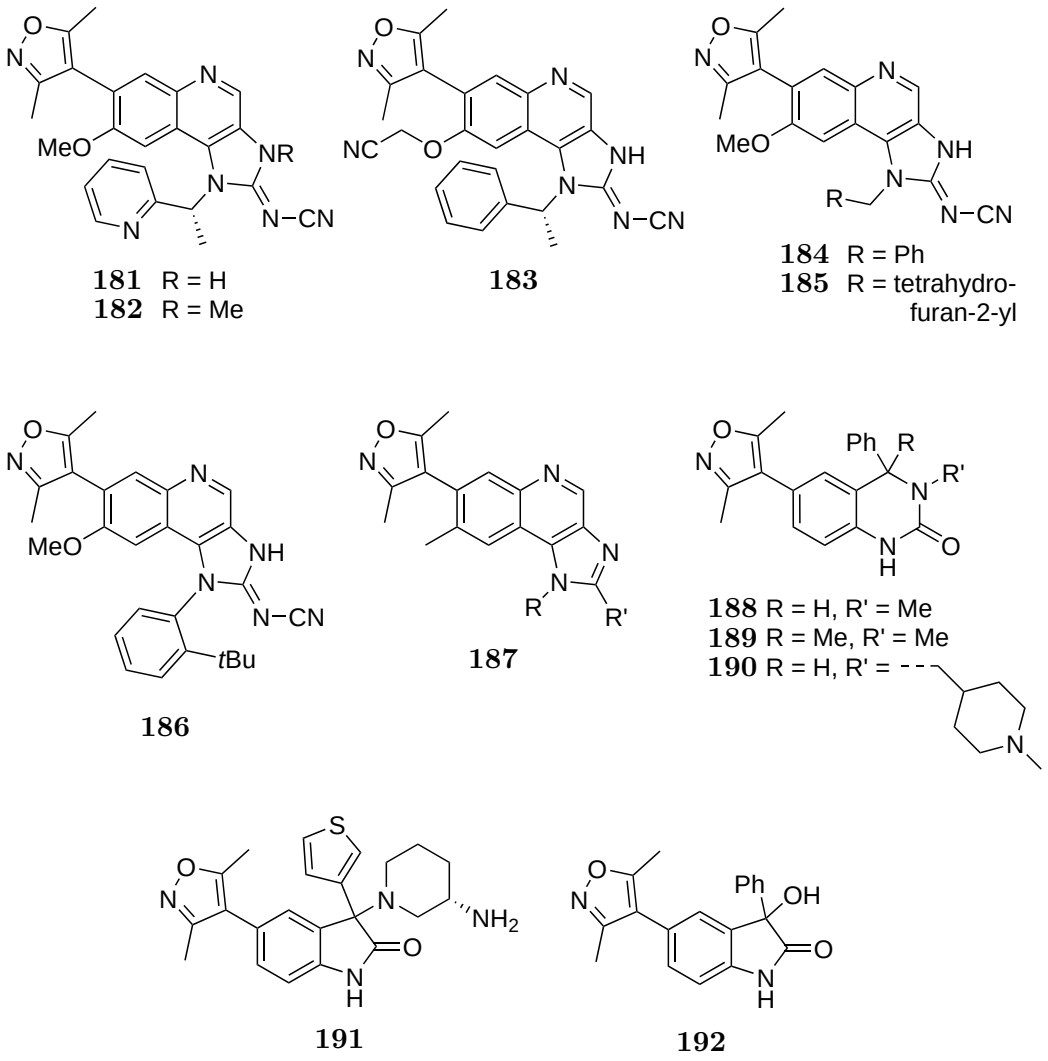

Figure 2.10 3,5-Dimethylisoxazole compounds described in the patent literature.

collection of dihydroquinazolinones were also disclosed, of which **188** (K_D 44 nM) was a closely matched compound to PNZ5, although **189** and **190** had higher affinities (31 nM).[247] Finally, the indolinones **191** and **192**, the latter of which is an isomer of **92**, had affinities for BRD4(1) measured at 8 nM and 51 nM respectively.[248]

Ligands bearing alternative acetyl-lysine mimics were also reported in the patent literature. A series of benzodiazepines with exocyclic ureas as the acetyl lysine mimic have been reported, of which **193**–**195** have 10 nM affinities for BRD4(1) [Figure 2.11].[249] Engelhardt and co-workers have disclosed two further series of compounds: a pyridinone family of which **196** was the most potent ligand;[250] and a triazolopyrazine family of which **197** was the most potent ligand.[251] Both these compounds were found to have an affinity of 9 nM for BRD4(1). Alternatively, from a family of substituted-triazolodiazepines, **198** and **199** were identified with 10 nM affinities.[252] The benzophenone **200** was the ligand with the most potential reported here;[253] this small,

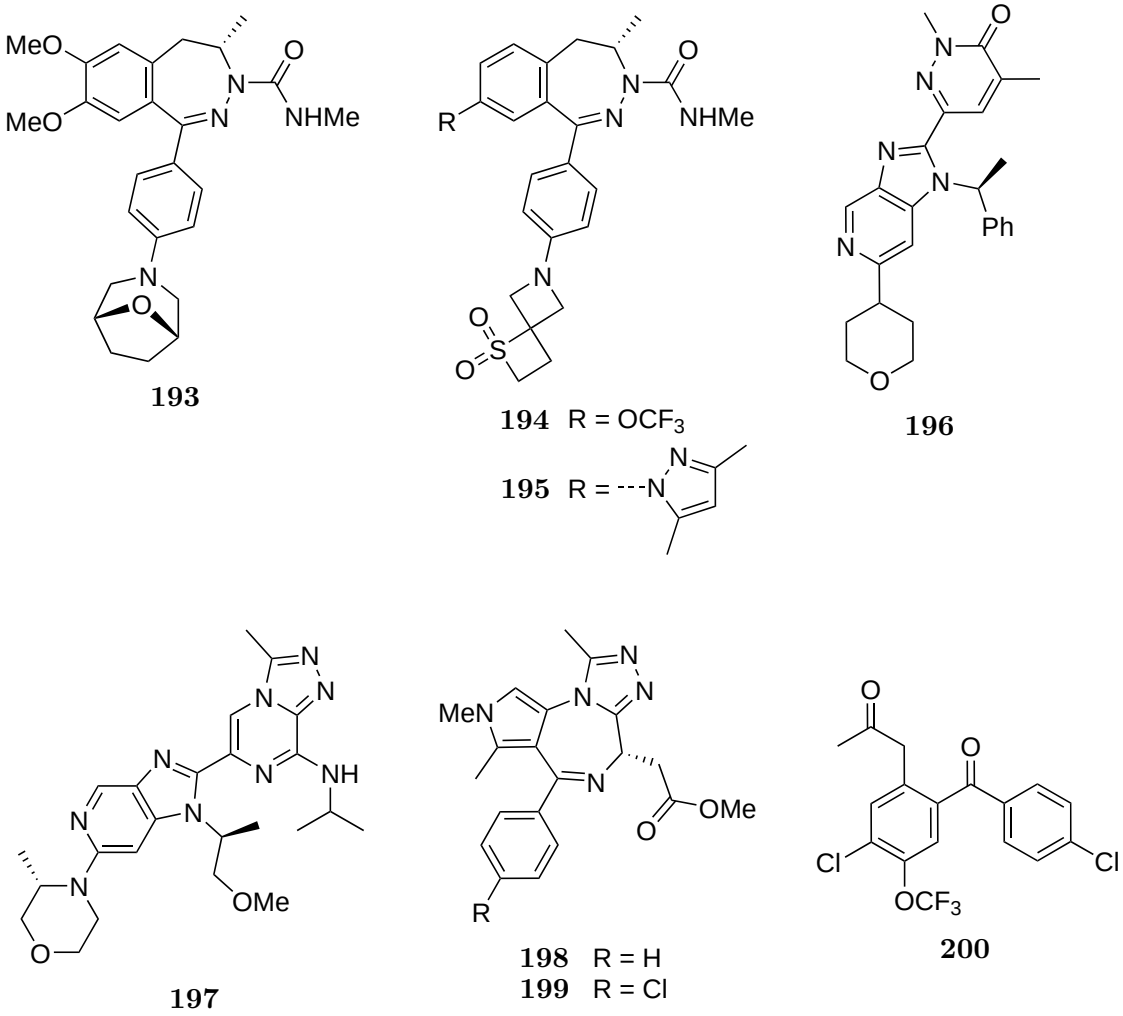

Figure 2.11 Compounds described with alternate acetyl lysine mimics.

flexible ligand, which features only arenes and no heterocycles, has a 10 nM activity against BRD4(1), and offers many opportunities for further optimisation to attain a pM affinity.

Finally, a last set of compounds disclosed by Engelhardt and coworkers holds the current benchmark for BRD4(1) affinity. Of all the compounds previously reported, none had demonstrated an affinity stronger than PNZ5; namely, less than 5 nM. However, a family of triazolopyridazines reported by Engelhardt *et al* included the compounds **201**–**205**, all of which have a reported IC_{50} of 3 nM [Figure 2.12].[254] At this point in time, these remain the most potent ligands described against BRD4(1).

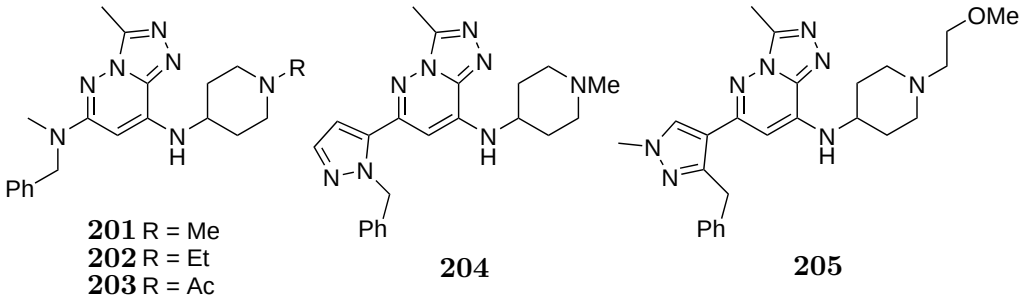

Figure 2.12 Potent ligands of BRD4(1).

2.4 Biological activity of PNZ5

Preliminary research using PNZ5 identified a potential role for this in the treatment of some forms of gastric cancer, the second leading cause of cancer-deaths.[255] Towards the identification of new anti-cancer compounds, collaborators at the SGC established and characterised three new gastric cancer cell lines, obtained from primary gastric adenocarcinoma (ACP02, diffuse type and ACP03, intestinal type) and peritoneal carcinomatosis (AGP01, ascitic fluid). To assess the ability of bromodomain inhibitors to modulate gastric cancer, 19 epigenetic probes were screened against these cell lines in an initial cytotoxicity assay, with inhibition of growth assessed after 72 h. Of these, the pan-BET inhibitor (+)-JQ1 and PNZ5 both demonstrated strong antiproliferative activity. The cytotoxic activities of (+)-JQ1 and PNZ5 were assessed as a function of concentration against these cell lines, and again both compounds showed strong cytotoxic effects against all three cell lines assayed [Figure 2.13]. Although these are only preliminary results, further research is ongoing to fully examine the potential of these compounds as therapies to treat gastric cancer.

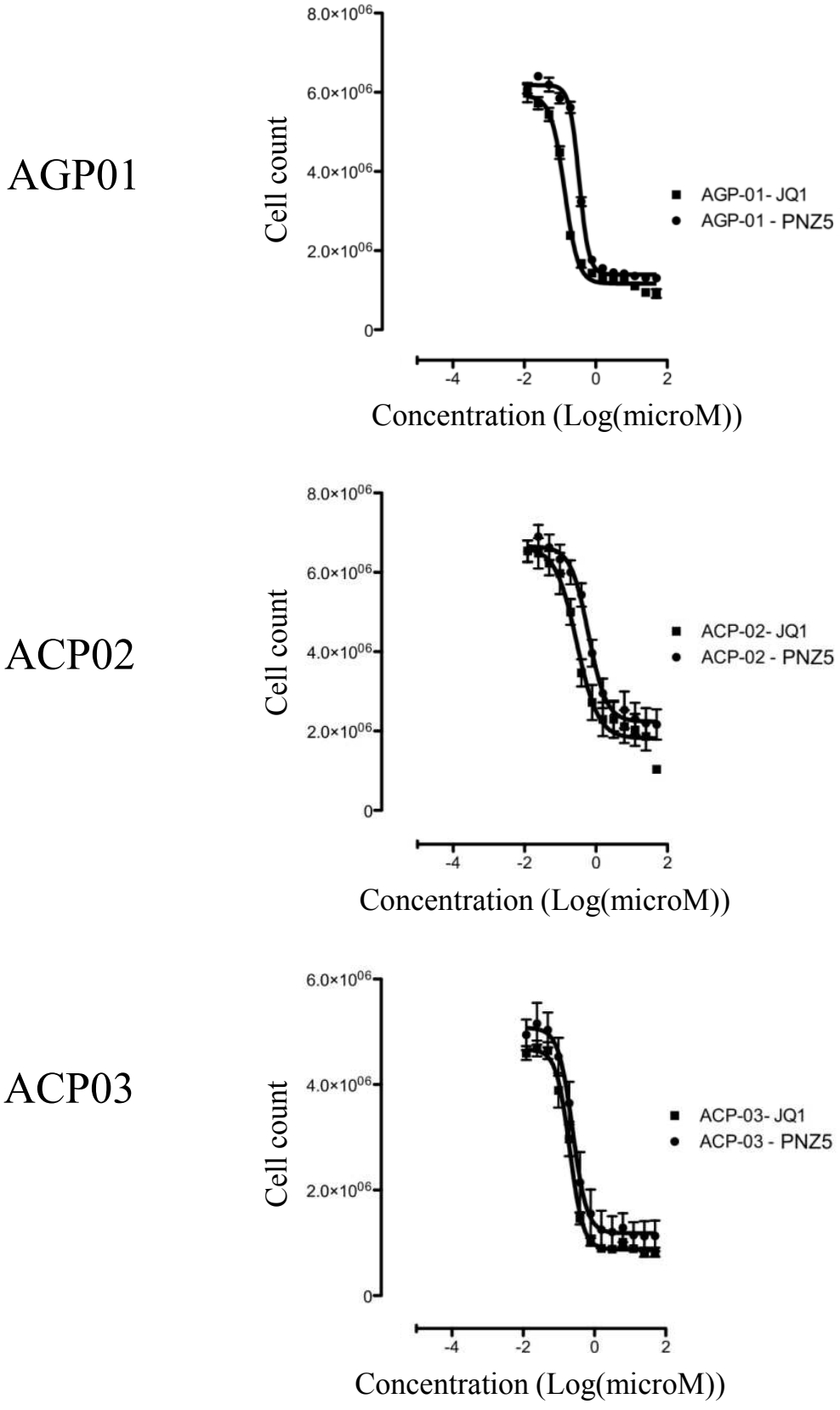

Figure 2.13 *in vitro* cytotoxic activity of (+)-JQ-1 and PNZ5 in gastric cancer cell lines after 72 hours of exposure. Experiments were performed by collaborators at the SGC in triplicate, with means and SEM displayed.

Chapter 3

BRD9

3.1 Project origin

3.1.1 Fragment lead

A novel bromodomain-binding motif was identified as the result of fragment screening. Collaborators at the SGC and researchers at the University of Cambridge screened a library of fragments against the bromodomain protein PCAF by a number of NMR-based methods,[256] including: saturation-transfer difference, which measures the transfer of magnetisation from the protein to bound ligands by the nuclear Overhauser effect;[257] water-ligand observed by gradient spectroscopy, where transfer of magnetisation from water in and around the binding site to a ligand is measured;[258] and a Carr-Purcell-Meiboom-Gill sequence, which measures changes in relaxation time as a function of binding.[259,260] From these, 1-methylquinolone (**206**) [Figure 3.1], was identified as a fragment hit against PCAF, with a ΔT_m of 4.5 °C at 1 mM (DSF), and a K_D of 320 μM (ITC). An initial SAR study identified **207** as a more potent ligand with improved binding affinities (ΔT_m 5.7 °C at 1 mM (DSF), K_D 30 μM (ITC)). This

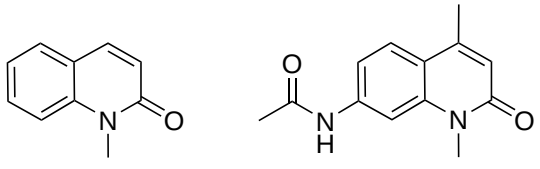

206 **207**

Figure 3.1 Lead compounds against PCAF as measured by NMR-based assays.

quinolone fragment had not previously been linked to bromodomain binding, and presented an opportunity to develop a novel family of bromodomain probes.

To assess the key binding elements of **206** and to identify areas for optimisation, a co-crystal structure with PCAF was obtained [Figure 3.2]. The structure revealed the *N*-methyl quinolone acted as an acetyl-lysine mimic, with H-bonds to the key asparagine residue N803 and tyrosine Y760 through one of the four conserved binding site water molecules [Figure 3.2a]. The importance of the planar and hydrophobic nature of the quinolone core was seen by the narrow pocket in which it resides, bound by Y809 and V752 [Figure 3.2b]. Although the development of substituents that mimic the conserved water molecules of the binding pocket could have yielded significant increases in potency, displacement of these molecules may have been prevented by the enthalpic barrier to dissociation. The C4 position was orientated towards an opening of the pocket, as demonstrated by the tolerance of the *C4*-methyl group of **207**; the improvement in binding seen with this compound may have resulted from increased hydrophobic interactions with the neighbouring A757 residue. The C7 position was alternatively orientated towards a large hydrophobic pocket, in which the methyl acetamide substituent of **207** would be located.

3.1.2 Preliminary research by L. Vieira

Lucas Vieira, a visiting researcher under my supervision from the Federal University of São Carlos, began the exploration of SAR around the lead compound **207**. Through a range of methods, an initial series of compounds (**207**–**215**) were synthesised for screening by DSF; the screening concentration was lowered to 10 μM, at which level the matched compound **207** now displayed a ΔT_m within the experimental error of the assay (-0.2 °C) [Table 3.1]. Methylation of the exocyclic amide (**208**) gave a substantial boost in binding, with the greatest ΔT_m of 2.1 °C observed; this was likely a result of better complementarity with the largely hydrophobic pocket in which it resides. Saturation of the pyridone (**209**) and derivatisation of the C4 methyl (**210**–**215**) were both found to be detrimental to binding (ΔT_m -0.6 – 0.4 °C). The crystal structure of PCAF shows a significant narrowing of the protein around the C4 methyl group, which would result in many of these derivatives sterically clashing with the protein and lowering their affinity.

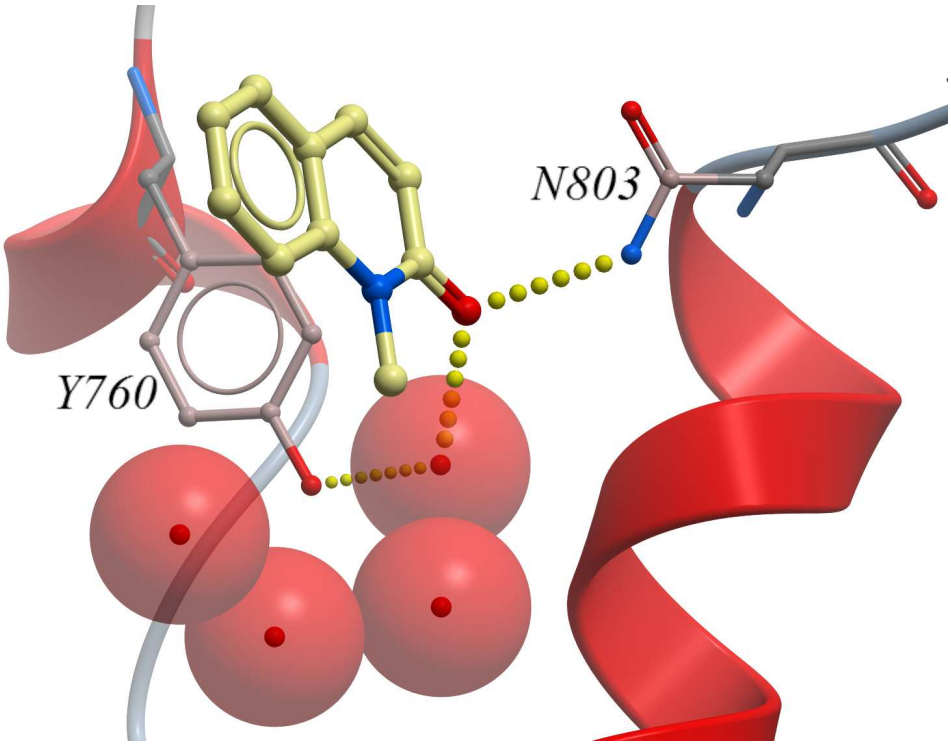

(a) Compound **206** with key H-bonds (yellow balls) to N803 and Y760 (ball and sticks) through a structural water molecule.

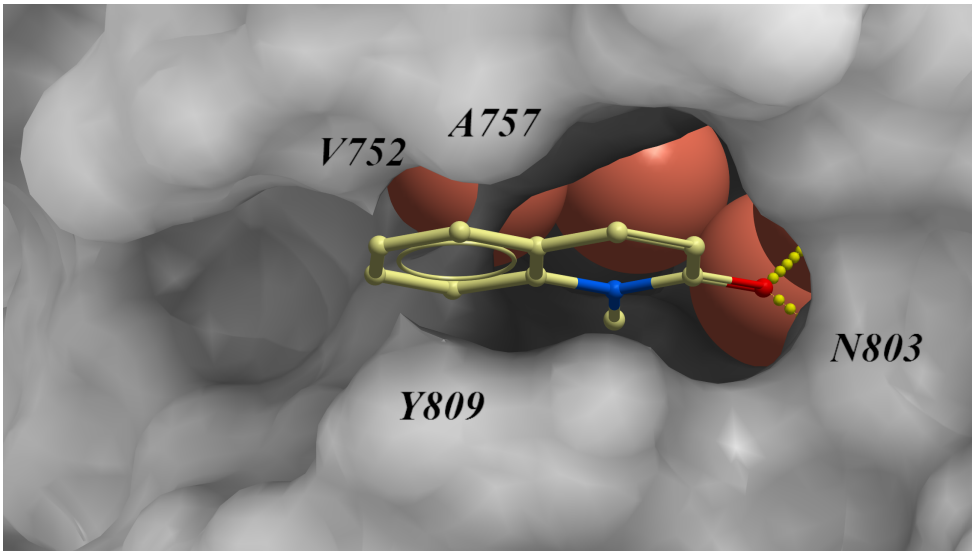

(b) The electrostatic surface of the binding pocket shows space for the C4 and C7 substituents of **207**.

Figure 3.2 Co-crystal structure of **206** bound to the bromodomain of PCAF with key H-bonds (dotted yellow line) and conserved water molecules (red spheres). Obtained by collaborators at the SGC. [Crystal data unpublished].

Table 3.1 First series of compounds synthesised by L. Vieira screened against PCAF by DSF.

Compound		ΔT_m	Compound		ΔT_m
Structure	#	(°C)	Structure	#	(°C)
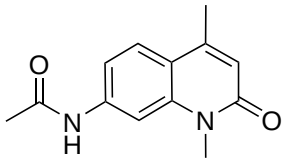	**207**	-0.2	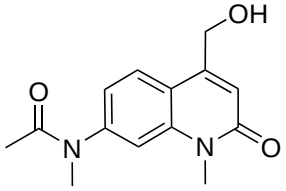	**212**	0.3
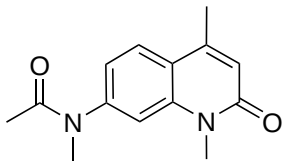	**208**	2.1	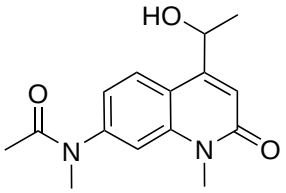	**213**	-0.3
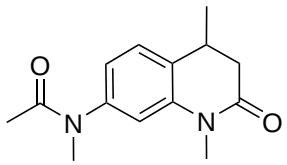	**209**	0.4	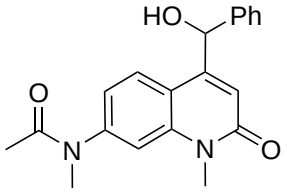	**214**	0.2
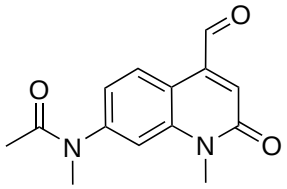	**210**	-0.6	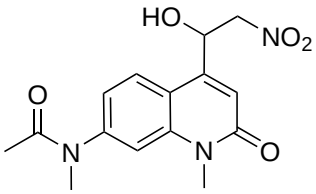	**215**	-0.1
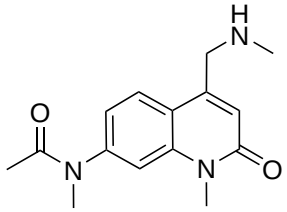	**211**	0.2			

All compounds were tested at 10 μM. Performed by collaborators at the SGC.

Further optimisation of the C7 position was pursued to identify the optimal scaffold for occupation of the neighbouring pocket. Towards this, a range of *N*-heterocycles were to be attached to the quinolone at the C7 position and screened for affinity. To synthesise the quinolone moiety, 3-bromoaniline was condensed with ethyl acetoacetate to give the amide **216** [Scheme 3.1]. By use of an acid-catalysed dehydrative cyclisation in neat H_2SO_4,[261] **217** was obtained, before methylation with NaH and MeI yielded the bromo-quinolone **218**. This aryl bromide was used in a palladium-catalysed Buchwald-Hartwig coupling with a range of heterocycles to generate the family of compounds **219**–**222** for testing.[262]

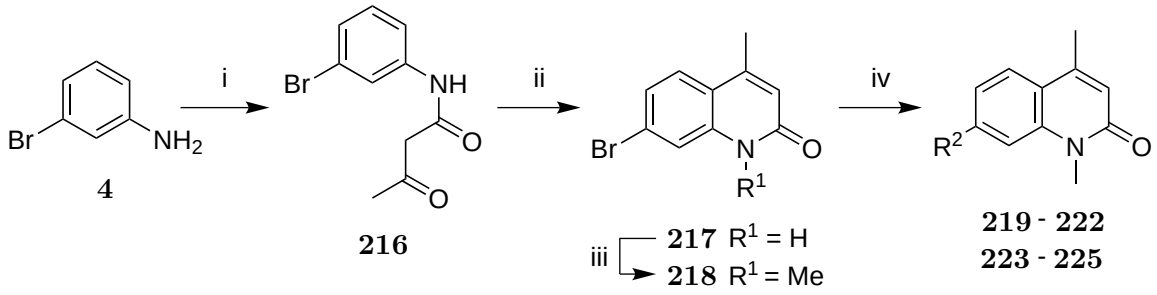

Reagents and Conditions: i. ethyl acetoacetate, xylenes, reflux, 16 h, 30%; ii. H_2SO_4, 95 °C, 2 h, 80%; iii. NaH, MeI, DMF, rt, 12 h, 80%; iv. *N*-heterocycle, $Pd(OAc)_2$, Xantphos, Cs_2CO_3, 1,4-dioxane, 110 °C, 36 h, 5-96%.

Scheme 3.1 Synthesis of *C7*-heterocyclic derivatives against PCAF.

When screening this family of compounds, an alternative activity was discovered. Initially these compounds were assayed against PCAF; however, a uniformly poor affinity (ΔT_m 0.2 – 0.6 °C) was observed [Table 3.2]. As part of a selectivity screen against other bromodomain proteins, these compounds fortuitously showed activity against BRD9 instead: saturated scaffolds (**219**–**221**, 4.0 – 5.9 °C) showed higher activity than an unsaturated reference compound (**222**, 3.8 °C), with the δ-lactam **220** showing the highest affinity. This activity against BRD9 was confirmed by ITC, with a K_D of 612 nM measured. Reinvestigating the lead compounds, the quinolone **206** was found to have a K_D of 5 μM against BRD9 by ITC, in comparison to the

Table 3.2 Second series of compounds synthesised by L. Vieira.

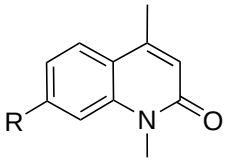

Compound		**ΔT_m (°C)**		**Compound**		**BRD9**
R	#	PCAF	BRD9*	R	#	ΔT_m (°C)*
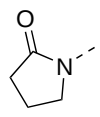	**219**	0.2	4.0 ± 0.7 (4)	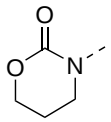	**223**	2.5 ± 0.4 (4)
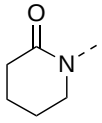	**220**	0.6	5.9 ± 0.5 (4)	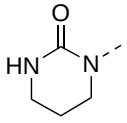	**224**	6.1 ± 0.7 (4)
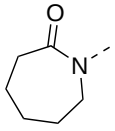	**221**	0.2	4.4 ± 0.3 (4)	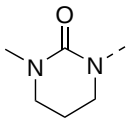	**225**	1.6 ± 0.5 (4)
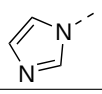	**222**	0.4	3.8 ± 0.4 (4)			

*Mean ΔT_m ± SEM (number of measurements). All compounds were tested at 10 μM.

Performed by collaborators at the SGC.

320 μM K_D against PCAF. Knowledge about the biological activity of BRD9 was extremely limited [Section 1.1.3], compounded by the fact that no selective inhibitors had been described for the protein. The considerable affinity of **220** gave confidence that, with optimisation, this could be developed into the first probe for the BRD9 protein; this became the focus of the further research efforts. To investigate if the δ-lactam motif was the ideal scaffold, further related heterocycles were assessed (**223**–**225**); although **224** showed a marginally greater ΔT_m (6.1 °C), this was within the statistical error of the affinity of **220**. Given the hydrophobic nature of the pocket and the abundance of chemical methods available towards synthesising substituted δ-lactams, the piperidinone **220** was chosen as the scaffold for elaboration.

To investigate postions for substitution to be explored at, a co-crystal structure of the piperidone **220** with BRD9 was obtained [Figure 3.3]. In the structure of **220** bound to BRD9, the quinolone carbonyl displayed H-bonds to N100 and Y57, mediated through one of the conserved water molecules, with the bicyclic core residing in a narrow cleft bound by V49 and Y106. Interestingly, the carbonyl of the piperidone was found to be close to, but not in, H-bonding distance with the hydroxyl of Y106, a bond that could potentially be achieved through elaboration of the scaffold which would add considerably to the potency of the ligands.

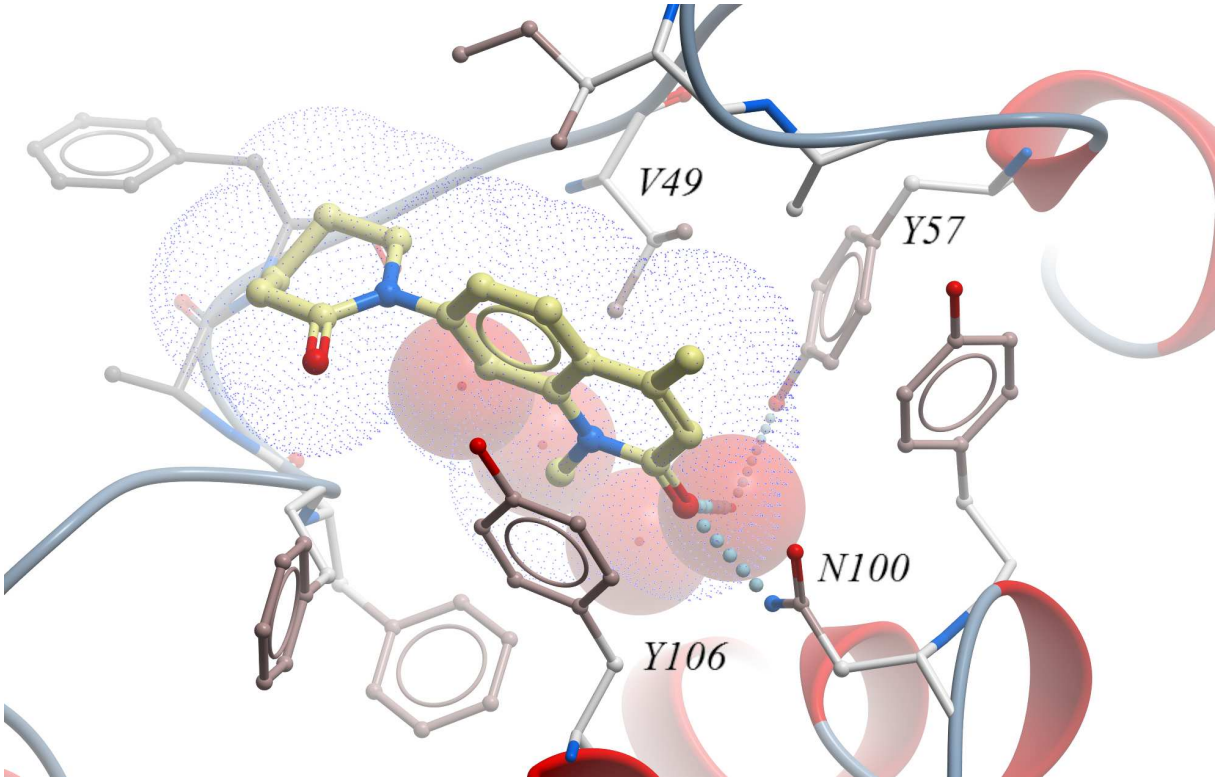

Figure 3.3 Co-crystal structure of **220** bound to BRD9 with conserved water molecules (red balls and spheres) and key H-bonds (dotted blue lines) [PDB ID: 4Z6H].

In addition to this, there also appeared to be space between the C7-heterocycle and the surrounding hydrophobic cavity that could be further exploited for selectivity and potency.

A final series of compounds synthesised by L. Vieira explored the optimal substitution pattern around the δ-lactam scaffold. Using the MCR described previously [Section 1.2.1.1], a range of aldehydes and nitroesters (**226**) were combined with NH_4OAc in ethanol and heated to furnish nitrolactams of the general form **227** in a single pot [Scheme 3.2].[130] The nitro group was then reduced with a nickel borohydride catalyic system,[263] the resulting amine was Boc-protected (**228**), and this compound was then used with **218** in a Buchwald-Hartwig coupling to yield compounds of the form **229** for testing. In some cases, the Boc group was also removed with a TFA treatment to yield the parent amine for testing. Compounds **230**–**234** were screened by DSF against BRD9 for potency and BRD4 for selectivity [Table 3.3]. All the compounds that were tested demonstrated uniform selectivity for BRD9 (ΔT_m 2.8 – 6.2 °C) over BRD4 (ΔT_m -0.5 – 0.3 °C). These affinities confirmed both the presence of space around the lactam for exploration and also the compatibility of the amino substituent that arose from the synthetic method. Of the patterns assessed, R_2 substitution was found to give the greatest affinities (**233**: 6.2 °C, **234**: 5.8 °C). Although there was no difference within experimental error between these compounds in terms of potency against BRD9, the phenyl substituent was expected to offer greater complimentarity with the binding pocket, prompting the use of this substitution pattern in further development.

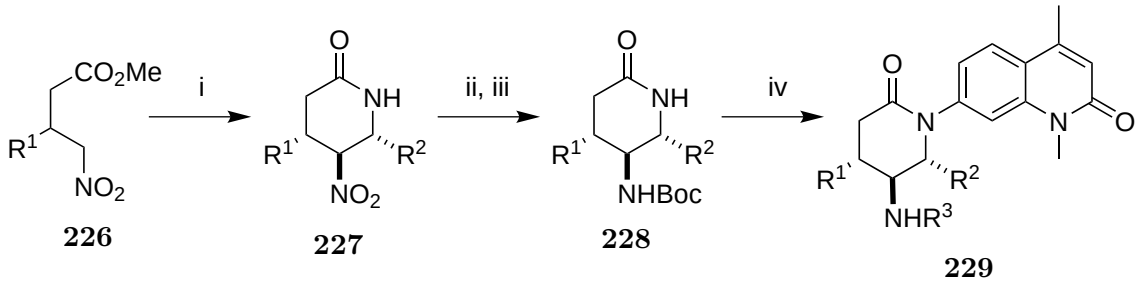

Reagents and Conditions: i. Aldehyde, NH_4OAc, EtOH, 90 °C, 20 h, 30-89%; ii. $NiCl_2 \cdot 6\,H_2O$, $NaBH_4$, MeOH, 0 °C, 30 min; iii. Boc_2O, rt, 14 h, 39-90% (2 steps); iv. **218**, $Pd(OAc)_2$, Xantphos, Cs_2CO_3, 1,4-dioxane, 110 °C, 36 h, 2-75%.

Scheme 3.2 Synthesis of substituted δ-lactam derivatives.

As the activity observed to date was obtained with racemic samples, the presence of an enantiomeric preference was examined by L. Vieira. Towards identifying this, the phenyl compound **234** was resolved into the component enantiomers (–)-**234** and (+)-**234** by preparative chiral HPLC. DSF screening against BRD9 showed a strong stereochemical preference for the

Table 3.3 Third series of compounds synthesised by L. Vieira screened against BRD9 and BRD4(1) by DSF.

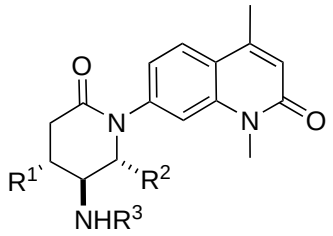

	Substituents			ΔT_m (°C)*		ITC
Compound	R^1	R^2	R^3	BRD9	BRD4(1)	(nM)
230	Me	H	Boc	3.0 ± 0.3 (4)	0.2 ± 0.2 (7)	
231	Me	Me	Boc	4.8 ± 1.2 (4)		
232	Me	Me	H	4.8 ± 0.7 (4)	0.1 ± 0.1 (3)	
233	H	Me	Boc	6.2 ± 0.7 (4)	0.3 ± 0.3 (3)	
234	H	Ph	Boc	5.8 ± 0.6 (4)	-0.6 ± 0.2 (3)	
(–)-**234**	H	Ph	Boc	4.7 ± 1.3 (3)	-0.5 ± 0.1 (3)	493
(+)-**234**	H	Ph	Boc	0.9 ± 0.1 (3)	-0.6 ± 0.2 (3)	

*Mean ΔT_m ± SEM (number of measurements). All compounds were tested at 10 μM. Performed by collaborators at the SGC.

(–)-enantiomer over the (+)-enantiomer (4.7 °C vs 0.9 °C). Given the chiral nature of the BRD9 protein and the proximity of the stereogenic centers to the binding pocket, a stereochemical preference was to be expected. The enhanced affinity of (–)-**234** was confirmed by ITC, where a K_D of 493 nM was observed. These enantiomeric differences in activity highlighted the importance of the stereogenic centers in these ligands, optimally orientating substituents to avoid steric clashes whilst also maximising binding interactions with the protein.

The absolute stereochemistry of (–)-**234** was determined by x-ray crystallography. A co-crystal structure was obtained from BRD9 and racemic **234**, albeit with only a 2.3 Å resolution [Figure 3.4]; when the electron density for the ligand was solved, the desired stereochemistry was identified as 2*S*,3*R*. In addition to the binding elements described previously, the phenyl ring was observed to occupy a hydrophobic cavity bound by F47, P48, V49 and I53. The NHBoc substituent was also found to be orientated such that the nonpolar *tert*-butyl group occupied a hydrophobic groove bound by G43, A46 and F47. As a result of the new substituents, the entire ligand was displaced slightly in the binding pocket such that the lactam carbonyl was now in H-bond distance of Y106. Unexpectedly, a second new H-bond was also seen to be formed between the NH of the amino group and the backbone carbonyl of G43. To highlight the part

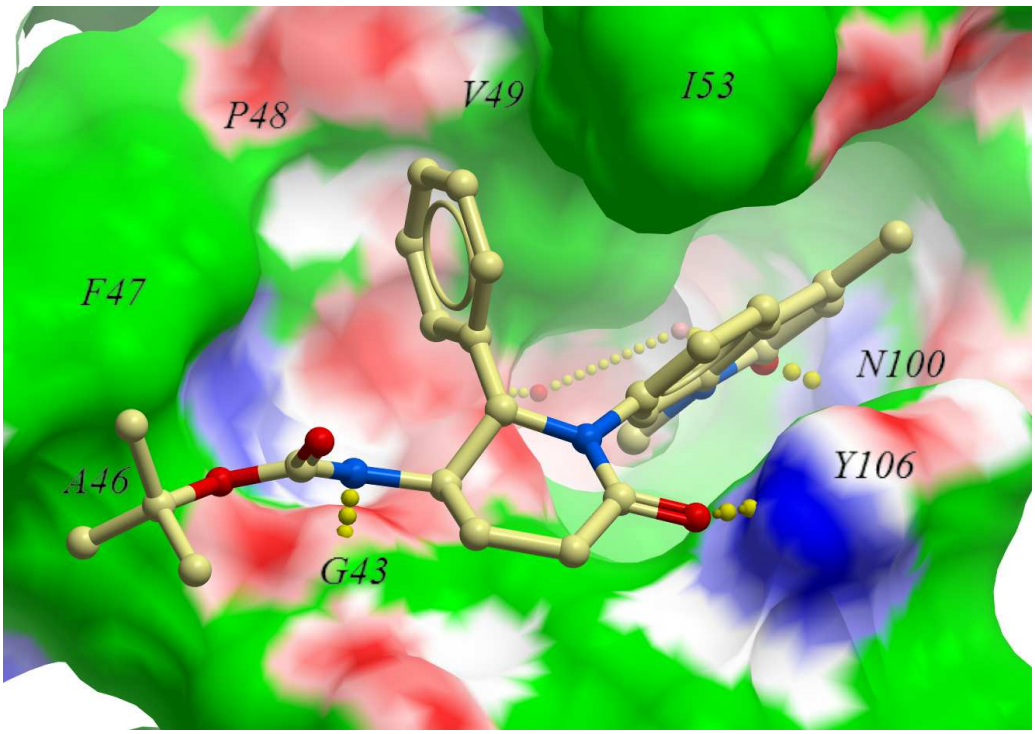

Figure 3.4 Co-crystal structure of **234** bound to BRD9 with conserved water molecules (red balls) and key H-bonds (dotted yellow lines). Obtained by collaborators at the SGC.

that chemistry can play in probe development, it is important to note here that this amino group was not targeted for inclusion in these molecules, but was instead only incorporated as a result of the synthetic methodology used.

3.1.3 Aim

The objective for this project was to convert the best lead compound of L. Vieira into an epigenetic probe against BRD9. Given the absolute stereochemistry of **234** was known, optimisation was to be performed using single enantiomer material. Using known methodology,[141] an enantioselective nitro-Mannich reaction would allow the synthesis of enriched **235** that could then be recrystallised to a single enantiomer [Scheme 3.3]. SAR around the aryl ring was then to be explored through varying the Michael acceptor in this step. The starting material **13** was designed such that the nitro-Mannich product **235**, upon deprotection, would cyclise to form the nitrolactam **236**,[264] intercepting the existing synthesis by L. Vieira. These enantiopure lactams have been synthesised previously through a six-step synthesis from stoichiometric quantities of enantiopure Andersen reagent;[265–268] our approach would only require 4 steps, use catalytic quantities of chiral reagents and the stereochemistry would be set in the antepenultimate step

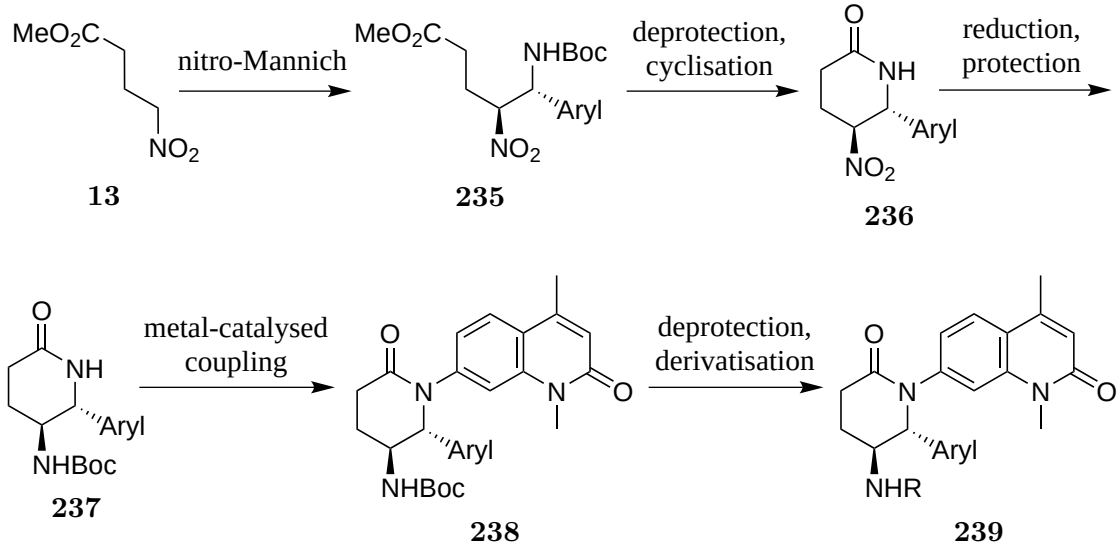

Scheme 3.3 General synthetic plan towards 2*S*,3*R*-enriched compounds.

rather than at the beginning of the synthesis. Reduction of the nitro group followed by Boc protection would then give the lactams **237**, which could undergo a metal-catalysed coupling to give the advanced intermediates **238**. A late-stage deprotection would then allow derivatisation of the amino group as the final step of the synthesis. Exploration of SAR around the amino and aryl substituents was to be performed until a potent and selective probe was obtained.

3.2 Development of a BRD9 probe with a six-membered ring scaffold

3.2.1 Synthesis of 2*S*,3*R*-series

The enantioselective nitro-Mannich reaction described by Johnson *et al.* was to be used to obtain 2*S*,3*R*-enriched material. This reaction, described previously [Section 1.2.2.2], was chosen as it would furnish material featuring the correct relative and absolute stereochemistry of the two stereogenic centers, with the absolute stereochemistry dictated by the choice of the cinchona-derived catalyst [Scheme 3.4]. Although substrates bearing esters had not been trialled in the reaction, this functionality was not expected to interfere with the nitro-Mannich reaction. Using the optimised conditions, nitroalkane **13** and amidosulfone **240** were combined using TBAB as a phase-transfer catalyst to give the racemic nitro-Mannich product **241** in good yield (91%) and dr (>20:1) [Table 3.4], confirming the compatibility of the desired substrates.

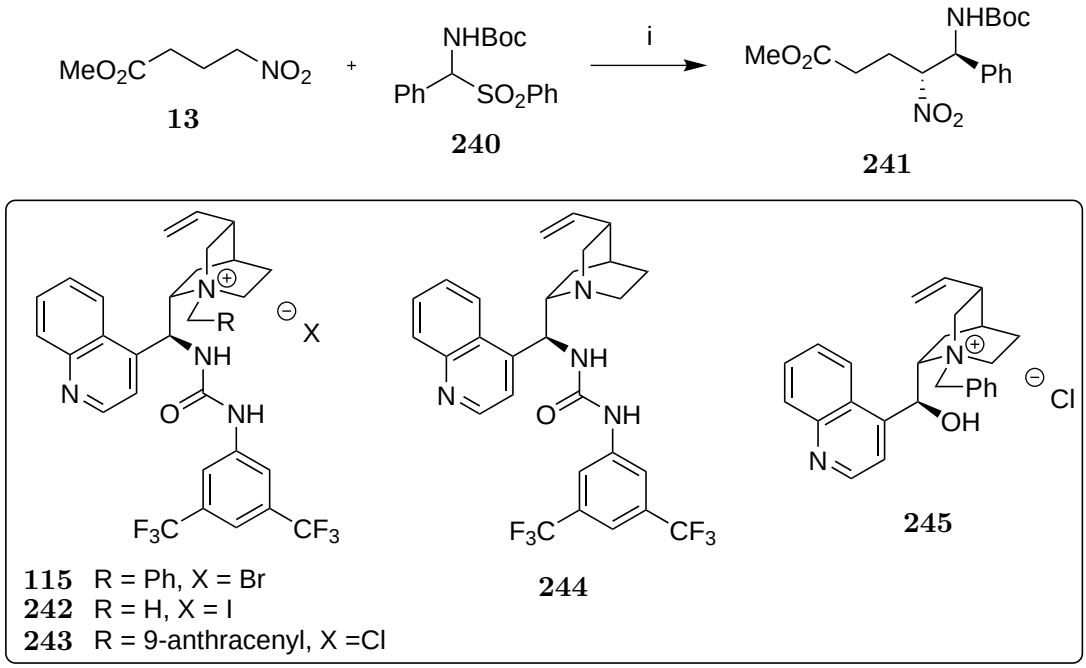

Reagents and Conditions: i. **13** (5 eq), **240** (1 eq), KOH (5 eq), catalyst (5 mol%), TBME, -20 °C, 16 h.

Scheme 3.4 Nitro-Mannich reaction towards 2*S*,3*R*-enriched material.

Table 3.4 Nitro-Mannich reaction towards 2*S*,3*R*-enriched material.

240 (mg)	**Catalyst**	**Yield** (%)	**dr**	**ee** (%)*
20	TBAB	91%	>20:1	0%
20	**115**	69%	9:1	84%
20	**242**	54%	12:1	66%
20	**243**	20%	14:1	82%
20	**244**	15%	2:1	8%
20	**245**	0%		
400	**115**	91%	8:1	91%
		(21%	14:1	98%)**
2000	**115**	80%	1.4:1	83%
		(15%	12:1	97%)**

*ee for major diastereomer reported.

**After recrystallisation.

Trialling a range of cinchona alkaloid-derived PTCs developed by Johnson *et al.* (**115**, **242** and **243**), the benzyl bromide-derived catalyst **115** gave the highest selectivity (84% ee), in accordance with the published research. The importance of the bifunctional nature of this catalyst, acting as both a Brønsted base/H-bond donor and as a phase-transfer catalyst, was confirmed by screening the commercial catalysts **244** and **245**, which gave low or no reactivity respectively under these conditions.

A curious trend was observed when this reaction was scaled up. On a small (20 mg) scale, the reaction proceeded with good dr (9:1) and ee (84%). Increasing to a medium (400 mg) scale, whilst dr was approximately the same (8:1) the ee peaked at 91%. Further scaling to a large (2 g) scale saw this trend reverse, with the ee dropping (83%) and the dr sharply decreasing (1.4:1). Phase-transfer catalysis is highly susceptible to a number of variables that homogenous catalysis is not.[269] On a small scale, the surface area:volume ratio of the solid particles in the liquid is significant, as, if only a few large crystals are used, the bulk of the catalyst molecules may be inaccessible to the reactants in the liquid phase. In contrast, maintaining physical homogeneity, and a high interface area:volume ratio, of biphasic systems on a larger scale becomes difficult, with local disparities in catalyst concentration occuring. These factors can both act to influence the effective catalyst concentration and hence the enantiocontrol of the reaction. As the magnitude of these factors are quantity-dependent, optimisation of the scale used may yield further improvements. Notwithstanding this, the enantioenriched material obtained from the large-scale reaction was viewed as acceptable and was successfully recrystallised from methanol to obtain (2*S*,3*R*)-**241** in 97% ee and 12:1 dr for further use.

This enantioenriched material was then progressed to intercept the existing synthesis of L. Vieira. The Boc group of **241** was removed with TFA to reveal an amine, which, in the presence of aqueous $NaHCO_3$ could react with the ester in an intramolecular cyclisation, giving (2*S*,3*R*)-**246** as a single diastereomer [Scheme 3.5]. The absolute stereochemistry of this was confirmed by comparing the optical rotation with literature values.[268] From here, the existing synthesis of L. Vieira was applied [Scheme 3.2]: the nitro group was reduced and protected with a Boc group to yield (2*S*,3*R*)-**247**; and through the condensation of ethyl acetoacetate

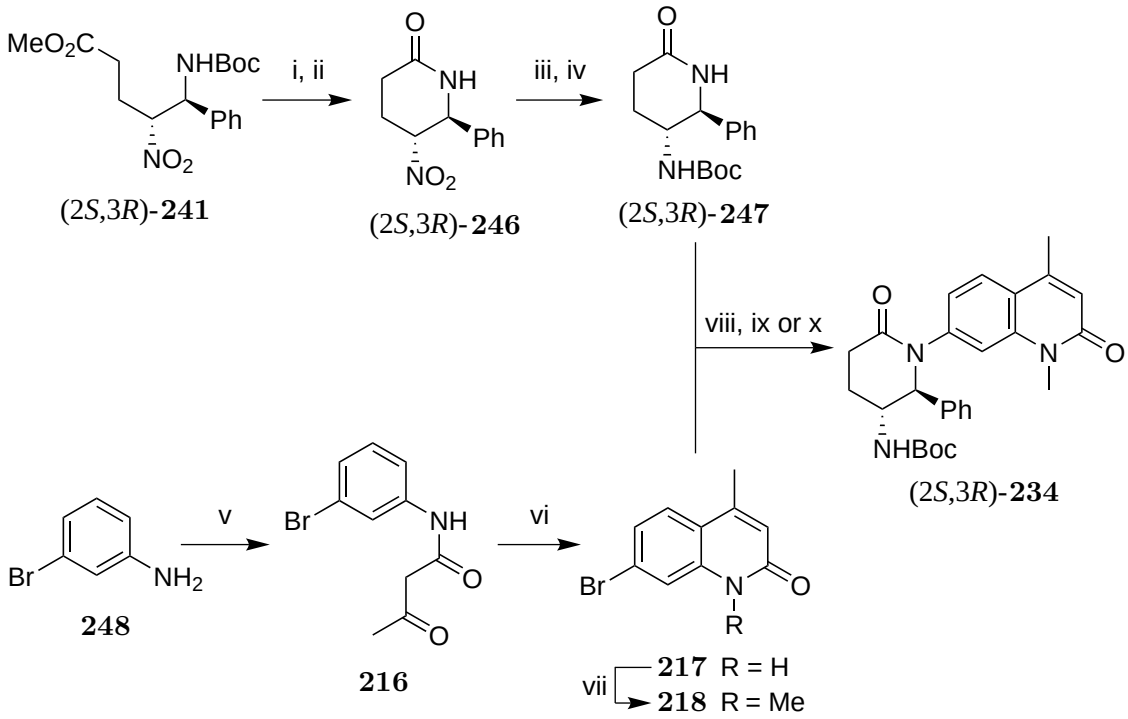

Reagents and Conditions: i. TFA, CH_2Cl_2, rt, 3h; ii. $NaHCO_{3(aq)}$, CH_2Cl_2, rt, 6 h, 66% (2 steps); iii. $NaBH_4$, $NiCl_2 \cdot 6\,H_2O$, MeOH, 0 °C, 30 min; iv. Boc_2O, rt, 14 h, 96% (2 steps); v. ethyl acetoacetate, xylenes, reflux, 16 h, 24%; vi. H_2SO_4, 95 °C, 2 h, 88%; vii. NaH, MeI, DMF, rt, 12 h, 84%; viii. $Pd(OAc)_2$, Xantphos, Cs_2CO_3, 1,4-dioxane, 110 °C, 36 h, 3%; ix. CuI, *N,N'*-dimethylethylenediamine, K_2CO_3, toluene, 110 °C, 36 h, 0%; x. CuI, (+/-)-*trans*-1,2-diaminocyclohexane, K_3PO_4, 1,4-dioxane, 97 °C, 42 h, 60%.

Scheme 3.5 Synthesis of (2*S*,3*R*)-**234**.

with 3-bromoaniline, cyclisation with H_2SO_4 and methylation with NaH and MeI, **218** was prepared for use in the coupling reaction.

The existing coupling method used by L. Vieira proved problematic with these substrates. Previously, L. Vieira had used a palladium-catalysed Buchwald-Hartwig coupling to attach the various *N*-heterocycles to **218**, with products typically obtained in good yields [Scheme 3.2];[262] however, α-phenyl groups on the heterocycles were found to be highly detrimental to the coupling reaction, with the use of **247** yielding only 2% product, a result that was subsequently confirmed here with a 3% yield [Scheme 3.5]. With the PPh_2 substituents of Xantphos, the quinoline system and the lactam with an α-phenyl group all competing for space around the palladium, the low reactivity observed is likely due to steric crowding preventing approach of one or other reagent into the catalyst complex.[270,271] Related substrates to these, however, have shown activity in copper-catalysed Goldberg couplings with smaller ligands.[272] Although no reactivity was observed with a CuI/*N,N'*-dimethylethylenediamine/K_2CO_3/toluene system, significant coupling was achieved using (+/-)-*trans*-1,2-diaminocyclohexane as a ligand with CuI as the metal source, K_3PO_4 as the base and 1,4-dioxane as the solvent,[273] successfully demon-

strating the desired coupling in a reasonable yield (60%). Although in principle the reaction is catalytic, stoichiometric equivalents were used to maximise the amount of (2*S*,3*R*)-**234** obtained.

The coupled material was converted into a number of simple amino-derivatives, which uncovered a fundamental issue. To explore alternative substitution of the amino substituent, the Boc group was first removed using TFA to give the primary amine (2*S*,3*R*)-**249**, which could then be derivatised [Scheme 3.6]: an Eschweiler-Clarke methylation yielded dimethylamine (2*S*,3*R*)-**250**; acetylation with acetic anhydride yielded the acetamide (2*S*,3*R*)-**251**; and condensation with chloroformates yielded the carbamates (2*S*,3*R*)-**252**–**254**. When these compounds were screened against BRD9 by DSF, however, no ΔT_m greater than 1 °C was observed [Table 3.5].

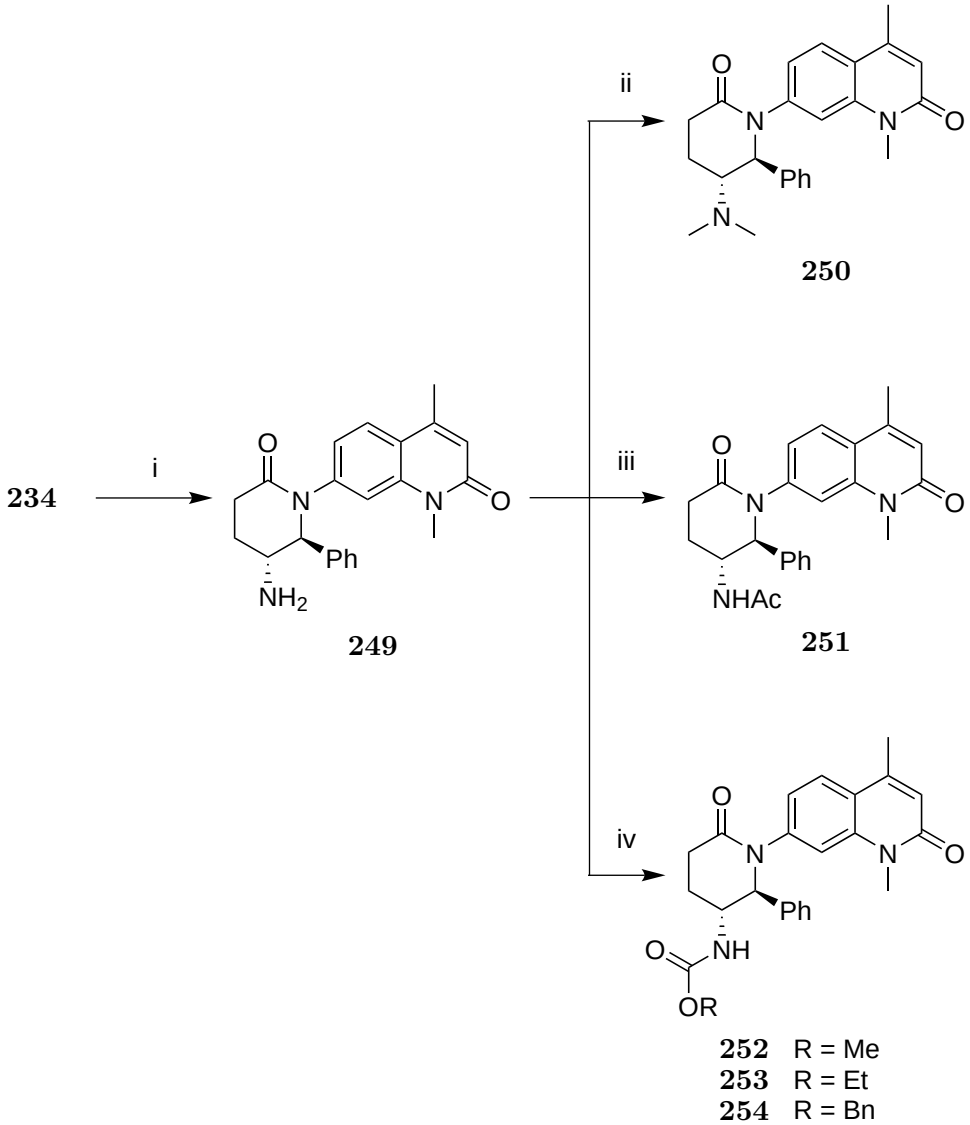

Reagents and Conditions: i. TFA, CH_2Cl_2, rt, 1h, 85%; ii. HCOOH, H_2CO, 95 °C, 14 h, 62%; iii. Ac_2O, NEt_3, CH_2Cl_2, rt, 16 h, 96%; iv. ROCOCl, NEt_3, CH_2Cl_2, rt, 1.5 h, (+)-**252**: 94%, (+)-**253**: 96%, (–)-**254**: 56%.

Scheme 3.6 Synthesis of novel (2*S*,3*R*)-derivatives.

Although this could have been due to incompatibility of the new substituents with the binding site, affinities this low were unexpected given the superficial location of the substitution and because conformational changes would facilitate some limited binding of unfavourable ligands. When both the parent amine, (2*S*,3*R*)-**249**, and the matched compound (2*S*,3*R*)-**234** also proved inactive (0.6 and 1.0 °C, respectively), the absolute stereochemistry of (–)-**234** was questioned. When the optical rotation of (2*S*,3*R*)-**234** was found to match the inactive enantiomer (+)-**234**, it became apparent that the absolute stereochemistry assigned to (–)-**234** was wrong, and the source of the error was to be identified. As an aside, these findings highlighted the importance of chirality in these compounds, and gave negative control compounds for use as a reference when assessing the activity of other probes.

Table 3.5 Screen of novel (2*S*,3*R*)-derivatives against BRD9 by DSF.

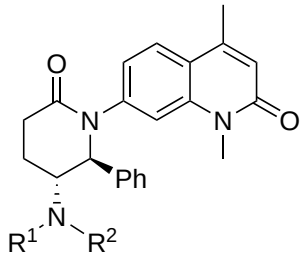

Compound			$\Delta\mathbf{T}_\mathrm{m}$
#	R^1	R^2	(°C)*
(2*S*,3*R*)-**250**	Me	Me	0.9 ± 0.3 (3)
(2*S*,3*R*)-**251**	Ac	H	0.4 ± 0.3 (3)
(2*S*,3*R*)-**252**	COOMe	H	0.8 ± 0.3 (3)
(2*S*,3*R*)-**253**	COOEt	H	0.9 ± 0.1 (3)
(2*S*,3*R*)-**254**	COOBn	H	0.8 ± 0.3 (3)
(2*S*,3*R*)-**249**	H	H	0.6 ± 0.2 (3)
(2*S*,3*R*)-**234**	Boc	H	1.0 ± 0.1 (3)

*Mean ΔT_m ± SEM (number of measurements).

All compounds were tested at 10 μM.

Performed by collaborators at the SGC.

The original assignment of the wrong stereochemistry was a result of both low crystal resolution and conformational flexibility. Returning to the original 2.3 Å co-crystal structure, it was found that both enantiomers can be described by the ligand electron density observed [Figure 3.5], which was a result of two synergistic factors. Firstly, a conformational ring flip around the

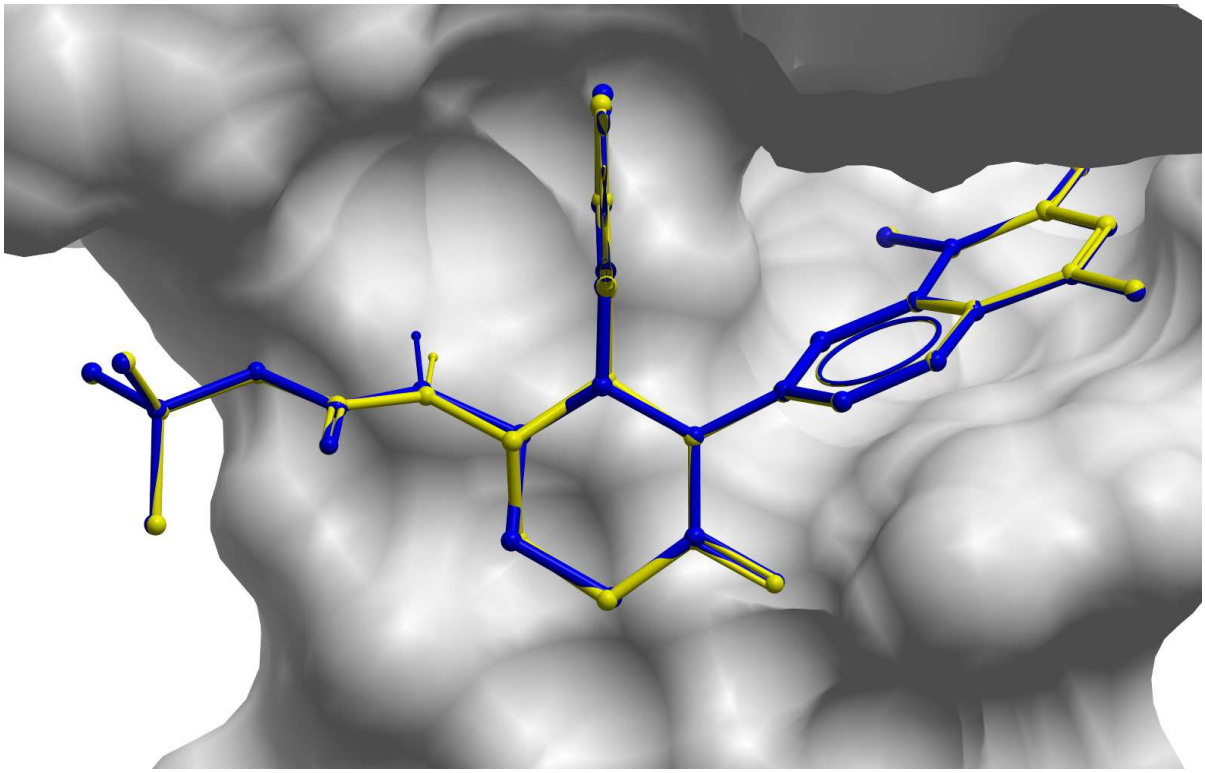

(a) From the top the enantiomers appear to directly overlay with substituents of the δ-lactam ring overlapping.

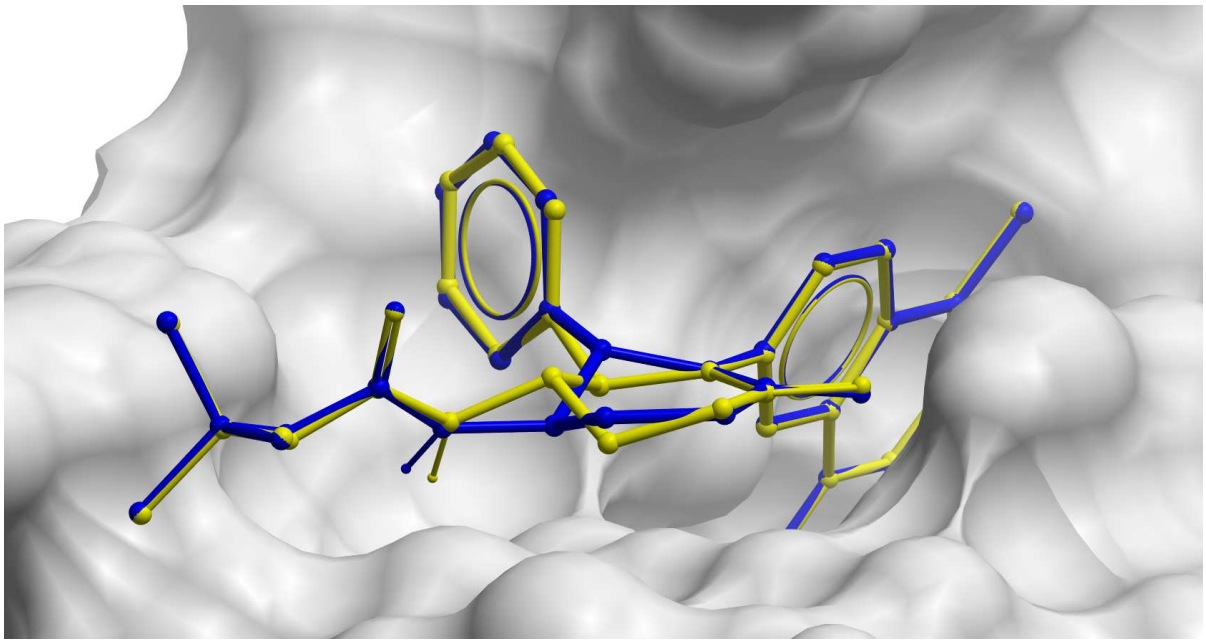

(b) From the side, the conformational changes around the δ-lactam, which were required to allow the substituents of the enantiomers to overlay, can be observed.

Figure 3.5 The original 2.3 Å co-crystal structure of BRD9 with both enantiomers of **234** modeled to fit the measured electron density. The (2*S*,3*R*)-enantiomer is in blue and the (2*R*,3*S*)-enantiomer is in yellow.

lactam scaffold allowed the two enantiomers to position their substituents such that they both fit the crystal data; the substituents of the ring appear to overlap almost identically [Figure 3.5a], despite the lactam scaffold at the core of the enantiomers differing considerably [Figure 3.5b]. Distinguishing the enantiomers by the spatial differences in the core would usually be achieved using the electron density; however, given the low resolution of this co-crystal, the density adequately described both and, unfortunately, the inactive enantiomer was modeled first. Pleasingly, however, a new co-crystal structure of **234** with BRD9 was obtained with a 1.95 Å resolution that confirmed the 2*R*,3*S* absolute stereochemistry and demonstrated all the same binding elements as described previously [Figure 3.6].

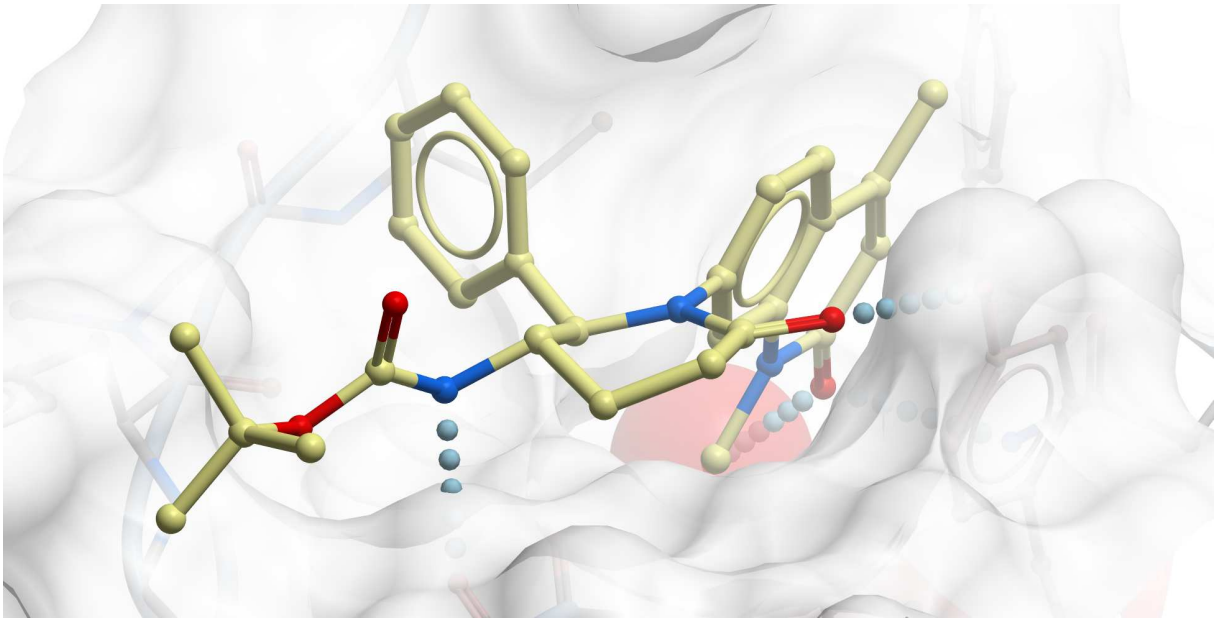

Figure 3.6 A 1.95 Å co-crystal structure of (2*R*,3*S*)-**234** bound to BRD9 with key H-bonds (teal dotted lines) and conserved water molecules (red sphere). [PDB ID: 4Z6I].

3.2.2 Optimisation with racemic material

A small number of racemic derivatives were rapidly synthesised to confirm the reason for the inactivity of the 2*S*,3*R*-series. Using the MCR described previously [Section 1.2.1.1], benzaldehyde, NH_4OAc and nitroalkane **13** were combined to furnish the nitrolactam **246** in a single pot exclusively as the *trans*-isomer [Scheme 3.7].[130] As before, and with comparable yields, the nitro group was reduced and the resulting amine was Boc-protected to give **247**, which was then coupled with the bromoquinolone **218** in a Goldberg coupling to yield **234**. Screening this compound by DSF against BRD9 showed a return of biological activity (ΔT_m

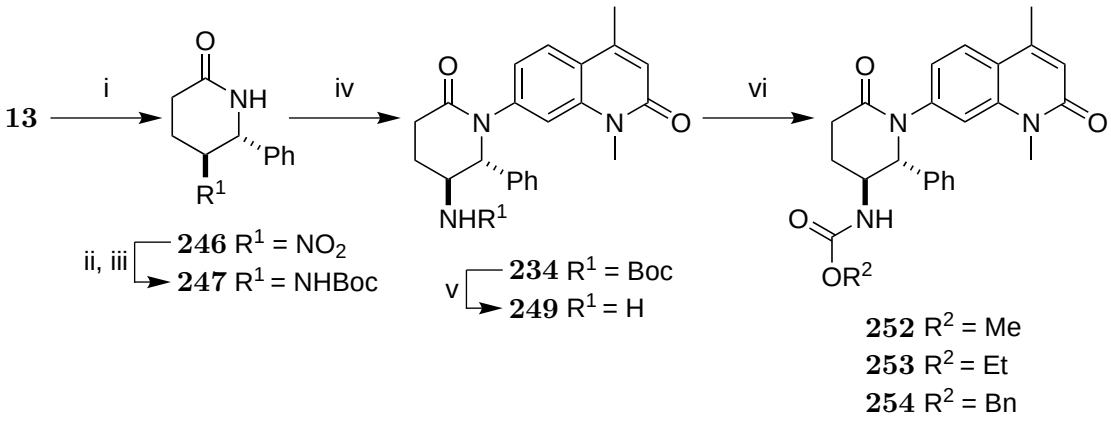

Reagents and Conditions: i. Benzaldehyde, NH_4OAc, EtOH, 90 °C, 20 h, 70%; ii. $NiCl_2 \cdot 6\,H_2O$, $NaBH_4$, MeOH, 0 °C, 30 min; iii. Boc_2O, rt, 14 h, 61% (2 steps); iv. **218**, CuI, (+/−)-*trans*-1,2-diaminocyclohexane, K_3PO_4, 1,4-dioxane, 97 °C, 42 h, 55%; v. TFA, CH_2Cl_2, rt, 1 h, 56%; vi. ROCOCl, NEt_3, CH_2Cl_2, rt, 1.5 h, 66-77%.

Scheme 3.7 Synthesis of racemic amino-derivatives.

3.2 °C) [Table 3.6]. This result was lower than previously measured (5.8 °C), potentially as a result of ageing of the protein stocks, differences in sample quality or other experimental variation. Removing the Boc group of **234** with TFA gave the primary amine **249** that was derivatised with a range of chloroformates to furnish **252**–**254**. Although the data for these compounds showed no statistical improvement upon those for the Boc compound (2.9–3.6 °C), they did show affinity for BRD9, in comparison to the (2*S*,3*R*)-analogs, the most important observation.

Table 3.6 Screening of racemic amino-derivatives against BRD9 by DSF.

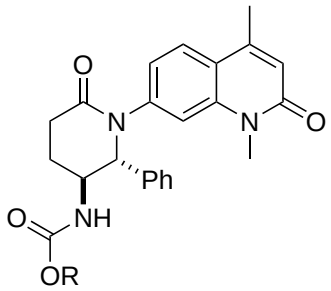

Compound		$\Delta \mathbf{T}_\mathrm{m}$
#	R	(°C)*
234	*t*Bu	3.2 ± 0.6 (3)
252	Me	2.9 ± 0.3 (3)
253	Et	2.9 ± 0.4 (3)
254	Bn	3.6 ± 0.6 (3)

*Mean ΔT_m ± SEM (number of measurements).
All compounds were tested at 10 μM.
Performed by collaborators at the SGC.

Although the absolute stereochemistry of the active enantiomers was now confirmed, optimisation was continued using racemic material in the interest of speed. Incorporation of the

enantioselective nitro-Mannich reaction to give enantioenriched materials resulted in a three-step synthesis to obtain the nitrolactam **246**; through the use of the nitro-Mannich/lactamisation cascade, the racemic nitrolactams could be obtained in a singe step [Section 1.2.1.1]. To facilitate the exploration of SAR, this MCR was used, in the first instance to obtain aryl derivatives. Using a range of benzaldehydes, nitrolactams **255**–**262** were obtained, and these were then reduced and Boc protected to give **263**–**270** [Scheme 3.8]. Coupling of these with **218** lead to a new range of derivatives, **271**–**278**, for testing. *para*-Methoxy substitution was poorly tolerated (1.1 °C) compared to other smaller *para*-substituents (**272**, **275** and **278**, 2.7–4.5 °C), suggesting only limited steric substitution was permitted at this position [Table 3.7]. *para*-Chloro substitution gave the highest affinity of all the compounds screened,

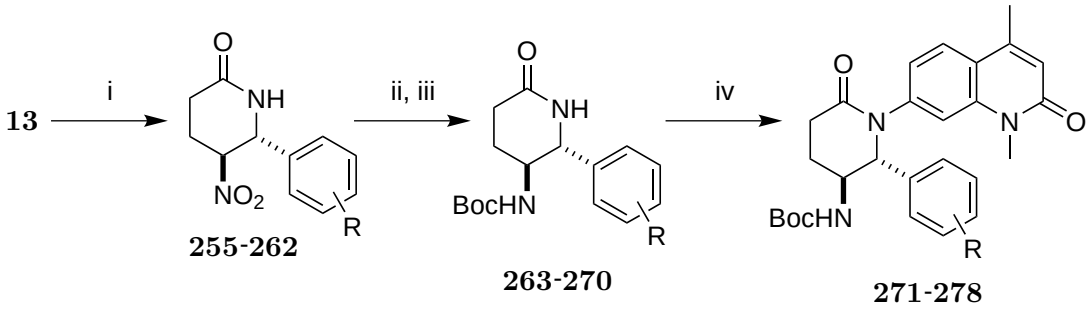

Reagents and Conditions: i. R-C_6H_4-CHO, NH_4OAc, EtOH, 90 °C, 20 h, 26-92%; ii. $NiCl_2 \cdot 6\,H_2O$, $NaBH_4$, MeOH, 0 °C, 30 min; iii. Boc_2O, rt, 14 h, 65-91% (2 steps); iv. **218**, CuI, (+/-)-*trans*-1,2-diaminocyclohexane, K_3PO_4, 1,4-dioxane, 97 °C, 42 h, 7-65%.

Scheme 3.8 Synthesis of racemic aryl-derivatives.

Table 3.7 Screening of racemic aryl-derivatives against BRD9 by DSF.

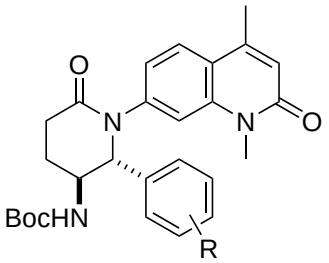

Compound		ΔT_m
#	R	(°C)*
271	*p*-OMe	1.1 ± 0.2 (5)
272	*p*-Me	2.7 ± 0.2 (5)
273	*o*-F	3.2 ± 0.2 (5)
274	*m*-F	3.0 ± 0.3 (5)
275	*p*-F	2.9 ± 0.1 (5)
276	*o*-Cl	2.7 ± 0.1 (5)
277	*m*-Cl	3.5 ± 0.5 (5)
278	*p*-Cl	4.5 ± 0.8 (5)

*Mean ΔT_m ± SEM (number of measurements).
All compounds were tested at 10 μM.
Performed by collaborators at the SGC.

although this did not improve upon the phenyl compound **234** within the error of the assay (4.5 ± 0.8 vs 3.2 ± 0.6). Nonetheless, *para*-chloro substitution was retained because, although it yielded no improvement in potency, it was expected that the increased complementarity with the binding site would offer advances in selectivity over other bromodomain proteins.

With the optimal aryl group selected, SAR around the amino-substituent was explored to optimise H-bonding with G43. Scaling up the synthesis gave significant quantities of the new *para*-chloro lead compound **278**, which was readily deprotected with HCl to give the amine **279** [Scheme 3.9]. This amine was then derivatised using various reagents: reaction with acid chlorides yielded the amides **280**–**284**; reaction with chloroformates yielded the carbamates **285** and **286**; reaction with sulfonyl chlorides yielded the sulfonamides **287**–**291**; reaction with isocyanates yielded the ureas **292**–**296**; and reaction with isothiocyanates yielded the thioureas **297** and **298**. When screening these against BRD9 by DSF, the most stark observation was that no one chemical class showed superior binding over any other [Table 3.8]. Each chemical class showed a range of affinities for different pendant groups (amides **280**–**284**: 0.9 – 4.6 °C; carbamates **285** and **286**: 4.5 – 6.1 °C; sulfonamides **287**–**291**: 3.4 – 6.2 °C; ureas **292**–**296**: 3.2 – 5.4 °C; thioureas **297** and **298**: 5.4 – 5.5 °C), however, with the exception of the amides, these ranges broadly overlapped. As an aside, the *para*-chloro carbamates (**285** and **286**: 4.5 – 6.1 °C) appeared to show generally higher affinities than their phenyl equivalents (**234** and **252** – **254**: 2.9 – 3.6 °C), supporting the earlier decision to include the *para*-chloro group.

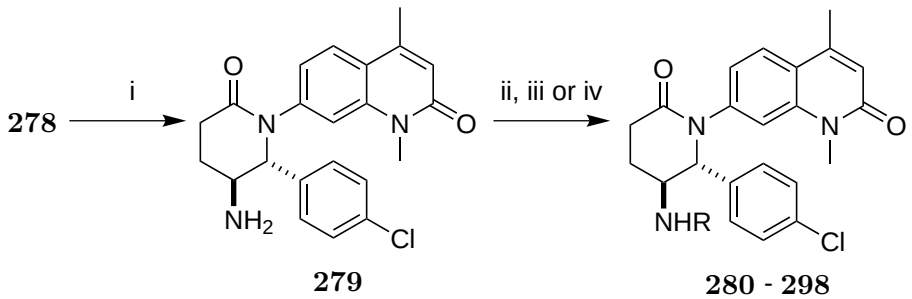

Reagents and Conditions: i. $HCl_{(dioxane)}$, rt, 11 h, 96%; ii. RCl, NEt_3, CH_2Cl_2, rt, 6 h, 12-78%; iii. RNCO, CH_2Cl_2, rt, 15 h, 16-40%; iv. RNCS, CH_2Cl_2, rt, 15 h, 26-40%.

Scheme 3.9 Synthesis of racemic *para*-chlorophenyl amino-derivatives.

Table 3.8 Screen of racemic *para*-chlorophenyl amino-derivatives against BRD9 by DSF.

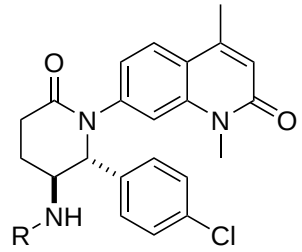

Compound #	R	ΔT_m (°C)*	Compound #	R	ΔT_m (°C)*
280	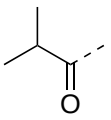	2.1 ± 0.7 (4)	**289**	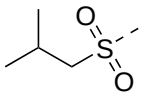	6.2 ± 0.6 (4)
281	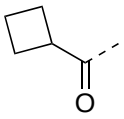	3.1 ± 0.5 (4)	**290**	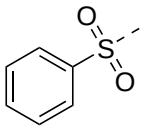	5.0 ± 0.4 (4)
282	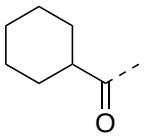	0.9 ± 0.5 (4)	**291**	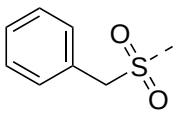	3.4 ± 0.2 (2)
283	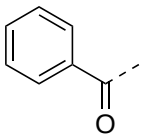	4.6 ± 0.7 (2)	**292**	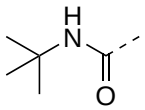	3.2 ± 0.5 (4)
284	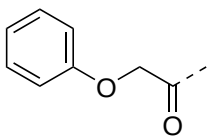	2.8 ± 0.7 (4)	**293**	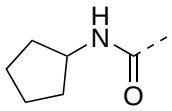	3.8 ± 0.7 (4)
278	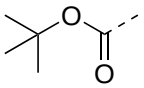	4.5 ± 0.8 (5)	**294**	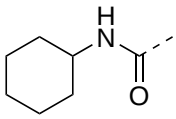	4.2 ± 0.7 (4)
285	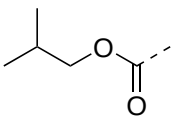	5.2 ± 0.5 (4)	**295**	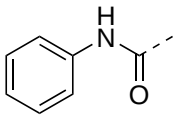	5.4 ± 0.7 (4)
286	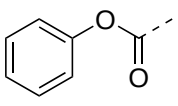	6.1 ± 1.8 (4)	**296**	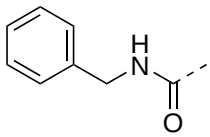	4.1 ± 0.9 (4)
287	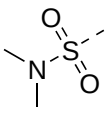	3.7 ± 0.1 (2)	**297**	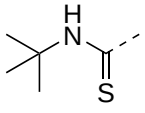	5.5 ± 0.9 (3)
288	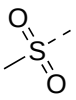	4.7 ± 0.5 (4)	**298**	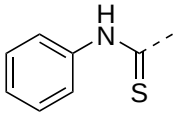	5.4 ± 0.5 (3)

*Mean ΔT_m ± SEM (number of measurements). All compounds were tested at 10 μM. Performed by collaborators at the SGC.

The trends observed likely arose from a combination of factors. Given the H-bond to G43 is greatly influenced by the *N*-functional group, binding affinities were expected to broadly reflect the Brønsted acidity of the chemical classes; instead, binding affinity was found to be dependent on both the type of functional group and the attached substituents. Although the latter dependence could be due to optimisation of hydrophobic interactions of the pendant group with the groove in which it occupies, an alternative hypothesis was proposed based around the conformation of the *N*-substituent dictating the presentation of the hydrogen bond donor. Because of the structural constraints of the binding pocket, each functional group/pendant group pair is limited in the conformations it can adopt, potentially none of which are ideal for H-bonding to the carbonyl of G43. This may explain why the amides, with less conformational freedom as a result of a shorter linkage, demonstrated generally lower affinities. It is prudent to highlight that the conformation of the protein is not independent of the ligand and will undergo small conformational changes to assist in ligand binding.

To identify the most potent species, the four best compounds were resolved into their component enantiomers for further testing. The carbamate **278**, the amide **283**, the sulfonamide **289** and the urea **295**, each presenting a different chemical class, were resolved by preparative HPLC into their component enantiomers. As assessed by DSF assay, one enantiomer showed preference over the second enantiomer (4.8–6.2 °C vs 0.9–1.3 °C), except for **283**, where, surprisingly, both enantiomers were equipotent within experimental error (5.2 ± 0.8 vs 4.1 ± 0.3) [Table 3.9]; it is unclear if this was a result of limitations in the DSF assay or conformational flexibility as seen for the (2*S*,3*R*)-series previously. This aside, the affinity for BRD9 of the most active enantiomer of each compound was measured in a more accurate ITC assay, which allowed a number of conclusions to be drawn: comparing the active enantiomer of the *para*-chlorophenyl species ((–)-**278**) to the phenyl equivalent ((–)-**234**) vindicated the inclusion of this substituent (247 nM vs. 493 nM); the limitations of the DSF assay were highlighted, as (+)-**295** had the second highest ΔT_m shift (5.3 °C) but a K_D of only 1.0 μM; and, most importantly, (–)-**289** was found to have a K_D of 99 nM, fulfilling the sub-100 nM potency requirements for an SGC probe. This compound was named, and hereafter referred to as, LP99 (**L**ucas Vieira **P**eter Clark **99** nM).[274]

A co-crystal structure of LP99 confirmed the absolute stereochemistry and distinct binding elements of the probe. As for the latter crystal structures, this demonstrated the desired 2*R*,3*S*

Table 3.9 Activity of single enantiomer derivatives against BRD9 by DSF and ITC.

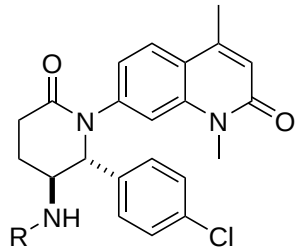

Compound R	#	ΔT_m (°C)*	K_D (nM)
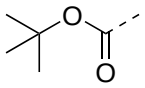	(+)-**278**	0.9 ± 0.4 (6)	
	(–)-**278**	4.8 ± 0.3 (6)	247
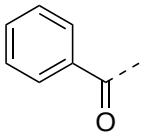	(+)-**283**	5.2 ± 0.8 (5)	200
	(–)-**283**	4.1 ± 0.3 (5)	
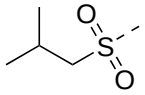	(+)-**289**	1.2 ± 0.2 (6)	
	(–)-**289** [LP99]	6.2 ± 0.4 (9)	99
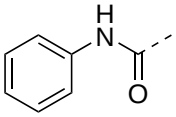	(+)-**295**	5.3 ± 0.6 (6)	1010
	(–)-**295**	1.3 ± 0.6 (6)	

*Mean ΔT_m ± SEM (number of measurements). All compounds were tested at 10 μM. Performed by collaborators at the SGC.

absolute stereochemistry [Figure 3.7]. The H-bonds developed through the synthesis were all apparent: the quinolone carbonyl accepts H-bonds from both N100 and Y57 mediated through one of the conserved water molecules; the lactam carbonyl accepts a H-bond from the hydroxyl of Y106; and the NH of the sulfonamide donates a H-bond to the peptide carbonyl of G43. Further, the *para*-chlorophenyl ring demonstrated good complementarity with the hydrophobic cavity bound by F47, P48, V49 and I53. Finally, the *iso*-butyl tail of the sulfonamide closely binds in the hydrophobic groove defined largely by F47. Although the ligand could potentially be further developed to include a polar interaction with the imidazole of H42, LP99 was selected as a chemical probe candidate against BRD9.

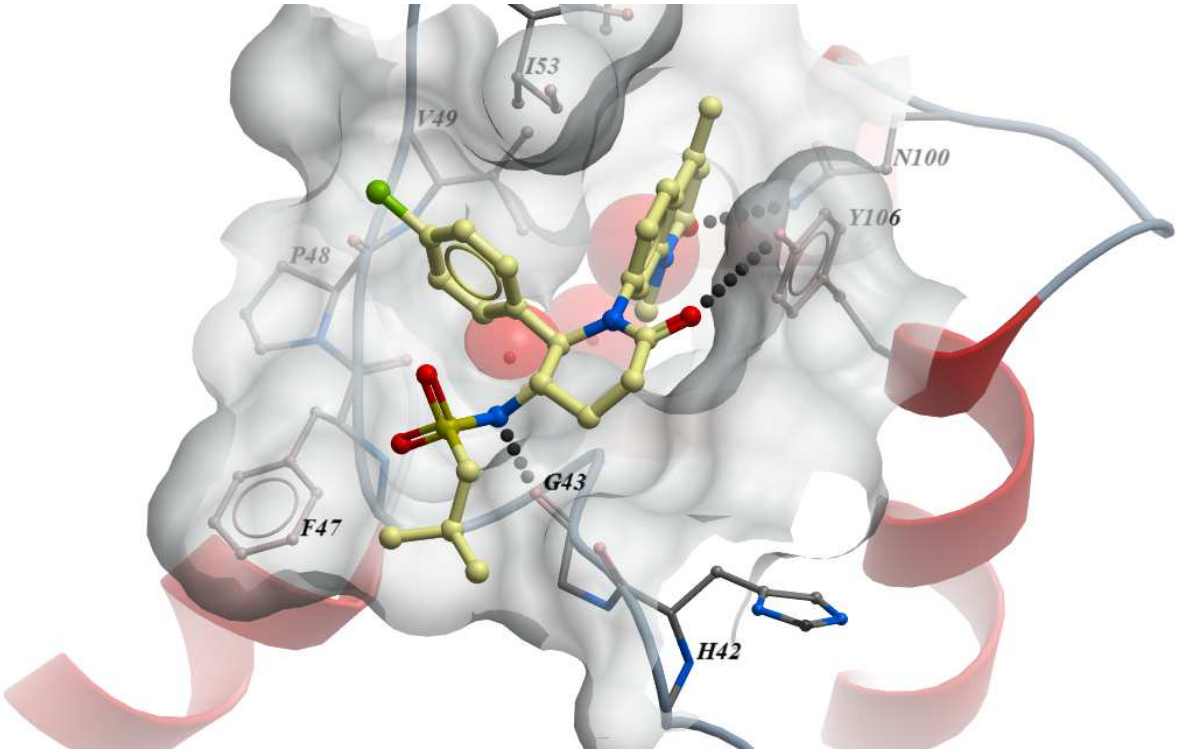

Figure 3.7 A 1.7 Å co-crystal structure of LP99 with the bromodomain of BRD9 with key H-bonds (black dotted lines) and conserved water molecules (red balls and spheres). Obtained by collaborators at the SGC.

3.2.3 Enantioenriched synthesis of LP99

Having identified the optimal substitution and confirmed the absolute stereochemistry, an enantioselective approach was initiated to ultimately allow for the large scale synthesis of LP99. Enantioenriched material was to be obtained using the same organocatalysed nitro-Mannich reaction as for the opposite enantiomer. Using the pseudo-enantiomeric catalyst **299**, the phenyl-substituted amidosulfone **240** was converted to the nitro-Mannich product **241** with excellent dr (14:1) and good ee for the major diastereomer (82%) [Scheme 3.10]; this ee was similar to that achieved with the alternative catalyst (82% vs 84%), highlighting the pseudo-enantiomeric behaviour of the cinchona alkaloids. A reaction with *para*-chlorophenyl-substituted amidosulfone **300** using TBAB as the PTC yielded the desired racemic product **301**, albeit with a dr that, worringly, favoured the *cis*-diastereomer (*trans*-**301**:*cis*-**301**, 1:1.5). Reassuringly, performing this reaction with the organocatalyst **299** on a small scale (0.06 mmol) yielded the desired product with selectivity in favour of the desired *trans*-diastereomer (*trans*-**301**:*cis*-**301**, 7:1), and with a good ee (85%) for the major diastereomer.

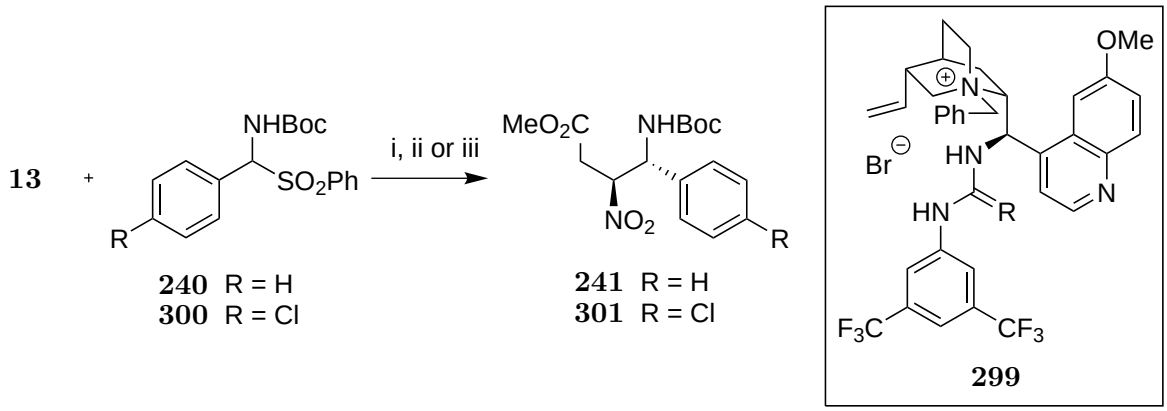

Reagents and Conditions: i. **13** (5 eq), **240** (1 eq), KOH (5 eq), **299** (5 mol%), TBME, -20°C, 16 h, 88%, dr 14:1, ee 82%/28% ii. **13** (5 eq), **300** (1 eq), KOH (5 eq), TBAB (5 mol%), TBME, -20°C, 16 h, 58%, dr 1:1.5; iii. **13** (5 eq), **300** (0.06 mmol, 1 eq), KOH (5 eq), **299** (5 mol%), TBME, -20°C, 16 h, 54%, dr 7:1; ee 85%.

Scheme 3.10 Nitro-Mannich reaction towards 2*R*,3*S*-enriched material.

On scale up, epimerisation of the stereocenter bearing the nitro group became a significant issue. When this reaction was performed on a 16 mmol scale, initial indications were positive, with a crude dr of 6:1 observed in favour of the desired diastereomer [Scheme 3.11]. However, as attempts were made to purify the material through FCC and recrystallisation, the dr decreased to 2:1. It soon became apparent that the stereocenter α to the nitro group was epimerising, with time and handling, to the undesired *cis*-diastereomer; through tautomerisation the C3 proton can be removed to form a nitronate that, on reprotonation, would epimerise and compromise the stereochemical integrity. This was not seen with the equivalent phenyl compound **241**, and thus this observation was attributed to the inductive effects of the *para*-chloro group increasing the acidity of the C3 proton and facilitating this process. The ee for this reaction was not measured as, due to the mixed origin of the enantiomers, it would be unrepresentative of the selectivity of the reaction.

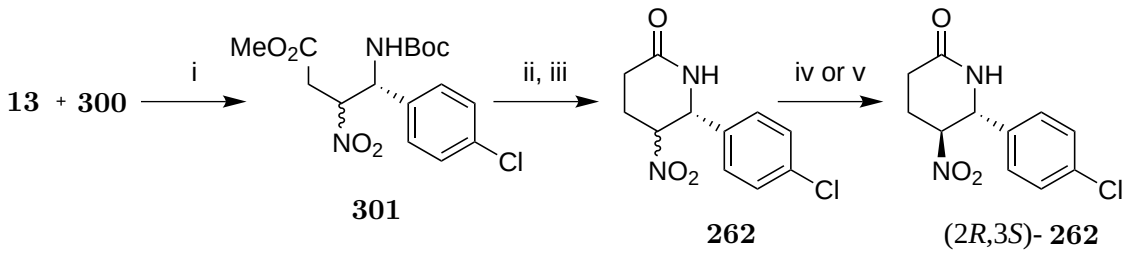

Reagents and Conditions: i. **13** (5 eq), **300** (16 mmol, 1 eq), KOH (5 eq), **299** (5 mol%), TBME, -20 °C, 16 h, 67%, dr 2:1; ii. TFA, CH_2Cl_2, rt, 3h; iii. $NaHCO_{3(aq)}$, CH_2Cl_2, rt, 6 h, 73% (2 steps), dr 2.5:1; iv. DBU (10 mol%), CH_2Cl_2, rt, 2.5 d, dr 12:1; v. iPr$_2$EtN (10 mol%), CH_2Cl_2, rt, 3 d, dr 12:1.

Scheme 3.11 Epimerisation of C3 towards 2*R*,3*S*-enriched material.

Measures were taken to minimise the impact of this issue, firstly by developing a method to recover the epimerised material. It was believed the nitrolactam **262** would show an equilibrium preference for the *trans*-diastereomer as the C3-substituent would preferentially adopt an equatorial position to minimise 1,3-diaxial strain with other substituents on the ring. Given the C2 proton can not readily be removed, it was envisioned that under the appropriate conditions epimerisation of C3 would reinstate the desired *trans*-arrangement. As before, the nitro-Mannich product **301** was deprotected with TFA and cyclised with assistance from a mild $NaHCO_{3(aq)}$ treatment to yield the nitrolactam **262** [Scheme 3.11]. This material already showed a slightly higher dr, evidence that base-catalysed epimerisation favoured the *trans*-diastereomer. Given the slow epimerisation seen under biphasic conditions with the weak base $NaHCO_3$, the stronger homogenous bases DBU and Hünig's base were trialled in dichloromethane. DBU catalysed the epimerisation at a faster rate (2.5 d vs 3 d), but pleasingly both bases coalesced on an equilibrium dr of 12:1 in favour of the *trans*-diastereomer.

With an efficient recovery method available, the nitro-Mannich reaction was studied more closely. All species present after work-up of the nitro-Mannich reaction were identified by NMR spectroscopy [Scheme 3.12]: the amidosulfone substrate **300** was never observed, attesting to complete conversion to the active species *in situ*; the hydroxy-adduct of the imine (**302**), an artifact of isolation following the aqueous work-up, was present; and the hydrolysis product of the imine (**303**), which could result from decomposition during the reaction or during isolation from **302**, was also identified. From the amounts of these species observed, conversion to the product **301** could be assessed [full data are reported in Section 6.1.1].

Before being able to optimise selectivity at C2, a metric to assess the enantioselectivity at this center was required. With considerable epimerisation occurring, it was necessary to measure selectivity for 2*R* over 2*S* for both diastereomers; the excess of 2*R*,3*S* and 2*R*,3*R* over 2*S*,3*R* and 2*S*,3*S* had to be identified. The relative amount of each enantiomer of the two diastereomers (*trans*: 2*R*,3*S* and 2*S*,3*R*; *cis*: 2*R*,3*R* and 2*S*,3*S*) could be measured by UV absorbances from analytical chiral HPLC, whereas the relative amount of each diastereomer could be assessed from the dr measured by NMR spectroscopy. Although comparing the integration of the four enantiomeric peaks from the HPLC spectrum alone would be operationally simpler, diastereomers may not absorb UV light equally and hence they can not be directly compared.

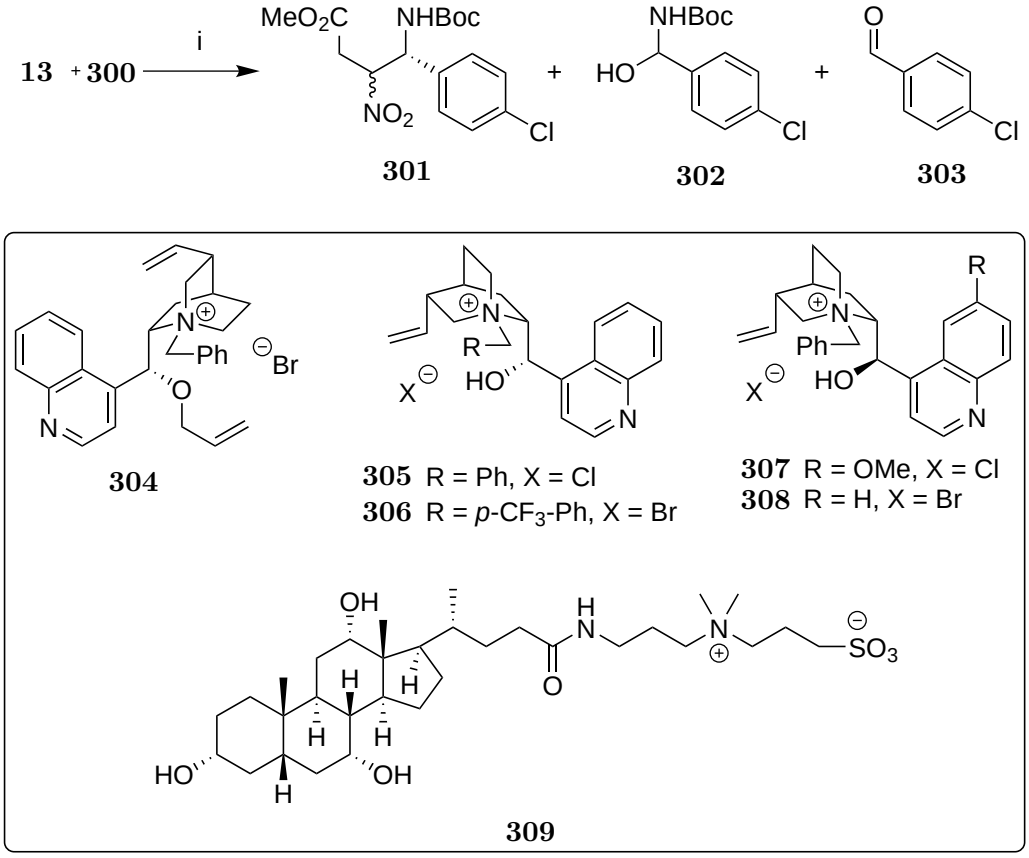

Reagents and Conditions: i. **13** (5 eq), **300** (1 eq), base, catalyst (5 mol%), TBME, -20°C, 16 h.

Scheme 3.12 Optimisation of the nitro-Mannich reaction towards 2*R*-enriched material from **300**.

Instead, the dr can be used to scale the integrations of the diastereomeric pairs, allowing the relative composition of the four enantiomers to be calculated. From this, the excess of the two 2*R* enantiomers over the two 2*S* enantiomers could be calculated to give an estimate of the stereoselectivity at C2. This metric is referred to as the epimeric excess, and has been established previously to report the enantioselectivity at one stereogenic center independent of others in the molecule.[275–277]

Optimisation of the epimeric excess at C2 was explored first using compound **300**. A range of commercial PTCs (**304**–**309**) were trialled in the reaction [Scheme 3.12]; although product was formed in all cases, no epimeric excess greater than 10% was observed [Table 3.10]. In comparison, using the bifunctional PTC catalyst **299** under the standard conditions gave an epimeric excess at C2 of 88%. The effect of varying the identity and loading of the base was then explored: most bases showed a limited difference in selectivity between loadings of 1.5 and 5 equivalents; and there was also only minimal differences between the best bases screened (KOH: 88%, K_2HPO_4: 87%, K_2CO_3: 89%). The best conditions with respect to epimeric

Table 3.10 Optimisation of the nitro-Mannich reaction towards 2*R*-enriched material from **300**.

Scale		**Base**		**Conversion**	**epimeric excess**$_{C2}$
(mmol)	**Catalyst**	Species	eq	(%)	(%)*
0.06	**304**	KOH	5	74	0
0.06	**305**	KOH	5	88	-4
0.06	**306**	KOH	5	81	1
0.06	**307**	KOH	5	87	4
0.06	**308**	KOH	5	72	10
0.06	**309**	KOH	5	91	3
0.06	**299**	KOH	5	76	88
0.06	**299**	KOH	1.5	78	88
0.06	**299**	Cs_2CO_3	5	98	82
0.06	**299**	Cs_2CO_3	1.5	99	81
0.06	**299**	K_2HPO_4	5	47	87
0.06	**299**	K_2HPO_4	1.5	84	86
0.06	**299**	KF	5	72	86
0.06	**299**	KF	1.5	81	79
0.06	**299**	K_2CO_3	5	88	89
0.06	**299**	K_2CO_3	1.5	90	88
15.9	**299**	K_2CO_3	5	80	84

*calculated from the integration of the absorbances of the four enantiomers by UV spectroscopy scaled by dr as measured by NMR spectroscopy.

excess (K_2CO_3, 5 eq) were used henceforth to maximise the chance of recrystallisation to a single enantiomer. Upon scale up to 15.9 mmol, although the yield and dr stayed high, the epimeric selectivity dropped to 84%. After deprotection, cyclisation and epimerisation to the nitrolactam **262**, despite exhaustive attempts the material could not be recrystallised to a single enantiomer; during each recrystallisation, the majority of the material would instead solidify with a lower enantiopurity than that with which it started. This has been shown to occur in cases where the racemate is more crystalline than the single enantiomers, or alternatively where both enantiomers crystallise simultaneously to form a conglomerate.[278] Although the mother liquor was conversely being enriched in this process, the small amount of material obtained was not synthetically useful.

An alternative substrate was explored to assess if the epimeric excess could be maintained at the larger scale. The amidosulfone **300** had been used to date for reasons of stability and handling. However, to convert this to the actual substrate **310** *in situ* requires superstoichiometric equivalents of base that could potentially catalyse a background reaction. Using **310** directly as the substrate allowed the catalytic screening of many other basic organocatalysts developed by or used in the Dixon group [Scheme 3.13]: the cinchona-derived ureas and thioureas (**311**–**315**);

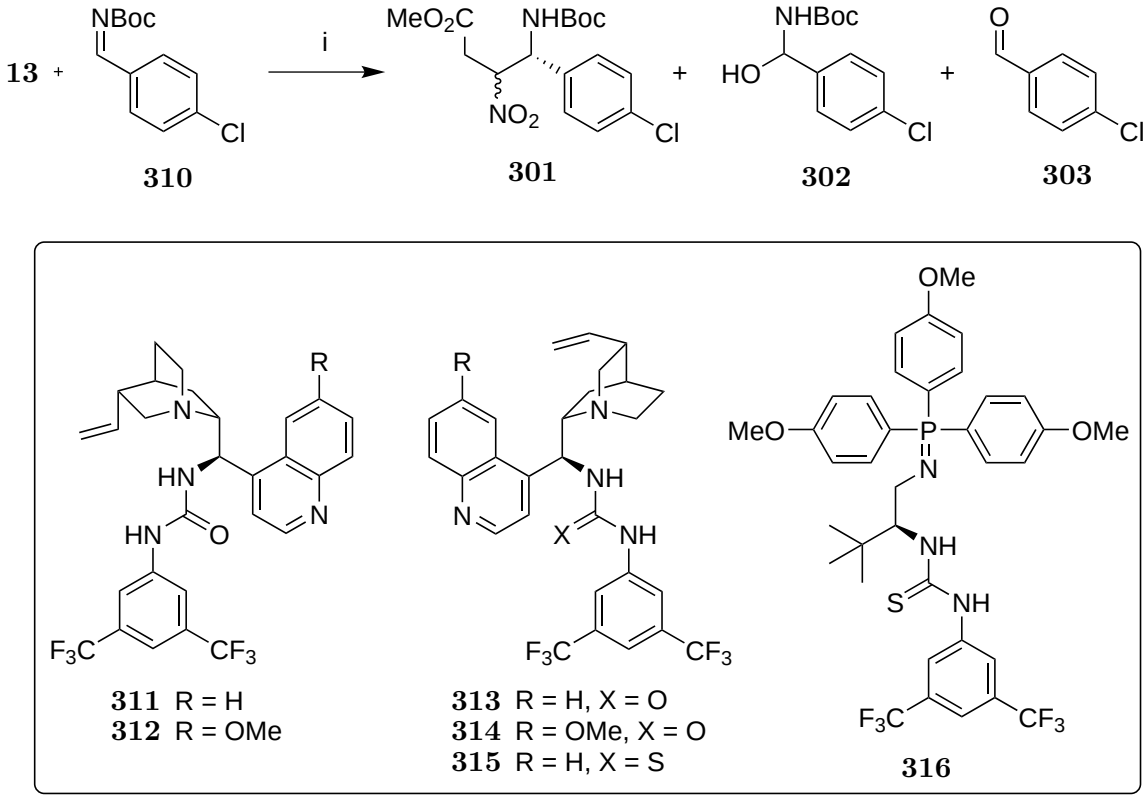

Reagents and Conditions: i. **13** (5 eq), **310** (1 eq), base (where applicable), catalyst (10 mol%), TBME, -20°C, 16 h.

Scheme 3.13 Optimisation of the nitro-Mannich reaction towards 2*R*-enriched material from **310**.

the recently reported iminophosphorane BIMP **316**;[143] and finally Takemoto's catalyst (**317**). The catalysts were screened at an increased loading of 10 mol%, but, whilst conversion varied greatly with catalyst (39–90%), there were no improvements in epimeric excess [Table 3.11]. In a final optimisation attempt, substoichiometric loadings of K_2CO_3 with **299** were explored, with the scale increased to identify results that would be synthetically useful. A small increase in epimeric excess (92%) was obtained with a base loading of 0.25 equivalents. Most gratifyingly, this selectivity was largely retained on the preparative scale, with an epimeric excess of 90% obtained, giving enriched material with which to complete the synthesis.

The enantioenriched material obtained was progressed to complete the synthesis of LP99. Using the method developed previously, **301** was deprotected, cyclised and epimirised under base-catalysis to yield **262** with a dr of 12:1; the minor diastereomer was subsequently separated by FCC [Scheme 3.14]. At this step, the material was found to have an ee of 90%, confirming the validity, and accuracy, of the epimeric excess metric. However, recrystallisation of this 90% ee material to a single enantiomer was attempted repeatedly, with many different solvents and

Table 3.11 Optimisation of the nitro-Mannich reaction towards 2*R*-enriched material from **310**.

Scale		Base		Conversion	epimeric excess$_{C2}$
(mmol)	**Catalyst**	Species	eq	(%)	(%)*
0.06	**311**			39	57
0.06	**312**			52	63
0.06	**313**			80	-61
0.06	**314**			61	-73
0.06	**315**			43	-54
0.06	**316**			90	-61
0.40	**299**	K_2CO_3	1	42	87
0.40	**299**	K_2CO_3	0.25	39	92
0.40	**299**	K_2CO_3	0.1	47	91
3.00	**299**	K_2CO_3	0.25	83	90

*ee for each diastereomer scaled by dr to give relative composition of the four enantiomers, from which the excess of 2*R* over 2*S* can be calculated.

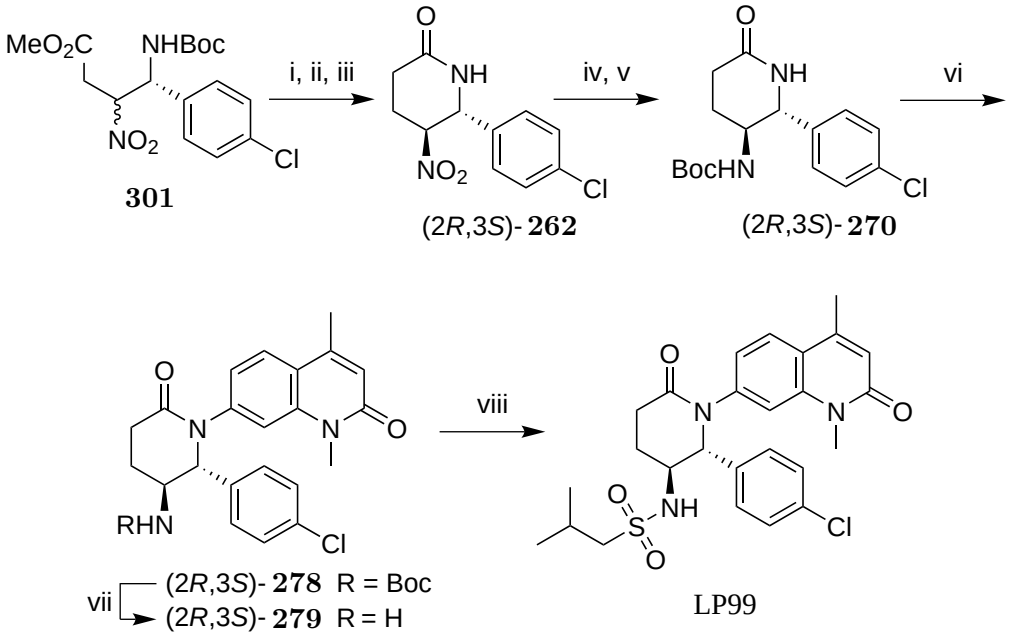

Reagents and Conditions: i. TFA, CH_2Cl_2, rt, 3h; ii. $NaHCO_{3(aq)}$, CH_2Cl_2, rt, 6 h; iii. DBU (10 mol%), CH_2Cl_2, rt, 2.5 d, 73% (3 steps), dr >20:1, ee 90%; iv. $NiCl_2 \cdot 6H_2O$, $NaBH_4$, MeOH, 0 °C, 30 min; v. Boc_2O, rt, 14 h, 74% (2 steps); vi. **218**, CuI, (+/-)-*trans*-1,2-diaminocyclohexane, K_3PO_4, 1,4-dioxane, 97 °C, 42 h, 65%; vii. $HCl_{(dioxane)}$, rt, 11 h, 96%; viii. *i*$BuSO_2Cl$, NEt_3, CH_2Cl_2, rt, 6 h, 78%.

Scheme 3.14 Enantioenriched synthesis of LP99.

combination of solvents, at this and every subsequent step in the synthesis of LP99, without success. Whether the proportion of (2*R*,3*S*)-material was below a critical level necessary for single enantiomeric crystallisation, or whether the racemate was more crystalline than the single enantiomer, recrystallisation to a single enantiomer was unsuccessful. In future, recrystallising the amine **279** as a salt with chiral acids may be successful. Although this could question the utility of the enantioselective synthesis entirely, 95% of the material synthesised, purified and carried through this enriched synthesis bore the correct absolute stereochemistry. In the end, LP99 was readily resolved by preparative HPLC to a single enantiomer for biological testing.

3.3 Biological activity of LP99 and BRD7/9

3.3.1 Biological validation of the probe LP99

Collaborators at the SGC performed a number of biological experiments to validate LP99, beginning with a DSF assay to assess selectivity. A DSF assay against the 49 expressible bromodomains was performed using LP99 [Figure 3.8. For full data, see Section 6.2.1]. In addition to a significant ΔT_m shift with BRD9, a strong affinity for BRD7 (9.9 °C), the most closely related bromodomain protein, was seen. The K_D for LP99 against BRD7 was measured as 909 nM by ITC, below the 30:1 selectivity threshold and necessitating the report of LP99 as a dual BRD7/9 probe. Beyond this, no ΔT_m >1 °C was observed, including for other closely structurally-related members of subfamily IV. It is pertinent to note that this is the only conclusion that can be drawn from this data; as thermal stabilisation of the protein and binding of a ligand are not directly linked properties, a ligand may potently bind a protein and compete with intrinsic ligands without conveying any change in thermal stability. As a result, the absence of shifts with other bromodomain proteins does not necessarily signify that LP99 does not bind them. Selectivity would be better assessed by an activity-based assay, however these require a larger amount of protein and largely remain to be developed.

LP99 inhibition of chromatin binding was demonstrated using a FRAP assay. BRD9 binds

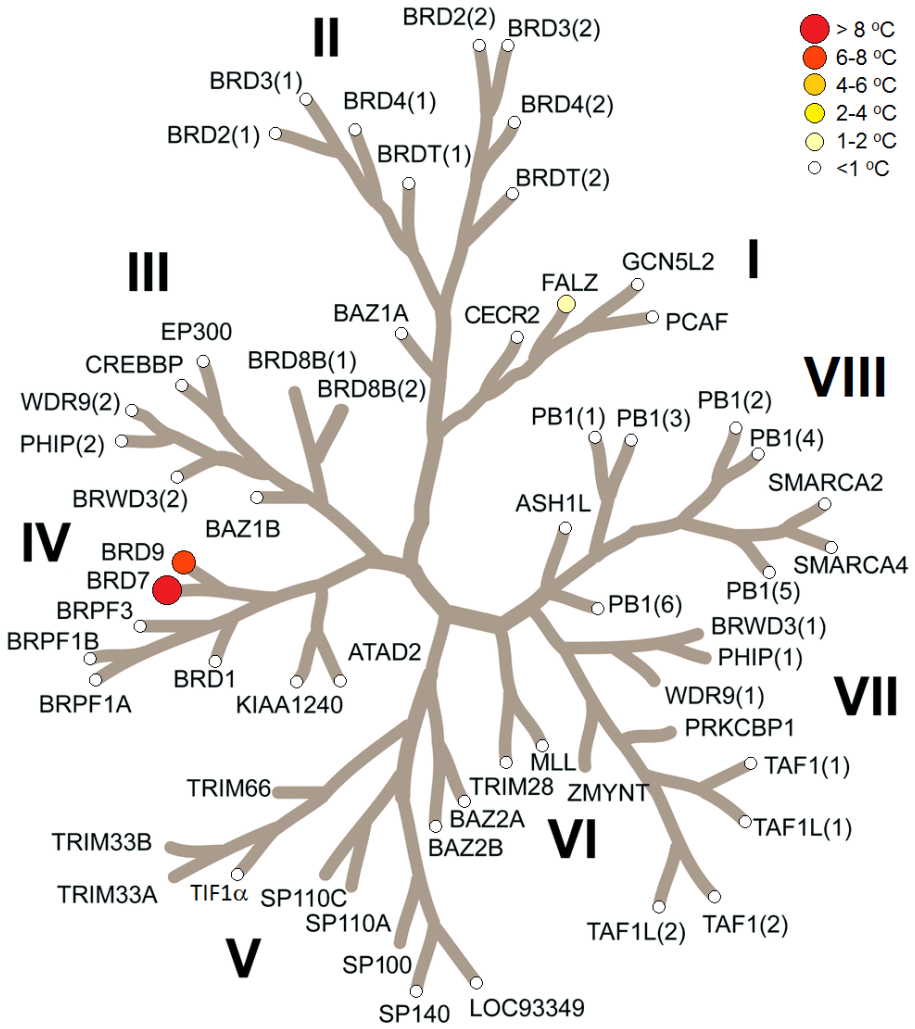

Figure 3.8 DSF assay of LP99 against 49 expressible bromodomains (ΔT_m, °C). Performed by collaborators at the SGC. Reproduced with permission from John Wiley & Sons, Inc.[274]

chromatin via its bromodomain, retarding the mobility of the protein in cells. If the bromodomain is bound by a small molecule ligand, the ability of the protein to diffuse through the cell, visualised through a GFP tag, would be heightened. As part of a FRAP assay [Section 1.3.4], U2OS cells were transfected with an eGFP-BRD9 construct. Upon photo-bleaching, the half-life of recovery of fluorescence was 1.3 s [Figure 3.9]; cells transfected with a N100F mutant that can not bind chromatin demonstrated a faster recovery of 1.1 s, as the mobility of this protein was not hindered by bromodomain binding. Suberoylanilide hydroxamic acid (SAHA), a broad-spectrum histone-deacetylase inhibitor, was added to increase global histone acetylation, increasing the prevalence of binding partners for bromodomains; this acted to increase $t_{1/2}$ for the vehicle control but not the N100F mutant (1.8 s and 1.1 s respectively). Treatment with LP99 showed a dose-dependent effect on FRAP recovery time, with a dose of 0.80 μM simulating that of the N100F mutant, and confirming LP99 inhibited the binding of bromodomains. In comparison to previous assays, this was the first demonstration of LP99

having an effect in cells, and boded well for future discovery.

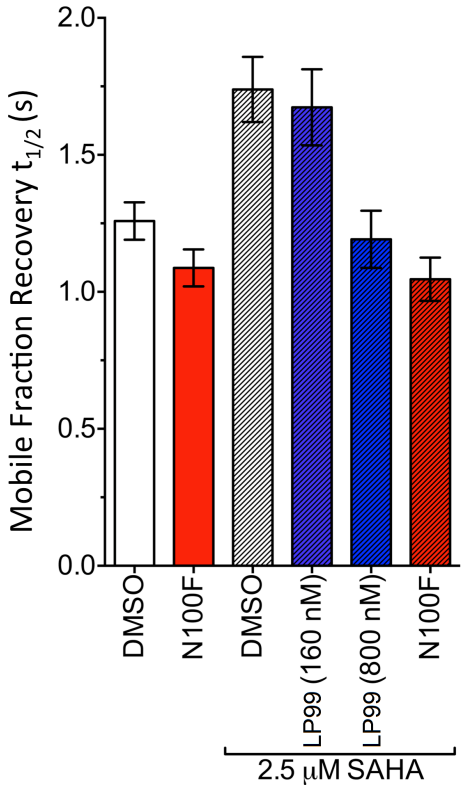

Figure 3.9 FRAP assay of U20S cells transfected with an eGFP-BRD9 construct and treated with LP99. Performed by collaborators at the SGC. Reproduced with permission from John Wiley & Sons, Inc.[274]

Building on the demonstration of cellular target interaction in the FRAP assay, a NanoBRET assay was used to demonstrate direct inhibition of BRD7/9-histone binding. A FRAP assay, whilst easier to perform, has no inherent information confirming the actual binding partner of the transfected protein. A NanoBRET assay [Section 1.3.6], however, confirms the binding partners through specifying both tagged biomolecules. Collaborators at the Promega Corporation expressed BRD7 and BRD9 with nanoluciferase donor tags, and histones H3.3 and H4 with fluorescently labeled HaloTag fusions as acceptors. The observation of BRET, as observed through a high BRET ratio ($\text{fluorescence}_{\text{acceptor}}$: $\text{fluorescence}_{\text{donor}}$), between these particles in the absence of LP99 confirmed they were within 10 nM of each other, and were hence assumed to be binding [Figure 3.10]. LP99 showed a dose-dependent inhibition of BRET, seen through a decrease in the BRET ratio, confirming disruption to the binding of BRD7 and BRD9 to the histones. All combinations of bromodomain and histone constructs showed IC_{50} values in the low μM range [Table 3.12]. Taken together with the FRAP assay, these results demonstrated that LP99 inhibits the cellular binding of BRD7 and BRD9 to histone, a direct demonstration

of biological activity of the probe.

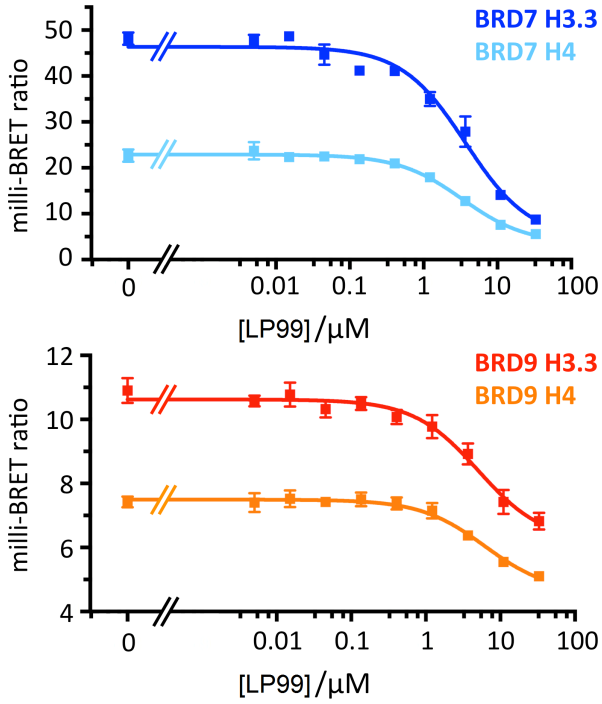

Figure 3.10 NanoBRET assay of HEK293 cells transfected with Nano-Luc-BRD7 and BRD9 proteins and Histone H3.3- and H4-HaloTag fusions and treated with LP99. Performed by collaborators at the Promega Corporation. Reproduced with permission from John Wiley & Sons, Inc.[274]

Table 3.12 Screening data obtained from NanoBRET assay

Bromodomain	**Histone**	**IC_{50} (μM)***
BRD7	H3.3	3.7 ± 0.27 (4)
BRD7	H4	3.3 ± 0.20 (4)
BRD9	H3.3	5.1 ± 0.50 (4)
BRD9	H4	6.2 ± 0.59 (4)

*Mean IC_{50} ± SEM (number of measurements)

Performed by collaborators at the Promega Corporation

Finally, LP99 was demonstrated to not be inherently cytotoxic to cells. For the probe to be of use biologically, it needed to be tolerated by cells without inducing immediate death. HeLa cells were treated with LP99 and cell proliferation was assessed at 24 and 72 hours using WST-1 to measure superoxide dismutase activity as a measure of cell metabolism.[279] For all concentrations less than 33 μM, LP99 was found to be non-toxic to cells [Figure 3.11]. As LP99 was shown to be potent and selective for BRD7/9, with cellular biological activity for which the mode of action was known, and as the compound was not readily cytotoxic to cells, this compound was classed as a probe for BRD7/9, and used to elucidate the biological roles of

these proteins.

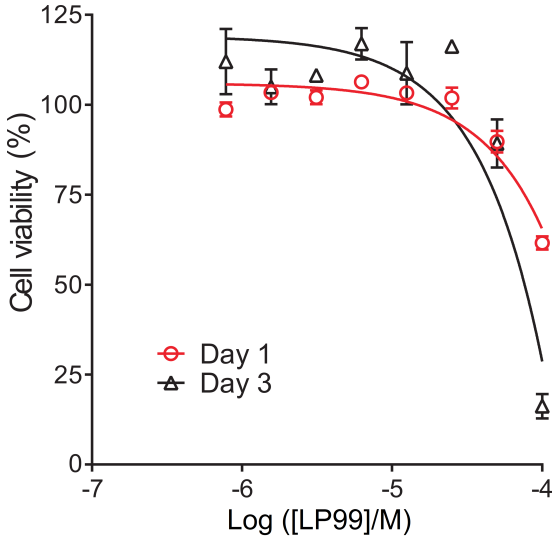

Figure 3.11 Cell viability of HeLa cells after treatment with LP99. Performed by collaborators at the SGC. Reproduced with permission from John Wiley & Sons, Inc.[274]

3.3.2 Biological activity of LP99 and the role of BRD7/9

LP99 was screened against the NCI60 panel to assess any *in vitro* anti-cancer activity. The US National Cancer Institute 60 human tumour cell line anticancer drug screen (NCI60) is a screening panel used to assess the activity of small molecules against human cancers.[280] The effect of small molecules on 60 different cancer cell lines, which encompasses leukemia, non-small cell lung cancer, colon cancer, central nervous system cancer, melanoma, ovarian cancer, renal cancer, prostate cancer and breast cancer tumours, is assessed by the change in growth of the cancer cells. Screening at an initial concentration of 10 μM, growth inhibition of more than 90% would be a significant result, prompting further research. However, when LP99 was screened against the NCI60 panel, no significant growth inhibition was observed for any of the 60 cell lines [Figure 3.12. Full data available in Section 6.2.2]. In the current form, LP99 is not amenable for use as an anti-cancer compound, and suggests targeting of BRD7/9 may be ineffective in treating cancer.

Although ineffective in cancer pathologies, LP99 demonstrated a previously unidentified role of BRD7/9 in inflammatory pathways. At the start of this project, BRD7 and BRD9 had only been implicated in various cancerous states [Sections 1.1.2 & 1.1.3]. As an initial screen

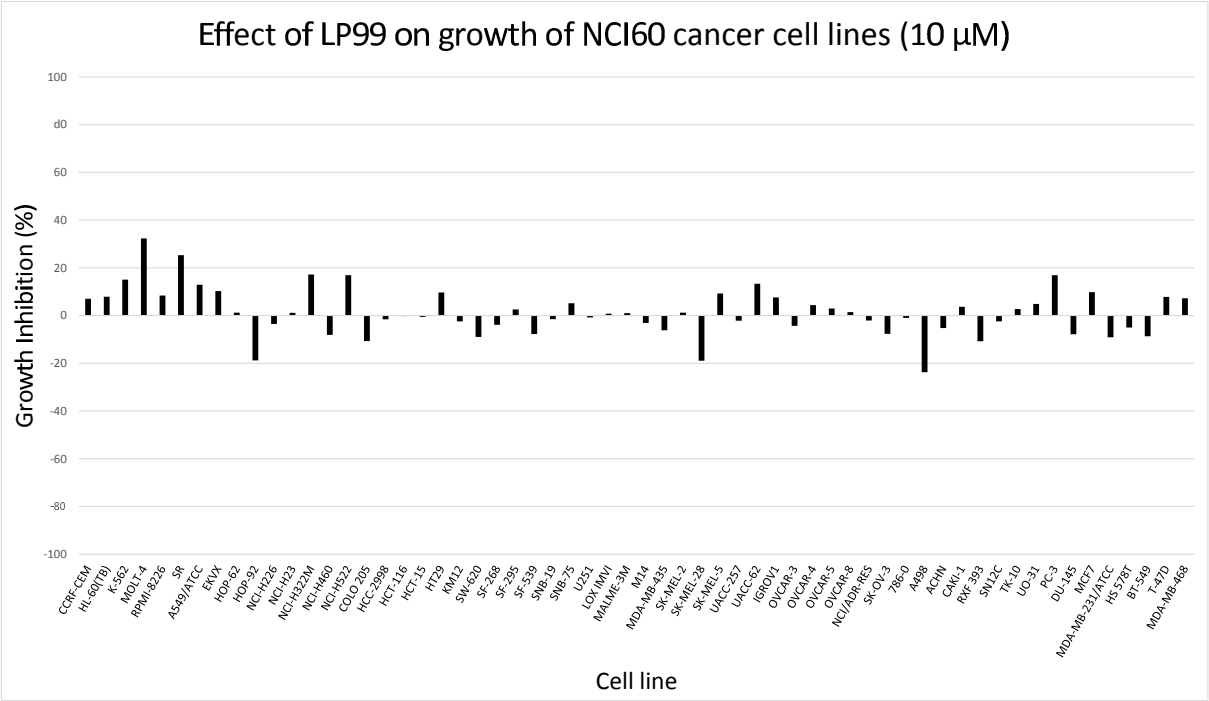

Figure 3.12 Activity of LP99 in NCI60 panel. Assay performed by the National Cancer Institute.

towards assessing other roles of these bromodomain proteins, the effect of LP99 on the secretion of the pro-inflammatory cytokine interleukin 6 (IL-6) from human THP-1 monocytic cells was measured. Stimulation with lipopolysaccharide, an endotoxin that binds cells and induces an immune response, was found to significantly increase IL-6 secretion compared to the vehicle [Figure 3.13]. In a dose-dependent manner, LP99 decreased IL-6 expression, the first evidence that BRD7 and BRD9 are potential targets for anti-inflammatory treatment; this suggests that small molecule BRD7/9 inhibitors may find future use as anti-inflammatory drugs. Although this is the only preliminary research available on the roles of BRD7/9, LP99 has been supplied to over 27 research groups and organisations for biological elucidation. Further understanding of the role of these proteins is greatly anticipated.

3.3.3 Probes reported since completion of work

Soon after the completion of our research, three other BRD9 probes were described. I-BRD9, the product of GSK and the University of Strathclyde, appeared in the chemical literature concurrently with our manuscript [Figure 3.14].[281] The amidine moiety acts as the acetyl lysine mimic, with an IC_{50} of 50 nM against BRD9 as measured by FRET assay, with a reputedly

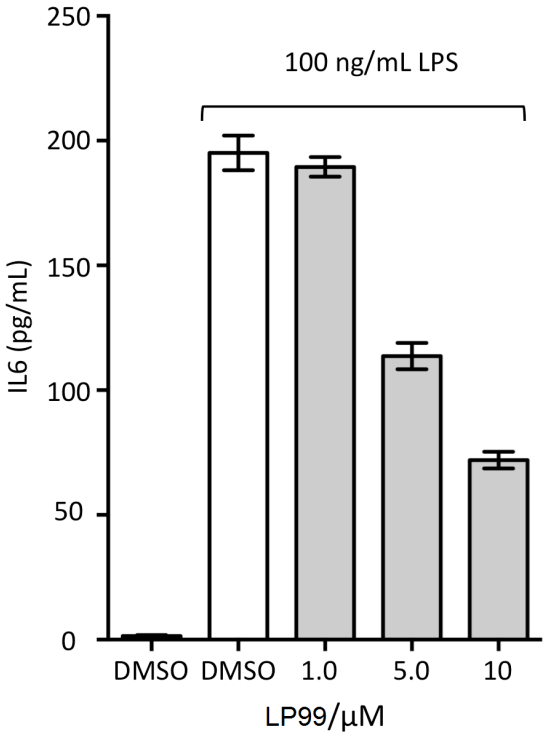

Figure 3.13 IL-6 secretion from human THP-1 monocytic cells stimulated with LPS and treated with LP99. Performed by collaborators at the SGC.

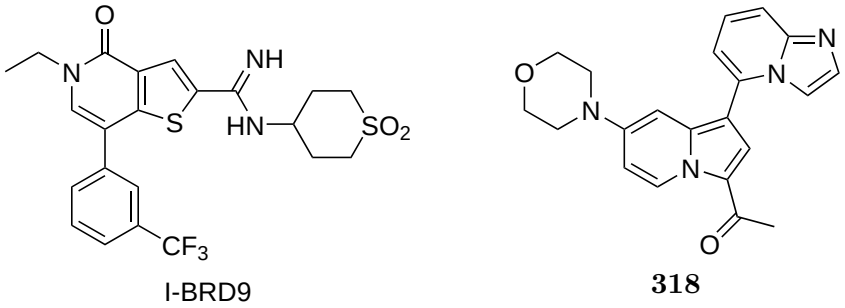

Figure 3.14 Recently reported BRD9 inhibitors.

70-fold selectivity over other bromodomain proteins, including a 200-fold selectivity over BRD7, as assessed by a BROMO*scan* assay. Binding to endogenous BRD9 was confirmed using a Cellzome chemoproteomic competition binding assay, in which cell or tissue lysates are used to measure the competition of the ligand with nonselective sepharose-bound bromodomain inhibitors for native BRD9; this gave an estimate of the IC_{50} as 80 nM. Finally, cellular activity of I-BRD9 was demonstrated through a NanoBRET assay, with a 160 nM affinity measured. To date, this probe has not seen further application in the literature towards understanding the function of BRD9.

Shortly after the appearance of this literature, a BRD7/9 probe from Boehringer Ingelheim,

BI-9564, was added to the SGC list of epigenetic probes. As the research detailing the development of activity of this probe has yet to be published, only limited information is available. The SGC has reported that the probe was the result of a fragment-based screen and optimised by structure-guided design. It is reported to bind BRD9 with a K_D of 14 nM and BRD7 with a K_D of 239 nM as assessed by ITC, with an affinity of >100 μM against other BET family members as assessed by AlphaScreen. Cellular activity has been demonstrated through a FRAP assay, with a cellular IC_{50} of 0.1 μM against BRD9 and 1 μM against BRD7. Off-target activity against CECR2, a bromodomain from subfamily I, has been observed on the isolated protein but this is not observed *in vitro*.

Finally, Hay *et al* presented the newest BRD7/9 probe. Arising from research targeting BAZ2A and BAZ2B bromodomain proteins,[282] a lead against BRD9 was optimised through a structure-based program to yield the acylpyrrole **318**.[283] The ketone moiety acts as an acetyl lysine mimic, with the compound displaying an affinity of 68 nM against BRD9, and a slightly weaker activity of 368 nM against BRD7, as assessed by ITC. This probe was found to be selective for BRD7/9 over other bromodomain proteins, as assessed by DSF, with no other bromodomains showing a ΔT_m shift of greater than 2 °C. Activity was confirmed in cellular FRAP assays, with a dose-dependent decrease in recovery time as a function of **318** concentration. As for I-BRD9, this compound has yet to be used to confirm further biological activity of BRD7/9, but hopefully new research will be published in due course. Use of these probes in an IL-6 assay would be useful to confirm the role of BRD7/9 in inflammatory processes.

3.4 Development of a BRD9 probe with a five-membered ring scaffold

3.4.1 Fragment lead

During previous screening attempts, a lead structure against a malarial bromodomain was identified. As discussed before [Section 1.1.5], only limited information is available regarding the malarial bromodomain proteins, with no ligands yet described to elucidate their role. In the

course of screening compounds made by L. Vieira for selectivity amongst other bromodomain proteins, the five-membered heterocyclic compounds **222** and **319** showed activity against *Plasmodium falciparum* bromodomain protein 3 (*Pf*BDP3), with ΔT_m of 3.1 °C and 2.1 °C respectively [Table 3.13]. An enantioselective synthesis from L-pyroglutamic acid gave (*S*)-**319**, which was found to have a ΔT_m of 3.7 °C. Given the absence of, and need for, inhibitors against malarial bromodomains, these compounds were to be used as leads in the design and synthesis of inhibitors of *Pf*BDP3.

Table 3.13 Compounds synthesised by L. Vieira screened against *Pf*BDP3 by DSF.

Compound		ΔT_m
Structure	#	(°C)
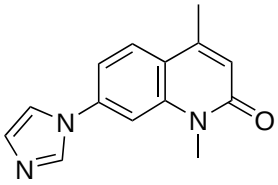	**222**	3.1
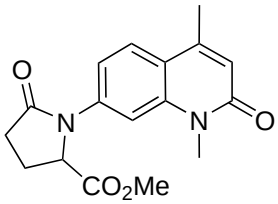	**319**	2.1
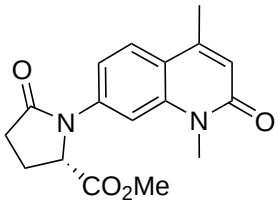	(*S*)-**319**	3.7

All compounds were tested at 10 μM.

Performed by collaborators at the SGC.

3.4.2 Preliminary research by S. Consalvi

Sara Consalvi, a visiting researcher under my supervision from Sapienza – Università di Roma, initially explored further derivatisation of the quinolone without success. Previous exploration of substitution of the C4-methyl group was limited to polar substituents [Table 3.1], despite the hydrophobic nature of the pocket surrounding this group. The nonpolar ethyl-substituted derivative **320** was obtained but showed significantly less affinity than the parent compound **218** against *Pf*BDP3 [Table 3.14]. Taken in conjunction with the poor affinity of the polar derivatives **210**–**215** (-0.6–0.3 °C), it was concluded that steric interactions, rather than

electrostatic effects, govern the tolerance of C4 substituents.

Table 3.14 Quinolone derivatives synthesised by S. Consalvi screened against *Pf*BDP3 by DSF.

Compound		$\Delta\mathbf{T}_m$	**Compound**		$\Delta\mathbf{T}_m$
Structure	#	(°C)	Structure	#	(°C)
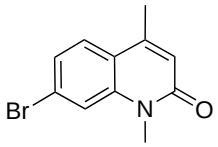	**218**	3.8	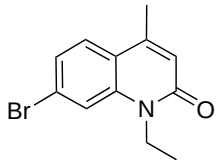	**321**	0.7
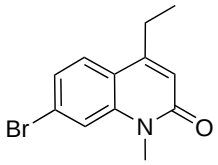	**320**	1.5	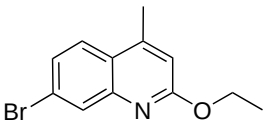	**322**	1.4

All compounds were tested at 10 μM. Performed by collaborators at the SGC.

The *N*-methyl group, which orientates towards the four conserved water molecules of the binding pocket, had not previously been explored. The ethylated species **321**, and the isomeric byproduct **322**, both showed negligible activity against *Pf*BDP3 (0.7 and 1.4 °C) [Table 3.14], potentially as a result of the ligands being unable to replicate the H-bonds lost by displacement of one of the water molecules. Although H-bonding substituents may replace these binding elements, the physical act of displacing the water is also important; although models have demonstrated cosolvent-exchange with these structural water molecules,[284] these ligands are considerably larger, potentially blocking egress of the water from the narrow binding pocket and preventing their displacement. Further, if these water molecules were incorporated during protein folding, displacement would not occur without significant protein unfolding.

In exploring SAR around the γ-lactam scaffold, the optimal substitution from the δ-lactam series (2-phenyl-3-amino) was to be assessed in the first instance. Using research completed by S. Pelletier [Section 1.2.1.2],[131] the nitroalkane **23** was combined with aryl imines (**323**) and benzoic acid to generate nitro-γ-lactams (**324**) in a one-pot procedure [Scheme 3.15]. The PMP-protecting group was removed by oxidation with ceric ammonium nitrate (CAN) to give the nitrolactams **325**.[285] As per the δ-lactam synthesis [Scheme 3.8], the nitro group of **325** was reduced and Boc protected to give **326**, which was then coupled with the bromoquinolone **218** to give 5-membered lactam species for testing (**327**). In addition, the Boc-group could

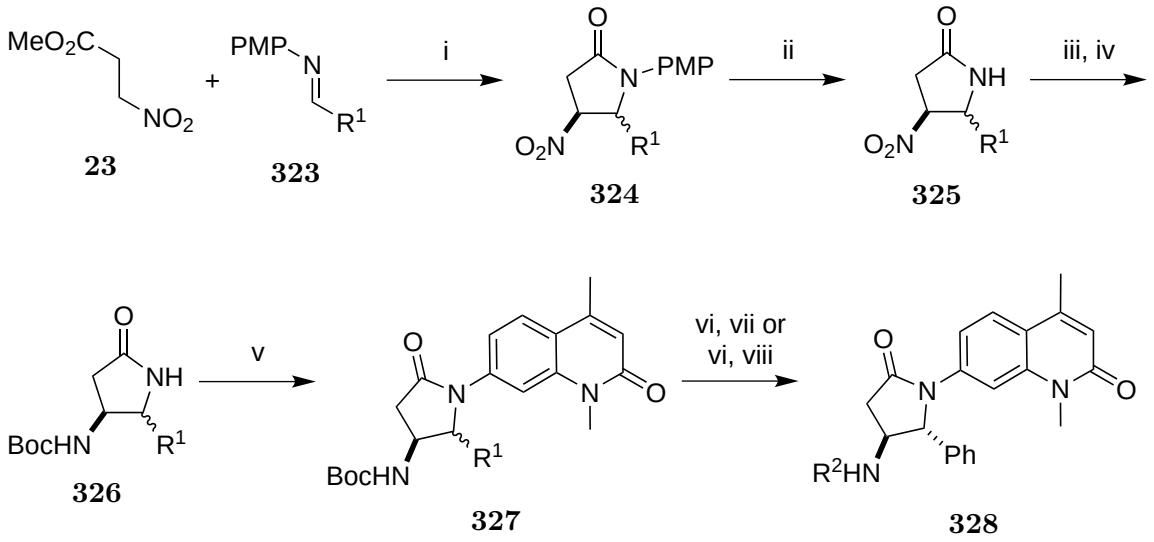

Reagents and Conditions: i. benzoic acid (10 mol%), toluene, 70 °C, 3 d, 40-55%; ii. CAN, MeCN, H_2O, 0 °C, 40 min, 67-73%; iii. $NiCl_2 \cdot 6\,H_2O$, $NaBH_4$, MeOH, 0 °C, 30 min; iv. Boc_2O, rt, 14 h, 67-87% (2 steps); v. **218**, CuI, K_3PO_4, (+/-)-*trans*-1,2-diaminocyclohexane, 1,4-dioxane, 97 °C, 42 h, 67-76%; vi. $HCl_{(1,4\text{–dioxane})}$ rt, 16 h, 96%; vii. R^2Cl, NEt_3, DCM, rt, 16 h, 20-26% or R^3NCO, DCM, rt, 15 h, 18%.

Scheme 3.15 Synthesis of γ-lactam derivatives for testing against *Pf*BDP3.

be removed with HCl and the resulting amine reacted with sulfonyl chlorides, chloroformates and isonitriles to give a range of compounds of the general form **328** for testing against *Pf*BDP3.

These compounds were then screened against *Pf*BDP3 and other bromodomain proteins by DSF assays to assess their affinity. When reviewing the binding of the equivalent *cis*- (**329**) and *trans*-species (**330**) to assess any diastereomeric differences, both were found to have negligible activity against *Pf*BDP3 (-0.7 °C) [Table 3.15]; The parent amine, **331**, tested to assess whether this was due to steric complications, was similarly inactive (-0.1 °C). However, when these compounds were screened by DSF against BRD9, **330** was identified to be a significantly better ligand for this protein than the probe LP99 (8.7 °C vs 6.2 °C). The enantiomers were resolved by preparative HPLC and the (+)-enantiomer was identified as the active enantiomer by DSF (9.7 °C). This affinity was confirmed by ITC, where a K_D of 30 nM was measured, a considerable improvement on LP99. As an aside, given both the (–)-enantiomer of **330** and the *cis*-species **329** showed some degree of binding (2.3 °C and 2.8 °C), this tolerance for less favourable ligands suggested the presence of space around the ligand that could be further exploited for optimisation.

Applying further optimisation from the δ-lactam series was unsuccessful in increasing the

Table 3.15 γ-lactam derivatives synthesised by S. Consalvi screened against *Pf*BDP3 and BRD9 by DSF and ITC.

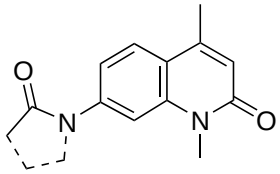

Compound		***Pf*BDP3**	**BRD9**	
Structure	#	ΔT_m (°C)	ΔT_m (°C)*	K_D (nM)
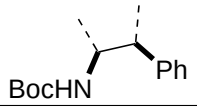	**329**	-0.7	2.8 ± 0.4 (8)	
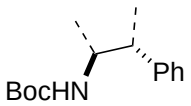	**330**	-0.7	8.7 ± 0.5 (8)	
	(+)-**330**		9.7 ± 0.5 (5)	30
	(–)-**330**		2.3 ± 0.2 (5)	
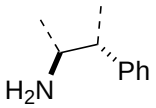	**331**	-0.1	4.4 ± 0.3 (8)	
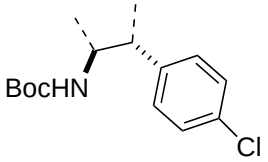	**332**		7.0	
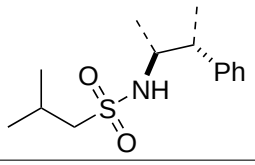	**333**		7.0	
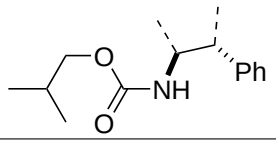	**334**		8.1	
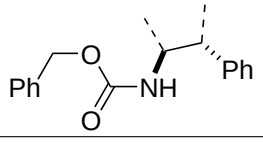	**335**		5.5	
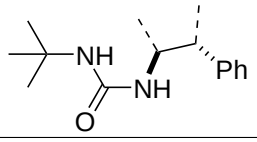	**336**		6.1	

*Where multiple measurements recorded, mean ΔT_m ± SEM (number of measurements) is reported. All compounds were tested at 10 μM by collaborators at the SGC.

affinity of these pyrrolidinone-based ligands. As per LP99, a *para*-chloro group was installed on the C2-phenyl (**332**), however this offered no improvement in binding (ΔT_m 7.0 °C). Exploring derivatisation of the amino group instead with the optimal substituents from the δ-lactam series led to the synthesis and testing of **333**–**336**, which similarly showed no improvement on the initial hit (5.5–8.1 °C). In changing the scaffold, the spatial positioning of the substituents of

the ligand change considerably, due to differences in conformation of the ring and bond angles. Given the gross scale of the changes, the optimisation for one scaffold would likely not match the optimisation for another. An SAR study encompassing a wider range of derivatisations was therefore pursued to identify parts of the lead compound where affinity could be improved.

3.4.3 Aim

The objective for this project was to explore chemical space around the chemical lead **330** towards an intellectual property claim on this motif. To explore further points of optimisation around the scaffold, a significantly broader set of diversifications were to be explored. The DSF assay previously used for screening was to be replaced with a competitive binding assay, which would give more accurate and biologically-relevant data. Having identified the best derivative, the selectivity of the ligand for BRD9 over other expressible bromodomains was also to be assessed by a competitive binding assay. Finally, it was our intention to file an intellectual property application surrounding this scaffold towards the ultimate development of a pharmaceutical.

3.4.4 Synthesis of five-membered ring derivatives

Alternative derivatisation of the exocyclic phenyl ring was first examined. In the synthesis of the lead compound, S. Consalvi used a number of the nitro-Mannich/lactamisation cascades developed by Pelletier *et al* [Section 1.2.1.2]. The shortest route to the desired compounds would involve synthesising the lactam around the C7-aniline equivalent of the quinolone, but S. Consalvi found no reactivity of this substrate in these reactions. Instead, S. Pelletier also developed a form of the reaction that utilised NH_4OAc as the nitrogen source to furnish *N*-unsubstituted lactams that would be compatible with the Goldberg coupling used previously to attach the quinolone [Scheme Scheme 1.4.3]. However, this reaction had only been demonstrated with isobutyraldehyde, and attempts to perform this using furfural to obtain the nitrolactam **337** were unsuccessful [Scheme 3.16.1]. Shifting from a small branched aliphatic chain to a heterocycle is a substantial change in electronics and sterics, so the result was not entirely surprising.

1. Protecting group-free synthesis

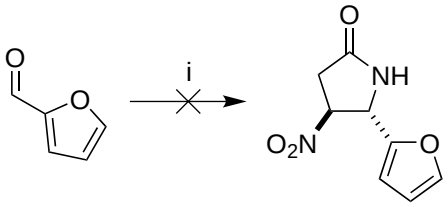

337

---

2. With preformed imine

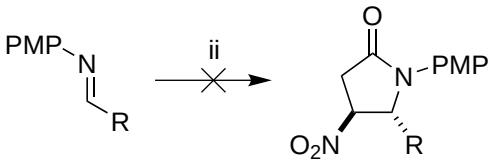

338 R = cyclohexyl
339 R = furyl

---

3. With *in situ* imine formation

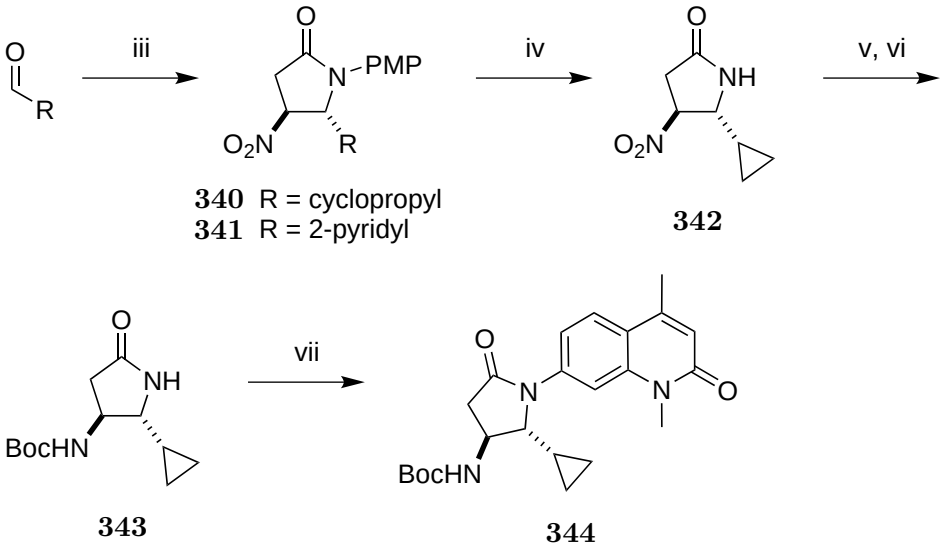

340 R = cyclopropyl
341 R = 2-pyridyl

342

343

344

---

4. *C3*-Alkylation

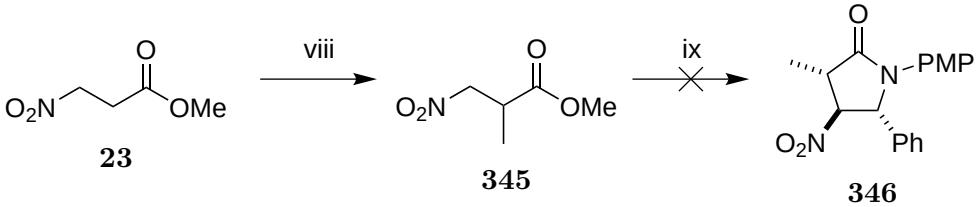

23

345

346

Reagents and Conditions: i. **23**, NH_4OAc, MeOH, 55 °C, 24 h, 0%; ii. **23**, benzoic acid (10 mol%), toluene, 70 °C, 3 d, 0%; iii. **23**, *p*-anisidine, benzoic acid (10 mol%), toluene, 70 °C, 4 d, **340**: 27%, **341**: 16%, **347**: 0%; iv. CAN, MeCN, H_2O, 0 °C, 40 min, 66%; v. $NiCl_2 \cdot 6\,H_2O$, $NaBH_4$, MeOH, 0 °C, 30 min; vi. Boc_2O, rt, 14 h, 87% (2 steps); vii. **218**, CuI, K_3PO_4, (+/-)-*trans*-1,2-diaminocyclohexane, 1,4-dioxane, 97 °C, 42 h, 72%; viii. LDA, MeI, DMPU, rt, 14 h, 23%; ix. *p*-anisidine, benzaldehyde, benzoic acid (10 mol%), toluene, 70 °C, 4 d, 0%.

Scheme 3.16 Nitro-Mannich/lactamisation cascades for the synthesis of γ-lactam derivatives

Methods using a *N*-protecting group were more successful. S. Pelletier also developed reactions using a *N*-PMP group that could be oxidatively cleaved. One such method, as used by S. Consalvi, involved the preformation of the imines [Schemes Scheme 1.4.2, Scheme 3.15]; attempts using the imines derived from cyclohexanecarbaldehyde and furfural were however unsuccessful in yielding **338** or **339**. Instead, trialling a method with *in situ* generation of the imine was more successful [Scheme Scheme 1.4.1], with the cyclopropyl species **340** and the pyridine species **341** both obtained from their respective aldehydes [Scheme 3.16.3]. Removal of the PMP-group with a CAN oxidation successfully yielded the deprotected cyclopropane compound **342**,[285] but not the pyridine derivative. This could be a result of oxidation of the pyridine system by the cerium species, but pyridine may also act as a ligand for cerium, a complexation that would affect isolation of the product and increase the rate of undesired side reactions through tethering of the oxidative species to the substrate.[286] Notwithstanding this, as per the δ-lactam synthesis, the nitro group of **342** was reduced and Boc protected to give **343**, which was then coupled with bromoquinolone **218** to give the cyclopropyl-substituted species **344** for testing.

Derivatisation of the C3 position of the lactam was targeted last. In an extension of her work, S. Pelletier demonstrated that alkyl substituents on the nitroester reagent were tolerated, giving compounds with a high *trans*/*trans* stereochemistry but lower yields [Section 1.2.1.2].[133] Towards this, the nitroalkane **23** was methylated with LDA and MeI to give **345** in low yield, due to formation of the dimethylated species [Scheme 3.16.4]. Trialling **345** under the optimised nitro-Mannich/lactamisation conditions unfortunately yielded none of the desired product **346**. This methyl group would likely add additional conformational strain to both the nitro-Mannich reaction and the cyclisation, which could potentially inhibit the progress of these reactions. Recently, an alternative methodology has been reported that yields compounds of the form **346** through a copper-catalysed conjugate addition/nitro-Mannich/lactamisation cascade.[285] Copper-catalysed conjugate addition of a diorgano zinc reagent to a nitroalkene (**348**) yielded substituted nitronate anions **349** [Scheme 3.17]. These could then readily undergo a nitro-Mannich reaction with PMP-protected imines to give β-nitroamines **350** that can spontaneously cyclise, resulting in the formation of 1,3,5-trisubstituted 4-nitro-pyrrolidin-2-ones **351** in reasonable yields (33–84%) as single diastereomers. Through the use of Cu-chiral ligand complexes, the reaction could be performed enantioselectively, with an ee of 89% demonstrated

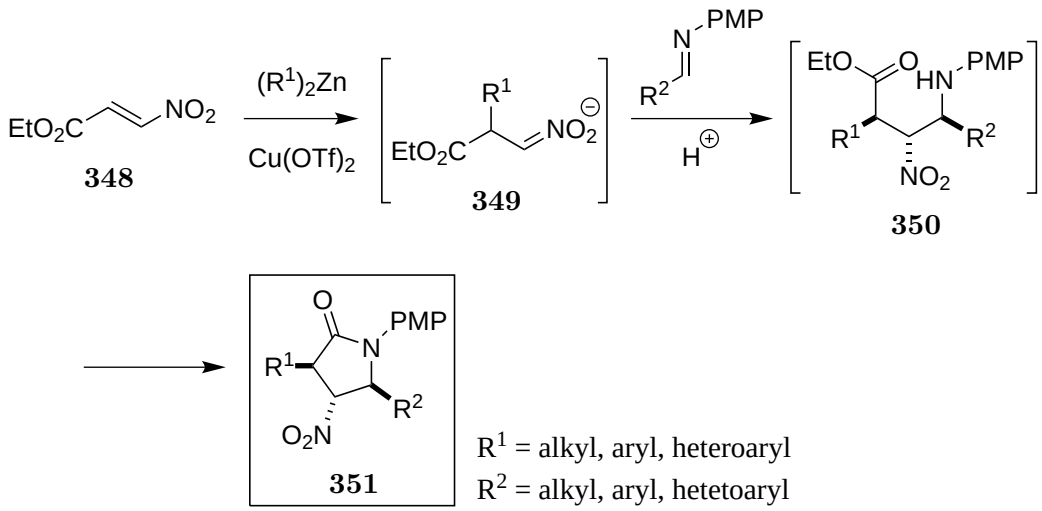

Scheme 3.17 Cu-catalysed conjugate addition/nitro-Mannich/lactamisation cascade.

from one example.

A range of amino-substituents were then synthesised with the aim to optimise H-bonding interactions with the protein. The amino-substituent of the valerolactam series was shown to be H-bonding with the backbone carbonyl of G43, however changing the scaffold would necessarily change the position of this group. Inspection of the crystal structure of BRD9 showed that there was another backbone carbonyl, specificially that of residue H42, to which the NH could hydrogen-bond, either instead of or cooperatively with G43. Towards synthesising derivatives to optimise these interactions, nitrolactam **352** from S. Consalvi was reduced to give an amine that was Boc-protected to yield **353** [Scheme 3.18]. This was then coupled with the bromoquinolone **218** in a Goldberg coupling to give **330**; the Boc group was then removed with HCl to furnish the amine **331** for further derivatisation. Reaction with *iso*-butylchloroformate gave the carbamate **334** and with *tert*-butylisocyanide gave the urea **336**: these compounds, matched to those made by S. Consalvi, were to act as controls to validate the new assay. A range of novel compounds, **354**–**357**, were also obtained through reaction of **331** with an acid chloride, sulfonyl chlorides and a chloroformate. Additionally, to explore the *para*-chlorophenyl series, substrate **332** from S. Consalvi was deprotected to give the amine **358** for derivatisation: reaction with trifluoroacetyl chloride gave **359**; with *iso*-butylchloroformate yielded **360**; and reaction with methyl and *iso*-butyl sulfonyl chlorides gave **361** and **362** respectively. Finally, to further explore chemical space around the amino substituent, **330** was doubly substituted on the amino group with NaH and MeI to give the diamine **363** for testing.

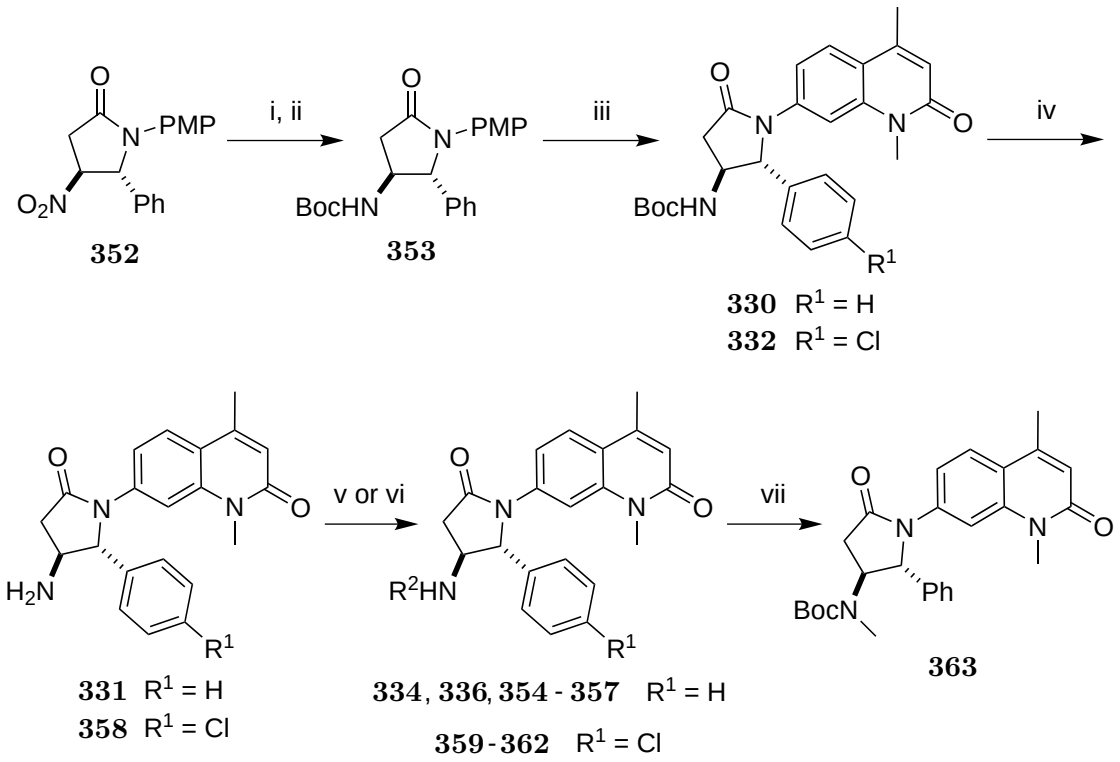

Reagents and Conditions: i. $NiCl_2 \cdot 6\,H_2O$, $NaBH_4$, MeOH, 0 °C, 30 min; ii. Boc_2O, rt, 14 h, 24% (2 steps); iii. **218**, CuI, K_3PO_4, (+/-)-*trans*-1,2-diaminocyclohexane, 1,4-dioxane, 97 °C, 42 h, **330**: 40%; iv. HCl, 1,4-dioxane, 16 h, **331**: 87%, **358**: 85%; v. R^2Cl, NEt_3, DCM, rt, 16 h, 11–91%; vi. *t*BuNCO, DCM, rt, 15 h, **336**: 92%; vii. NaH, MeI, DMF, rt, 2 h, 37%.

Scheme 3.18 Synthesis of γ-lactam *N*-derivatives.

The two amide carbonyls were then targeted in an attempt to modify the strength of the H-bonds. Thiocarbonyls have been found to be less basic than carbonyls with respect to accepting H-bonds;[287] although deliberately weakening the H-bonds would seem counter-intuitive, loosening these constraints may enable the ligand to adopt a slightly different position with better global binding interactions. Generation of the sulfa-analogue building blocks was readily achieved with Lawesson's reagent to yield thiolactam **364** and thioquinolone **365** [Scheme 3.19.1 & Scheme 3.19.2]. These were then coupled in a Goldberg reaction in all combinations to give the thionylated species **366**–**369**. Although **366** was readily obtained from the Goldberg reaction, couplings with the pyrrolidine-2-thione **364** yielded the *S*-linked species **368** and **370** [Scheme 3.19.3]. Copper-catalysed C_{aryl}-S bond forming reactions are prevalent in the literature,[288] although they are less common with these substrates. Given the steric hindrance of the phenyl group to access to the nitrogen atom as opposed to the relatively unhindered exocyclic sulfur, the preference seen here was perhaps not surprising. Synthesis of the dithio derivative **369** was alternatively realised from direct thionylation of **330** using Lawesson's reagent [Scheme 3.19.4].

1. Lactam thionylation

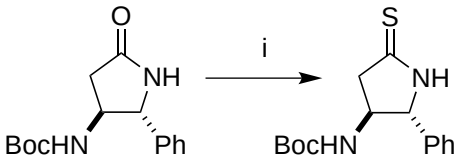

353 **364**

2. Quinolone thionylation

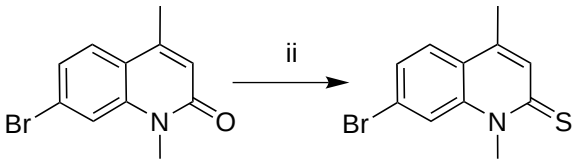

218 **365**

3. Coupling of thiocarbonyl species

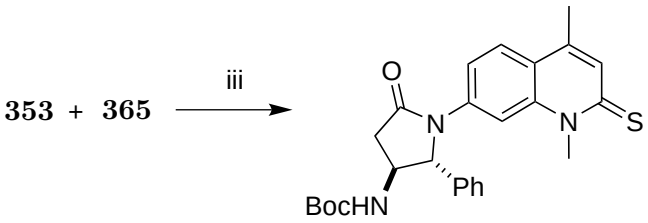

366

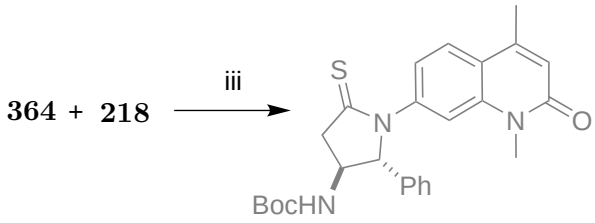

367

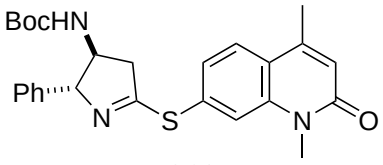

368

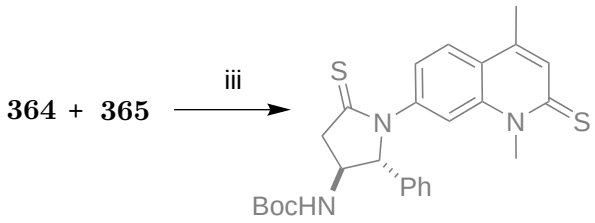

369

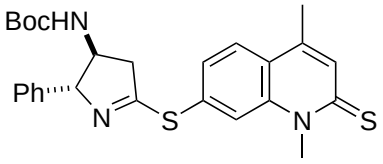

370

4. Direct thionylation

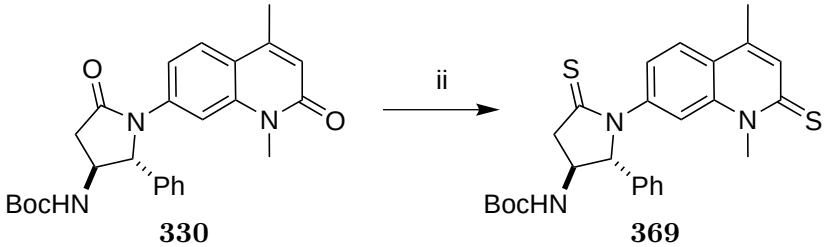

330 **369**

Reagents and Conditions: i. Lawesson's reagent, THF, rt, 4 h, 88%; ii. Lawesson's reagent, toluene, reflux 2 d, **365**: 83%, **369**: 19%; iii. CuI, K_3PO_4, (+/-)-*trans*-1,2-diaminocyclohexane, 1,4-dioxane, 97 °C, 42 h, **366**: 38%, **368**: 17%, **370**: 10%.

Scheme 3.19 Synthesis of thiocarbonyl species.

Finally, the effect of heteroatoms in the 5-membered ring was explored. It was originally desired to make the 2-oxazolidone and 2-imidazolidone equivalents **371** and **372**, with only a CH_2 replaced for the heteroatom to avoid loss of any existing binding elements [Figure 3.15]; however, the lack of direct literature precedent for these compounds encouraged the design of more simple analogues. In the interest of exploring whether the inclusion of these heteroatoms resulted in significant new binding interactions, **373** and **374** were to instead be synthesised with the NHBoc substituent omitted.

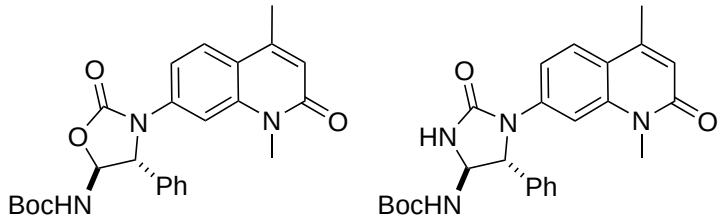

371

372

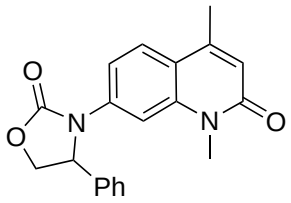

373

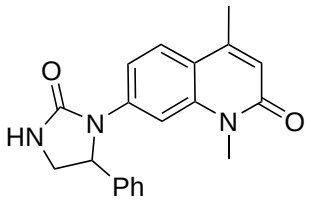

374

Figure 3.15 Ideal and actual heterocyclic derivatives for testing.

Synthesis of the 2-oxazolidone-scaffold was more readily achieved than that of the 2-imidazolidone. 2-Phenylglycinol was reduced with $LiAlH_4$ to an alcohol that could be cyclised with diethylcarbonate to yield **375**;[289] coupling of this with the bromoquinolone **218** gave the desired product **373** directly [Scheme 3.20.1]. Meanwhile, phenylglyoxal was condensed with urea and cyclised under acid catalysis to yield the hydantoin **376**;[290] this was reduced with $LiAlH_4$ to give the cyclic urea **377** for coupling [Scheme 3.20.2].[291] As the coupling reaction could proceed through either nitrogen, a Boc-protection strategy was originally planned: it was expected that the use of a stoichiometric equivalent of Boc_2O would lead to the selective protection of the sterically more accessible N1 position; the N3 position would remain unprotected and hence available for coupling with **218**. Unfortunately, only the diprotected species **378** was observed. Although protection of one nitrogen would be expected to decrease the nucleophilicity of the other through inductive effects, plus the inherent steric hindrance at N3, this preference appeared to be superseded by solubility effects; **377** is highly insoluble, but Boc-protection greatly increased solubility and hence exposure of the N3 nitrogen to the

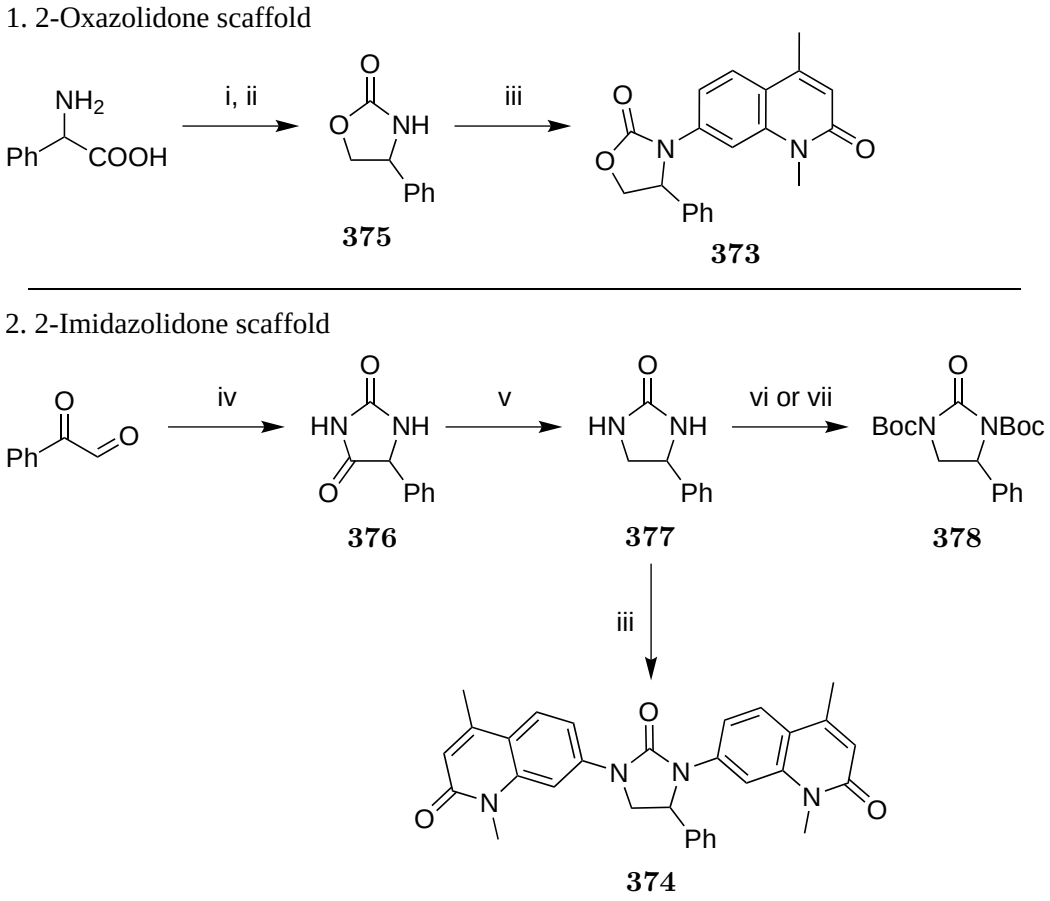

Reagents and Conditions: i. $LiAlH_{4(THF)}$, THF; ii. $(EtO)_2CO$, NaOMe, 40% (2 steps); iii. CuI, K_3PO_4, (+/-)-*trans*-1,2-diaminocyclohexane, 1,4-dioxane, 97 °C, 42 h, **373**: 86%, **374**: 19%, iv. urea, ethylacetoacetate, conc HCl, EtOH, 12%; v. $LiAlH_{4(THF)}$, THF, 92%; vi. Boc_2O, DMAP, THF; vii. NaH, THF then Boc_2O.

Scheme 3.20 Synthesis of species with heterocyclic scaffolds.

remaining Boc_2O. A protection-free coupling was attempted in the hope that, statistically, some of the desired product may be obtained; however, only the dimer **374** was obtained, likely due to similar solubility reasons. Nonetheless, compound **374** was tested to assess any new binding information that could be obtained from this species.

3.4.5 Biological testing of derivatives by BROMO*scan* assay

The compounds obtained were assessed by a BROMO*scan* assay. To give more accurate and biologically-relevant data, a BROMO*scan* competitive binding assay was performed by DiscoveRx Corporation [Section 1.3.3]. Given the significant differences to the DSF assays used previously for screening, **334** and **336** were included as reference samples, alongside a sample of **330** prepared by S. Consalvi. Using this assay, a measure of binding affinity for each compound was obtained in the form of IC_{50} values [Table 3.16. For full data, see Section 6.2.3].

Table 3.16 Screening of five-membered ring species against BRD9 by BROMO*scan* assay.

Compound		IC_{50}	**Compound**		IC_{50}
Structure	#	(nM)	Structure	#	(nM)
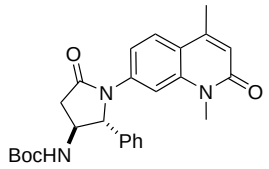	**330**	3400	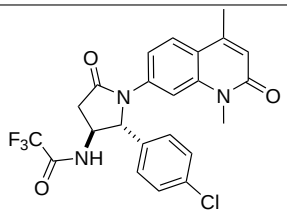	**359**	870
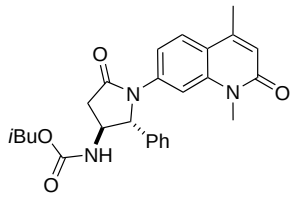	**334**	1200	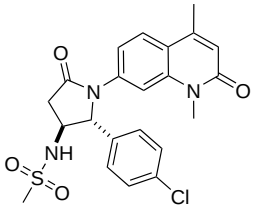	**361**	130
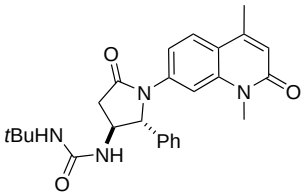	**336**	800	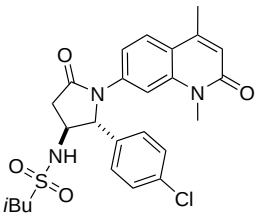	**362**	450
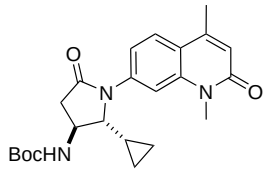	**344**	4500	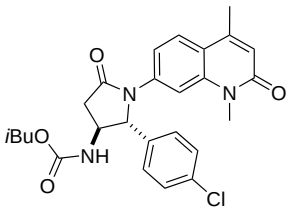	**360**	2400
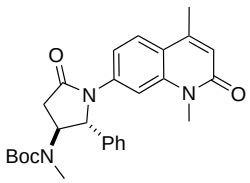	**363**	71000	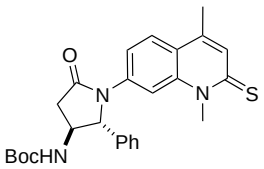	**366**	290
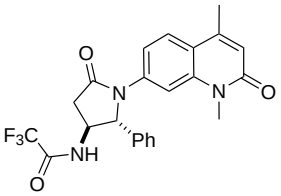	**354**	700	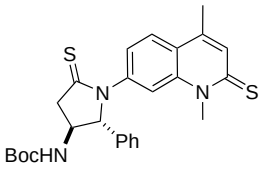	**369**	300
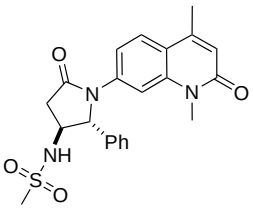	**355**	210	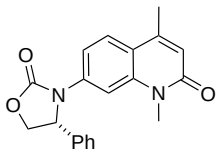	**373**	4900
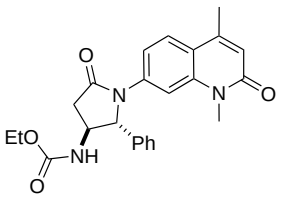	**357**	170	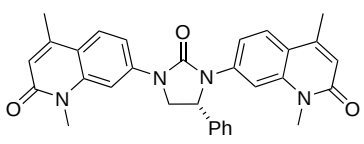	**374**	890

Performed by collaborators at DiscoveRx Corporation.

It is pertinent to note here that at the highest dilutions a number of the compounds displayed solubility issues and precipitated out of solution. Where appropriate, these data points were omitted when fitting curves to the data to allow accurate measures of IC_{50} to be obtained.

Testing of the control compounds against BRD9 highlighted an error with one of them. Of the compounds synthesised by S. Consalvi, a K_D was only determined for **330**, hence this represented the only direct comparison available to equate differences between the assays. The value obtained from this assay, 3.4 μM, was 113x that of the previous ITC assay (30 nM); this increase is far beyond experimental differences and suggested instead that there was a problem with the sample. By DSF, the other controls **334** and **336** have lower affinity than **330** (8.1 and 6.1 °C vs 8.7 °C), however they both have a greater affinity as assessed by the BROMO*scan* assay (1200 and 800 nM respectively), confirming an issue with the sample of **330**. Given the time lapse between the original synthesis by S. Consalvi and the performance of the BROMO*scan* assay, degration of the compound was a distinct possibility. As replacement of the carbonyls with thiocarbonyls should be a subtle effect, from the sulfa-analogues **366** and **369** (IC_{50} 290 nM and 300 nM) it was extrapolated that the actual affinity of **330** for BRD9 in this assay was probably closer to 300 nM; this approximation of thionylation having only a limited effect sees some validation in the small difference in affinity between **366** and **369** (10 nM). Although a direct reference to compounds previously screened against this protein by DSF assay was not available, conclusions could still be drawn from the biologically-relevant data obtained from this assay.

The exact substitution of the ring at the C5 position of the lactam was found to be immaterial, but the nature of the ring was important. *para*-Chlorophenyl substitution was found to have an ambivalent effect on potency when compared to phenyl counterparts: the *para*-chloro substituent was favoured with a methyl sulfonamide group (*para*-Cl **361**: 130 nM, phenyl **355**: 210 nM), disfavoured with an isobutyl carbamate (*para*-Cl **360**: 2400 nM, phenyl **334**: 1200 nM), and no significant preference was seen with a trifluoromethyl amide substituent (*para*-Cl **359**: 870 nM, phenyl **354**: 700 nM). These results showed that, unlike with the δ-lactam series, a *para*-chloro substituent did not benefit from increased binding interactions compared to a simple proton. The nature of the ring, however, was more important, as seen by the cyclopropyl species displaying a significantly lower affinity for BRD9 (**344**: 4500 nM, **330**: $\sim$ 300 nM).

This was likely due to the planar nature of the aromatic ring being more compatible with the flat cavity surrounding this substituent; also, being larger, the phenyl ring would benefit from more hydrophobic interactions with the predominantly non-polar residues in the pocket than the smaller, puckered cyclopropyl substituent. In the absence of forming new strong H-bonds in the pocket, exploring other unsaturated aromatic rings may yield subtle increases in affinity in the future.

As for the δ-lactam series of compounds, N-substitution showed no significant trend amongst functional groups. Within the 2-phenyl series of compounds, carbamates were found to be simultaneously the best (**357**: 170 nM) and the worst (**334**: 1200 nM) compounds. Within the *para*-chloro series, although the two sulfonamides were found to be the strongest binders (**361**: 130 nM, **362**: 450 nM), the small sample size (four compounds) questioned whether this was a significant result. Notwithstanding this, optimisation of the N-substituent revealed a number of ligands with improved affinity, with the methylsulfoxide **361** the best compound identified to date (130 nM). Given the tolerance of the substituents tested, and that both the functional group motif and the pendant group determine the affinity, it can be imagined that a more populous screen of N-substituents may yield further subtle increases in affinity for BRD9.

The most conclusive observation from these results was of the detriment to binding of double N-substitution. **363**, which bears both a methyl and a Boc group on the exocyclic amine, was found to have an IC_{50} of 71 μM, 14 times worse than the next weakest ligand. The H-bond that usually exists between the amino group and a peptide carbonyl can not be formed with this species as the amine can not act as a H-bond donor when doubly substituted. Further, this weak affinity could also have been attributed to steric clashes between the methyl group and the peptide backbone, preventing the ligand adopting the standard binding mode. Synthesis of the equivalent carbonate compound, which would remove H-bond donor functionality without introducing steric issues, would allow the relative importance of these two aspects to be quantified.

Finally, the most intriguing results came from the heteroatom derivatives. Although changing a nonpolar CH_2 group for a more polar O or NR group in a largely hydrophobic pocket would modulate binding, it was expected that loss of the H-bond from the omitted NHBoc substituent

in these compounds would have the most significant effect on affinity. This hypothesis held for the carbamate compound **373**, where the affinity was approximately 16x weaker (4900 nM) than **330**; the dimeric urea species **374**, however, displayed only a 3-fold decrease in binding (890 nM). Due to the ligand being buried in the binding site, this dimeric ligand was not expected to be able to bind two bromodomains simultaneously; instead, the prospect of a novel binding interaction was raised. Although there could be more hydrophobic interactions with the protein from the increased surface area of the ligand, inspection of the binding pocket reveals a flexible histidine residue (H158) that could potentially H-bond with the second quinoline motif, which could account for why, despite the loss of the NHBoc H-bond, this compound still had significant binding. Further study of this potential new interaction should be explored, as, in addition to increasing potency of the ligand, this may offer a solution to selectivity for BRD9 over BRD7 as the latter protein does not contain this histidine residue.

Despite some successes, this project was not pursued further. A number of potent compounds had been identified, chief amongst them **361** (130 nM), **357** (170 nM) and **355** (210 nM), as assessed by a metric that was a direct measure of biological activity. In addition to these advances, a number of areas for future improvement were also identified, with formation of a new H-bond to H158 a potential solution for BRD7/9 selectivity. Unfortunately, given the lack of ligands with affinities below 100 nM from this assay, this work, and the corresponding application for protection of intellectual property, has not been progressed further at this time.

Chapter 4

PCAF

4.1 Project origin

4.1.1 Lead compounds

Researchers from Constellation Pharmaceuticals disclosed structures detailing their progress towards PCAF inhibitors. Their progress was summarised in two general structures, **379** and **380** [Figure 4.1], with the best example of each family having affinities of 50 nM and 10 nM respectively (K_D, ITC). Although the exact structures of these lead compounds were not revealed, a number of structural elements could be assessed. Each family featured a different acetyl lysine mimic – **379** a triazinedione and **380** a phthalazinone – to replicate the H-bond to N803 of acetyl lysine recognition.[292] The significant polarity and steric differences between these bioisosteres suggested that many other acetyl lysine mimics may be tolerated by the binding site. Both families also feature variable-length pendant chains, attached

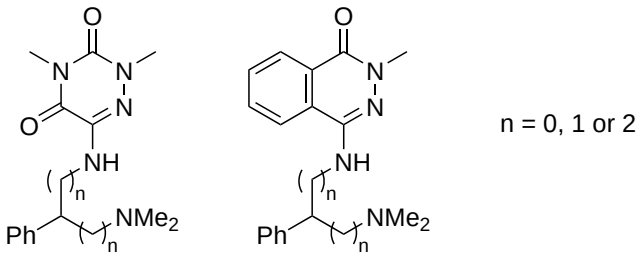

Figure 4.1 Disclosed general structures from Constellation Pharmaceuticals. The exact structure of the lead compounds was not presented.

through a secondary amine, that bear both a phenyl ring and a terminal tertiary amine. The tolerance of the large phenyl substituent and the variable length of the alkyl chain suggested the presence of either a large binding pocket that could accommodate the substituents or that the chain was orientated out of the binding site. In comparison, the presence of the secondary and tertiary amines raised the possibility of H-bonds being formed with the protein. Visualisation of these ligands in the binding site was necessary to confirm these hypotheses.

Computational docking with the protein allowed for some understanding of the binding mode. Collaborators at the SGC docked one of the triazinedione family of compounds, **381** [Figure 4.2], with the X-ray crystal structure of the bromodomain of PCAF [Figure 4.3]. As absolute stereochemistry had been not disclosed, both enantiomers of **381** were docked, with the surprising result that both could potentially bind the bromodomain. Each enantiomer was able to replicate the key bonds of acetyl lysine recognition, with the C3 carbonyl of the triazinedione positioned to H-bond with both N803 and one of the conserved water molecules, which in turn H-bonds to Y760 [Figures 4.3a, 4.3b]. Furthermore, in both enantiomers the nitrogen linking the bioisostere and the pendant chain was found to be in proximity to the residue E756, with which a H-bond could be formed. There were substantial differences in the pendant chain between the two enantiomers, with one enantiomer orientating the tertiary amine into a pocket and the phenyl ring out of the binding site, whilst the other showed the reverse [Figures 4.3c, 4.3d]. In the case of (*R*)-**381**, the phenyl ring closely fitted the pocket whilst the amine was exposed for favourable interactions with the polar solvent. However, in the case of (*S*)-**381**, the tertiary amine had the potential to form a H-bond with one of the H-bond acceptors embedded in the pocket: both the E750 and E756 residues are in close proximity to this amine, in addition to a number of carbonyls of the peptide chain. Synthesis of related ligands could be used to confirm these proposed binding elements.

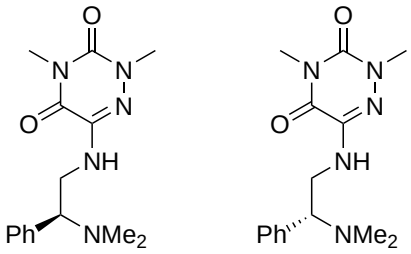

(*S*)-**381** (*R*)-**381**

Figure 4.2 Representative lead compound modeled.

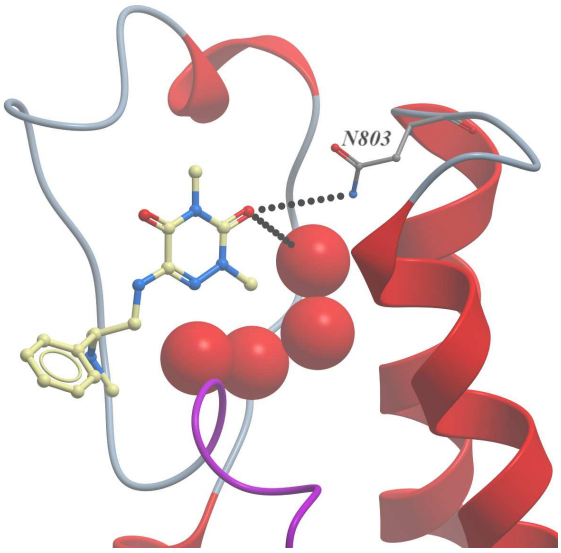

(a) Potential binding mode of (*S*)-**381**

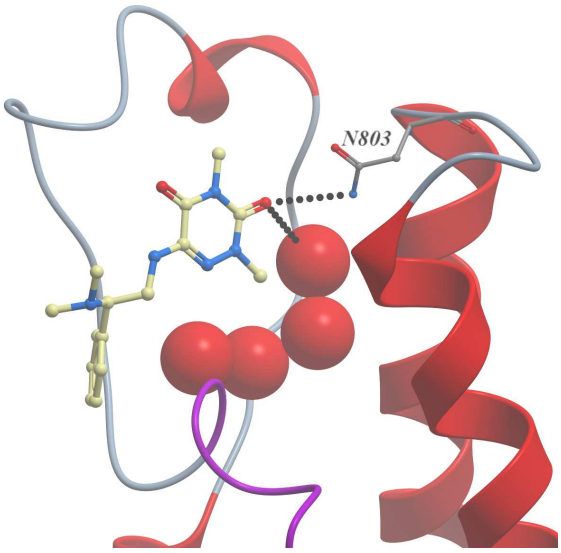

(b) Potential binding mode of (*R*)-**381**

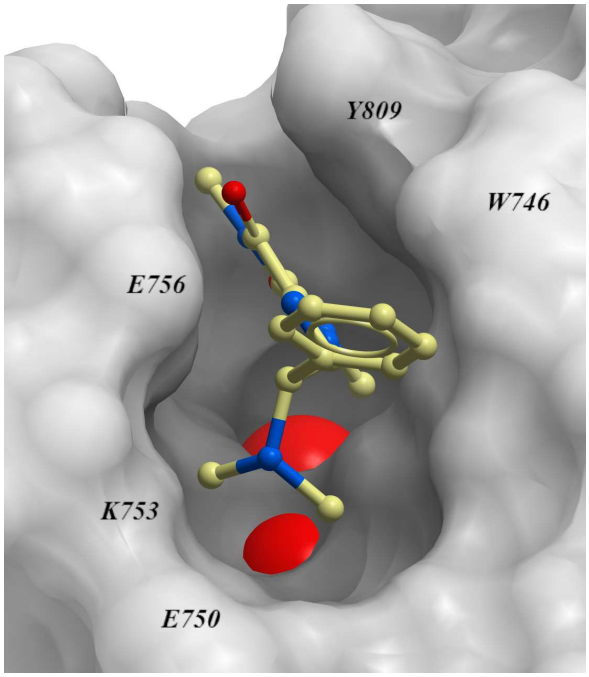

(c) Dimethylamine substituent of (*S*)-**381** occupying pocket

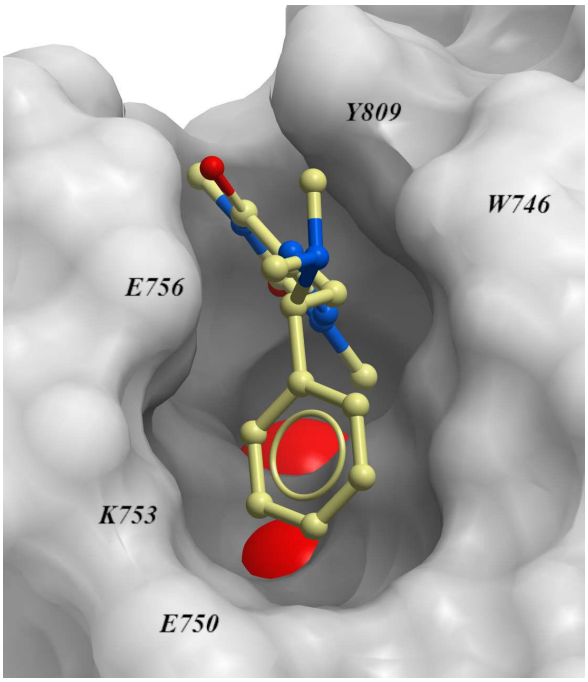

(d) Phenyl substituent of (*R*)-**381** occupying pocket

Figure 4.3 Enantiomers of **381** docked with PCAF, with key potential H-bonds for acetyl lysine recognition (black dots) and water molecules (red spheres). Docking calculations performed with Molsoft ICM by collaborators at the SGC. [PDB ID: 1N72]

4.1.2 Aim

The aim of this research was to confirm key binding elements from the general lead structures **379** and **380** towards a future PCAF probe. This was to be achieved through the synthesis of a series of related compounds for biological validation. Given the tolerance demonstrated by the binding site, three established acetyl lysine bioisosteres were to be explored: [1,2,4]triazolo[4,3-*b*]pyridazines (**382**),[108] [1,2,4]triazolo[4,3-*a*]phthalazines (**383**),[112] and ethyl [1,2,4]triazolo[4,3-*b*]pyridazin-8-yl carbamates (**384**) [Figure 4.4].[112,293] These were to be coupled in all combinations with a range of amines, including 1-phenylethan-1-amine (**385**), N^1,N^1-dimethyl-3-phenylpropane-1,3-diamine (**386**) and N^1,N^1-dimethyl-1-phenylethane-1,2-diamine (**387**), to begin a preliminary exploration of SAR around the pendant chain. In addition to attempting to replicate the activities reported by Constellation Pharmaceuticals, exploration of various acetyl lysine mimics and pendant chains was hoped to provide insight into the binding elements of these ligands; the importance of the terminal tertiary amine, the positioning of the phenyl ring and the effect of chain length were all to be assessed. Through measuring the biological activity of these compounds, SAR would be assessed to guide the future design of a PCAF probe.

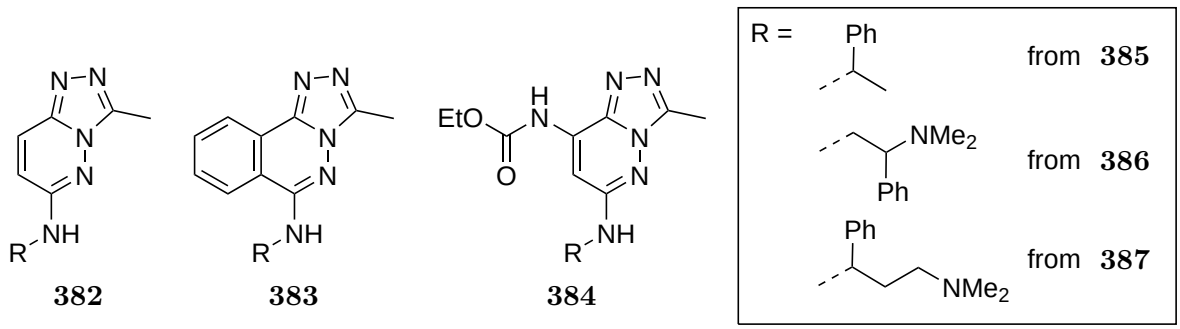

382 **383** **384**

Figure 4.4 Families of compounds targeted against PCAF.

4.2 Synthesis of derivatives against PCAF

In the first instance, synthesis of the pyridazine-based family of compounds (**382**) was attempted. Given the modular nature of the compounds to be made, a general synthetic pathway was

proposed centered around the condensation of the acetyl lysine mimic as an aryl chloride with the amine of the pendant chain [Exemplified in Scheme 4.1]. Related chlorides have been shown to react through both S_NAr mechanisms with nucleophiles and in metal-mediated coupling reactions,[294] allowing many methods to be explored to form the desired linkage. A reported method that detailed heating the amine and chloride in *n*BuOH was trialled,[295] however only the ether **388** was formed [Scheme 4.1]. Avoiding a nucleophilic solvent, the aryl chloride **389** and the simple amine **385** were heated in *N*-methylpyrrolidone (NMP) with NEt_3 as a base to successfully yield **390**. This general method was amenable to a range of amines, with **391** and **392** both readily synthesised for testing from their respective amines. With these compounds attained, similar methods were to be trialled with the remaining series of compounds.

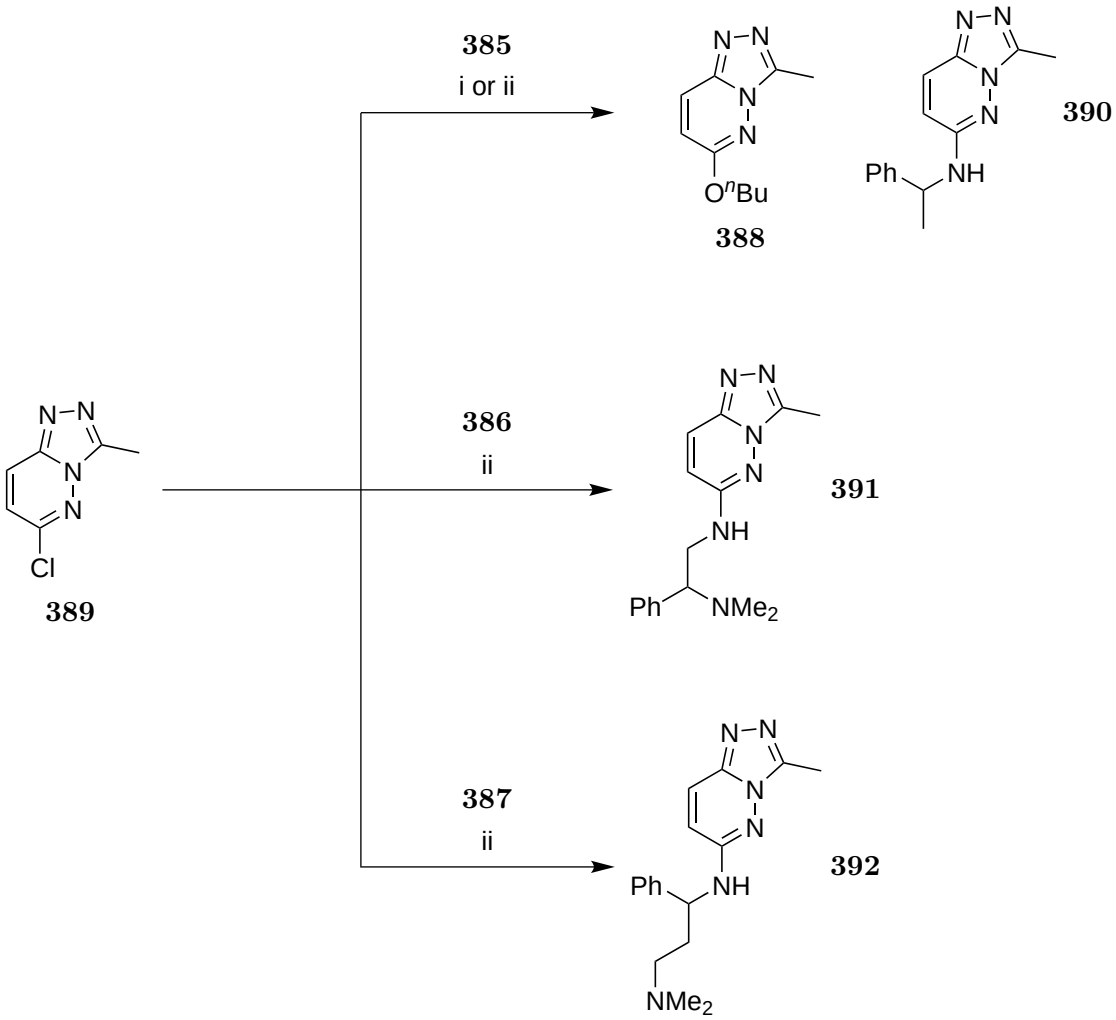

Reagents and Conditions: i. K_2CO_3, *n*BuOH, reflux, 14 h, **388**: 52%, **390**: 0%; ii. NEt_3, NMP, 120 °C, 36 h, **390**: 32%, **392**: 11%, **391**: 33%.

Scheme 4.1 Synthesis of pyridazine-based derivatives.

The synthesis of the phthalazine family of compounds (**383**) proved more problematic. 1,4-Dichlorophthalazine **393** was refluxed with hydrazine and cyclised with acetyl chloride to give the chloride **394** as a starting material for derivatisation with the amines **385**–**387** [Scheme 4.2].[111] Attempting the same NMP/NEt_3 method with **385** as before, however, resulted in no observed formation of **395**. The lower reactivity of **394** may be caused by the phthalazine system both sterically hindering incoming nucleophiles and decreasing the electrophilicity of the carbon to be derivatised through electron donation. Use of a stronger base, NaOH, was similarly unsuccessful;[296] formation of a lithium amide with *n*BuLi, however, readily furnished the desired product **395**. Applying the same method, albeit with an increased loading of lithium amide, allowed **396** to also be obtained. At the same time, alternative methods to this product were also explored: a palladium-coupled method using $Pd(OAc)_2$,

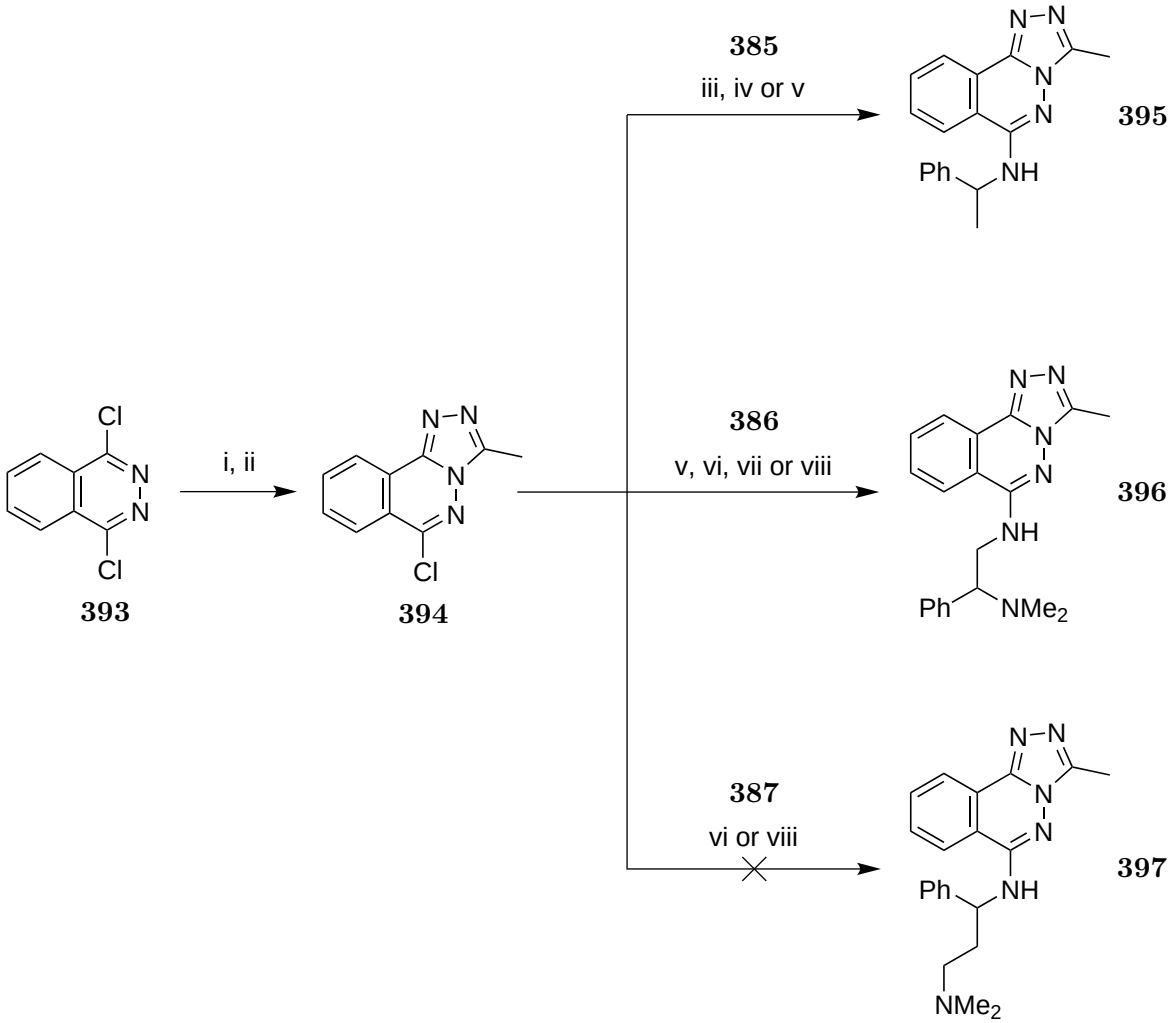

Reagents and Conditions: i. $N_2H_4 \cdot H_2O$, EtOH, reflux, 30 min; ii. AcCl, NEt_3, 1,4-dioxane, 110 °C, 14 h, 64% (2 steps); iii. NEt_3, NMP, 130 °C, 18 h, 0%; iv. NaOH, DMF, 100 °C, 2 h, 0%; v. Amine (1.6 eq), *n*BuLi (1.5 eq), THF, rt, 16 h, **395**: 36%, **396**: 0%; vi. Amine (5 eq), *n*BuLi (4.8 eq), THF, rt, 16 h, **396**: 73%, **397**: 0%, ; vii. $Pd(OAc)_2$, Xantphos, K_2CO_3, 1,4-dioxane, reflux, 16 h, 56%; viii. Amine, KI, HCl, EtOH, 110 °C, 16 h, **396**: 89%, **397**: 0%.

Scheme 4.2 Synthesis of phthalazine-based derivatives.

Xantphos and K_2CO_3 furnished the product in 56% yield;[297] and a method using catalytic KI and HCl, which forms a more reactive aryl iodide *in situ*, gave the product in an 89% yield.[298] To obtain the final compound of the family, **397**, both the *n*BuLi and KI methods with trialled with **386**; however, no reaction was observed. Given the related amine **385** successfully reacted under more mild conditions, steric hindrance of the α-phenyl group was not believed to be at fault; instead, an intramolecular H-bond between the primary and tertiary amines was believed to be formed, acting to decrease the nucleophilicity of the primary amine and preventing the reaction progressing. Use of an additive to disrupt this H-bond may prove beneficial to the synthesis of **397** in the future.

Despite the success with the previous families, none of the pyridazinyl carbamates **384** were obtained pure for testing. Reaction of the aniline **398** with ethyl chloroformate gave the parent chloride **399** for derivatisation [Scheme 4.3]; using catalytic KI and HCl, the highest yielding method for the phthalazines [Scheme 4.2], **400**–**402** were successfully formed; however, an impurity appeared with each of them that could not be removed despite the exploration of many different chromatographic systems. To avoid formation of the impurity in the first case, the other methods used for the phthalazine series were trialled with the amine **385**, but in all cases **400** was isolated as a mixture. The impurity was eventually identified as the aniline **403**, a hydrolysis product resulting from cleavage of the ethyl carbamate group. As the ratio of **403**:**400** increased with handling, the conclusion was drawn that the ethyl carbamate was not stable to the purification conditions – predominantly combinations of MeOH, CH_2Cl_2 and NEt_3 – employed for these highly polar compounds. Future syntheses may be able to minimise this problem through employing a protecting group whilst attaching the pendant chain, before having ethyl carbamate formation as the final step of the synthesis. This notwithstanding, a range of pyridazine-based and phthalazine-based compounds were obtained for testing.

4.3 Biological testing of derivatives against PCAF

All the compounds obtained were screened against PCAF to assess their affinity for the bromodomain. The results obtained from the DSF assay suggested the general affinity of these

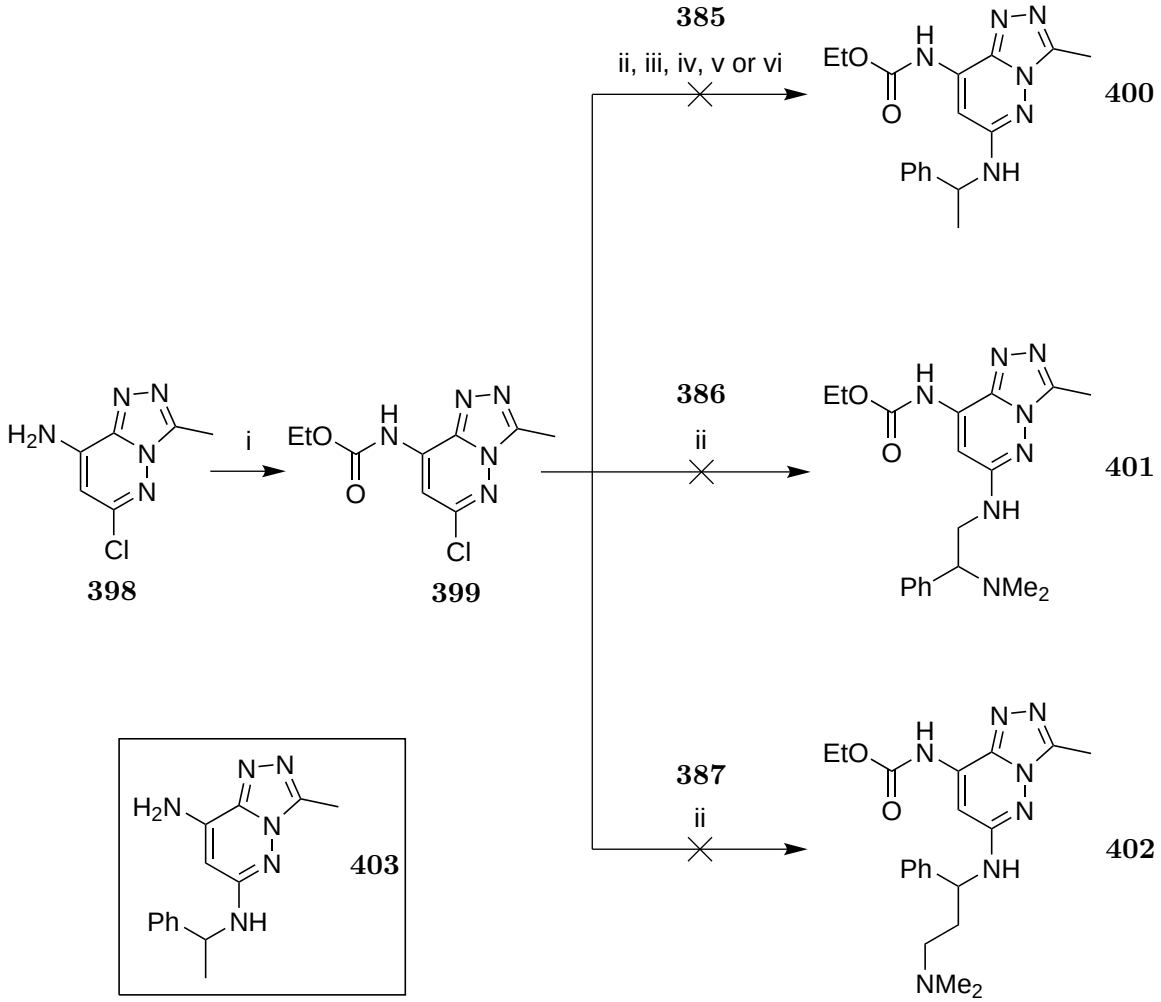

Reagents and Conditions: i. ethylchloroformate, K_2CO_3, toluene, reflux, 2 d, 56%; ii. Amine, KI, HCl, EtOH, 110 °C, 16 h, **400**: 0%, **401**: 0%, **402**: 0%; iii. Amine, NEt_3, NMP, 130 °C, 18 h, 0%; iv. Amine (1.6 eq), *n*BuLi (1.5 eq), THF, rt, 16 h, 0%; v. Amine (5 eq), *n*BuLi (4.8 eq), THF, rt, 16 h, 0%; vi. Amine, $Pd(OAc)_2$, Xantphos, K_2CO_3, 1,4-dioxane, reflux, 16 h, 0%.

Scheme 4.3 Synthesis of pyridazinyl carbamate-based derivatives.

compounds for PCAF was very low [Table 4.1]: no ΔT_m greater than 2 °C was observed. The pyridazines (**388**–**392**) showed a uniform low stabilisation of the protein – no thermal shift greater than 0.1 °C was observed. Because of the low activity of this family of compounds, no conclusions on the effect of the pendant group could be drawn. Although the phthalazine-based derivative **395** showed negligible affinity (0.2 °C), **396** was observed to cause a 1.7 °C thermal shift; this affinity was confirmed through an ITC assay, from which a K_D of 1.0 μM with PCAF was measured.

Despite the paucity of positive results, some conclusions could be drawn about the binding elements necessary for PCAF affinity. **391** and **396** bear the same pendant chain but have significantly different activities (0.1 vs 1.7 °C), with the more active compound having a larger

Table 4.1 Screening of compounds against PCAF by DSF and ITC assays.

Compound Structure	#	$\Delta\mathbf{T}_m$ (°C)	**Compound** Structure	#	$\Delta\mathbf{T}_m$ (°C)	$\boldsymbol{K}_D$ (μM)
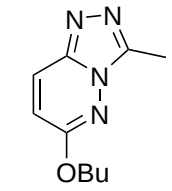	**388**	0.0	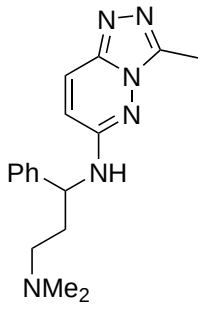	**392**	0.1	
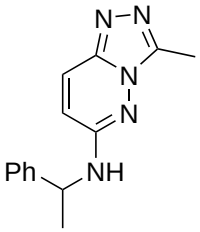	**390**	0.1	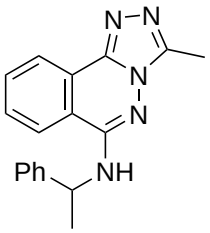	**395**	0.2	
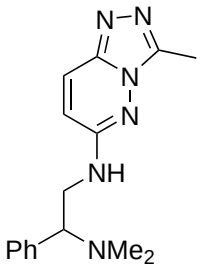	**391**	0.1	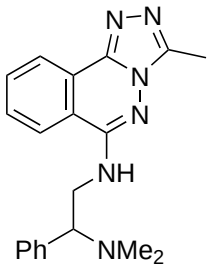	**396**	1.7	1.0

All compounds were tested at 10 μM. Performed by collaborators at the SGC.

aromatic system as part of the acetyl lysine mimic; this significant difference in activities could be reconciled by the possibility that **396** was involved in π-π interactions with the tyrosine residue Y809 in the binding pocket [Figure 4.3]. These two rings systems could adopt an edge-to-face arrangement that would act to increase the enthalpy of **396** binding relative to **391**. Focusing instead on the effect of the pendant chain, the two phthalazine-based compounds **395** and **396** also had considerably different affinities (0.2 vs 1.7 °C). Unfortunately, because the position of the phenyl ring, the length of the chain and the presence of the tertiary amine were changed simultaneously, the binding element, or elements, responsible for this difference could not be identified from these compounds alone.

More compounds need to be tested against PCAF for further conclusions to be drawn. The best compound identified here, **396**, was found to have a K_D of 1.0 μM, significantly weaker

than the disclosed Constellation Pharmaceutical compounds (**379**: 50 nM, **380**: 10 nM). The synthesis and testing of matched compounds to **396** that differ only in the attachment point of the phenyl ring could identify the ideal position for this group; subsequently SAR could be explored around the ring to find the optimal substitution pattern. Also, given the prevalence of H-bond donors and acceptors in the pocket surrounding the tertiary amine, derivatisation of the terminal position with alternative H-bonding groups, especially those able to form multiple H-bonds simultaneously, may prove fruitful in obtaining a probe against the PCAF protein.

4.4 Further research by L. Trulli and M. Moustakim

This research was being progressed by colleagues towards a PCAF probe at the time of writing. Laura Trulli, a visiting researcher under my supervision from Sapienza – Università di Roma, and Moses Moustakim, of the University of Oxford, had begun synthetic work on new families of compounds for testing. Each researcher was pursuing a different acetyl lysine bioisostere: L. Trulli was continuing the work with [1,2,4]triazolo[4,3-*a*]phthalazines, **404** [Figure 4.5]; and M. Moustakim was pursuing the synthesis of ethyl [1,2,4]triazolo[4,3-*b*]pyridazin-8-yl carbamates, **405**. In both cases, a range of *N*-substituents were to be explored to investigate optimisation of the terminal H-bond and the effect of the position and identity of the phenyl ring. Synthetic work was still ongoing, but some preliminary results from L. Trulli had become available.

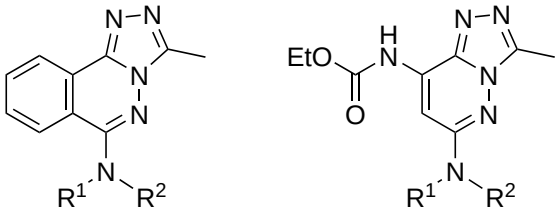

404 **405**

Figure 4.5 Families of compounds to be explored by L. Trulli and M. Moustakim.

A new range of phthalazine-based ligands with different pendant groups allowed some of the binding parameters to be explored further. A range of phthlazine-based compounds, **406**–**411**, synthesised by L. Trulli were assessed by DSF against PCAF [Table 4.2]. The piperazine-bearing compound **406** showed no activity in this assay (ΔT_m -0.5 °C, DSF): although many variables were changed with this compound, it was expected that the loss of H-bond donor capacity at the

Table 4.2 First series of compounds synthesised by L. Trulli screened against PCAF by DSF.

Compound Structure	#	ΔT_m (°C)	Compound Structure	#	ΔT_m (°C)
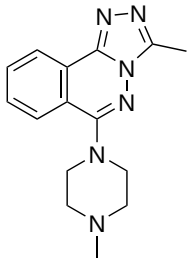	**406**	-0.5	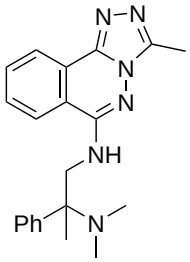	**407**	0.7
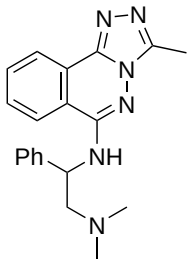	**408**	0.4	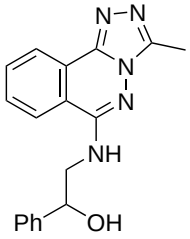	**409**	0.1
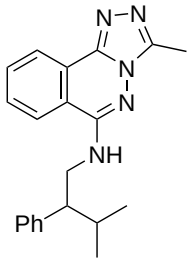	**410**	1.0	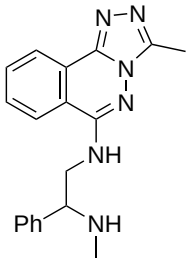	**411**	2.1

All compounds were tested at 10 μM. Performed by collaborators at the SGC.

nitrogen attaching the piperazine to the phthalazine, and the cyclisation-induced conformation, were the most crucial elements. In comparing the related compounds **408** (0.4 °C) and **396** (1.7 °C), it was observed that attachment of the phenyl at the β-position was favoured over the α-position. Similarly, comparing **410**, which lacks the terminal nitrogen and hence the ability to H-bond, with **396** (1.0 °C vs 1.7 °C) highlights the importance of H-bonding with the terminal amine. Introducing a quarternary center, as in **407**, was detrimental to binding (0.7 °C), likely due to steric clashes in the binding site with E756 (Figure 4.3c). However, most importantly, the methyl amine **411** was identified as having the highest affinity for PCAF seen to date, with a ΔT_m of 2.1 °C; this affinity is to be confirmed in due course by an ITC assay. The increased affinity of this compound can be attributed to the ability of this group to both accept and donate H-bonds simultaneously, allowing an additional interaction over **396**. Although the alcohol **409** could be argued to be an even better substituent as it would be capable of forming three H-bonds, the capacity of oxygen and nitrogen to form strong H-bonds are different,

highlighted by the poor affinity of **409** (0.1 °C). An x-ray co-crystal structure is to be obtained to confirm the binding mode, however, these results do provisionally support the hypothesis that optimising the terminal H-bonding group may be the best method to increase the affinity of these compounds against PCAF. Exploration of alternative H-bonding substituents is ongoing.

Chapter 5

Conclusion

BRD4

A probe compound against BRD4(1) was successfully developed. A fragment, **48**, bearing 3,5-dimethylisoxazole as an acetyl lysine mimic had been identified as a lead against BRD4(1), with an IC_{50} of 1.3 μM. Through investigating an alternative scaffold and the SAR around this, the development of a BRD4(1) probe was envisaged. In the first instance, a range of isoindolinone derivatives were synthesised to validate the new scaffold. Compound **60**, an intermediate towards our intended SAR, showed a 100-fold increase in affinity for BRD4(1) over **48**, with an IC_{50} of 13 nM, validating the alternative scaffold used. Another intermediate, the nitromethyl compound **73**, also displayed a high affinity for BRD4(1), with an IC_{50} of 20 nM. Building on these results, chemical methods to derivatise these leads towards the further investigation of SAR were first proven on a model system lacking the 3,5-dimethylisoxazole moiety; subsequent application of these methods to the real compound allowed a range of *C3*- and *N*-substituted derivatives to be obtained. However, it was found that substitution at the C3 position was unfavourable, and that a proton in this position conveyed the greatest affinity. Further, the methyl group already installed on the nitrogen was identified as conveying the greatest affinity from those substituents tested. Resolution of the most potent species identified PNZ5 as a probe against BRD4(1), with a K_D of 5 nM. A co-crystal structure with BRD4(1) showed that, in addition to the isoxazole mimicking the H-bonding of acetyl lysine recognition, new H-bonds were formed between the carbonyl of the isoindolinone and both the network of conserved water molecules in the base of the binding pocket and also a proximal lysine residue, mediated

through another water molecule. The small nature of this probe and the number of strong binding interactions resulted in a high ligand efficiency, ideal for further pharmaceutical development.

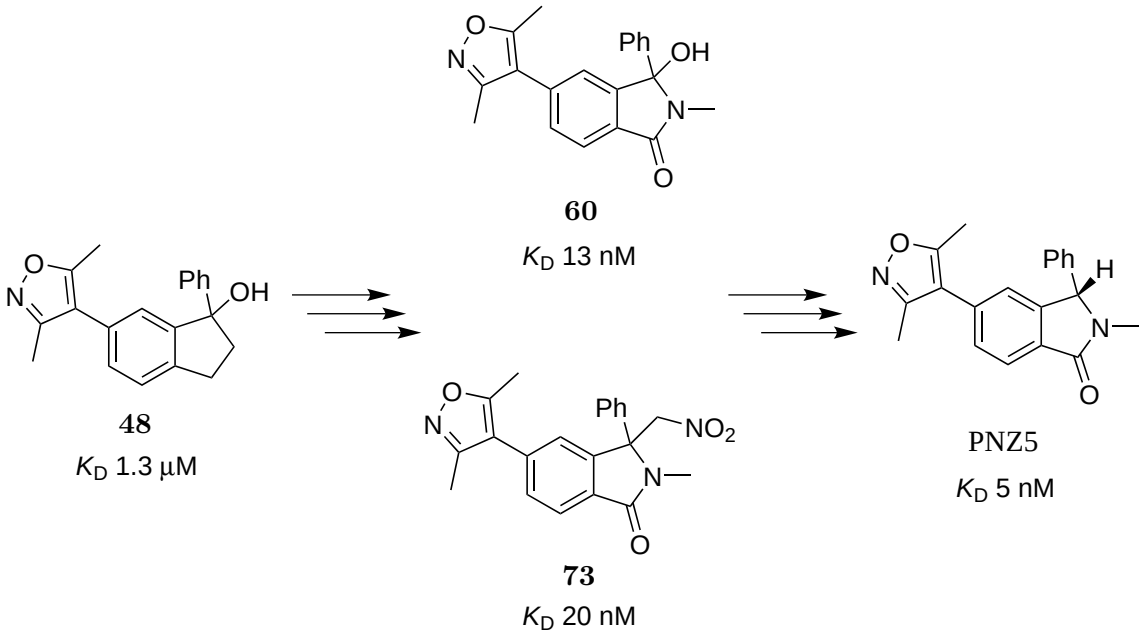

Figure 5.1 Probe development against BRD4(1)

Exploration of asymmetric chemical syntheses had only limited success. An enantioselective nitro-Mannich reaction towards the active enantiomer of **73** was explored using a range of organocatalysts. After optimisation, the reaction could be performed on a model compound with a BINOL-derived phosphoric acid catalyst to give a nitro-Mannich product in 62% ee. Unfortunately, application of these optimised conditions to the real system resulted in no reactivity being observed. In a similar process, an enantioselective Hantzsch reduction with organocatalysts was explored. After extensive optimisation of the reaction on a model system, the reduced product could be obtained in a 90% ee when using a reduced-backbone BINOL-derived phosphoric acid catalyst and a di-*tert*-butyl substituted Hantzsch ester. Applying these conditions to a system bearing the 3,5-dimethylisoxazole, an ee of 79% was obtained. Subsequent *N*-methylation to complete the enriched synthesis of PNZ5 was, however, unsuccessful under the conditions tried. Finally, an alternative synthesis to PNZ5 was explored, starting from a symmetrical molecule that could undergo a desymmetrising directed-*ortho*-acylation to avoid the regioselectivity issues of the existing synthesis. A variety of methods and directing groups were explored, however *ortho*-acylation was not achieved. Eventually, an alternative method appeared in the literature that could be used to successfully form this linkage.

Preliminary biological testing suggested a potential therapeutic application for PNZ5. As there had been significant progress in understanding the role of BRD4 during the completion of this research, PNZ5 was tested directly for therapeutic applications. It was found that PNZ5 had significant cytotoxic activity against a number of gastric cancer cell lines that had proven resistant to many existing therapies. Although these are only preliminary results, PNZ5 may yet show therapeutic application in the treatment of gastric cancer through inhibition of BRD4.

BRD7/9

A probe compound against BRD7/9 was successfully developed. A researcher under my supervision developed (–)-**234** as a lead compound against BRD9, with the active enantiomer displaying a K_D of 493 nM and an apparent absolute stereochemistry of 2*S*,3*R* as assigned by x-ray crystallography. Through exploring SAR around the phenyl ring and the *N*-substituent, development of a probe against BRD9 was envisaged, with use of an enantioenriched synthesis. Using a cinchona-derived bifunctional phase transfer catalyst in a nitro-Mannich reaction, single enantiomer (2*S*,3*R*)-intermediates were obtained. When testing a series of *N*-derivatives, however, these proved to have no affinity for BRD9. Through various means, it was identified that the original stereochemical assignment was erroneous, and that the active enantiomer instead had a 2*R*,3*S* absolute stereochemistry. Pursuing optimisation on racemic material, SAR around the phenyl ring was explored, with a *para*-chloro substituent identified that could potentially increase selectivity. Optimisation of the amino substituent was then performed, and, upon resolution of the enantiomers, LP99 was identified as a high affinity ligand against BRD9, with a K_D of 99 nM. Through the use of a pseudoenantiomeric catalyst to that used

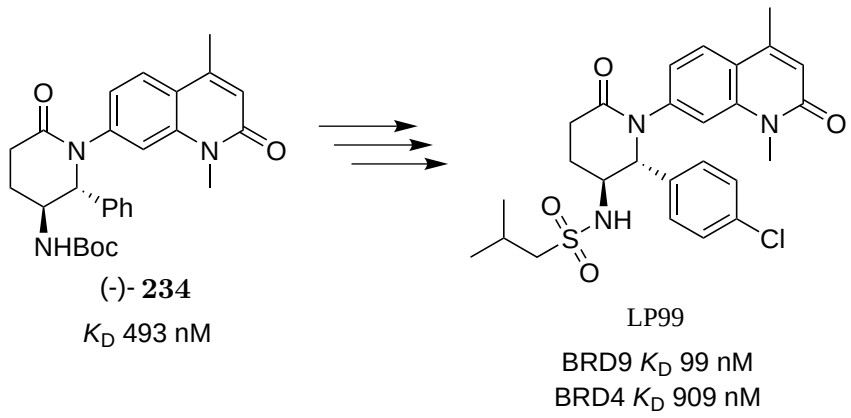

Figure 5.2 Probe development against BRD9

previously, an enantioenriched synthesis of LP99 was achieved in 90% ee.

LP99 was used in the elucidation of the biochemical role of BRD7/9. When assessing the selectivity of this compound, an affinity of 909 nM was measured against BRD7, prompting LP99 to be reported as the first dual BRD7/9 probe. Beyond this, LP99 proved to be highly selective for BRD7/9 amongst all expressible bromodomain proteins. Through a number of assays, cellular inhibition of BRD7/9 binding to chromatin by LP99 was observed. Although only limited activity against a panel of cancer cell lines was evidenced, LP99 was observed to inhibit the secretion of inflammatory cytokines, identifying a previously unknown role of BRD7/9 in the regulation of inflammatory processes.

An improved probe against BRD9 was explored through a related scaffold. A second researcher under my supervision, whilst developing compounds against malarial bromodomains, identified (+)-**330** as having significant activity against BRD9, with the active enantiomer displaying a K_{D} of 30 nM. It was envisaged that exploring SAR around many points of the molecule, including optimisation of the phenyl and amino substituents, replacement of the carbonyls with thiocarbonyls, and investigating alternative heterocyclic scaffolds, may yield compounds with increased affinity. A family of molecules were synthesised and tested against BRD9 using an alternative BROMO*scan* assay. The affinity of (+)-**330** in this assay showed a greatly decreased affinity, IC_{50} of 3.4 μM, however this was believed to be largely due to problems with the original sample. Although there were many promising observations, including the potential benefit of using an imidazolidinone scaffold, **361** was identified as having the highest affinity for BRD9, with an IC_{50} of 130 nM as assessed by a BROMO*scan* assay.

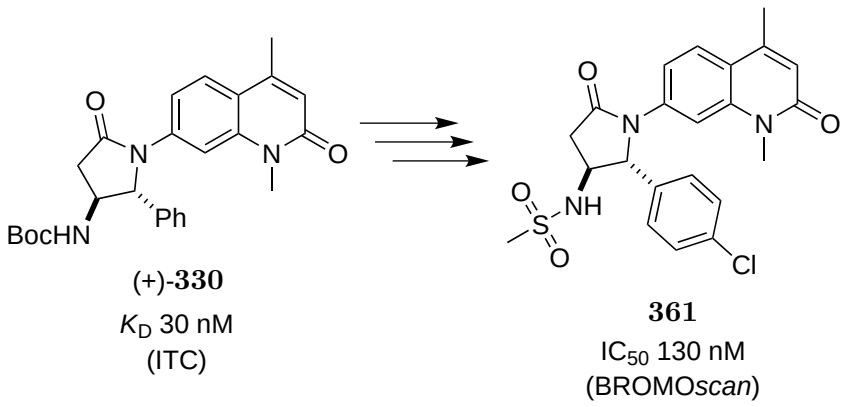

Figure 5.3 Alternative probe development against BRD9

PCAF

Disclosed structures of lead compounds against PCAF were investigated towards the future development of a PCAF probe. Ligands of the general form **379** and **380** were disclosed by researchers at Constellation Pharmaceuticals as lead structures against PCAF, with the best ligand in each series having a K_D of 50 nM and 10 nM respectively. A range of compounds bearing different acetyl lysine mimics and pendant amine chains were targeted to validate these structures. Although synthesis of a range of pyridazine- and phthalazine-based derivatives was largely successful, a family of pyridazinyl carbamates was not realised due to stability issues. Screening of the compounds against PCAF revealed the pyridazine-based compounds to be inactive, however the phthalazine-based ligand **396** demonstrated a K_D of 1 μM against PCAF. Although this was significantly weaker than those disclosed, a number of key binding elements have potentially been identified, including π-π-stacking of the phthalazine acetyl lysine mimic with a neighbouring tyrosine residue, in addition to potential H-bonds between the secondary amine and a glutamic acid and between the tertiary amine and one of the numerous H-bonding groups in the surrounding pocket. Research is ongoing to progress **396** into a PCAF probe, however preliminary results have been used to confirm a number of binding elements.

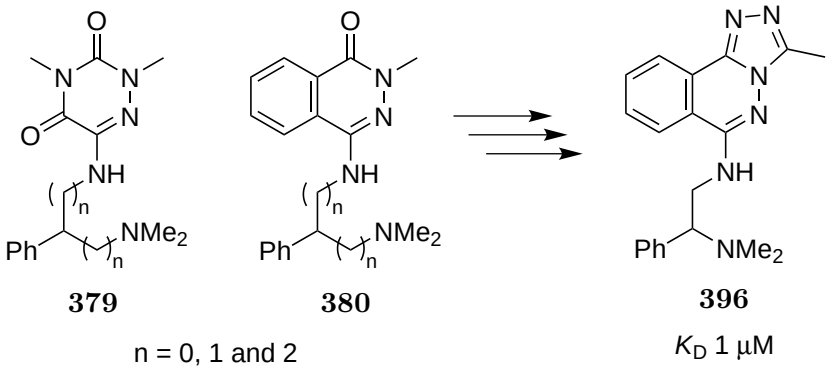

Figure 5.4 Probe development against PCAF

Summary

A number of novel bromodomain ligands have been developed and used to discover previously unknown activity of the bromodomain proteins targeted. Through the use of structure-based drug design programs, biophysical assays and appropriate chemical methods, new probes have

been developed against the bromodomain proteins BRD4, BRD7 and BRD9, in addition to a lead compound against PCAF, proteins for which no selective probes had been reported at the outset of this research. Although knowledge of the role of BRD4 has been assessed through genetic experiments and through the use of existing pan-BET inhibitors, PNZ5 was able to demonstrate a potential therapy for gastric cancer through modulation of BRD4. LP99, the first reported probe for BRD7/9, was developed and demonstrated that inhibition of the bromodomain of these proteins could result in their dissociation from chromatin in cells. Further, LP99 was used to illustrate a role of BRD7 and BRD9 in inflammatory processes, as evidenced through bromodomain inhibition modulating cytokine expression, identifying a new target for anti-inflammatory therapies. Finally, progress was made towards a potent ligand for the PCAF protein. Although much is already known about the activity of this protein, selective probes of PCAF may find use in treatment of one or more of the many pathologies with which it is associated.

Chapter 6

Appendixes

6.1 Supplementary chemical data

6.1.1 Optimisation of nitro-Mannich reaction towards 2*R*-enriched material.

Table 6.1 Optimisation of nitro-Mannich reaction towards 2*R*-enriched material

	Scale		**Base**		**Conversion (%)**				**ee**$_{\text{diastereomer}}$ (%)		**epimeric excess**$_{C2}$[‡]
Substrate	(mmol)	**Catalyst**	Species	eq	**301**	**302**	**303**	**d.r.**[†]	*trans*	*cis*	(%)
300	0.06	**304**	KOH	5	74	22	4	1:3	0	0	0
300	0.06	**305**	KOH	5	88	9	3	1:3	-8	-2	-4
300	0.06	**306**	KOH	5	81	13	6	1:1	-3	4	1
300	0.06	**307**	KOH	5	87	10	3	1:1	6	3	4
300	0.06	**308**	KOH	5	72	25	3	1:1	5	15	10
300	0.06	**309**	KOH	5	91	9	0	1:2	2	4	3
300	0.06	**299**	KOH	5	76	14	10	3:1	90	83	88
300	0.06	**299**	KOH	1.5	78	20	2	7:1	90	74	88
300	0.06	**299**	Cs_2CO_3	5	98	1	1	5:1	87	58	82
300	0.06	**299**	Cs_2CO_3	1.5	99	1	0	4:1	86	62	81
300	0.06	**299**	K_2HPO_4	5	47	42	11	12:1	89	61	87
300	0.06	**299**	K_2HPO_4	1.5	84	8	8	11:1	88	58	86
300	0.06	**299**	KF	5	72	18	10	13:1	88	58	86
300	0.06	**299**	KF	1.5	81	11	8	12:1	83	33	79
300	0.06	**299**	K_2CO_3	5	88	4	8	5:1	91	78	89
300	0.06	**299**	K_2CO_3	1.5	90	3	7	10:1	90	67	88
300	15.9	**299**	K_2CO_3	5	80	9	11	7:1	84	80	84
310	0.06	**311**			39	53	8	2:1	59	52	57
310	0.06	**312**			52	39	9	2:1	65	58	63
310	0.06	**313**			80	10	9	2:1	-63	-57	-61
310	0.06	**314**			61	31	8	2:1	-76	-67	-73
310	0.06	**315**			43	46	10	1:1	-62	-41	-54
310	0.06	**316**			90	3	7	5:1	-62	-58	-61
310	0.08	**317**			66	31	4	4:1	86	72	83
310	0.40	**299**	K_2CO_3	1	42	51	7	4:1	89	80	87
310	0.40	**299**	K_2CO_3	0.25	39	53	8	8:1	92	90	92
310	0.40	**299**	K_2CO_3	0.1	47	45	8	5:1	91	90	91
310	3.00	**299**	K_2CO_3	0.25	83	5	12	7:1	90	90	90

[†] *trans*:*cis*; [‡] ee for each diastereomer scaled by dr to give relative composition of the four enantiomers, from which the excess of 2*R* over 2*S* can be calculated.

6.2 Supplementary biological data

6.2.1 Selectivity screen of LP99

Table 6.2 Screening of LP99 against expressable bromodomain proteins by DSF

#	ΔT_m (°C)*	#	ΔT_m (°C)*
ASH1L	-0.4 ± 0.3 (3)	EP300	-0.3 ± 0.2 (3)
ATAD2	-0.4 ± 0.3 (3)	FALZ	1.0 ± 0.4 (3)
BAZ1A	-0.9 ± 0.5 (3)	GCN5L2	-0.5 ± 0.1 (3)
BAZ1B	-0.7 ± 0.1 (3)	KIAA1240	0.3 ± 0.0 (3)
BAZ2A	-0.6 ± 0.1 (3)	LOC93349	0.7 ± 0.1 (3)
BAZ2B	-0.1 ± 0.0 (3)	MLL	0.5 ± 0.1 (3)
BRD1	-0.1 ± 0.1 (3)	PB1(1)	-0.4 ± 0.1 (3)
BRD2(1)	-0.2 ± 0.3 (3)	PB1(2)	0.0 ± 0.1 (3)
BRD2(2)	-0.2 ± 0.0 (3)	PB1(3)	0.6 ± 0.1 (3)
BRD3(1)	-0.1 ± 0.1 (3)	PB1(4)	0.1 ± 0.1 (3)
BRD3(2)	-0.3 ± 0.0 (3)	PB1(5)	-0.1 ± 0.1 (3)
BRD4(1)	0.0 ± 0.1 (3)	PB1(6)	0.0 ± 0.1 (3)
BRD4(2)	-0.2 ± 0.1 (3)	PCAF	-0.2 ± 0.1 (3)
BRD7(1)	9.9 ± 0.1 (3)	PHIP(2)	-1.0 ± 0.3 (3)
BRD7(2)	9.9 ± 0.6 (3)	SMARCA2	0.3 ± 0.1 (3)
BRD9(1)	6.8 ± 0.6 (4)	SMARCA4	0.2 ± 0.0 (3)
BRD9(2)	6.5 ± 0.1 (3)	SP140	0.3 ± 0.1 (3)
BRDT(1)	-0.2 ± 0.1 (3)	TAF1(1)	0.2 ± 0.0 (3)
BRDT(2)	0.0 ± 0.1 (3)	TAF1(2)	0.8 ± 0.2 (3)
BRPF1A	-0.4 ± 0.2 (3)	TAF1L(1)	0.2 ± 0.0 (3)
BRPF1B	-0.2 ± 0.1 (3)	TAF1L(2)	0.0 ± 0.1 (3)
BRPF3	-0.2 ± 0.1 (3)	TIF1α	0.0 ± 0.1 (6)
BRWD3(2)	-0.2 ± 0.5 (3)	TRIM28	-0.3 ± 0.3 (3)
CECR2	0.1 ± 0.1 (6)	WDR9(2)	-0.8 ± 0.2 (3)
CREBBP	-0.5 ± 0.1 (3)		

*Mean ΔT_m ± SEM (number of measurements). All compounds were tested at 10 μM. Performed by collaborators at the SGC.

6.2.2 Activity of LP99 in NCI60 panel. Assay performed by the National Cancer Institute.

Table 6.3 Activity of LP99 in NCI60 panel against human cancer cell lines at 10 μM concentration.

Type of cancer	Cell line	Δ Growth (%)
Leukemia	CCRF-CEM	6.99
	HL-60(TB)	7.90
	K-562	15.05
	MOLT-4	32.30
	RPMI-8226	8.35
	SR	25.27
Non-Small Cell Lung Cancer	A549/ATCC	12.88
	EKVX	10.27
	HOP-62	1.24
	HOP-92	-18.80
	NCI-H226	-3.52
	NCI-H23	1.15
	NCI-H322M	17.23
	NCI-H460	-8.07
	NCI-H5SS	16.92
Colon Cancer	COLO 205	-10.66
	HCC-2998	-1.55
	HCT-116	-0.24
	HCT-15	-0.57
	HT29	9.71
	KW12	-2.41
	SW-620	-8.95
CNS Cancer	SF-268	-3.87
	SF-295	2.56
	SF-539	-7.76
	SNB-19	-1.50
	SNB-75	5.19
	U251	-0.80
Melanoma	LOX IMVI	0.81
	MALME-3M	0.99
	M14	-3.12
	MDA-MB-435	-6.18
	SK-MEL-2	1.20
	SK-MEL-28	-18.95
	SK-MEL-5	9.23

Type of cancer	**Cell line**	**Δ Growth (%)**
Melanoma	UACC-257	-2.15
	UACC-62	13.34
Ovarian Cancer	IGROV1	7.63
	OVCAR-3	-4.31
	OVCAR-4	4.37
	OVCAR-5	2.94
	OVCAR-8	1.44
	NCI/ADR-RES	-2.10
	SK-OV-3	-7.68
Renal Cancer	786-0	-0.99
	A498	-23.70
	ACHN	-5.25
	CAKI-1	3.63
	RXF 393	-10.72
	SN12C	-2.41
	TK-10	2.70
	UO-31	4.91
Prostate Cancer	PC-3	16.92
	DU-145	-7.78
Breast Cancer	MCF7	9.83
	MDA-MB-231/ATCC	-9.10
	HS 578T	-5.03
	BT-549	-8.68
	T-47D	7.79
	MDA-MB-468	7.24

6.2.3 Results of BROMO*scan* assay of 5-membered ring species against BRD9.

Curve images for 5-membered ring species against BRD9 from BROMO*scan* assay. The amount of bromodomain protein (y-axis) was measured by qPCR and is plotted against the corresponding compound concentration (x-axis) in nM in log10 scale. Data points marked with an "x" were not used for IC_{50} determination. *Nb*: Although K_D is listed on the graphs, this is incorrect and should instead by listed as IC_{50}, as the inhibition of protein binding to the solid support is measured and not the binding kinetics of the ligand to the bromodomain.

- Compound **330**

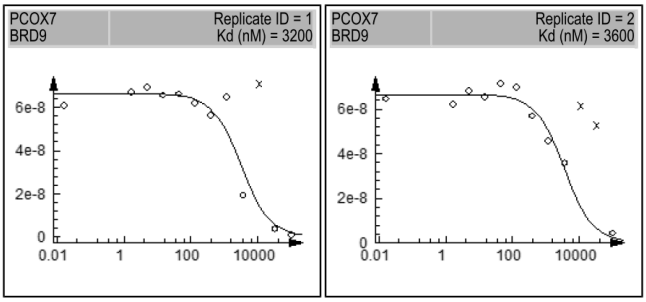

- Compound **334**

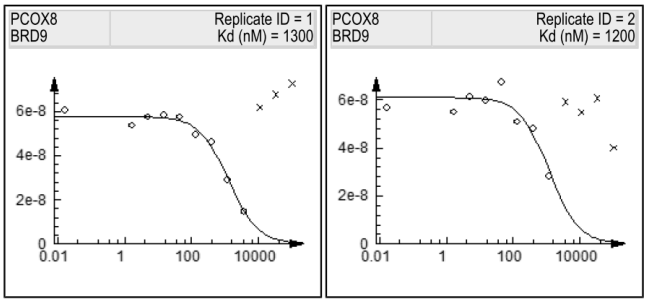

- Compound **336**

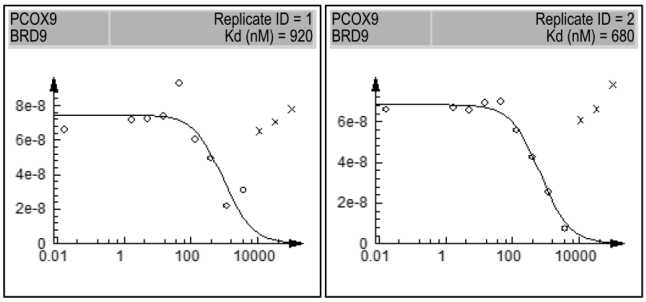

- Compound **344**

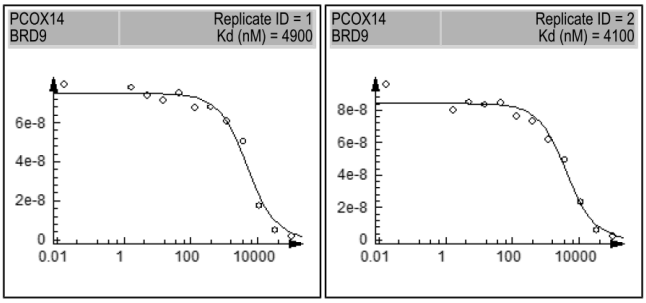

- Compound **354**

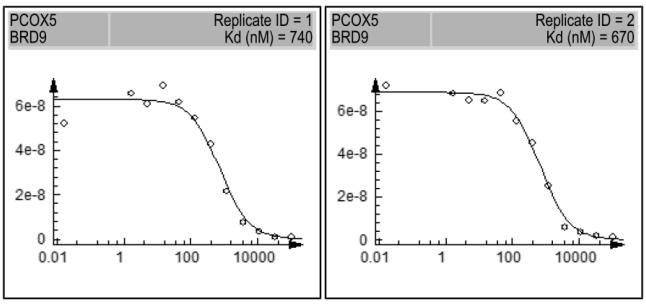

- Compound **355**

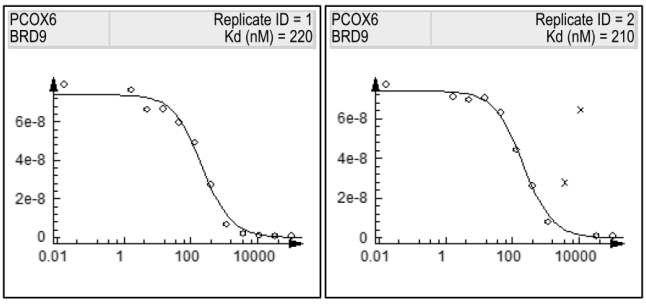

- Compound **357**

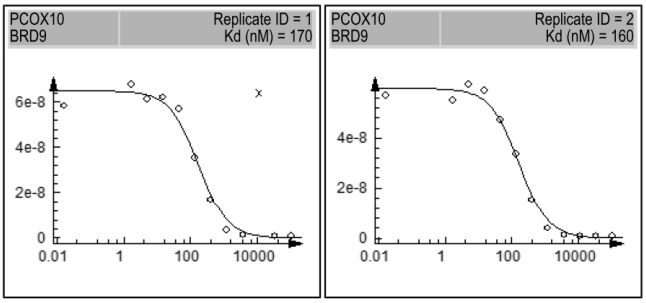

- Compound **359**

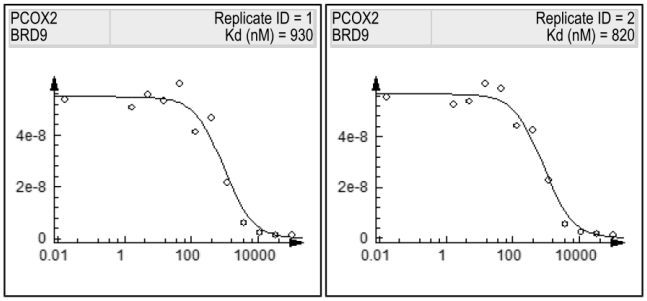

- Compound **360**

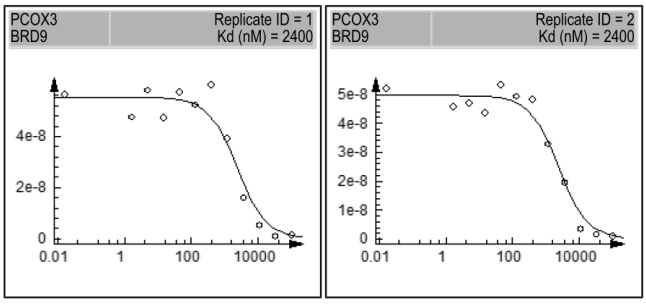

- Compound **361**

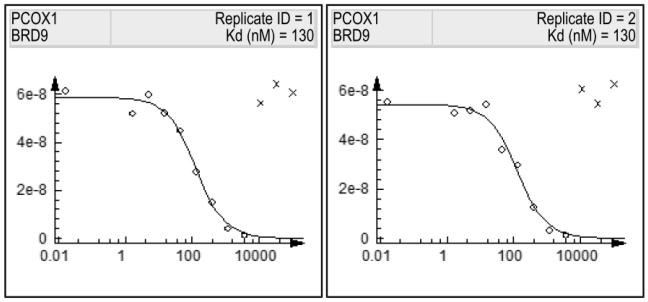

- Compound **362**

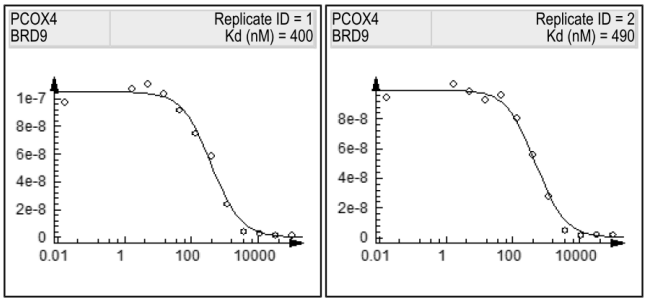

- Compound **363**

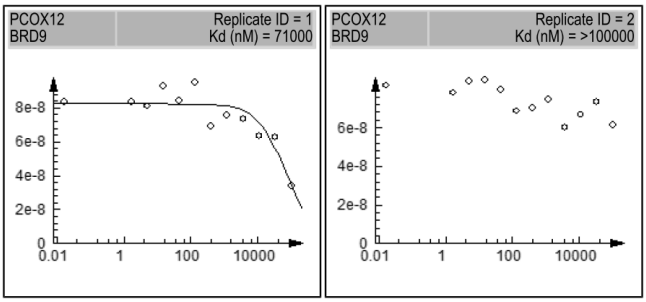

- Compound **366**

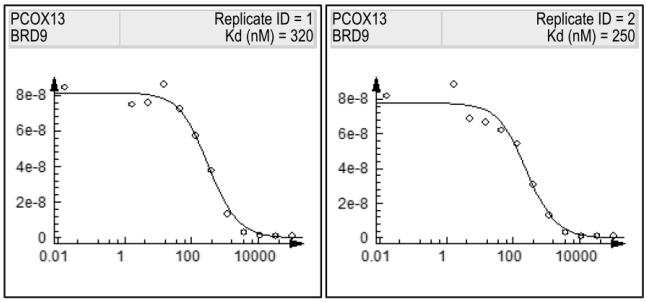

- Compound **369**

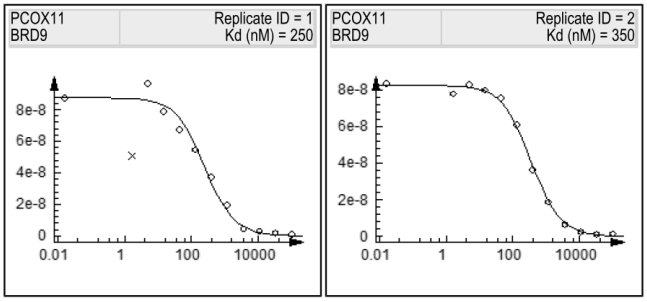

- Compound **373**

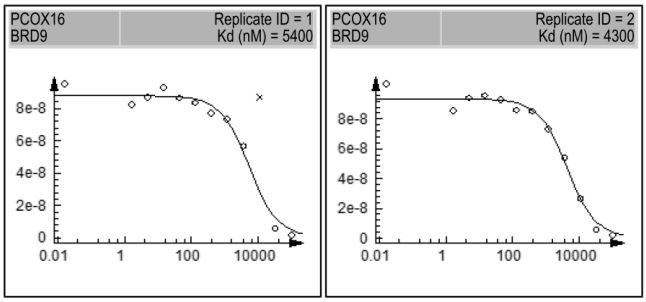

- Compound **374**

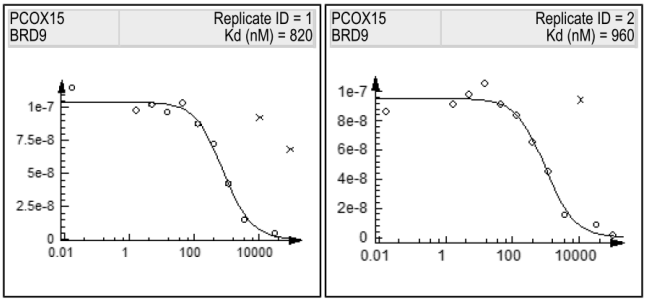

Chapter 7

Experimental

7.1 General experimental

Inert conditions are defined as reactions performed under argon (zero grade) in oven- and vacuum-dried glassware using standard vacuum line techniques and dry solvents, which have been passed through activated alumina columns. Degassing of solvents was achieved by bubbling through argon for 15 minutes with sonication. Reactions were monitored by TLC using Merck silica gel 60 F254 plates and visualized by fluorescence quenching under UV light (254 nm) & by staining with potassium permanganate solution. Chromatographic purification was performed on VWR 60 silica gel 40-63 μM using technical grade solvents that were used as supplied. Reagents used were obtained from commercial suppliers or purified according to standard procedures with the following exceptions. Anhydrous 1,4-dioxane was dried over 3Å-molecular sieves. The cinchona alkaloid-derived phase-transfer catalysts were prepared by Dr Kayli Johnson or prepared according to literature methods.[141] The chiral phosphoric and sulfonic acid catalysts were prepared by Dr Michael Muratore, Dr Lie Shi, Dr Pavol Jakubec and Dr Alexander Gregory or prepared according to literature methods.[299–301] The advanced starting materials used in Section 3.4 were prepared by Dr Sara Consalvi.

NMR spectra were recorded on either a Bruker AVII400, a Bruker AVIII400 or a Bruker AVII 500, with ^{13}C cyroprobe, spectrometer. Chemical shifts (δ) are reported in ppm with the solvent resonance as the internal standard where appropriate. Data are reported as follows: multiplicity [s = singlet, d = doublet, t = triplet, q = quartet, quin = quintet, sxt = sextet, spt = septet, m = multiplet, br = broad], coupling constants (J) in hertz (Hz), integration, assignment. Two-dimensional spectroscopy (COSY, HSQC and HMBC) was performed to assist in structural elucidation but the data are not reported here. High-resolution electrospray ionisation mass spectra (HR-ESI-MS) were recorded on a Bruker Daltonics MicroTOF mass spectrometer. Low-resolution electrospray ionisation mass spectra (LR-ESI-MS) were recorded on a Waters LCT Premier mass spectrometer. Infrared spectra were recorded on a Bruker Tensor 27 FT-IR spectrometer as a thin film, with only selected maximum absorbances reported in cm^{-1}. Optical rotations were recorded using a Perkin Elmer 341 polarimeter; absolute optical rotations are quoted as $[\alpha]_{\mathrm{D}}^{\mathrm{T}}$ where concentrations (c) are in g/100 mL, D refers to the D-line of sodium (589 nm), and temperatures (T) are given in degrees Celsius (°C). Melting points (Mpt) were obtained on a Leica Galen III Hot-stage melting point apparatus and

microscope and on a Kofler hot block and are reported uncorrected. Enantiomeric excesses were determined by HPLC analysis on an Agilent 1200 Series instrument employing chiral stationary phase columns. The same instrument was used in the separation of enantiomers using a semipreparative chiral stationary phase column.

Compound names were generated using the ACD/I-Lab service according to IUPAC nomenclature. Position numbering is for the purposes of assignment only and does not reflect IUPAC numbering conventions.

7.2 BRD4

5-Bromo-2-benzofuran-1,3-dione (**54**)
NaOH (9.6 g, 240 mmol) was dissolved in H_2O (90 mL), phthalic anhydride (20 g, 120 mmol) was added and the reaction mixture was stirred at rt until homogenous. The reaction was cooled to 0 °C, Br_2 (6.8 mL, 132 mmol) was added dropwise and the reaction mixture was stirred at 90 °C for 6 h. The reaction was cooled at 3 °C for 24 h, the resultant precipitate was filtered off, washed with H_2O (3 x 50 mL) and dried under vacuum. $SOCl_2$ (35 mL, 480 mmol) was added and the reaction mixture was stirred at reflux for 2.5 h. The reaction mixture was filtered through Celite, concentrated and recrystallised (EtOAc) to yield **54** (14.6 g, 48%) as a pale yellow powder.

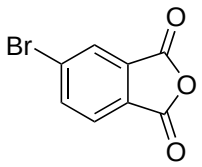

Mpt: 104-105 °C (lit. 106-107 °C); ^{1}H-NMR ($CDCl_3$): δ_H 8.17 (d, J = 2.0 Hz, 1H), 8.05 (dd, J = 8.0, 1.5 Hz, 1H), 7.90 (d, J = 8.0 Hz, 1H); ^{13}C-NMR ($CDCl_3$): δ_C 161.9, 161.6, 139.3, 12.9, 131.5, 129.8, 128.9, 126.8; LR-ESI-MS: $C_8H_3BrO_3Na$ $[M+Na]^+$ m/z found 248.9 calcd 248.9. Data are in accordance with literature values.[180]

6-Bromo-3-hydroxy-2-methyl-3-phenylisoindolin-1-one (**56**) and **5-bromo-3-hydroxy-2-methyl-3-phenylisoindolin-1-one** (**57**)
Method A. **58** (470 mg, 1.6 mmol) was dissolved in $MeNH_2$ (5.0 mL, 33 weight% ethanolic soln) and the reaction mixture was stirred at reflux for 14 h. The reaction mixture was concentrated and purification by FCC (20% EtOAc/PE) yielded **57** (320 mg, 68%) as a white solid.
Method B. NaOH (3.5 g, 87 mmol) was dissolved in H_2O (36 mL), phthalic anhydride (7.2 g, 43 mmol) was added and the solution was stirred until homogenous. The solution was cooled to 0 °C, Br_2 (2.5 mL, 46 mmol) in H_2O (3.6 mL) was added dropwise and the reaction mixture was stirred at 90 °C for 6 h. The reaction mixture was cooled to 3 °C for 24 h, the resultant precipitate was filtered, washed with H_2O (3 x 50 mL) and dried. $SOCl_2$ (14.5 mL) was added and the reaction mixture was stirred at reflux for 2.5 h. The reaction mixture was concentrated, dissolved in EtOAc (200 mL), filtered and concentrated. Benzene (55 mL) and $AlCl_3$ (6.6 g, 49 mmol) were added and the reaction mixture was stirred at rt for 12 h. The reaction mixture was poured over ice (200 mL) and the aqueous phase was extracted with EtOAc (4 x 200 mL). The combined organic extracts were washed with brine (100 mL), dried over Na_2SO_4, filtered and concentrated. Under inert conditions, the crude material was dissolved in THF (120 mL), $SOCl_2$ (3.9 mL, 54 mmol) and a catalytic amount of DMF (15 drops) were added and the

reaction mixture was stirred at rt for 4 h. The reaction mixture was concentrated, $MeNH_2$ (16 mL, 160 mmol, 33 weight% ethanolic soln) was added and the reaction mixture was stirred at rt for 14 h. The reaction mixture was concentrated and EtOAc (200 mL) was added. The organic phase was washed with H_2O (2 x 200 mL), brine (200 mL), dried over Na_2SO_4, filtered and concentrated. Purification by FCC (10% EtOAc/PE) yielded **57** (1.1 g, 6.9%) and **56** (790 mg, 5.1%) as white solids. Recrystallisation of each sample (EtOAc) yielded **57** (860 mg, 5.6%) and **56** (470 mg, 3.1%) as white crystals.

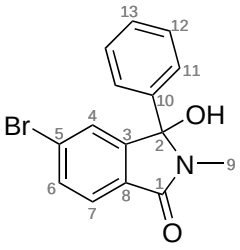

57: Mpt: 190-192 °C; ^{1}H-NMR ($CDCl_3$): δ_H 7.60 (d, J = 8.0 Hz, 1H, C(7)H), 7.58 (dd, J = 8.0, 1.5 Hz, 1H, C(6)H), 7.46 (d, J = 1.5 Hz, 1H, C(4)H), 7.41-7.35 (m, 5H, C(11)H, C(12)H & C(13)H), 2.80 (s, 3H, C(9)H_3); ^{13}C-NMR ($CDCl_3$): δ_C 166.6 (C(1)), 150.3 (C(3)), 137.0 (C(8)), 133.0 (C(6)), 129.2 (C(10)), 128.9 (C(11)), 128.8 (C(13)), 127.2 (C(5)), 126.2 (C(4)),125.9 (C(12)), 124.7 (C(7)), 90.5 (C(2)), 24.1 (C(9)); IR ν_{max} 3209, 1680, 1429, 1065, 699; LR-ESI-MS: $C_{15}H_{12}BrNO_2Na$ $[M+Na]^+$ *m/z* found 340.0 calcd 340.0, $C_{15}H_{11}BrNO_2$ $[M-H]^-$ *m/z* found 316.0 calcd 316.0; HR-ESI-MS: $C_{15}H_{12}BrNO_2Na$ $[M+Na]^+$ *m/z* found 339.9941 calcd 339.9944 error = 0.7 ppm.

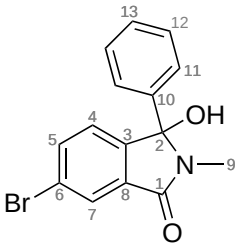

56: Mpt: 170-171 °C; ^{1}H-NMR ($CDCl_3$): δ_H 7.61 (dd, J = 8.0, 1.7 Hz, 1H, C(5)H), 7.50 (d, J = 1.6 Hz, 1H, C(7)H), 7.38-7.32 (m, 5H, C(11)H, C(12)H & C(13)H), 7.19 (d, J = 8.2 Hz, 1H, C(4)H), 2.71 (s, 3H, C(9)H_3); ^{13}C-NMR ($CDCl_3$): δ_C 166.6 (C(1)), 147.7 (C(3)), 137.3 (C(8)), 135.7 (C(5)), 131.7 (C(10)), 128.7 (C(11)), 128.7 (C(13)), 125.9 (C(7)), 125.8 (C(12)), 124.0 (C(4)), 123.5 (C(6)), 90.9 (C(2)), 24.1 (C(9)); IR ν_{max} 3238, 3068, 2925, 1688, 1443, 1085, 763; LR-ESI-MS: $C_{15}H_{12}BrNO_2Na$ $[M+Na]^+$ *m/z* found 340.0 calcd 340.0, $C_{15}H_{11}BrNO_2$ $[M-H]^-$ *m/z* found 316.0 calcd 316.0; HR-ESI-MS: $C_{15}H_{12}BrNO_2Na$ $[M+Na]^+$ *m/z* found 339.9944 calcd 339.9940 error = 0.9 ppm.

Methyl 2-benzoyl-4-bromobenzoate (**58**)

Under inert conditions, **54** (34.7 g, 150 mmol) was dissolved in benzene (206 mL) and the solution was cooled to 0 °C. $AlCl_3$ (42 g, 310 mmol) was added in portions and the reaction mixture was stirred at rt for 24 h. The reaction mixture was poured into ice water (1 L) and extracted with EtOAc (3 x 500 mL). The combined organic extracts were dried over Na_2SO_4, filtered and concentrated. Separately $SOCl_2$ (28 mL, 380 mmol) was added dropwise to MeOH (115 mL) at 0 °C. The original material was added to this solution and the reaction mixture was stirred at rt for 14 h. The reaction mixture was concentrated and EtOAc (500 mL) was added. The organic phase was washed with H_2O (2 x 500 mL), dried over Na_2SO_4, filtered and concentrated. EtOAc (200 mL) was added, the solution was passed through a plug of silica and the silica was washed with EtOAc (500 mL). The combined eluent was concentrated and recrystallisation (MeOH) yielded **58** (21.7 g, 44%) as an opaque oil.

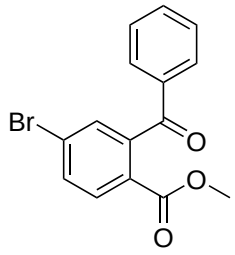

Mpt: 124.1-124.6 °C (lit. 125 °C); ^{1}H-NMR ($CDCl_3$): δ_H 7.93 (d, J = 8.5 Hz, 1H), 7.75 (dd, J = 8.0, 1.0 Hz, 2H), 7.72 (dd, J = 8.5, 2.0 Hz, 1H), 7.58 (tt, J = 7.5, 1.0 Hz, 1H), 7.55 (d, J = 2.0 Hz, 1H), 7.46 (t, J = 8.0 Hz, 2H), 3.62 (s, 3H); ^{13}C-NMR ($CDCl_3$): δ_C 195.2, 165.6, 143.3, 136.6, 133.4, 132.7, 131.6, 130.7, 129.2, 128.6, 127.9, 127.5, 52.3; LR-ESI-MS: $C_{15}H_{11}BrO_3Na$ $[M+Na]^+$ *m/z* found 341.0 calcd 341.0. Data are in accordance with literature values.[302]

6-(3,5-Dimethyl-1,2-oxazol-4-yl)-3-hydroxy-2-methyl-3-phenylisoindolin-1-one (**59**)
In a pressure tube under inert conditions, **56** (50 mg, 0.16 mmol), KOAc (31 mg, 0.31 mmol) and $PdCl_2$ (1.4 mg, 0.0080 mmol) were combined. 3,5-dimethylisoxazole (23 μL, 0.24 mmol) was added to DMAc (0.75 mL) under inert conditions and the solution was degassed. This solution was added to the tube, the tube was sealed and the reaction mixture was stirred at 130 °C for 6 h. The reaction mixture was passed through a plug of Celite and the Celite was washed with CH_2Cl_2 (20 mL). The combined filtrate was concentrated and EtOAc (50 mL) was added. The organic phase was washed with H_2O (2 x 50 mL), dried over Na_2SO_4, filtered and concentrated. Purification by FCC (25% EtOAc/PE) yielded **59** (33 mg, 62%) as a white solid.

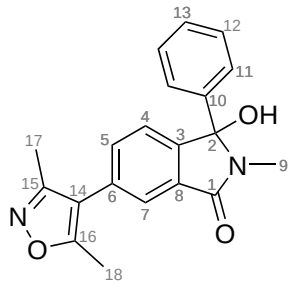

Mpt: 205-206 °C; ^{1}H-NMR ($CDCl_3$): δ_H 7.64 (d, J = 1.0 Hz, 1H, C(7)H), 7.45-7.30 (m, 7H, C(4)H, C(5)H, C(11)H, C(12)H & C(13)H), 2.69 (s, 3H, C(9)H_3), 2.39 (s, 3H, C(18)H_3), 2.21 (s, 3H, C(17)H_3); ^{13}C-NMR ($CDCl_3$): δ_C 167.2 (C(1)), 165.9 (C(16)), 158.4 (C(15)), 148.0 (C(3)), 137.6 (C(8), 133.2 (C(5)), 132.0 (C(10)), 131.0 (C(6)), 128.8 (C(11)), 128.7 (C(13)), 125.9 (C(12)), 123.5 (C(7)), 123.3 (C(4)), 115.7 (C(14)), 91.0 (C(2)), 24.0 (C(9)), 11.6 (C(18)), 10.8 (C(17)); IR ν_{max} 3063, 2932, 1688, 1450, 1385, 1056, 765; LR-ESI-MS: $C_{20}H_{19}N_2O_3$ $[M+H]^+$ *m/z* found 335.1 calcd 335.1, $C_{20}H_{18}N_2O_3Na$ $[M+Na]^+$ *m/z* found 357.0 calcd 357.1, $C_{20}H_{17}N_2O_3$ $[M-H]^-$ *m/z* found 333.1 calcd 333.1; HR-ESI-MS: $C_{20}H_{18}N_2O_3Na$ $[M+Na]^+$ *m/z* found 357.1200 calcd 357.1210 error = 2.7 ppm.

5-(3,5-Dimethyl-1,2-oxazol-4-yl)-3-hydroxy-2-methyl-3-phenylisoindolin-1-one (**60**)
Method A. In a pressure tube under inert conditions, **57** (1.28 g, 4.2 mmol), KOAc (0.83 g, 8.5 mmol) and $PdCl_2$ (38 mg, 0.21 mmol) were combined. 3,5-dimethylisoxazole (0.62 mL, 6.4 mmol) was added to DMAc (20 mL) under inert conditions and the solution was degassed. This solution was added to the tube, the tube was sealed and the reaction mixture was stirred at 130 °C for 6 h. The reaction mixture was passed through a plug of Celite and the Celite was washed with CH_2Cl_2 (50 mL). The combined filtrate was concentrated and EtOAc (250 mL) was added. The organic phase was washed with H_2O (2 x 250 mL), dried over Na_2SO_4, filtered and concentrated. Purification by FCC (33% EtOAc/PE) yielded **60** (1.17 g, 87%) as a white solid.
Method B. **61** (120 mg, 0.36 mmol) was dissolved in $MeNH_2$ (3 mL, 33 weight% ethanolic soln) and the reaction mixture was stirred at reflux for 16 h. The reaction mixture was concentrated and purification by FCC (50% EtOAc/PE) yielded **60** (29.8 mg, 25%) as a white solid.

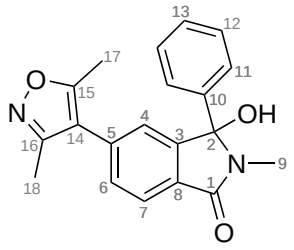

Mpt: 198-199 °C; ^{1}H-NMR ($CDCl_3$): δ_H 7.66 (d, J = 8.0 Hz, 1H, C(7)H), 7.41-7.29 (m, 5H, C(11)H, C(12)H & C(13)H), 7.25 (dd, J = 8.0, 1.5 Hz, 1H, C(6)H), 7.19 (s, 1H, C(4)H), 5.02 (br s, 1H, OH), 2.64 (s, 3H, C(9)H_3), 2.33 (s, 3H, C(17)H_3), 2.16 (s, 3H, C(18)H_3); ^{13}C-NMR ($CDCl_3$): δ_C 167.4 (C(1)), 165.8 (C(15)), 158.2 (C(16))), 149.9 (C(3)), 137.7 (C(8)), 135.0 (C(5)), 129.9 (C(6)), 129.2 (C(10)), 128.7 (C(11) or C(12)), 128.6 (C(13)), 125.9 (C(11) or C(12)), 123.5 (C(7)), 123.3 (C(4)), 115.9 (C(14)), 91.0 (C(2)), 24.0 (C(9)), 11.6 (C(17)), 10.7 (C(18)); IR ν_{max} 2923, 2852, 1682, 1451, 1055, 699; LR-ESI-MS: $C_{20}H_{18}N_2O_3Na$ $[M+Na]^+$ *m/z* found 357.1 calcd 357.0, $C_{20}H_{17}N_2O_3$ $[M-H]^-$ *m/z* found 333.1 calcd 333.1; HR-ESI-MS: $C_{20}H_{18}N_2O_3Na$ $[M+Na]^+$ *m/z* found 357.1201 calcd 357.1210 error = 2.3 ppm.

Methyl 2-benzoyl-4-(3,5-dimethyl-1,2-oxazol-4-yl)benzoate (**61**)

In a pressure tube under inert conditions, **58** (300 mg, 0.94 mmol), KOAc (190 mg, 1.9 mmol) and $PdCl_2$ (8.3 mg, 0.05 mmol) were combined. Separately 3,5-dimethylisoxazole (0.14 mL, 1.4 mmol) was added to DMAc (4.5 mL) under inert conditions and the solution was degassed. This solution was added to the tube, the tube was sealed and the reaction mixture was stirred at 130 °C for 6 h. The reaction mixture was passed through a plug of Celite and the Celite was washed with CH_2Cl_2 (50 mL). The combined filtrate was concentrated and dissolved in EtOAc (150 mL). The organic phase was washed with H_2O (2 x 150 mL), dried over Na_2SO_4, filtered and concentrated. Purification by FCC (16% EtOAc/hexane) yielded **61** (250 mg, 80%) as a pale yellow oil.

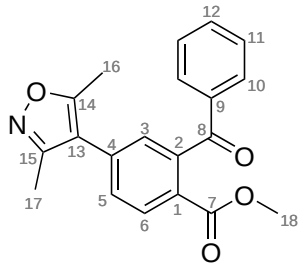

^{1}H-NMR ($CDCl_3$): δ_H 8.13 (d, J = 8.0 Hz, 1H, C(6)H), 7.81-7.76 (m, 2H, C(10)H), 7.59 (tt, J = 7.5, 1.5 Hz, 1H, C(12)H), 7.50-7.44 (m, 3H, C(5)H and C(11)H), 7.30 (d, J = 1.5 Hz, 1H, C(3)H), 3.64 (s, 3H, C(18)H_3), 2.45 (s, 3H, C(16)H_3), 2.31 (s, 3H, C(17)H_3); ^{13}C-NMR ($CDCl_3$): δ_C 196.4 (C(8)), 166.2 (C(14)), 165.9 (C(7)), 158.2 (C(15)), 142.4 (C(2)), 136.9 (C(9)), 135.1 (C(4)), 133.4 (C(12)), 130.7 (C(6)), 129.9 (C(5)), 129.2 (C(10)), 128.7 (C(11)), 128.1 (C(1)), 128.0 (C(3)), 115.2 (C(13)), 52.3 (C(18)), 11.8 (C(16)), 10.9 (C(17)); IR ν_{max} 3060, 2953, 2928, 1720, 1673, 1274, 1090, 708; LR-ESI-MS: $C_{20}H_{18}NO_4$ $[M+H]^+$ *m/z* found 336.1 calcd 336.1, $C_{20}H_{17}NO_4Na$ $[M+Na]^+$ *m/z* found 358.1 calcd 358.1; HR-ESI-MS: $C_{20}H_{17}NO_4Na$ $[M+Na]^+$ *m/z* found 358.1038 calcd 358.1050 error = 3.3 ppm.

3-Hydroxy-3-phenyl-2,3-dihydro-1*H*-isoindol-1-one (**62**)

Phthalimide (2.00 g, 13.6 mmol) was dissolved in CH_2Cl_2 (34 mL) and the solution was cooled to 0 °C. PhMgBr (40.8 mL, 40.8 mmol, 1M THF) was added slowly and the reaction mixture was stirred at rt for 5 h. NH_4Cl was added (34 mL, sat. aq. soln), the organic phase was separated and the aqueous phase was extracted with CH_2Cl_2 (3 x 30 mL). The combined organic phase was dried over Na_2SO_4, filtered and concentrated. Recrystallisation (EtOAc) **62** (2.38 g, 78%) as a white powder.

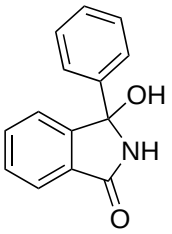

Mpt: 158.0-159.5 °C (lit. 165 °C); ^{1}H-NMR ($CDCl_3$): δ_H 7.57-7.52 (m, 3H), 7.49 (td, J = 7.5, 1.0 Hz, 1H), 7.38 (dd, J = 7.5, 1.0 Hz, 1H), 7.36-7.30 (m, 4H), 7.09 (br s, 1H), 4.59 (br s, 1H); ^{13}C-NMR ($CDCl_3$): δ_C 169.8, 149.9, 139.8, 133.2, 129.5, 129.4, 128.6, 128.6, 125.5, 123.6, 122.9, 88.2; LR-ESI-MS: $C_{14}H_{12}NO_2$ $[M+H]^+$ m/z found 226.1 calcd 226.1, $C_{14}H_{11}NO_2Na$ $[M+Na]^+$ m/z found 248.1 calcd 248.1. Data are in accordance with literature values.[303]

3-Methoxy-3-phenyl-2,3-dihydro-1*H*-isoindol-1-one (**63**)

Compound **62** (370 mg, 1.64 mmol) was dissolved in MeOH (25 mL), concentrated H_2SO_4 (50 μL, 0.82 mmol) was added and the reaction mixture was stirred at reflux for 1 d. EtOAc (20 mL) was added, the organic phase was washed with $NaHCO_3$ (3 x 25 mL, sat. aq. soln), dried over Na_2SO_4, filtered and concentrated. Purification by FCC (0.5% MeOH/CH_2Cl_2) yielded **63** (293, 75%) as colourless crystals.

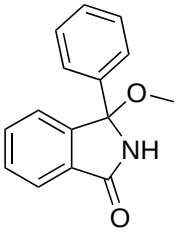

Mpt: 132.8-134.1 °C (lit. 136 °C); ^{1}H-NMR ($CDCl_3$): δ_H 7.84 (d, J = 7.0 Hz, 1H), 7.59-7.46 (m, 4H), 7.38-7.28 (m, 4H), 7.01 (br s, 1H), 3.15 (s, 3H); ^{13}C-NMR ($CDCl_3$): δ_C 169.9, 146.5, 139.9, 132.9, 131.1, 129.6, 128.6, 128.5, 125.5, 123.7, 123.2, 92.2, 50.3; LR-ESI-MS: $C_{15}H_{14}NO_2$ $[M+H]^+$ m/z found 240.1 calcd 240.1. Data are in accordance with literature values.[187]

3-(Nitromethyl)-3-phenyl-2,3-dihydro-1*H*-isoindol-1-one (**64**)

Method A. Under inert condtions, **62** (100 mg, 0.44 mmol) was dissolved in nitromethane (1 mL), BEMP (12 μL, 0.044 mmol) was added and the reaction mixture was stirred at reflux for 66 h. EtOAc (20 mL) was added, the organic phase was washed with H_2O (3 x 20 mL), dried over Na_2SO_4, filtered and concentrated. Purification by FCC (0.5% MeOH/CH_2Cl_2) yielded **64** (13 mg, 11%) as a white solid.

Method B. Under inert condtions, **62** (100 mg, 0.44 mmol) was dissolved in nitromethane (1 mL), DPP (11 mg, 0.044 mmol) was added and the reaction mixture was stirred at reflux for 66 h. EtOAc (20 mL) was added, the organic phase was washed with $NaHCO_3$ (3 x 20 mL, sat. aq. soln), dried over Na_2SO_4, filtered and concentrated. Purification by FCC (0.5% MeOH/CH_2Cl_2) yielded **64** (28 mg, 24%) as a white solid.

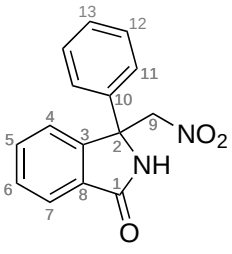

Mpt: 190.2-190.9 °C; ^{1}H-NMR ($(CD_3)_2CO$): δ_H 8.46 (br s, 1H, NH), 7.80 (dt, J = 8.0, 1.0 Hz, 1H, C(4)H), 7.76-7.70 (m, 3H, C(7)H & C(12)H), 7.63 (td, J = 7.5, 1.0 Hz, 1H, C(6)H), 7.54 (td, J = 7.5, 1.0 Hz, 1H, C(5)H), 7.45-7.39 (m, 2H, C(11)H), 7.34 (ddt, J = 8.0, 6.5, 1.0 Hz, 1H, C(13)H), 5.80 (d, J = 13.5 Hz, 1H, C(9)H_a), 5.41 (d, J = 13.5 Hz, 1H, C(9)H_b); ^{13}C-NMR ($(CD_3)_2CO$): δ_C 169.6 (C(1)), 148.2 (C(8)), 140.3 (C(10)), 133.3 (C(5)), 131.9 (C(3)), 130.1 (C(6)), 130.1 (C(12)), 129.2 (C(7)), 126.1 (C(11)), 124.6 (C(13)), 124.3 (C(4)), 81.5 (C(9)), 66.1 (C(2)); IR ν_{max} 3216, 2921, 2360, 1703, 1554, 700; LR-ESI-MS: $C_{15}H_{13}N_2O_3$ $[M+H]^+$ m/z found 269.1 calcd 269.1, $C_{15}H_{12}N_2O_3Na$ $[M+Na]^+$ m/z found 291.1 calcd 291.1; HR-ESI-MS: $C_{15}H_{13}N_2O_3$ $[M+H]^+$ m/z found 269.09207 calcd 269.09215 error = 0.24 ppm; Analytical HPLC separation (stationary phase: Chiralpak AD-H, solvent composition: hexane:iso-propanol 85:15, flow rate: 1 mL.min^{-1},

injection concentration: 1 mg.mL^{-1}, injection volume: 10 μL, λ: 210 nm): t_1 = 30.9 min, t_2 = 34.3 min.

3-Phenyl-2,3-dihydro-1*H*-isoindol-1-one (**65**)

Compound **62** (25 mg, 0.11 mmol) was dissolved in toluene (5 mL), **68** (35 mg, 0.14 mmol) and DPP (1.4 mg, 0.0055 mmol) were added and the reaction mixture was stirred at rt for 20 h. EtOAc (20 mL) was added, the organic phase was washed with NH_4Cl (3 x 20 mL, sat. aq. soln), H_2O (3 x 20 mL), dried over Na_2SO_4, filtered and concentrated. Purification by FCC (0.5% MeOH/CH_2Cl_2) yielded **65** (18 mg, 78%) as a white solid.

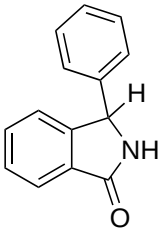

Mpt: 218.0-218.7 °C (lit. 219 °C); ^{1}H-NMR ($CDCl_3$): δ_H 7.90 (dd, J = 6.5, 1.0 Hz, 1H), 7.52 (td, J = 7.5, 1.5 Hz, 1H), 7.48 (td, J = 7.5, 1.0 Hz, 1H), 7.40-7.30 (m, 3H), 7.29-7.23 (m, 3H), 6.80 (br s, 1H), 5.64 (s, 1H); ^{13}C-NMR ($CDCl_3$): δ_C 171.0, 147.9, 138.4, 132.3, 130.7, 129.1, 128.6, 128.4, 126.8, 123.8, 123.3, 60.8; LR-ESI-MS: $C_{14}H_{12}NO$ $[M+H]^+$ *m/z* found 210.1 calcd 210.1; Analytical HPLC separation (stationary phase: Chiralpak AD, solvent composition: hexane:iso-propanol 85:15, flow rate: 1 mL.min^{-1}, injection concentration: 1 mg.mL^{-1}, injection volume: 10 μL, λ: 210 nm): t_1 = 7.7 min, t_2 = 11.9 min. Data are in accordance with literature values.[304]

2-Methyl-3-(nitromethyl)-3-phenylisoindolin-1-one (**66**)

Under inert conditions, **71** (100 mg, 0.42 mmol) was dissolved in nitromethane (3 mL), DPP (21 mg, 0.084 mmol) was added and the reaction mixture was stirred at reflux for 36 h. The reaction mixture was concentrated and purification by FCC (0.5% MeOH/CH_2Cl_2) yielded **66** (90 mg, 76%) as a white solid.

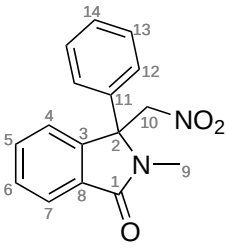

Mpt: 145-147 °C; ^{1}H-NMR ($CDCl_3$): δ_H 7.89 (dd, J = 7.0, 1.0 Hz, 1H, C(4)*H*), 7.55 (td, J = 7.5, 1.0 Hz, 1H, C(6)*H*), 7.51 (td, J = 7.5, 1.0 Hz, 1H, C(5)*H*), 7.42-7.37 (m, 3H, C(12)*H* & C(14)*H*), 7.33 (dd, J = 7.5, 1.0 Hz, 1H, C(7)*H*), 7.09-7.06 (m, 2H, C(13)*H*), 5.52 (d, J = 11.5 Hz, 1H, C(10)H_a), 5.33 (d, J = 11.5 Hz, 1H , C(10)H_b), 3.00 (s, 3H, C(9)H_3); ^{13}C-NMR ($CDCl_3$): δ_C 168.1 (*C*(1)), 145.5 (*C*(3)), 136.1 (*C*(8)), 132.4 (*C*(6)), 131.0 (*C*(11)), 129.6 (*C*(12)), 129.5 (*C*(14)), 129.1 (*C*(5)), 125.4 (*C*(13)), 124.1 (*C*(4)), 122.4 (*C*(7)), 76.99 (*C*(10)), 68.9 (*C*(2)), 25.2 (*C*(9)); IR ν_{max} 3032, 2975, 1693, 1551, 1376, 694; LR-ESI-MS: $C_{16}H_{14}N_2O_3Na$ $[M+Na]^+$ *m/z* found 305.1 calcd 305.1, $C_{16}H_{13}N_2O_3$ $[M-H]^-$ *m/z* found 281.1 calcd 281.1; HR-ESI-MS: $C_{16}H_{14}N_2O_3Na$ $[M+Na]^+$ *m/z* found 305.0894 calcd 305.0897 error = 1.0 ppm; Analytical HPLC separation (stationary phase: Chiralpak OD-H, solvent composition: hexane:iso-propanol 80:20, flow rate: 1 mL.min^{-1}, injection concentration: 1 mg.mL^{-1}, injection volume: 10 μL, λ: 210 nm): t_1 = 26.2 min, t_2 = 31.5 min.

2-Methyl-3-phenyl-2,3-dihydro-1*H*-isoindol-1-one (**67**)

Compound **71** (25 mg, 0.105 mmol) was dissolved in toluene (5 mL), **68** (33 mg, 0.13 mmol) was added and the reaction mixture was stirred at rt for 3 d. EtOAc (10 mL) was added, the organic phase was washed with $NaHCO_3$ (2 x 10 mL, sat. aq. soln), NH_4Cl (2 x 10 mL, sat. aq. soln) and H_2O (2 x 10 mL), dried over Na_2SO_4, filtered and concentrated. Purification by

FCC (0.5% MeOH/CH_2Cl_2) yielded **67** (23 mg, 98%) as a white solid.

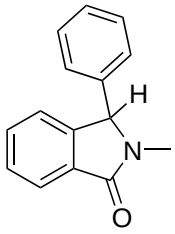

Mpt: 97.4-99.4 °C (lit. 101 °C); ^{1}H-NMR ($CDCl_3$): δ_H 7.51 (d, J = 7.5 Hz, 1H), 7.46 (t, J = 7.5 Hz, 1H), 7.39-7.29 (m, 7H), 4.84 (br s, 1H), 2.60 (s, 3H); ^{13}C-NMR ($CDCl_3$): δ_C 168.0, 149.0, 138.0, 132.5, 129.9, 129.2, 128.6, 128.4, 125.9, 123.0, 122.8, 91.0, 23.9; LR-ESI-MS: $C_{15}H_{13}NONa$ $[M+Na]^+$ *m/z* found 246.1 calcd 246.1; Analytical HPLC separation (stationary phase: Chiralpak OD, solvent composition: hexane:iso-propanol 98:2, flow rate: 1 mL.min^{-1}, injection concentration: 1 mg.mL^{-1}, injection volume: 10 μL, λ: 210 nm): t_1 = 15.7 min, t_2 = 18.8 min. Data are in accordance with literature values.[304]

Diethyl 2,6-dimethyl-1,4-dihydropyridine-3,5-dicarboxylate (**68**)

Ethyl acetoacetate (2.53 mL, 20 mmol), paraformaldehyde (300 mg, 10 mmol) and NH_4OAc (1.16 g, 15 mmol) were combined and stirred at 80 °C for 15 min. Cold H_2O (10 mL) was added and the resultant precipitate was filtered. Recrystallisation (MeOH) yielded **68** (1.47 g, 58%) as a yellow powder.

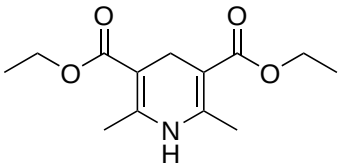

Mpt: 181.2-183.2 °C (lit. 185-186 °C); ^{1}H-NMR ($CDCl_3$): δ_H 5.24 (br s, 1H), 4.17 (q, J = 7.0 Hz, 4H), 3.27 (s, 2H), 2.19 (s, 6H), 1.29 (t, J = 7.0 Hz, 6H); ^{13}C-NMR ($CDCl_3$): δ_C 168.0, 144.8, 99.5, 59.6, 24.8, 19.2, 14.5; LR-ESI-MS: $C_{13}H_{18}NO_4$ $[M-H]^-$ *m/z* found 252.2 calcd 252.1. Data are in accordance with literature values.[305]

2-Benzoylbenzoic acid (**70**)

Phthalic anhydride (4.0 g, 27 mmol) was dissolved in benzene (60 mL), $AlCl_3$ (7.2 g, 54 mmol) was added and the reaction mixture was stirred at rt for 14 h. The reaction mixture was poured over ice (200 g), acidified with concentrated HCl and the aqueous phase was extracted with Et_2O (4 x 100 mL). The combined organic extracts were washed with H_2O (3 x 100 mL) then extracted with $NaHCO_3$ (3 x 100 mL, sat. aq. soln). The combined aqueous extracts were washed with Et_2O (3 x 50 mL), acidified with concentrated HCl and the resulting precipitate was filtered to yield **70** (5.66 g, 93%) as a white solid.

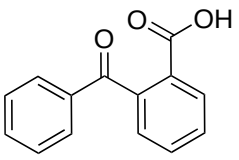

Mpt: 123-124 °C (lit. 124-125 °C); ^{1}H-NMR ($CDCl_3$): δ_H 8.09 (d, J = 8.0 Hz, 1H), 7.73 (d, J = 7.5 Hz, 2H), 7.67 (t, J = 8.0 Hz, 1H), 7.61-7.52 (m, 2H), 7.45-7.36 (m, 3H); ^{13}C-NMR ($CDCl_3$): δ_C 197.1, 169.9, 142.5, 137.0, 133.2, 133.1, 130.9, 129.5, 129.4, 128.4, 127.9, 127.7; LR-ESI-MS: $C_{14}H_{10}O_3Na$ $[M+Na]^+$ *m/z* found 249.0 calcd 249.1, $C_{14}H_9O_3$ $[M-H]^-$ *m/z* found 225.1 calcd 225.1. Data are in accordance with literature values.[306]

3-Hydroxy-2-methyl-3-phenylisoindolin-1-one (**71**)

Under inert conditions, **70** (1.0 g, 4.4 mmol) was dissolved in THF (13 mL), $SOCl_2$ (0.64 mL, 8.8 mmol) and a catalytic amount of DMF (10 drops) were added and the reaction mixture was stirred at rt for 4 h. The reaction mixture was concentrated, $MeNH_2$ (11 mL, 33 weight% ethanolic soln) was added and the reaction mixture was stirred at rt for 14 h. EtOAc (100 mL) was added, the organic phase was washed with H_2O (3 x 50 mL), brine (50 mL), dried over Na_2SO_4, filtered and concentrated. Purification by FCC (CH_2Cl_2) yielded **71** (760 mg, 72%) as a white solid.

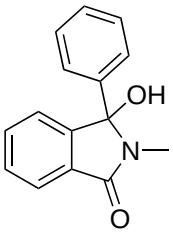

Mpt: 189-190 °C (lit. 187-188 °C); ^{1}H-NMR ($CDCl_3$): δ_H 7.65 (d, J = 7.0 Hz, 1H), 7.48 (t, J = 7.0 Hz, 1H), 7.43-7.30 (m, 7H), 2.70 (s, 3H); ^{13}C-NMR ($CDCl_3$): δ_C 165.1, 151.8, 137.9, 132.6, 130.0, 129.4, 128.7, 128.5, 125.9, 123.2, 122.7, 91.0, 23.9; LR-ESI-MS: $C_{15}H_{13}NO_2Na$ $[M+Na]^+$ *m/z* found 262.1 calcd 262.1, $C_{15}H_{12}NO_2$ $[M-H]^-$ *m/z* found 238.1 calcd 238.1. Data are in accordance with literature values.[307]

5-(3,5-Dimethyl-1,2-oxazol-4-yl)-2-methyl-3-(nitromethyl)-3-phenylisoindolin-1-one (73)

Under inert conditions, **60** (303 mg, 0.9 mmol) was dissolved in nitromethane (6.3 mL), DPP (45 mg, 0.18 mmol) was added and the reaction mixture was stirred at reflux for 2 d. The reaction mixture was concentrated and EtOAc (150 mL) was added. The organic phase was washed with H_2O (2 x 150 mL), dried over Na_2SO_4, filtered and concentrated. Purification by FCC (1% MeOH/CH_2Cl_2) yielded **73** (304 mg, 89%) as a colourless oil.

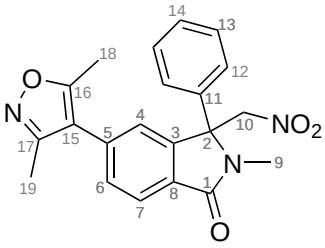

^{1}H-NMR ($CDCl_3$): δ_H 7.94 (d, J = 7.5 Hz, 1H, C(7)H), 7.44-7.36 (m, 4H, C(12)H & C(13)H), 7.19 (d, J = 0.5 Hz, 1H, C(4)H), 7.12-7.09 (m, 2H, C(6)H & C(14)H), 5.56 (d, J = 11.5 Hz, 1H, C(10)Ha), 5.34 (d, J = 11.5 Hz, 1H, C(10)Hb), 3.02 (s, 3H, C(9)H_3), 2.38 (s, 3H, C(18)H_3), 2.23 (s, 3H, C(19)H_3); ^{13}C-NMR ($CDCl_3$): δ_C 167.5 (C(1)), 165.9 (C(16)), 158.3 (C(17)), 146.0 (C(3)), 135.8 (C(8)), 134.9 (C(5)), 130.4 (C(14)), 130.2 (C(11)), 129.7 (C(12) or C(13)), 129.4 (C(6)), 125.4 (C(12) or C(13)), 124.5 (C(7)), 123.2 (C(4)), 115.9 (C(15)), 76.8 (C(10)), 69.0 (C(2)), 25.2 (C(9)), 11.6 (C(18)), 10.7 (C(19)); IR ν_{max} 3062, 2965, 2360, 1690, 1553, 1375, 699; LR-ESI-MS: $C_{21}H_{20}N_3O_4$ $[M+H]^+$ *m/z* found 378.1 calcd 378.1, $C_{21}H_{19}N_3O_4Na$ $[M+Na]^+$ *m/z* found 400.1 calcd 400.1; HR-ESI-MS: $C_{21}H_{19}N_3O_4Na$ $[M+Na]^+$ *m/z* found 400.1264 calcd 400.1268 error = 1.0 ppm; Analytical HPLC separation (stationary phase: Chiralpak AD, solvent composition: hexane:iso-propanol 80:20, flow rate: 0.9 mL.min^{-1}, injection concentration: 1.1 mg.mL^{-1}, injection volume: 10 μL, λ: 210 nm): t_1 = 22.4 min, t_2 = 25.9 min.

***N*-[(6-(3,5-Dimethyl-1,2-oxazol-4-yl)-2-methyl-3-oxo-1-phenyl-2,3-dihydro-1*H*-isoindol-1-yl)methyl]acetamide (74)**

Compound **73** (30 mg, 0.079 mmol) was suspended in AcOH (1 mL), the solution was cooled to 0 °C, freshly ground zinc (52 mg, 0.79 mmol) was added in portions and the reaction mixture was stirred at reflux for 14 h. The reaction mixture was concentrated and purification by FCC (1.5% MeOH/CH_2Cl_2) yielded **74** (17 mg, 55%) as a white solid.

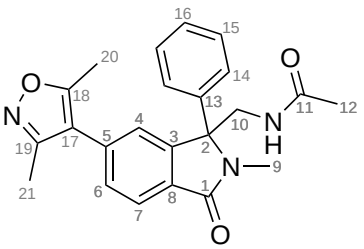

Mpt: 230.4-232.4 °C; ^{1}H-NMR ($CDCl_3$): δ_H 7.85 (d, J = 7.5 Hz, 1H, C(7)H), 7.41-7.30 (m, 4H, C(6)H, C(15)H & C(16)H), 7.21 (d, J = 7.5 Hz, 2H, C(14)H), 7.15 (s, 1H, C(4)H), 6.03 (br s, 1H, NH), 4.99-4.90 (m, 1H, C(10)H_a), 3.96 (d, J = 13.5 Hz, 1H, C(10)H_b), 2.90 (s, 3H, C(9)H_3), 2.39 (s, 3H, C(20)H_3), 2.22 (s, 3H, C(21)H_3), 1.75 (s, 3H, C(12)H_3); ^{13}C-NMR ($CDCl_3$): δ_C 170.7 (C(11)), 169.2 (C(1)), 166.5 (C(18)), 158.8 (C(19)), 149.0 (C(3)), 137.5 (C(8)), 135.2 (C(5)), 131.0 (C(13)), 129.8 (C(6)), 129.8 (C(15)), 129.1 (C(16)), 126.4 (C(14)), 123.9 (C(7)), 123.7 (C(4)), 116.4 (C(17)), 71.1 (C(2)), 40.7 (C(10)), 25.7 (C(9)), 23.3 (C(12)),

12.1 (*C*(20)), 11.3 (*C*(21)); IR ν_{max} 3339, 3068, 2928, 1672, 697; LR-ESI-MS: $C_{23}H_{24}N_3O_3$ $[M+H]^+$ *m/z* found 390.2 calcd 390.1; HR-ESI-MS: $C_{23}H_{23}N_3O_3Na$ $[M+Na]^+$ *m/z* found 412.1632 calcd 412.1634 error = 0.6 ppm.

3-(Aminomethyl)-5-(3,5-dimethyl-1,2-oxazol-4-yl)-2-methyl-3-phenyl-2,3-dihydro-1*H*-isoindol-1-one (**75**)

Compound **73** (50 mg, 0.13 mmol) was dissolved in MeOH (4 mL), a solution of NH_4Cl (72.2 mg, 1.35 mmol) in H_2O (0.5 mL) and freshly-ground zinc powder (88.4 mg, 1.35 mmol) were added and the reaction mixture was stirred at 60 °C for 17 h. 1M HCl (10 mL) was added, the reaction mixture was filtered and volatiles were removed. H_2O (10 mL) was added and the aqueous phase was washed with EtOAc (3 x 20 mL). The aqueous phase was basified with 1M NaOH and extracted with EtOAc (3 x 20 mL). The combined organic extracts were dried over Na_2SO_4, filtered and concentrated to yield **75** (39 mg, 85%) as a white powder.

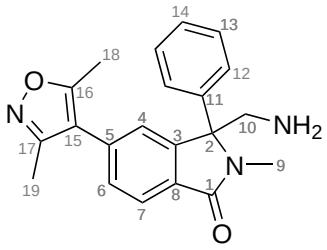

Mpt: 201.0-203.0 °C; ^{1}H-NMR ($CDCl_3$): δ_H 7.95 (d, J = 8.0 Hz, 1H, C(7)*H*), 7.39-7.30 (m, 4H, C(6)*H*, C(13)*H* & C(14)*H*), 7.18 (d, J = 7.5 Hz, 2H, C(12)*H*), 7.09 (s, 1H, C(4)*H*), 3.85 (d, J = 13.9 Hz, 1H, C(10)H_a), 3.63 (d, J = 13.9 Hz, 1H, C(10)H_b), 2.89 (s, 3H, C(9)H_3), 2.34 (s, 3H, C(18)H_3), 2.19 (s, 3H, C(19)H_3); ^{13}C-NMR ($CDCl_3$): δ_C 168.8 (*C*(1)), 165.7 (*C*(16)), 158.2 (*C*(17)), 148.6 (*C*(3)), 137.7 (*C*(8)), 134.8 (*C*(5)), 131.2 (*C*(11)), 129.5 (*C*(6)), 129.2 (*C*(13)), 128.5 (*C*(14)), 126.1 (*C*(12)), 125.8 (*C*(7)), 124.1 (*C*(4)), 116.0 (*C*(15)), 71.4 (*C*(2)), 44.2 (*C*(10)), 25.1 (*C*(9)), 11.7 (*C*(18)), 10.8 (*C*(19)); IR ν_{max} 3394, 3330, 3060, 2927, 1693, 1378, 700; LR-ESI-MS: $C_{21}H_{22}N_3O_2$ $[M+H]^+$ *m/z* found 348.2 calcd 348.1; HR-ESI-MS: $C_{21}H_{22}N_3O_2$ $[M+H]^+$ *m/z* found 348.1707 calcd 348.1707 error = 0.2 ppm.

5-(3,5-Dimethyl-1,2-oxazol-4-yl)-2-methyl-3-[(dimethylamino)methyl]-3-phenyl-2,3-dihydro-1*H*-isoindol-1-one (**76**)

Compound **75** (39 mg, 0.11 mmol) was suspended in H_2O (1 mL), formic acid (12 μL, 0.31 mmol) was added and the solution was cooled to 0 °C. Formaldehyde (23 μL, 0.34 mmol) was added dropwise and the reaction mixture was stirred at reflux for 7 h. The reaction mixture was basified with 1M NaOH and the aqueous phase was extracted with EtOAc (3 x 10 mL). The combined organic extracts were dried over Na_2SO_4, filtered and concentrated. Purification by FCC (0.5% MeOH/CH_2Cl_2) yielded **76** (38 mg, 92%) as a white solid.

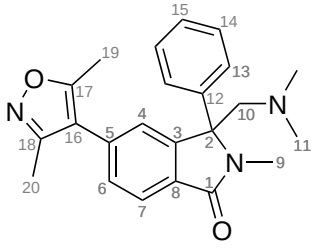

Mpt: 169.3-171.0 °C; ^{1}H-NMR ($CDCl_3$): δ_H 8.00 (d, J = 7.5 Hz, 1H, C(7)*H*), 7.46-7.34 (m, 4H, C(6)*H*, C(14)*H* & C(15)*H*), 7.28 (dd, J = 8.0, 2.0 Hz, 2H, C(13)*H*), 7.14 (s, 1H, C(4)*H*), 3.55 (d, J = 13.5 Hz, 1H, C(10)H_a), 3.40 (d, J = 14.0 Hz, 1H, C(10)H_b), 2.99 (s, 3H, C(9)H_3), 2.41 (s, 3H, C(19)H_3), 2.26 (s, 3H, C(20)H_3), 2.11 (s, 6H, C(11)H_3); ^{13}C-NMR ($CDCl_3$): δ_C 168.7 (*C*(1)), 165.5 (*C*(17)), 158.3 (*C*(18)), 150.2 (*C*(3)), 139.1 (*C*(8)), 133.6 (*C*(5)), 131.1 (*C*(12)), 129.0 (*C*(14)), 128.9 (*C*(6)), 128.1 (*C*(15)), 125.8 (*C*(13)), 123.8 (*C*(7)), 122.7 (*C*(4)), 116.2 (*C*(16)), 70.4 (*C*(2)), 62.1 (*C*(10)), 47.6 (*C*(11)), 25.7 (*C*(9)), 11.6 (*C*(19)), 10.7 (*C*(20)); IR ν_{max} 2825, 2778, 1697, 1379, 701; LR-ESI-MS: $C_{23}H_{26}N_3O_2$ $[M+H]^+$ *m/z* found 376.2 calcd 376.2; HR-ESI-MS: $C_{23}H_{26}N_3O_2$ $[M+H]^+$ *m/z* found 376.2020 calcd 376.2016 error = 1.0 ppm.

6-(3,5)-Dimethyl-1,2-oxazol-4-yl)-2-methyl-3-oxo-1-phenyl-2,3-dihydro-1*H*-isoindole-1-carbonitrile (**77**)

Method A. Under inert conditions, **73** (90 mg, 0.24 mmol) was dissolved in THF (2.4 mL), *n*-Bu_4NI (4.4 mg, 0.012 mmol), BnBr (31.2 μL, 0.26 mmol) and KOH (14 mg, 0.25 mmol) were added and the reaction mixture was stirred at rt for 3 h. H_2O (10 mL) was added and the aqueous phase was extracted with EtOAc (4 x 10 mL). The combined organic extracts were dried over Na_2SO_4, filtered and concentrated. FCC (3% MeOH/CH_2Cl_2) gave crude **412**. This material was dissolved in THF (2.5 mL), NEt_3 (183 μL, 1.30 mmol) and $SOCl_2$ (50 μL, 0.65 mmol) were added and the reaction mixture was stirred at rt for 12 h. H_2O (10 mL) was added and the aqueous phase was extracted with EtOAc (3 x 10 mL). The combined organic extracts were dried over Na_2SO_4, filtered and concentrated. Purification by FCC (25% EtOAc/hexane) yielded **77** (31.3 mg, 38%) as a white powder.

Method B. Under inert conditions in a pressure tube, **60** (330 mg, 0.99 mmol) was dissolved in THF (7.3 mL), *t*-BuNC (131 μL, 1.14 mmol) and pTsOH$\cdot H_2O$ (19 mg, 0.099 mmol) were added, the tube was sealed and the reaction mixture was stirred at 120 °C for 15 h. EtOAc (50 mL) was added, the organic phase was washed with H_2O (3 x 50mL), dried over Na_2SO_4, filtered and concentrated. Purification by FCC (1.5% MeOH/CH_2Cl_2) yielded **77** (254 mg, 75%) as a white powder.

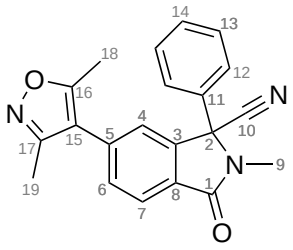

Mpt: 147.8-149.2 °C; ^{1}H-NMR ($CDCl_3$): δ_H 8.01 (dd, J = 8.0, 0.5 Hz, 1H, C(7)H), 7.48 (dd, J = 8.0, 1.5 Hz, 1H, C(6)H), 7.47-7.43 (m, 3H, C(13)H & C(14)H), 7.43-7.34 (m, 2H, C(12)H), 7.21 (dd, J = 1.5, 0.5 Hz, 1H, C(4)H), 3.05 (s, 3H, C(9)H_3), 2.37 (s, 3H, C(18)H_3), 2.21 (s, 3H, C(19)H_3); ^{13}C-NMR ($CDCl_3$): δ_C 166.9 (C(1)), 166.1 (C(16)), 158.1 (C(17)), 144.6 (C(3)), 136.1 (C(8)), 133.1 (C(5)), 131.1 (C(6)), 130.3 (C(14)), 129.8 (C(13)), 129.0 (C(11)), 125.9 (C(12)), 124.8 (C(7)), 123.3 (C(4)), 116.0 (C(15)), 115.5 (C(10)), 66.3 (C(2)), 26.0 (C(9)), 11.7 (C(18)), 10.8 (C(19)); IR ν_{max} 2918, 2322, 2207, 1703, 1359, 1011, 692; LR-ESI-MS: $C_{21}H_{18}N_3O_2$ $[M+H]^+$ *m/z* found 344.1 calcd 344.1; HR-ESI-MS: $C_{21}H_{17}N_3O_2Na$ $[M+Na]^+$ *m/z* found 366.1213 calcd 366.1209 error = 1.1 ppm.

6-(3,5-Dimethyl-1,2-oxazol-4-yl)-2-methyl-3-oxo-1-phenyl-2,3-dihydro-1*H*-isoindole-1-carboxamide (**78**)

Compound **77** (375 mg, 1.09 mmol) was dissolved in CH_2Cl_2 (31 mL), concentrated H_2SO_4 (7.8 mL) was added and the reaction mixture was stirred at reflux for 15 h. H_2O (35 mL) was added, the organic phase was separated and the aqueous phase was extracted with CH_2Cl_2 (3 x 35 mL). The combined organic phase was dried over Na_2SO_4, filtered and concentrated to yield **78** (318 mg, 81%) as a white solid.

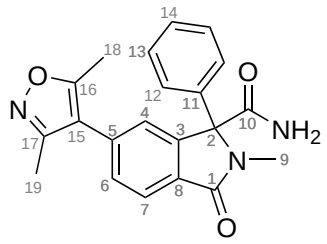

Mpt: >265 °C; ^{1}H-NMR ($CDCl_3$): δ_H 7.95 (d, J = 8.0 Hz, 1H, C(7)H), 7.51 (d, J = 1.0 Hz, 1H, C(4)H), 7.46 (dd, J = 7.5, 1.5 Hz, 1H, C(6)H), 7.39-7.33 (m, 3H, C(13)H & C(14)H), 7.16-7.13 (m, 2H, C(12)H), 6.27 (br s, 1H, NH), 5.67 (br s, 1H, NH), 2.93 (s, 3H, C(9)H_3), 2.40 (s, 3H, C(18)H_3), 2.26 (s, 3H, C(19)H_3); ^{13}C-NMR ($CDCl_3$): δ_C 171.2 (C(10)), 168.7 (C(1)), 166.0 (C(16)), 158.2 (C(17)), 146.5 (C(3)), 136.0 (C(8)), 135.4 (C(5)), 130.1 (C(6)), 129.8 (C(11)), 129.0 (C(14)), 128.9 (C(13)), 128.3 (C(12)), 124.4 (C(4)), 124.1 (C(7)), 115.8 (C(15)), 75.7 (C(2)), 26.9 (C(9)), 11.8 (C(18)), 10.8 (C(19)); IR ν_{max} 3351, 3156, 2924, 1682, 1374, 699; LR-ESI-MS: $C_{21}H_{20}N_3O_3$ $[M+H]^+$ m/z found 362.1 calcd 362.1; HR-ESI-MS: $C_{21}H_{19}N_3O_3Na$ $[M+Na]^+$ m/z found 384.1319 calcd 384.1308 error = 2.8 ppm.

5-(3,5-Dimethyl-1,2-oxazol-4-yl)-2-methyl-3-phenyl-2,3-dihydro-1*H*-isoindol-1-one (**81**), **(*S*)-5-(3,5-dimethyl-1,2-oxazol-4-yl)-2-methyl-3-phenyl-2,3-dihydro-1*H*-isoindol-1-one** ((–)-**81**/PNZ5) and **(*R*)-5-(3,5-dimethyl-1,2-oxazol-4-yl)-2-methyl-3-phenyl-2,3-dihydro-1*H*-isoindol-1-one** ((+)-**81**)

Method A. Compound **78** (25 mg, 0.07 mmol) was dissolved in THF (2 mL), concentrated HCl (0.2 mL) was added and the reaction was heated at reflux for 20 h. H_2O (20 mL) was added and the aqueous phase was extracted with EtOAc (3 x 20 mL). The combined organic extracts were dried over Na_2SO_4, filtered and concentrated. Purification by FCC (1% MeOH/CH_2Cl_2) yielded **81** (16.9 mg, 47%) as a colourless oil.

Method B. Under inert conditions, **60** (200 mg, 0.60 mmol) was dissolved in CH_2Cl_2 (3.6 mL) and the solution was cooled to 0 °C. TFA (0.6 mL) was added dropwise and the reaction mixture was stirred at 0 °C for 5 min. A solution of Et_3SiH (192 μL, 1.2 mmol) in CH_2Cl_2 (1.2 mL) was added slowly over 5 min and the reaction mixture was stirred at rt for 4 h. The reaction mixture was concentrated, $NaHCO_{3(aq)}$ (20 mL) and CH_2Cl_2 (20 mL) were added and the organic phase was separated. The organic phase was washed with H_2O (2 x 20 mL), dried over Na_2SO_4, filtered and concentrated. Purification by FCC (1% MeOH/CH_2Cl_2) yielded **81** (64 mg, 34%) as a colourless oil.

Method C. Compound **60** (55 mg, 0.16 mmol) was dissolved in toluene (5 mL), **68** (52 mg, 0.21 mmol) and DPP (2.0 mg, 0.008 mmol) were added and the reaction mixture was stirred at rt for 7 d. EtOAc (20 mL) was added, the organic phase was washed with $NH_4Cl_{(aq)}$ (2 x 20 mL) and H_2O (2 x 20 mL), dried over Na_2SO_4, filtered and concentrated. Purification by FCC (1% MeOH/CH_2Cl_2) yielded **81** (52 mg, 98%) as a colourless oil.

The enantiomers of **81** were preparatively resolved by HPLC (stationary phase: Semipreparative Chiralpak AD, solvent composition: hexane:iso-propanol 70:30, flow rate: 1.15 mL.min^{-1}, injection concentration: 16.5 mg.mL^{-1}, injection volume: 100 μL, λ: 220 nm) with the enantiomers eluting at 43.9 min ((–)-**81**/PNZ5) and 55.2 min ((+)-**81**).

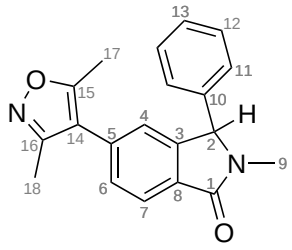

^{1}H-NMR ($CDCl_3$): δ_H 7.36 (dd, J = 7.5, 0.5 Hz, 1H, C(7)H), 7.40-7.29 (m, 5H, C(11)H, C(12)H & C(13)H), 7.24 (dd, J = 7.5, 1.5 Hz, 1H, C(6)H), 7.18 (s, 1H, C(4)H), 5.33 (s, 1H, C(2)H), 2.63 (s, 3H, C(9)H_3), 2.32 (s, 3H, C(17)H_3), 2.14 (s, 3H, C(18)H_3); ^{13}C-NMR ($CDCl_3$): δ_C 167.3 (C(1)), 165.8 (C(15)), 158.1 (C(16)), 149.9 (C(3)), 137.8 (C(8)), 134.9 (C(5)), 129.7 (C(6)), 129.2 (C(10)), 128.7 (C(12)), 128.6 (C(13)), 125.8 (C(11)), 123.4 (C(7)), 123.2 (C(4)), 115.9 (C(14)), 90.9 (C(2)), 23.9 (C(9)), 11.6 (C(17)), 10.6 (C(18)); IR ν_{max} 3449, 2929, 2867, 1685, 1421, 702; LR-ESI-MS: $C_{20}H_{19}N_2O_2$ $[M+H]^+$ m/z found 319.1 calcd 319.2, $C_{20}H_{18}N_2O_2Na$ $[M+Na]^+$ m/z found 341.1 calcd 341.1; HR-ESI-MS: $C_{20}H_{19}N_2O_2$ $[M+H]^+$ m/z found 319.14410 calcd 319.14432 error = 0.67 ppm; Analytical HPLC separation (stationary phase: Chiralpak AD, solvent composition: hexane:iso-propanol 80:20, flow rate: 1 mL.min^{-1}, injection concentration: 1 mg.mL^{-1}, injection volume: 10 μL, λ: 220 nm): t_1 = 13.5 min, t_2 = 17.4 min.

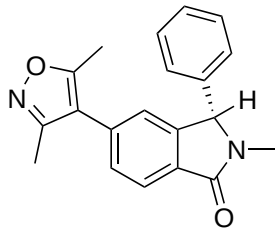

(–)-**413**: $[\alpha]_D{}^{20}$ - 25 (c 0.36, $CHCl_3$); Analytical HPLC ee determination: t_1 = 99.903, t_2 = 0.097, ee = >99%.

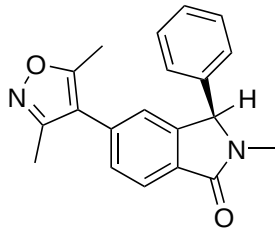

(+)-**81**: $[\alpha]_D{}^{20}$ + 15 (c 0.21, $CHCl_3$); Analytical HPLC ee determination: t_1 = 0.079, t_2 = 99.921, ee = >99%.

2-Benzyl-5-(3,5-dimethyl-1,2-oxazol-4-yl)-3-hydroxy-3-phenylisoindolin-1-one (**83**)
61 (18 mg, 0.05 mmol) was dissolved in EtOH (0.5 mL), benzylamine (0.5 mL) was added and the reaction mixture was stirred at 60 °C for 16 h. The reaction mixture was concentrated and purification by FCC (25% EtOAc/PE) yielded **83** (13 mg, 61%) as a white solid.

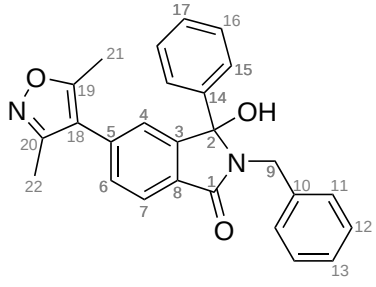

Mpt: 184-185 °C; ^{1}H-NMR ($CDCl_3$): δ_H 7.88 (d, J = 8.0 Hz, 1H, C(7)H), 7.38-7.35 (m, 2H, C(12)H), 7.34 (dd, J = 8.0, 1.5 Hz, 1H, C(6)H), 7.32-7.28 (m, 3H, C(11)H & C(13)H), 7.25-7.22 (m, 2H, C(16)H), 7.20-7.14 (m, 3H, C(15)H & C(17)H), 7.13 (d, J = 1.0 Hz, 1H, C(4)H), 4.79 (d, J = 15.0 Hz, 1H, C(9)H_a), 4.10 (d, J = 15.0 Hz, 1H, C(9)H_b), 2.30 (s, 3H, C(21)H_3), 2.14 (s, 3H, C(22)H_3); ^{13}C-NMR ($CDCl_3$): δ_C 167.2 (C(1)), 166.8 (C(19)), 158.1 (C(20)), 149.8 (C(3)), 138.0 (C(8)), 137.9 (C(5)), 135.3 (C(14)), 130.2 (C(6)), 129.4 (C(10)), 128.7 (C(16)), 128.6 (C(13)), 128.6 (C(11)), 128.3 (C(15)), 127.2 (C(17)), 126.2 (C(12)), 123.9 (C(7)), 123.1 (C(4)), 115.9 (C(18)), 91.6 (C(2)), 43.1 (C(9)), 11.6 (C(21)), 10.7 (C(22)); IR ν_{max} 3063, 3032, 2925, 1700, 1409, 1055, 640; LR-ESI-MS: $C_{26}H_{22}N_2O_3Na$ $[M+Na]^+$ m/z found 433.1 calcd 433.2, $C_{26}H_{21}N_2O_3$ $[M-H]^-$ m/z found 409.1 calcd 409.2; HR-ESI-MS: $C_{26}H_{22}N_2O_3Na$ $[M+Na]^+$ m/z found 433.1517 calcd

433.1523 error = 1.2 ppm.

2-[2-(Diethylamino)ethyl]-5-(3,5)-dimethyl-1,2-oxazol-4-yl)-3-hydroxyl-3-phenyl-2,3-dihydro-1*H*-isoindol-1-one (**84**)

Compound **61** (101 mg, 0.30 mmol) was dissolved in EtOH (4 mL), *N,N*-diethylethylenediamine (1 mL) was added and the reaction mixture was stirred at reflux for 14 h. The reaction mixture was concentrated and purification by FCC (50% EtOAc/PE) yielded **84** (20 mg, 16%) as an opaque oil.

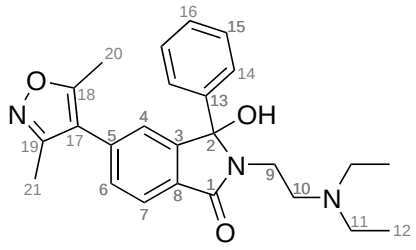

^{1}H-NMR ($CDCl_3$): δ_H 7.87 (d, J = 8.0 Hz, 1H, C(7)H), 7.44 (dd, J = 7.5, 1.5 Hz, 2H, C(14)H), 7.39-7.32 (m, 3H, C(15)H & C(16)H), 7.30 (dd, J = 8.0, 1.5 Hz, 1H, C(6)H), 7.08 (d, J = 1.0 Hz, 1H, C(4)H), 4.12-4.04 (m, 1H, OH), 2.95-2.78 (m, 2H, C(9)H), 2.70-2.59 (m, 2H, C(10)H), 2.49-2.37 (m, 4H, C(11)H_2), 2.33 (s, 3H, C(20)H_3), 2.18 (s, 3H, C(21)H_3), 1.04 (t, J = 7.0 Hz, 6H, C(12)H_3); ^{13}C-NMR ($CDCl_3$): δ_C 181.5 (C(1)), 165.7 (C(18)), 158.3 (C(19)), 149.5 (C(3)), 140.6 (C(8)), 135.0 (C(5)), 129.4 (C(6)), 128.8 (C(13)), 128.6 (C(15)), 128.3 (C(16)), 126.3 (C(14)), 123.7 (C(7)), 122.9 (C(4)), 116.1 (C(17)), 89.7 (C(2)), 52.3 (C(11)), 45.7 (C(9)), 37.7 (C(10)), 11.7 (C(20)), 10.8 (C(21)), 10.0 (C(12)); IR ν_{max} 2973, 1699, 1625, 1385, 1060, 704; LR-ESI-MS: $C_{25}H_{30}N_3O_3$ $[M+H]^+$ *m/z* found 420.2 calcd 420.3, $C_{25}H_{29}N_3O_3Na$ $[M+Na]^+$ *m/z* found 442.2 calcd 442.2; HR-ESI-MS: $C_{25}H_{29}N_3O_3Na$ $[M+Na]^+$ *m/z* found 442.2101 calcd 442.2107 error = 1.7 ppm.

2-Benzoyl-*N*-(2,2-dimethoxyethyl)-4-(3,5-dimethyl-1,2-oxazol-4-yl)benzamide (**85**) and **2-(2,2-dimethoxyethyl)-5-(3,5-dimethyl-1,2-oxazol-4-yl)-3-hydroxy-3-phenyl-2,3-dihydro-1*H*-isoindol-1-one** (**86**)

Compound **61** (103 mg, 0.31 mmol) was dissolved in EtOH (4 mL), aminoacetaldehyde dimethyl acetal (1 mL) and NEt_3 (0.1 mL) were added and the reaction mixture was stirred at reflux for 14 h. The reaction mixture was concentrated and purification by iterative FCC (50% EtOAc/PE then 5% MeOH/EtOAc) yielded **85** (47 mg, 37%) and **86** (21 mg, 18%) as opaque oils.

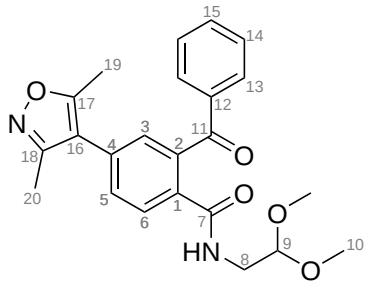

85: ^{1}H-NMR ($CDCl_3$): δ_H 8.07 (d, J = 8.0 Hz, 1H, C(3)H), 7.74 (dd, J = 8.5, 1.5 Hz, 2H, C(13)H), 7.47 (tt, J = 7.5, 1.5 Hz, 1H, C(15)H), 7.38-7.31 (m, 3H, C(5)H & C(14)H), 7.10 (d, J = 2.0 Hz, 1H, C(3)H), 6.21 (br s, 1H, NH), 4.31 (t, J = 5.5 Hz, 1H, C(9)H), 3.19 (s, 6H, C(10)H_3), 2.53 (d, J = 5.5 Hz, 2H, C(8)H_2), 2.39 (s, 3H, C(19)H_3), 2.25 (s, 3H, C(20)H_3); ^{13}C-NMR ($CDCl_3$): δ_C 198.5 (C(11)), 171.4 (C(7)), 165.6 (C(17)), 158.3 (C(18)), 141.9 (C(2)), 137.6 (C(12)), 135.3 (C(4)), 132.6 (C(15)), 132.4 (C(1)), 130.5 (C(5)), 129.4 (C(6)), 129.2 (C(14)), 128.3 (C(13)), 126.8 (C(3)), 115.6 (C(16)), 100.7 (C(9)), 54.2 (C(10)), 40.2 (C(8)), 11.6 (C(19)), 10.8 (C(20)); IR ν_{max} 2935, 1671, 1581, 1374, 1235, 1075, 731, 702; LR-ESI-MS: $C_{23}H_{25}N_2O_5$ $[M+H]^+$ *m/z* found 409.2 calcd 409.2; HR-ESI-MS: $C_{23}H_{24}N_2O_5Na$ $[M+Na]^+$ *m/z* found 431.15774 calcd 431.15782 error = 0.15 ppm.

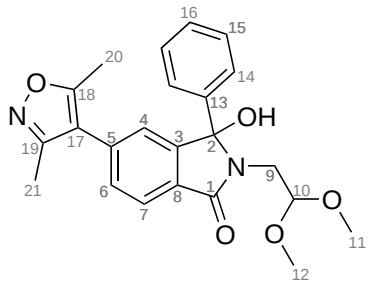

86: ^{1}H-NMR ($CDCl_3$): δ_H 7.90 (dd, J = 7.5, 0.5 Hz, 1H, C(7)H), 7.42-7.32 (m, 6H, C(6)H, C(14)H, C(15)H & C(16)H), 7.13 (d, J = 0.8 Hz, 1H, C(4)H), 5.48 (br s, 1H, OH), 4.65 (dd, J = 6.9, 3.2 Hz, 1H, C(10)H), 4.07 (dd, J = 15.0, 3.0 Hz, 1H, C(9)H_a), 3.44 (s, 3H, C(11)H_3), 3.43 (s, 3H, C(12)H_3), 2.92 (dd, J = 15.0, 7.0 Hz, 1H, C(9)H_b), 2.34 (s, 3H, C(20)H_3), 2.20 (s, 3H, C(21)H_3), ^{13}C-NMR ($CDCl_3$): δ_C 167.9 (C(1)), 165.8 (C(18)), 158.3 (C(19)), 150.1 (C(3)), 139.0 (C(8)), 135.4 (C(5)), 129.9 (C(6)), 128.8 (C(15)), 128.7 (C(16)), 128.6 (C(16)), 126.1 (C(14)), 123.9 (C(7)), 123.0 (C(4)), 116.0 (C(17)), 102.3 (C(10)), 90.8 (C(2)), 55.4 (C(11)), 54.7 (C(12)), 41.6 (C(9)), 11.7 (C(20)), 10.8 (C(21)); IR ν_{max} 3317, 2935, 1703, 1626, 1409, 1124, 1059, 703; LR-ESI-MS: $C_{23}H_{25}N_2O_5$ $[M+H]^+$ m/z found 409.2 calcd 409.2; HR-ESI-MS: $C_{23}H_{24}N_2O_5Na$ $[M+Na]^+$ m/z found 431.15774 calcd 431.15786 error = 0.24 ppm.

5-(3,5)-Dimethyl-1,2-oxazol-4-yl)-3-hydroxy-2-(2-hydroxyethyl)-3-phenyl-2,3-dihydro-1*H*-isoindol-1-one (**87**) and **8-(3,5-dimethyl-1,2-oxazol-4-yl)-9b-phenyl-2,3-dihydro[1,3]oxazolo[2,3-*a*]isoindol-5(9b*H*)-one** (**88**)

Compound **61** (120 mg, 0.36 mmol) was dissolved in EtOH (3 mL), ethanolamine (1 mL) was added and the reaction mixture was stirred at reflux for 14 h. EtOAc (20 mL) was added, the organic phase was washed with 1M HCl (3 x 20 mL), H_2O (3 x 20 mL), dried over Na_2SO_4, filtered and concentrated. Purification by iterative FCC (25% EtOAc/PE then 1% MeOH/EtOAc) yielded **87** (18 mg, 14%) and **88** (32 mg, 26%) as opaque oils.

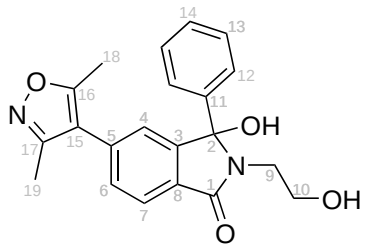

87: ^{1}H-NMR ($CDCl_3$): δ_H 7.81 (d, J = 7.5 Hz, 1H, C(7)H), 7.41-7.33 (m, 5H, C(12)H, C(13)H & C(14)H), 7.32 (dd, J = 8.0, 1.5 Hz, 1H, C(6)H), 7.13 (d, J = 0.5 Hz, 1H, C(4)H), 3.91 (ddd, J = 15.0, 3.5, 3.0 Hz, 1H, C(9)H_a), 3.81-3.69 (m, 2H, C(10)H_2), 3.01 (ddd, J = 15.0, 8.5, 3.5 Hz, 1H, C(9)H_b), 2.32 (s, 3H, C(18)H_3), 2.16 (s, 3H, C(19)H_3); ^{13}C-NMR ($CDCl_3$): δ_C 168.3 (C(1)), 165.8 (C(16)), 159.2 (C(17)), 150.0 (C(3)), 138.6 (C(8)), 135.3 (C(5)), 130.0 (C(6)), 128.9 (C(14)), 128.8 (C(13)), 128.7 (C(11)), 126.1 (C(12)), 123.7 (C(7)), 123.1 (C(4)), 116.0 (C(15)), 90.8 (C(2)), 61.5 (C(10)), 42.2 (C(9)), 11.6 (C(18)), 10.7 (C(19)); IR ν_{max} 3374, 1700, 1624, 1409, 1057, 704; LR-ESI-MS: $C_{21}H_{21}N_2O_4$ $[M+H]^+$ m/z found 365.1 calcd 365.2, $C_{21}H_{20}N_2O_4Na$ $[M+Na]^+$ m/z found 387.1 calcd 387.1, $C_{21}H_{19}N_2O_4$ $[M-H]^-$ m/z found 363.0 calcd 363.1; HR-ESI-MS: $C_{21}H_{21}N_2O_4$ $[M+H]^+$ m/z found 365.1496 calcd 365.1497 error = 0.45 ppm.

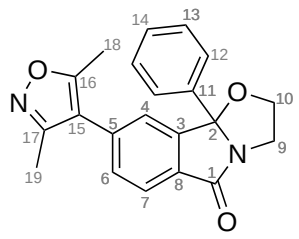

88: ^{1}H-NMR ($CDCl_3$): δ_H 7.86 (dd, J = 8.0, 0.5 Hz, 1H, C(7)H), 7.61 (dd, J = 8.5, 1.5 Hz, 2H, C(12)H), 7.44-7.38 (m, 3H, C(13)H & C(14)H), 7.38 (dd, J = 8.0, 1.5 Hz, 1H, C(6)H), 7.15 (d, J = 0.5 Hz, 1H, C(4)H), 4.45-4.37 (m, 1H, C(10)H_a), 4.21-4.12 (m, 2H, C(10)H_b & C(9)H_a), 3.35-3.28 (m, 1H, C(9)H_b), 2.34 (s, 3H, C(18)H_3), 2.19 (s, 3H, C(19)H_3); ^{13}C-NMR ($CDCl_3$): δ_C 173.3 (C(1)), 165.9 (C(16)), 158.2 (C(17)), 147.5 (C(3)), 137.6 (C(8)), 135.8 (C(5)), 130.8 (C(6)), 130.2 (C(11)), 129.0 (C(14)), 128.8 (C(13)), 125.6 (C(12)), 124.7 (C(7)), 123.9 (C(4)), 115.8 (C(15)), 100.2 (C(2)), 70.2 (C(10)), 41.6 (C(9)), 11.6 (C(18)), 10.7 (C(19)); IR ν_{max} 3059, 2360, 2161,

1722, 1620, 1342, 1041, 702; LR-ESI-MS: $C_{21}H_{19}N_2O_3$ $[M+H]^+$ *m/z* found 347.1 calcd 347.1; HR-ESI-MS: $C_{21}H_{19}N_2O_3$ $[M+H]^+$ *m/z* found 347.13902 calcd 347.1392 error = 0.49 ppm.

2-Benzoyl-*N*-(1,3-dihydroxy-2-methylpropan-2-yl)-4-(3,5-dimethyl-1,2-oxazol-4-yl)benzamide (**89**)

Compound **61** (101 mg, 0.30 mmol) was dissolved in EtOH (5 mL), 2-amino-2-methyl-1,3-propanediol (1.0 g, 9.5 mmol) and NEt_3 (0.1 mL) were added and the reaction mixture was stirred at reflux for 2 d. The reaction mixture was concentrated and purification by FCC (1% $MeOH/CH_2Cl_2$) yielded **89** (52 mg, 42%) as an opaque oil.

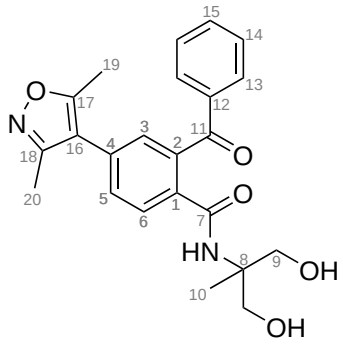

^{1}H-NMR ($CDCl_3$): δ_H 7.82 (dd, J = 8.5, 1.5 Hz, 2H, C(13)H), 7.72 (d, J = 8.0 Hz, 1H, C(6)H), 7.61 (tt, J = 7.5, 1.5 Hz, 1H, C(15)H), 7.47 (t, J = 8.0 Hz, 2H, C(14)H), 7.44 (dd, J = 8.0, 2.0 Hz, 1H, C(5)H), 7.33 (d, J = 2.0 Hz, 1H, C(3)H), 6.68 (br s, 1H, NH), 4.00 (br s, 2H, OH), 3.70 (d, J = 11.5 Hz, 2H, C(9)H_a), 3.58 (d, J = 11.5 Hz, 2H, C(9)H_b), 2.40 (s, 3H, C(19)H_3), 2.25 (s, 3H, C(20)H_3), 1.15 (s, 3H, C(10)H_3); ^{13}C-NMR ($CDCl_3$): δ_C 197.1 (C(11)), 168.9 (C(7)), 166.0 (C(17)), 158.2 (C(18)), 138.8 (C(2)), 136.5 (C(12)), 136.3 (C(4)), 133.8 (C(15)), 132.5 (C(1)), 131.0 (C(5)), 130.1 (C(14)), 129.6 (C(6)), 128.6 (C(13)), 127.9 (C(3)), 115.2 (C(16)), 67.5 (C(9)), 59.0 (C(8)), 19.0 (C(10)), 11.6 (C(19)), 10.7 (C(20)); IR ν_{max} 2916, 2358, 1702, 1417, 1059, 701; LR-ESI-MS: $C_{23}H_{25}N_2O_5$ $[M+H]^+$ *m/z* found 409.2 calcd 409.2, $C_{23}H_{24}N_2O_5Na$ $[M+Na]^+$ *m/z* found 431.2 calcd 431.2, $C_{23}H_{23}N_2O_5$ $[M-H]^-$ *m/z* found 407.1 calcd 407.2; HR-ESI-MS: $C_{23}H_{25}N_2O_5$ $[M+H]^+$ *m/z* found 409.17580 calcd 409.17659 error = 1.97 ppm.

5-(3,5-Dimethyl-1,2-oxazol-4-yl)-3-phenyl-2,3-dihydro-1*H*-isoindol-1-one (**91**)

Method A. Compound **61** (62 mg, 0.15 mmol) was dissolved in EtOH (2 mL), allylamine (0.5 mL) was added and the reaction mixture was stirred at reflux for 36 h. The reaction mixture was concentrated and purification by FCC (35% EtOAc/PE) yielded **91** (16 mg, 29%) as a white solid.

Method B. Compound **92** (20 mg, 0.062 mmol) was dissolved in CH_2Cl_2 (2.5 mL), **119** (24 mg, 0.078 mmol) and DPP (0.8 mg, 0.0003 mmol) were added and the reaction mixture was stirred at rt for 36 h. The reaction mixture was concentrated and purification by preparative TLC (5% $MeOH/CH_2Cl_2$) yielded **91** (10 mg, 53%) as a white solid.

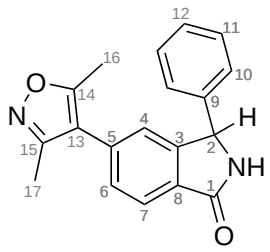

Mpt: 72.0-72.4 °C; ^{1}H-NMR ($CDCl_3$): δ_H 7.91 (d, J = 8.0 Hz, 1H, C(7)H), 7.66 (br s, 1H, NH), 7.39-7.28 (m, 6H, C(6)H, C(10)H, C(11)H & C(12)H), 7.10 (s, 1H, C(4)H), 5.69 (s, 1H, C(2)H), 2.34 (s, 3H, C(16)H_3), 2.19 (s, 3H, C(17)H_3); ^{13}C-NMR ($CDCl_3$): δ_C 170.8 (C(1)), 165.7 (C(14)), 158.2 (C(15)), 148.6 (C(3)), 138.0 (C(8)), 134.7 (C(5)), 130.1 (C(9)), 129.2 (C(6)), 129.1 (C(11)), 128.6 (C(12)), 126.7 (C(10)), 124.1 (C(7)), 123.7 (C(4)), 116.0 (C(13)), 60.8 (C(2)), 11.6 (C(16)), 10.7 (C(17)); IR ν_{max} 3201, 3063, 2928, 1696, 1620, 730, 701; LR-ESI-MS: $C_{19}H_{17}N_2O_2$ $[M+H]^+$ *m/z* found 305.1 calcd 305.1; $C_{19}H_{16}N_2O_2Na$ $[M+Na]^+$ *m/z* found 327.1 calcd 327.1; HR-ESI-MS: $C_{19}H_{17}N_2O_2$ $[M+H]^+$ *m/z* found 305.12955 calcd 305.12860 error = 3.11 ppm; Analytical HPLC separation (stationary phase: Chiralpak AD, solvent composition: hexane:iso-propanol

60:40, flow rate: 1 mL.min^{-1}, injection concentration: 1 mg.mL^{-1}, injection volume: 10 μL, λ: 220 nm): t_1 = 21.7 min, t_2 = 24.5 min.

5-(3,5-Dimethyl-1,2-oxazol-4-yl)-3-hydroxy-3-phenyl-2,3-dihydro-1*H*-isoindol-1-one (92)

Compound **61** (553 mg, 1.65 mmol) was dissolved in 1,4-dioxane (1.1 mL), $NH_4OH_{(aq)}$ (1.1 ml, 28%) was added and the reaction mixture was stirred at 80 °C for 20 h. EtOAc (100 mL) was added, the organic phase was washed with H_2O (3 x 100 mL), dried over Na_2SO_4, filtered and concentrated. Purification by FCC (25% EtOAc/PE) yielded **92** (81 mg, 15%) as an opaque oil.

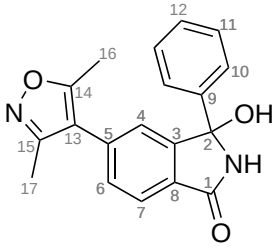

^{1}H-NMR ($CDCl_3$): δ_H 7.79 (d, J = 8.0 Hz, 1H, C(7)H), 7.58 (dd, J = 8.0, 2.0 Hz, 2H, C(10)H), 7.41-7.36 (m, 3H, C(11)H & C(12)H), 7.34 (dd, J = 8.0, 1.5 Hz, 1H, C(6)H), 7.24 (s, 1H, C(4)H), 6.85 (br s, 1H, NH), 3.97 (br s, 1H, OH), 2.36 (s, 3H, C(16)H_3), 2.21 (s, 3H, C(17)H_3); ^{13}C-NMR ($CDCl_3$): δ_C 169.6 (C(1)), 165.9 (C(14)), 158.1 (C(15)), 150.8 (C(3)), 139.7 (C(8)), 135.7 (C(5)), 129.9 (C(6)), 128.7 (C(12)), 128.7 (C(11)), 128.4 (C(9)), 125.4 (C(10)), 123.9 (C(7)), 123.3 (C(8)), 115.8 (C(13)), 88.2 (C(2)), 11.6 (C(16)), 10.7 (C(17)); IR ν_{max} 3251, 2358, 2341, 1702, 1620, 1417, 1059, 701; LR-ESI-MS: $C_{19}H_{17}N_2O_3$ $[M+H]^+$ m/z found 321.1 calcd 321.1, $C_{19}H_{16}N_2O_3Na$ $[M+Na]^+$ m/z found 343.1 calcd 343.1, $C_{19}H_{15}N_2O_3$ $[M-H]^-$ m/z found 319.0 calcd 319.1; HR-ESI-MS: $C_{19}H_{17}N_2O_3$ $[M+H]^+$ m/z found 321.12337 calcd 321.12350 error = 0.42 ppm.

Dimethyl 2,6-diethyl-1,4-dihydropyridine-3,5-dicarboxylate (117)

Methyl propionylacetate (260 mg, 2.0 mmol), paraformaldehyde (30 mg, 1.0 mmol) and NH_4OAc (116 mg, 1.5 mmol) were combined and stirred at 80 °C for 15 min. Cold H_2O (10 mL) was added and the resultant precipitate was filtered. Recrystallisation (MeOH) yielded **117** (138 mg, 55%) as yellow prisms.

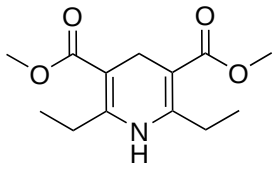

Mpt: 132.0-132.2 °C (lit. 129-131 °C); ^{1}H-NMR ($CDCl_3$): δ_H 5.29 (br s, 1H), 3.71 (s, 6H), 3.28 (s, 2H), 2.62 (q, J = 7.5 Hz, 4H), 1.16 (t, J = 7.5 Hz, 6H); ^{13}C-NMR ($CDCl_3$): δ_C 167.9, 151.0, 98.2, 51.0, 25.6, 24.9, 12.6; LR-ESI-MS: $C_{13}H_{18}NO_4$ $[M-H]^-$ m/z found 252.1 calcd 252.1, $C_{13}H_{19}NO_4Na$ $[M+Na]^+$ m/z found 276.1 calcd 276.1. Data are in accordance with literature values.[308]

Dimethyl 2,6-dimethyl-1,4-dihydropyridine-3,5-dicarboxylate (118)

Methyl acetoacetate (0.81 mL, 7.5 mmol), paraformaldehyde (113 mg, 3.8 mmol) and NH_4OAc (436 mg, 5.7 mmol) were combined and stirred at 80 °C for 30 min. Cold H_2O (10 mL) was added and the resultant precipitate was filtered. Recrystallisation (MeOH) yielded **118** (619 mg, 73%) as yellow crystals.

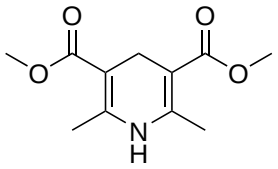

Mpt: 229.3-229.8 °C (lit. 230-231 °C); ^{1}H-NMR ($CDCl_3$): δ_H 5.17 (br s, 1H), 3.71 (s, 6H), 3.28 (s, 2H), 2.21 (s, 6H); ^{13}C-NMR ($CDCl_3$): δ_C 168.4, 145.1, 99.3, 51.0, 24.8, 19.1; LR-ESI-MS: $C_{11}H_{15}NO_4Na$ $[M+Na]^+$ m/z found 248.1 calcd 248.1, $C_{11}H_{14}NO_4$ $[M-H]^-$ m/z found 224.1 calcd 224.1. Data are in accordance with literature values.[309]

Di-*tert*-butyl 2,6-dimethyl-1,4-dihydropyridine-3,5-dicarboxylate (**119**)

tert-Butyl acetoacetate (1.25 mL, 7.5 mmol), paraformaldehyde (113 mg, 3.8 mmol) and NH_4OAc (436 mg, 5.7 mmol) were combined and stirred at 80 °C for 30 min. Cold H_2O (10 mL) was added and the resultant precipitate was filtered. Recrystallisation (MeOH) yielded **119** (293 mg, 25%) as a yellow powder.

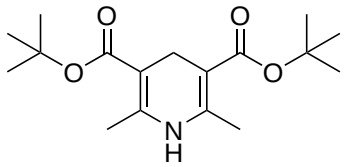

Mpt: 147.8-149.7 °C (lit. 151-153 °C); ^{1}H-NMR ($CDCl_3$): δ_H 5.11 (br s, 1H), 3.19 (s, 2H), 2.16 (s, 6H), 1.50 (s, 18H); ^{13}C-NMR ($CDCl_3$): δ_C 167.6, 143.8, 100.9, 79.4, 28.4, 25.4, 19.2; LR-ESI-MS: $C_{17}H_{26}NO_4$ $[M\text{-}H]^-$ *m/z* found 308.1 calcd 308.2, $C_{17}H_{27}NO_4Na$ $[M+Na]^+$ *m/z* found 332.1 calcd 332.2. Data are in accordance with literature values.[308]

Di(adamantan-1-yl) 2,6-dimethyl-1,4-dihydropyridine-3,5-dicarboxylate (**121**)

Adamantan-1-yl 3-oxobutanoate (580 mg, 2.45 mmol), paraformaldehyde (37 mg, 1.23 mmol) and NH_4OAc (143 mg, 1.85 mmol) were combined and stirred at 80 °C for 15 min. Cold H_2O (10 mL) was added and the resultant precipitate was filtered. Recrystallisation (MeOH) yielded **121** (619 mg, 73%) as a pale yellow powder.

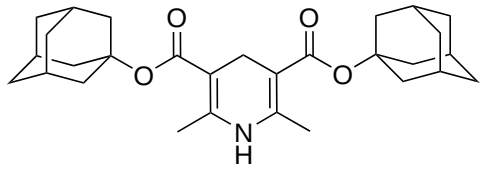

Mpt: 214.1-216.0 °C (lit. 216 °C); ^{1}H-NMR ($CDCl_3$): δ_H 5.00 (br s, 1H), 2.80 (s, 2H), 2.27 (s, 6H), 2.19-2.13 (m, 18H), 1.75-1.62 (m, 12H); ^{13}C-NMR ($CDCl_3$): δ_C 167.3, 143.7, 100.9, 79.5, 41.7, 36.3, 30.8, 25.4, 19.3; LR-ESI-MS: $C_{29}H_{38}NO_4$ $[M\text{-}H]^-$ *m/z* found 464.2 calcd 464.3. Data are in accordance with literature values.[310]

***tert*-Butyl methyl 2,6-dimethyl-1,4-dihydropyridine-3,5-dicarboxylate** (**122**)

Methyl acetoacetate (2.8 mL, 26 mmol), *tert*-butyl acetoacetate (4.31 mL, 26 mmol), NH_4OAc (2.0 g, 26 mmol) and hexamethylenetetramine (3.64 g, 26 mmol) were combined and stirred at 100 °C for 30 min. The reaction mixture was concentrated and CH_2Cl_2 (100 mL) was added. The organic phase was washed with H_2O (3 x 100 mL), dried over Na_2SO_4, filtered and concentrated. Purification by iterative FCC (5% MeOH/CH_2Cl_2 then 6%EtOAc/PE) yielded **122** (137 mg, 2%) as yellow crystals.

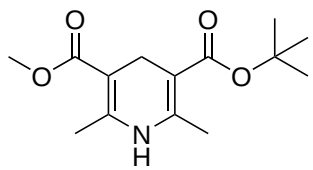

Mpt: 75.0-76.2 °C (no Mpt reported in lit.); ^{1}H-NMR ($CDCl_3$): δ_H 5.08 (br s, 1H), 3.93 (s, 3H), 2.84 (s, 3H), 2.82 (s, 3H), 2.20 (s, 1H), 2.17 (s, 1H), 1.62 (s, 9H); ^{13}C-NMR ($CDCl_3$): δ_C 166.5, 165.4, 161.8, 140.8, 124.8, 122.6, 82.3, 52.3, 28.4, 28.2, 25.0, 24.9; LR-ESI-MS: $C_{14}H_{20}NO_4$ $[M\text{-}H]^-$ *m/z* found 266.1 calcd 266.1. Data are in accordance with literature values.[311]

Ethyl 4-(3,5-dimethyl-1,2-oxazol-4-yl)benzoate (**126**)

In a pressure tube under inert conditions, ethyl 4-bromobenzoate (6.63 mL, 40.6 mmol), KOAc (7.97 g, 81.2 mmol) and $PdCl_2$ (72 mg, 0.406 mmol) were combined. 3,5-dimethylisoxazole (5.97 mL, 60.9 mmol) was added to DMAc (100 mL) under inert conditions and the solution was degassed. This solution was added to the tube, the tube was sealed and the reaction mixture

was stirred at 130 °C for 16 h. The reaction mixture was passed through a plug of Celite and the Celite was washed with CH_2Cl_2 (200 mL). The combined filtrate was concentrated and EtOAc (250 mL) was added. The organic phase was washed with H_2O (2 x 250 mL), dried over Na_2SO_4, filtered and concentrated. Purification by FCC (8% EtOAc/PE) yielded **126** (9.22 g, 93%) as a white powder.

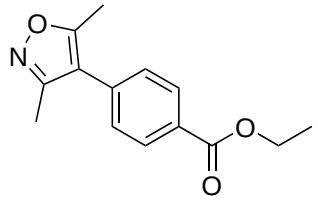

Mpt: 69.6-70.8 °C (lit. 71.1-72.2 °C); ^{1}H-NMR ($CDCl_3$): δ_H 8.05 (d, J = 8.5 Hz, 2H), 7.26 (d, J = 8.5 Hz, 2H), 4.33 (q, J = 7.0 Hz, 2H), 2.36 (s, 3H), 2.22 (s, 3H), 1.34 (t, J = 7.0 Hz, 3H); ^{13}C-NMR ($CDCl_3$): δ_C 166.1, 165.7, 158.4, 135.1, 130.0, 129.5, 128.8, 116.0, 61.1, 14.3, 11.7, 10.8; LR-ESI-MS: $C_{14}H_{16}NO_3$ $[M+H]^+$ *m/z* found 246.1 calcd 246.1, $C_{14}H_{15}NO_3Na$ $[M+Na]^+$ *m/z* found 268.1 calcd 268.1. Data are in accordance with literature values.[312]

4-(3,5-Dimethyl-1,2-oxazol-4-yl)-*N*-methylbenzamide (**127**)

In a pressure tube, **126** (0.5 g, 2.0 mmol) and $MeNH_2$ (4 mL, 40 mmol, sat. ethanolic soln) were combined, the tube was sealed and the reaction mixture was stirred at 70 °C for 18 h. The reaction mixture was concentrated and purification by FCC (80% EtOAc/PE) yielded **127** (335 mg, 71%) as a white powder.

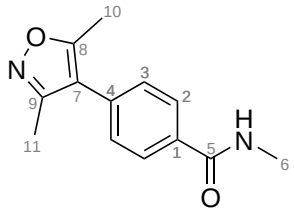

Mpt: 142.6-143.8 °C; ^{1}H-NMR ($CDCl_3$): δ_H 7.86 (d, J = 8.5 Hz, 2H, C(2)H), 7.29 (d, J = 8.5 Hz, 2H, C(3)H), 6.70 (br s, 1H, NH), 3.01 (d, J = 5.0 Hz, 3H, C(6)H_3), 2.39 (s, 3H, C(10)H_3), 2.24 (s, 3H, C(11)H_3); ^{13}C-NMR ($CDCl_3$): δ_C 167.6 (C(5)), 165.5 (C(8)), 158.3 (C(9)), 133.6 (C(4)), 133.5(C(1)), 129.0 (C(2)), 127.4 (C(3)), 115.9 (C(7)), 26.8 (C(6)), 11.5 (C(10)), 10.7 (C(11)); IR ν_{max} 3274, 2362, 1626, 1558, 1316, 687; LR-ESI-MS: $C_{13}H_{15}N_2O_2$ $[M+H]^+$ *m/z* found 231.1 calcd 231.1, $C_{13}H_{14}N_2O_2Na$ $[M+Na]^+$ *m/z* found 253.1 calcd 253.1; HR-ESI-MS: $C_{13}H_{15}N_2O_2$ $[M+H]^+$ *m/z* found 231.11390 calcd 231.11288 error = 4.4 ppm.

4-(3,5-Dimethyl-1,2-oxazol-4-yl)benzoic acid (**128**)

Compound **126** (1.1 g, 4.1 mmol) was dissolved in NaOH (20.4 mL, 2M ethanolic soln) and the reaction mixture was stirred at reflux for 24 h. H_2O (200 mL) was added, the aqueous phase was washed with Et_2O (3 x 200 mL) and acidifed with concentrated HCl. Et_2O (200 mL) was added and the organic phase was washed with H_2O (3 x 200 mL), dried over Na_2SO_4, filtered and concentrated to yield **128** (0.91 g, 94%) as a white solid.

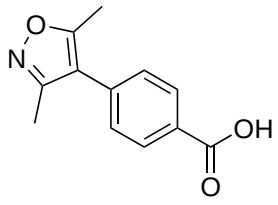

Mpt: 130.6-131.9 °C (lit. 130 °C); ^{1}H-NMR (DMSO): δ_H 13.03 (br s, 1H), 8.02 (d, J = 8.5 Hz, 2H), 7.53 (d, J = 8.5 Hz, 2H), 2.44 (s, 3H), 2.25 (s, 3H); ^{13}C-NMR (DMSO): δ_C 167.0, 165.8, 158.0, 134.5, 129.7, 129.6, 128.9, 115.3, 11.5, 10.5; LR-ESI-MS: $C_{12}H_{10}NO_3$ $[M-H]^-$ *m/z* found 216.1 calcd 216.1. Data are in accordance with literature values.[313]

7.3 BRD9

Methyl 4-nitrobutanoate (**13**)

Methyl acrylate (4.2 mL, 46 mmol) was suspended in nitromethane (12.5 mL, 230 mmol), K_2CO_3 (0.63 g, 4.6 mmol) was added and the reaction mixture was stirred at rt for 16 hours. The reaction mixture was filtered and the fitrate was concentrated. Purification by FCC (20% EtOAc/PE) yielded **13** (1.6 g, 47%) as a yellow liquid.

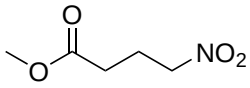

^{1}H-NMR ($CDCl_3$): δ_H 4.49 (t, J = 6.5 Hz, 2H), 3.72 (s, 3H), 2.49 (t, J = 7.0 Hz, 2H), 2.33 (quin, J = 7.0 Hz, 2H); ^{13}C-NMR ($CDCl_3$): δ_C 169.8, 74.3, 51.9, 30.2, 22.3; LR-ESI-MS: $C_5H_9NO_4Na$ $[M+Na]^+$ *m/z* found 170.1 calcd 170.1. Data are in accordance with literature values.[314]

***N*-(3-Bromophenyl)-3-oxobutanamide** (**216**)

m-Bromoaniline (20.1 mL, 184 mmol) was dissolved in xylenes (87 mL), ethyl acetoacetate (14.6 mL, 115 mmol) was added and the reaction mixture was stirred at reflux for 16 hours. The reaction mixture was cooled, Na_2CO_3 (500 mL, sat. aq. soln) was added and the aqueous phase was extracted with CH_2Cl_2 (3 x 500 mL). The combined organic extracts were dried over Na_2SO_4, filtered and concentrated. Trituration with hexane and cooling to 0 °C yielded **216** (7.16 g, 24%) as a white powder.

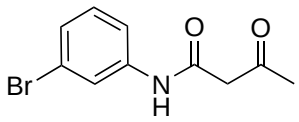

Mpt: 109.8-110.8 °C; ^{1}H-NMR ($CDCl_3$): δ_H 9.29 (br s, 1H), 7.83 (s, 1H), 7.44 (d, J = 8.0 Hz, 1H), 7.25 (d, J = 8.0 Hz, 1H), 7.18 (t, J = 8.0 Hz, 1H), 3.60 (s, 2H), 2.33 (s, 3H); ^{13}C-NMR ($CDCl_3$): δ_C 205.3, 163.5, 138.7, 130.2, 127.5, 123.0, 122.6, 118.6, 49.3, 31.3; LR-ESI-MS: $C_{10}H_{10}BrNO_2$ $[M+H]^+$ *m/z* found 255.9 calcd 256.0. Data are in accordance with literature values.[315]

7-Bromo-4-methylquinolin-2(1*H*)-one (**217**)

Compound **216** (5.0 g, 19.5 mmol) was suspended in concentrated sulfuric acid (23.4 mL) and the reaction mixture was stirred at 95 °C for 2 h. The reaction mixture was poured into water (2.3L) and the resulting precipitate was filtered off to yield **217** (4.0 g, 88%) as a white opaque oil.

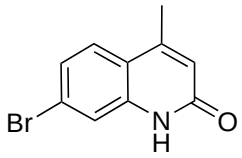

^{1}H-NMR ($CDCl_3$): δ_H 11.68 (br s, 1H), 7.65 (d, J = 8.5 Hz, 1H), 7.47 (d, J = 2.0 Hz, 1H), 7.35 (dd, J = 8.5, 2.0 Hz, 1H), 6.43 (d, J = 1.0 Hz, 1H), 2.40 (d, J = 1.0 Hz, 3H); ^{13}C-NMR ($(CD_3)_2SO$): δ_C 161.5, 147.7, 139.8, 126.8, 124.4, 123.3, 121.3, 118.7, 117.5, 18.4; LR-ESI-MS: $C_{10}H_9BrNO$ $[M+H]^+$ *m/z* found 238.0 calcd 237.9. Data are in accordance with literature values.[315]

7-Bromo-1,4-dimethylquinolin-2(1*H*)-one (**218**)

Compound **217** (4.0 g, 16.8 mmol) was dissolved in DMF (200 mL), MeI (1.15 mL, 18.5 mmol) and NaH (0.81 g, 20.2 mmol, 60% dispersion in mineral oil) were added and the reaction mixture was stirred at rt for 12 h. H_2O (10 mL) was slowly added and the reaction mixture was concentrated. EtOAc (250 mL) was added and the organic phase was washed with H_2O (3 x 250 mL), dried over Na_2SO_4, filtered and concentrated. Trituration (hexane/EtOAc) yielded **218** (3.57 g, 84%) as white crystals.

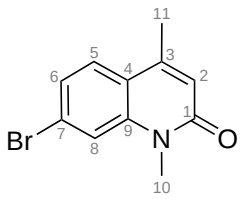

Mpt: 105.7-107.3 °C; ^{1}H-NMR ($CDCl_3$): δ_H 7.55 (d, J = 7.5 Hz, 1H, C(5)H), 7.53 (s, 1H, C(8)H), 7.37 (dd, J = 8.5, 2.0 Hz, 1H, C(6)H), 6.61 (d, J = 1.0 Hz, 1H, C(2)H), 3.68 (s, 3H, C(10)H_3), 2.45 (d, J = 1.0 Hz, 3H, C(11)H_3); ^{13}C-NMR ($CDCl_3$): δ_C 161.9 (C(1)), 146.0 (C(4)), 139.2 (C(9)), 126.5 (C(5)), 125.1 (C(6)), 124.8 (C(7)), 121.4 (C(2)), 120.3 (C(3)), 117.4 (C(2)), 29.4 (C(10)), 18.9 (C(11)); IR ν_{max} 2364, 1640, 1581, 937, 842, 813; LR-ESI-MS: $C_{11}H_{11}BrNO$ $[M+H]^+$ m/z found 252.0 calcd 252.0; HR-ESI-MS: $C_{11}H_{11}BrNO$ $[M+H]^+$ m/z found 252.0019 calcd 252.0033 error = 0.48 ppm.

***tert*-Butyl [(2*R**,3*S**)-1-(1,4-dimethyl-2-oxo-1,2-dihydroquinolin-7-yl)-6-oxo-2-phenylpiperidin-3-yl]carbamate (234) & *tert*-butyl [(2*S*,3*R*)-1-(1,4-dimethyl-2-oxo-1,2-dihydroquinolin-7-yl)-6-oxo-2-phenylpiperidin-3-yl]carbamate ((+)-234)**

Method A. In a pressure tube under inert conditions, **247** (30 mg, 0.10 mmol), **218** (39 mg, 0.15 mmol) and K_3PO_4 (43.7 mg, 0.21 mmol) were combined. 1,4-dioxane (0.4 mL) was added and the solution was degassed. (+/-)-*trans*-1,2-diaminocyclohexane (12.4 μL, 0.10 mmol) and CuI (19.6 mg, 0.10 mmol) were added, the tube was sealed and the reaction mixture was stirred at 97 °C for 42 h. The reaction mixture was passed through a plug of Celite and the Celite was washed with CH_2Cl_2 (50 mL). The combined filtrate was concentrated and purification by FCC (15% isopropanol/PE) yielded **234** (26.1 mg, 55%) as a pale yellow opaque oil.

Method B. Under inert conditions, (–)-**247** (25 mg, 0.086 mmol), **218** (18 mg, 0.072 mmol), Xantphos (5.7 mg, 0.011 mmol) and Cs_2CO_3 (33 mg, 0.101 mmol) were combined. 1,4-dioxane (0.5 mL) and $Pd(OAc)_2$ (1.6 mg, 0.0072 mmol) were added and the reaction mixture was stirred at 110 °C for 36 h. The reaction mixture was passed through a plug of Celite and the Celite was washed with CH_2Cl_2 (15 mL). The combined filtrate was concentrated and purification by FCC (1% MeOH/CH_2Cl_2) yielded (+)-**234** (2.0 mg, 3%) as a pale yellow opaque oil.

Method C. In a pressure tube under inert conditions, (–)-**247** (390 mg, 1.34 mmol), **218** (508 mg, 2.02 mmol) and K_3PO_4 (570 mg, 2.69 mmol) were combined. 1,4-dioxane (13.4 mL) was added and the solution was degassed. (+/-)-*trans*-1,2-diaminocyclohexane (0.161 mL, 1.34 mmol) and CuI (256 mg, 1.34 mmol) were added, the tube was sealed and the reaction mixture was stirred at 97 °C for 42 h. The reaction mixture was passed through a plug of Celite and the Celite was washed with CH_2Cl_2 (500 mL). The combined filtrate was concentrated and purification by iterative FCC (15% isopropanol/PE then 0.5% MeOH/CH_2Cl_2) yielded (+)-**234** (369 mg, 60%) as a pale yellow opaque oil.

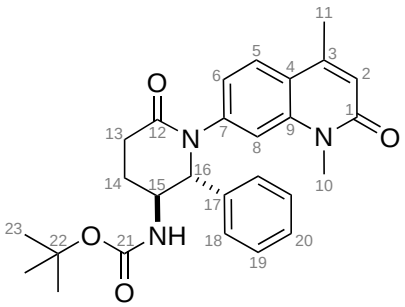

234: ^{1}H-NMR ($CDCl_3$): δ_H 7.60 (d, J = 8.5 Hz, 1H, C(5)H), 7.42-7.36 (m, 4H, C(18)H & C(19)H), 7.31 (app. sxt, J = 4.5 Hz, 1H, C(20)H), 7.15 (d, J = 1.0 Hz, 1H, C(8)H), 7.08 (dd, J = 8.5, 1.5 Hz, 1H, C(6)H), 6.52 (d, J = 1.0 Hz, 1H, C(2)H), 5.23 (d, J = 6.0 Hz, 1H, C(16)H), 4.08 (br s, 1H, C(15)H), 3.50 (s, 3H, C(10)H_3), 2.84 (ddd, J = 19.0, 8.0, 2.5 Hz, 1H, C(13)H_a), 2.74 (ddd, J = 19.0, 10.5, 8.0 Hz, 1H, C(13)H_b), 2.38 (d, J = 1.0 Hz, 3H, C(11)H_3), 2.22-2.11 (m, 1H, C(14)H_a), 1.89-1.80 (m, 1H, C(14)H_b), 1.50 (s, 9H, C(23)H_3); ^{13}C-NMR ($CDCl_3$): δ_C 169.7 (C(12)), 162.0 (C(1)), 155.4 (C(21)), 145.8 (C(4)), 144.2 (C(7)), 140.3 (C(9)), 138.8 (C(17)), 128.9 (C(19)), 128.2 (C(20)), 126.7 (C(18)), 125.9 (C(5)), 121.1 (C(2)),

120.7 (*C*(6)), 120.1 (*C*(3)), 113.0 (*C*(8)), 80.5 (*C*(22)), 69.1 (*C*(16)), 51.2 (*C*(15)), 29.1 (*C*(10)), 28.4 (*C*(23)), 27.9 (*C*(13)), 20.9 (*C*(14)), 18.8 (*C*(11)); IR ν_{max} 3274, 2976, 2362, 1703, 1650, 1594, 1169, 732; LR-ESI-MS: $C_{27}H_{32}N_3O_4$ $[M+H]^+$ *m/z* found 462.2 calcd 462.3; $C_{27}H_{31}N_3O_4Na$ $[M+Na]^+$ *m/z* found 484.2 calcd 484.2; HR-ESI-MS: $C_{27}H_{32}N_3O_4$ $[M+H]^+$ *m/z* found 462.23873 calcd 462.23869 error = 0.21 ppm.

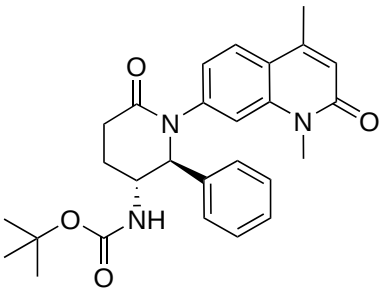

(+)-**234**: $[\alpha]_D{}^{20}$ + 13 (*c* 1.0, $CHCl_3$).

Methyl (4*S,5*R**)-5-[(*tert*-butoxycarbonyl)amino]-4-nitro-5-phenyl-pentanoate (241)**

Method A. Compound **13** (43 mg, 0.29 mmol) was dissolved in TBME (0.58 mL), **240** (20 mg, 0.058 mmol), TBAB (1.0 mg, 0.003 mmol) was added and the solution was cooled to -78 °C. KOH (16 mg, 0.29 mmol) was added and the reaction mixture was stirred at -20 °C for 14 h. $NaHCO_3$ (5 mL, sat. aq. soln) was added and the aqueous phase was extracted with CH_2Cl_2 (3 x 5 mL). The combined organic extracts were dried over Na_2SO_4, filtered and concentrated. Purification by FCC (CH_2Cl_2) yielded **241** (24 mg, 91%, dr >20:1) as a white solid.

Method B. Compound **13** (0.85 g, 5.75 mmol) was dissolved in TBME (11.5 mL), **240** (400 mg, 1.15 mmol) and **115** (41 mg, 0.058 mmol) were added and the solution was cooled to -78 °C. KOH (16 mg, 0.29 mmol) was added and the reaction mixture was stirred at -20 °C for 14 h. $NaHCO_3$ (5 mL, sat. aq. soln) was added and the aqueous phase was extracted with CH_2Cl_2 (3 x 5 mL). The combined organic extracts were dried over Na_2SO_4, filtered and concentrated. Purification by FCC (CH_2Cl_2) yielded **241** (24 mg, 91%, dr 8:1, ee 91%) as a white solid. Recrystallisation (MeOH) yielded **241** (85 mg, 21%, dr 14:1, ee 98%) as a white solid.

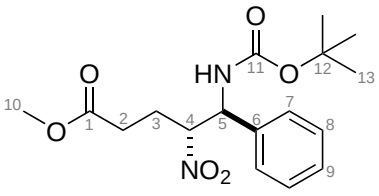

Mpt: 88.8-89.7 °C; ^{1}H-NMR ($CDCl_3$): δ_H 7.39-7.31 (m, 3H, C(8)*H* & C(9)*H*), 7.25 (d, *J* = 6.5 Hz, 2H, C(7)*H*), 5.19 (br s, 2H, C(5)*H* & N*H*), 4.95 (br s, 1H, C(4)*H*), 3.69 (s, 3H, C(10)H_3), 2.48 (ddd, *J* = 16.0, 6.5, 5.5 Hz, 1H, C(2)H_a), 2.37-2.22 (m, 3H, C(2)H_b & C(3)H_2), 1.44 (s, 9H, C(13)H_3); ^{13}C-NMR ($CDCl_3$): δ_C 172.4 (*C*(1)), 154.9 (*C*(11)), 136.4 (*C*(6)), 129.1 (*C*(8)), 128.8 (*C*(9)), 126.8 (*C*(7)), 90.2 (*C*(4)), 80.7 (*C*(12)), 56.9 (*C*(5)), 51.9 (*C*(10)), 29.8 (*C*(2)), 28.2 (*C*(13)), 25.1 (*C*(3)); IR ν_{max} 2923, 2825, 2363, 1716, 1653, 1558, 1258, 701; LR-ESI-MS: $C_{17}H_{24}N_2O_6Na$ $[M+Na]^+$ *m/z* found 375.2 calcd 375.2; HR-ESI-MS: $C_{17}H_{24}N_2O_6Na$ $[M+Na]^+$ *m/z* found 375.15266 calcd 375.15253 error = 0.35 ppm; Analytical HPLC separation (stationary phase: Chiralpak OD, solvent composition: hexane:isopropanol 96:4, flow rate: 1 mL.min^{-1}, injection concentration: 2 mg.mL^{-1}, injection volume: 5 μL, λ: 210 nm): t_1 = 14.6 min (*cis*), t_2 = 15.7 min (*trans*), t_3 = 16.5 min (*cis*), t_4 = 18.9 min (*trans*).

(5*S, 6*R**)-5-Nitro-6-phenyl-piperidin-2-one (246) & (5*R*, 6*S*)-5-nitro-6-phenyl-piperidin-2-one ((–)-246)**

Method A. Compound **13** (2 g, 13.6 mmol) was dissolved in EtOH (5 mL), benzaldehyde (1.39 mL, 13.6 mmol) and NH_4OAc (2.1 g, 27.2 mmol) were added and the reaction mixture was stirred at 90 °C for 20 h. The reaction mixture was concentrated and recrystallisation (EtOAc) yielded **246** (2.11 g, 70%) as a white solid.

Method B. Under inert conditions, **241** (50 mg, 0.14 mmol) was dissolved in CH_2Cl_2 (1.8 mL), TFA (54 μL, 0.71 mmol) was added and the reaction mixture was stirred at rt for 3 h. The reaction mixture was concentrated, CH_2Cl_2 (1.1 mL) and $NaHCO_3$ (0.74 mL, sat. aq. soln) were added and the reaction mixture was stirred at rt for 6 h. The reaction mixture was acidified with 1M HCl, the organic phase was separated and the aqueous phase was extracted with EtOAc (3 x 5 mL). The combined organic phases were washed with H_2O (2 x 20 mL), dried over Na_2SO_4, filtered and concentrated. Purification by FCC (1.2% MeOH/CH_2Cl_2) yielded (–)-**246** (21 mg, 66%) as a white solid.

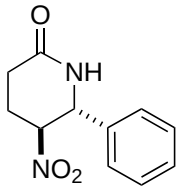

Mpt: 142.0-143.2 °C (lit. 141 °C); ^{1}H-NMR ($CDCl_3$): δ_H 7.45-7.39 (m, 3H), 7.34-7.31 (m, 2H), 6.08 (br s, 1H), 5.27 (dd, J = 6.0, 1.5 Hz, 1H), 4.72 (ddd, J = 8.0, 6.0, 3.5 Hz, 1H), 2.68-2.52 (m, 3H), 2.38-2.30 (m, 1H); ^{13}C-NMR ($CDCl_3$): δ_C 169.6, 137.3, 129.4, 126.6, 126.5, 85.2, 58.9, 27.8, 23.3; LR-ESI-MS: $C_{11}H_{13}N_2O_3$ $[M+H]^+$ *m/z* found 221.2 calcd 221.1; Analytical HPLC separation (stationary phase: Chiralpak OD, solvent composition: hexane:isopropanol 85:15, flow rate: 1 mL.min^{-1}, injection concentration: 1.4 mg.mL^{-1}, injection volume: 5 μL, λ: 210 nm): t_1 = 30.5 min, t_2 = 37.7 min.

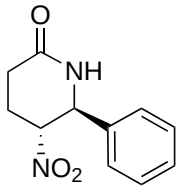

(–)-**246**: $[\alpha]_D^{20}$ - 54 (*c* 1.0, $CHCl_3$), lit. - 56. Data are in accordance with literature values.[268]

***tert*-Butyl [(2*R**,3*S**)-6-oxo-2-phenylpiperidin-3-yl]carbamate (247) & *tert*-butyl [(2*S*,3*R*)-6-oxo-2-phenylpiperidin-3-yl]carbamate ((–)-247)**

Method A. Compound **246** (1.475 g, 6.70 mmol) was dissolved in MeOH (44 mL) and the solution was cooled to 0 °C. $NiCl_2 \cdot 6\,H_2O$ (80 mg, 0.33 mmol) was added and the solution was stirred at 0 °C for 5 min. $NaBH_4$ (1.1 g, 26.8 mmol) was added in portions and the reaction mixture was stirred at 0 °C for 30 min. Boc_2O (1.75 g, 8.03 mmol) was added and the reaction mixture was stirred at rt for 14 h. H_2O (50 mL) was added and the volatiles were removed. The remaining aqueous phase was extracted with EtOAc (5 x 100 mL), the combined organic extracts were dried over Na_2SO_4, filtered and concentrated. Purification by FCC (1% MeOH/CH_2Cl_2) yielded **247** (1.18 g, 61%) as a white solid.

Method B. Compound (–)-**246** (308 mg, 1.4 mmol) was dissolved in MeOH (9.3 mL) and the solution was cooled to 0 °C. $NiCl_2 \cdot 6\,H_2O$ (16.6 mg, 0.07 mmol) was added and the solution was stirred at 0 °C for 5 min. $NaBH_4$ (212 mg, 5.60 mmol) was added in portions and the reaction mixture was stirred at 0 °C for 30 min. Boc_2O (366 mg, 1.68 mmol) was added and the reaction mixture was stirred at rt for 14 h. H_2O (20 mL) was added and the volatiles were removed. The remaining aqueous phase was extracted with EtOAc (5 x 50 mL), the combined organic extracts were dried over Na_2SO_4, filtered and concentrated. Purification by FCC (2% MeOH/CH_2Cl_2) yielded (–)-**247** (392 mg, 96%) as a white solid.

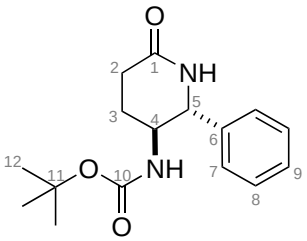

247: Mpt: 205.1-207.0 °C; ^{1}H-NMR ($CDCl_3$): δ_H 7.40-7.29 (m, 5H, C(7)*H*, C(8)*H* & C(9)*H*), 6.20 (br s, 1H, N*H*), 4.98 (br s, 1H, N*H*), 4.53 (br s, 1H, C(5)*H*), 3.91 (br s, 1H, C(4)*H*), 2.55 (t, J = 7.0 Hz, 2H, C(2)H_2), 2.00 (dtd, J = 14.0, 7.0, 3.0 Hz, 1H, C(3)H_a), 1.83 (dq, J = 14.0, 7.0 Hz, 1H, C(3)H_b), 1.37 (d, J = 2.0 Hz, 9H, C(12)H_3); ^{13}C-NMR ($CDCl_3$): δ_C 171.3 (*C*(1)), 155.0 (*C*(10)), 139.8 (*C*(6)), 128.8 (*C*(8)), 128.2 (*C*(9)), 126.7 (*C*(7)), 80.0 (*C*(11)), 61.9 (*C*(5)), 50.8 (*C*(4)), 28.2 (*C*(12)), 28.2 (*C*(2)), 23.3 (*C*(3)); IR ν_{max} 3276, 2976, 2247, 1698, 1655, 1366, 1168, 732, 700; LR-ESI-MS: $C_{16}H_{23}N_2O_3$ $[M+H]^+$ *m/z* found 291.2 calcd 291.2, $C_{16}H_{22}N_2O_3Na$ $[M+Na]^+$ *m/z* found 313.1 calcd 313.2; HR-ESI-MS: $C_{16}H_{22}N_2O_3Na$ $[M+Na]^+$ *m/z* found 313.1523 calcd 313.1512 error = 0.81 ppm.

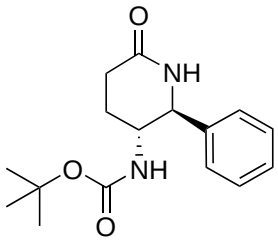

(–)-**247**: $[\alpha]_D{}^{20}$ - 22 (*c* 1.0, $CHCl_3$).

7-[(2*R,3*S**)-3-Amino-6-oxo-2-phenylpiperidin-1-yl]-1,4-dimethylquino-lin-2(1*H*)-one** (**249**) & **7-[(2*S*,3*R*)-3-amino-6-oxo-2-phenylpiperidin-1-yl]-1,4-dimethylquinolin-2(1*H*)-one** ((+)-**249**)

Method A. Under inert conditions, **234** (71.6 mg, 0.16 mmol) was dissolved in CH_2Cl_2 (1.5 mL), TFA (2.5 mL) was added and the reaction mixture was stirred at rt for 1 h. The reaction mixture was concentrated, 1M HCl (2 mL) was added and the aqueous phase was washed with CH_2Cl_2 (3 x 5 mL). The aqueous phase was basified with 2M NaOH and the aqueous phase was extracted with CH_2Cl_2 (5 x 5 mL). The combined organic extracts were dried over Na_2SO_4, filtered and concentrated. Purification by FCC (3.5% MeOH/CH_2Cl_2) yielded **249** (31.2 mg, 56%) as a white solid.

Method B. Under inert conditions, (+)-**234** (380 mg, 0.82 mmol) was dissolved in CH_2Cl_2 (9 mL), TFA (9 mL) was added and the reaction mixture was stirred at rt for 1 h. The reaction mixture was concentrated, 1M HCl (8 mL) was added and the aqueous phase was washed with CH_2Cl_2 (3 x 25 mL). The aqueous phase was basified with 2M NaOH and the aqueous phase was extracted with CH_2Cl_2 (5 x 25 mL). The combined organic extracts were dried over Na_2SO_4, filtered and concentrated to yield (+)-**249** (240 mg, 85%) as a white solid.

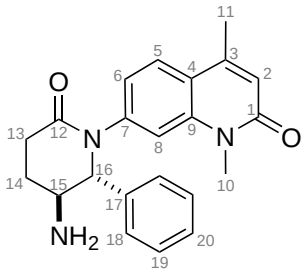

249: ^{1}H-NMR ($CDCl_3$): δ_H 7.53 (d, J = 8.5 Hz, 1H, C(5)*H*), 7.34-7.20 (m, 5H, C(18)*H*, C(19)*H* & C(20)*H*), 7.02 (br s, 1H, C(8)*H*), 7.01 (dd, J = 9.0, 2.0 Hz, 1H, C(6)*H*), 6.47 (d, J = 1.0 Hz, 1H, C(2)*H*), 4.66 (d, J = 6.0 Hz, 1H, C(16)*H*), 3.46 (s, 3H, C(10)H_3), 3.42 (br s, 1H, C(15)*H*), 2.85 (dt, J = 18.5, 6.5 Hz, 1H, C(13)H_a), 2.77 (dt, J = 18.5, 7.0 Hz, 1H, C(13)H_b), 2.33 (d, J = 1.0 Hz, 3H, C(11)H_3), 2.19-2.10 (m, 1H, C(14)H_a), 1.93-1.85 (m, 1H, C(14)H_b); ^{13}C-NMR ($CDCl_3$): δ_C 170.4 (*C*(12)), 162.0 (*C*(1)), 145.9 (*C*(3)), 143.7 (*C*(7)), 140.0 (*C*(9)), 139.1 (*C*(17)), 128.8 (*C*(19)), 128.2 (*C*(20)), 127.4 (*C*(18)), 125.6 (*C*(5)), 121.2 (*C*(2)), 120.8 (*C*(6)), 119.8 (*C*(4)), 113.8 (*C*(8)), 73.0 (*C*(16)), 52.6 (*C*(15)), 29.7 (*C*(13)), 29.0 (*C*(10)),

26.2 (*C*(14)), 18.8 (*C*(11)); IR ν_{max} 3363, 2944, 1645, 1591, 729; LR-ESI-MS: $C_{22}H_{24}N_3O_2$ $[M+H]^+$ *m/z* found 362.2 calcd 362.2, $C_{22}H_{23}N_3O_2Na$ $[M+Na]^+$ *m/z* found 384.3 calcd 384.2; HR-ESI-MS: $C_{22}H_{24}N_3O_2$ $[M+H]^+$ *m/z* found 362.18651 calcd 362.18630 error = 0.51 ppm.

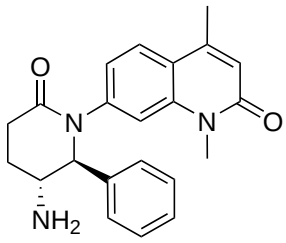

(+)-**249**: $[\alpha]_D^{20}$ +51 (*c* 1.0, $CHCl_3$).

7-[(2*S*,3*R*)-3-(Dimethylamino)-6-oxo-2-phenylpiperidin-1-yl]-1,4-dimethylquinolin-2(1*H*)-one ((+)-**250**)

Compound (+)-**249** (17.4 mg, 0.055 mmol) was dissolved in formaldehyde (0.5 mL), formic acid (0.5 mL) was added and the reaction mixture was stirred at 95 °C for 14 h. The reaction mixture was concentrated and purification by FCC (4% MeOH/CH_2Cl_2) yielded (+)-**250** (11.5 mg, 62%) as a tan opaque oil.

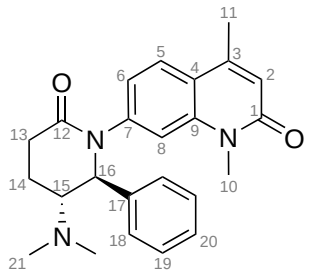

^{1}H-NMR ($CDCl_3$): δ_H 7.60 (d, J = 8.5 Hz, 1H, C(5)*H*), 7.40 (t, J = 8.0 Hz, 2H, C(19)*H*), 7.34-7.29 (m, 3H, C(18)*H* & C(20)*H*), 7.13 (d, J = 1.5 Hz, 1H, C(8)*H*), 7.08 (dd, J = 8.5, 2.0 Hz, 1H, C(6)*H*), 6.52 (d, J = 1.0 Hz, 1H, C(2)*H*), 5.05 (br s, 1H, C(16)*H*), 3.46 (s, 3H, C(10)H_3), 2.80 (ddd, J = 18.0, 10.0, 7.0 Hz, 1H, C(13)H_a), 2.66 (br s, 1H, C(15)*H*), 2.62 (ddd, J = 18.0, 6.5, 5.0 Hz, 1H, C(13)H_b), 2.45 (s, 6H, C(21)H_3), 2.38 (d, J = 1.0 Hz, 3H, C(11)H_3), 2.08-1.91 (m, 2H, C(14)H_2); ^{13}C-NMR ($CDCl_3$): δ_C 171.3 (*C*(12)), 162.1 (*C*(1)), 145.9 (*C*(4)), 144.8 (*C*(7)), 140.9 (*C*(9)), 140.2 (*C*(17)), 128.8 (*C*(19)), 127.9 (*C*(20)), 126.9 (*C*(18)), 125.8 (*C*(5)), 120.9 (*C*(2)), 120.4 (*C*(6)), 119.9 (*C*(3)), 112.8 (*C*(8)), 66.6 (*C*(16)), 66.1 (*C*(15)), 42.9 (*C*(21)), 29.1 (*C*(13)), 29.0 (*C*(10)), 19.1 (*C*(14)), 18.8 (*C*(11)); IR ν_{max} 2959, 2823, 2777, 1653, 1596, 732; LR-ESI-MS: $C_{24}H_{28}N_3O_2$ $[M+H]^+$ *m/z* found 390.2 calcd 390.2; HR-ESI-MS: $C_{24}H_{28}N_3O_2$ $[M+H]^+$ *m/z* found 390.21760 calcd 390.21881 error = 3.09 ppm.

***N*-[(2*S*,3*R*)-1-(1,4-Dimethyl-2-oxo-1,2-dihydroquinolin-7-yl)-6-oxo-2-phenylpiperidin-3-yl]acetamide** ((+)-**251**)

Compound (+)-**249** (17.8 mg, 0.055 mmol) was dissolved in CH_2Cl_2 (0.25 mL), NEt_3 (10 μL, 0.08 mmol) and acetic anhydride (16 μL, 0.17 mmol) were added and the reaction mixture was stirred at rt for 16 h. H_2O (10 mL) was added and the aqueous phase was extracted with CH_2Cl_2 (3 x 10 mL). The combined organic extracts were dried over Na_2SO_4, filtered and concentrated. Purification by FCC (3% MeOH/CH_2Cl_2) yielded (+)-**251** (19.1 mg, 96%) as an opaque oil.

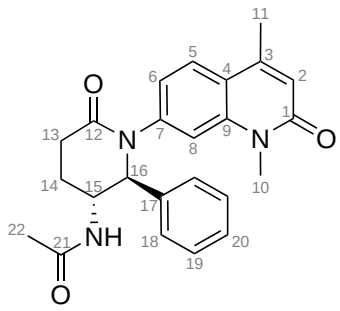

^{1}H-NMR ($CDCl_3$): δ_H 7.54 (d, J = 8.5 Hz, 1H, C(5)H), 7.42-7.35 (m, 4H, C(18)H & C(19)H), 7.34-7.27 (m, 1H, C(20)H), 7.12 (d, J = 1.5 Hz, 1H, C(8)H), 7.03 (dd, J = 8.5, 1.5 Hz, 1H, C(6)H), 6.49 (s, 1H, C(2)H), 5.19 (br s, 1H, C(16)H), 4.42 (dq, J = 7.0, 3.5 Hz, 1H, C(15)H), 3.40 (s, 3H, C(10)H_3), 2.82 (dd, J = 9.0, 5.5 Hz, 2H, C(13)H_2), 2.36 (s, 3H, C(11)H_3), 2.16 (dtd, J = 14.5, 9.5, 4.0 Hz, 1H, C(14)H_a), 2.08 (s, 3H, C(22)H_3), 1.90-1.80 (m, 1H, C(14)H_b); ^{13}C-NMR ($CDCl_3$): δ_C 170.6 (C(21)), 170.1 (C(12)), 161.9 (C(1)), 146.0 (C(4)), 144.1 (C(7)), 140.1 (C(9)), 138.6 (C(17)), 128.9 (C(19)), 128.2 (C(20)), 126.6 (C(18)), 125.7 (C(5)), 121.0 (C(2)), 120.5 (C(6)), 120.0 (C(3)), 113.1 (C(8)), 69.2 (C(16)), 49.8 (C(15)), 29.0 (C(10)), 28.1 (C(13)), 23.3 (C(22)), 20.8 (C(14)), 18.8 (C(11)); IR ν_{max} 3292, 3061, 2947, 1644, 1591, 730; LR-ESI-MS: $C_{24}H_{26}N_3O_3$ $[M+H]^+$ m/z found 404.2 calcd 404.2, $C_{24}H_{25}N_3O_3Na$ $[M+Na]^+$ m/z found 426.2 calcd 426.2; HR-ESI-MS: $C_{24}H_{26}N_3O_3$ $[M+H]^+$ m/z found 404.19687 calcd 404.19687 error = 0.0 ppm; $[\alpha]_D^{20}$ +26 (c 1.0, $CHCl_3$).

Methyl [(2*R,3*S**)-1-(1,4-Dimethyl-2-oxo-1,2-dihydroquinolin-7-yl)-6-oxo-2-phenylpiperidin-3-yl]carbamate** (**252**) & **methyl [(2*S*,3*R*)-1-(1,4-dimethyl-2-oxo-1,2-dihydroquinolin-7-yl)-6-oxo-2-phenylpiperidin-3-yl]carbamate** ((+)-**252**)

Method A. Compound **249** (10 mg, 0.028 mmol) was dissolved in CH_2Cl_2 (0.22 mL), NEt_3 (20 μL, 0.14 mmol) and methyl chloroformate (20 μL, 0.26 mmol) were added and the reaction mixture was stirred at rt for 1.5 h. H_2O (10 mL) was added and the aqueous phase was extracted with CH_2Cl_2 (3 x 10 mL). The combined organic extracts were dried over Na_2SO_4, filtered and concentrated. Purification by FCC (1.5% MeOH/CH_2Cl_2) yielded **252** (7.7 mg, 66%) as a pale yellow solid.

Method B. Compound (+)-**249** (18.0 mg, 0.050 mmol) was dissolved in CH_2Cl_2 (0.25 mL), NEt_3 (20 μL, 0.14 mmol) and methyl chloroformate (20 μL, 0.26 mmol) were added and the reaction mixture was stirred at rt for 1.5 h. H_2O (10 mL) was added and the aqueous phase was extracted with CH_2Cl_2 (3 x 10 mL). The combined organic extracts were dried over Na_2SO_4, filtered and concentrated. Purification by FCC (1.5% MeOH/CH_2Cl_2) yielded (+)-**252** (19.7 mg, 94%) as a pale yellow solid.

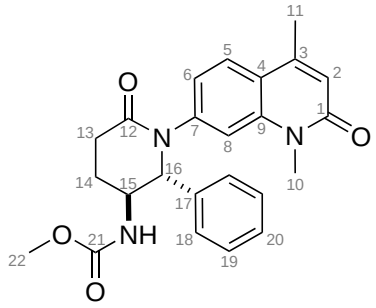

252: Mpt: 117.6-118.4 °C; ^{1}H-NMR ($CDCl_3$): δ_H 7.57 (d, J = 8.5 Hz, 1H, C(5)H), 7.43-7.28 (m, 5H, C(18)H, C(19)H & C(20)H), 7.13 (d, J = 2.0 Hz, 1H, C(8)H), 7.06 (dd, J = 8.5, 2.0 Hz, 1H, C(6)H), 6.51 (d, J = 1.0 Hz, 1H, C(2)H), 5.78 (br s, 1H, NH), 5.21 (br s, 1H, C(16)H), 4.16 (br s, 1H, C(15)H), 3.74 (s, 3H, C(22)H_3), 3.45 (s, 3H, C(10)H_3), 2.88-2.79 (m, 1H, C(13)H_a), 2.79 (ddd, J = 19.0, 10.5, 7.0 Hz, 1H, C(13)H_b), 2.36 (d, J = 1.0 Hz, 3H, C(11)H_3), 2.23-2.11 (m, 1H, C(14)H_a), 1.93-1.82 (m, 1H, C(14)H_b); ^{13}C-NMR ($CDCl_3$): δ_C 169.8 (C(12)), 162.0 (C(1)), 156.6 (C(21)), 145.9 (C(4)), 144.1 (C(7)), 140.1 (C(9)), 138.8 (C(17)), 129.0 (C(19)), 128.3 (C(20)), 126.7 (C(18)), 125.8 (C(5)), 121.0 (C(2)), 120.5 (C(6)), 120.0 (C(3)), 113.0 (C(8)), 69.3 (C(16)), 52.4 (C(22)), 51.6 (C(15)), 29.0 (C(10)), 28.0 (C(13)), 21.2 (C(14)), 18.8 (C(11)); IR ν_{max} 3273, 2950, 1713, 1646, 1592, 729; LR-ESI-MS: $C_{24}H_{26}N_3O_4$ $[M+H]^+$ m/z found 420.2 calcd 420.2,

$C_{24}H_{25}N_3O_4Na$ $[M+Na]^+$ *m/z* found 442.1 calcd 442.2; HR-ESI-MS: $C_{24}H_{26}N_3O_4$ $[M+H]^+$ *m/z* found 420.19178 calcd 420.19193 error = 0.34 ppm.

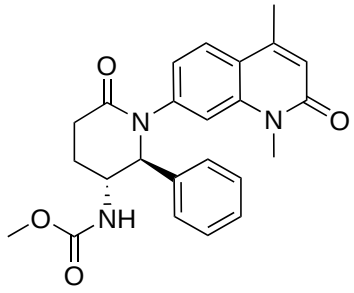

(+)-**252**: $[\alpha]_D{}^{20}$ +17 (*c* 1.0, $CHCl_3$).

Ethyl [(2*R,3*S**)-1-(1,4-dimethyl-2-oxo-1,2-dihydroquinolin-7-yl)-6-oxo-2-phenylpiperidin-3-yl]carbamate** (**253**) & **ethyl [(2*S*,3*R*)-1-(1,4-dimethyl-2-oxo-1,2-dihydroquinolin-7-yl)-6-oxo-2-phenylpiperidin-3-yl]carbamate**((+)-**253**)

Method A. Compound **249** (10 mg, 0.028 mmol) was dissolved in CH_2Cl_2 (0.22 mL), NEt_3 (20 μL, 0.14 mmol) and ethyl chloroformate (20 μL, 0.21 mmol) were added and the reaction mixture was stirred at rt for 1.5 h. H_2O (10 mL) was added and the aqueous phase was extracted with CH_2Cl_2 (3 x 10 mL). The combined organic extracts were dried over Na_2SO_4, filtered and concentrated. Purification by FCC (1.5% MeOH/CH_2Cl_2) yielded **253** (9.2 mg, 77%) as an opaque oil.

Method B. Compound (+)-**249** (16.5 mg, 0.046 mmol) was dissolved in CH_2Cl_2 (0.25 mL), NEt_3 (20 μL, 0.14 mmol) and ethyl chloroformate (20 μL, 0.21 mmol) were added and the reaction mixture was stirred at rt for 1.5 h. H_2O (10 mL) was added and the aqueous phase was extracted with CH_2Cl_2 (3 x 10 mL). The combined organic extracts were dried over Na_2SO_4, filtered and concentrated. Purification by FCC (1.5% MeOH/CH_2Cl_2) yielded (+)-**253** (19.1 mg, 96%) as an opaque oil.

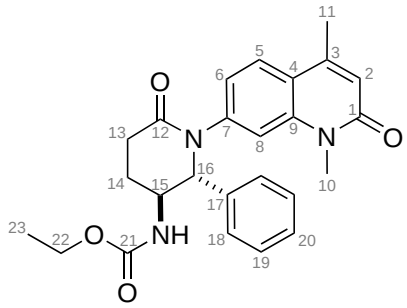

253: ^{1}H-NMR ($CDCl_3$): δ_H 7.58 (d, J = 8.5 Hz, 1H, C(5)H), 7.42-7.29 (m, 5H, C(18)H, C(19)H & C(20)H), 7.14 (d, J = 1.5 Hz, 1H, C(8)H), 7.07 (dd, J = 8.5, 1.5 Hz, 1H, C(6)H), 6.52 (d, J = 1.0 Hz, 1H, C(2)H), 5.62 (br s, 1H, NH), 5.24 (br s, 1H, C(16)H), 4.19 (q, J = 7.0 Hz, 2H, C(22)H_2), 4.15 (br s, 1H, C(15)H), 3.46 (s, 3H, C(10)H_3), 2.88-2.78 (m, 1H, C(13)H_a), 2.76 (ddd, J = 19.0, 10.5, 7.0 Hz, 1H, C(13)H_b), 2.37 (d, J = 1.0 Hz, 3H, C(11)H_3), 2.24-2.11 (m, 1H, C(14)H_a), 1.96-1.82 (m, 1H, C(14)H_b), 1.29 (t, J = 7.0 Hz, 3H, C(23)H_3); ^{13}C-NMR ($CDCl_3$): δ_C 169.7 (*C*(12)), 162.0 (*C*(1)), 156.2 (*C*(21)), 145.9 (*C*(4)), 144.2 (*C*(7)),140.2 (*C*(9)), 138.8 (*C*(17)), 129.0 (*C*(19)), 128.2 (*C*(20)), 126.7 (*C*(18)), 125.8 (*C*(5)), 121.0 (*C*(2)), 120.5 (*C*(6)), 120.0 (*C*(3)), 113.0 (*C*(8)), 69.3 (*C*(16)), 61.3 (*C*(22)), 51.5 (*C*(15)), 29.0 (*C*(10)), 27.9 (*C*(13)), 21.1 (*C*(14)), 18.8 (*C*(11)), 14.6 (*C*(23)); IR ν_{max} 3273, 2979, 1709, 1648, 1593, 730; LR-ESI-MS: $C_{25}H_{28}N_3O_4$ $[M+H]^+$ *m/z* found 434.2 calcd 434.2, $C_{25}H_{27}N_3O_4Na$ $[M+Na]^+$ *m/z* found 456.2 calcd 456.2; HR-ESI-MS: $C_{25}H_{28}N_3O_4$ $[M+H]^+$ *m/z* found 434.20743 calcd 434.20734 error = 0.22 ppm.

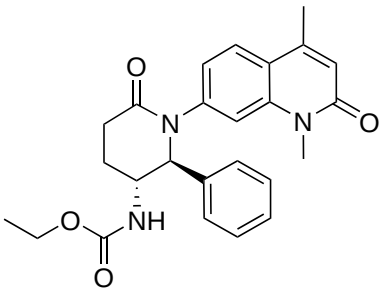

(+)-**253**: $[\alpha]_D^{20}$ +11 (*c* 1.0, $CHCl_3$).

Benzyl [(2*R,3*S**)-1-(1,4-dimethyl-2-oxo-1,2-dihydroquinolin-7-yl)-6-oxo-2-phenylpiperidin-3-yl]carbamate** (**254**) & **benzyl [(2*S*,3*R*)-1-(1,4-dimethyl-2-oxo-1,2-dihydroquinolin-7-yl)-6-oxo-2-phenylpiperidin-3-yl]carbamate**((–)-**254**)

Method A. Compound **249** (10 mg, 0.028 mmol) was dissolved in CH_2Cl_2 (0.22 mL), NEt_3 (20 μL, 0.14 mmol) and benzyl chloroformate (20 μL, 0.14 mmol) were added and the reaction mixture was stirred at rt for 1.5 h. H_2O (10 mL) was added and the aqueous phase was extracted with CH_2Cl_2 (3 x 10 mL). The combined organic extracts were dried over Na_2SO_4, filtered and concentrated. Purification by FCC (1.5% MeOH/CH_2Cl_2) yielded **254** (9.3 mg, 68%) as a white solid.

Method B. Compound (+)-**249** (17.5 mg, 0.048 mmol) was dissolved in CH_2Cl_2 (0.25 mL), NEt_3 (20 μL, 0.14 mmol) and benzyl chloroformate (20 μL, 0.14 mmol) were added and the reaction mixture was stirred at rt for 1.5 h. H_2O (10 mL) was added and the aqueous phase was extracted with CH_2Cl_2 (3 x 10 mL). The combined organic extracts were dried over Na_2SO_4, filtered and concentrated. Purification by FCC (1.5% MeOH/CH_2Cl_2) yielded (–)-**254** (13.5 mg, 56%) as a white solid.

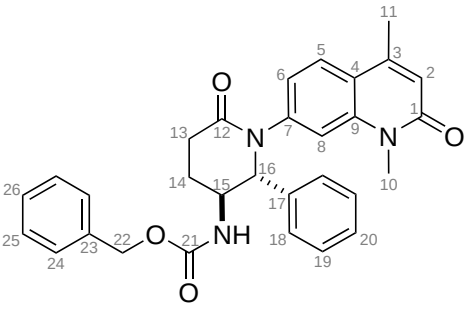

254: Mpt: 106.0-106.9 °C; ^{1}H-NMR ($CDCl_3$): δ_H 7.55 (d, J = 8.5 Hz, 1H, C(5)H), 7.43-7.29 (m, 10H, C(18)H, C(19)H, C(20)H, C(24)H, C(25)H & C(26)H), 7.10 (br s, 1H, C(8)H), 7.01 (dd, J = 8.5, 1.5 Hz, 1H, C(6)H), 6.52 (s, 1H, C(2)H), 5.67 (br s, 1H, NH), 5.23 (br s, 1H, C(16)H), 5.19 (d, J = 12.0 Hz, 1H, C(22)H_a), 5.15 (d, J = 12.0 Hz, 1H, C(22)H_b), 4.17 (br s, 1H, C(15)H), 3.41 (s, 3H, C(10)H_3), 2.89-2.76 (m, 1H, C(13)H_a), 2.74 (ddd, J = 19.0, 10.0, 7.5 Hz, 1H, C(13)H_b), 2.36 (s, 3H, C(11)H_3), 2.23-2.12 (m, 1H, C(14)H_a), 1.93-1.83 (m, 1H, C(14)H_b); ^{13}C-NMR ($CDCl_3$): δ_C 169.6 (*C*(12)), 162.0 (*C*(1)), 155.9 (*C*(21)), 145.8 (*C*(4)), 144.1 (*C*(7)), 140.2 (*C*(9)), 138.7 (*C*(17)), 136.0 (*C*(23)), 129.0 (*C*(25)), 128.6 (*C*(19)), 128.4 (*C*(26)), 128.3 (*C*(20)), 128.2 (*C*(18)), 126.7 (*C*(24)), 125.8 (*C*(5)), 121.0 (*C*(2)), 120.4 (*C*(6)), 120.0 (*C*(3)), 112.9 (*C*(8)), 69.2 (*C*(16)), 67.1 (*C*(22)), 51.6 (*C*(15)), 29.0 (*C*(10)), 27.9 (*C*(13)), 21.1 (*C*(14)), 18.8 (*C*(11)); IR ν_{max} 3264, 3033, 2949, 1712, 1646, 1592, 730; LR-ESI-MS: $C_{30}H_{30}N_3O_4$ $[M+H]^+$ *m/z* found 496.2 calcd 496.2, $C_{30}H_{29}N_3O_4Na$ $[M+Na]^+$ *m/z* found 518.2 calcd 518.2; HR-ESI-MS: $C_{30}H_{30}N_3O_4$ $[M+H]^+$ *m/z* found 496.22308 calcd 496.22309 error = 0.02 ppm.

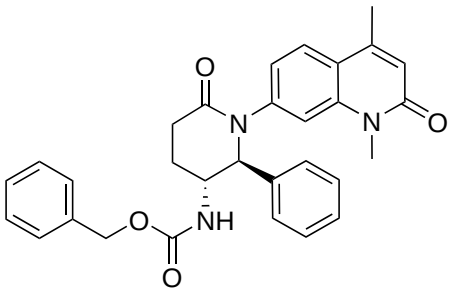

(–)-**254**: $[\alpha]_D^{20}$ -14 (*c* 1.0, $CHCl_3$).

(5*R,6*S**)-6-(4-methoxyphenyl)-5-nitropiperidin-2-one** (**255**)

Compound **13** (106 mg, 0.72 mmol) was dissolved in EtOH (0.23 mL), 4-methoxybenzaldehyde (88 μL, 0.72 mmol) and NH_4OAc (111 mg, 1.44 mmol) were added and the reaction mixture was stirred at reflux for 24 h. The reaction mixture was concentrated and purification by FCC (CH_2Cl_2) yielded **255** (43 mg, 26%) as a white powder.

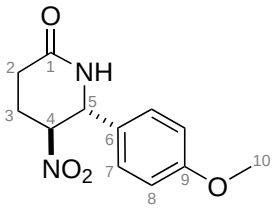

Mpt: 187.8-188.9 °C; ^{1}H-NMR ($CDCl_3$): δ_H 7.24 (d, J = 8.5 Hz, 2H, C(7)H), 6.93 (d, J = 9.0 Hz, 2H, C(8)H), 5.97 (br s, 1H, NH), 5.16 (dd, J = 6.5, 1.0 Hz, 1H, C(5)H), 4.69 (ddd, J = 8.5, 6.5, 3.5 Hz, 1H, C(4)H), 3.81 (s, 3H, C(10)H_3), 2.73-2.50 (m, 3H, C(2)H_2 & C(3)H_a), 2.41-2.32 (m, 1H, C(3)H_b); ^{13}C-NMR ($CDCl_3$): δ_C 169.6 (*C*(1)), 160.4 (*C*(9)), 129.0 (*C*(6)), 127.9 (*C*(7)), 114.8 (*C*(8)), 85.6 (*C*(4)), 58.7 (*C*(5)), 55.4 (*C*(10)), 28.0 (*C*(2)), 23.9 (*C*(3)); IR ν_{max} 3167, 3010, 1651, 1256, 820, 623; LR-ESI-MS: $C_{12}H_{15}N_2O_4$ $[M+H]^+$ *m/z* found 251.1 calcd 251.0, $C_{12}H_{14}N_2O_4Na$ $[M+Na]^+$ *m/z* found 273.0 calcd 273.1; HR-ESI-MS: $C_{12}H_{15}N_2O_4$ $[M+H]^+$ *m/z* found 251.10263 calcd 251.10233 error = 1.23 ppm.

(5*R,6*S**)-6-(4-Methylphenyl)-5-nitropiperidin-2-one** (**256**)

Compound **13** (106 mg, 0.72 mmol) was dissolved in EtOH (0.23 mL), 4-methylbenzaldehyde (85 μL, 0.72 mmol) and NH_4OAc (111 mg, 1.44 mmol) were added and the reaction mixture was stirred at reflux for 24 h. The reaction mixture was concentrated and purification by FCC (0.5% MeOH/CH_2Cl_2) yielded **256** (145 mg, 86%) as a white powder.

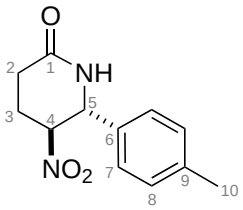

Mpt: 168.0-168.8 °C; ^{1}H-NMR ($CDCl_3$): δ_H 7.22 (d, J = 8.5 Hz, 2H, C(8)H), 7.20 (d, J = 9.0 Hz, 2H, C(7)H), 6.26 (br s, 1H, NH), 5.20 (dd, J = 6.0, 1.5 Hz, 1H, C(5)H), 4.69 (ddd, J = 7.5, 6.0, 4.0 Hz, 1H, C(4)H), 2.70-2.47 (m, 3H, C(2)H_2 & C(3)H_a), 2.36 (s, 3H, C(10)H_3), 2.35-2.27 (m, 1H, C(3)H_b); ^{13}C-NMR ($CDCl_3$): δ_C 169.8 (*C*(1)), 139.4 (*C*(6)), 134.3 (*C*(9)), 130.0 (*C*(8)), 126.4 (*C*(7)), 85.3 (*C*(4)), 58.7 (*C*(5)), 27.8 (*C*(2)), 23.4 (*C*(3)), 21.1 (*C*(10)); IR ν_{max} 3208, 3080, 2913, 1660, 1547, 1387, 741; LR-ESI-MS: $C_{12}H_{15}N_2O_3$ $[M+H]^+$ *m/z* found 235.1 calcd 235.1, $C_{12}H_{14}N_2O_3Na$ $[M+Na]^+$ *m/z* found 257.0 calcd 257.1; HR-ESI-MS: $C_{12}H_{14}N_2O_3Na$ $[M+Na]^+$ *m/z* found 257.08966 calcd 257.08920 error = 1.79 ppm.

(5*R,6*S**)-6-(2-Fluorophenyl)-5-nitropiperidin-2-one** (**257**)

Compound **13** (106 mg, 0.72 mmol) was dissolved in EtOH (0.23 mL), 2-fluorobenzaldehyde (76 μL, 0.72 mmol) and NH_4OAc (111 mg, 1.44 mmol) were added and the reaction mixture was stirred at reflux for 24 h. The reaction mixture was concentrated and purification by FCC (CH_2Cl_2) yielded **257** (139 mg, 81%) as a white powder.

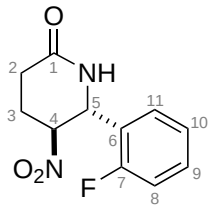

Mpt: 166.3-167.4 °C; ^{1}H-NMR ($CDCl_3$): δ_H 7.40 (dddd, J = 8.0, 7.5, 5.5, 1.5 Hz, 1H, C(9)H), 7.35 (td, J = 7.5, 1.5 Hz, 1H, C(8)H), 7.24 (td, J = 7.5, 1.0 Hz, 1H, C(11)H), 7.14 (ddd, J = 10.5, 8.5, 1.0 Hz, 1H, C(10)H), 6.47 (br s, 1H, NH), 5.66 (t, J = 3.5 Hz, 1H, C(5)H), 4.85 (dt, J = 5.5, 4.0 Hz, 1H, C(4)H), 2.62-2.55 (m, 3H, C(2)H_2 & C(3)H_a), 2.28-2.18 (m, 1H, C(3)H_b); ^{13}C-NMR ($CDCl_3$): δ_C 170.1 (C(1)), 159.7 (d, J = 252.7 Hz, C(7)), 131.1 (d, J = 7.9 Hz, C(11)), 128.1 (d, J = 3.2 Hz, C(9)), 125.1 (d, J = 3.2 Hz, C(10)), 124.9 (d, J = 12.7 Hz, C(6)), 116.3 (d, J = 21.5 Hz, C(8)), 82.0 (C(4)), 53.1 (C(5)), 27.2 (C(2)), 22.1 (C(3)); IR ν_{max} 3216, 3078, 2929, 1662, 1551, 771; LR-ESI-MS: $C_{11}H_{12}FN_2O_3$ [M+H]$^+$ *m/z* found 239.1 calcd 239.1, $C_{11}H_{11}FN_2O_3Na$ [M+Na]$^+$ *m/z* found 261.0 calcd 261.1; HR-ESI-MS: $C_{11}H_{11}FN_2O_3Na$ [M+Na]$^+$ *m/z* found 261.06459 calcd 261.06452 error = 0.30 ppm.

(5*R,6*S**)-6-(3-Fluorophenyl)-5-nitropiperidin-2-one (258)**

Compound **13** (106 mg, 0.72 mmol) was dissolved in EtOH (0.23 mL), 3-fluorobenzaldehyde (76 μL, 0.72 mmol) and NH_4OAc (111 mg, 1.44 mmol) were added and the reaction mixture was stirred at reflux for 24 h. The reaction mixture was concentrated and purification by FCC (CH_2Cl_2) yielded **258** (45 mg, 26%) as a pale yellow oil.

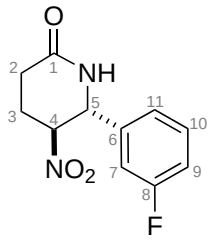

^{1}H-NMR ($CDCl_3$): δ_H 7.41 (td, J = 8.0, 6.0 Hz, 1H, C(10)H), 7.12 (dd, J = 7.0, 1.0 Hz, 1H, C(7)H), 7.13-7.03 (m, 2H, C(9)H & C(11)H), 6.77 (br s, 1H, NH), 5.30 (dd, J = 5.5, 1.0 Hz, 1H, C(5)H), 4.71 (ddd, J = 7.5, 6.0, 4.0 Hz, 1H, C(4)H), 2.72-2.53 (m, 3H, C(2)H_2 & C(3)H_a), 2.37-2.27 (m, 1H, C(3)H_b); ^{13}C-NMR ($CDCl_3$): δ_C 170.2 (C(1)), 163.2 (d, J = 248.8 Hz, C(8)), 139.9 (d, J = 6.4 Hz, C(6)), 131.2 (d, J = 7.9 Hz, C(10)), 122.2 (d, J = 3.2 Hz, C(11)), 116.5 (d, J = 21.5 Hz, C(7)), 113.7 (d, J = 23.0 Hz, C(9)), 84.7 (C(4)), 58.3 (d, J = 2.4 Hz, C(5)), 27.6 (C(2)), 23.1 (C(3)); IR ν_{max} 3183, 3052, 1656, 1551, 790, 695; LR-ESI-MS: $C_{11}H_{12}FN_2O_3$ [M+H]$^+$ *m/z* found 239.1 calcd 239.1, $C_{11}H_{11}FN_2O_3Na$ [M+Na]$^+$ *m/z* found 261.0 calcd 261.1; HR-ESI-MS: $C_{11}H_{11}FN_2O_3Na$ [M+Na]$^+$ *m/z* found 261.06459 calcd 261.06458 error = 0.06 ppm.

(5*R,6*S**)-6-(4-Fluorophenyl)-5-nitropiperidin-2-one (259)**

Compound **13** (106 mg, 0.72 mmol) was dissolved in EtOH (0.23 mL), 4-fluorobenzaldehyde (77 μL, 0.72 mmol) and NH_4OAc (111 mg, 1.44 mmol) were added and the reaction mixture was stirred at reflux for 24 h. The reaction mixture was concentrated and purification by FCC (CH_2Cl_2) yielded **259** (132 mg, 77%) as a white powder.

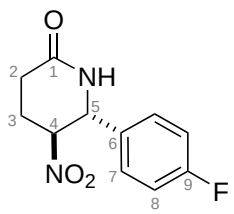

Mpt: 101.7-103.2 °C; ^{1}H-NMR ($CDCl_3$): δ_H 7.31 (dd, J = 8.5, 5.0 Hz, 2H, C(7)H), 7.17 (br s, 1H, NH), 7.12 (t, J = 8.5 Hz, 2H, C(8)H), 5.25 (dd, J = 6.0, 1.0 Hz, 1H, C(5)H), 4.68 (ddd, J = 8.0, 6.0, 3.5 Hz, 1H, C(4)H), 2.72-2.51 (m, 3H, C(2)H_2 & C(3)H_a), 2.37-2.28 (m, 1H, C(3)H_b); ^{13}C-NMR ($CDCl_3$): δ_C 170.8 (C(1)), 163.1 (d, J = 248.0 Hz, C(9)), 132.8 (d, J = 3.2 Hz, C(6)), 128.4 (d, J 8.7 = Hz, C(7)), 116.5 (d, J = 22.3 Hz, C(8)), 85.1 (C(4)), 58.2 (C(5)), 27.6 (C(2)), 23.3 (C(3)); IR ν_{max} 3210, 2950, 1680, 1542, 1202, 780; LR-ESI-MS: $C_{11}H_{12}FN_2O_3$ [M+H]$^+$ *m/z* found 239.1 calcd 239.1, $C_{11}H_{11}FN_2O_3Na$ [M+Na]$^+$ *m/z* found 261.0 calcd 261.1; HR-ESI-MS: $C_{11}H_{11}FN_2O_3Na$ [M+Na]$^+$ *m/z* found 261.06459 calcd 261.06470 error = 0.40 ppm.

(5*R,6*S**)-6-(2-Chlorophenyl)-5-nitropiperidin-2-one** (**260**)

Compound **13** (106 mg, 0.72 mmol) was dissolved in EtOH (0.23 mL), 2-chlorobenzaldehyde (81 μL, 0.72 mmol) and NH_4OAc (111 mg, 1.44 mmol) were added and the reaction mixture was stirred at reflux for 24 h. The reaction mixture was concentrated and purification by FCC (CH_2Cl_2) yielded **260** (49 mg, 27%) as pale yellow crystals.

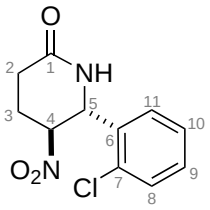

Mpt: 163.7-164.9 °C; ^{1}H-NMR ($CDCl_3$): δ_H 7.45 (dd, J = 7.0, 1.5 Hz, 1H, C(8)H), 7.42-7.33 (m, 3H, C(9)H, C(10)H & C(11)H), 6.83 (br s, 1H, NH), 5.85 (t, J = 2.5 Hz, 1H, C(5)H), 4.87-4.83 (m, 1H, C(4)H), 2.58 (ddd, J = 6.5, 4.0, 1.5 Hz, 1H, C(2)H_a), 2.56-2.46 (m, 2H, C(2)H_b & C(3)H_a), 2.15-2.07 (m, 1H, C(3)H_b); ^{13}C-NMR ($CDCl_3$): δ_C 170.4 (C(1)), 135.3 (C(6)), 132.3 (C(7)), 130.5 (C(11)), 130.3 (C(8)), 128.1 (C(9)), 127.8 (C(10)), 80.7 (C(4)), 55.3 (C(5)), 26.6 (C(2)), 20.7 (C(3)); IR ν_{max} 3210, 2927, 1660, 1549, 1330, 767; LR-ESI-MS: $C_{11}H_{12}ClN_2O_3$ $[M+H]^+$ *m/z* found 255.1 calcd 255.0, $C_{11}H_{11}ClN_2O_3Na$ $[M+Na]^+$ *m/z* found 277.0 calcd 277.0; HR-ESI-MS: $C_{11}H_{11}ClN_2O_3Na$ $[M+Na]^+$ *m/z* found 277.03504 calcd 277.03489 error = 0.58 ppm.

(5*R,6*S**)-6-(3-Chlorophenyl)-5-nitropiperidin-2-one** (**261**)

Compound **13** (106 mg, 0.72 mmol) was dissolved in EtOH (0.23 mL), 3-chlorobenzaldehyde (81 μL, 0.72 mmol) and NH_4OAc (111 mg, 1.44 mmol) were added and the reaction mixture was stirred at reflux for 24 h. The reaction mixture was concentrated and purification by FCC (0.5% MeOH/CH_2Cl_2) yielded **261** (125 mg, 69%) as a yellow solid.

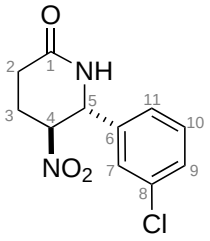

Mpt: 110.1-111.3 °C; ^{1}H-NMR ($CDCl_3$): δ_H 7.39-7.36 (m, 2H, C(9)H & C(10)H), 7.35 (s, 1H, C(7)H), 7.24-7.21 (m, 1H, C(11)H), 6.01 (br s, 1H, NH), 5.27 (d, J = 6.0 Hz, 1H, C(5)H), 4.71 (ddd, J = 7.5, 6.0, 4.0 Hz, 1H, C(4)H), 2.68-2.55 (m, 3H, C(2)H_2 & C(3)H_a), 2.35 (dddd, J = 11.5, 7.5, 3.5, 2.5 Hz, 1H, C(3)H_b); ^{13}C-NMR ($CDCl_3$): δ_C 172.6 (C(1)), 147.9 (C(6)), 135.0 (C(8)), 130.8 (C(7)), 129.8 (C(10)), 126.8 (C(11)), 124.8 (C(9)), 84.8 (C(4)), 58.4 (C(5)), 26.8 (C(2)), 23.3 (C(3)); IR ν_{max} 3065, 2901, 1654, 1549, 786, 695; LR-ESI-MS: $C_{11}H_{12}ClN_2O_3$ $[M+H]^+$ *m/z* found 255.1 calcd 255.0, $C_{11}H_{11}ClN_2O_3Na$ $[M+Na]^+$ *m/z* found 277.0 calcd 277.0; HR-ESI-MS: $C_{11}H_{11}ClN_2O_3Na$ $[M+Na]^+$ *m/z* found 277.03504 calcd 277.03492 error = 0.47 ppm.

(5*R,6*S**)-6-(4-Chlorophenyl)-5-nitropiperidin-2-one** (**262**)

Method A. Compound **13** (4.08 g, 27.8 mmol) was dissolved in EtOH (9.0 mL), 4-chlorobenzaldehyde (3.90 g, 27.8 mmol) and NH_4OAc (4.28 g, 55.5 mmol) were added and the reaction mixture was stirred at reflux for 20 h. The reaction mixture was concentrated and recrystallisation (EtOAc) yielded **262** (7.24 g, 92%) as a white powder.

Method B. Compound **301** (3.84 g, 10.9 mmol) was dissolved in CH_2Cl_2 (140 mL), TFA (4.2 mL, 54.5 mmol) was added and the reaction mixture was stirred at rt for 6 h. The reaction mixture was concentrated, $NaHCO_3$ (56 mL, sat. aq. soln) and CH_2Cl_2 (84 mL) were added and the reaction mixture was stirred at rt for 6 h. The reaction mixture was acidified with 1M HCl, the organic phase was separated and the aqueous phase was extracted with EtOAc (3 x 250 mL). The combined organic phases were dried over Na_2SO_4, filtered and concentrated.

The residue was dissolved in CH_2Cl_2 (56 mL), DBU (0.16 mL, 1.09 mmol) was added and the reaction mixture was stirred at rt for 4 d. The reaction mixture was acidified with 1M HCl, the organic phase was separated and the aqueous phase was extracted with CH_2Cl_2 (3 x 100 mL). The combined organic phases were dried, filtered and concentrated. Purification by FCC (0.5% MeOH/CH_2Cl_2) yielded **262** (2.03 g, 73%) as a white powder with a dr >20:1.

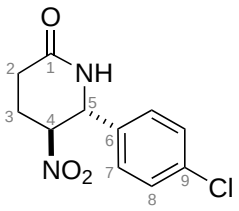

Mpt: 138.1-139.3 °C; ^{1}H-NMR ($CDCl_3$): δ_H 7.42 (d, J = 8.5 Hz, 2H, C(7)H), 7.29 (d, J = 8.5 Hz, 2H, C(8)H), 5.84 (br s, 1H, NH), 5.24 (d, J = 6.5 Hz, 1H, C(5)H), 4.68 (ddd, J = 7.5, 6.5, 4.0 Hz, 1H, C(4)H), 2.74-2.55 (m, 3H, C(2)H_2 & C(3)H_a), 2.40-2.31 (m, 1H, C(3)H_b); ^{13}C-NMR ($CDCl_3$): δ_C 169.6 (C(1)), 135.8 (C(6)), 135.5 (C(9)), 129.7 (C(8)), 127.9 (C(7)), 85.1 (C(4)), 58.4 (C(5)), 27.8 (C(2)), 23.5 (C(3)); IR ν_{max} 3166, 3043, 2897,1653, 1555, 843, 818, 622; LR-ESI-MS: $C_{11}H_{12}ClN_2O_3$ $[M+H]^+$ *m/z* found 255.1 calcd 255.0, $C_{11}H_{11}ClN_2O_3Na$ $[M+Na]^+$ *m/z* found 277.0 calcd 277.0; HR-ESI-MS: $C_{11}H_{11}ClN_2O_3Na$ $[M+Na]^+$ *m/z* found 277.03504 calcd 277.03494 error = 0.36 ppm; Analytical HPLC separation (stationary phase: Chiralpak OD-H, solvent composition: hexane:isopropanol 70:30, flow rate: 1 mL.min^{-1}, injection concentration: 1 mg.mL^{-1}, injection volume: 10 μL, λ: 210 nm): t_1 = 24.8 min, t_2 = 31.2 min.

***tert*-Butyl [(2*R**,3*S**)-2-(4-methoxyphenyl)-6-oxopiperidin-3-yl]carbamate (263)**

Compound **255** (45.0 mg, 0.18 mmol) was dissolved in MeOH (1.2 mL) and the solution was cooled to 0 °C. $NiCl_2 \cdot 6\,H_2O$ (2.1 mg, 0.009 mmol) was added and the solution was stirred at 0 °C for 5 min. $NaBH_4$ (27.0 mg, 0.72 mmol) was added in portions and the reaction mixture was stirred at 0 °C for 30 min. Boc_2O (47.0 mg, 0.22 mmol) was added and the reaction mixture was stirred at rt for 14 h. H_2O (10 mL) was added and the volatiles were removed. The remaining aqueous phase was extracted with EtOAc (3 x 10 mL), the combined organic extracts were dried over Na_2SO_4, filtered and concentrated. Purification by FCC (2.5% MeOH/CH_2Cl_2) yielded **263** (42.0 mg, 73%) as a white powder.

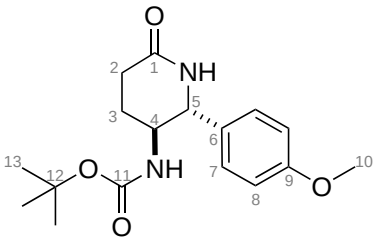

Mpt: 226.8-228.6 °C; ^{1}H-NMR ($CDCl_3$): δ_H 7.24 (d, J = 8.5 Hz, 2H, C(7)H), 6.89 (d, J = 8.5 Hz, 2H, C(8)H), 6.03 (br s, 1H, NH), 4.87 (d, J = 7.0 Hz, 1H, NH), 4.44 (br s, 1H, C(5)H), 3.85 (br s, 1H, C(4)H), 3.74 (s, 3H, C(10)H_3), 2.57-2.51 (m, 2H, C(2)H_2), 2.03 (dtd, J = 13.5, 7.0, 3.5 Hz, 1H, C(3)H_a), 1.82 (dtd, J = 14.5, 7.0, 7.0 Hz, 1H, C(3)H_b), 1.36 (s, 9H, C(13)H_3); ^{13}C-NMR ($CDCl_3$): δ_C 171.2 (C(1)), 159.5 (C(9)), 155.0 (C(11)), 131.7 (C(6)), 127.9 (C(7)), 114.1 (C(8)), 79.9 (C(12)), 60.4 (C(5)), 55.3 (C(10)), 53.4 (C(4)), 28.5 (C(2)), 28.2 (C(13)), 21.0 (C(3)); IR ν_{max} 3378, 2980, 1675, 1513, 1163, 838; LR-ESI-MS: $C_{17}H_{25}N_2O_4$ $[M+H]^+$ *m/z* found 321.2 calcd 321.2, $C_{17}H_{24}N_2O_4Na$ $[M+Na]^+$ *m/z* found 343.0 calcd 343.1; HR-ESI-MS: $C_{17}H_{24}N_2O_4Na$ $[M+Na]^+$ *m/z* found 343.16283 calcd 343.16247 error = 1.03 ppm.

***tert*-Butyl [(2*R**,3*S**)-2-(4-methylphenyl)-6-oxopiperidin-3-yl]carbamate (264)**

Compound **256** (135 mg, 0.58 mmol) was dissolved in MeOH (5 mL) and the solution was cooled to 0 °C. $NiCl_2 \cdot 6\,H_2O$ (6.8 mg, 0.03 mmol) was added and the solution was stirred at 0 °C for 5 min. $NaBH_4$ (87 mg, 2.3 mmol) was added in portions and the reaction mixture was stirred at 0 °C for 30 min. Boc_2O (151 mg, 0.69 mmol) was added and the reaction mixture was stirred

at rt for 14 h. H_2O (40 mL) was added and the volatiles were removed. The remaining aqueous phase was extracted with EtOAc (3 x 40 mL), the combined organic extracts were dried over Na_2SO_4, filtered and concentrated. Purification by FCC (1.5% MeOH/CH_2Cl_2) yielded **264** (159 mg, 91%) as a white powder.

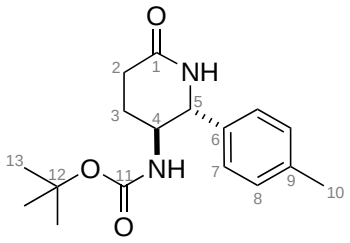

Mpt: 210.9-212.3 °C; ^{1}H-NMR ($CDCl_3$): δ_H 7.21 (d, J = 8.0 Hz, 2H, C(8)H), 7.17 (d, J = 8.0 Hz, 2H, C(7)H), 6.16 (br s, 1H, NH), 4.97 (br s, 1H, NH), 4.49 (br s, 1H, C(5)H), 3.87 (br s, 1H, C(4)H), 2.58-2.52 (m, 2H, C(2)H_2), 2.34 (s, 3H, C(10)H_3), 2.00 (dtd, J = 14.0, 7.0, 3.5 Hz, 1H, C(3)H_a), 1.81 (dtd, J = 14.5, 7.0, 6.5 Hz, 1H, C(3)H_b), 1.37 (s, 9H, C(13)H_3); ^{13}C-NMR ($CDCl_3$): δ_C 171.3 (C(1)), 155.0 (C(11)), 138.0 (C(6)), 136.8 (C(9)), 129.4 (C(7)), 126.6 (C(8)), 79.9 (C(12)), 61.6 (C(5)), 50.8 (C(4)), 28.4 (C(2)), 28.2 (C(13)), 23.4 (C(3)), 21.0 (C(10)); IR ν_{max} 3387, 2936, 1673, 1511, 1164, 727; LR-ESI-MS: $C_{17}H_{25}N_2O_3$ $[M+H]^+$ *m/z* found 305.2 calcd 305.1, $C_{17}H_{24}N_2O_3Na$ $[M+Na]^+$ *m/z* found 327.1 calcd 327.2; HR-ESI-MS: $C_{17}H_{24}N_2O_3Na$ $[M+Na]^+$ *m/z* found 327.16791 calcd 327.16733 error = 1.79 ppm.

***tert*-Butyl [(2*R**,3*S**)-2-(2-fluorophenyl)-6-oxopiperidin-3-yl]carbamate (265)**

Compound **257** (117 mg, 0.49 mmol) was dissolved in MeOH (3.2 mL) and the solution was cooled to 0 °C. $NiCl_2 \cdot 6\,H_2O$ (5.8 mg, 0.025 mmol) was added and the solution was stirred at 0 °C for 5 min. $NaBH_4$ (74 mg, 1.96 mmol) was added in portions and the reaction mixture was stirred at 0 °C for 30 min. Boc_2O (129 mg, 0.59 mmol) was added and the reaction mixture was stirred at rt for 14 h. H_2O (30 mL) was added and the volatiles were removed. The remaining aqueous phase was extracted with EtOAc (3 x 30 mL), the combined organic extracts were dried over Na_2SO_4, filtered and concentrated. Purification by FCC (1.5% MeOH/CH_2Cl_2) yielded **265** (126.1 mg, 84%) as a white powder.

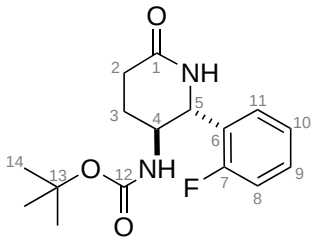

Mpt: 180.0-181.6 °C; ^{1}H-NMR ($CDCl_3$): δ_H 7.41-7.28 (m, 2H, C(9)H & C(11)H), 7.19 (t, J = 7.5 Hz, 1H, C(10)H), 7.06 (dd, J = 10.0, 8.5 Hz, 1H, C(8)H), 6.05 (br s, 1H, NH), 4.85 (br s, 1H, NH), 4.76 (d, J = 5.0 Hz, 1H, C(5)H), 4.03-3.93 (m, 1H, C(4)H), 2.62-2.54 (m, 2H, C(2)H_2), 2.10-2.02 (m, 1H, C(3)H_a), 1.95-1.85 (m, 1H, C(3)H_b), 1.33 (s, 9H, C(14)H_3); ^{13}C-NMR ($CDCl_3$): δ_C 171.5 (C(1)), 160.3 (d, J = 250.3 Hz, C(7)), 154.8 (C(12)), 130.0 (d, J = 8.7 Hz, C(9)), 128.1 (d, J = 9.4 Hz, C(11)), 126.6 (d, J = 18.3 Hz, C(6)), 124.7 (d, J = 3.2 Hz, C(10)), 116.7 (d, J = 22.3 Hz, C(8)), 79.8 (C(13)), 55.6 (d, J = 7.2 Hz, C(5)), 50.1 (C(4)), 29.0 (C(2)), 28.1 (C(14)), 25.3 (C(3)); IR ν_{max} 3361, 2976, 1687, 1668, 1173, 760; LR-ESI-MS: $C_{16}H_{22}FN_2O_3$ $[M+H]^+$ *m/z* found 309.2 calcd 309.1, $C_{16}H_{21}FN_2O_3Na$ $[M+Na]^+$ *m/z* found 331.1 calcd 331.1; HR-ESI-MS: $C_{16}H_{21}FN_2O_3Na$ $[M+Na]^+$ *m/z* found 331.14284 calcd 331.14268 error = 0.52 ppm.

***tert*-Butyl [(2*R**,3*S**)-2-(3-fluorophenyl)-6-oxopiperidin-3-yl]carbamate (266)**

Compound **258** (47 mg, 0.20 mmol) was dissolved in MeOH (1.3 mL) and the solution was cooled to 0 °C. $NiCl_2 \cdot 6\,H_2O$ (2.3 mg, 0.01 mmol) was added and the solution was stirred at 0 °C for 5 min. $NaBH_4$ (29.8 mg, 0.79 mmol) was added in portions and the reaction mixture was stirred at 0 °C for 30 min. Boc_2O (52 mg, 0.24 mmol) was added and the reaction mixture was

stirred at rt for 14 h. H_2O (10 mL) was added and the volatiles were removed. The remaining aqueous phase was extracted with EtOAc (3 x 10 mL), the combined organic extracts were dried over Na_2SO_4, filtered and concentrated. Purification by FCC (1.5% MeOH/CH_2Cl_2) yielded **266** (46.8 mg, 77%) as white needles.

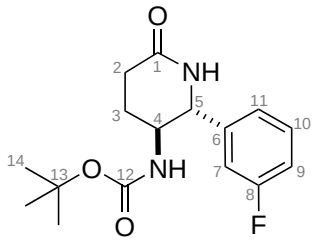

Mpt: 178.1-179.4 °C; ^{1}H-NMR ($CDCl_3$): δ_H 7.35 (td, J = 8.0, 6.0 Hz, 1H, C(10)H), 7.15 (d, J = 7.5 Hz, 1H, C(11)H), 7.08-6.98 (m, 2H, C(7)H & C(9)H), 6.14 (br s, 1H, NH), 4.89 (br s, 1H, NH), 4.55 (br s, 1H, C(5)H), 3.90 (br s, 1H, C(4)H), 2.64-2.43 (m, 2H, C(2)H_2), 2.00 (dtd, J = 14.0, 7.0, 3.5 Hz, 1H, C(3)H_a), 1.84 (dq, J = 14.0, 7.0 Hz, 1H, C(3)H_b), 1.39 (s, 9H, C(14)H_3); ^{13}C-NMR ($CDCl_3$): δ_C 171.1 (C(1)), 163.0 (d, J = 247.2 Hz, C(8)), 154.9 (C(12)), 142.5 (d, J = 7.2 Hz, C(6)), 130.4 (d, J = 7.9 Hz, C(10)), 122.3 (d, J = 4.0 Hz, C(11)), 115.2 (d, J = 20.7 Hz, C(9)), 113.9 (d, J = 22.3 Hz, C(7)), 80.1 (C(13)), 61.4 (C(5)), 50.7 (C(4)), 28.2 (C(14)), 28.1 (C(2)), 23.4 (C(3)); IR ν_{max} 3363, 2985, 1679, 1524, 1234, 1156, 855; LR-ESI-MS: $C_{16}H_{21}FN_2O_3Na$ [M+Na]$^+$ *m/z* found 331.1 calcd 331.1; HR-ESI-MS: $C_{16}H_{21}FN_2O_3Na$ [M+Na]$^+$ *m/z* found 331.14284 calcd 331.14248 error = 1.13 ppm.

***tert*-Butyl [(2*R**,3*S**)-2-(4-fluorophenyl)-6-oxopiperidin-3-yl]carbamate (267)**

Compound **259** (118 mg, 0.50 mmol) was dissolved in MeOH (5 mL) and the solution was cooled to 0 °C. $NiCl_2 \cdot 6\,H_2O$ (5.9 mg, 0.025 mmol) was added and the solution was stirred at 0 °C for 5 min. $NaBH_4$ (76 mg, 2.0 mmol) was added in portions and the reaction mixture was stirred at 0 °C for 30 min. Boc_2O (131 mg, 0.60 mmol) was added and the reaction mixture was stirred at rt for 14 h. H_2O (30 mL) was added and the volatiles were removed. The remaining aqueous phase was extracted with EtOAc (3 x 30 mL), the combined organic extracts were dried over Na_2SO_4, filtered and concentrated. Purification by FCC (1.5% MeOH/CH_2Cl_2) yielded **267** (123.7 mg, 81%) as a white powder.

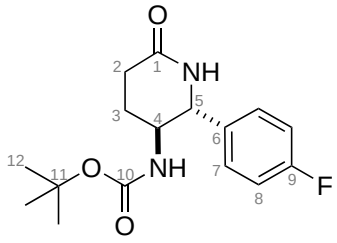

Mpt: 223.5-225.2 °C; ^{1}H-NMR ($CDCl_3$): δ_H 7.32 (dd, J = 8.5, 5.0 Hz, 2H, C(7)H), 7.06 (t, J = 8.5 Hz, 2H, C(8)H), 6.20 (br s, 1H, NH), 4.89 (br s, 1H, NH), 4.49 (br s, 1H, C(5)H), 3.87 (br s, 1H, C(4)H), 2.63-2.51 (m, 2H, C(2)H_2), 2.01 (tdd, J = 10.5, 7.0, 3.5 Hz, 1H, C(3)H_a), 1.88-1.77 (m, 1H, C(3)H_b), 1.37 (s, 9H, C(12)H_3); ^{13}C-NMR ($CDCl_3$): δ_C 171.2 (C(1)), 162.6 (d, J = 247.0 Hz, C(9)), 154.9 (C(10)), 135.5 (d, J = 3.2 Hz, C(6)), 128.5 (d, J = 7.9 Hz, C(7)), 115.7 (d, J = 21.5, C(8)), 80.1 (C(11)), 61.4 (C(5)), 50.8 (C(4)), 28.4 (C(2)), 28.2 (C(12)), 23.7 (C(3)); IR ν_{max} 3382, 1676, 1515, 1234, 836; LR-ESI-MS: $C_{16}H_{22}FN_2O_3$ [M+H]$^+$ *m/z* found 309.2 calcd 309.1, $C_{16}H_{21}FN_2O_3Na$ [M+Na]$^+$ *m/z* found 331.1 calcd 331.1; HR-ESI-MS: $C_{16}H_{21}FN_2O_3Na$ [M+Na]$^+$ *m/z* found 331.14284 calcd 331.14244 error = 1.23 ppm.

***tert*-Butyl [(2*R**,3*S**)-2-(2-chlorophenyl)-6-oxopiperidin-3-yl]carbamate (268)**

Compound **260** (47 mg, 0.19 mmol) was dissolved in MeOH (1.3 mL) and the solution was cooled to 0 °C. $NiCl_2 \cdot 6\,H_2O$ (2.2 mg, 0.009 mmol) was added and the solution was stirred at 0 °C for 5 min. $NaBH_4$ (28 mg, 0.74 mmol) was added in portions and the reaction mixture was stirred at 0 °C for 30 min. Boc_2O (48 mg, 0.22 mmol) was added and the reaction mixture was stirred at rt for 14 h. H_2O (10 mL) was added and the volatiles were removed. The remaining

aqueous phase was extracted with EtOAc (3 x 10 mL), the combined organic extracts were dried over Na_2SO_4, filtered and concentrated. Purification by FCC (1.5% MeOH/CH_2Cl_2) yielded **268** (43 mg, 72%) as a white powder.

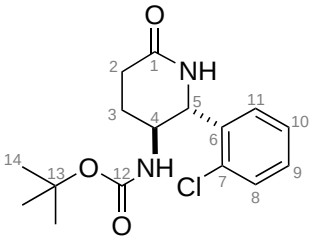

Mpt: 206.4-208.4 °C; ^{1}H-NMR ($CDCl_3$): δ_H 7.41 (d, J = 7.5 Hz, 1H, C(8)H), 7.37 (td, J = 7.5, 1.0 Hz, 1H, C(11)H), 7.32 (dd, J = 7.5, 1.5 Hz, 1H, C(10)H), 7.27 (ddd, J = 8.0, 7.0, 1.5 Hz, 1H, C(9)H), 6.12 (br s, 1H, NH), 4.91 (br s, 1H, NH), 4.89 (d, J = 5.0 Hz, 1H, C(5)H), 4.09-4.00 (m, 1H, C(4)H), 2.58-2.53 (m, 2H, C(2)H_2), 1.99 (dtd, J = 13.0, 6.5, 3.5 Hz, 1H, C(3)H_a), 1.97-1.85 (m, 1H, C(3)H_b), 1.33 (s, 9H, C(14)H_3); ^{13}C-NMR ($CDCl_3$): δ_C 171.6 (C(1)), 154.7 (C(12)), 136.8 (C(6)), 133.2 (C(7)), 129.9 (C(11)), 129.5 (C(9)), 128.4 (C(8)), 127.5 (C(10)), 79.8 (C(13)), 58.5 (C(5)), 49.8 (C(4)), 28.8 (C(2)), 28.2 (C(14)), 24.8 (C(3)); IR ν_{max} 3375, 1688, 1662, 1512, 1172, 758; LR-ESI-MS: $C_{16}H_{21}ClN_2O_3Na$ $[M+Na]^+$ *m/z* found 347.1 calcd 347.0; HR-ESI-MS: $C_{16}H_{21}ClN_2O_3Na$ $[M+Na]^+$ *m/z* found 347.11329 calcd 347.11301 error = 0.82 ppm.

***tert*-Butyl [(2*R**,3*S**)-2-(3-chlorophenyl)-6-oxopiperidin-3-yl]carbamate (269)**

Compound **261** (157 mg, 0.62 mmol) was dissolved in MeOH (4.1 mL) and the solution was cooled to 0 °C. $NiCl_2 \cdot 6\,H_2O$ (7.3 mg, 0.03 mmol) was added and the solution was stirred at 0 °C for 5 min. $NaBH_4$ (94 mg, 2.5 mmol) was added in portions and the reaction mixture was stirred at 0 °C for 30 min. Boc_2O (162 mg, 0.74 mmol) was added and the reaction mixture was stirred at rt for 14 h. H_2O (40 mL) was added and the volatiles were removed. The remaining aqueous phase was extracted with EtOAc (3 x 40 mL), the combined organic extracts were dried over Na_2SO_4, filtered and concentrated. Purification by FCC (1.5% MeOH/CH_2Cl_2) yielded **269** (119 mg, 60%) as white crystals.

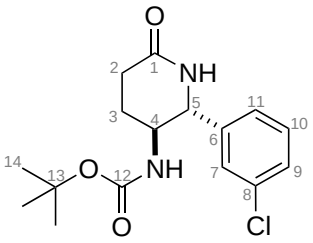

Mpt: 209.3-211.1 °C; ^{1}H-NMR ($CDCl_3$): δ_H 7.42-7.30 (m, 4H, C(7)H, C(9)H, C(10)H & C(11)H), 5.98 (br s, 1H, NH), 4.80 (br s, 1H, NH), 4.53 (br s, 1H, C(5)H), 3.89 (br s, 1H, C(4)H), 2.68-2.50 (m, 2H, C(2)H_2), 2.08-1.97 (m, 1H, C(3)H_a), 1.86 (dq, J = 13.5, 6.5 Hz, 1H, C(3)H_b), 1.39 (s, 9H, C(14)H_3); ^{13}C-NMR ($CDCl_3$): δ_C 175.1 (C(1)), 152.6 (C(12)), 141.9 (C(6)), 132.5 (C(10)), 130.2 (C(10)), 128.8 (C(7)), 128.5 (C(11)), 127.0 (C(9)), 81.4 (C(13)), 61.5 (C(5)), 50.6 (C(4)), 30.8 (C(2)), 28.2 (C(14)), 23.5 (C(3)); IR ν_{max} 3359, 2983, 1678, 1528, 1161, 795; LR-ESI-MS: $C_{16}H_{22}ClN_2O_3$ $[M+H]^+$ *m/z* found 325.1 calcd 325.0, $C_{16}H_{21}ClN_2O_3Na$ $[M+Na]^+$ *m/z* found 347.0 calcd 347.1; HR-ESI-MS: $C_{16}H_{21}ClN_2O_3Na$ $[M+Na]^+$ *m/z* found 347.11329 calcd 347.11249 error = 2.32 ppm.

***tert*-Butyl [(2*R**,3*S**)-2-(4-chlorophenyl)-6-oxopiperidin-3-yl]carbamate (270)**

Compound **262** (101 mg, 0.72 mmol) was dissolved in MeOH (3.2 mL) and the solution was cooled to 0 °C. $NiCl_2 \cdot 6\,H_2O$ (5.8 mg, 0.02 mmol) was added and the solution was stirred at 0 °C for 5 min. $NaBH_4$ (74 mg, 2.0 mmol) was added in portions and the reaction mixture was stirred at 0 °C for 30 min. Boc_2O (129 mg, 0.59 mmol) was added and the reaction mixture was stirred at rt for 14 h. H_2O (30 mL) was added and the volatiles were removed. The remaining aqueous phase was extracted with EtOAc (3 x 30 mL), the combined organic extracts were dried

over Na_2SO_4, filtered and concentrated. Purification by FCC (1.5% MeOH/CH_2Cl_2) yielded **270** (130 mg, 65%) as a white powder.

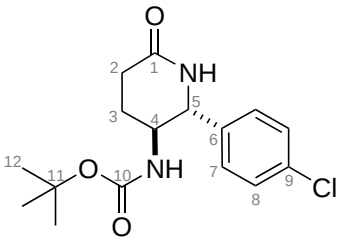

Mpt: 233.9-235.9 °C; ^{1}H-NMR (CD_3OD): δ_H 7.70 (d, J = 1.0 Hz, 1H, NH), 7.38 (d, J = 8.5 Hz, 2H, C(7)H), 7.27 (d, J = 8.5 Hz, 2H, C(8)H), 7.11 (d, J = 8.0 Hz, 1H, NH), 4.31 (d, J = 6.5 Hz, 1H, C(5)H), 3.56-3.47 (m, 1H, C(4)H), 2.41-2.26 (m, 2H, C(2)H_2), 1.76-1.61 (m, 2H, C(3)H_2), 1.27 (s, 9H, C(12)H_3); ^{13}C-NMR (CD_3OD): δ_C 179.6 (C(1)), 150.2 (C(10)), 141.4 (C(6)), 138.5 (C(8)), 137.7 (C(7)), 132.6 (C(9)), 87.5 (C(11)), 69.2 (C(5)), 60.7 (C(4)), 38.5 (C(2)), 37.7 (C(12)), 34.2 (C(3)); IR ν_{max} 3380, 2382, 1675, 1514, 1493, 1163, 841; LR-ESI-MS: $C_{16}H_{21}ClN_2O_3Na$ $[M+Na]^+$ m/z found 347.1 calcd 347.0; HR-ESI-MS: $C_{16}H_{21}ClN_2O_3Na$ $[M+Na]^+$ m/z found 347.11329 calcd 347.11298 error = 0.91 ppm.

***tert*-Butyl [(2*R**,3*S**)-1-(1,4-dimethyl-2-oxo-1,2-dihydroquinolin-7-yl)-2-(4-methoxyphenyl)-6-oxopiperidin-3-yl]carbamate (271)**

In a pressure tube under inert conditions, **263** (39.0 mg, 0.12 mmol), **218** (46.0 mg, 0.18 mmol) and K_3PO_4 (52.0 mg, 0.24 mmol) were combined. 1,4-dioxane (1.2 mL) was added and the solution was degassed. (+/-)-*trans*-1,2-diaminocyclohexane (15 μL, 0.12 mmol) and CuI (23.0 mg, 0.12 mmol) were added, the tube was sealed and the reaction mixture was stirred at 97 °C for 42 h. The reaction mixture was passed through a plug of Celite and the Celite was washed with CH_2Cl_2 (30 mL). The combined filtrate was concentrated and purification by iterative FCC (20% isopropanol/hexane then 2% MeOH/CH_2Cl_2) yielded **271** (17.3 mg, 28%) as a pale yellow opaque oil.

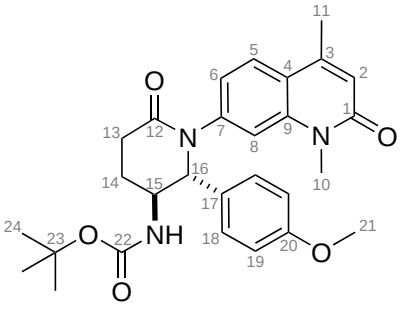

^{1}H-NMR ($CDCl_3$): δ_H 7.60 (d, J = 8.5 Hz, 1H, C(5)H), 7.28 (d, J = 8.5 Hz, 2H, C(18)H), 7.15 (d, J = 1.5 Hz, 1H, C(8)H), 7.06 (dd, J = 8.5, 1.5 Hz, 1H, C(6)H), 6.90 (d, J = 8.5 Hz, 2H, C(19)H), 6.52 (d, J = 1.0 Hz, 1H, C(2)H), 5.25-5.18 (m, 1H, C(16)H), 4.05-3.99 (m, 1H, C(15)H), 3.79 (s, 3H, C(21)H_3), 3.52 (s, 3H, C(10)H_3), 2.82 (ddd, J = 19.0, 8.0, 3.0 Hz, 1H, C(13)H_a), 2.72 (ddd, J = 19.0, 10.5, 8.0 Hz, 1H, C(13)H_b), 2.38 (d, J = 0.5 Hz, 3H, C(11)H_3), 2.22-2.12 (m, 1H, C(14)H_a), 1.88-1.76 (m, 1H, C(14)H_b), 1.49 (s, 9H, C(24)H_3); ^{13}C-NMR ($CDCl_3$): δ_C 169.6 (C(12)), 162.0 (C(1)), 159.3 (C(20)), 155.4 (C(22)), 145.9 (C(4)), 144.2 (C(7)), 140.2 (C(9)), 130.6 (C(17)), 127.9 (C(18)), 125.8 (C(5)), 121.2 (C(2)), 120.7 (C(6)), 120.0 (C(3)), 114.2 (C(19)), 113.0 (C(8)), 80.3 (C(23)), 68.6 (C(16)), 55.3 (C(21)), 51.3 (C(15)), 29.1 (C(10)), 28.4 (C(24)), 28.0 (C(13)), 21.0 (C(14)), 18.1 (C(11)); IR ν_{max} 3278, 2975, 2360, 2341, 1704, 1650, 1594, 1512, 1249, 1172; LR-ESI-MS: $C_{28}H_{34}N_3O_5$ $[M+H]^+$ m/z found 492.3 calcd 492.4; $C_{28}H_{33}N_3O_5Na$ $[M+Na]^+$ m/z found 514.2 calcd 514.2; HR-ESI-MS: $C_{28}H_{33}N_3O_5Na$ $[M+Na]^+$ m/z found 514.23124 calcd 514.23011 error = 2.22 ppm.

***tert*-Butyl [(2*R**,3*S**)-1-(1,4-dimethyl-2-oxo-1,2-dihydroquinolin-7-yl)-2-(4-methylphenyl)-6-oxopiperidin-3-yl]carbamate (272)**

In a pressure tube under inert conditions, **264** (37.1 mg, 0.12 mmol), **218** (46.0 mg, 0.18 mmol) and K_3PO_4 (52.0 mg, 0.24 mmol) were combined. 1,4-dioxane (1.2 mL) was added and the

solution was degassed. (+/-)-*trans*-1,2-diaminocyclohexane (15 μL, 0.12 mmol) and CuI (23.0 mg, 0.12 mmol) were added, the tube was sealed and the reaction mixture was stirred at 97 °C for 42 h. The reaction mixture was passed through a plug of Celite and the Celite was washed with CH_2Cl_2 (30 mL). The combined filtrate was concentrated and purification by iterative FCC (25% isopropanol/hexane then 1.5% MeOH/CH_2Cl_2) yielded **272** (26.2 mg, 45%) as a pale yellow opaque oil.

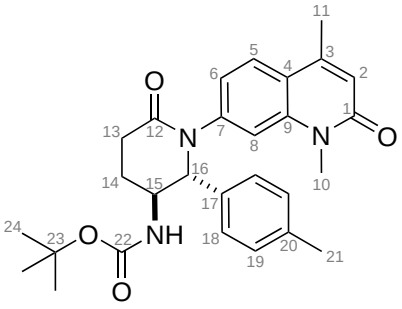

^{1}H-NMR ($CDCl_3$): δ_H 7.60 (d, J = 8.5 Hz, 1H, C(5)H), 7.26 (d, J = 7.0 Hz, 2H, C(19)H), 7.19 (s, 1H, C(8)H), 7.17 (dd, J = 5.0, 1.5 Hz, 2H, C(18)H), 7.07 (dd, J = 8.5, 1.0 Hz, 1H, C(6)H), 6.52 (d, J = 0.5 Hz, 1H, C(2)H), 5.26 (br s, 1H, C(16)H), 4.04 (br s, 1H, C(15)H), 3.51 (s, 3H, C(10)H_3), 2.82 (ddd, J = 19.0, 8.0, 2.5 Hz, 1H, C(13)H_a), 2.72 (ddd, J = 19.0, 10.5, 7.5 Hz, 1H, C(13)H_b), 2.37 (s, 3H, C(11)H_3), 2.33 (s, 3H, C(21)H_3), 2.21-2.11 (m, 1H, C(14)H_a), 1.87-1.78 (m, 1H, C(14)H_b), 1.50 (s, 9H, C(24)H_3); ^{13}C-NMR ($CDCl_3$): δ_C 169.7 (C(12)), 162.0 (C(1)), 155.4 (C(22)), 145.8 (C(4)), 144.3 (C(7)), 140.2 (C(9)), 137.9 (C(20)), 135.7 (C(17)), 129.5 (C(18)), 126.6 (C(19)), 125.8 (C(5)), 121.0 (C(2)), 120.6 (C(6)), 120.0 (C(3)), 113.1 (C(8)), 80.3 (C(23)), 68.9 (C(16)), 53.4 (C(15)), 29.1 (C(10)), 28.4 (C(24)), 27.8 (C(13)), 21.0 (C(21)), 20.9 (C(14)), 18.8 (C(11)); IR ν_{max} 3277, 2976, 1704, 1649, 1594, 1168, 731; LR-ESI-MS: $C_{28}H_{34}N_3O_4$ $[M+H]^+$ m/z found 476.3 calcd 476.3, $C_{28}H_{33}N_3O_4Na$ $[M+Na]^+$ m/z found 498.3 calcd 498.2; HR-ESI-MS: $C_{28}H_{33}N_3O_4Na$ $[M+Na]^+$ m/z found 498.23633 calcd 498.23474 error = 3.18 ppm.

tert-Butyl [(2*R,3*S**)-1-(1,4-dimethyl-2-oxo-1,2-dihydroquinolin-7-yl)-2-(2-fluorophenyl)-6-oxopiperidin-3-yl]carbamate (273)**

In a pressure tube under inert conditions, **265** (37.6 mg, 0.12 mmol), **218** (46.0 mg, 0.18 mmol) and K_3PO_4 (52.0 mg, 0.24 mmol) were combined. 1,4-dioxane (1.2 mL) was added and the solution was degassed. (+/-)-*trans*-1,2-diaminocyclohexane (15 μL, 0.12 mmol) and CuI (23.0 mg, 0.12 mmol) were added, the tube was sealed and the reaction mixture was stirred at 97 °C for 42 h. The reaction mixture was passed through a plug of Celite and the Celite was washed with CH_2Cl_2 (30 mL). The combined filtrate was concentrated and purification by iterative FCC (30% isopropanol/hexane then 1% MeOH/CH_2Cl_2) yielded **273** (13.9 mg, 24%) as a pale yellow opaque oil.

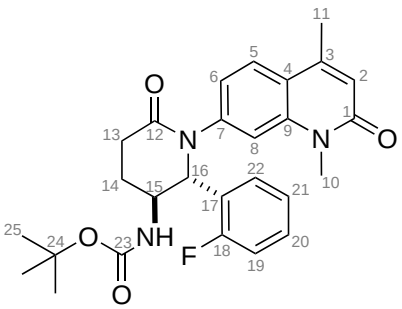

^{1}H-NMR ($CDCl_3$): δ_H 7.59 (d, J = 8.5 Hz, 1H, C(5)H), 7.36 (td, J = 7.5, 1.0 Hz, 1H, C(22)H), 7.29-7.26 (m, 1H, C(20)H), 7.15 (td, J = 7.5, 1.0 Hz, 1H, C(21)H), 7.13 (d, J = 1.5 Hz, 1H, C(8)H), 7.05 (dd, J = 8.5, 1.5 Hz, 1H, C(6)H), 7.03 (ddd, J = 11.0, 8.0, 0.5 Hz, 1H, C(19)H), 6.52 (d, J = 1.0 Hz, 1H, C(2)H), 5.40 (br s, 1H, NH), 5.09 (d, J = 5.0 Hz, 1H, C(16)H), 4.22-4.15 (m, 1H, C(15)H)3.52 (s, 3H, C(10)H_3), 2.86 (ddd, J = 19.0, 7.5, 5.5 Hz, 1H, C(13)H_a), 2.77 (ddd, J = 19.0, 8.5, 7.5 Hz, 1H, C(13)H_b), 2.38 (d, J = 1.0 Hz, 3H, C(11)H_3), 2.23-2.14 (m, 1H, C(14)H_a), 2.03-1.94 (m, 1H, C(14)H_b), 1.43 (s, 9H, C(25)H_3); ^{13}C-NMR ($CDCl_3$): δ_C 169.7 (C(12)), 162.0 (C(1)), 160.1 (d, J = 248.0 Hz, C(18)), 155.0 (C(23)), 145.8 (C(4)),

143.5 (*C*(7)), 140.2 (*C*(9)), 130.2 (d, *J* = 7.9 Hz, *C*(20)), 128.7 (d, *J* = 3.2 Hz, *C*(22)), 125.9 (*C*(5)), 124.4 (d, *J* = 3.2 Hz, *C*(21)), 121.2 (*C*(2)), 120.7 (*C*(6)), 120.2 (*C*(3)), 116.1 (d, *J* = 21.5 Hz, *C*(19)), 113.1 (*C*(8)), 107.4 (d, *J* = 20.7 Hz, *C*(17)), 77.2 (*C*(24)), 64.5 (*C*(16)), 50.0 (*C*(15)), 29.1 (*C*(10)), 28.8 (*C*(13)), 28.3 (*C*(25)), 23.1 (*C*(14)), 18.8 (*C*(11)); IR ν_{max} 3276, 2977, 1705, 1650, 1593, 1168, 730; LR-ESI-MS: $C_{27}H_{31}FN_3O_4$ $[M+H]^+$ *m/z* found 480.2 calcd 480.3, $C_{27}H_{30}FN_3O_4Na$ $[M+Na]^+$ *m/z* found 502.2 calcd 502.2; HR-ESI-MS: $C_{27}H_{31}FN_3O_4$ $[M+H]^+$ *m/z* found 480.22931 calcd 480.22833 error = 2.04 ppm.

***tert*-Butyl [(2*R**,3*S**)-1-(1,4-dimethyl-2-oxo-1,2-dihydroquinolin-7-yl)-2-(3-fluorophenyl)-6-oxopiperidin-3-yl]carbamate (274)**

In a pressure tube under inert conditions, **266** (37.6 mg, 0.12 mmol), **218** (46.0 mg, 0.18 mmol) and K_3PO_4 (52.0 mg, 0.24 mmol) were combined. 1,4-dioxane (1.2 mL) was added and the solution was degassed. (+/-)-*trans*-1,2-diaminocyclohexane (15 μL, 0.12 mmol) and CuI (23.0 mg, 0.12 mmol) were added, the tube was sealed and the reaction mixture was stirred at 97 °C for 42 h. The reaction mixture was passed through a plug of Celite and the Celite was washed with CH_2Cl_2 (30 mL). The combined filtrate was concentrated and purification by iterative FCC (30% isopropanol/hexane then 1.5% MeOH/CH_2Cl_2) yielded **274** (17.6 mg, 30%) as a pale yellow opaque oil.

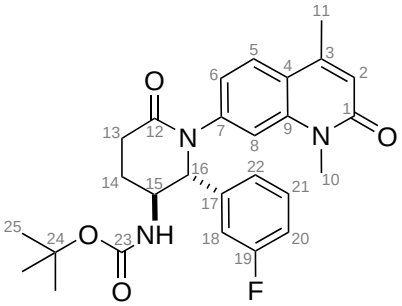

^{1}H-NMR ($CDCl_3$): δ_H 7.62 (d, *J* = 8.5 Hz, 1H, C(5)*H*), 7.36 (td, *J* = 8.0, 5.5 Hz, 1H, C(21)*H*), 7.19 (d, *J* = 7.5 Hz, 1H, C(22)*H*), 7.16 (d, *J* = 1.5 Hz, 1H, C(8)*H*), 7.11 (d, *J* = 9.0 Hz, 1H, C(18)*H*), 7.06 (dd, *J* = 8.5, 1.0 Hz, 1H, C(6)*H*), 7.00 (td, *J* = 8.5, 2.5 Hz, 1H, C(20)*H*), 6.53 (d, *J* = 1.0 Hz, 1H, C(2)*H*), 5.35 (br s, 1H, N*H*), 5.23 (br s, 1H, C(16)*H*), 4.06 (br s, 1H, C(15)*H*), 3.54 (s, 3H, C(10)H_3), 2.84 (ddd, *J* = 19.0, 8.0, 3.0 Hz, 1H, C(13)H_a), 2.74 (ddd, *J* = 19.0, 10.5, 8.0 Hz, 1H, C(13)H_b), 2.39 (d, *J* = 0.5 Hz, 3H, C(11)H_3), 2.20-2.11 (m, 1H, C(14)H_a), 1.90-1.82 (m, 1H, C(14)H_b), 1.50 (s, 9H, C(25)H_3); ^{13}C-NMR ($CDCl_3$): δ_C 169.5 (*C*(12)), 163.1 (d, *J* = 248.8 Hz, *C*(19)), 162.0 (*C*(1)), 155.4 (*C*(23)), 145.8 (*C*(4)), 144.0 (*C*(7)), 141.5 (d, *J* = 6.4 Hz, *C*(17)), 140.3 (*C*(9)), 130.6 (d, *J* = 7.9 Hz, *C*(21)), 126.0 (*C*(5)), 122.4 (d, *J* = 3.2 Hz, *C*(22)), 121.2 (*C*(2)), 120.6 (*C*(6)), 120.2 (*C*(3)), 115.2 (d, *J* = 20.7 Hz, *C*(20)), 113.9 (d, *J* = 22.3 Hz, *C*(18)), 113.1 (*C*(8)), 80.5 (*C*(24)), 68.5 (*C*(16)), 51.1 (*C*(15)), 29.1 (*C*(10)), 28.4 (*C*(25)), 27.8 (*C*(13)), 21.0 (*C*(14)), 18.8 (*C*(11)); IR ν_{max} 3282, 2977, 1704, 1650, 1593, 1169, 731; LR-ESI-MS: $C_{27}H_{31}FN_3O_4$ $[M+H]^+$ *m/z* found 480.2 calcd 480.3, $C_{27}H_{30}FN_3O_4Na$ $[M+Na]^+$ *m/z* found 502.2 calcd 502.2; HR-ESI-MS: $C_{27}H_{31}FN_3O_4$ $[M+H]^+$ *m/z* found 480.22931 calcd 480.22834 error = 1.87 ppm.

***tert*-Butyl [(2*R**,3*S**)-1-(1,4-dimethyl-2-oxo-1,2-dihydroquinolin-7-yl)-2-(4-fluorophenyl)-6-oxopiperidin-3-yl]carbamate (275)**

In a pressure tube under inert conditions, **267** (37.6 mg, 0.12 mmol), **218** (46.0 mg, 0.18 mmol) and K_3PO_4 (52.0 mg, 0.24 mmol) were combined. 1,4-dioxane (1.2 mL) was added and the solution was degassed. (+/-)-*trans*-1,2-diaminocyclohexane (15 μL, 0.12 mmol) and CuI (23.0 mg, 0.12 mmol) were added, the tube was sealed and the reaction mixture was stirred at 97 °C for 42 h. The reaction mixture was passed through a plug of Celite and the Celite was washed

with CH_2Cl_2 (30 mL). The combined filtrate was concentrated and purification by iterative FCC (30% isopropanol/hexane then 1.5% MeOH/CH_2Cl_2) yielded **275** (10.8 mg, 19%) as a pale yellow opaque oil.

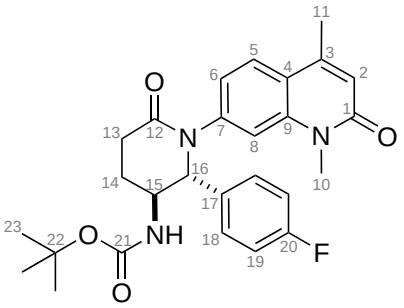

^{1}H-NMR ($CDCl_3$): δ_H 7.61 (d, J = 8.5 Hz, 1H, C(5)H), 7.36 (t, J = 7.0 Hz, 2H, C(18)H), 7.13 (d, J = 1.5 Hz, 1H, C(8)H), 7.08 (t, J = 8.5 Hz, 2H, C(19)H), 7.04 (dd, J = 8.5, 1.5 Hz, 1H, C(6)H), 6.54 (d, J = 1.0 Hz, 1H, C(2)H), 5.12 (d, J = 6.5 Hz, 1H, C(16)H), 4.03 (br s, 1H, C(15)H), 3.54 (s, 3H, C(10)H_3), 2.84 (ddd, J = 19.0, 7.5, 2.5 Hz, 1H, C(13)H_a), 2.73 (ddd, J = 18.5, 10.0, 8.0 Hz, 1H, C(13)H_b), 2.39 (d, J = 1.0 Hz, 3H, C(11)H_3), 2.19-2.11 (m, 1H, C(14)H_a), 1.88-1.82 (m, 1H, C(14)H_b), 1.50 (s, 9H, C(23)H_3); ^{13}C-NMR ($CDCl_3$): δ_C 169.5 (C(12)), 162.4 (d, J = 247.0 Hz, C(20)), 162.0 (C(1)), 155.4 (C(21)), 145.9 (C(4)), 144.0 (C(7)), 140.3 (C(9)), 134.5 (d, J = 2.9 Hz, C(17)), 128.5 (d, J = 8.6 Hz, C(18)), 126.0 (C(5)), 121.2 (C(2)), 120.7 (C(6)), 120.2 (C(3)), 115.9 (d, J = 21.0 Hz, C(19)), 113.0 (C(8)), 80.5 (C(22)), 68.5 (C(16)), 53.4 (C(15)), 29.1 (C(10)), 28.4 (C(23)), 27.9 (C(13)), 21.0 (C(14)), 18.9 (C(11)); IR ν_{max} 3284, 2977, 1704, 1652, 1595, 1168, 732; LR-ESI-MS: $C_{27}H_{31}FN_3O_4$ $[M+H]^+$ *m/z* found 480.2 calcd 480.3, $C_{27}H_{30}FN_3O_4Na$ $[M+Na]^+$ *m/z* found 502.3 calcd 502.2; HR-ESI-MS: $C_{27}H_{30}FN_3O_4Na$ $[M+Na]^+$ *m/z* found 502.21126 calcd 502.21002 error = 2.46 ppm.

***tert*-Butyl [(2*R**,3*S**)-2-(2-chlorophenyl)-1-(1,4-dimethyl-2-oxo-1,2-dihydroquinolin-7-yl)-6-oxopiperidin-3-yl]carbamate (276)**

In a pressure tube under inert conditions, **268** (39.6 mg, 0.12 mmol), **218** (46.0 mg, 0.18 mmol) and K_3PO_4 (52.0 mg, 0.24 mmol) were combined. 1,4-dioxane (1.2 mL) was added and the solution was degassed. (+/-)-*trans*-1,2-diaminocyclohexane (15 μL, 0.12 mmol) and CuI (23.0 mg, 0.12 mmol) were added, the tube was sealed and the reaction mixture was stirred at 97 °C for 42 h. The reaction mixture was passed through a plug of Celite and the Celite was washed with CH_2Cl_2 (30 mL). The combined filtrate was concentrated and purification by iterative FCC (25% isopropanol/hexane then 1.5% MeOH/CH_2Cl_2) yielded **276** (4.2 mg, 7%) as a pale yellow opaque oil.

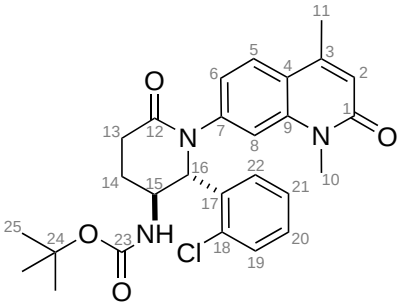

^{1}H-NMR ($CDCl_3$): δ_H 7.59 (d, J = 8.5 Hz, 1H, C(5)H), 7.44 (d, J = 7.5 Hz, 1H, C(19)H), 7.33-7.28 (m, 2H, C(20)H & C(22)H), 7.22 (td, J = 7.5, 1.0 Hz, 1H, C(21)H), 7.12 (d, J = 1.5 Hz, 1H, C(8)H), 7.07 (dd, J = 8.5, 1.5 Hz, 1H, C(6)H), 6.53 (d, J = 1.0 Hz, 1H, C(2)H), 5.52 (br s, 1H, NH), 4.94 (d, J = 8.0 Hz, 1H, C(16)H), 4.31-4.25 (m, 1H, C(15)H), 3.54 (s, 3H, C(10)H_3), 2.91-2.80 (m, 2H, C(13)H_2), 2.38 (d, J = 0.5 Hz, 3H, C(11)H_3), 2.17-2.12 (m, 1H, C(14)H_a), 2.07-2.00 (m, 1H, C(14)H_b), 1.41 (s, 9H, C(25)H_3); ^{13}C-NMR ($CDCl_3$): δ_C 170.0 (C(12)), 162.0 (C(1)), 154.7 (C(23)), 145.9 (C(4)), 143.3 (C(7)), 140.2 (C(9)), 135.7 (C(17)), 133.2 (C(18)), 130.3 (C(22)), 129.6 (C(21)), 128.9 (C(19)), 127.1 (C(20)), 125.8 (C(5)), 121.1 (C(2)), 120.7 (C(6)), 120.1 (C(3)), 112.7 (C(8)), 80.2 (C(24)), 66.2 (C(16)), 53.4 (C(15)), 29.4 (C(13)), 29.2 (C(10)), 28.3 (C(25)), 23.7 (C(14)), 18.9 (C(11)); IR ν_{max} 3281,

2976, 1706, 1652, 1594, 1168, 731; LR-ESI-MS: $C_{27}H_{31}ClN_3O_4$ $[M+H]^+$ *m/z* found 496.2 calcd 496.1, $C_{27}H_{30}ClN_3O_4Na$ $[M+Na]^+$ *m/z* found 518.2 calcd 518.2; HR-ESI-MS: $C_{27}H_{31}ClN_3O_4$ $[M+H]^+$ *m/z* found 496.19976 calcd 496.19867 error = 2.20 ppm.

***tert*-Butyl [(2*R**,3*S**)-2-(3-chlorophenyl)-1-(1,4-dimethyl-2-oxo-1,2-dihydroquinolin-7-yl)-6-oxopiperidin-3-yl]carbamate (277)**

In a pressure tube under inert conditions, **269** (39.6 mg, 0.12 mmol), **218** (46.0 mg, 0.18 mmol) and K_3PO_4 (52.0 mg, 0.24 mmol) were combined. 1,4-dioxane (1.2 mL) was added and the solution was degassed. (+/-)-*trans*-1,2-diaminocyclohexane (15 μL, 0.12 mmol) and CuI (23.0 mg, 0.12 mmol) were added, the tube was sealed and the reaction mixture was stirred at 97 °C for 42 h. The reaction mixture was passed through a plug of Celite and the Celite was washed with CH_2Cl_2 (30 mL). The combined filtrate was concentrated and purification by iterative FCC (25% isopropanol/hexane then 1% MeOH/CH_2Cl_2) yielded **277** (26.8 mg, 60%) as a pale yellow opaque oil.

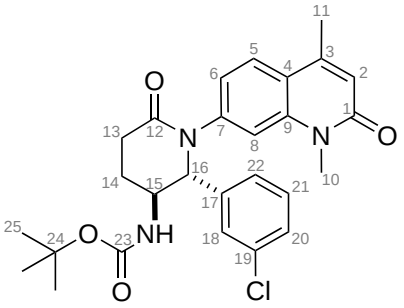

^{1}H-NMR ($CDCl_3$): δ_H 7.62 (d, J = 8.5 Hz, 1H, C(5)H), 7.38 (br s, 1H, C(18)H), 7.34-7.26 (m, 3H, C(20)H, C(21)H & C(22)H), 7.16 (d, J = 1.5 Hz, 1H, C(8)H), 7.04 (dd, J = 8.5, 1.0 Hz, 1H, C(6)H), 6.53 (s, 1H, C(2)H), 5.32 (br s, 1H, C(16)H), 4.05 (br s, 1H, C(15)H), 3.54 (s, 3H, C(10)H_3), 2.84 (ddd, J = 19.0, 8.0, 2.0 Hz, 1H, C(13)H_a), 2.74 (ddd, J = 19.0, 10.5, 8.0 Hz, 1H, C(13)H_b), 2.38 (s, 3H, C(11)H_3), 2.19-2.10 (m, 1H, C(14)H_a), 1.90-1.77 (m, 1H, C(14)H_b), 1.50 (s, 9H, C(25)H_3); ^{13}C-NMR ($CDCl_3$): δ_C 169.5 (*C*(12)), 162.0 (*C*(1)), 155.4 (*C*(23)), 145.8 (*C*(4)), 143.9 (*C*(7)), 140.9 (*C*(9)), 140.4 (*C*(17)), 135.0 (*C*(19)), 130.2 (*C*(21)), 128.4 (*C*(22)), 127.0 (*C*(18)), 126.0 (*C*(5)), 124.9 (*C*(20)), 121.2 (*C*(2)), 120.6 (*C*(6)), 120.2 (*C*(3)), 113.2 (*C*(8)), 80.5 (*C*(24)), 68.5 (*C*(16)), 53.4 (*C*(15)), 29.1 (*C*(10)), 28.3 (*C*(25)), 27.8 (*C*(13)), 20.9 (*C*(14)), 18.8 (*C*(10)); IR ν_{max} 3280, 2976, 1704, 1650, 1594, 1168, 731; LR-ESI-MS: $C_{27}H_{31}ClN_3O_4$ $[M+H]^+$ *m/z* found 496.2 calcd 496.1, $C_{27}H_{30}ClN_3O_4Na$ $[M+Na]^+$ *m/z* found 518.2 calcd 518.2; HR-ESI-MS: $C_{27}H_{31}ClN_3O_4$ $[M+H]^+$ *m/z* found 496.19976 calcd 496.19867 error = 2.20 ppm.

***tert*-Butyl [(2*R**,3*S**)-2-(4-chlorophenyl)-1-(1,4-dimethyl-2-oxo-1,2-dihydroquinolin-7-yl)-6-oxopiperidin-3-yl]carbamate (278), *tert*-butyl[(2*R*,3*S*)-2-(4-chlorophenyl)-1-(1,4-dimethyl-2-oxo-1,2-dihydroquinolin-7-yl)-6-oxopiperidin-3-yl]carbamate ((–)-278) & *tert*-butyl [(2*S*,3*R*)-2-(4-chlorophenyl)-1-(1,4-dimethyl-2-oxo-1,2-dihydroquinolin-7-yl)-6-oxo-piperidin-3-yl]carbamate ((+)-278)**

In a pressure tube under inert conditions, **270** (205 mg, 0.63 mmol), **218** (239 mg, 0.95 mmol) and K_3PO_4 (268 mg, 1.26 mmol) were combined. 1,4-dioxane (6.3 mL) was added and the solution was degassed. (+/-)-*trans*-1,2-diaminocyclohexane (76 μL, 0.63 mmol) and CuI (120 mg, 0.63 mmol) were added, the tube was sealed and the reaction mixture was stirred at 97 °C for 42 h. The reaction mixture was passed through a plug of Celite and the Celite was washed with CH_2Cl_2 (100 mL). The combined filtrate was concentrated and purification by FCC (0.5% MeOH/CH_2Cl_2) yielded **278** (205 mg, 65%) as a white powder. The enantiomers of **278** were preparatively resolved by HPLC (stationary phase: Semipreparative Chiralpak AD,

solvent composition: hexane:isopropanol 80:20, flow rate: 3 mL.min^{-1}, injection concentration: 15 mg.mL^{-1}, injection volume: 100 μL, λ: 220 nm) with the enantiomers eluting at 23.4 min ((–)-**278**) and 42.1 min ((+)-**278**).

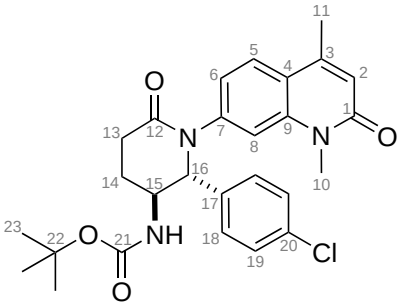

278: Mpt: 138.2-139.6 °C; ^{1}H-NMR ($CDCl_3$): δ_H 7.61 (d, J = 8.5 Hz, 1H, C(5)H), 7.40-7.31 (m, 4H, C(18)H & C(19)H), 7.14 (d, J = 1.5 Hz, 1H, C(8)H), 7.03 (dd, J = 8.5, 1.5 Hz, 1H, C(6)H), 6.54 (d, J = 1.0 Hz, 1H, C(2)H), 5.32 (br s, 1H, NH), 5.13 (d, J = 6.0 Hz, 1H, C(16)H), 4.03 (d, J = 6.0 Hz, 1H, C(15)H), 3.55 (s, 3H, C(10)H_3), 2.83 (ddd, J = 19.0, 8.0, 3.0 Hz, 1H, C(13)H_a), 2.72 (ddd, J = 19.0, 10.5, 8.0 Hz, 1H, C(13)H_b), 2.39 (d, J = 1.0 Hz, 3H, C(11)H_3), 2.18-2.10 (m, 1H, C(14)H_a), 1.90-1.82 (m, 1H, C(14)H_b), 1.50 (s, 9H, C(23)H_3); ^{13}C-NMR ($CDCl_3$): δ_C 169.5 (C(12)), 162.0 (C(1)), 155.4 (C(21)), 145.8 (C(4)), 143.9 (C(7)), 140.3 (C(9)), 137.3 (C(17)), 134.1 (C(20)), 129.1 (C(19)), 128.1 (C(18)), 126.0 (C(5)), 121.2 (C(2)), 120.6 (C(6)), 120.2 (C(3)), 113.0 (C(8)), 80.5 (C(22)), 68.6 (C(16)), 51.2 (C(15)), 29.1 (C(10)), 28.3 (C(23)), 27.9 (C(13)), 21.0 (C(14)), 18.8 (C(11)); IR ν_{max} 3282, 2976, 1704, 1650, 1594, 1168, 731; LR-ESI-MS: $C_{27}H_{31}ClN_3O_4$ [M+H]$^+$ *m/z* found 496.2 calcd 496.2, $C_{27}H_{30}ClN_3O_4Na$ [M+Na]$^+$ *m/z* found 518.3 calcd 518.2; HR-ESI-MS: $C_{27}H_{31}ClN_3O_4$ [M+H]$^+$ *m/z* found 496.19976 calcd 496.19868 error = 2.40 ppm; Analytical HPLC separation (stationary phase: Chiralpak AD, solvent composition: hexane:isopropanol 80:20, flow rate: 1 mL.min^{-1}, injection concentration: 1 mg.mL^{-1}, injection volume: 10 μL, λ: 220 nm): t_1 = 13.0 min, t_2 = 24.2 min.

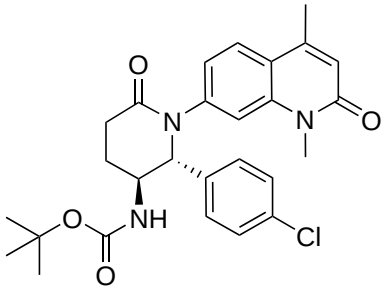

(–)-**278**: $[\alpha]_D^{20}$ - 21 (*c* 0.17, $CHCl_3$); Analytical HPLC ee determination: t_1 = 99.97, t_2 = 0.03, ee = >99%.

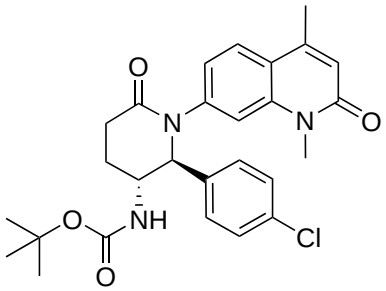

(+)-**278**: $[\alpha]_D^{20}$ + 20 (*c* 0.17, $CHCl_3$); Analytical HPLC ee determination: t_1 = 0.10, t_2 = 99.9, ee = >99%.

7-[(2*R,3*S**)-3-Amino-2-(4-chlorophenyl)-6-oxopiperidin-1-yl]-1,4-dimethylquinolin-2(1*H*)-one** (**279**)

Compound **278** (654 mg, 1.32 mmol) was dissolved in HCl (10 mL, sat. 1,4-dioxane soln) and the reaction mixture was stirred at rt for 11 h. The reaction mixture was concentrated, EtOAc (5 mL) was added and the solution was concentrated. 1M HCl (10 mL) was added and the aqueous phase was washed with CH_2Cl_2 (3 x 10 mL). The aqueous phase was basified with Na_2CO_3 and extracted with CH_2Cl_2 (3 x 10 mL, sat. aq. soln). The combined organic extracts

were dried over Na_2SO_4, filtered and concentrated to yield **279** (502 mg, 96%) as an opaque oil.

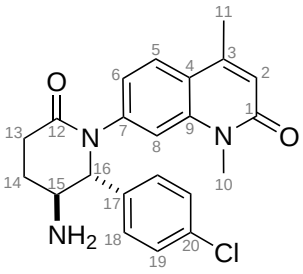

^{1}H-NMR ($CDCl_3$): δ_H 7.53 (d, J = 8.5 Hz, 1H, C(5)H), 7.26 (d, J = 8.0 Hz, 2H, C(18)H), 7.18 (d, J = 8.0 Hz, 2H, C(19)H), 7.03 (d, J = 1.0 Hz, 1H, C(8)H), 6.95 (dd, J = 8.5, 1.0 Hz, 1H, C(6)H), 6.48 (s, 1H, C(2)H), 5.95 (br s, 1H, NH), 4.66 (d, J = 6.0 Hz, 1H, C(16)H), 3.50 (s, 3H, C(10)H_3), 3.36 (br s, 1H, C(15)H), 2.88-2.70 (m, 2H, C(13)H_2), 2.34 (s, 3H, C(11)H_3), 2.14-2.06 (m, 1H, C(14)H_a), 1.94-1.83 (m, 1H, C(14)H_b); ^{13}C-NMR ($CDCl_3$): δ_C 170.2 (C(12)), 161.9 (C(1)), 145.8 (C(4)), 143.4 (C(7)), 140.1 (C(9)), 137.7 (C(17)), 133.9 (C(20)), 128.9 (C(19)), 128.7 (C(18)), 125.7 (C(5)), 121.1 (C(2)), 121.0 (C(6)), 119.9 (C(3)), 113.6 (C(8)), 72.3 (C(16)), 52.7 (C(15)), 29.8 (C(13)), 29.1 (C(10)), 26.5 (C(14)), 18.7 (C(11)); IR ν_{max} 3367, 3293, 2943, 2882, 2238, 1644, 1590, 725; LR-ESI-MS: $C_{22}H_{23}ClN_3O_2$ $[M+H]^+$ m/z found 396.1 calcd 396.2, $C_{22}H_{22}ClN_3O_2Na$ $[M+Na]^+$ m/z found 418.1 calcd 418.1; HR-ESI-MS: $C_{22}H_{23}ClN_3O_2$ $[M+H]^+$ m/z found 396.14733 calcd 396.14642 error = 2.29 ppm.

_N_-[(2_R_*,3_S_*)-2-(4-Chlorophenyl)-1-(1,4-dimethyl-2-oxo-1,2-dihydroquinolin-7-yl)-6-oxopiperidin-3-yl]-2-methylpropanamide (**280**)

Compound **279** (20 mg, 0.051 mmol) was dissolved in CH_2Cl_2 (0.22 mL), NEt_3 (20 μL, 0.14 mmol) and isobutyryl chloride (20 μL, 0.19 mmol) were added and the reaction mixture was stirred at rt for 2 h. H_2O (10 mL) was added and the aqueous phase was extracted with CH_2Cl_2 (3 x 10 mL). The combined organic extracts were dried over Na_2SO_4, filtered and concentrated. Purification by FCC (10% isopropanol/hexane) and preparative TLC (8% MeOH/CH_2Cl_2) yielded **280** (4.1 mg, 18%) as a white powder.

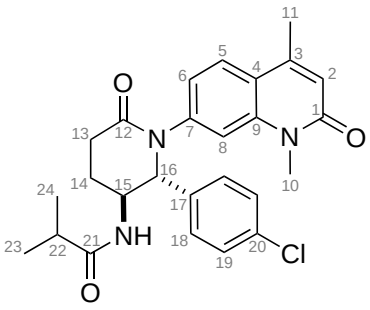

Mpt: 136.0-137.2 °C; ^{1}H-NMR ($CDCl_3$): δ_H 7.60 (d, J = 8.5 Hz, 1H, C(5)H), 7.35 (d, J = 2.0 Hz, 4H, C(18)H & C(19)H), 7.09 (d, J = 2.0 Hz, 1H, C(8)H), 6.98 (dd, J = 8.5, 2.0 Hz, 1H, C(6)H), 6.53 (s, 1H, C(2)H), 6.03 (d, J = 6.5 Hz, 1H, NH), 5.29 (d, J = 3.0 Hz, 1H, C(16)H), 4.31 (ddd, J = 10.5, 4.0, 3.5 Hz, 1H, C(15)H), 3.52 (s, 3H, C(10)H_3), 2.86 (ddd, J = 19.0, 8.0, 3.0 Hz, 1H, C(13)H_a), 2.74 (ddd, J = 19.0, 10.5, 7.5 Hz, 1H, C(13)H_b), 2.46 (spt, J = 7.0 Hz, 1H, C(22)H), 2.38 (s, 3H, C(11)H_3), 2.17 (dddd, J = 15.0, 11.0, 8.0, 3.5 Hz, 1H, C(14)H_a), 1.86 (dddd, J = 12.0, 7.5, 6.5, 3.5 Hz, 1H, C(14)H_b), 1.21 (d, J = 7.0 Hz, 3H, C(23)H_3), 1.20 (d, J = 7.0 Hz, 3H, C(24)H_3); ^{13}C-NMR ($CDCl_3$): δ_C 177.7 (C(21)), 169.6 (C(12)), 162.1 (C(1)), 146.0 (C(4)), 143.8 (C(7)), 140.5 (C(9)), 137.3 (C(17)), 134.4 (C(20)), 129.3 (C(19)), 128.3 (C(18)), 126.2 (C(5)), 121.5 (C(2)), 120.5 (C(6)), 120.4 (C(3)), 113.1 (C(8)), 68.3 (C(16)), 50.1 (C(15)), 35.9 (C(22)), 29.3 (C(10)), 28.2 (C(13)), 21.0 (C(14)), 20.1 (C(23)), 19.6 (C(24)), 19.0 (C(11)); IR ν_{max} 3305, 2967, 1647, 1592, 730; LR-ESI-MS: $C_{26}H_{29}ClN_3O_3$ $[M+H]^+$ m/z found 466.2 calcd 466.1, $C_{26}H_{28}ClN_3O_3Na$ $[M+Na]^+$ m/z found 488.1 calcd 488.2; HR-ESI-MS: $C_{26}H_{29}ClN_3O_3$ $[M+H]^+$ m/z found 466.18920 calcd 466.18893 error = 0.56 ppm.

_N_-[(2_R_*,3_S_*)-2-(4-chlorophenyl)-1-(1,4-dimethyl-2-oxo-1,2-dihydroquinolin-7-yl)-6-oxopiperidin-3-yl]cyclobutanecarboxamide (**281**)

Compound **279** (20 mg, 0.051 mmol) was dissolved in CH_2Cl_2 (0.22 mL), NEt_3 (20 μL, 0.14

mmol) and cyclobutanecarbonyl chloride (20 μL, 0.18 mmol) were added and the reaction mixture was stirred at rt for 2 h. H_2O (10 mL) was added and the aqueous phase was extracted with CH_2Cl_2 (3 x 10 mL). The combined organic extracts were dried over Na_2SO_4, filtered and concentrated. Purification by FCC (1% MeOH/CH_2Cl_2) and preparative TLC (40% isopropanol/hexane) yielded **281** (3.8 mg, 16%) as a white powder.

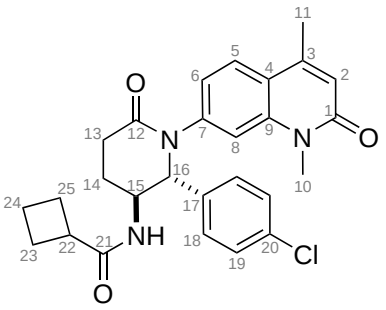

Mpt: 131.9-133.6 °C; ^{1}H-NMR ($CDCl_3$): δ_H 7.60 (d, J = 8.5 Hz, 1H, C(5)H), 7.37-7.33 (m, 4H, C(18)H & C(19)H), 7.08 (d, J = 2.0 Hz, 1H, C(8)H), 6.97 (dd, J = 8.5, 2.0 Hz, 1H, C(6)H), 6.53 (d, J = 1.0 Hz, 1H, C(2)H), 5.92 (d, J = 7.0 Hz, 1H, NH), 5.29 (d, J = 2.5 Hz, 1H, C(16)H), 4.34-4.29 (m, 1H, C(15)H), 3.52 (s, 3H, C(10)H_3), 3.09 (dtd, J = 17.0, 8.5, 1.0 Hz, 1H, C(22)H), 2.84 (ddd, J = 19.0, 8.0, 3.0 Hz, 1H, C(13)H_a), 2.72 (ddd, J = 19.0, 10.5, 8.0 Hz, 1H, C(13)H_b), 2.38 (d, J = 1.0 Hz, 3H, C(11)H_3), 2.36-2.26 (m, 2H, C(23)H_2), 2.26-2.12 (m, 3H, C(14)H_a & C(25)H_2), 2.08-1.99 (m, 1H, C(24)H_a), 1.97-1.89 (m, 1H, C(24)H_b), 1.88-1.62 (m, 1H, C(14)H_b); ^{13}C-NMR ($CDCl_3$): δ_C 175.6 (C(21)), 169.6 (C(12)), 162.1 (C(1)), 146.0 (C(4)), 143.9 (C(7)), 140.5 (C(9)), 137.3 (C(17)), 134.3 (C(20)), 129.3 (C(19)), 128.2 (C(18)), 126.2 (C(5)), 121.5 (C(2)), 120.5 (C(6)), 120.4 (C(3)), 113.1 (C(8)), 68.4 (C(16)), 50.2 (C(15)), 40.0 (C(22)), 29.3 (C(10)), 28.2 (C(13)), 25.6 (C(23)), 25.3 (C(25)), 21.0 (C(14)), 19.0 (C(11)), 18.4 (C(24)); IR ν_{max} 3300, 2945, 2360, 1647, 1592, 725; LR-ESI-MS: $C_{27}H_{29}ClN_3O_3$ $[M+H]^+$ *m/z* found 478.2 calcd 478.2, $C_{27}H_{28}ClN_3O_3Na$ $[M+Na]^+$ *m/z* found 500.2 calcd 500.2; HR-ESI-MS: $C_{27}H_{29}ClN_3O_3$ $[M+H]^+$ *m/z* found 478.18920 calcd 478.18845 error = 1.57 ppm.

_N_-[(2_R_*,3_S_*)-2-(4-chlorophenyl)-1-(1,4-dimethyl-2-oxo-1,2-dihydroquinolin-7-yl)-6-oxopiperidin-3-yl]cyclohexanecarboxamide (**282**)

Compound **279** (20 mg, 0.051 mmol) was dissolved in CH_2Cl_2 (0.22 mL), NEt_3 (20 μL, 0.14 mmol) and cyclohexanecarbonyl chloride (20 μL, 0.15 mmol) were added and the reaction mixture was stirred at rt for 2 h. H_2O (10 mL) was added and the aqueous phase was extracted with CH_2Cl_2 (3 x 10 mL). The combined organic extracts were dried over Na_2SO_4, filtered and concentrated. Purification by FCC (15% isopropanol/hexane) and preparative TLC (40% isopropanol/hexane) yielded **282** (3.0 mg, 12%) as a colourless oil.

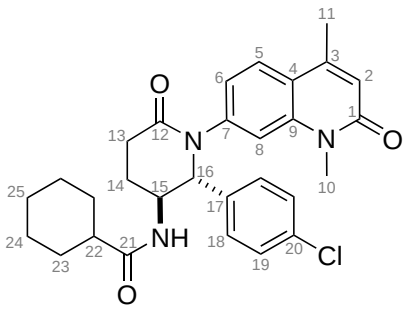

^{1}H-NMR ($CDCl_3$): δ_H 7.57 (d, J = 8.5 Hz, 1H, C(5)H), 7.38 (d, J = 8.5 Hz, 2H, C(18)H), 7.14 (d, J = 8.5 Hz, 2H, C(19)H), 7.07 (d, J = 1.5 Hz, 1H, C(8)H), 6.96 (dd, J = 8.5, 2.0 Hz, 1H, C(6)H), 6.52 (d, J = 1.0 Hz, 1H, C(2)H), 5.23 (d, J = 5.5 Hz, 1H, C(16)H), 4.96 (d, J = 7.5 Hz, 1H, NH), 4.79-4.70 (m, 1H, C(15)H), 3.51 (s, 3H, C(10)H_3), 2.93-2.88 (m, 2H, C(13)H_a & C(13)H_b), 2.37 (d, J = 1.0 Hz, 3H, C(11)H_3), 2.04-1.85 (m, 2H, C(14)H_a & C(14)H_b), 1.82-1.73 (m, 3H, C(22)H & C(24)H_a), 1.70-1.64 (m, 2H, C(24)H_b), 1.44-1.32 (m, 2H, C(25)H_2), 1.28-1.17 (m, 4H, C(23)H_2); ^{13}C-NMR ($CDCl_3$): δ_C 176.0 (C(21)), 169.2 (C(12)), 162.2 (C(1)), 144.8 (C(4)), 144.0 (C(7)), 140.5 (C(9)), 137.1 (C(17)), 134.9 (C(20)), 129.9 (C(19)), 129.0 (C(18)), 126.2 (C(5)), 121.4 (C(2)), 121.0 (C(6)), 120.8 (C(3)), 113.3

(C(8)), 65.1 (C(16)), 47.5 (C(15)), 31.0 (C(13)), 29.8 (C(22)), 29.6 (C(25)), 29.4 (C(10)), 25.7 (C(23)), 25.7 (C(24)), 22.5 (C(14)), 19.0 (C(11)); IR ν_{max} 3481, 3289, 2929, 1648, 1593, 721; LR-ESI-MS: $C_{29}H_{33}ClN_3O_3$ $[M+H]^+$ *m/z* found 506.2 calcd 506.2, $C_{29}H_{32}ClN_3O_3Na$ $[M+Na]^+$ *m/z* found 528.2 calcd 528.2; HR-ESI-MS: $C_{29}H_{32}ClN_3O_3Na$ $[M+Na]^+$ *m/z* found 528.20244 calcd 528.20186 error = 1.13 ppm.

***N*-[(2*R**,3*S**)-2-(4-chlorophenyl)-1-(1,4-dimethyl-2-oxo-1,2-dihydroquinolin-7-yl)-6-oxopiperidin-3-yl]benzamide (283), *N*-[(2*R*,3*S*)-2-(4-chlorophenyl)-1-(1,4-dimethyl-2-oxo-1,2-dihydroquinolin-7-yl)-6-oxo-piperidin-3-yl]benzamide** ((+)-**283**) & ***N*-[(2*S*,3*R*)-2-(4-chlorophenyl)-1-(1,4-dimethyl-2-oxo-1,2-dihydroquinolin-7-yl)-6-oxopiperidin-3-yl]benz-amide** ((–)-**283**)

Compound **279** (20 mg, 0.051 mmol) was dissolved in CH_2Cl_2 (0.22 mL), NEt_3 (20 μL, 0.14 mmol) and benzoyl chloride (20 μL, 0.076 mmol) were added and the reaction mixture was stirred at rt for 6 h. H_2O (10 mL) was added and the aqueous phase was extracted with CH_2Cl_2 (3 x 10 mL). The combined organic extracts were dried over Na_2SO_4, filtered and concentrated. Purification by FCC (1.5% MeOH/CH_2Cl_2) and preparative TLC (3% MeOH/EtOAc) yielded **283** (10.4 mg, 40%) as a colourless oil. The enantiomers of **283** were preparatively resolved by HPLC (stationary phase: Semipreparative Chiralpak AD, solvent composition: hexane:isopropanol 30:70, flow rate: 1.8 mL.min^{-1}, injection concentration: 20 mg.mL^{-1}, injection volume: 100 μL, λ: 220 nm) with the enantiomers eluting at 19.0 min ((+)-**283**) and 22.0 min ((–)-**283**).

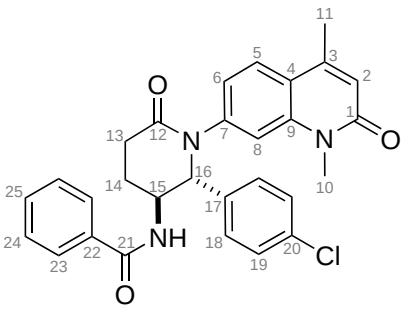

283: ^{1}H-NMR ($CDCl_3$): δ_H 7.84 (d, J = 7.0 Hz, 2H, C(23)H), 7.57 (tt, J = 7.5, 1.0 Hz, 1H, C(25)H), 7.56 (d, J = 9.0 Hz, 1H, C(5)H), 7.48 (dd, J = 8.0, 7.0 Hz, 2H, C(24)H), 7.40-7.38 (m, 4H, C(18)H & C(19)H), 7.06 (d, J = 1.5 Hz, 1H, C(8)H), 7.00 (dd, J = 8.5, 1.5 Hz, 1H, C(6)H), 6.93 (d, J = 6.5 Hz, 1H, NH), 6.49 (d, J = 0.5 Hz, 1H, C(2)H), 5.46-5.43 (m, 1H, C(16)H), 4.57-4.52 (m, 1H, C(15)H), 3.36 (s, 3H, C(10)H_3), 2.86 (dd, J = 6.5, 5.0 Hz, 1H, C(13)H_a), 2.83 (dd, J = 6.5, 1.5 Hz, 1H, C(13)H_b), 2.35 (d, J = 1.0 Hz, 3H, C(11)H_3), 2.23 (dddd, J = 14.0, 10.0, 9.5, 4.0 Hz, 1H, C(14)H_a), 1.97 (ddt, J = 14.0, 5.5, 5.0 Hz, 1H, C(14)H_b); ^{13}C-NMR ($CDCl_3$): δ_C 169.8 (C(12)), 168.1 (C(21)), 162.1 (C(1)), 146.0 (C(4)), 144.0 (C(7)), 140.5 (C(9)), 137.3 (C(17)), 134.4 (C(20)), 133.8 (C(22)), 132.4 (C(25)), 129.4 (C(19)), 129.0 (C(24)), 128.2 (C(18)), 127.1 (C(23)), 126.2 (C(5)), 121.3 (C(2)), 120.6 (C(6)), 120.4 (C(3)), 113.0 (C(8)), 68.2 (C(16)), 50.8 (C(15)), 29.2 (C(10)), 28.2 (C(13)), 21.2 (C(14)), 19.0 (C(11)); IR ν_{max} 3294, 2946, 2360, 2342, 1646, 1592, 727; LR-ESI-MS: $C_{29}H_{27}ClN_3O_3$ $[M+H]^+$ *m/z* found 500.2 calcd 500.2, $C_{29}H_{26}ClN_3O_3Na$ $[M+Na]^+$ *m/z* found 522.2 calcd 522.2; HR-ESI-MS: $C_{29}H_{26}ClN_3O_3Na$ $[M+Na]^+$ *m/z* found 522.1555 calcd 522.1559 error = 0.7 ppm; Analytical HPLC separation (stationary phase: Chiralpak AD, solvent composition: hexane:isopropanol 60:40, flow rate: 1 mL.min^{-1}, injection concentration: 10 mg.mL^{-1}, injection volume: 100 μL, λ: 220 nm): t_1 = 14.5 min, t_2 = 32.3 min.

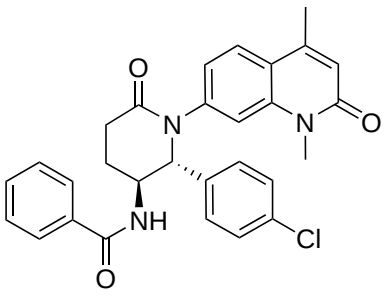

(+)-**283**: $[\alpha]_D^{20}$ + 4 (*c* 0.14, $CHCl_3$); Analytical HPLC ee determination: t_1 = 99.48, t_2 = 0.52, ee = 99%.

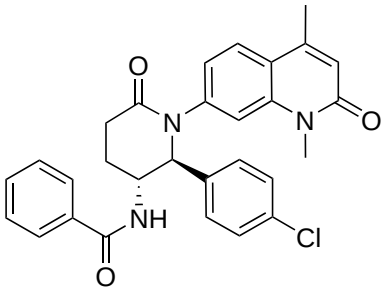

(–)-**283**: $[\alpha]_D^{20}$ - 5 (*c* 0.13, $CHCl_3$); Analytical HPLC ee determination: t_1 = 0.46, t_2 = 99.54, ee = >99%.

***N*-[(2*R**,3*S**)-2-(4-chlorophenyl)-1-(1,4-dimethyl-2-oxo-1,2-dihydroquinolin-7-yl)-6-oxopiperidin-3-yl]-2-phenoxyacetamide** (**284**)

Compound **279** (20 mg, 0.051 mmol) was dissolved in CH_2Cl_2 (0.22 mL), NEt_3 (20 μL, 0.14 mmol) and phenoxyacetyl chloride (20 μL, 0.15 mmol) were added and the reaction mixture was stirred at rt for 2 h. H_2O (10 mL) was added and the aqueous phase was extracted with CH_2Cl_2 (3 x 10 mL). The combined organic extracts were dried over Na_2SO_4, filtered and concentrated. Purification by FCC (15% isopropanol/hexane) and preparative TLC (isopropanol) yielded **284** (3.8 mg, 14%) as a colourless oil.

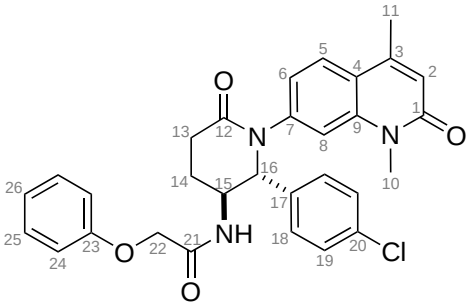

^{1}H-NMR ($CDCl_3$): δ_H 7.56 (d, J = 8.5 Hz, 1H, C(5)H), 7.35 (d, J = 8.5 Hz, 2H, C(18)H), 7.33 (d, J = 8.5 Hz, 2H, C(25)H), 7.30 (d, J = 8.5 Hz, 2H, C(19)H), 7.06 (tt, J = 7.5, 1.0 Hz, 1H, C(26)H), 7.05 (d, J = 2.0 Hz, 1H, C(8)H), 7.03 (d, J = 7.5 Hz, 1H, NH), 6.92 (dd, J = 8.5, 1.0 Hz, 2H, C(24)H), 6.89 (dd, J = 8.5, 2.0 Hz, 1H, C(6)H), 6.53 (d, J = 1.0 Hz, 1H, C(2)H), 5.13 (d, J = 4.0 Hz, 1H, C(16)H), 4.59 (d, J = 15.0 Hz, 1H, C(22)H_a), 4.53 (d, J = 15.5 Hz, 1H, C(22)H_b), 4.50-4.45 (m, 1H, C(15)H), 3.45 (s, 3H, C(10)H_3), 2.85 (ddd, J = 19.0, 7.5, 4.0 Hz, 1H, C(13)H_a), 2.74 (ddd, J = 19.0, 9.5, 7.5 Hz, 1H, C(13)H_b), 2.38 (d, J = 1.0 Hz, 3H, C(11)H_3), 2.25-2.16 (m, 1H, C(14)H_a), 2.01-1.94 (m, 1H, C(14)H_b); ^{13}C-NMR ($CDCl_3$): δ_C 169.6 (*C*(21)), 168.7 (*C*(12)), 162.1 (*C*(1)), 157.0 (*C*(23)), 145.9 (*C*(4)), 143.6 (*C*(7)), 140.4 (*C*(9)), 137.1 (*C*(17)), 134.6 (*C*(20)), 130.2 (*C*(25)), 129.5 (*C*(19)), 128.3 (*C*(18)), 126.2 (*C*(5)), 122.8 (*C*(26)), 121.5 (*C*(2)), 120.4 (*C*(3)), 120.3 (*C*(6)), 114.8 (*C*(24)), 113.0 (*C*(8)), 68.6 (*C*(16)), 67.6 (*C*(22)), 49.9 (*C*(15)), 29.2 (*C*(10)), 28.5 (*C*(13)), 21.8 (*C*(14)), 19.0 (*C*(11)); IR ν_{max} 3284, 3059, 2948, 1652, 1594, 724; LR-ESI-MS: $C_{30}H_{29}ClN_3O_4$ $[M+H]^+$ *m/z* found 530.2 calcd 530.2, $C_{30}H_{28}ClN_3O_4Na$ $[M+Na]^+$ *m/z* found 552.3 calcd 552.2; HR-ESI-MS: $C_{30}H_{29}ClN_3O_4$ $[M+H]^+$ *m/z* found 530.18411 calcd 530.18329 error = 1.55 ppm.

2-Methylpropyl [(2*R,3*S**)-2-(4-chlorophenyl)-1-(1,4-dimethyl-2-oxo-1,2-dihydroquinolin-7-yl)-6-oxopiperidin-3-yl]carbamate (285)**

Compound **279** (20 mg, 0.051 mmol) was dissolved in CH_2Cl_2 (0.22 mL), NEt_3 (20 μL, 0.14 mmol) and isobutyl chloroformate (20 μL, 0.15 mmol) were added and the reaction mixture was stirred at rt for 2 h. H_2O (10 mL) was added and the aqueous phase was extracted with CH_2Cl_2 (3 x 10 mL). The combined organic extracts were dried over Na_2SO_4, filtered and concentrated. Purification by FCC (15% isopropanol/hexane) and preparative TLC (40% isopropanol/hexane) yielded **285** (6.0 mg, 24%) as a white powder.

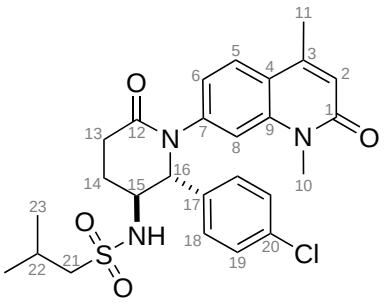

Mpt: 216.2-218.0 °C; ^{1}H-NMR ($CDCl_3$): δ_H 7.60 (d, J = 8.5 Hz, 1H, C(5)H), 7.36 (d, J = 8.5 Hz, 2H, C(18)H), 7.31 (d, J = 8.5 Hz, 2H, C(19)H), 7.12 (d, J = 2.0 Hz, 1H, C(8)H), 7.01 (dd, J = 8.5, 1.5 Hz, 1H, C(6)H), 6.53 (d, J = 0.5 Hz, 1H, C(2)H), 5.36-5.31 (m, 1H, C(16)H), 5.26 (br s, 1H, NH), 4.12-4.07 (m, 1H, C(15)H), 3.91 (d, J = 6.5 Hz, 2H, C(22)H_2), 3.52 (s, 3H, C(10)H_3), 2.84 (ddd, J = 19.0, 8.0, 3.5 Hz, 1H, C(13)H_a), 2.74 (ddd, J = 19.0, 10.0, 8.0 Hz, 1H, C(13)H_b), 2.38 (s, 3H, C(11)H_3), 2.22-2.11 (m, 1H, C(14)H_a), 1.99-1.86 (m, 2H, C(14)H_b & C(23)H), 0.95 (d, J = 6.5 Hz, 6H, C(24)H_3); ^{13}C-NMR ($CDCl_3$): δ_C 169.6 (C(12)), 162.1 (C(1)), 161.0 (C(21)), 146.0 (C(4)), 144.0 (C(7)), 143.3 (C(9)), 137.4 (C(17)), 134.4 (C(20)), 129.4 (C(19)), 128.2 (C(18)), 126.2 (C(5)), 121.4 (C(2)), 120.6 (C(6)), 120.4 (C(3)), 113.1 (C(8)), 71.8 (C(22)), 70.2 (C(16)), 51.7 (C(15)), 29.3 (C(10)), 28.2 (C(13)), 28.1 (C(23)), 22.1 (C(14)), 19.2 (C(24)), 19.0 (C(11)); IR ν_{max} 3272, 2959, 1711, 1649, 1593, 722; LR-ESI-MS: $C_{27}H_{31}ClN_3O_4$ $[M+H]^+$ *m/z* found 496.2 calcd 496.2, $C_{27}H_{30}ClN_3O_4Na$ $[M+Na]^+$ *m/z* found 518.2 calcd 518.2; HR-ESI-MS: $C_{27}H_{30}ClN_3O_4Na$ $[M+Na]^+$ *m/z* found 518.18171 calcd 518.18108 error = 1.18 ppm.

Phenyl [(2*R,3*S**)-2-(4-chlorophenyl)-1-(1,4-dimethyl-2-oxo-1,2-dihydroquinolin-7-yl)-6-oxopiperidin-3-yl]carbamate (286)**

Compound **279** (20 mg, 0.051 mmol) was dissolved in CH_2Cl_2 (0.22 mL), NEt_3 (20 μL, 0.14 mmol) and phenyl chloroformate (20 μL, 0.076 mmol) were added and the reaction mixture was stirred at rt for 2 h. H_2O (10 mL) was added and the aqueous phase was extracted with CH_2Cl_2 (3 x 10 mL). The combined organic extracts were dried over Na_2SO_4, filtered and concentrated. Purification by FCC (2% MeOH/CH_2Cl_2) and preparative TLC (2.5% MeOH/EtOAc) yielded **286** (9.8 mg, 38%) as an opaque oil.

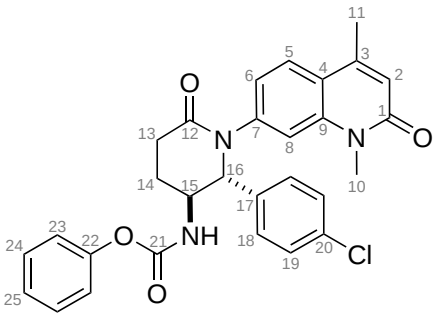

^{1}H-NMR ($CDCl_3$): δ_H 7.61 (d, J = 8.5 Hz, 1H, C(5)H), 7.41-7.31 (m, 6H, C(18)H, C(19)H & C(24)H), 7.25 (t, J = 7.5 Hz, 1H, C(25)H), 7.16 (s, 1H, C(8)H), 7.12 (d, J = 8.0 Hz, 2H, C(23)H), 7.05 (d, J = 8.0 Hz, 1H, C(6)H), 6.54 (s, 1H, C(2)H), 5.96 (d, J = 6.0 Hz, 1H, NH), 5.35 (br s, 1H, C(16)H), 4.17 (br s, 1H, C(15)H), 3.50 (s, 3H, C(10)H_3), 2.88 (ddd, J = 15.5, 8.0, 3.5 Hz, 1H, C(13)H_a), 2.82 (ddd, J = 19.0, 10.0, 7.5 Hz, 1H, C(13)H_b), 2.38 (s, 3H, C(11)H_3), 2.25-2.18 (m, 1H, C(14)H_a), 2.01-1.95 (m, 1H, C(14)H_b); ^{13}C-NMR ($CDCl_3$): δ_C 169.7 (C(12)), 162.2 (C(1)), 154.7 (C(21)), 150.7 (C(22)), 146.0 (C(4)), 143.9 (C(7)), 140.5 (C(9)), 137.5 (C(17)), 134.5 (C(20)), 129.7 (C(24)), 129.4 (C(19)), 128.3 (C(18)), 126.2

(C(5)), 126.0 (C(25)), 121.5 (C(23)), 121.4 (C(2)), 120.6 (C(6)), 120.4 (C(3)), 113.2 (C(8)), 68.5 (C(16)), 52.1 (C(15)), 29.3 (C(10)), 28.1 (C(13)), 21.2 (C(14)), 19.0 (C(11)); IR ν_{max} 3254, 2361, 1649, 1593, 1491, 1202, 727; LR-ESI-MS: $C_{29}H_{27}ClN_3O_4$ $[M+H]^+$ *m/z* found 516.2 calcd 516.2, $C_{29}H_{26}ClN_3O_4Na$ $[M+Na]^+$ *m/z* found 538.2 calcd 538.2; HR-ESI-MS: $C_{29}H_{26}ClN_3O_4Na$ $[M+Na]^+$ *m/z* found 538.1504 calcd 538.1511 error = 1.3 ppm.

_N_-[(2_R_*,3_S_*)-2-(4-Chlorophenyl)-1-(1,4-dimethyl-2-oxo-1,2-dihydroquinolin-7-yl)-6-oxopiperidin-3-yl]-_N_,_N_-dimethylsulfuric diamide (287)

Compound **279** (20 mg, 0.051 mmol) was dissolved in CH_2Cl_2 (0.22 mL), NEt_3 (20 μL, 0.14 mmol) and *N*,*N*-dimethylsulfamoyl chloride (20 μL, 0.19 mmol) were added and the reaction mixture was stirred at rt for 6 h. H_2O (10 mL) was added and the aqueous phase was extracted with CH_2Cl_2 (3 x 10 mL). The combined organic extracts were dried over Na_2SO_4, filtered and concentrated. Purification by FCC (3% MeOH/CH_2Cl_2) and preparative TLC (3% MeOH/EtOAc) yielded **287** (5.7 mg, 22%) as an opaque oil.

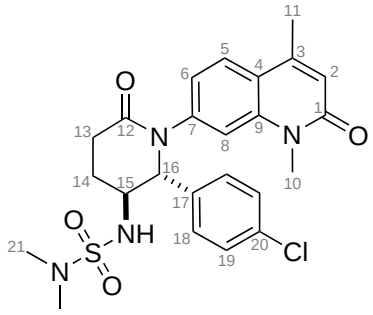

^{1}H-NMR ($CDCl_3$): δ_H 7.60 (d, J = 8.5 Hz, 1H, C(5)H), 7.36 (d, J = 8.5 Hz, 1H, C(18)H), 7.34 (d, J = 1.5 Hz, 1H, C(8)H), 7.26 (d, J = 8.5 Hz, 1H, C(19)H), 7.12 (dd, J = 8.5, 1.5 Hz, 1H, C(6)H), 6.56 (s, 1H, C(2)H), 5.55 (d, J = 6.5 Hz, 1H, NH), 5.35 (br s, 1H, C(16)H), 3.79 (br s, 1H, C(15)H), 3.56 (s, 3H, C(10)H_3), 2.84-2.73 (m, 8H, C(13)H_2 & C(21)H_3), 2.38 (s, 3H, C(11)H_3), 2.19-2.12 (m, 1H, C(14)H_a), 1.85-1.78 (m, 1H, C(14)H_b); ^{13}C-NMR ($CDCl_3$): δ_C 169.7 (C(12)), 162.2 (C(1)), 146.2 (C(4)), 143.8 (C(7)), 140.5 (C(9)), 137.2 (C(17)), 134.5 (C(20)), 129.4 (C(19)), 128.2 (C(18)), 126.1 (C(5)), 121.4 (C(2)), 121.1 (C(6)), 120.5 (C(3)), 113.5 (C(8)), 69.8 (C(16)), 54.4 (C(15)), 38.2 (C(21)), 29.5 (C(10)), 27.8 (C(13)), 21.8 (C(14)), 19.0 (C(11)); IR ν_{max} 3148, 2889, 2361, 2341, 1649, 1593, 1329, 1149, 722; LR-ESI-MS: $C_{24}H_{28}ClN_4O_4S$ $[M+H]^+$ *m/z* found 503.2 calcd 503.3, $C_{24}H_{27}ClN_4O_4SNa$ $[M+Na]^+$ *m/z* found 525.1 calcd 525.1; HR-ESI-MS: $C_{24}H_{27}ClN_4O_4SNa$ $[M+H]^+$ *m/z* found 525.1334 calcd 525.1336 error = 0.4 ppm.

_N_-[(2_R_*,3_S_*)-2-(4-Chlorophenyl)-1-(1,4-dimethyl-2-oxo-1,2-dihydroquinolin-7-yl)-6-oxopiperidin-3-yl]methanesulfonamide (288)

Compound **279** (20 mg, 0.051 mmol) was dissolved in CH_2Cl_2 (0.22 mL), NEt_3 (20 μL, 0.14 mmol) and methanesulfonyl chloride (20 μL, 0.25 mmol) were added and the reaction mixture was stirred at rt for 2 h. H_2O (10 mL) was added and the aqueous phase was extracted with CH_2Cl_2 (3 x 10 mL). The combined organic extracts were dried over Na_2SO_4, filtered and concentrated. Purification by FCC (30% isopropanol/hexane) and preparative TLC (isopropanol) yielded **288** (7.2 mg, 30%) as white crystals.

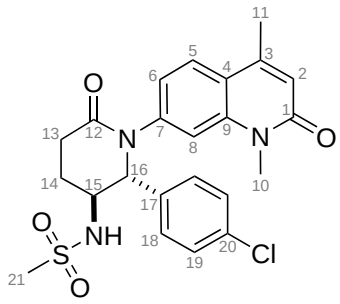

Mpt: 154.9-155.8 °C; ^{1}H-NMR ($CDCl_3$): δ_H 7.59 (d, J = 8.5 Hz, 1H, C(5)H), 7.35 (d, J = 9.0 Hz, 2H, C(18)H), 7.32 (d, J = 2.0 Hz, 1H, C(8)H), 7.27 (d, J = 9.5 Hz, 2H, C(19)H), 7.11 (dd, J = 8.5, 2.0 Hz, 1H, C(6)H), 6.53 (d, J = 1.0 Hz, 1H, C(2)H), 6.50 (d, J = 8.5 Hz, 1H, NH), 5.27 (br s, 1H, C(16)H), 3.87-3.83 (m, 1H, C(15)H), 3.54 (s, 3H, C(10)H_3), 2.91 (s, 3H, C(21)H_3), 2.80 (ddd, J = 19.0, 8.5, 3.5 Hz, 1H, C(13)H_a), 2.74 (ddd, J = 19.0, 10.5, 7.5 Hz, 1H, C(13)H_b), 2.37 (d, J = 0.5 Hz, 3H, C(11)H_3), 2.17-2.07 (m, 1H, C(14)H_a), 1.82-1.74 (m, 1H, C(14)H_b); ^{13}C-NMR ($CDCl_3$): δ_C 170.1 (C(12)), 162.1 (C(1)), 146.0 (C(4)), 143.7 (C(7)), 140.6 (C(9)), 136.9 (C(17)), 134.6 (C(20)), 129.5 (C(19)), 128.2 (C(18)), 126.1 (C(5)), 121.6 (C(2)), 121.0 (C(6)), 120.5 (C(3)), 113.6 (C(8)), 70.9 (C(16)), 53.9 (C(15)), 41.9 (C(21)), 29.5 (C(10)), 27.8 (C(13)), 22.2 (C(14)), 19.0 (C(11)); IR ν_{max} 3148, 2920, 2361, 2341, 1648, 1592, 1327, 1150, 730; LR-ESI-MS: $C_{23}H_{25}ClN_3O_4S$ $[M+H]^+$ *m/z* found 474.1 calcd 474.1, $C_{23}H_{24}ClN_3O_4SNa$ $[M+Na]^+$ *m/z* found 496.0 calcd 496.1; HR-ESI-MS: $C_{23}H_{25}ClN_3O_4S$ $[M+H]^+$ *m/z* found 474.12488 calcd 474.12421 error = 1.42 ppm.

***N*-[(2*R**,3*S**)-2-(4-Chlorophenyl)-1-(1,4-dimethyl-2-oxo-1,2-dihydroquinolin-7-yl)-6-oxopiperidin-3-yl]-2-methylpropane-1-sulfonamide** (**289**), ***N*-[(2*R*,3*S*)-2-(4-chlorophenyl)-1-(1,4-dimethyl-2-oxo-1,2-dihydroquino-lin-7-yl)-6-oxopiperidin-3-yl]-2-methylpropane-1-sulfonamide**((–)-**289**/LP99)) & ***N*-[(2*S*,3*R*)-2-(4-chlorophenyl)-1-(1,4-dimethyl-2-oxo-1,2-dihydroquinolin-7-yl)-6-oxopiperidin-3-yl]-2-methylpropane-1-sulfonamide** ((+)-**289**)

Compound **279** (132 mg, 0.33 mmol) was dissolved in CH_2Cl_2 (1.33 mL), NEt_3 (130 μL, 0.93 mmol) and isobutylsulfonyl chloride (131 μL, 1.00 mmol) were added and the reaction mixture was stirred at rt for 3 h. H_2O (25 mL) was added and the aqueous phase was extracted with CH_2Cl_2 (3 x 25 mL). The combined organic extracts were dried over Na_2SO_4, filtered and concentrated. Purification by FCC (12.5% isopropanol/hexane) yielded **289** (134 mg, 78%) as a white powder. The enantiomers of **289** were preparatively resolved by HPLC (stationary phase: Semipreparative Chiralpak AD, solvent composition: hexane:isopropanol 60:40, flow rate: 1 mL.min^{-1}, injection concentration: 6 mg.mL^{-1}, injection volume: 100 μL, λ: 220 nm) with the enantiomers eluting at 10.8 min ((–)-**289**/LP99) and 20.7 min ((+)-**289**).

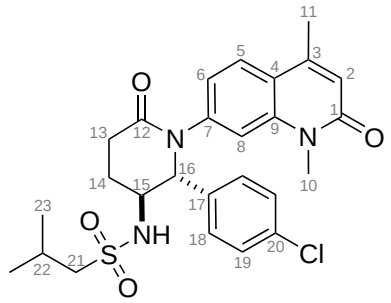

289: Mpt: 137.6-139.6 °C; ^{1}H-NMR ($CDCl_3$): δ_H 7.59 (d, J = 8.5 Hz, 1H, C(5)H), 7.35 (d, J = 8.5 Hz, 2H, C(18)H), 7.33 (d, J = 2.0 Hz, 1H, C(8)H), 7.27 (d, J = 8.5 Hz, 2H, C(19)H), 7.11 (d, J = 8.5 Hz, 1H, C(6)H), 6.53 (d, J = 0.5 Hz, 1H, NH), 5.27 (br s, 1H, C(16)H), 3.84 (br s, 1H, C(15)H), 3.55 (s, 3H, C(10)H_3), 2.90-2.68 (m, 4H, C(13)H_2 & C(21)H_2), 2.37 (s, 3H, C(11)H_3), 2.27-2.09 (m, 2H, C(14)H_a), 1.82-1.73 (m, 1H, C(14)H_b), 1.06 (dd, J = 7.0, 3.0 Hz, 6H, C(23)H_3); ^{13}C-NMR ($CDCl_3$): δ_C 169.7 (C(12)), 162.1 (C(1)), 146.0 (C(4)), 143.8 (C(7)), 140.6 (C(9)), 137.0 (C(17)), 134.6 (C(20)), 129.4 (C(19)), 128.2 (C(18)), 126.1 (C(5)), 121.6 (C(2)), 121.0 (C(6)), 120.5 (C(3)), 113.6 (C(8)), 71.1 (C(16)), 62.0 (C(21)), 53.9 (C(15)), 29.5 (C(10)), 27.7 (C(13)), 25.1 (C(22)), 22.7 (C(23)), 22.6 (C(14)), 19.0 (C(11)); IR ν_{max} 3157, 2960, 2361, 2340, 1649, 1593, 1325, 1144, 725; LR-ESI-MS: $C_{26}H_{31}ClN_3O_4S$ $[M+H]^+$ *m/z* found 516.2 calcd 516.2, $C_{26}H_{30}ClN_3O_4SNa$

$[M+Na]^+$ *m/z* found 538.2 calcd 538.2; HR-ESI-MS: $C_{26}H_{30}ClN_3O_4SNa$ $[M+Na]^+$ *m/z* found 538.1538 calcd 538.1533 error = 0.85 ppm; Analytical HPLC separation (stationary phase: Chiralpak AD, solvent composition: hexane:isopropanol 60:40, flow rate: 1 mL.min^{-1}, injection concentration: 1 mg.mL^{-1}, injection volume: 10 μL, λ: 220 nm): t_1 = 7.2 min, t_2 = 14.2 min.

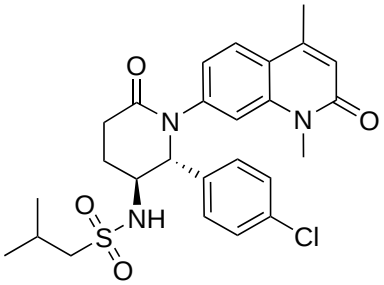

(–)-**289**/LP99: $[\alpha]_D{}^{20}$ - 61 (*c* 0.09, $CHCl_3$); Analytical HPLC ee determination: t_1 = 99.84, t_2 = 0.16, ee = >99%.

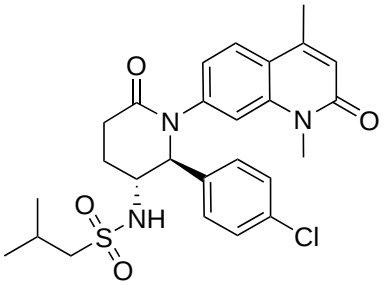

(+)-**289**: $[\alpha]_D{}^{20}$ + 53 (*c* 0.09, $CHCl_3$); Analytical HPLC ee determination: t_1 = 0.17, t_2 = 99.83, ee = >99%.

***N*-[(2*R**,3*S**)-2-(4-Chlorophenyl)-1-(1,4-dimethyl-2-oxo-1,2-dihydroquinolin-7-yl)-6-oxopiperidin-3-yl]benzenesulfonamide (290)**

Compound **279** (20 mg, 0.051 mmol) was dissolved in CH_2Cl_2 (0.22 mL), NEt_3 (20 μL, 0.14 mmol) and benzenesulfonyl chloride (20 μL, 0.16 mmol) were added and the reaction mixture was stirred at rt for 2 h. H_2O (10 mL) was added and the aqueous phase was extracted with CH_2Cl_2 (3 x 10 mL). The combined organic extracts were dried over Na_2SO_4, filtered and concentrated. Purification by FCC (2% MeOH/CH_2Cl_2) and preparative TLC (isopropanol) yielded **290** (7.3 mg, 27%) as a colourless oil.

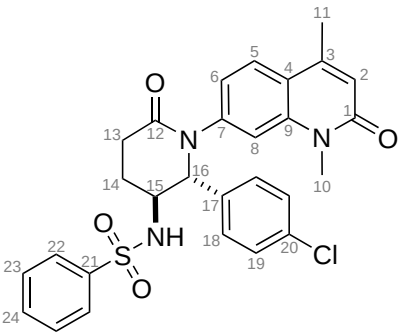

^{1}H-NMR ($CDCl_3$): δ_H 7.86 (dd, *J* = 8.0, 1.0 Hz, 2H, C(22)*H*), 7.56 (tt, *J* = 7.5, 1.0 Hz, 1H, C(24)*H*), 7.55 (d, *J* = 8.5 Hz, 1H, C(5)*H*), 7.44 (t, *J* = 8.0 Hz, 2H, C(23)*H*), 7.29 (d, *J* = 8.5 Hz, 2H, C(18)*H*), 7.25 (d, *J* = 2.0 Hz, 1H, C(8)*H*), 7.14 (d, *J* = 8.5 Hz, 2H, C(19)*H*), 7.03 (dd, *J* = 8.5, 2.0 Hz, 1H, C(6)*H*), 6.77 (d, *J* = 7.0 Hz, 1H, N*H*), 6.53 (d, *J* = 1.0 Hz, 1H, C(2)*H*), 5.16 (br s, 1H, C(16)*H*), 3.66-3.60 (m, 1H, C(15)*H*), 3.44 (s, 3H, C(10)H_3), 2.82-2.77 (m, 2H, C(13)H_2), 2.37 (d, *J* = 1.0 Hz, 3H, C(11)H_3), 2.04 (dtd, *J* = 14.0, 9.5, 3.5 Hz, 1H, C(14)H_a), 1.66-1.62 (m, 1H, C(14)H_b); ^{13}C-NMR ($CDCl_3$): δ_C 170.4 (*C*(12)), 162.1 (*C*(1)), 146.0 (*C*(4)), 143.8 (*C*(7)), 140.5 (*C*(21)), 140.4 (*C*(9)), 136.8 (*C*(17)), 134.5 (*C*(20)), 133.2 (*C*(24)), 129.4 (*C*(23)), 129.4 (*C*(19)), 128.1 (*C*(18)), 127.0 (*C*(22)), 126.0 (*C*(5)), 121.5 (*C*(2)), 120.9 (*C*(6)), 120.4 (*C*(3)), 113.5 (*C*(8)), 70.1 (*C*(16)), 53.6 (*C*(15)), 29.4 (*C*(10)), 27.7 (*C*(13)), 21.8 (*C*(14)), 19.0 (*C*(11)); IR ν_{max} 3096, 2919, 2362, 1647, 1591, 1160, 724; LR-ESI-MS: $C_{28}H_{27}ClN_3O_4S$ $[M+H]^+$ *m/z* found 536.1 calcd 536.2, $C_{28}H_{26}ClN_3O_4SNa$ $[M+Na]^+$ *m/z* found 558.2 calcd 558.1; HR-ESI-MS: $C_{28}H_{27}ClN_3O_4S$ $[M+H]^+$ *m/z* found 536.14053 calcd

536.13983 error = 1.31 ppm.

***N*-[(2*R**,3*S**)-2-(4-Chlorophenyl)-1-(1,4-dimethyl-2-oxo-1,2-dihydroquinolin-7-yl)-6-oxopiperidin-3-yl]-1-phenylmethanesulfonamide** (**291**)

Compound **279** (20 mg, 0.051 mmol) was dissolved in CH_2Cl_2 (0.22 mL), NEt_3 (20 μL, 0.14 mmol) and phenylmethanesulfonyl chloride (20 μL, 0.10 mmol) were added and the reaction mixture was stirred at rt for 6 h. H_2O (10 mL) was added and the aqueous phase was extracted with CH_2Cl_2 (3 x 10 mL). The combined organic extracts were dried over Na_2SO_4, filtered and concentrated. Purification by FCC (1% MeOH/EtOAc) and preparative TLC (80% EtOAc/PE) yielded **291** (13.8 mg, 50%) as a colourless oil.

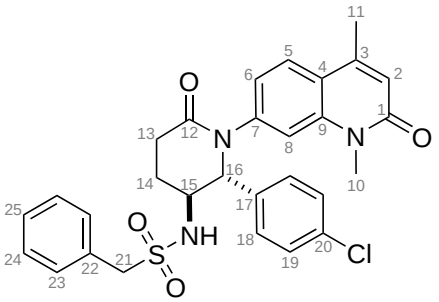

^{1}H-NMR ($CDCl_3$): δ_H 7.60 (d, J = 8.5 Hz, 1H, C(5)H), 7.37-7.29 (m, 9H, C(18)H, C(19)H, C(23)H, C(24)H & C(25)H), 7.13 (s, 1H, C(8)H), 7.09 (dd, J = 9.0, 1.5 Hz, 1H, C(6)H), 6.56 (s, 1H, C(2)H), 6.06 (d, J = 7.5 Hz, 1H, NH), 5.18 (br s, 1H, C(16)H), 4.35 (d, J = 13.5 Hz, 1H, C(21)H_a), 4.27 (d, J = 14.0 Hz, 1H, C(21)H_b), 3.54 (s, 3H, C(10)H_3), 3.39-3.35 (m, 1H, C(15)H), 2.68 (ddd, J = 19.5, 8.5, 1.5 Hz, 1H, C(13)H_a), 2.61 (ddd, J = 19.0, 10.5, 7.5 Hz, 1H, C(13)H_b), 2.37 (s, 3H, C(11)H_3), 1.89-1.80 (m, 1H, C(14)H_a), 1.57-1.51 (m, 1H, C(14)H_b); ^{13}C-NMR ($CDCl_3$): δ_C 169.9 (*C*(12)), 162.1 (*C*(1)), 146.2 (*C*(4)), 144.0 (*C*(7)), 140.5 (*C*(9)), 136.8 (*C*(17)), 134.4 (*C*(20)), 130.8 (*C*(23)), 129.4 (*C*(19)), 129.2 (*C*(25)), 129.2 (*C*(22)), 129.0 (*C*(24)), 127.9 (*C*(18)), 126.1 (*C*(5)), 121.3 (*C*(2)), 121.0 (*C*(6)), 120.6 (*C*(3)), 113.5 (*C*(8)), 71.0 (*C*(16)), 60.6 (*C*(21)), 54.3 (*C*(15)), 29.6 (*C*(10)), 27.3 (*C*(13)), 21.3 (*C*(14)), 19.0 (*C*(11)); IR ν_{max} 2918, 1648, 1593, 1456, 1328, 1152, 729; LR-ESI-MS: $C_{29}H_{28}ClN_3O_4SNa$ $[M+Na]^+$ *m/z* found 572.1 calcd 572.2; HR-ESI-MS: $C_{29}H_{28}ClN_3O_4SNa$ $[M+Na]^+$ *m/z* found 572.1381 calcd 572.1387 error = 1.0 ppm.

1-*tert*-Butyl-3-[(2*R,3*S**)-2-(4-chlorophenyl)-1-(1,4-dimethyl-2-oxo-1,2-dihydroquinolin-7-yl)-6-oxopiperidin-3-yl]urea** (**292**)

Compound **279** (20 mg, 0.051 mmol) was dissolved in CH_2Cl_2 (0.22 mL), *tert*-butylisocyanate (5.8 μL, 0.051 mmol) was added and the reaction mixture was stirred at rt for 15 h. The reaction mixture was concentrated and purification by FCC (1.5% MeOH/CH_2Cl_2) and preparative TLC (35% isopropanol/hexane) yielded **292** (7.8 mg, 31%) as a white solid.

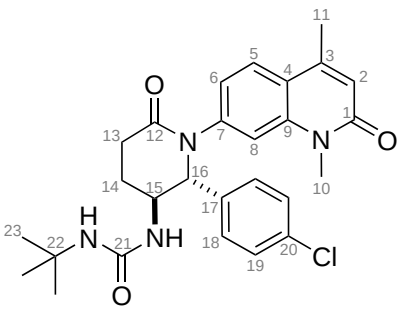

Mpt: 159.8-160.0 °C; ^{1}H-NMR ($CDCl_3$): δ_H 7.53 (d, J = 8.5 Hz, 1H, C(5)H), 7.32-7.23 (m, 4H, C(18)H & C(19)H), 7.10 (d, J = 1.5 Hz, 1H, C(8)H), 6.98 (dd, J = 8.5, 1.5 Hz, 1H, C(6)H), 6.46 (s, 1H, C(2)H), 5.64 (br s, 1H, NH), 5.27 (br s, 1H, C(16)H), 4.06 (d, J = 2.0 Hz, 1H, C(15)H), 3.43 (s, 3H, C(10)H_3), 2.67 (dd, J = 19.0, 7.5 Hz, 1H, C(13)H_a), 2.59-2.47 (m, 1H, C(13)H_b), 2.31 (s, 3H, C(11)H_3), 2.00-1.88 (m, 1H, C(14)H_a), 1.60-1.52 (m, 1H, C(14)H_b), 1.29 (s, 9H, C(23)H_3); ^{13}C-NMR ($CDCl_3$): δ_C 168.4 (*C*(12)), 162.0 (*C*(1)), 157.3 (*C*(21)), 146.1 (*C*(4)), 144.1 (*C*(7)), 140.3 (*C*(9)), 137.0 (*C*(17)), 133.9 (*C*(20)), 129.1 (*C*(19)), 127.8 (*C*(18)), 126.0 (*C*(5)), 121.2 (*C*(2)), 120.8 (*C*(6)), 120.4 (*C*(3)), 113.0 (*C*(8)), 69.6 (*C*(16)), 50.4 (*C*(22)),

49.8 (*C*(15)), 29.5 (*C*(23)), 29.2 (*C*(10)), 27.7 (*C*(13)), 20.4 (*C*(14)), 18.9 (*C*(11)); IR ν_{max} 3370, 2963, 1645, 1589, 1556, 731; LR-ESI-MS: $C_{27}H_{32}ClN_4O_3$ $[M+H]^+$ *m/z* found 495.2 calcd 495.3, $C_{27}H_{31}ClN_4O_3Na$ $[M+Na]^+$ *m/z* found 517.3 calcd 517.2; HR-ESI-MS: $C_{27}H_{32}ClN_4O_3$ $[M+H]^+$ *m/z* found 495.21575 calcd 495.21475 error = 2.0 ppm.

1-[(2*R,3*S**)-2-(4-chlorophenyl)-1-(1,4-dimethyl-2-oxo-1,2-dihydroquinolin-7-yl)-6-oxopiperidin-3-yl]-3-cyclopentylurea** (**293**)

Compound **279** (20 mg, 0.051 mmol) was dissolved in CH_2Cl_2 (0.22 mL), cyclopentylisocyanate (5.7 μL, 0.051 mmol) was added and the reaction mixture was stirred at rt for 15 h. The reaction mixture was concentrated and purification by FCC (20% isopropanol/hexane) and preparative TLC (40% isopropanol/hexane) yielded **293** (6.6 mg, 26%) as a colourless oil.

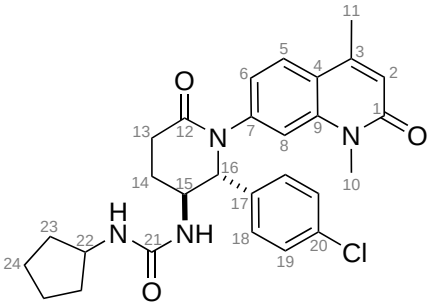

^{1}H-NMR ($CDCl_3$): δ_H 7.58 (d, J = 8.5 Hz, 1H, C(5)*H*), 7.39-7.30 (m, 4H, C(18)*H* & C(19)*H*), 7.14 (d, J = 2.0 Hz, 1H, C(8)*H*), 7.03 (dd, J = 8.5, 2.0 Hz, 1H, C(6)*H*), 6.51 (d, J = 1.0 Hz, 1H, C(2)*H*), 5.78 (d, J = 6.5 Hz, 1H, N*H*), 5.33-5.27 (m, 2H, C(16)*H* & N*H*), 4.19-4.14 (m, 1H, C(15)*H*), 4.07 (tdt, J = 7.0, 7.0, 6.5 Hz, 1H, C(22)*H*), 3.47 (s, 3H, C(10)H_3), 2.73 (ddd, J = 19.5, 8.5, 1.5 Hz, 1H, C(13)H_a), 2.59 (ddd, J = 19.5, 11.0, 8.5 Hz, 1H, C(13)H_b), 2.37 (d, J = 1.0 Hz, 3H, C(11)H_3), 2.09-1.91 (m, 3H, C(14)H_a & C(23)H_a), 1.72-1.58 (m, 5H, C(14)H_b, C(24)H_2), 1.35 (dq, J = 12.5, 6.5 Hz, 2H, C(23)H_b); ^{13}C-NMR ($CDCl_3$): δ_C 170.9 (*C*(12)), 162.0 (*C*(1)), 157.9 (*C*(21)), 146.1 (*C*(4)), 144.2 (*C*(7)), 140.5 (*C*(9)), 137.2 (*C*(17)), 134.1 (*C*(20)), 129.3 (*C*(19)), 128.0 (*C*(18)), 126.1 (*C*(5)), 121.5 (*C*(2)), 120.8 (*C*(6)), 120.5 (*C*(3)), 113.1 (*C*(8)), 69.8 (*C*(16)), 52.1 (*C*(22)), 50.2 (*C*(15)), 33.7 (*C*(23)), 29.3 (*C*(10)), 27.9 (*C*(13)), 23.8 (*C*(24)), 20.6 (*C*(14)), 19.0 (*C*(11)); IR ν_{max} 3364, 2956, 2361, 1645, 1591, 1556, 729; LR-ESI-MS: $C_{28}H_{32}ClN_4O_3$ $[M+H]^+$ *m/z* found 507.2 calcd 507.2, $C_{28}H_{31}ClN_4O_3Na$ $[M+Na]^+$ *m/z* found 529.2 calcd 529.2; HR-ESI-MS: $C_{28}H_{32}ClN_4O_3$ $[M+H]^+$ *m/z* found 507.21575 calcd 507.21487 error = 1.72 ppm.

1-[(2*R,3*S**)-2-(4-chlorophenyl)-1-(1,4-dimethyl-2-oxo-1,2-dihydroquinolin-7-yl)-6-oxopiperidin-3-yl]-3-cyclohexylurea** (**294**)

Compound **279** (20 mg, 0.051 mmol) was dissolved in CH_2Cl_2 (0.22 mL), cyclohexylisocyanate (6.5 μL, 0.051 mmol) was added and the reaction mixture was stirred at rt for 15 h. The reaction mixture was concentrated and purification by FCC (15% isopropanol/hexane) then preparative TLC (40% isopropanol/hexane) yielded **294** (5.2 mg, 20%) as white crystals.

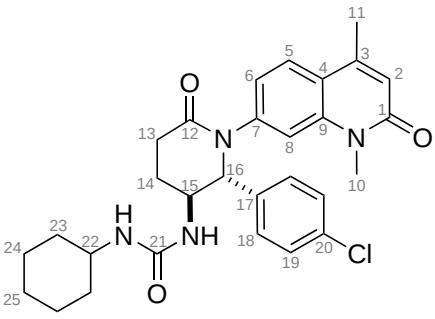

Mpt: 145.2-146.9 °C; ^{1}H-NMR ($CDCl_3$): δ_H 7.59 (d, J = 8.5 Hz, 1H, C(5)*H*), 7.38-7.31 (m, 4H, C(18)*H* & C(19)*H*), 7.15 (d, J = 2.0 Hz, 1H, C(8)*H*), 7.03 (dd, J = 8.5, 2.0 Hz, 1H, C(6)*H*), 6.52 (d, J = 1.0 Hz, 1H, C(2)*H*), 5.70 (d, J = 6.5 Hz, 1H, N*H*), 5.33 (br s, 1H, C(16)*H*), 5.13 (d, J = 8.0 Hz, 1H, N*H*), 4.18-4.13 (m, 1H, C(15)*H*), 3.67-3.57 (m, 1H, C(22)*H*), 3.50 (s, 3H, C(10)H_3), 2.74 (ddd, J = 19.0, 8.5, 1.5 Hz, 1H, C(13)H_a), 2.60 (ddd, J = 19.0, 11.0, 8.5 Hz, 1H, C(13)H_b), 2.38 (d, J = 1.0 Hz, 3H, C(11)H_3), 2.11-1.98 (m, 1H,

C(14)H_a), 1.96-1.87 (m, 2H, C(23)H_a), 1.76-1.67 (m, 6H, C(14)H_b, C(24)H_2 & C(25)H_a), 1.44-1.32 (m, 1H, C(25)H_b), 1.21-1.03 (m, 2H, C(23)H_b); ^{13}C-NMR ($CDCl_3$): δ_C 169.3 (*C*(12)), 161.9 (*C*(1)), 157.3 (*C*(21)), 145.9 (*C*(4)), 144.0 (*C*(7)), 140.4 (*C*(9)), 137.1 (*C*(17)), 134.0 (*C*(20)), 129.1 (*C*(19)), 127.8 (*C*(18)), 126.0 (*C*(5)), 121.4 (*C*(2)), 120.6 (*C*(6)), 120.4 (*C*(3)), 113.0 (*C*(8)), 69.7 (*C*(16)), 50.1 (*C*(15)), 48.9 (*C*(22)), 33.9 (*C*(23)), 29.1 (*C*(10)), 27.7 (*C*(13)), 25.6 (*C*(24)), 24.9 (*C*(25)), 20.4 (*C*(14)), 18.9 (*C*(11)); IR ν_{max} 3364, 2930, 2853, 1645, 1591, 1555, 730; LR-ESI-MS: $C_{29}H_{34}ClN_4O_3$ $[M+H]^+$ *m/z* found 521.2 calcd 521.3, $C_{29}H_{33}ClN_4O_3Na$ $[M+Na]^+$ *m/z* found 543.2 calcd 543.2; HR-ESI-MS: $C_{29}H_{34}ClN_4O_3$ $[M+H]^+$ *m/z* found 521.23140 calcd 521.23096 error = 0.84 ppm.

1-[(2*R,3*S**)-2-(4-chlorophenyl)-1-(1,4-dimethyl-2-oxo-1,2-dihydroquinolin-7-yl)-6-oxopiperidin-3-yl]-3-phenylurea** (**295**), **1-[(2*R*,3*S*)-2-(4-chlorophenyl)-1-(1,4-dimethyl-2-oxo-1,2-dihydroquinolin-7-yl)-6-oxo-piperidin-3-yl]-3-phenylurea** ((+)-**295**) & **1-[(2*S*,3*R*)-2-(4-chlorophenyl)-1-(1,4-dimethyl-2-oxo-1,2-dihydroquinolin-7-yl)-6-oxopiperidin-3-yl]-3-phenylurea** ((–)-**295**)

Compound **279** (20 mg, 0.051 mmol) was dissolved in CH_2Cl_2 (0.22 mL), phenylisocyanate (5.5 μL, 0.051 mmol) was added and the reaction mixture was stirred at rt for 15 h. The reaction mixture was concentrated and purification by FCC (2% MeOH/CH_2Cl_2) and preparative TLC (5% MeOH/CH_2Cl_2) yielded **295** (10.4 mg, 40%) as a colourless oil.

The enantiomers of **295** were preparatively resolved by HPLC (stationary phase: Semipreparative Chiralpak AD, solvent composition: hexane:isopropanol 70:30, flow rate: 3 mL.min^{-1}, injection concentration: 12 mg.mL^{-1}, injection volume: 100 μL, λ: 220 nm) with the enantiomers eluting at 18.8 min ((+)-**295**) and 23.3 min ((–)-**295**).

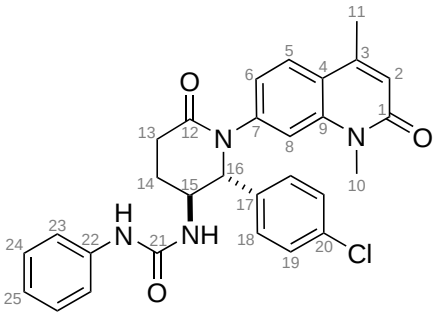

295: ^{1}H-NMR ($CDCl_3$): δ_H 7.86 (s, 1H, N*H*), 7.52 (d, *J* = 8.5 Hz, 1H, C(5)*H*), 7.40-7.23 (m, 8H, C(18)*H*, C(19)*H*, C(23)*H* & C(24)*H*), 7.12 (d, *J* = 1.5 Hz, 1H, C(8)*H*), 7.07 (dd, *J* = 8.5, 2.0 Hz, 1H, C(6)*H*), 7.03 (tt, *J* = 7.0, 1.0 Hz, 1H, C(25)*H*), 6.46 (d, *J* = 0.5 Hz, 1H, C(2)*H*), 6.41 (d, *J* = 6.5 Hz, 1H, N*H*), 5.36 (br s, 1H, C(16)*H*), 4.28-4.24 (m, 1H, C(15)*H*), 3.29 (s, 3H, C(10)H_3), 2.81 (ddd, *J* = 19.5, 9.0, 1.0 Hz, 1H, C(13)H_a), 2.65 (ddd, *J* = 19.0, 10.5, 8.5 Hz, 1H, C(13)H_b), 2.29 (d, *J* = 0.5 Hz, 3H, C(11)H_3), 2.13-2.02 (m, 1H, C(14)H_a), 1.69-1.65 (m, 1H, C(14)H_b); ^{13}C-NMR ($CDCl_3$): δ_C 171.4 (*C*(12)), 161.8 (*C*(1)), 155.4 (*C*(21)), 145.9 (*C*(4)), 143.7 (*C*(7)), 140.5 (*C*(9)), 138.9 (*C*(22)), 136.4 (*C*(17)), 134.2 (*C*(20)), 129.2 (*C*(19)), 129.0 (*C*(24)), 127.7 (*C*(18)), 126.2 (*C*(5)), 123.0 (*C*(25)), 121.5 (*C*(2)), 120.6 (*C*(3)), 120.5 (*C*(6)), 118.9 (*C*(23)), 112.8 (*C*(8)), 69.7 (*C*(16)), 49.7 (*C*(15)), 29.0 (*C*(10)), 27.7 (*C*(13)), 20.1 (*C*(14)), 18.8 (*C*(11)); IR ν_{max} 3344, 2950, 2361, 2341, 1645, 1596, 1550, 732; LR-ESI-MS: $C_{29}H_{28}ClN_4O_3$ $[M+H]^+$ *m/z* found 515.2 calcd 515.2, $C_{29}H_{27}ClN_4O_3Na$ $[M+Na]^+$ *m/z* found 537.2 calcd 537.2; HR-ESI-MS: $C_{29}H_{27}ClN_4O_3Na$ $[M+Na]^+$ *m/z* found 537.1664 calcd 537.1669 error = 1.0 ppm; Analytical HPLC separation (stationary phase: Chiralpak AD, solvent composition: hexane:isopropanol 80:20, flow rate: 1 mL.min^{-1}, injection concentration: 1 mg.mL^{-1}, injection volume: 10 μL, λ: 220 nm): t_1 = 24.8 min, t_2 = 29.1 min.

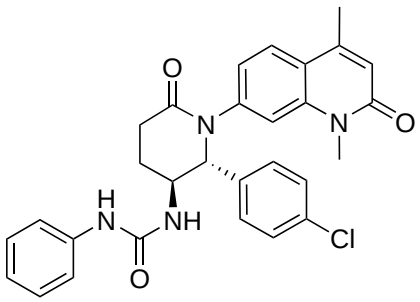

(+)-**295**: $[\alpha]_D{}^{20}$ + 9 (*c* 0.08, $CHCl_3$); Analytical HPLC ee determination: t_1 = 99.94, t_2 = 0.06, ee = >99%.

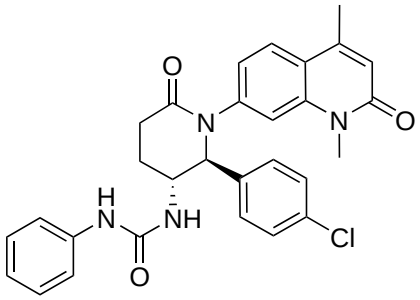

(–)-**295**: $[\alpha]_D{}^{20}$ - 11 (*c* 0.11, $CHCl_3$); Analytical HPLC ee determination: t_1 = 0.79, t_2 = 99.21, ee = 98%.

1-Benzyl-3-[(2*R,3*S**)-2-(4-chlorophenyl)-1-(1,4-dimethyl-2-oxo-1,2-dihydroquinolin-7-yl)-6-oxopiperidin-3-yl]urea** (**296**)

Compound **279** (20 mg, 0.051 mmol) was dissolved in CH_2Cl_2 (0.22 mL), benzylisocyanate (6.2 μL, 0.051 mmol) was added and the reaction mixture was stirred at rt for 15 h. The reaction mixture was concentrated and purification by FCC (15% isopropanol/hexane) and preparative TLC (30% isopropanol/hexane) yielded **296** (4.2 mg, 16%) as a colourless oil.

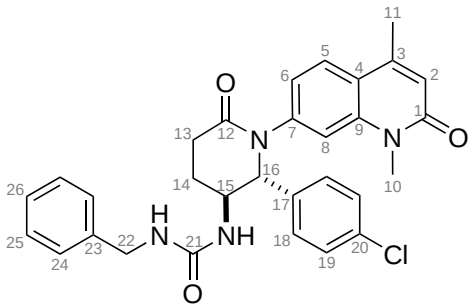

^{1}H-NMR ($CDCl_3$): δ_H 7.53 (d, J = 8.5 Hz, 1H, C(5)H), 7.37-7.25 (m, 9H, C(18)H, C(19)H, C(24)H, C(25)H & C(26)H), 7.09 (d, J = 1.5 Hz, 1H, C(8)H), 6.95 (dd, J = 8.5, 1.5 Hz, 1H, C(6)H), 6.50 (s, 1H, C(2)H), 6.03 (d, J = 5.5 Hz, 1H, NH), 5.74 (s, 1H, NH), 5.28 (br s, 1H, C(16)H), 4.38 (s, 2H, C(22)H), 4.20-4.16 (m, 1H, C(15)H), 3.36 (s, 3H, C(10)H_3), 2.62 (ddd, J = 19.0, 8.5, 1.5 Hz, 1H, C(13)H_a), 2.53 (ddd, J = 19.0, 10.0, 8.0 Hz, 1H, C(13)H_b), 2.36 (s, 3H, C(11)H_3), 2.01-1.91 (m, 1H, C(14)H_a), 1.61-1.58 (m, 1H, C(14)H_b); ^{13}C-NMR ($CDCl_3$): δ_C 170.9 (*C*(12)), 161.8 (*C*(1)), 157.8 (*C*(21)), 145.8 (*C*(4)), 143.8 (*C*(7)), 140.3 (*C*(9)), 139.4 (*C*(17)), 136.8 (*C*(23)), 134.0 (*C*(20)), 129.1 (*C*(19)), 128.7 (*C*(25)), 127.8 (*C*(18)), 127.4 (*C*(26)), 127.2 (*C*(24)), 126.0 (*C*(5)), 121.5 (*C*(2)), 120.4 (*C*(3)), 120.4 (*C*(6)), 113.0 (*C*(8)), 69.6 (*C*(16)), 50.0 (*C*(15)), 44.0 (*C*(22)), 29.0 (*C*(10)), 27.6 (*C*(13)), 20.3 (*C*(14)), 18.9 (*C*(11)); IR ν_{max} 3363, 2920, 2361, 1645, 1588, 1558, 723; LR-ESI-MS: $C_{30}H_{30}ClN_4O_3$ $[M+H]^+$ *m/z* found 529.2 calcd 529.2, $C_{30}H_{29}ClN_4O_3Na$ $[M+Na]^+$ *m/z* found 551.2 calcd 551.2; HR-ESI-MS: $C_{30}H_{30}ClN_4O_3$ $[M+H]^+$ *m/z* found 529.20010 calcd 529.19965 error = 0.85 ppm.

1-*tert*-Butyl-3-[(2*R,3*S**)-2-(4-chlorophenyl)-1-(1,4-dimethyl-2-oxo-1,2-dihydroquinolin-7-yl)-6-oxopiperidin-3-yl]thiourea** (**297**)

Compound **279** (20 mg, 0.051 mmol) was dissolved in CH_2Cl_2 (0.22 mL), *tert*-butylisothiocyanate (6.4 μL, 0.051 mmol) was added and the reaction mixture was stirred at rt

for 15 h. The reaction mixture was concentrated and purification by iterative preparative TLC (40% isopropanol/hexane then 5% MeOH/CH_2Cl_2) yielded **297** (6.7 mg, 26%) as an opaque oil.

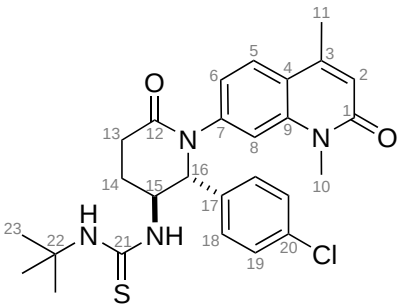

^{1}H-NMR ($CDCl_3$): δ_H 7.55 (d, J = 8.5 Hz, 1H, C(5)H), 7.37 (d, J = 8.5 Hz, 2H, C(18)H), 7.30 (d, J = 8.5 Hz, 2H, C(19)H), 7.09 (d, J = 1.5 Hz, 1H, C(8)H), 6.99 (dd, J = 8.5, 2.0 Hz, 1H, C(6)H), 6.66 (br s, 1H, NH), 6.46 (d, J = 1.0 Hz, 1H, C(2)H), 5.80 (br s, 1H, C(16)H), 4.75-4.69 (m, 1H, C(15)H), 3.46 (s, 3H, C(10)H_3), 2.76 (dd, J = 19.5, 8.5 Hz, 1H, C(13)H_a), 2.52 (ddd, J = 19.5, 11.0, 8.5 Hz, 1H, C(13)H_b), 2.32 (d, J = 0.5 Hz, 3H, C(11)H_3), 2.09-1.96 (m, 1H, C(14)H_a), 1.70-1.61 (m, 1H, C(14)H_b), 1.45 (s, 9H, C(23)H_3); ^{13}C-NMR ($CDCl_3$): δ_C 181.5 (C(21)), 176.2 (C(12)), 161.9 (C(1)), 145.9 (C(4)), 143.7 (C(7)), 140.4 (C(9)), 136.9 (C(17)), 134.1 (C(20)), 129.2 (C(19)), 127.6 (C(18)), 126.0 (C(5)), 121.4 (C(2)), 120.4 (C(6)), 120.4 (C(3)), 112.5 (C(8)), 67.8 (C(16)), 62.2 (C(22)), 53.2 (C(15)), 29.7 (C(10)), 29.5 (C(23)), 27.8 (C(13)), 20.3 (C(14)), 18.9 (C(11)); IR ν_{max} 3336, 2961, 1645, 1592, 1540, 731; LR-ESI-MS: $C_{27}H_{32}ClN_4O_2S$ $[M+H]^+$ m/z found 511.2 calcd 511.3; $C_{27}H_{31}ClN_4O_2SNa$ $[M+Na]^+$ m/z found 533.1 calcd 533.2; HR-ESI-MS: $C_{27}H_{32}ClN_4O_2S$ $[M+H]^+$ m/z found 511.19290 calcd 511.19254 error = 0.72 ppm.

1-Phenyl-3-[(2*R,3*S**)-2-(4-chlorophenyl)-1-(1,4-dimethyl-2-oxo-1,2-dihydroquinolin-7-yl)-6-oxopiperidin-3-yl]thiourea** (**298**)

Compound **279** (20 mg, 0.051 mmol) was dissolved in CH_2Cl_2 (0.22 mL), phenylisothiocyanate (6.0 μL, 0.051 mmol) was added and the reaction mixture was stirred at rt for 15 h. The reaction mixture was concentrated and purification by iterative preparative TLC (40% isopropanol/hexane then 5% MeOH/CH_2Cl_2) yielded **298** (10.7 mg, 40%) as an opaque oil.

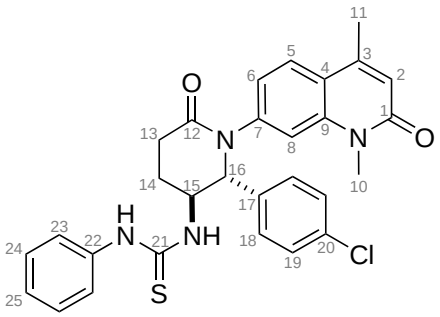

^{1}H-NMR ($CDCl_3$): δ_H 8.48 (br s, 1H, NH), 7.56 (d, J = 8.5 Hz, 1H, C(5)H), 7.49-7.36 (m, 6H, C(18)H, C(19)H & C(24)H), 7.31-7.26 (m, 3H, C(23)H & C(25)H), 7.16 (br s, 1H, NH), 7.10 (d, J = 1.5 Hz, 1H, C(8)H), 7.02 (dd, J = 8.5, 2.0 Hz, 1H, C(6)H), 6.53 (d, J = 1.0 Hz, 1H, C(2)H), 5.79 (br s, 1H, C(16)H), 4.87 (dq, J = 7.0, 3.0 Hz, 1H, C(15)H), 3.43 (s, 3H, C(10)H_3), 2.83 (ddd, J = 18.5, 9.0, 1.5 Hz, 1H, C(13)H_a), 2.56 (ddd, J = 19.0, 10.5, 9.0 Hz, 1H, C(13)H_b), 2.37 (d, J = 0.5 Hz, 3H, C(11)H_3), 2.15 (dddd, J = 14.5, 11.0, 9.0, 4.0 Hz, 1H, C(14)H_a), 1.87-1.78 (m, 1H, C(14)H_b); ^{13}C-NMR ($CDCl_3$): δ_C 181.3 (C(21)), 170.4 (C(12)), 162.0 (C(1)), 146.0 (C(4)), 143.8 (C(7)), 140.6 (C(9)), 137.1 (C(22)), 136.7 (C(17)), 134.4 (C(20)), 129.9 (C(24)), 129.4 (C(19)), 127.8 (C(18)), 127.1 (C(25)), 126.3 (C(5)), 124.7 (C(23)), 121.6 (C(2)), 120.6 (C(3)), 120.4 (C(6)), 112.7 (C(8)), 67.9 (C(16)), 54.0 (C(15)), 29.3 (C(10)), 28.0 (C(13)), 20.4 (C(14)), 19.0 (C(11)); IR ν_{max} 3316, 6057, 2949, 1647, 1592, 1537, 729; LR-ESI-MS: $C_{29}H_{28}ClN_4O_2S$ $[M+H]^+$ m/z found 531.2 calcd 531.2, $C_{29}H_{27}ClN_4O_2SNa$ $[M+Na]^+$ m/z found 553.0 calcd 553.1; HR-ESI-MS: $C_{29}H_{28}ClN_4O_2S$ $[M+H]^+$ m/z found 531.16160 calcd 531.16125 error = 0.65 ppm.

Methyl (4*S,5*R**)-5-[(*tert*-butoxycarbonyl)amino]-5-(4-chlorophenyl)-4-nitropentanoate (301)**

Method A. Compound **13** (43 mg, 0.29 mmol) was dissolved in TBME (0.58 mL), **300** (22.2 mg, 0.058 mmol) and TBAB (1.0 mg, 0.003 mmol) were added and the solution was cooled to -78 °C. KOH (16 mg, 0.29 mmol) was added and the reaction mixture was stirred at -20 °C for 14 h. $NaHCO_3$ (5 mL, sat. aq. soln) was added and the aqueous phase was extracted with CH_2Cl_2 (3 x 5 mL). The combined organic extracts were dried over Na_2SO_4, filtered and concentrated. Purification by FCC (66% CH_2Cl_2/hexane) yielded **301** (13 mg, 58%, dr *cis*:*trans* 1.46:1) as a colourless oil.

Method B. Compound **13** (6.68 g, 45.4 mmol) was dissolved in TBME (90.6 mL), **300** (2.18 g, 9.08 mmol) and **299** (0.68 g, 0.91 mmol) were added and the solution was cooled to -78 °C. K_2CO_3 (6.27 g, 45.4 mmol) was added and the reaction mixture was stirred at -20 °C for 36 h. $NaHCO_3$ (25 mL, sat. aq. soln) was added and the aqueous phase was extracted with CH_2Cl_2 (7 x 25 mL). The combined organic extracts were dried over Na_2SO_4, filtered and concentrated. Purification by FCC (50% Et_2O/PE) yielded **301** (2.46 g, 70%, dr *cis*:*trans* 1:7, ee_{cis} 90%, ee_{trans} 90%) as a colourless oil.

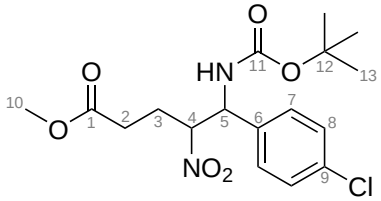

^{1}H-NMR ($CDCl_3$): δ_H 7.36 (dd, J = 8.5, 5.5 Hz, 2H, C(8)H), 7.23 (dd, J = 8.5, 4.0 Hz, 2H, C(7)H), 5.70 (br s, 1H, NH), 5.18 (br s, 1H, C(5)H), 4.94 (br s, 1H, C(4)H), 3.72 (s, 3H, C(10)H_3), 2.54-2.25 (m, 4H, C(2)H_2 & C(3)H_2), 1.45 (s, 9H, C(13)H_3); ^{13}C-NMR ($CDCl_3$): δ_C 172.0 (C(1)), 154.9 (C(11)), 135.7 (C(6)), 134.4 (C(9)), 129.3 (C(8)), 127.7 (C(7)), 90.4 (C(4)), 80.7 (C(12)), 55.3 (C(5)), 52.0 (C(10)), 29.5 (C(2)), 28.2 (C(13)), 26.3 (C(3)); IR ν_{max} 3379, 2977, 1736, 1707, 1682, 1551, 1163, 830; LR-ESI-MS: $C_{17}H_{24}ClN_2O_6$ $[M+H]^+$ *m/z* found 387.1 calcd 387.2; HR-ESI-MS: $C_{17}H_{24}ClN_2O_6$ $[M+H]^+$ *m/z* found 387.1317 calcd 387.1321 error = 0.49 ppm; Analytical HPLC separation (stationary phase: Chiralpak AD, solvent composition: hexane:isopropanol 85:15, flow rate: 0.5 mL.min^{-1}, injection concentration: 2 mg.mL^{-1}, injection volume: 5 μL, λ: 210 nm): t_1 = 26.5 min (*cis*), t_2 = 28.1 min (*cis*), t_3 = 32.2 min (*trans*), t_4 = 34.0 min (*trans*).

***tert*-Butyl (1-(1,4-dimethyl-2-oxo-1,2-dihydroquinolin-7-yl)-5-oxo-2-phenylpyrrolidin-3-yl)carbamate (330)**

In a pressure tube under inert conditions, **353** (100 mg, 0.36 mmol), **218** (137 mg, 0.54 mmol) and K_3PO_4 (154 mg, 0.72 mmol) were combined. 1,4-dioxane (3.6 mL) was added and the solution was degassed. (+/-)-*trans*-1,2-diaminocyclohexane (43 μL, 0.36 mmol) and CuI (69 mg, 0.36 mmol) were added, the tube was sealed and the reaction mixture was stirred at 97 °C for 42 h. The reaction mixture was passed through a plug of Celite and the Celite was washed with CH_2Cl_2 (30 mL). The combined filtrate was concentrated and purification by FCC (10% isopropanol/PE) yielded **330** (64 mg, 40%) as a white solid.

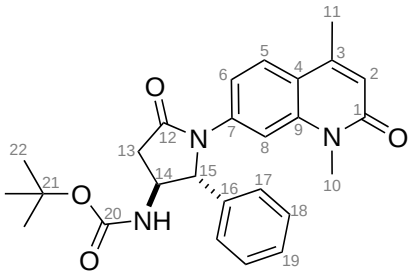

Mpt: 194.8-196.1 °C; ^{1}H-NMR ($CDCl_3$): δ_H 8.06 (br s, 1H, C(8)H), 7.52 (d, J = 9.0 Hz, 1H, C(5)H), 7.43-7.29 (m, 5H, C(17)H, C(18)H & C(19)H), 7.13 (dd, J = 9.0, 2.0 Hz, 1H, C(6)H), 6.49 (s, 1H, C(2)H), 5.27 (br s, 1H, C(15)H), 4.15 (t, J = 7.0 Hz, 1H, C(14)H), 3.57 (s, 3H, C(10)H_3), 3.11 (dd, J = 17.5, 7.0 Hz, 1H, C(13)H_a), 2.46 (d, J = 17.5 Hz, 1H, C(13)H_b), 2.36 (s, 3H, C(11)H_3), 1.49 (s, 9H, C(22)H_3); ^{13}C-NMR ($CDCl_3$): δ_C 171.8 (C(12)), 162.3 (C(1)), 155.2 (C(20)), 145.8 (C(4)), 140.2 (C(7)), 140.1 (C(9)), 135.1 (C(16)), 129.3 (C(18)), 128.8 (C(19)), 126.8 (C(17)), 125.6 (C(5)), 120.3 (C(2)), 118.2 (C(3)), 114.4 (C(6)), 106.5 (C(8)), 80.3 (C(21)), 66.0 (C(15)), 47.9 (C(14)), 36.4 (C(13)), 29.1 (C(10)), 28.2 (C(22)), 18.7 (C(11)); IR ν_{max} 3304, 2924, 1705, 1640, 1519, 1443, 1289, 1166, 1013, 840, 701; LR-ESI-MS: $C_{26}H_{30}N_3O_4$ $[M+H]^+$ *m/z* found 448.2 calcd 448.2; HR-ESI-MS: $C_{26}H_{30}N_3O_4$ $[M+H]^+$ *m/z* found 448.22308 calcd 448.22318 error = 0.17 ppm.

7-(3-Amino-5-oxo-2-phenylpyrrolidin-1-yl)-1,4-dimethylquinolin-2(1*H*)-one (331)

Compound **330** (288 mg, 0.64 mmol) was dissolved in HCl (4.3 mL, 4M 1,4-dioxane soln) and the reaction mixture was stirred at rt for 16 h. The reaction mixture was concentrated then co-evaporated with EtOAc (4 x 10 mL). 1M HCl (20 mL) was added and the aqueous phase was washed with $CHCl_3$ (3 x 20 mL). The aqueous phase was basified with Na_2CO_3 (sat. aq. soln) and extracted with $CHCl_3$ (3 x 20 mL). The combined organic extracts were dried over Na_2SO_4, filtered and concentrated to yield **331** (194 mg, 87%) as a white powder.

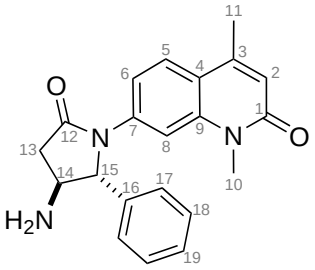

Mpt: 93.0-93.7 °C; ^{1}H-NMR ($CDCl_3$): δ_H 7.71 (d, J = 2.0 Hz, 1H, C(8)H), 7.53 (d, J = 8.5 Hz, 1H, C(5)H), 7.36 (t, J = 7.0 Hz, 2H, C(18)H), 7.33-7.20 (m, 4H, C(6)H, C(17)H & C(19)H), 6.48 (s, 1H, C(2)H), 4.95 (d, J = 3.5 Hz, 1H, C(15)H), 3.60 (ddd, J = 7.0, 4.5, 4.0 Hz, 1H, C(14)H), 3.55 (s, 3H, C(10)H_3), 3.07 (dd, J = 17.0, 7.0 Hz, 1H, C(13)H_a), 2.48 (dd, J = 17.0, 5.0 Hz, 1H, C(13)H_b), 2.36 (d, J = 1.0 Hz, 3H, C(11)H_3); ^{13}C-NMR ($CDCl_3$): δ_C 173.3 (C(12)), 162.3 (C(1)), 145.9 (C(4)), 140.1 (C(7)), 140.1 (C(9)), 138.4 (C(16)), 129.3 (C(18)), 128.4 (C(19)), 125.9 (C(17)), 125.4 (C(5)), 120.1 (C(2)), 118.1 (C(3)), 115.1 (C(6)), 107.2 (C(8)), 73.4 (C(15)), 54.7 (C(14)), 40.8 (C(13)), 29.2 (C(10)), 18.7 (C(11)); IR ν_{max} 3349, 2920, 2361, 1694, 1643, 1581, 1416, 1392, 702; LR-ESI-MS: $C_{21}H_{22}N_3O_2$ $[M+H]^+$ *m/z* found 348.2 calcd 348.2; HR-ESI-MS: $C_{21}H_{22}N_3O_2$ $[M+H]^+$ *m/z* found 348.17065 calcd 348.17067 error = 0.08 ppm.

2-Methylpropyl (1-(1,4-dimethyl-2-oxo-1,2-dihydroquinolin-7-yl)-5-oxo-2-phenylpyrrolidin-3-yl)carbamate (334)

Compound **331** (20 mg, 0.058 mmol) was dissolved in CH_2Cl_2 (0.58 mL), isobutylchloroformate (22 μL, 0.17 mmol) and NEt_3 (24 μL, 0.17 mmol) were added and the reaction mixture was stirred at rt for 16 h. H_2O (10 mL) was added and the organic phase was separated. The aqueous phase was extracted with CH_2Cl_2 (3 x 5 mL), the combined organic extracts were dried over Na_2SO_4, filtered and concentrated. Purification by FCC (1% MeOH/CH_2Cl_2) yielded **334** (19 mg, 74%) as a white solid.

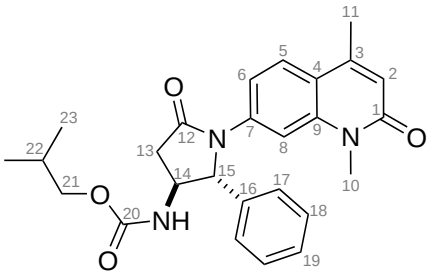

Mpt: 221.3-221.9 °C; ^{1}H-NMR ($CDCl_3$): δ_H 8.10 (br s, 1H, C(8)H), 7.45-7.28 (m, 6H, C(5)H, C(17)H, C(18)H & C(19)H), 7.03 (br s, 1H, C(6)H), 6.44 (s, 1H, C(2)H), 6.30 (br s, 1H, NH), 5.37 (s, 1H, C(15)H), 4.21 (t, J = 7.0 Hz, 1H, C(14)H), 3.97 (dd, J = 10.5, 6.5 Hz, 1H, C(21)H_a), 3.90 (dd, J = 10.0, 7.0 Hz, 1H, C(21)H_b), 3.48 (s, 3H, C(10)H_3), 3.11 (dd, J = 17.5, 7.5 Hz, 1H, C(13)H_a), 2.54 (d, J = 17.5 Hz, 1H, C(13)H_b), 2.31 (d, J = 1.0 Hz, 3H, C(11)H_3), 1.95 (spt, J = 6.5 Hz, 1H, C(22)H), 0.95 (d, J = 7.0 Hz, 6H, C(23)H_3); ^{13}C-NMR ($CDCl_3$): δ_C 173.1 (C(12)), 162.3 (C(1)), 156.6 (C(20)), 145.8 (C(4)), 140.3 (C(7)), 140.1 (C(9)), 137.4 (C(16)), 129.3 (C(18)), 128.4 (C(19)), 125.7 (C(17)), 125.3 (C(5)), 119.8 (C(2)), 117.8 (C(3)), 113.5 (C(6)), 105.4 (C(8)), 71.5 (C(21)), 70.8 (C(15)), 53.4 (C(14)), 37.3 (C(13)), 29.2 (C(10)), 28.0 (C(22)), 19.0 (C(23)), 18.6 (C(11)); IR ν_{max} 3276, 2961, 1702, 1646, 1593, 1375, 1250, 731; LR-ESI-MS: $C_{26}H_{30}N_3O_4$ [M+H]$^+$ *m/z* found 448.2 calcd 448.2; HR-ESI-MS: $C_{26}H_{30}N_3O_4$ [M+H]$^+$ *m/z* found 448.22309 calcd 448.22244 error = 1.43 ppm.

1-*tert*-Butyl-3-(1-(1,4-dimethyl-2-oxo-1,2-dihydroquinolin-7-yl)-5-oxo-2-phenyl-pyrrolidin-3-yl)urea (**336**)

Compound **331** (25 mg, 0.072 mmol) was dissolved in CH_2Cl_2 (0.31 mL), *tert*-butylisocyanate (8.3 μL, 0.072 mmol) was added and the reaction mixture was stirred at rt for 16 h. The reaction mixture was concentrated and purification by FCC (1% MeOH/CH_2Cl_2) yielded **336** (29.6 mg, 92%) as an opaque oil.

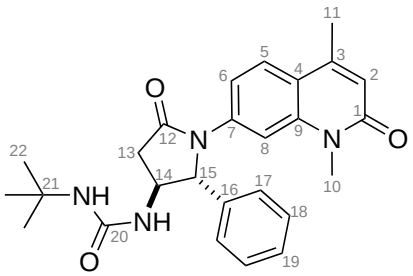

^{1}H-NMR ($CDCl_3$): δ_H 8.41 (d, J = 1.5 Hz, 1H, C(8)H), 7.36-7.31 (m, 3H, C(17)H & C(19)H), 7.30-7.23 (m, 3H, C(5)H & C(18)H), 6.70 (dd, J = 9.0, 2.0 Hz, 1H, C(6)H), 6.53 (d, J = 7.5 Hz, 1H, NH), 6.40 (s, 1H, C(2)H), 5.27 (s, 1H, C(15)H), 4.31 (t, J = 7.0 Hz, 1H, C(14)H), 3.46 (s, 3H, C(10)H_3), 3.02 (dd, J = 17.5, 7.0 Hz, 1H, C(13)H_a), 2.44 (d, J = 17.5 Hz, 1H, C(13)H_b), 2.28 (s, 3H, C(11)H_3), 1.41 (s, 9H, C(22)H_3); ^{13}C-NMR ($CDCl_3$): δ_C 174.3 (C(12)), 162.6 (C(1)), 157.4 (C(20)), 146.5 (C(4)), 140.8 (C(7)), 139.7 (C(9)), 137.2 (C(16)), 129.1 (C(18)), 128.0 (C(19)), 125.7 (C(17)), 125.0 (C(5)), 118.6 (C(2)), 117.1 (C(3)), 112.8 (C(6)), 104.3 (C(8)), 71.3 (C(15)), 52.1 (C(14)), 50.3 (C(21)), 37.9 (C(13)), 29.6 (C(22)), 29.4 (C(10)), 18.7 (C(11)); IR ν_{max} 3298, 2976, 2362, 2342, 1704, 1653, 1594, 1374; LR-ESI-MS: $C_{26}H_{31}N_4O_3$ [M+H]$^+$ *m/z* found 447.2 calcd 447.3; HR-ESI-MS: $C_{26}H_{31}N_4O_3$ [M+H]$^+$ *m/z* found 447.23907 calcd 447.23919 error = 0.29 ppm.

5-Cyclopropyl-1-(4-methoxyphenyl)-4-nitropyrrolidin-2-one (**340**)

Under inert conditions, **23** (83 μL, 0.75 mmol) was dissolved in toluene (15 mL), *p*-anisidine (139 mg, 1.13 mmol), benzoic acid (9.2 mg, 0.075 mmol) and cyclopropane carboxaldehyde (84 μL, 1.13 mmol) were added and the reaction mixture was stirred at 70 °C for 4 d. Na_2CO_3 (20 mL, sat. aq. soln) was added and the organic phase was separated. The aqueous phase was extracted with EtOAc (3 x 20 mL), the combined organic phase was dried over Na_2SO_4, filtered and concentrated. Purification by FCC (50% EtOAc/PE) yielded **340** (57 mg, 27%) as a brown

oil.

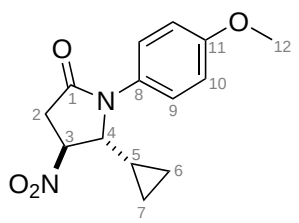

^{1}H-NMR ($CDCl_3$): δ_H 7.21 (d, J = 9.0 Hz, 2H, C(9)H), 6.93 (d, J = 9.0 Hz, 2H, C(10)H), 5.10 (ddd, J = 7.5, 3.5, 2.5 Hz, 1H, C(3)H), 3.82 (s, 3H, C(12)H_3), 3.73 (dd, J = 10.0, 2.0 Hz, 1H, C(4)H), 3.23 (dd, J = 18.0, 3.5 Hz, 1H, C(2)H_a), 3.17 (dd, J = 18.0, 8.0 Hz, 1H, C(2)H_b), 0.96 (ddt, J = 17.5, 8.0, 5.0 Hz, 1H, C(5)H), 0.63-0.54 (m, 2H, C(6)H_a & C(7)H_a), 0.32 (ddt, J = 9.5, 5.0, 2.5 Hz, 1H, C(6)H_b), 0.13 (ddt, J = 9.5, 4.5, 3.0 Hz, 1H, C(7)H_b), ^{13}C-NMR ($CDCl_3$): δ_C 169.0 (C(1)), 158.8 (C(11)), 129.3 (C(8)), 127.6 (C(9)), 114.6 (C(10)), 83.5 (C(3)), 70.7 (C(4)), 55.4 (C(12)), 35.4 (C(2)), 14.8 (C(5)), 5.8 (C(6)), 1.0 (C(7)); IR ν_{max} 3007, 2838, 1699, 1552,, 1511, 1247, 831; LR-ESI-MS: $C_{14}H_{17}N_2O_4$ $[M+H]^+$ *m/z* found 277.1 calcd 277.1, $C_{14}H_{16}N_2O_4Na$ $[M+Na]^+$ *m/z* found 299.0 calcd 299.1; HR-ESI-MS: $C_{14}H_{17}N_2O_4$ $[M+H]^+$ *m/z* found 277.11828 calcd 277.11826 error = 0.1 ppm.

1-(4-Methoxyphenyl)-4-nitro-5-(pyridin-2-yl)pyrrolidin-2-one (**341**)

Under inert conditions, **23** (83 μL, 0.75 mmol) was dissolved in toluene (15 mL), *p*-anisidine (139 mg, 1.13 mmol), benzoic acid (9.2 mg, 0.075 mmol) and 2-pyridinecarboxaldehyde (107 μL, 1.13 mmol) were added and the reaction mixture was stirred at 70 °C for 4 d. Na_2CO_3 (20 mL, sat. aq. soln) was added and the organic phase was separated. The aqueous phase was extracted with EtOAc (3 x 20 mL), the combined organic phase was dried over Na_2SO_4, filtered and concentrated. Purification by FCC (40% EtOAc/PE) yielded **341** (37 mg, 16%) as a brown oil.

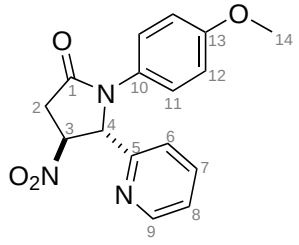

^{1}H-NMR ($CDCl_3$): δ_H 8.65 (d, J = 4.5 Hz, 1H, C(9)H), 7.64 (td, J = 7.5, 1.5 Hz, 1H, C(7)H), 7.28 (dd, J = 7.0, 5.0 Hz, 1H, C(8)H), 7.19-7.12 (m, 3H, C(6)H & C(11)H), 6.82 (d, J = 9.0 Hz, 2H, C(12)H), 5.66 (d, J = 1.0 Hz, 1H, C(4)H), 5.32 (dt, J = 8.0, 1.5 Hz, 1H, C(3)H), 3.75 (s, 3H, C(14)H_3), 3.45 (dd, J = 18.0, 8.0 Hz, 1H, C(2)H_a), 3.30 (dd, J = 18.0, 2.0 Hz, 1H, C(2)H_b); ^{13}C-NMR ($CDCl_3$): δ_C 169.8 (C(1)), 158.1 (C(13)), 155.5 (C(5)), 150.7 (C(9)), 137.1 (C(7)), 129.4 (C(10)), 125.7 (C(11)), 124.0 (C(8)), 122.3 (C(6)), 114.4 (C(12)), 82.8 (C(3)), 69.1 (C(4)), 55.4 (C(14)), 35.8 (C(2)); IR ν_{max} 2934, 2838, 2359, 1706, 1555, 1513, 1250; LR-ESI-MS: $C_{16}H_{16}N_3O_4$ $[M+H]^+$ *m/z* found 314.1 calcd 314.1, $C_{16}H_{15}N_3O_4Na$ $[M+Na]^+$ *m/z* found 336.0 calcd 336.1; HR-ESI-MS: $C_{16}H_{16}N_3O_4$ $[M+H]^+$ *m/z* found 314.11353 calcd 314.11356 error = 0.07 ppm.

5-Cyclopropyl-4-nitropyrrolidin-2-one (**342**)

Compound **340** (57 mg, 0.21 mmol) was dissolved in acetonitrile (3.6 mL) and the solution was cooled to 0 °C. A solution of ceric ammonium nitrate (339 mg, 0.62 mmol) in H_2O (3.6 mL) was added and the reaction mixture was stirred at 0 °C for 40 min. The volatiles were removed and the remaining aqueous phase was extracted with EtOAc (3 x 20 mL). The combined organic extracts were dried over Na_2SO_4, filtered and concentrated. Purification by FCC (40% EtOAc/PE) yielded **342** (23 mg, 66%) as an orange oil.

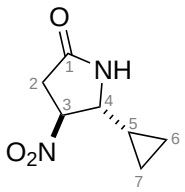

^{1}H-NMR ($CDCl_3$): δ_H 7.38 (br s, 1H, NH), 5.05 (ddd, J = 8.5, 4.0, 3.0 Hz, 1H, C(3)H), 3.58 (dd, J = 8.5, 3.0 Hz, 1H, C(4)H), 3.07 (dd, J = 18.0, 4.0 Hz, 1H, C(2)H_a), 2.93 (dd, J = 18.0, 8.5 Hz, 1H, C(2)H_b), 1.03 (qt, J = 8.0, 5.0 Hz, 1H, C(5)H), 0.72-0.62 (m, 2H, C(6)H_a & C(7)H_a), 0.49-0.33 (m, 2H, C(6)H_b & C(7)H_b); ^{13}C-NMR ($CDCl_3$): δ_C 173.0 (C(1)), 85.1 (C(3)), 63.4 (C(4)), 34.7 (C(2)), 15.5 (C(5)), 2.9 (C(6)), 2.0 (C(7)); IR ν_{max} 3241, 2922, 2360, 2342, 1702, 1554, 669; LR-ESI-MS: $C_7H_{10}N_2O_3Na$ [M+Na]$^+$ *m/z* found 193.1 calcd 193.1; HR-ESI-MS: $C_7H_{11}N_2O_3$ [M+H]$^+$ *m/z* found 171.07642 calcd 171.07648 error = 0.33 ppm.

***tert*-Butyl (2-cyclopropyl-5-oxopyrrolidin-3-yl)carbamate (343)**

Compound **342** (20.3 mg, 0.12 mmol) was dissolved in MeOH (0.8 mL) and the solution was cooled to 0 °C. $NiCl_2 \cdot 6\,H_2O$ (1.4 mg, 0.006 mmol) was added and the solution was stirred at 0 °C for 5 min. $NaBH_4$ (18.0 mg, 0.48 mmol) was added in portions and the reaction mixture was stirred at 0 °C for 30 min. Boc_2O (31.2 mg, 0.14 mmol) was added and the reaction mixture was stirred at rt for 14 h. H_2O (5 mL) was added and the volatiles were removed. The remaining aqueous phase was extracted with EtOAc (3 x 5 mL), the combined organic extracts were dried over Na_2SO_4, filtered and concentrated. Purification by FCC (3% MeOH/CH_2Cl_2) yielded **343** (24.9 mg, 87%) as a colourless oil.

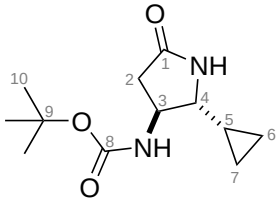

^{1}H-NMR ($CDCl_3$): δ_H 6.73 (br s, 1H, NH), 4.98 (br s, 1H, NH), 4.20 (br s, 1H, C(3)H), 2.88 (dd, J = 8.0, 4.0 Hz, 1H, C(4)H), 2.76 (dd, J = 17.5, 8.0 Hz, 1H, C(2)H_a), 2.19 (dd, J = 17.0, 5.5 Hz, 1H, C(2)H_b), 1.44 (s, 9H, C(10)H_3), 0.96-0.85 (m, 1H, C(5)H), 0.61-0.49 (m, 2H, C(6)H_a & C(7)H_a), 0.39-0.33 (m, 1H, C(7)H_b), 0.25-0.18 (m, 1H, C(6)H_b); ^{13}C-NMR ($CDCl_3$): δ_C 175.4 (C(1)), 155.1 (C(8)), 79.9 (C(9)), 65.9 (C(4)), 52.7 (C(3)), 37.3 (C(2)), 28.3 (C(10)), 14.4 (C(5)), 2.2 (C(6)), 1.9 (C(7)); IR ν_{max} 3276, 2979, 2932, 1686, 1531, 1366, 1280, 1168, 732; LR-ESI-MS: $C_{12}H_{21}N_2O_3$ [M+H]$^+$ *m/z* found 241.2 calcd 241.1, $C_{12}H_{20}N_2O_3Na$ [M+Na]$^+$ *m/z* found 263.1 calcd 263.1; HR-ESI-MS: $C_{12}H_{21}N_2O_3$ [M+H]$^+$ *m/z* found 241.15647 calcd 241.15466 error = 0.02 ppm.

***tert*-Butyl (2-cyclopropyl-1-(1,4-dimethyl-2-oxo-1,2-dihydroquinolin-7-yl)-5-oxopyrrolidin-3-yl)carbamate (344)**

In a pressure tube under inert conditions, **343** (24.9 mg, 0.10 mmol), **218** (39.2 mg, 0.16 mmol) and K_3PO_4 (44.1 mg, 0.21 mmol) were combined. 1,4-dioxane (1.04 mL) was added and the solution was degassed. (+/-)-*trans*-1,2-diaminocyclohexane (12.5 μL, 0.10 mmol) and CuI (19.8 mg, 0.10 mmol) were added, the tube was sealed and the reaction mixture was stirred at 97 °C for 42 h. The reaction mixture was passed through a plug of Celite and the Celite was washed with CH_2Cl_2 (30 mL). The combined filtrate was concentrated and purification by FCC (15% isopropanol/PE) yielded **344** (30.8 mg, 72%) as a yellow opaque oil.

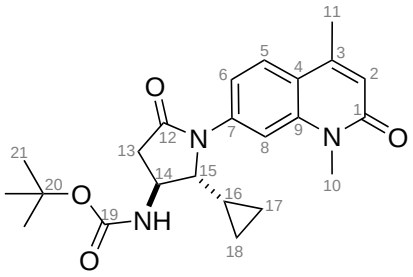

^{1}H-NMR ($CDCl_3$): δ_H 7.69 (br s, 1H, C(8)H), 7.62 (d, J = 8.5 Hz, 1H, C(5)H), 7.18 (dd, J = 8.5, 1.5 Hz, 1H, C(6)H), 6.53 (s, 1H, C(2)H), 5.42 (d, J = 7.0 Hz, 1H, NH), 4.25 (t, J = 7.5 Hz, 1H, C(14)H), 3.66-3.60 (m, 1H, C(15)H), 3.63 (s, 3H, C(10)H_3), 3.12 (dd, J = 17.5, 7.5 Hz, 1H, C(13)H_a), 2.45 (dd, J = 15.0, 2.0 Hz, 1H, C(13)H_b), 2.42 (s, 3H, C(11)H_3), 1.47 (s, 9H, C(21)H_3), 0.98-0.86 (m, 1H, C(16)H), 0.61-0.39 (m, 3H, C(17)H_a, C(18)H_2), 0.27-0.17 (m, 1H, C(17)H_b); ^{13}C-NMR ($CDCl_3$): δ_C 172.0 (C(12)), 162.2 (C(1)), 155.2 (C(19)), 145.9 (C(4)), 140.3 (C(7)), 140.1 (C(9)), 125.5 (C(5)), 120.5 (C(2)), 119.0 (C(3)), 116.9 (C(6)), 109.6 (C(8)), 80.1 (C(20)), 71.8 (C(15)), 50.6 (C(14)), 38.3 (C(13)), 29.3 (C(10)), 28.4 (C(21)), 18.8 (C(11)), 14.0 (C(16)), 5.2 (C(17)), 1.5 (C(18)); IR ν_{max} 3288, 2976, 2924, 1696, 1653, 1592, 731; LR-ESI-MS: $C_{23}H_{30}N_3O_4$ $[M+H]^+$ *m/z* found 412.2 calcd 412.2, $C_{23}H_{29}N_3O_4Na$ $[M+Na]^+$ *m/z* found 434.2 calcd 434.2; HR-ESI-MS: $C_{23}H_{30}N_3O_4$ $[M+H]^+$ *m/z* found 412.22308 calcd 412.22238 error = 1.7 ppm.

Methyl 2-methyl-3-nitropropanoate (**345**)

Under inert conditions, diisopropylamine (0.46 mL, 3.3 mmol) was dissolved in THF (5.0 mL) and the solution was cooled to -10 °C. *n*-BuLi (1.88 mL, 3.0 mmol, 1.6M hexane soln) was added dropwise and the reaction mixture was stirred at 0 °C for 30 min. The reaction was cooled to -78 °C, 1,3-dimethyl-3,4,5,6-tetrahydro-2(1H)-pyrimidinone (1.82 mL) and a solution of **23** (162 μL, 1.5 mmol) in THF (1.0 mL) were added dropwise and the reaction mixture was stirred at -78 °C for 30 min. MeI (140 μL, 2.3 mmol) was added and the reaction mixture was stirred at rt for 14 h. 1M HCl (50 mL) was slowly added and the aqueous phase was extracted with Et_2O (5 x 50 mL). The combined organic extracts were washed with H_2O (2 x 250 mL) and $NaHCO_3$ (250 mL, sat. aq. soln), dried over Na_2SO_4, filtered and concentrated. Purification by FCC (5% EtOAc/PE) yielded **345** (51 mg, 23%) as a colourless oil.

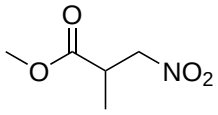

^{1}H-NMR ($CDCl_3$): δ_H 4.73 (dd, J = 14.0, 8.0 Hz, 1H), 4.42 (dd, J = 14.0, 6.0 Hz, 1H), 3.75 (s, 3H), 3.28 (dqd, J = 8.0, 7.5, 5.5 Hz, 1H), 1.30 (d, J = 7.5 Hz, 3H); ^{13}C-NMR ($CDCl_3$): δ_C 172.9, 76.3, 52.5, 37.5, 14.3; LR-ESI-MS: $C_5H_9NO_4Na$ $[M+Na]^+$ *m/z* found 170.0 calcd 170.0;. Data are in accordance with literature values.[133]

***tert*-Butyl (5-oxo-2-phenylpyrrolidin-3-yl)carbamate** (**353**)

Compound **352** (720 mg, 3.5 mmol) was dissolved in MeOH (23 mL) and the solution was cooled to 0 °C. $NiCl_2 \cdot 6\,H_2O$ (42 mg, 0.18 mmol) was added and the solution was stirred at 0 °C for 5 min. $NaBH_4$ (530 mg, 14 mmol) was added in portions and the reaction mixture was stirred at 0 °C for 30 min. Boc_2O (916 mg, 4.2 mmol) was added and the reaction mixture was stirred at rt for 16 h. A solution of brine (sat. aq. soln):$NaHCO_3$ (sat. aq. soln):EtOAc (200 mL, 2:1:2) was added and the organic phase was separated. The aqueous phase was extracted with EtOAc (5 x 150 mL), the combined organic extracts were dried over Na_2SO_4, filtered and concentrated. Purification by FCC (66% EtOAc/PE) yielded **353** (235 mg, 24%) as a white solid.

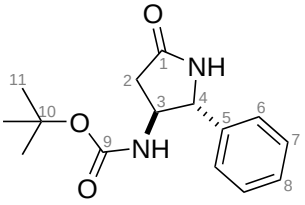

Mpt: 187.2-188.0 °C; ^{1}H-NMR (CD_3OD): δ_H 7.41-7.28 (m, 5H, C(6)*H*, C(7)*H* & C(8)*H*), 4.57 (d, J = 4.5 Hz, 1H, C(4)*H*), 4.03 (d, J = 5.0 Hz, 1H, C(3)*H*), 2.72 (dd, J = 17.0, 8.0 Hz, 1H, C(2)H_a), 2.30 (dd, J = 17.0, 5.5 Hz, 1H, C(2)H_b), 1.42 (s, 9H, C(11)H_3); ^{13}C-NMR (CD_3OD): δ_C 178.5 (*C*(1)), 157.9 (*C*(9)), 141.7 (*C*(5)), 130.0 (*C*(7)), 129.2 (*C*(8)), 127.2 (*C*(6)), 80.6 (*C*(10)), 66.1 (*C*(4)), 57.2 (*C*(3)), 37.6 (*C*(2)), 28.8 (*C*(11)); IR ν_{max} 3392, 2983, 1695, 1509, 1454, 1273, 1169, 1003, 687; LR-ESI-MS: $C_{15}H_{20}N_2O_3Na$ $[M+Na]^+$ *m/z* found 299.1 calcd 299.1; HR-ESI-MS: $C_{15}H_{20}N_2O_3Na$ $[M+Na]^+$ *m/z* found 299.13661 calcd 299.13667 error = 0.12 ppm.

***N*-[1-(1,4-Dimethyl-2-oxo-1,2-dihydroquinolin-7-yl)-5-oxo-2-phenyl-pyrrolidin-3-yl]-2,2,2-trifluoroacetamide (354)**

Compound **331** (20 mg, 0.058 mmol) was dissolved in CH_2Cl_2 (0.58 mL), trifluoroacetic anhydride (24 μL, 0.17 mmol) and NEt_3 (24 μL, 0.17 mmol) were added and the reaction mixture was stirred at rt for 16 h. H_2O (10 mL) was added and the organic phase was separated. The aqueous phase was extracted with CH_2Cl_2 (3 x 5 mL), the combined organic extracts were dried over Na_2SO_4, filtered and concentrated. Purification by FCC (0.5% MeOH/CH_2Cl_2) yielded **354** (21.6 mg, 85%) as a white solid.

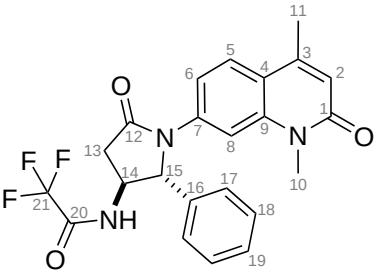

Mpt: 246.0-246.3 °C; ^{1}H-NMR ($CDCl_3$): δ_H 10.36 (d, J = 7.5 Hz, 1H, N*H*), 8.46 (d, J = 2.0 Hz, 1H, C(8)*H*), 7.40-7.27 (m, 5H, C(17)*H*, C(18)*H* & C(19)*H*), 7.23 (d, J = 9.0 Hz, 1H, C(5)*H*), 6.54 (dd, J = 9.0, 2.0 Hz, 1H, C(6)*H*), 6.26 (d, J = 1.0 Hz, 1H, C(2)*H*), 5.32 (br s, 1H, C(15)*H*), 4.56 (t, J = 7.5 Hz, 1H, C(14)*H*), 3.27 (s, 3H, C(10)H_3), 3.16 (dd, J = 18.0, 7.5 Hz, 1H, C(13)H_a), 2.70 (d, J = 18.0 Hz, 1H, C(13)H_b), 2.25 (d, J = 0.5 Hz, 3H, C(11)H_3); ^{13}C-NMR ($CDCl_3$): δ_C 173.0 (*C*(12)), 162.5 (*C*(1)), 157.9 (q, J = 38.1 Hz, *C*(20)), 146.5 (*C*(4)), 140.2 (*C*(7)), 139.6 (*C*(9)), 136.8 (*C*(16)), 129.5 (*C*(18)), 128.7 (*C*(19)), 125.4 (*C*(17)), 125.0 (*C*(5)), 118.7 (*C*(2)), 117.3 (*C*(3)), 116.0 (q, J = 287.7 Hz, *C*(21)), 112.7 (*C*(6)), 104.2 (*C*(8)), 69.6 (*C*(15)), 51.7 (*C*(14)), 37.3 (*C*(13)), 29.3 (*C*(10)), 18.7 (*C*(11)); IR ν_{max} 3216, 3062, 2924, 1705, 1643, 1373, 1210, 1181, 1153, 731; LR-ESI-MS: $C_{23}H_{21}F_3N_3O_3$ $[M+H]^+$ *m/z* found 444.2 calcd 444.1; HR-ESI-MS: $C_{23}H_{21}F_3N_3O_3$ $[M+H]^+$ *m/z* found 444.15295 calcd 444.15271 error = 0.55 ppm.

***N*-[1-(1,4-Dimethyl-2-oxo-1,2-dihydroquinolin-7-yl)-5-oxo-2-phenyl-pyrrolidin-3-yl]methanesulfonamide (355)**

Compound **331** (20 mg, 0.058 mmol) was dissolved in CH_2Cl_2 (0.58 mL), methanesulfonyl chloride (13.4 μL, 0.17 mmol) and NEt_3 (24 μL, 0.17 mmol) were added and the reaction mixture was stirred at rt for 16 h. H_2O (10 mL) was added and the organic phase was separated. The aqueous phase was extracted with CH_2Cl_2 (3 x 5 mL), the combined organic extracts were dried over Na_2SO_4, filtered and concentrated. Purification by FCC (1.25% MeOH/CH_2Cl_2) yielded **355** (20.7 mg, 84%) as a white powder.

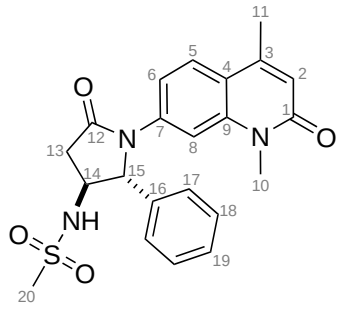

Mpt: 226.8-227.4 °C; ^{1}H-NMR ($CDCl_3$): δ_H 8.53-8.49 (m, 2H, C(8)*H* & N*H*), 7.35-7.24 (m, 5H, C(17)*H*, C(18)*H* & C(19)*H*), 7.13 (d, J = 9.0 Hz, 1H, C(5)*H*), 6.59 (d, J = 0.5 Hz, 1H, C(2)*H*), 6.55 (dd, J = 9.0, 2.0 Hz, 1H, C(6)*H*), 5.48 (br s, 1H, C(15)*H*), 4.05 (t, J = 8.5 Hz, 1H, C(14)*H*), 3.53 (s, 3H, C(10)H_3), 3.12 (dd, J = 18.0, 8.0 Hz, 1H, C(13)H_a), 3.10 (s, 3H, C(20)H_3), 2.67 (d, J = 18.0 Hz, 1H, C(13)H_b), 2.23 (d, J = 1.0 Hz, 3H, C(11)H_3); ^{13}C-NMR ($CDCl_3$): δ_C 173.1 (*C*(12)), 162.9 (*C*(1)), 146.5 (*C*(4)), 140.1 (*C*(7)), 139.6 (*C*(9)), 137.2 (*C*(16)), 129.4 (*C*(18)), 128.5 (*C*(19)), 125.5 (*C*(17)), 124.7 (*C*(5)), 118.8 (*C*(2)), 117.2 (*C*(3)), 112.9 (*C*(6)), 104.3 (*C*(8)), 71.6 (*C*(15)), 54.6 (*C*(14)), 42.1 (*C*(20)), 38.1 (*C*(13)), 29.7 (*C*(10)), 18.6 (*C*(11)); IR ν_{max} 3063, 3029, 2933, 1664, 1556, 753, 702; LR-ESI-MS: $C_{22}H_{24}N_3O_4S$ $[M+H]^+$ *m/z* found 426.1 calcd 426.2; HR-ESI-MS: $C_{22}H_{24}N_3O_4S$ $[M+H]^+$ *m/z* found 426.1482 calcd 426.1480 error = 0.45 ppm.

_N_-[1-(1,4-Dimethyl-2-oxo-1,2-dihydroquinolin-7-yl)-5-oxo-2-phenyl-pyrrolidin-3-yl]-1,1,1-trifluoromethanesulfonamide (356)

Compound **331** (20 mg, 0.058 mmol) was dissolved in CH_2Cl_2 (0.58 mL), trifluoromethanesulfonyl chloride (18 μL, 0.17 mmol) and NEt_3 (24 μL, 0.17 mmol) were added and the reaction mixture was stirred at rt for 16 h. H_2O (10 mL) was added and the organic phase was separated. The aqueous phase was extracted with CH_2Cl_2 (3 x 5 mL), the combined organic extracts were dried over Na_2SO_4, filtered and concentrated. Purification by FCC (80% EtOAc/hexane) yielded **356** (3.0 mg, 11%) as an opaque oil.

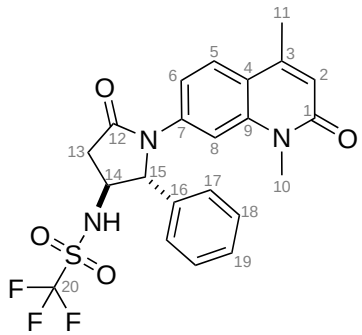

^{1}H-NMR ($CDCl_3$): δ_H 8.66 (br s, 1H, C(8)*H*), 7.38-7.30 (m, 3H, C(17)*H* & C(19)*H*), 7.23-7.18 (m, 3H, C(5)*H* & C(18)*H*), 6.50 (d, J = 1.0 Hz, 1H, C(2)*H*), 6.44 (d, J = 9.0 Hz, 1H, C(6)*H*), 5.37 (br s, 1H, C(15)*H*), 4.20 (d, J = 7.5 Hz, 1H, C(14)*H*), 3.43 (s, 3H, C(10)H_3), 3.14 (dd, J = 18.0, 7.5 Hz, 1H, C(13)H_a), 2.76 (d, J = 18.0 Hz, 1H, C(13)H_b), 2.29 (d, J = 0.5 Hz, 3H, C(11)H_3); ^{13}C-NMR ($CDCl_3$): δ_C 172.6 (*C*(12)), 163.1 (*C*(1)), 147.2 (*C*(4)), 140.2 (*C*(7)), 139.5 (*C*(9)), 136.3 (*C*(16)), 129.6 (*C*(18)), 128.9 (*C*(19)), 125.3 (*C*(17)), 124.9 (*C*(5)), 119.9 (d, J = 320.4 Hz, *C*(20)), 118.2 (*C*(2)), 117.2 (*C*(3)), 112.6 (*C*(6)), 104.0 (*C*(8)), 71.5 (*C*(15)), 55.9 (*C*(14)), 38.4 (*C*(13)), 29.8 (*C*(10)), 18.7 (*C*(11)); IR ν_{max} 3033, 2921, 2360, 2342, 1712, 1641, 1577, 1377, 1193; LR-ESI-MS: $C_{22}H_{21}F_3N_3O_4S$ $[M+H]^+$ *m/z* found 480.1 calcd 480.1; $C_{22}H_{20}F_3N_3O_4SNa$ $[M+Na]^+$ *m/z* found 502.1 calcd 502.1; HR-ESI-MS: $C_{22}H_{21}F_3N_3O_4S$ $[M+H]^+$ *m/z* found 480.11994 calcd 480.11963 error = 0.64 ppm.

Ethyl (1-(1,4-dimethyl-2-oxo-1,2-dihydroquinolin-7-yl)-5-oxo-2-phenyl-pyrrolidin-3-yl)carbamate (357)

Compound **331** (11 mg, 0.032 mmol) was dissolved in CH_2Cl_2 (1.0 mL), ethylchloroformate (3 μL, 0.035 mmol) and K_2CO_3 (9.0 mg, 0.064 mmol) were added and the reaction mixture was stirred at rt for 16 h. H_2O (10 mL) was added and the organic phase was separated. The aqueous phase was extracted with CH_2Cl_2 (3 x 5 mL), the combined organic extracts were dried over Na_2SO_4, filtered and concentrated. Purification by FCC (1% MeOH/CH_2Cl_2) yielded **357**

(1.6 mg, 12%) as a colourless oil.

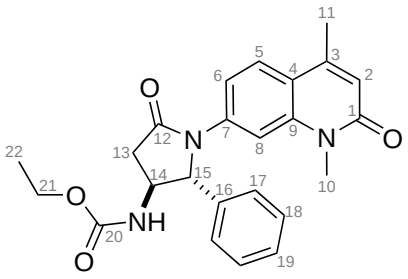

^{1}H-NMR ($CDCl_3$): δ_H 8.09 (br s, 1H, C(8)H), 7.47-7.28 (m, 6H, C(5)H, C(17)H, C(18)H & C(19)H), 7.05 (dd, J = 9.0, 2.0 Hz, 1H, C(6)H), 6.45 (d, J = 1.0 Hz, 1H, C(2)H), 6.06 (br s, 1H, NH), 5.37 (br s, 1H, C(15)H), 4.28-4.17 (m, 3H, C(14)H & C(21)H_2), 3.50 (s, 3H, C(10)H_3), 3.12 (dd, J = 18.0, 7.5 Hz, 1H, C(13)H_a), 2.52 (d, J = 17.5 Hz, 1H, C(13)H_b), 2.33 (d, J = 1.0 Hz, 3H, C(11)H_3), 1.30 (t, J = 7.0 Hz, 3H, C(22)H_3); ^{13}C-NMR ($CDCl_3$): δ_C 175.7 (C(12)), 162.3 (C(1)), 154.7 (C(20)), 145.8 (C(4)), 140.3 (C(7)), 140.1 (C(9)), 137.4 (C(16)), 129.3 (C(18)), 128.4 (C(19)), 125.7 (C(17)), 125.4 (C(5)), 119.9 (C(2)), 117.8 (C(3)), 113.5 (C(6)), 105.5 (C(8)), 70.8 (C(15)), 61.3 (C(21)), 53.4 (C(14)), 37.3 (C(13)), 29.2 (C(10)), 18.7 (C(11)), 14.6 (C(22)); IR ν_{max} 3282, 2978, 2360, 2343, 1706, 1653, 1594, 1375, 1253; LR-ESI-MS: $C_{24}H_{26}N_3O_4$ $[M+H]^+$ m/z found 420.2 calcd 420.2; $C_{24}H_{25}N_3O_4Na$ $[M+Na]^+$ m/z found 442.2 calcd 442.2; HR-ESI-MS: $C_{24}H_{25}N_3O_4Na$ $[M+Na]^+$ m/z found 442.17373 calcd 442.17358 error = 0.32 ppm.

7-[3-Amino-2-(4-chlorophenyl)-5-oxopyrrolidin-1-yl]-1,4-dimethyl-quinolin-2(1*H*)-one (358)

Compound **332** (288 mg, 0.64 mmol) was dissolved in HCl (4.3 mL, 4M in 1,4-dioxane) and the reaction mixture was stirred at rt for 16 h. The reaction mixture was concentrated then co-evaporated with EtOAc (4 x 10 mL). HCl (20 mL, 1M in H_2O) was added and the aqueous phase was washed with $CHCl_3$ (3 x 20 mL). The aqueous phase was basified with Na_2CO_3 (sat. aq. soln) and extracted with $CHCl_3$ (3 x 20 mL). The combined organic extracts were dried over Na_2SO_4, filtered and concentrated to yield **358** (185 mg, 85%) as a grey solid.

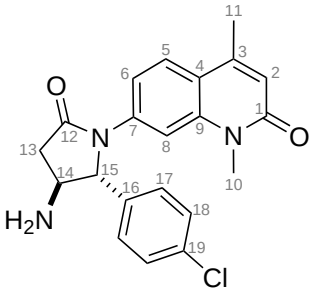

Mpt: 187.9-188.6 °C; ^{1}H-NMR ($CDCl_3$): δ_H 7.75 (d, J = 2.0 Hz, 1H, C(8)H), 7.53 (d, J = 9.0 Hz, 1H, C(5)H), 7.33 (d, J = 8.5 Hz, 2H, C(18)H), 7.21 (d, J = 8.5 Hz, 2H, C(17)H), 7.10 (dd, J = 8.5, 2.0 Hz, 1H, C(6)H), 6.50 (d, J = 1.0 Hz, 1H, C(2)H), 4.94 (d, J = 4.0 Hz, 1H, C(15)H), 3.60-3.53 (m, 1H, C(14)H), 3.59 (s, 3H, C(10)H_3), 3.04 (dd, J = 17.0, 7.0 Hz, 1H, C(13)H_a), 2.48 (dd, J = 17.0, 5.5 Hz, 1H, C(13)H_b), 2.37 (d, J = 1.0 Hz, 3H, C(11)H_3); ^{13}C-NMR ($CDCl_3$): δ_C 173.1 (C(12)), 162.3 (C(1)), 145.8 (C(4)), 140.2 (C(7)), 139.7 (C(9)), 136.9 (C(16)), 134.3 (C(19)), 129.5 (C(18)), 127.3 (C(17)), 125.5 (C(5)), 120.3 (C(2)), 118.3 (C(3)), 114.9 (C(6)), 107.3 (C(8)), 72.6 (C(15)), 54.8 (C(14)), 40.8 (C(13)), 29.2 (C(10)), 18.7 (C(11)); IR ν_{max} 3360, 2920, 1698, 1646, 1591, 1392, 731; LR-ESI-MS: $C_{21}H_{21}ClN_3O_2$ $[M+H]^+$ m/z found 382.1 calcd 382.1, $C_{21}H_{20}ClN_3O_2Na$ $[M+Na]^+$ m/z found 404.1 calcd 404.1; HR-ESI-MS: $C_{21}H_{21}ClN_3O_2$ $[M+H]^+$ m/z found 382.1317 calcd 382.1316 error = 0.23 ppm.

***N*-[2-(4-Chlorophenyl)-1-(1,4-dimethyl-2-oxo-1,2-dihydroquinolin-7-yl)-5-oxo-pyrrolidin-3-yl]-2,2,2-trifluoroacetamide (359)**

Compound **358** (20 mg, 0.052 mmol) was dissolved in CH_2Cl_2 (0.52 mL), trifluoroacetic anhydride (21.8 μL, 0.16 mmol) and NEt_3 (23 μL, 0.16 mmol) were added and the reaction mixture was stirred at rt for 16 h. H_2O (5 mL) was added and the organic phase was separated.

The aqueous phase was extracted with CH_2Cl_2 (3 x 5 mL), the combined organic extracts were dried over Na_2SO_4, filtered and concentrated. Purification by FCC (60% EtOAc/PE) yielded **359** (18 mg, 72%) as a white powder.

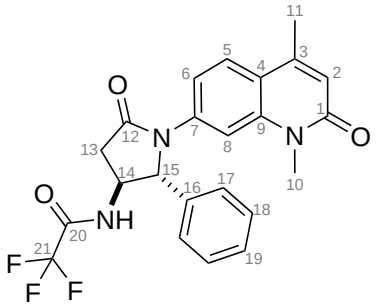

Mpt: 244.1-244.9 °C; ^{1}H-NMR ($(CD_3)_2SO$): δ_H 10.24 (d, J = 5.0 Hz, 1H, NH), 7.76 (d, J = 2.0 Hz, 1H, C(8)H), 7.66 (d, J = 9.0 Hz, 1H, C(5)H), 7.44-7.39 (m, 4H, C(17)H & C(18)H), 7.37 (dd, J = 9.0, 2.0 Hz, 1H, C(6)H), 6.42 (s, 1H, C(2)H), 5.57 (d, J = 2.5 Hz, 1H, C(15)H), 4.32 (br s, 1H, C(14)H), 3.46 (s, 3H, C(10)H_3), 3.33 (d, J = 1.0 Hz, 3H, C(11)H_3), 3.20 (dd, J = 17.5, 8.5 Hz, 1H, C(13)H_a), 2.68 (dd, J = 18.0, 3.5 Hz, 1H, C(13)H_b); ^{13}C-NMR ($(CD_3)_2SO$): δ_C 172.1 (C(12)), 160.9 (C(1)), 156.9 (C(20)), 146.1 (C(4)), 139.7 (C(7)), 139.7 (C(9)), 137.6 (C(16)), 132.6 (C(19)), 128.9 (C(18)), 128.3 (C(17)), 125.8 (C(5)), 119.4 (C(21)), 119.3 (C(2)), 117.2 (C(3)), 115.1 (C(6)), 106.8 (C(8)), 67.9 (C(15)), 51.2 (C(14)), 35.9 (C(13)), 28.8 (C(10)), 18.2 (C(11)); IR ν_{max} 3212, 3058, 2361, 1704, 1649, 1556, 1215, 1181, 1151; LR-ESI-MS: $C_{23}H_{20}ClF_3N_3O_3$ $[M+H]^+$ *m/z* found 478.1 calcd 478.1, $C_{23}H_{19}ClF_3N_3O_3Na$ $[M+Na]^+$ *m/z* found 500.1 calcd 500.1; HR-ESI-MS: $C_{23}H_{20}ClF_3N_3O_3$ $[M+H]^+$ *m/z* found 478.11398 calcd 478.11389 error = 0.19 ppm.

***N*-[2-(4-Chlorophenyl)-1-(1,4-dimethyl-2-oxo-1,2-dihydroquinolin-7-yl)-5-oxo-pyrrolidin-3-yl]methanesulfonamide (361)**

Compound **358** (20 mg, 0.052 mmol) was dissolved in CH_2Cl_2 (0.52 mL), methanesulfonyl chloride (13 μL, 0.16 mmol) and NEt_3 (23 μL, 0.16 mmol) were added and the reaction mixture was stirred at rt for 16 h. H_2O (5 mL) was added and the organic phase was separated. The aqueous phase was extracted with CH_2Cl_2 (3 x 5 mL), the combined organic extracts were dried over Na_2SO_4, filtered and concentrated. Purification by FCC (1.25% MeOH/CH_2Cl_2) yielded **361** (22 mg, 91%) as an opaque oil.

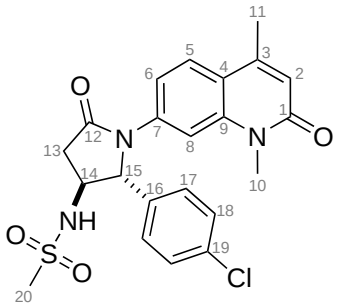

^{1}H-NMR ($CDCl_3$): δ_H 8.63 (d, J = 9.5 Hz, 1H, NH), 8.55 (d, J = 2.0 Hz, 1H, C(8)H), 7.28 (d, J = 8.5 Hz, 2H, C(18)H), 7.21 (d, J = 8.5 Hz, 2H, C(17)H), 7.12 (d, J = 9.0 Hz, 1H, C(5)H), 6.60 (d, J = 1.0 Hz, 1H, C(2)H), 6.46 (dd, J = 9.0, 2.0 Hz, 1H, C(6)H), 5.47 (br s, 1H, C(15)H), 4.01 (t, J = 8.5 Hz, 1H, C(14)H), 3.54 (s, 3H, C(10)H_3), 3.11 (s, 3H, C(20)H_3), 3.08 (dd, J = 17.5, 8.0 Hz, 1H, C(13)H_a), 2.67 (d, J = 18.0 Hz, 1H, C(13)H_b), 2.23 (d, J = 1.0 Hz, 3H, C(11)H_3); ^{13}C-NMR ($CDCl_3$): δ_C 173.0 (C(12)), 162.9 (C(1)), 146.5 (C(4)), 139.9 (C(7)), 139.6 (C(9)), 135.8 (C(16)), 134.4 (C(19)), 129.5 (C(18)), 127.0 (C(17)), 124.7 (C(5)), 118.9 (C(2)), 117.3 (C(3)), 112.6 (C(6)), 104.2 (C(8)), 71.1 (C(15)), 54.4 (C(14)), 42.1 (C(20)), 37.8 (C(13)), 29.7 (C(10)), 18.6 (C(11)); IR ν_{max} 3126, 2893, 1704, 1641, 1577, 1322, 1147, 727; LR-ESI-MS: $C_{22}H_{23}ClN_3O_4S$ $[M+H]^+$ *m/z* found 460.1 calcd 460.1, $C_{22}H_{22}ClN_3O_4SNa$ $[M+Na]^+$ *m/z* found 482.0 calcd 482.0; HR-ESI-MS: $C_{22}H_{23}ClN_3O_4S$ $[M+H]^+$ *m/z* found 460.10923 calcd 460.10915 error = 0.15 ppm.

2-Methylpropyl [2-(4-chlorophenyl)-1-(1,4-dimethyl-2-oxo-1,2-dihydro-quinolin-7-

yl)-5-oxopyrrolidin-3-yl]carbamate (**360**)

Compound **358** (20 mg, 0.052 mmol) was dissolved in CH_2Cl_2 (0.52 mL), isobutylchloroformate (20.4 μL, 0.16 mmol) and NEt_3 (23 μL, 0.16 mmol) were added and the reaction mixture was stirred at rt for 16 h. H_2O (5 mL) was added and the organic phase was separated. The aqueous phase was extracted with CH_2Cl_2 (3 x 5 mL), the combined organic extracts were dried over Na_2SO_4, filtered and concentrated. Purification by FCC (0.75% MeOH/CH_2Cl_2) yielded **360** (22 mg, 87%) as a white powder.

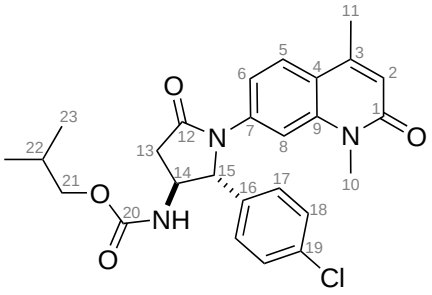

Mpt: 127.4-128.0 °C; ^{1}H-NMR ($CDCl_3$): δ_H 8.15 (s, 1H, C(8)H), 7.35-7.21 (m, 5H, C(5)H, C(17)H & C(18)H), 6.80 (dd, J = 9.0, 1.5 Hz, 1H, C(6)H), 6.66 (d, J = 6.0 Hz, 1H, NH), 6.37 (d, J = 1.0 Hz, 1H, C(2)H), 5.29 (br s, 1H, C(15)H), 4.12 (t, J = 7.0 Hz, 1H, C(14)H), 3.93 (dd, J = 10.5, 6.5 Hz, 1H, C(21)H_a), 3.85 (dd, J = 10.0, 6.5 Hz, 1H, C(21)H_b), 3.42 (s, 3H, C(10)H_3), 3.01 (dd, J = 18.0, 7.5 Hz, 1H, C(13)H_a), 2.53 (d, J = 18.0 Hz, 1H, C(13)H_b), 2.24 (d, J = 0.5 Hz, 3H, C(11)H_3), 1.91 (tspt, J = 7.0, 6.5 Hz, 1H, C(22)H), 0.90 (d, J = 6.5 Hz, 6H, C(23)H_3); ^{13}C-NMR ($CDCl_3$): δ_C 173.1 (*C*(12)), 162.3 (*C*(1)), 156.7 (*C*(20)), 145.8 (*C*(4)), 140.1 (*C*(7)), 140.1 (*C*(9)), 136.0 (*C*(16)), 134.2 (*C*(19)), 129.5 (*C*(18)), 127.1 (*C*(17)), 125.3 (*C*(5)), 119.7 (*C*(2)), 117.7 (*C*(3)), 113.1 (*C*(6)), 105.2 (*C*(8)), 71.5 (*C*(21)), 70.2 (*C*(15)), 53.2 (*C*(14)), 37.1 (*C*(13)), 29.2 (*C*(10)), 28.0 (*C*(22)), 19.0 (*C*(23)), 18.6 (*C*(11)); IR ν_{max} 3270, 2961, 1699, 1645, 1592, 1373, 1249, 729; LR-ESI-MS: $C_{26}H_{29}ClN_3O_4$ $[M+H]^+$ *m/z* found 482.2 calcd 482.2, $C_{26}H_{28}ClN_3O_4Na$ $[M+Na]^+$ *m/z* found 504.1 calcd 504.2; HR-ESI-MS: $C_{26}H_{29}ClN_3O_4$ $[M+H]^+$ *m/z* found 482.18411 calcd 482.18404 error = 0.12 ppm.

***N*-[2-(4-Chlorophenyl)-1-(1,4-dimethyl-2-oxo-1,2-dihydroquinolin-7-yl)-5-oxo-pyrrolidin-3-yl]-2-methylpropane-1-sulfonamide** (**362**)

Compound **358** (20 mg, 0.052 mmol) was dissolved in CH_2Cl_2 (0.52 mL), isobutanesulfonyl chloride (20.5 μL, 0.16 mmol) and NEt_3 (23 μL, 0.16 mmol) were added and the reaction mixture was stirred at rt for 16 h. H_2O (5 mL) was added and the organic phase was separated. The aqueous phase was extracted with CH_2Cl_2 (3 x 5 mL), the combined organic extracts were dried over Na_2SO_4, filtered and concentrated. Purification by FCC (1% MeOH/CH_2Cl_2) yielded **362** (13 mg, 49%) as an opaque oil.

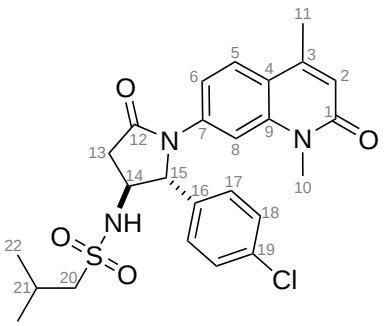

^{1}H-NMR ($CDCl_3$): δ_H 8.61 (d, J = 2.0 Hz, 1H, C(8)H), 8.44 (d, J = 9.5 Hz, 1H, NH), 7.28 (d, J = 8.5 Hz, 2H, C(18)H), 7.22 (d, J = 9.0 Hz, 2H, C(17)H), 7.12 (d, J = 9.0 Hz, 1H, C(5)H), 6.67 (d, J = 1.0 Hz, 1H, C(2)H), 6.44 (dd, J = 9.0, 2.0 Hz, 1H, C(6)H), 5.47 (s, 1H, C(15)H), 3.99 (t, J = 8.5 Hz, 1H, C(14)H), 3.59 (s, 3H, C(10)H_3), 3.08 (dd, J = 18.0, 8.0 Hz, 1H, C(13)H_a), 3.05 (d, J = 7.0 Hz, 2H, C(20)H_2), 2.65 (d, J = 18.0 Hz, 1H, C(13)H_b), 2.36 (tspt, J = 7.0, 6.5 Hz, 1H, C(21)H), 2.24 (d, J = 0.5 Hz, 3H, C(11)H_3), 1.16 (d, J = 6.5 Hz, 6H, C(22)H_3); ^{13}C-NMR ($CDCl_3$): δ_C 173.0 (*C*(12)), 163.0 (*C*(1)), 146.5 (*C*(4)), 139.9 (*C*(7)), 139.7 (*C*(9)), 135.9 (*C*(16)), 134.3 (*C*(19)), 129.5 (*C*(18)), 127.1 (*C*(17)), 124.7 (*C*(5)), 119.0 (*C*(2)), 117.3 (*C*(3)), 112.6 (*C*(6)), 104.2 (*C*(8)), 71.5 (*C*(15)), 62.3 (*C*(20)), 54.4 (*C*(14)), 37.8 (*C*(13)), 29.8

(*C*(10)), 25.0 (*C*(21)), 22.6 (*C*(22)), 18.6 (*C*(11)); IR ν_{max} 3129, 2963, 2361, 1707, 1644, 1579, 1374, 731; LR-ESI-MS: $C_{25}H_{29}ClN_3O_4S$ $[M+H]^+$ *m/z* found 502.2 calcd 502.2; HR-ESI-MS: $C_{25}H_{29}ClN_3O_4S$ $[M+H]^+$ *m/z* found 502.15618 calcd 502.15621 error = 0.06 ppm.

***tert*-Butyl methyl(1-(1,4-dimethyl-2-oxo-1,2-dihydroquinolin-7-yl)-5-oxo-2-phenylpyrrolidin-3-yl)carbamate (363)**

Compound **330** (35.2 mg, 0.079 mmol) was dissolved in DMF (0.4 mL) and the solution was cooled to 0 °C. NaH (4.4 mg, 0.11 mmol, 60% dispersion in mineral oil) was added and the reaction mixture was stirred at 0 °C for 30 min. MeI (6.8 μL, 0.11 mmol) was added and the reaction mixture was stirred at rt for 2 h. H_2O (20 mL) was added and the aqueous phase was extracted with Et_2O (3 x 20 mL). The combined organic extracts were washed with brine (2 x 60 mL), dried over Na_2SO_4, filtered and concentrated. Purification by FCC (40% EtOAc/PE) and preparative TLC (EtOAc) yielded **363** (13.4 mg, 37%) as an opaque oil.

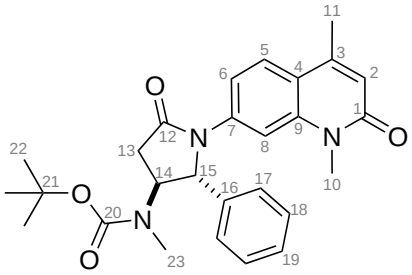

^{1}H-NMR ($CDCl_3$): δ_H 7.75 (br s, 1H, C(8)*H*), 7.54 (d, *J* = 9.0 Hz, 1H, C(5)*H*), 7.35 (t, *J* = 7.0 Hz, 2H, C(18)*H*), 7.32-7.23 (m, 3H, C(17)*H* & C(19)*H*), 7.23 (dd, *J* = 9.0, 2.0 Hz, 1H, C(6)*H*), 6.50 (s, 1H, C(2)*H*), 5.20 (d, *J* = 2.5 Hz, 1H, C(15)*H*), 4.64 (br s, 1H, C(14)*H*), 3.56 (s, 3H, C(10)H_3), 3.05 (dd, *J* = 18.0, 9.0 Hz, 1H, C(13)H_a), 2.94 (br s, 3H, C(23)H_3), 2.80 (dd, *J* = 18.0, 5.0 Hz, 1H, C(13)H_b), 2.37 (s, 3H, C(11)H_3), 1.39 (s, 9H, C(22)H_3); ^{13}C-NMR ($CDCl_3$): δ_C 170.0 (*C*(12)), 162.3 (*C*(1)), 153.4 (*C*(20)), 145.8 (*C*(4)), 140.2 (*C*(7)), 140.2 (*C*(9)), 133.1 (*C*(16)), 129.3 (*C*(18)), 128.4 (*C*(19)), 125.7 (*C*(17)), 125.5 (*C*(5)), 120.3 (*C*(2)), 118.3 (*C*(3)), 114.9 (*C*(6)), 107.3 (*C*(8)), 80.8 (*C*(21)), 69.3 (*C*(15)), 58.0 (*C*(14)), 35.0 (*C*(13)), 29.7 (*C*(23)), 29.2 (*C*(10)), 28.3 (*C*(22)), 18.7 (*C*(11)); IR ν_{max} 2922, 2851, 2361, 1696, 1658, 1597, 1368; LR-ESI-MS: $C_{27}H_{32}N_3O_4$ $[M+H]^+$ *m/z* found 462.2 calcd 462.3; $C_{27}H_{31}N_3O_4Na$ $[M+Na]^+$ *m/z* found 484.2 calcd 484.2; HR-ESI-MS: $C_{27}H_{32}N_3O_4$ $[M+H]^+$ *m/z* found 462.2387 calcd 462.2388 error = 0.21 ppm.

***tert*-Butyl (5-thioxo-2-phenylpyrrolidin-3-yl)carbamate (364)**

Under inert conditions, **353** (32 mg, 0.12 mmol) was dissolved in THF (0.23 mL), Lawesson's reagent (23.4 mg, 0.058 mmol) was added portionwise over 15 min and the reaction mixture was stirred at rt for 4 h. The reaction mixture was concentrated and purification by FCC (5% EtOAc/CH_2Cl_2) yielded **364** (30 mg, 88%) as a white solid.

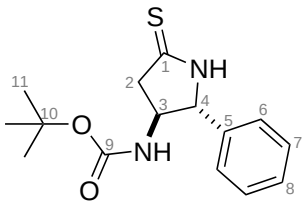

Mpt: 168.0-168.7 °C; ^{1}H-NMR ($CDCl_3$): δ_H 8.51 (br s, 1H, N*H*), 7.40 (t, *J* = 7.5 Hz, 2H, C(7)*H*), 7.36-7.31 (m, 3H, C(6)*H* & C(8)*H*), 5.08 (br s, 1H, C(4)*H*), 4.97 (br s, 1H, N*H*), 4.23-4.16 (m, 1H, C(3)*H*), 3.27 (dd, *J* = 18.0, 6.0 Hz, 1H, C(2)H_a), 2.79 (d, *J* = 18.0 Hz, 1H, C(2)H_b), 1.46 (s, 9H, C(11)H_3); ^{13}C-NMR ($CDCl_3$): δ_C 203.9 (*C*(1)), 155.0 (*C*(9)), 137.6 (*C*(5)), 129.1 (*C*(7)), 128.5 (*C*(8)), 125.8 (*C*(6)), 80.4 (*C*(10)), 72.0 (*C*(4)), 58.1 (*C*(3)), 47.5 (*C*(2)), 28.3 (*C*(11)); IR ν_{max} 3246, 2979, 2360, 1688, 1509, 1165, 732; LR-ESI-MS: $C_{15}H_{20}N_2O_2SNa$ $[M+Na]^+$ *m/z* found 315.1 calcd 315.1; HR-ESI-MS: $C_{15}H_{20}N_2O_2SNa$ $[M+Na]^+$ *m/z* found 315.11377 calcd 315.11384 error = 0.19 ppm.

7-Bromo-1,4-dimethylquinoline-2(1*H*)-thione (**365**)

Under inert conditions, **218** (100 mg, 0.40 mmol) was dissolved in toluene (4 mL), Lawesson's reagent (96 mg, 0.24 mmol) was added and the reaction mixture was stirred at reflux for 2 d. The reaction mixture was concentrated and purification by FCC (CH_2Cl_2) yielded **365** (88 mg, 83%) as a yellow powder.

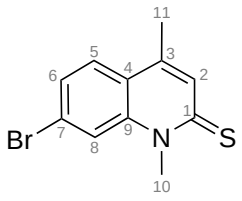

Mpt: 184.2-185.3 °C; ^{1}H-NMR ($CDCl_3$): δ_H 7.70 (d, J = 1.5 Hz, 1H, C(8)H), 7.59-7.55 (m, 2H, C(2)H & C(5)H), 7.44 (dd, J = 8.5, 2.0 Hz, 1H, C(6)H), 4.23 (s, 3H, C(10)H_3), 2.38 (s, 3H, C(11)H_3); ^{13}C-NMR ($CDCl_3$): δ_C 184.5 (C(1)), 141.1 (C(9)), 138.8 (C(4)), 133.6 (C(2)), 127.0 (C(5)), 126.5 (C(6)), 125.4 (C(7)), 123.5 (C(3)), 118.8 (C(8)), 37.7 (C(10)), 18.2 (C(11)); IR ν_{max} 3044, 2928, 1609, 1591, 1541, 1338, 1317, 1157, 1106, 1055; LR-ESI-MS: $C_{11}H_{11}BrNS$ $[M+H]^+$ *m/z* found 268.0 calcd 268.0, $C_{11}H_{10}BrNSNa$ $[M+Na]^+$ *m/z* found 290.0 calcd 290.0; HR-ESI-MS: $C_{11}H_{11}BrNS$ $[M+H]^+$ *m/z* found 267.9790 calcd 267.9791 error = 0.5 ppm.

***tert*-Butyl (1-(1,4-dimethyl-2-thioxo-1,2-dihydroquinolin-7-yl)-5-oxo-2-phenylpyrrolidin-3-yl)carbamate** (**366**)

In a pressure tube under inert conditions, **353** (14.1 mg, 0.051 mmol), **365** (21 mg, 0.077 mmol) and K_3PO_4 (22 mg, 0.10 mmol) were combined. 1,4-dioxane (0.51 mL) was added and the solution was degassed. (+/-)-*trans*-1,2-diaminocyclohexane (6.1 μL, 0.051 mmol) and CuI (9.2 mg, 0.051 mmol) were added, the tube was sealed and the reaction mixture was stirred at 97 °C for 42 h. The reaction mixture was passed through a plug of Celite and the Celite was washed with CH_2Cl_2 (30 mL). The combined filtrate was concentrated and purification by FCC (10% isopropanol/PE then separately 0.25% MeOH/CH_2Cl_2) yielded **366** (9.0 mg, 38%) as a yellow oil.

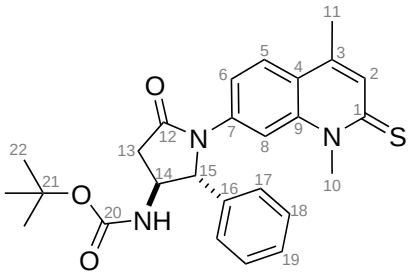

^{1}H-NMR ($CDCl_3$): δ_H 8.33 (br s, 1H, C(8)H), 7.58 (d, J = 9.0 Hz, 1H, C(5)H), 7.50 (s, 1H, C(2)H), 7.42-7.31 (m, 5H, C(17)H, C(18)H & C(19)H), 7.23 (dd, J = 9.0, 1.5 Hz, 1H, C(6)H), 5.37 (br s, 1H, NH), 5.34 (d, J = 6.0 Hz, 1H, C(15)H), 4.17 (t, J = 6.5 Hz, 1H, C(14)H), 4.13 (s, 3H, C(10)H_3), 3.13 (dd, J = 17.5, 7.5 Hz, 1H, C(13)H_a), 2.49 (d, J = 17.5 Hz, 1H, C(13)H_b), 2.34 (s, 3H, C(11)H_3), 1.49 (s, 9H, C(22)H_3); ^{13}C-NMR ($CDCl_3$): δ_C 184.2 (C(1)), 173.2 (C(12)), 155.3 (C(20)), 140.9 (C(9)), 140.7 (C(7)), 139.1 (C(4)), 137.0 (C(16)), 132.5 (C(2)), 129.4 (C(18)), 128.5 (C(19)), 125.8 (C(5)), 125.7 (C(17)), 121.3 (C(3)), 115.7 (C(6)), 107.0 (C(8)), 80.6 (C(21)), 70.9 (C(15)), 53.3 (C(14)), 37.7 (C(10)), 37.3 (C(13)), 28.4 (C(22)), 18.1 (C(11)); IR ν_{max} 3322, 2977, 2357, 1702, 1614, 1164, 702; LR-ESI-MS: $C_{26}H_{30}N_3O_3S$ $[M+H]^+$ *m/z* found 464.2 calcd 464.1, $C_{26}H_{29}N_3O_3SNa$ $[M+Na]^+$ *m/z* found 486.2 calcd 486.2; HR-ESI-MS: $C_{26}H_{29}N_3O_3SNa$ $[M+Na]^+$ *m/z* found 486.18218 calcd 486.18195 error = 0.49 ppm.

***tert*-Butyl {5-[(1,4-dimethyl-2-oxo-1,2-dihydroquinolin-7-yl)sulfanyl]-2-phenyl-3,4-dihydro-2*H*-pyrrol-3-yl}carbamate** (**368**)

In a pressure tube under inert conditions, **364** (15 mg, 0.051 mmol), **218** (19.4 mg, 0.077 mmol)

and K_3PO_4 (22 mg, 0.10 mmol) were combined. 1,4-dioxane (0.51 mL) was added and the solution was degassed. (+/-)-*trans*-1,2-diaminocyclohexane (6.1 μL, 0.051 mmol) and CuI (9.7 mg, 0.051 mmol) were added, the tube was sealed and the reaction mixture was stirred at 97 °C for 42 h. The reaction mixture was passed through a plug of Celite and the Celite was washed with CH_2Cl_2 (30 mL). The combined filtrate was concentrated and purification by FCC (0.75% MeOH/CH_2Cl_2) yielded **368** (4.0 mg, 17%) as a colourless oil.

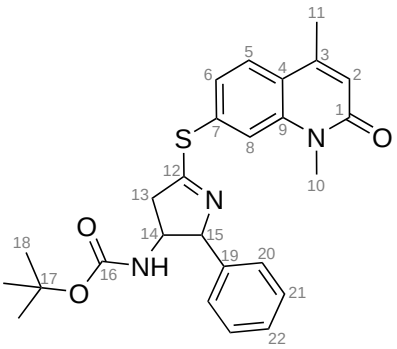

^{1}H-NMR ($CDCl_3$): δ_H 7.76 (d, J = 1.5 Hz, 1H, C(8)H), 7.71 (d, J = 8.5 Hz, 1H, C(5)H), 7.50 (dd, J = 8.5, 1.5 Hz, 1H, C(6)H), 7.34 (t, J = 7.5 Hz, 2H, C(21)H), 7.29-7.23 (m, 3H, C(20)H & C(22)H), 6.62 (d, J = 1.0 Hz, 1H, C(2)H), 5.07 (br s, 1H, C(15)HNH), 4.88 (br s, 1H, NH), 4.21 (br s, 1H, C(14)H), 3.68 (s, 3H, C(10)H_3), 3.15 (dd, J = 17.5, 8.0 Hz, 1H, C(13)H_a), 2.64 (dd, J = 17.5, 4.0 Hz, 1H, C(13)H_b), 2.45 (d, J = 1.0 Hz, 3H, C(11)H_3), 1.44 (s, 9H, C(18)H_3); ^{13}C-NMR ($CDCl_3$): δ_C 171.8 (C(12)), 161.9 (C(1)), 155.1 (C(16)), 145.9 (C(4)), 140.4 (C(7)), 140.1 (C(9)), 131.7 (C(19)), 128.5 (C(21)), 127.5 (C(22)), 127.1 (C(6)), 126.1 (C(20)), 125.8 (C(5)), 122.1 (C(2)), 121.8 (C(3)), 119.8 (C(8)), 82.0 (C(15)), 80.0 (C(17)), 57.9 (C(14)), 45.5 (C(13)), 29.3 (C(10)), 28.3 (C(18)), 18.9 (C(11)); IR ν_{max} 3629, 2981, 2906, 2253, 1772, 1700, 1647, 787; LR-ESI-MS: $C_{26}H_{30}N_3O_3S$ $[M+H]^+$ *m/z* found 464.2 calcd 464.2; HR-ESI-MS: $C_{26}H_{30}N_3O_3S$ $[M+H]^+$ *m/z* found 464.20024 calcd 464.20042 error = 0.37 ppm.

***tert*-Butyl (1-(1,4-dimethyl-2-thioxo-1,2-dihydroquinolin-7-yl)-5-thioxo-2-phenylpyrrolidin-3-yl)carbamate (369)**

Under inert conditions, **330** (19 mg, 0.040 mmol) was dissolved in toluene (0.8 mL), Lawesson's reagent (19.5 mg, 0.048 mmol) was added and the reaction mixture was stirred at reflux for 2 d. The reaction mixture was filtered hot and concentrated. Purification by FCC (0.5% MeOH/CH_2Cl_2) yielded **369** (3.8 mg, 19%) as a yellow solid.

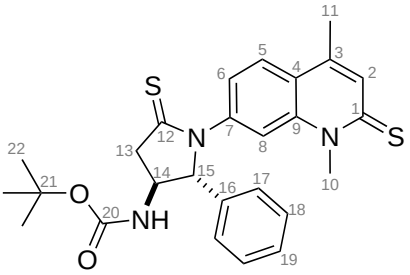

Mpt: 127.0-127.8 °C; ^{1}H-NMR ($CDCl_3$): δ_H 8.12 (br s, 1H, C(8)H), 7.70 (d, J = 9.0 Hz, 1H, C(5)H), 7.56 (d, J = 1.0 Hz, 1H, C(2)H), 7.43-7.32 (m, 6H, C(6)H, C(17)H, C(18)H & C(19)H), 5.52 (br s, 1H, NH), 5.08 (d, J = 5.0 Hz, 1H, C(15)H), 4.19 (br s, 1H, C(14)H), 4.14 (s, 3H, C(10)H_3), 3.67 (dd, J = 18.5, 7.0 Hz, 1H, C(13)H_a), 3.12 (dd, J = 18.5, 2.0 Hz, 1H, C(13)H_b), 2.37 (d, J = 1.0 Hz, 3H, C(11)H_3), 1.49 (s, 9H, C(22)H_3); ^{13}C-NMR ($CDCl_3$): δ_C 201.4 (C(12)), 184.5 (C(1)), 155.2 (C(20)), 141.4 (C(9)), 140.7 (C(7)), 138.6 (C(4)), 136.6 (C(16)), 133.9 (C(2)), 129.4 (C(18)), 128.9 (C(19)), 126.2 (C(5)), 125.9 (C(17)), 123.6 (C(3)), 120.2 (C(6)), 112.8 (C(8)), 80.7 (C(21)), 80.2 (C(15)), 55.5 (C(14)), 50.3 (C(13)), 37.8 (C(10)), 28.3 (C(22)), 18.1 (C(11)); IR ν_{max} 3257, 2975, 2928, 2360, 1711, 1614, 1159, 1057, 701; LR-ESI-MS: $C_{26}H_{30}N_3O_2S_2$ $[M+H]^+$ *m/z* found 480.2 calcd 480.1; HR-ESI-MS: $C_{26}H_{29}N_3O_2S_2Na$ $[M+Na]^+$ *m/z* found 502.1593 calcd 502.1595 error = 0.29 ppm.

***tert*-Butyl {5-[(1,4-dimethyl-2-thioxo-1,2-dihydroquinolin-7-yl)sulfanyl]-2-phenyl-**

3,4-dihydro-2*H*-pyrrol-3-yl}carbamate (**370**)

In a pressure tube under inert conditions, **364** (15 mg, 0.051 mmol), **365** (21 mg, 0.077 mmol) and K_3PO_4 (22 mg, 0.10 mmol) were combined. 1,4-dioxane (0.51 mL) was added and the solution was degassed. (+/-)-*trans*-1,2-diaminocyclohexane (6.1 μL, 0.051 mmol) and CuI (9.7 mg, 0.051 mmol) were added, the tube was sealed and the reaction mixture was stirred at 97 °C for 42 h. The reaction mixture was passed through a plug of Celite and the Celite was washed with CH_2Cl_2 (30 mL). The combined filtrate was concentrated and purification by FCC (5% isopropanol/PE) yielded **370** (2.4 mg, 10%) as a colourless oil.

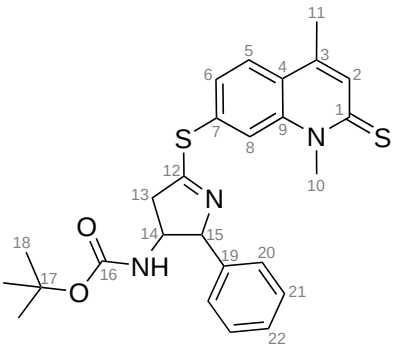

^{1}H-NMR ($CDCl_3$): δ_H 8.12 (br s, 1H, C(8)*H*), 7.70 (d, *J* = 9.0 Hz, 1H, C(5)*H*), 7.56 (d, *J* = 1.0 Hz, 1H, C(2)*H*), 7.41 (t, *J* = 7.5 Hz, 2H, C(21)*H*), 7.39-7.33 (m, 4H, C(6)*H*, C(20)*H* & C(22)*H*), 5.52 (br s, 1H, N*H*), 5.08 (d, *J* = 5.0 Hz, 1H, C(15)*H*), 4.22-4.17 (m, 1H, C(14)*H*), 4.14 (s, 3H, C(10)H_3), 3.67 (dd, *J* = 18.5, 7.0 Hz, 1H, C(13)H_a), 3.12 (dd, *J* = 18.5, 2.0 Hz, 1H, C(13)H_b), 2.37 (d, *J* = 1.0 Hz, 3H, C(11)H_3), 1.49 (s, 9H, C(18)H_3); ^{13}C-NMR ($CDCl_3$): δ_C 201.4 (*C*(12)), 184.5 (*C*(1)), 155.2 (*C*(16)), 141.4 (*C*(9)), 140.7 (*C*(7)), 138.6 (*C*(4)), 136.6 (*C*(19)), 133.9 (*C*(2)), 129.4 (*C*(21)), 128.9 (*C*(22)), 126.2 (*C*(5)), 125.9 (*C*(20)), 123.6 (*C*(3)), 120.2 (*C*(6)), 112.8 (*C*(8)), 80.7 (*C*(17)), 80.2 (*C*(15)), 55.5 (*C*(14)), 50.3 (*C*(13)), 37.8 (*C*(10)), 28.3 (*C*(18)), 18.1 (*C*(11)); IR ν_{max} 3398, 2978, 1696, 1610, 1164; LR-ESI-MS: $C_{26}H_{30}N_3O_2S_2$ $[M+H]^+$ *m/z* found 480.2 calcd 480.1; HR-ESI-MS: $C_{26}H_{29}N_3O_2S_2Na$ $[M+Na]^+$ *m/z* found 502.15934 calcd 502.15954 error = 0.41 ppm.

1,4-Dimethyl-7-(2-oxo-4-phenyl-1,3-oxazolidin-3-yl)quinolin-2(1*H*)-one(**373**)

In a pressure tube under inert conditions, **375** (50 mg, 0.31 mmol), **218** (116 mg, 0.46 mmol) and K_3PO_4 (130 mg, 0.61 mmol) were combined. 1,4-dioxane (3.1 mL) was added and the solution was degassed. (+/-)-*trans*-1,2-diaminocyclohexane (37 μL, 0.31 mmol) and CuI (58 mg, 0.31 mmol) were added, the tube was sealed and the reaction mixture was stirred at 97 °C for 42 h. The reaction mixture was passed through a plug of Celite and the Celite was washed with CH_2Cl_2 (50 mL). The combined filtrate was concentrated and purification by FCC (15% isopropanol/hexane) yielded **373** (88 mg, 86%) as an orange oil.

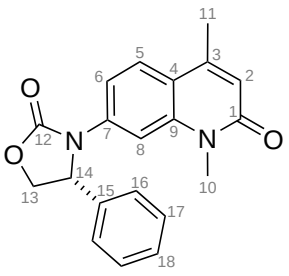

^{1}H-NMR ($CDCl_3$): δ_H 7.58-7.49 (m, 2H, C(5)*H* & C(8)*H*), 7.42-7.30 (m, 5H, C(16)*H*, C(17)*H* & C(18)*H*), 7.24 (dd, *J* = 9.0, 1.0 Hz, 1H, C(6)*H*), 6.45 (d, *J* = 6.0 Hz, 1H, C(2)*H*), 5.50 (dd, *J* = 9.0, 6.0 Hz, 1H, C(14)*H*), 4.85 (t, *J* = 9.0 Hz, 1H, C(13)H_a), 4.26 (dd, *J* = 9.0, 6.0 Hz, 1H, C(13)H_b), 3.51 (s, 3H, C(10)H_3), 2.34 (s, 3H, C(11)H_3); ^{13}C-NMR ($CDCl_3$): δ_C 162.2 (*C*(1)), 155.5 (*C*(12)), 145.8 (*C*(4)), 140.2 (*C*(9)), 139.0 (*C*(7)), 137.9 (*C*(15)), 129.6 (*C*(17)), 129.1 (*C*(18)), 126.0 (*C*(16)), 125.6 (*C*(5)), 120.0 (*C*(2)), 117.8 (*C*(3)), 113.6 (*C*(6)), 105.7 (*C*(8)), 69.7 (*C*(13)), 60.6 (*C*(14)), 29.1 (*C*(10)), 18.7 (*C*(11)); IR ν_{max} 2923, 1751, 1655, 1595, 1393, 730; LR-ESI-MS: $C_{20}H_{19}N_2O_3$ $[M+H]^+$ *m/z* found 335.1 calcd 335.1, $C_{20}H_{18}N_2O_3Na$ $[M+Na]^+$ *m/z* found 357.1 calcd 357.1; HR-ESI-MS: $C_{20}H_{19}N_2O_3$ $[M+H]^+$ *m/z* found 335.1390 calcd 335.1389 error = 0.22 ppm.

7,7'-(2-Oxo-4-phenylimidazolidine-1,3-diyl)bis(1,4-dimethylquinolin-2(1*H*)-one) (374)

In a pressure tube under inert conditions, **377** (34 mg, 0.21 mmol), **218** (79 mg, 0.31 mmol) and K_3PO_4 (89 mg, 0.42 mmol) were combined. 1,4-dioxane (2.1 mL) was added and the solution was degassed. (+/-)-*trans*-1,2-diaminocyclohexane (25 μL, 0.21 mmol) and CuI (40 mg, 0.21 mmol) were added, the tube was sealed and the reaction mixture was stirred at 97 °C for 42 h. The reaction mixture was passed through a plug of Celite and the Celite was washed with CH_2Cl_2 (50 mL). The combined filtrate was concentrated and purification by FCC (2% MeOH/CH_2Cl_2) yielded **374** (19.8 mg, 19%) as a yellow oil.

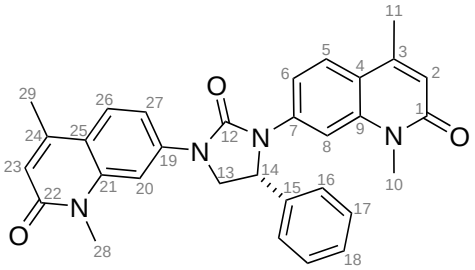

^{1}H-NMR ($CDCl_3$): δ_H 7.92 (d, J = 1.5 Hz, 1H, C(8)H or C(20)H), 7.70-7.66 (m, 2H, C(8)H or C(20)H and C(5)H or C(26)H), 7.56 (d, J = 9.0 Hz, 1H, C(5)H or C(26)H), 7.45-7.34 (m, 5H, C(6)H or C(27)H and C(16)H & C(18)H), 7.31 (td, J = 9.5, 2.0 Hz, 2H, C(17)H), 6.53 (s, 1H, C(2)H or C(23)H), 6.48 (s, 1H, C(2)H or C(23)H), 5.50 (dd, J = 9.0, 5.5 Hz, 1H, C(14)H), 4.53 (t, J = 9.0 Hz, 1H, C(13)H_a), 3.90 (dd, J = 9.0, 5.5 Hz, 1H, C(13)H_b), 3.73 (s, 3H, C(10)H_3 or C(28)H_3), 3.58 (s, 3H, C(10)H_3 or C(28)H_3), 2.45 (s, 3H, C(11)H_3 or C(29)H_3), 2.38 (s, 3H, C(11)H_3 or C(29)H_3); ^{13}C-NMR ($CDCl_3$): δ_C 162.5 (*C*(1) or *C*(22)), 162.3 (*C*(1) or *C*(22)), 154.9 (*C*(12)), 145.9 (*C*(4) or *C*(24)), 145.9 (*C*(4) or *C*(24)), 141.3 (*C*(7) or *C*(19)), 140.7 (*C*(7) or *C*(19)), 140.3 (*C*(9) or *C*(21)), 140.3 (*C*(9) or *C*(21)), 139.3 (*C*(15)), 129.6 (*C*(17)), 128.9 (*C*(18)), 126.0 (*C*(16)), 125.9 (*C*(5) or *C*(26)), 125.6 (*C*(5) or *C*(26)), 119.8 (*C*(2) or *C*(23)), 119.7 (*C*(2) or *C*(23)), 117.5 (*C*(3) or *C*(24)), 117.3 (*C*(3) or *C*(24)), 113.9 (*C*(6) or *C*(27)), 111.5 (*C*(6) or *C*(27)), 105.9 (*C*(8) or *C*(20)), 103.5 (*C*(8) or *C*(20)), 57.2 (*C*(14)), 51.5 (*C*(13)), 29.4 (*C*(10) or *C*(28)), 29.2 (*C*(10) or *C*(28)), 18.8 (*C*(11) or *C*(29)), 18.7 (*C*(11) or *C*(29)); IR ν_{max} 2946, 1645, 1583, 1389, 1255, 702; LR-ESI-MS: $C_{31}H_{29}N_4O_3$ $[M+H]^+$ *m/z* found 505.2 calcd 505.3, $C_{31}H_{28}N_4O_3Na$ $[M+Na]^+$ *m/z* found 527.3 calcd 527.2; HR-ESI-MS: $C_{31}H_{28}N_4O_3Na$ $[M+Na]^+$ *m/z* found 527.20536 calcd 527.20538 error = 0.04 ppm.

4-Phenyl-1,3-oxazolidin-2-one (375)

2-Phenylglycinol (226 mg, 1.64 mmol), diethyl carbonate (0.4 mL, 3.29 mmol) and sodium methoxide (4.4 mg, 0.082 mmol) were combined and the reaction mixture was stirred at reflux for 16 h. The reaction mixture was concentrated, H_2O (20 mL) was added and the aqueous phase was extracted with EtOAc (3 x 20 mL). The combined organic extracts were dried over Na_2SO_4, filtered and concentrated. Purification by FCC (5% EtOAc/CH_2Cl_2) yielded **375** (102 mg, 40%) as a white crystalline solid.

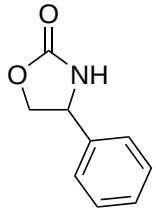

Mpt: 130.0-131.2 °C (lit. 131-132 °C); ^{1}H-NMR ($CDCl_3$): δ_H 7.42-7.31 (m, 5H), 6.62 (br s, 1H), 4.95 (t, J = 7.8 Hz, 1H), 4.71 (t, J = 8.8 Hz, 1H), 4.16 (dd, J = 8.6, 7.1 Hz, 1H); ^{13}C-NMR ($CDCl_3$): δ_C 160.0, 139.5, 129.1, 128.6, 125.9, 72.4, 56.3; LR-ESI-MS: $C_9H_{10}NO_2$ $[M+H]^+$ *m/z* found 164.1 calcd 164.1; Data are in accordance with literature values.[316]

5-Phenylimidazolidine-2,4-dione (376)

Phenylglyoxal monohydrate (1.5 g, 9.85 mmol) was dissolved in EtOH (49 mL), urea (1.18 g, 19.7 mmol), ethylacetoacetate (1.25 mL, 9.85 mmol) and conc HCl (1.77 mL) were added and the reaction mixture was stirred at reflux for 6 h. The reaction mixture was concentrated and the resulting solid was titurated (EtOH) to yield **376** (200 mg, 12%) as a white solid.

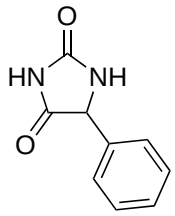

Mpt: 182.5-183.7 °C (lit. 183-184 °C); ^{1}H-NMR ($(CD_3)_2SO$): δ_H 10.79 (br s, 1H), 8.41 (s, 1H), 7.41 (tt, J = 7.0, 1.5 Hz, 2H), 7.37-7.31 (m, 3H), 5.16 (s, 1H); ^{13}C-NMR ($(CD_3)_2SO$): δ_C 174.2, 157.5, 136.1, 128.7, 128.2, 126.7, 61.2; LR-ESI-MS: $C_9H_9N_2O_2$ $[M+H]^+$ *m/z* found 177.1 calcd 177.1; Data are in accordance with literature values.[317]

4-Phenylimidazolidin-2-one (**377**)

Compound **376** (200 mg, 1.14 mmol) was dissolved in THF (22 mL), $LiAlH_4$ (4.5 mL, 4.5 mmol, 1M THF soln) was added slowly and the reaction mixture was stirred at reflux for 3 d. NaOH (100 mL, 2M aq. soln) was added slowly and the reaction mixture was filtered. The filtrate was extracted with EtOAc (3 x 150 mL), the combined organic extracts were dried over Na_2SO_4, filtered and concentrated to yield **377** (169 mg, 92%) as a white powder.

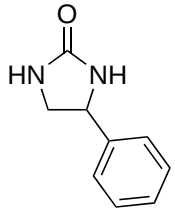

Mpt: 160.3-162.1 °C (lit. 161-162 °C); ^{1}H-NMR ($(CD_3)_2SO$): δ_H 7.40-7.25 (m, 5H), 6.86 (s, 1H), 6.32 (br s, 1H), 4.73 (t, J = 7.5 Hz, 1H), 3.71 (t, J = 8.5 Hz, 1H), 3.03 (ddd, J = 8.5, 7.0, 1.0 Hz, 1H); ^{13}C-NMR ($(CD_3)_2SO$): δ_C 163.5, 143.0, 128.5, 127.4, 126.0, 55.4, 48.8; LR-ESI-MS: $C_9H_{11}N_2O$ $[M+H]^+$ *m/z* found 162.1 calcd 162.1; Data are in accordance with literature values.[318]

7.4 PCAF

6-Butoxy-3-methyl[1,2,4]triazolo[4,3-*b*]pyridazine (**388**)

Compound **389** (25 mg, 0.15 mmol) was dissolved in *n*-butanol (1.5 mL), 1-phenylethan-1-amine (19 μL, 0.15 mmol) and K_2CO_3 (25 mg, 0.18 mmol) were added and the reaction mixture was stirred at reflux for 14 h. The reaction mixture was filtered and concentrated. Purification by FCC (EtOAc) yielded **388** (16 mg, 52%) as a crystalline white solid.

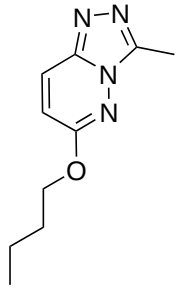

Mpt: 215.7-217.7 °C (lit. no Mpt reported in literature °C); ^{1}H-NMR ($CDCl_3$): δ_H 7.88 (d, J = 10.0 Hz, 1H), 6.72 (d, J = 10.0 Hz, 1H), 4.35 (t, J = 6.5 Hz, 2H), 2.70 (s, 3H), 1.80 (tt, J = 7.5, 6.5 Hz, 2H), 1.50 (sxt, J = 7.5 Hz, 2H), 0.99 (t, J = 7.5 Hz, 3H); ^{13}C-NMR ($CDCl_3$): δ_C 160.4, 147.0, 143.2, 125.9, 115.7, 67.7, 30.5, 19.1, 13.7, 9.6; LR-ESI-MS: $C_{10}H_{15}N_4O$ $[M+H]^+$ *m/z* found 207.1 calcd 207.1, $C_{10}H_{14}N_4Na$ $[M+Na]^+$ *m/z* found 229.1 calcd 229.1. Data are in accordance with available literature values.[319]

3-Methyl-*N*-(1-phenylethyl)[1,2,4]triazolo[4,3-*b*]pyridazin-6-amine (**390**)

Compound **389** (25 mg, 0.15 mmol) was dissolved in NMP (0.3 mL), 1-phenylethan-1-amine (38 μL, 0.30 mmol) and NEt_3 (83 μL, 0.60 mmol) were added and the reaction mixture was stirred at 120 °C for 36 h. H_2O (10 mL) was added and the aqueous phase was extracted with

EtOAc (3 x 10 mL). The combined organic extracts were washed with $NaHCO_3$ (2 x 10 mL, sat. aq. soln) and H_2O (2 x 10 mL), dried over Na_2SO_4, filtered, concentrated and purified by FCC (0.5% MeOH/0.5% NEt_3/CH_2Cl_2). The crude material was acidifed with HCl (1M aq. soln) and the aqueous phase was washed with CH_2Cl_2 (3 x 10 mL). The aqueous phase was basified with NaOH (2M aq. soln) and extracted with EtOAc (3 x 10 mL). The combined organic extracts were dried over Na_2SO_4, filtered and concentrated to yield **390** (12.1 mg, 32%) as a tan solid.

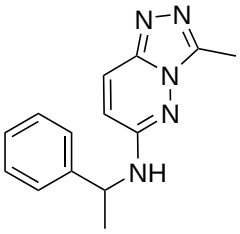

Mpt: 210.2-210.7 °C (no Mpt reported in literature); ^{1}H-NMR (CD_3OD): δ_H 7.70 (d, J = 10.0 Hz, 1H), 7.41 (dd, J = 7.5, 1.0 Hz, 2H), 7.30 (t, J = 7.5 Hz, 2H), 7.20 (tt, J = 7.5, 1.5 Hz, 1H), 6.85 (d, J = 10.0 Hz, 1H), 4.97 (q, J = 7.0 Hz, 1H), 2.49 (s, 3H), 1.55 (d, J = 7.0 Hz, 3H); ^{13}C-NMR (CD_3OD): δ_C 154.9, 145.9, 144.2, 144.1, 129.5, 128.2, 127.5, 123.9, 119.3, 52.6, 23.1, 9.3; LR-ESI-MS: $C_{14}H_{16}N_5$ $[M+H]^+$ *m/z* found 254.1 calcd 254.2; Data are in accordance with available literature values.[112]

***N*^{1},*N*^{1}-Dimethyl-*N*^{2}-(3-methyl[1,2,4]triazolo[4,3-*b*]pyridazin-6-yl)-1-phenylethane-1,2-diamine (391)**

Compound **389** (25 mg, 0.15 mmol) was dissolved in NMP (0.3 mL), N^1,N^1-dimethyl-1-phenylethane-1,2-diamine (26.8 mg, 0.16 mmol) and NEt_3 (83 μL, 0.60 mmol) were added and the reaction mixture was stirred at 120 °C for 36 h. H_2O (10 mL) was added and the aqueous phase was extracted with EtOAc (3 x 10 mL). The combined organic extracts were washed with $NaHCO_3$ (2 x 10 mL, sat. aq. soln) and H_2O (2 x 10 mL), dried over Na_2SO_4, filtered, concentrated and purified by FCC (0.5% MeOH/0.5% NEt_3/CH_2Cl_2). The crude material was acidifed with HCl (1M aq. soln) and the aqueous phase was washed with CH_2Cl_2 (3 x 10 mL). The aqueous phase was basified with NaOH (2M aq. soln) and extracted with EtOAc (3 x 10 mL). The combined organic extracts were dried over Na_2SO_4, filtered and concentrated to yield **391** (14.4 mg, 33%) as an orange amorphous solid.

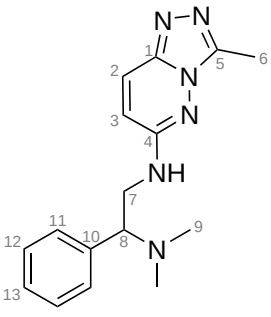

^{1}H-NMR ($CDCl_3$): δ_H 7.69 (d, J = 10.0 Hz, 1H, C(2)H), 7.39 (t, J = 7.5 Hz, 2H, C(12)H), 7.34 (tt, J = 7.5, 1.5 Hz, 1H, C(13)H), 7.29-7.27 (m, 2H, C(11)H), 6.53 (d, J = 9.5 Hz, 1H, C(3)H), 5.47 (t, J = 4.5 Hz, 1H, NH), 3.80 (ddd, J = 13.0, 8.0, 3.5 Hz, 1H, C(7)H_a), 3.70 (dd, J = 8.0, 5.5 Hz, 1H, C(8)H), 3.64 (dt, J = 12.5, 5.5 Hz, 1H, C(7)H_b), 2.64 (s, 3H, C(6)H_3), 2.24 (s, 6H, C(9)H_3); ^{13}C-NMR ($CDCl_3$): δ_C 153.3 (C(4)), 146.5 (C(5)), 142.8 (C(1)), 136.2 (C(10)), 128.7 (C(11)), 128.3 (C(12)), 127.9 (C(13)), 124.1 (C(2)), 115.8 (C(3)), 67.5 (C(8)), 42.6 (C(7)), 41.6 (C(9)), 9.6 (C(6)); IR ν_{max} 3256, 3059, 2936, 2779, 1627, 1574, 1509, 703; LR-ESI-MS: $C_{16}H_{21}N_6$ $[M+H]^+$ *m/z* found 297.2 calcd 297.2, $C_{16}H_{20}N_6Na$ $[M+Na]^+$ *m/z* found 319.1 calcd 319.2; HR-ESI-MS: $C_{16}H_{21}N_6$ $[M+H]^+$ *m/z* found 297.18222 calcd 297.18179 error = 0.86 ppm.

***N*^{3},*N*^{3}-Dimethyl-*N*^{1}-(3-methyl[1,2,4]triazolo[4,3-*b*]pyridazin-6-yl)-1-phenylpropane-1,3-diamine (392)**

Compound **389** (25 mg, 0.15 mmol) was dissolved in NMP (0.3 mL), N^1,N^1-dimethyl-3-phenylpropane-1,3-diamine (29 mg, 0.16 mmol) and NEt_3 (83 μL, 0.60 mmol) were added and

the reaction mixture was stirred at 120 °C for 36 h. H_2O (10 mL) was added and the aqueous phase was extracted with EtOAc (3 x 10 mL). The combined organic extracts were washed with $NaHCO_3$ (2 x 10 mL, sat. aq. soln) and H_2O (2 x 10 mL), dried over Na_2SO_4, filtered, concentrated and purified by FCC (0.5% MeOH/0.5% NEt_3/CH_2Cl_2). The crude material was acidifed with HCl (1M aq. soln) and the aqueous phase was washed with CH_2Cl_2 (3 x 10 mL). The aqueous phase was basified with NaOH (2M aq. soln) and extracted with EtOAc (3 x 10 mL). The combined organic extracts were dried over Na_2SO_4, filtered and concentrated to yield **392** (5.1 mg, 11%) as a colourless oil.

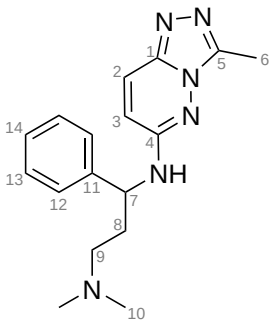

^{1}H-NMR ($CDCl_3$): δ_H 7.91 (d, J = 5.0 Hz, 1H, NH), 7.66 (d, J = 10.0 Hz, 1H, C(2)H), 7.36 (dd, J = 8.0, 1.5 Hz, 2H, C(12)H), 7.33 (t, J = 8.0 Hz, 2H, C(13)H), 7.24 (tt, J = 7.0, 1.5 Hz, 1H, C(14)H), 6.51 (d, J = 10.0 Hz, 1H, C(3)H), 4.96 (dt, J = 7.5, 5.0 Hz, 1H, C(7)H), 2.49 (ddd, J = 12.5, 8.0, 4.0 Hz, 1H, C(9)H_a), 2.46 (s, 3H, C(6)H_3), 2.43 (ddd, J = 12.5, 7.5, 4.5 Hz, 1H, C(9)H_b), 2.33 (s, 6H, C(10)H_3), 2.07 (dddd, J = 14.5, 8.0, 5.0, 4.5 Hz, 1H, C(8)H_a), 1.94 (dtd, J = 15.0, 7.5, 4.0 Hz, 1H, C(8)H_b); ^{13}C-NMR ($CDCl_3$): δ_C 152.7 (C(4)), 146.5 (C(5)), 142.7 (C(1) or C(11)), 142.6 (C(1) or C(11)), 128.4 (C(13)), 127.0 (C(14)), 126.4 (C(12)), 124.0 (C(2)), 115.9 (C(3)), 56.9 (C(9)), 56.9 (C(7)), 45.4 (C(10)), 32.7 (C(8)), 9.4 (C(6)); IR ν_{max} 3244, 3058, 2946, 2817, 1627, 1576, 1500, 1105, 701; LR-ESI-MS: $C_{17}H_{23}N_6$ $[M+H]^+$ *m/z* found 311.2 calcd 311.2, $C_{17}H_{22}N_6Na$ $[M+Na]^+$ *m/z* found 333.2 calcd 333.2; HR-ESI-MS: $C_{17}H_{23}N_6$ $[M+H]^+$ *m/z* found 311.19787 calcd 311.19785 error = 0.08 ppm.

6-Chloro-3-methyl[1,2,4]triazolo[3,4-*a*]phthalazine (**394**)

$N_2H_4 \cdot H_2O$ (0.53 mL, 11.0 mmol) was dissolved in EtOH (7.2 mL) and the solution was stirred at reflux for 30 min. **393** (300 mg, 1.4 mmol) was added and the reaction mixture was stirred at reflux for 30 min. The reaction mixture was filtered, the precipitate was washed with PE (2 x 100 mL) and dried. The precipitate was dissolved in 1,4-dioxane (14.3 mL), acetyl chloride (123 μL, 1.72 mmol) and NEt_3 (0.2 mL, 1.4 mmol) were added and the reaction mixture was stirred at 110 °C for 14 h. CH_2Cl_2 (100 mL) was added and the organic phase was washed with H_2O (3 x 100 mL), dried over Na_2SO_4, filtered and concentrated to yield **394** (212 mg, 64%) as a beige solid.

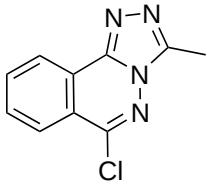

Mpt: 170.8-171.5 °C (lit. 169-170 °C); ^{1}H-NMR ($CDCl_3$): δ_H 8.68 (dd, J = 8.0, 0.5 Hz, 1H), 8.26 (d, J = 8.5 Hz, 1H), 8.00 (td, J = 7.5, 1.0 Hz, 1H), 7.87 (ddd, J = 8.5, 7.5, 1.0 Hz, 1H), 2.82 (s, 3H); ^{13}C-NMR ($CDCl_3$): δ_C 149.8, 147.8, 142.3, 134.8, 131.2, 127.4, 124.0, 123.5, 122.0, 9.8; LR-ESI-MS: $C_{10}H_8ClN_4$ $[M+H]^+$ *m/z* found 219.0 calcd 219.1, $C_{10}H_7ClN_4Na$ $[M+Na]^+$ *m/z* found 241.0 calcd 241.0. Data are in accordance with literature values.[111]

3-Methyl-*N*-(1-phenylethyl)[1,2,4]triazolo[3,4-*a*]phthalazin-6-amine (**395**)

Under inert conditions, 1-phenylethan-1-amine (14.8 μL, 0.11 mmol) was dissolved in THF (0.71 mL) and the solution was cooled to -78 °C. *n*-BuLi (66.5 μL, 0.11 mmol, 1.6M hexane soln) was added dropwise and the reaction mixture was stirred at -78 °C for 15 min. In a separate flask under inert conditions, **394** (15.6 mg, 0.071 mmol) was dissolved in THF (0.71 mL) and cooled to -78 °C. The solution from the initial flask was added dropwise and the reaction mixture was

stirred at rt for 12 h. H_2O (20 mL) was added slowly and the aqueous phase was extracted with EtOAc (5 x 20 mL). The combined organic extracts were dried over Na_2SO_4, filtered and concentrated. Purification by FCC (70% EtOAc/0.5% NEt_3/PE) yielded **395** (7.8 mg, 36%) as a white solid.

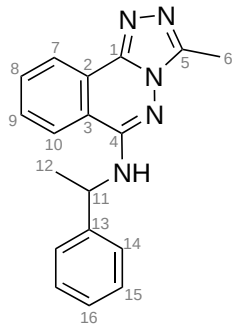

Mpt: 160.0-160.9 °C; ^{1}H-NMR ($CDCl_3$): δ_H 8.56 (dd, J = 8.0, 0.5 Hz, 1H, C(7)H), 7.83 (d, J = 8.0 Hz, 1H, C(10)H), 7.79 (ddd, J = 8.0, 7.5, 1.0 Hz, 1H, C(8)H), 7.68 (ddd, J = 8.0, 7.5, 1.5 Hz, 1H, C(9)H), 7.47 (dd, J = 7.5, 1.0 Hz, 2H, C(14)H), 7.35 (dd, J = 7.5, 7.5 Hz, 2H, C(15)H), 7.27 (tt, J = 7.5, 1.0 Hz, 1H, C(16)H), 5.51 (d, J = 5.5 Hz, 1H, NH), 5.23 (quin, J = 6.5 Hz, 1H, C(11)H), 2.61 (s, 3H, C(6)H_3), 1.71 (d, J = 7.0 Hz, 3H, C(12)H_3); ^{13}C-NMR ($CDCl_3$): δ_C 149.7 (C(4)), 147.3 (C(5)), 143.8 (C(13)), 141.8 (C(1)), 132.5 (C(8)), 129.9 (C(9)), 128.6 (C(15)), 127.4 (C(16)), 126.3 (C(14)), 124.2 (C(2)), 123.9 (C(7)), 122.1 (C(10)), 118.2 (C(3)), 51.7 (C(11)), 22.5 (C(12)), 9.7 (C(6)); IR ν_{max} 3246, 3066, 2933, 2361, 2341, 1550, 1509, 701; LR-ESI-MS: $C_{18}H_{18}H_5$ $[M+H]^+$ m/z found 304.2 calcd 304.2; HR-ESI-MS: $C_{18}H_{18}N_5$ $[M+H]^+$ m/z found 304.15567 calcd 304.15558 error = 0.31 ppm.

N^1,N^1-Dimethyl-N^2-(3-methyl[1,2,4]triazolo[3,4-a]phthalazin-6-yl)-1-phenylethane-1,2-diamine (**396**)

Method A. Under inert conditions, N^1,N^1-dimethyl-1-phenylethane-1,2-diamine (75 mg, 0.46 mmol) was dissolved in THF (1.83 mL) and the solution was cooled to -78 °C. n-BuLi (275 μL, 0.44 mmol, 1.6M hexane soln) was added dropwise and the reaction mixture was stirred at -78 °C for 15 min. In a separate flask under inert conditions, **394** (20 mg, 0.092 mmol) was dissolved in THF (0.92 mL) and cooled to -78 °C. The solution from the initial flask was added dropwise and the reaction mixture was stirred at rt for 12 h. H_2O (20 mL) was added slowly and the aqueous phase was extracted with EtOAc (5 x 20 mL). The combined organic extracts were dried over Na_2SO_4, filtered and concentrated. Purification by FCC (0.1% MeOH/0.5% NEt_3/CH_2Cl_2) yielded **396** (23 mg, 73%) as a colourless oil.

Method B. Compound **394** (20 mg, 0.092 mmol) was dissolved in 1,4-dioxane (0.51 mL), Xantphos (21.2 mg, 0.037 mmol), N^1,N^1-dimethyl-1-phenylethane-1,2-diamine (75 mg, 0.46 mmol), K_2CO_3 (63.2 mg, 0.46 mmol) and $Pd(OAc)_2$ (4.1 mg, 0.018 mmol) were added and the reaction mixture was stirred at reflux for 12 h. H_2O (20 mL) was added and the aqueous phase was extracted with EtOAc (3 x 20 mL). The combined organic extracts were dried over Na_2SO_4, filtered and concentrated. Purification by FCC (0.1% MeOH/0.5% NEt_3/CH_2Cl_2) yielded **396** (17.7 mg, 56%) as a colourless oil.

Method C. In a pressure tube, **394** (20 mg, 0.092 mmol) was dissolved in EtOH (0.2 mL), N^1,N^1-dimethyl-1-phenylethane-1,2-diamine (35 mg, 0.21 mmol), KI (1.5 mg, 0.009 mmol) and concentrated HCl (2 μL, 0.002 mmol) were added, the tube was sealed and the reaction mixture was stirred at 100 °C for 12 h. The reaction mixture was concentrated, NaOH (20 mL, 1M aq. soln) was added and the aqueous phase was extracted with EtOAc (3 x 20 mL). The combined organic extracts were dried over Na_2SO_4, filtered, concentrated and purified by FCC (0.25% MeOH/0.5% NEt_3/CH_2Cl_2). The crude material was acidifed with HCl (sat. aq. soln) and the aqueous phase was washed with CH_2Cl_2 (3 x 10 mL). The aqueous phase was basified with NaOH (2M aq. soln) and extracted with EtOAc (3 x 10 mL). The combined organic extracts

were dried over Na_2SO_4, filtered and concentrated to yield **396** (28.1 mg, 89%) as a colourless oil.

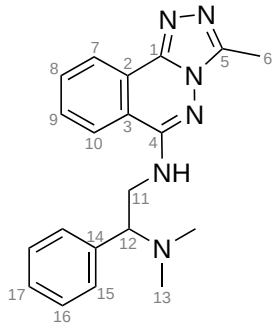

^{1}H-NMR ($CDCl_3$): δ_H 8.56 (dd, J = 8.0, 0.5 Hz, 1H, C(7)H), 7.79 (ddd, J = 8.0, 7.0, 1.5 Hz, 1H, C(8)H), 7.73 (d, J = 7.5 Hz, 1H, C(10)H), 7.68 (ddd, J = 8.0, 7.0, 1.5 Hz, 1H, C(9)H), 7.39 (ddt, J = 8.0, 6.5, 1.5 Hz, 2H, C(16)H), 7.36-7.31 (m, 3H, C(15)H & C(17)H), 6.12 (br s, 1H, NH), 3.89 (ddd, J = 12.5, 8.0, 3.0 Hz, 1H, C(11)H_a), 3.80 (dd, J = 8.0, 5.5 Hz, 1H, C(12)H), 3.75 (dt, J = 12.5, 5.5 Hz, 1H, C(11)H_b), 2.66 (s, 3H, C(6)H_3), 2.28 (s, 6H, C(13)H_3); ^{13}C-NMR ($CDCl_3$): δ_C 150.9 (C(4)), 147.2 (C(5)), 141.9 (C(1)), 136.3 (C(14)), 132.4 (C(8)), 129.9 (C(9)), 128.7 (C(15)), 128.3 (C(16)), 128.0 (C(17)), 124.1 (C(2)), 123.7 (C(7)), 122.3 (C(10)), 118.4 (C(3)), 67.5 (C(12)), 42.7 (C(11)), 41.6 (C(13)), 9.7 (C(6)); IR ν_{max} 3312, 3063, 2936, 2781, 2361, 1513, 731, 701; LR-ESI-MS: $C_{20}H_{23}N_6$ $[M+H]^+$ *m/z* found 347.2 calcd 347.2; HR-ESI-MS: $C_{20}H_{23}N_6$ $[M+H]^+$ *m/z* found 347.19787 calcd 347.19787 error = 0.00 ppm.

Ethyl (6-chloro-3-methyl[1,2,4]triazolo[4,3-*b*]pyridazin-8-yl)carbamate (**399**)

Compound **398** (20 mg, 0.11 mmol) was dissolved in toluene (1 mL), ethylchloroformate (104 μL, 1.1 mmol) and K_2CO_3 (156 mg, 1.1 mmol) were added and the reaction mixture was stirred at reflux for 2 d. H_2O (10 mL) was added and the aqueous phase was extracted with EtOAc (3 x 10 mL). The combined organic extracts were dried over Na_2SO_4, filtered and concentrated. Purification by FCC (0.1% MeOH/EtOAc) yielded **399** (15.7 mg, 56%) as a beige solid.

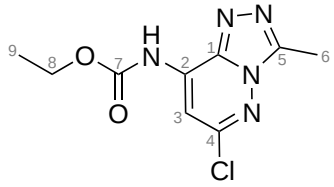

Mpt: 120.9-121.7 °C; ^{1}H-NMR ($CDCl_3$): δ_H 8.49 (br s, 1H, NH), 7.75 (s, 1H, C(3)H), 4.35 (q, J = 7.0 Hz, 2H, C(8)H_2), 2.79 (s, 3H, C(6)H_3), 1.37 (t, J = 7.0 Hz, 3H, C(9)H_3); ^{13}C-NMR ($CDCl_3$): δ_C 152.4 (C(4)), 151.0 (C(7)), 148.2 (C(2)), 138.5 (C(1)), 134.6 (C(5)), 103.4 (C(3)), 63.0 (C(8)), 14.2 (C(9)), 9.7 (C(6)); IR ν_{max} 3138, 2981, 1732, 1550, 1221, 725; LR-ESI-MS: $C_9H_{11}ClN_5O_2$ $[M+H]^+$ *m/z* found 256.1 calcd 256.1, $C_9H_{10}ClN_5O_2Na$ $[M+Na]^+$ *m/z* found 278.0 calcd 278.0; HR-ESI-MS: $C_9H_{11}ClN_5O_2$ $[M+H]^+$ *m/z* found 256.05958 calcd 256.05960 error = 0.09 ppm.

References

1. Schreiber, S. L. *Nat. Chem. Biol.* **2005**, *1*, 64–66.
2. Weiss, W. A.; Taylor, S. S.; Shokat, K. M. *Nat. Chem. Biol.* **2007**, *3*, 739–744.
3. Shamji, A.; Nghiem, P.; Schreiber, S. *Mol. Cell* **2003**, *12*, 271–280.
4. Sarbassov, D. D.; Ali, S. M.; Kim, D.-H.; Guertin, D. A.; Latek, R. R. et al. *Curr. Biol.* **2004**, *14*, 1296–1302.
5. Arrowsmith, C. H.; Audia, J. E.; Austin, C.; Baell, J.; Bennett, J. et al. *Nat. Chem. Biol.* **2015**, *11*, 536–541.
6. Choudhary, C.; Kumar, C.; Gnad, F.; Nielsen, M. L.; Rehman, M. et al. *Science* **2009**, *325*, 834–840.
7. Kouzarides, T.; Kouzarides, T. *EMBO J.* **2000**, *19*, 1176–1179.
8. Tamkun, J. W.; Deuring, R.; Scott, M. P.; Kissinger, M.; Pattatucci, M. et al. *Cell* **1992**, *68*, 561–572.
9. Haynes, S. R.; Dollard, C.; Winston, F.; Beck, S.; Trowsdale, J. et al. *Nucleic Acids Res.* **1992**, *20*, 2603.
10. Mujtaba, S.; Zeng, L.; Zhou, M.-M. *Oncogene* **2007**, *26*, 5521–5527.
11. Owen, D. J.; Ornaghi, P.; Yang, J. C.; Lowe, N.; Evans, P. R. et al. *EMBO J.* **2000**, *19*, 6141–6149.
12. Filippakopoulos, P.; Picaud, S.; Mangos, M.; Keates, T.; Lambert, J. P. et al. *Cell* **2012**, *149*, 214–231.
13. Muller, S.; Filippakopoulos, P.; Knapp, S. *Expert Rev. Mol. Med.* **2011**, *13*, e29.
14. Hewings, D. S.; Rooney, T. P. C.; Jennings, L. E.; Hay, D. A.; Schofield, C. J. et al. *J. Med. Chem.* **2012**, *55*, 9393–9413.
15. Florence, B.; Faller, D. V. *Front. Biosci.* **2001**, *6*, 1008–1018.
16. Matangkasombut, O.; Buratowski, R. M.; Swilling, N. W.; Buratowski, S. *Genes Dev.* **2000**, *14*, 951–962.
17. Denis, G. V.; Green, M. R. *Genes Dev.* **1996**, *10*, 261–271.
18. Wu, S. Y.; Chiang, C. M. *J. Biol. Chem.* **2007**, *282*, 13141–13145.
19. Krueger, B. J.; Varzavand, K.; Cooper, J. J.; Price, D. H. *PLoS One* **2010**, *5*, e12335.
20. Jang, M. K.; Mochizuki, K.; Zhou, M.; Jeong, H. S.; Brady, J. N. et al. *Mol. Cell* **2005**, *19*, 523–534.

21. Devaiah, B. N.; Lewis, B. A.; Cherman, N.; Hewitt, M. C.; Albrecht, B. K. et al. *Proc. Natl. Acad. Sci. U. S. A.* **2012**, *109*, 6927–6932.

22. Yang, Z.; He, N.; Zhou, Q. *Mol. Cell. Biol.* **2008**, *28*, 967–976.

23. Bolden, J. E.; Tasdemir, N.; Dow, L. E.; van Es, J. H.; Wilkinson, J. E. et al. *Cell Rep.* **2014**, *8*, 1919–1929.

24. Filippakopoulos, P.; Qi, J.; Picaud, S.; Shen, Y.; Smith, W. B. et al. *Nature* **2010**, *468*, 1067–1073.

25. Seal, J.; Lamotte, Y.; Donche, F.; Bouillot, A.; Mirguet, O. et al. *Bioorg. Med. Chem. Lett.* **2012**, *22*, 2968–2972.

26. Crawford, N. P. S.; Alsarraj, J.; Lukes, L.; Walker, R. C.; Officewala, J. S. et al. *Proc. Natl. Acad. Sci. U. S. A.* **2008**, *105*, 6380–6385.

27. Ott, C. J.; Kopp, N.; Bird, L.; Paranal, R. M.; Qi, J. et al. *Blood* **2012**, *120*, 2843–2852.

28. Lockwood, W. W.; Zejnullahu, K.; Bradner, J. E.; Varmus, H. *Proc. Natl. Acad. Sci. U. S. A.* **2012**, *109*, 19408–13.

29. Dawson, M. A.; Prinjha, R. K.; Dittmann, A.; Giotopoulos, G.; Bantscheff, M. et al. *Nature* **2011**, *478*, 529–533.

30. Zuber, J.; Shi, J.; Wang, E.; Rappaport, A. R.; Herrmann, H. et al. *Nature* **2011**, *478*, 524–528.

31. French, C. A.; Miyoshi, I.; Kubonishi, I.; Grier, H. E.; Perez-atayde, A. R. et al. *Cancer Res.* **2003**, 304–307.

32. French, C. A.; Ramirez, C. L.; Kolmakova, J.; Hickman, T. T.; Cameron, M. J. et al. *Oncogene* **2008**, *27*, 2237–2242.

33. Mertz, J. A.; Conery, A. R.; Bryant, B. M.; Sandy, P.; Balasubramanian, S. et al. *Proc. Natl. Acad. Sci. U. S. A.* **2011**, *108*, 16669–16674.

34. Lin, A.; Wang, S.; Nguyen, T.; Shire, K.; Frappier, L. *J. Virol.* **2008**, *82*, 12009–12019.

35. You, J.; Srinivasan, V.; Denis, G. V.; Harrington, W. J.; Ballestas, M. E. et al. *J. Virol.* **2006**, *80*, 8909–8919.

36. Helfer, C.; Yan, J.; You, J. *Viruses* **2014**, *6*, 3228–3249.

37. Bisgrove, D. A.; Mahmoudi, T.; Henklein, P.; Verdin, E. *Proc. Natl. Acad. Sci. U. S. A.* **2007**, *104*, 13690–13695.

38. Cuppen, E.; Van Ham, M.; Pepers, B.; Wieringa, B.; Hendriks, W. *FEBS Lett.* **1999**, *459*, 291–298.

39. Staal, A.; Enserink, J. M.; Stein, J. L.; Stein, G. S.; Van Wijnen, A. J. *J. Cell. Physiol.* **2000**, *185*, 269–279.

40. Middeljans, E.; Wan, X.; Jansen, P. W.; Sharma, V.; Stunnenberg, H. G. et al. *PLoS One* **2012**, *7*, e33834.

41. Kadoch, C.; Hargreaves, D. C.; Hodges, C.; Elias, L.; Ho, L. et al. *Nat. Genet.* **2013**, *45*, 592–601.

42. Kzhyshkowska, J.; Rusch, A.; Wolf, H.; Dobner, T. *Biochem. J.* **2003**, *371*, 385–393.

43. Burrows, A. E.; Smogorzewska, A.; Elledge, S. J. *Proc. Natl. Acad. Sci. U. S. A.* **2010**, *107*, 14280–14285.

44. Drost, J.; Mantovani, F.; Tocco, F.; Elkon, R.; Comel, A. et al. *Nat. Cell Biol.* **2010**, *12*, 380–389.

45. Sherr, C. J. *Science* **1996**, *274*, 1672–1677.

46. Sears, R. C.; Nevins, J. R. *J. Biol. Chem.* **2002**, *277*, 11617–11620.

47. Zhou, J.; Ma, J.; Zhang, B. C.; Li, X. L.; Shen, S. R. et al. *J. Cell. Physiol.* **2004**, *200*, 89–98.

48. Peng, C.; Liu, H. Y.; Zhou, M.; Zhang, L. M.; Li, X. L. et al. *Mol. Cell. Biochem.* **2007**, *303*, 141–149.

49. Park, Y. A.; Lee, J. W.; Kim, H. S.; Lee, Y. Y.; Kim, T. J. et al. *Clin. Cancer Res.* **2014**, *20*, 565–575.

50. Chiu, Y. H.; Lee, J. Y.; Cantley, L. C. *Mol. Cell* **2014**, *54*, 193–202.

51. Park, S. W.; Herrema, H.; Salazar, M.; Cakir, I.; Cabi, S. et al. *Cell Metab.* **2014**, *20*, 73–84.

52. Kikuchi, M.; Okumura, F.; Tsukiyama, T.; Watanabe, M.; Miyajima, N. et al. *Biochim. Biophys. Acta - Mol. Cell Res.* **2009**, *1793*, 1828–1836.

53. Harte, M. T.; Brien, G. J.; Ryan, N. M.; Gorski, J. J.; Savage, K. I. et al. *Cancer Res.* **2010**, *70*, 2538–2547.

54. Jones, S. E. *Breast Cancer Res. Treat.* **2002**, *75 Suppl 1*, 19–21.

55. Wu, W.-J.; Hu, K.-S.; Chen, D.-L.; Zeng, Z.-L.; Luo, H.-Y. et al. *Eur. J. Clin. Invest.* **2013**, *43*, 131–140.

56. Park, Y. A.; Lee, J. W.; Choi, J. J.; Jeon, H. K.; Cho, Y. et al. *Gynecol. Oncol.* **2012**, *124*, 125–133.

57. Xue, Z.; Zhao, J.; Niu, L.; An, G.; Guo, Y. et al. *PLoS One* **2015**, *10*, e0127682.

58. Li, D.; Yang, Y.; Zhu, G.; Liu, X.; Zhao, M. et al. *FEBS Lett.* **2015**, *589*, 2218–2223.

59. Tang, H.; Wang, Z.; Liu, Q.; Liu, X.; Wu, M. et al. *PLoS One* **2014**, *9*, e84146.

60. Hu, K.; Liao, D.; Wu, W.; Han, A.-J.; Shi, H.-J. et al. *Oncotarget* **2014**, *5*, 3088–3100.

61. Xu, Y.; Cao, W.; Zhou, M.; Li, C.; Luo, Y. et al. *Behav. Brain Res.* **2015**, *286*, 1–10.

62. Steilmann, C.; Cavalcanti, M. C. O.; Bartkuhn, M.; Pons-Kühnemann, J.; Schuppe, H. C. et al. *Reproduction* **2010**, *140*, 435–443.

63. Huang, H.-T.; Chen, S.-M.; Pan, L.-B.; Yao, J.; Ma, H.-T. *Oncol. Rep.* **2015**, *33*, 283–291.

64. Cleary, S. P.; Jeck, W. R.; Zhao, X.; Chen, K.; Selitsky, S. R. et al. *Hepatology* **2013**, *58*, 1693–1702.

65. Scotto, L.; Narayan, G.; Nandula, S. V.; Subramaniyam, S.; Kaufmann, A. M. et al. *Mol. Cancer* **2008**, *7*, 58–67.

66. Atkin, N. B. *Cytogenet. Cell Genet.* **2000**, *91*, 44–46.

67. Kang, J. U.; Koo, S. H.; Kwon, K. C.; Park, J. W.; Kim, J. M. *Cancer Genet. Cytogenet.* **2008**, *182*, 1–11.

68. Andersson, A. K.; Ma, J.; Wang, J.; Chen, X.; Gedman, A. L. et al. *Nat. Genet.* **2015**, *47*, 330–337.

69. Yang, X.-J.; Ogryzko, V. V.; Nishikawa, J.-I.; Howard, B. H.; Nakatani, Y. *Nature* **1996**, *382*, 319–324.

70. Jeanmougin, F.; Wurtz, J. M.; Le Douarin, B.; Chambon, P.; Losson, R. *Trends Biochem. Sci.* **1997**, *22*, 151–153.

71. Dhalluin, C.; Carlson, J. E.; Zeng, L.; He, C.; Aggarwal, A. K. et al. *Nature* **1999**, *399*, 491–496.

72. Xu, W.; Edmondson, D. G.; Roth, S. Y. *Mol. Cell. Biol.* **1998**, *18*, 5659–5669.

73. Nagy, Z.; Tora, L. *Oncogene* **2007**, *26*, 5341–5357.

74. Curtis, A. M.; Seo, S. B.; Westgate, E. J.; Rudic, R. D.; Smyth, E. M. et al. *J. Biol. Chem.* **2004**, *279*, 7091–7097.

75. Linares, L. K.; Kiernan, R.; Triboulet, R.; Chable-Bessia, C.; Latreille, D. et al. *Nat. Cell Biol.* **2007**, *9*, 331–338.

76. Farria, A.; Li, W.; Dent, S. Y. R. *Oncogene* **2015**, 1–13.

77. Lin, R.; Tao, R.; Gao, X.; Li, T.; Zhou, X. et al. *Mol. Cell* **2013**, *51*, 506–518.

78. Amakye, D.; Jagani, Z.; Dorsch, M. *Nat. Med.* **2013**, *19*, 1410–1422.

79. Infante, P.; Canettieri, G.; Gulino, A.; Di Marcotullio, L. *Trends Mol. Med.* **2014**, *20*, 416–418.

80. Malatesta, M.; Steinhauer, C.; Mohammad, F.; Pandey, D. P.; Squatrito, M. et al. *Cancer Res.* **2013**, *73*, 6323–6333.

81. Moran, E. *Curr. Opin. Genet. Dev.* **1993**, *3*, 63–70.

82. Ge, X.; Jin, Q.; Zhang, F.; Yan, T.; Zhai, Q. *Mol. Biol. Cell* **2009**, *20*, 419–427.

83. Gong, A.-Y.; Eischeid, A. N.; Xiao, J.; Zhao, J.; Chen, D. et al. *BMC Cancer* **2012**, *12*, 492.

84. Chen, L.-F.; Greene, W. C. *Nat. Rev. Mol. Cell Biol.* **2004**, *5*, 392–401.

85. Hayden, M. S.; Ghosh, S. *Genes Dev.* **2004**, *18*, 2195–2224.

86. Holmes, C. *Neuropathol. Appl. Neurobiol.* **2013**, *39*, 51–68.

87. Chen, L. F.; Fischle, W.; Verdin, E.; Greene, W. C. *Science* **2001**, *293*, 1653–1657.

88. Chen, L. F.; Mu, Y.; Greene, W. C. *EMBO J.* **2002**, *21*, 6539–6548.

89. Adams, M.; Sharmeen, L.; Kimpton, J.; Romeo, J. M.; Garcia, J. V. et al. *Proc. Natl. Acad. Sci. U. S. A.* **1994**, *91*, 3862–3866.

90. Benkirane, M.; Chun, R. F.; Xiao, H.; Ogryzko, V. V.; Howard, B. H. et al. *J. Biol. Chem.* **1998**, *273*, 24898–24905.

91. Deng, L.; de la Fuente, C.; Fu, P.; Wang, L.; Donnelly, R. et al. *Virology* **2000**, *277*, 278–295.

92. Kiernan, R. E.; Vanhulle, C.; Schiltz, L.; Adam, E.; Xiao, H. et al. *EMBO J.* **1999**, *18*, 6106–6118.

93. Kikuchi, H.; Nakayama, M.; Kawai, C.; Kuribayashi, F.; Mimuro, H. et al. *Microbiol. Immunol.* **2015**, *59*, 243–247.

94. Duclot, F.; Jacquet, C.; Gongora, C.; Maurice, T. *Neurosci. Lett.* **2010**, *475*, 179–183.

95. Park, S. Y.; Lee, Y. H.; Seong, A. R.; Lee, J.; Jun, W. et al. *Int. J. Mol. Med.* **2013**, *32*, 469–475.

96. Park, S.-Y.; Kim, M.-J.; Kim, Y. J.; Lee, Y.-H.; Bae, D. et al. *Int. J. Mol. Med.* **2015**, *35*, 1109–1118.

97. Dekker, F. J.; Ghizzoni, M.; van der Meer, N.; Wisastra, R.; Haisma, H. J. *Bioorg. Med. Chem.* **2009**, *17*, 460–466.

98. Zeng, L.; Li, J.; Muller, M.; Yan, S.; Mujtaba, S. et al. *J. Am. Chem. Soc.* **2005**, *127*, 2376–2377.

99. Wang, Q.; Wang, R.; Zhang, B.; Zhang, S.; Zheng, Y. et al. *Med. Chem. Commun.* **2013**, *4*, 737.

100. Andrews, K. T.; Tran, T. N.; Fairlie, D. P. *Curr. Pharm. Des.* **2012**, *18*, 3467–3479.

101. Merrick, C. J.; Duraisingh, M. T. *Eukaryot. Cell* **2010**, *9*, 1150–1158.

102. Fan, Q.; An, L.; Cui, L. *Eukaryot. Cell* **2004**, *3*, 264–276.

103. Josling, G. A.; Petter, M.; Oehring, S. C.; Gupta, A. P.; Dietz, O. et al. *Cell Host Microbe* **2015**, *17*, 741–751.

104. Chung, C. W.; Dean, A. W.; Woolven, J. M.; Bamborough, P. *J. Med. Chem.* **2012**, *55*, 576–586.

105. Lucas, X.; Wohlwend, D.; Hügle, M.; Schmidtkunz, K.; Gerhardt, S. et al. *Angew. Chem. Int. Ed.* **2013**, *52*, 14055–14059.

106. Hewings, D. S.; Wang, M.; Philpott, M.; Fedorov, O.; Uttarkar, S. et al. *J. Chem. Educ.* **2011**, *54*, 6761–6770.

107. Taylor, A. M.; Vaswani, R. G.; Gehling, V. S.; Hewitt, M. C.; Leblanc, Y. et al. *ACS Med. Chem. Lett.* **2015**, ASAP.

108. Fedorov, O.; Lingard, H.; Wells, C.; Monteiro, O. P.; Picaud, S. et al. *J. Med. Chem.* **2014**, *57*, 462–476.

109. Liu, H. *Faming Zhuanli Shenqing* **2014**, CN 104016986 (A).

110. Liu, H. *Faming Zhuanli Shenqing* **2014**, CN 103694244 (A).

111. Xue, D.-Q.; Zhang, X.-Y.; Wang, C.-J.; Ma, L.-Y.; Zhu, N. et al. *Eur. J. Med. Chem.* **2014**, *85*, 235–244.

112. Albrecht, B. K. *PCT Int. Appl.* **2012**, WO 2012/174487 A2.

113. Zhao, L.; Cao, D.; Chen, T.; Wang, Y.; Miao, Z. et al. *J. Med. Chem.* **2013**, *56*, 3833–3851.

114. Vidler, L. R.; Filippakopoulos, P.; Fedorov, O.; Picaud, S.; Martin, S. et al. *J. Med. Chem.* **2013**, *56*, 8073–8088.

115. Fish, P. V.; Filippakopoulos, P.; Bish, G.; Brennan, P. E.; Bunnage, M. E. et al. *J. Med. Chem.* **2012**, *55*, 9831–9837.

116. Dömling, A.; Wang, W.; Wang, K.; Do, A. *Chem. Rev.* **2012**, *112*, 3083–3135.

117. Biggs-Houck, J. E.; Younai, A.; Shaw, J. T. *Curr. Opin. Chem. Biol.* **2010**, *14*, 371–382.

118. Nishizawa, R.; Nishiyama, T.; Hisaichi, K.; Matsunaga, N.; Minamoto, C. et al. *Bioorg. Med. Chem. Lett.* **2007**, *17*, 727–731.

119. Liddle, J.; Allen, M. J.; Borthwick, A. D.; Brooks, D. P.; Davies, D. E. et al. *Bioorg. Med. Chem. Lett.* **2008**, *18*, 90–94.

120. Nair, P. P. S.; Chandrashekarappa, K. K. H.; Masagalli, J. N.; Nagaraja, P.; Mahadevan, K. M. *Int. J. Pharm. Pharm. Sci.* **2015**, *7*, 448–459.

121. Le Floch, C.; Le Gall, E.; Sengmany, S.; Renevret, P.; Léonel, E. et al. *Eur. J. Med. Chem.* **2015**, *89*, 654–670.

122. Frolova, L. V.; Magedov, I. V.; Romero, A. E.; Karki, M.; Otero, I. et al. *J. Med. Chem.* **2013**, *56*, 6886–6900.

123. Muehlstaedt, M.; Schulze, B. *J. Prakt. Chem.* **1975**, *317*, 919–925.

124. Bhagwatheeswaran, H.; Gaur, S. P.; Jain, P. C. *Synthesis (Stuttg).* **1976**, *1976*, 615–616.

125. Jakubec, P.; Cockfield, D. M.; Helliwell, M.; Raftery, J.; Dixon, D. J. *Beilstein J. Org. Chem.* **2012**, *8*, 567–578.

126. Jakubec, P.; Hawkins, A.; Felzmann, W.; Dixon, D. J. *J. Am. Chem. Soc.* **2012**, *134*, 17482–17485.

127. Jakubec, P.; Cockfield, D. M.; Dixon, D. J. *J. Am. Chem. Soc.* **2009**, *131*, 16632–16633.

128. Jakubec, P.; Kyle, A. F.; Calleja, J.; Dixon, D. J. *Tetrahedron Lett.* **2011**, *52*, 6094–6097.

129. Kyle, A. F.; Jakubec, P.; Cockfield, D. M.; Cleator, E.; Skidmore, J. et al. *Chem. Commun.* **2011**, *47*, 10037.

130. Desai, M. C.; Thadeio, P. F.; Lefkowitz, S. L. *Tetrahedron Lett.* **1993**, *34*, 5831–5834.

131. Pelletier, S. M.-c. One-pot Nitro-Mannich Cascade Reactions : New Methodologies and Synthetic Applications. Ph.D. thesis, University of Oxford, 2011.

132. Pelletier, S. M. C.; Ray, P. C.; Dixon, D. J. *Org. Lett.* **2009**, *11*, 4512–4515.

133. Pelletier, S. M.; Ray, P. C.; Dixon, D. J. *Org. Lett.* **2011**, *13*, 6406–6409.

134. Dalko, P. I., Ed. *Comprehensive Enantioselective Organocatalysis: Catalysts, Reactions and Applications, Volume 1: Privileged Catalysts*, 1st ed.; Wiley-VCH Verlag GbmH & Co. KGaA: Weinheim, Germany, 2013; p 237.

135. Dalko, P. I., Ed. *Comprehensive Enantioselective Organocatalysis: Catalysts, Reactions, and Applications, Volume 2: Activations*, 1st ed.; Wiley-VCH Verlag GbmH & Co. KGaA: Weinheim, Germany, 2013; p 717.

136. Dalko, P. I., Ed. *Comprehensive enantioselective Organocatalysis: Catalysts, Reactions and Applications, Volume 3: Reactions and Applications*, 1st ed.; Wiley-VCH Verlag GbmH & Co. KGaA: Weinheim, Germany, 2013; p 1438.

137. Zamfir, A.; Schenker, S.; Freund, M.; Tsogoeva, S. B. *Org. Biomol. Chem.* **2010**, *8*, 5262–5276.

138. Nakashima, D.; Yamamoto, H. *J. Am. Chem. Soc.* **2006**, *128*, 9626–9627.

139. Marcelli, T.; Hiemstra, H. *Synthesis (Stuttg).* **2010**, 1229–1279.

140. Hashimoto, T.; Maruoka, K. *Chem. Rev.* **2007**, *107*, 5656–5682.

141. Johnson, K. M.; Rattley, M. S.; Sladojevich, F.; Barber, D. M.; Nuñez, M. G. et al. *Org. Lett.* **2012**, *14*, 2492–2495.

142. Jakubec, P.; Muratore, M. E.; Aillaud, I.; Thompson, A. L.; Dixon, D. J. *Tetrahedron: Asymmetry* **2015**, *26*, 251–261.

143. Núñez, M. G.; Farley, A. J. M.; Dixon, D. J. *J. Am. Chem. Soc.* **2013**, *135*, 16348–16351.

144. Takemoto, Y. *Chem. Pharm. Bull.* **2010**, *58*, 593–601.

145. Henry, L. *Bull. Mem. l Acad. R. Med. Belgique* **1896**, *32*, 33.

146. Westermann, B. *Angew. Chem. Int. Ed.* **2003**, *42*, 151–153.

147. Marqués-López, E.; Merino, P.; Tejero, T.; Herrera, R. P. *Eur. J. Org. Chem.* **2009**, 2401–2420.

148. Noble, A.; Anderson, J. C. *Chem. Rev.* **2013**, *113*, 2887–2939.

149. Hantzsch, A. *Justus Liebigs Ann. Chem.* **1882**, *215*, 1–82.

150. de Vries, J. G.; Mršić, N. *Catal. Sci. Technol.* **2011**, *1*, 727–735.

151. Zheng, C.; You, S.-L. *Chem. Soc. Rev.* **2012**, *41*, 2498–2518.

152. Ouellet, S. G.; Walji, A. M.; MacMillan, D. W. C. *Acc. Chem. Res.* **2007**, *40*, 1327–1339.

153. Rueping, M.; Sugiono, E.; Azap, C.; Theissmann, T.; Bolte, M. *Org. Lett.* **2005**, *7*, 3781–3783.

154. Simon, L.; Goodman, J. M. *J. Am. Chem. Soc.* **2008**, *130*, 8741–8747.

155. ur Rahman, A.; Choudhary, M. I.; Thomson, W. J. *Bioassay Techniques for Drug Development*, 1st ed.; Taylor & Francis: Amsterdam, 2001; pp 1–214.

156. Hughes, J. P.; Rees, S. S.; Kalindjian, S. B.; Philpott, K. L. *Br. J. Pharmacol.* **2011**, *162*, 1239–1249.

157. Pantoliano, M. W.; Petrella, E. C.; Kwasnoski, J. D.; Lobanov, V. S.; Myslik, J. et al. *J. Biomol. Screen.* **2001**, *6*, 429–440.

158. Vedadi, M.; Niesen, F. H.; Allali-Hassani, A.; Fedorov, O. Y.; Finerty, P. J. et al. *Proc. Natl. Acad. Sci. U. S. A.* **2006**, *103*, 15835–15840.

159. Ericsson, U. B.; Hallberg, B. M.; De Titta, G. T.; Dekker, N.; Nordlund, P. *Anal. Biochem.* **2006**, *357*, 289–298.

160. Matulis, D.; Kranz, J. K.; Salemme, F. R.; Todd, M. J. *Biochemistry* **2005**, *44*, 5258–5266.

161. Wahlberg, E.; Karlberg, T.; Kouznetsova, E.; Markova, N.; Macchiarulo, A. et al. *Nat. Biotechnol.* **2012**, *30*, 283–288.

162. Fedorov, O.; Marsden, B.; Pogacic, V.; Rellos, P.; Müller, S. et al. *Proc. Natl. Acad. Sci. U. S. A.* **2007**, *104*, 20523–20528.

163. Niesen, F. H.; Berglund, H.; Vedadi, M. *Nat. Protoc.* **2007**, *2*, 2212–2221.

164. Ladbury, J. E.; Chowdhry, B. Z. *Chem. Biol.* **1996**, *3*, 791–801.

165. Jecklin, M. C.; Schauer, S.; Dumelin, C. E.; Zenobi, R. *J. Mol. Recognit.* **2009**, *22*, 319–329.

166. Cooper, M. A. *Anal. Bioanal. Chem.* **2003**, *377*, 834–842.

167. Quinn, E.; Wodicka, L.; Ciceri, P.; Pallares, G.; Pickle, E. et al. *Cancer Res.* **2013**, *73*, 4238.

168. DiscoveRx, Competitive Binding Technology - DiscoveRx. `http://www.discoverx.com/`.

169. Axelrod, D.; Koppel, D. E.; Schlessinger, J.; Elson, E.; Webb, W. W. *Biophys. J.* **1976**, *16*, 1055–1069.

170. Deschout, H.; Raemdonck, K.; Demeester, J.; De Smedt, S. C.; Braeckmans, K. *Pharm. Res.* **2014**, *31*, 255–270.

171. De Los Santos, C.; Chang, C.-W.; Mycek, M.-A.; Cardullo, R. A. *Mol. Reprod. Dev.* **2015**, *82*, 587–604.

172. Ullman, E. F.; Kirakossian, H.; Singh, S.; Wu, Z. P.; Irvin, B. R. et al. *Proc. Natl. Acad. Sci. U. S. A.* **1994**, *91*, 5426–5430.

173. Eglen, R. M.; Reisine, T.; Roby, P.; Rouleau, N.; Illy, C. et al. *Curr. Chem. Genomics* **2008**, *1*, 2–10.

174. Wigle, T. J.; Herold, J. M.; Senisterra, G. a.; Vedadi, M.; Kireev, D. B. et al. *J. Biomol. Screen.* **2010**, *15*, 62–71.

175. Xu, Y.; Piston, D. W.; Johnson, C. H. *Proc. Natl. Acad. Sci. U. S. A.* **1999**, *96*, 151–156.

176. Pfleger, K. D. G.; Eidne, K. *Nat. Methods* **2006**, *3*, 165–174.

177. Machleidt, T.; Woodroofe, C. C.; Schwinn, M. K.; Méndez, J.; Robers, M. B. et al. *ACS Chem. Biol.* **2015**, *10*, 1797–1804.

178. Hitko, C. W. *PCT Int. Appl.* **2014**, WO 2014/093677 A1.

179. Hay, D.; Fedorov, O.; Filippakopoulos, P.; Martin, S.; Philpott, M. et al. *Med. Chem. Commun.* **2012**, 140–144.

180. Norman, M. H.; Kelley, J. L.; Hollingsworth, E. B. *J. Med. Chem.* **1993**, *36*, 3417–3423.

181. Banno, Y.; Miyamoto, Y.; Sasaki, M.; Oi, S.; Asakawa, T. et al. *Bioorg. Med. Chem.* **2011**, *19*, 4953–4970.

182. Bowden, K.; Hiscocks, P.; Perjéssy, A. *J. Chem. Soc. Perkin Trans. 2 Phys. Org. Chem.* **1998**, *2*, 291–296.

183. Cueva, J. P.; Gallardo-Godoy, A.; Juncosa, J. I.; Vidi, P.; Lill, M. et al. *J. Med. Chem.* **2011**, *54*, 5508–5521.

184. Nishio, T.; Yamamoto, H. *J. Heterocycl. Chem.* **1995**, *32*, 883–891.

185. Fall, Y.; Reynaud, C.; Doucet, H.; Santelli, M. *Eur. J. Org. Chem.* **2009**, 4041–4050.

186. Ruan, Y.-P.; Chen, M.-D.; He, M.-Z.; Zhou, X.; Huang, P.-Q. *Synth. Commun.* **2004**, *34*, 853–861.

187. Wang, E. C.; Chen, H. F.; Feng, P. K.; Lin, Y. L.; Hsu, M. K. *Tetrahedron Lett.* **2002**, *43*, 9163–9165.

188. Felner, I.; Schenker, K. *Helv. Chim. Acta* **1969**, *52*, 1810–1815.

189. Chen, M.-W.; Chen, Q.-A.; Duan, Y.; Ye, Z.-S.; Zhou, Y.-G. *Chem. Commun.* **2012**, *48*, 1698.

190. Bamba, M. *PCT Int. Appl.* **2008**, WO 2008/153207 A1.

191. Petronzi, C.; Collarile, S.; Croce, G.; Filosa, R.; De Caprariis, P. et al. *Eur. J. Org. Chem.* **2012**, 5357–5365.

192. Kang, S. W.; Heo, E. Y.; Jun, J. G.; Kim, S. H. *Bull. Korean Chem. Soc.* **2004**, *25*, 1924–1928.

193. Wasserman, H. H.; Dion, R. P. *Tetrahedron Lett.* **1982**, *23*, 785–788.

194. Tivey, D. J. *J. Chem. Soc. Perkin Trans. 2 Phys. Org. Chem.* **1958**, *1958*, 2276–2282.

195. Liu, J.-J. *U.S. Pat. Appl. Publ.* **2011**, US 2011/0201635.

196. Spialter, L.; Pappalardo, J. A. *J. Org. Chem.* **1957**, *22*, 840–843.

197. Czekelius, C.; Carreira, E. M. *Angew. Chem. Int. Ed.* **2005**, *44*, 612–615.

198. Ghashghaei, O.; Manna, C. A.; Vicente-garcía, E.; Revés, M.; Lavilla, R. *Beilstein J. Org. Chem.* **2014**, *10*, 12–17.

199. Turner, R. *J. Am. Chem. Soc.* **1946**, *68*, 1607–1608.

200. Jhan, Y. H.; Kang, T. W.; Hsieh, J. C. *Tetrahedron Lett.* **2013**, *54*, 1155–1159.

201. Mustazza, C.; Borioni, A.; Sestili, I.; Sbraccia, M.; Rodomonte, A. et al. *J. Med. Chem.* **2008**, *51*, 1058–1062.

202. Moriconi, A.; Cesta, M. C.; Cervellera, M. N.; Aramini, A.; Coniglio, S. et al. *J. Med. Chem.* **2007**, *50*, 3984–4002.

203. Takeuchi, Y.; Fujisawa, H.; Noyori, R. *Org. Lett.* **2004**, *6*, 4607–4610.

204. Aebi, J. *PCT Int. Appl.* **2013**, WO 2013/079452.

205. Evans, A. R.; Taylor, G. A. *J. Chem. Soc. Perkin Trans. I* **1983**, 979–983.

206. Chaikittisilp, W.; Didas, S. A.; Kim, H.-j.; Jones, C. W. *Chem. Mater.* **2013**, *25*, 613–622.

207. Bujak, P.; Krompiec, S.; Malarz, J.; Krompiec, M.; Filapek, M. et al. *Tetrahedron* **2010**, *66*, 5972–5981.

208. Snieckus, V. *Chem. Rev.* **1990**, *90*, 879–933.

209. Hartung, C. G.; Snieckus, V. *Mod. Arene Chem.*; Wiley-VCH Verlag GbmH & Co. KGaA: Weinheim, Germany, 2002; Chapter 10, pp 330–367.

210. Smith, M. B.; March, J. *March's Advanced Organic Chemistry: Reactions, Mechanisms, and Structure, Sixth Edition*, 6th ed.; Wiley-Blackwell, 2006.

211. Sera, M.; Yamashita, M.; Ono, Y.; Tabata, T.; Muto, E. et al. *Org. Process Res. Dev.* **2014**, *18*, 446–453.

212. Beam, C. F.; Park, C. A.; Reames, D. C.; Miller, S. A.; Hauser, C. R. *J. Chem. Eng. Data* **1978**, *23*, 183–184.

213. Hardcastle, I. R.; Ahmed, S. U.; Atkins, H.; Farnie, G.; Golding, B. T. et al. *J. Med. Chem.* **2006**, *49*, 6209–6221.

214. Katritzky, A. R.; Fan, W.-Q. *Org. Prep. Proced. Int.* **1987**, *19*, 263–268.

215. Banerjee, A.; Santra, S. K.; Guin, S.; Rout, S. K.; Patel, B. K. *Eur. J. Org. Chem.* **2013**, *2013*, 1367–1376.

216. Park, J.; Park, E.; Kim, A.; Lee, Y.; Chi, K.-W. et al. *Org. Lett.* **2011**, *13*, 4390–4393.

217. Evans, P.; Nelson, J. D.; Stanley, A. L. *J. Org. Chem.* **1995**, *60*, 2298–2301.

218. Kochi, T.; Tazawa, A.; Honda, K.; Kakiuchi, F. *Chem. Lett.* **2011**, *40*, 1018–1020.

219. Basle, O.; Bidange, J.; Shuai, Q.; Li, C.-j. *Adv. Synth. Catal.* **2010**, *352*, 1145–1149.

220. Miao, J.; Ge, H. *Org. Lett.* **2013**, *15*, 2930–2933.

221. Li, Z. Y.; Li, D. D.; Wang, G. W. *J. Org. Chem.* **2013**, *78*, 10414–10420.

222. Powers, J. J.; Favor, D. A.; Rankin, T.; Sharma, R.; Pandit, C. et al. *Tetrahedron Lett.* **2009**, *50*, 1267–1269.

223. Takaoka, S.; Takaoka, N.; Minoshima, Y.; Huang, J. M.; Kubo, M. et al. *Tetrahedron* **2009**, *65*, 8354–8361.

224. Su, X.; Surry, D. S.; Spandl, R. J.; Spring, D. R. *Org. Lett.* **2008**, *10*, 2593–2596.

225. Sun, X.; Shan, G.; Sun, Y.; Rao, Y. *Angew. Chem. Int. Ed.* **2013**, *52*, 4440–4444.

226. Mei, T. S.; Giri, R.; Maugel, N.; Yu, J. Q. *Angew. Chem. Int. Ed.* **2008**, *47*, 5215–5219.

227. Parham, W. E.; Piccirilli, R. M. *J. Org. Chem.* **1976**, *41*, 1268–1269.

228. Li, X.; Fang, Y.; Deng, P.; Hu, J.; Li, T. et al. *Org. Lett.* **2011**, *13*, 4628–4631.

229. Stec, J.; Huang, Q.; Pieroni, M.; Kaiser, M.; Fomovska, A. et al. *J. Med. Chem.* **2012**, *55*, 3088–3100.

230. Shiina, I. *Tetrahedron* **2004**, *60*, 1587–1599.

231. Engelhardt, H. *PCT Int. Appl.* **2014**, WO 2014/154760 A1.

232. Sai, K. K. S.; O'Connor, M. J.; Klumpp, D. A. *Tetrahedron Lett.* **2011**, *52*, 2195–2198.

233. Picaud, S.; Da Costa, D.; Thanasopoulou, A.; Filippakopoulos, P.; Fish, P. V. et al. *Cancer Res.* **2013**, *73*, 3336–3346.

234. Sverdrup, F. M. *U.S. Pat. Appl. Publ.* **2015**, WO 2015/051035 A1.

235. Hanahan, D.; Weinberg, R. A. *Cell* **2011**, *144*, 646–674.

236. Delmore, J. E.; Issa, G. C.; Lemieux, M. E.; Rahl, P. B.; Shi, J. et al. *Cell* **2011**, *146*, 904–917.

237. Ciceri, P.; Müller, S.; O'Mahony, A.; Fedorov, O.; Filippakopoulos, P. et al. *Nat. Chem. Biol.* **2014**, *10*, 305–12.

238. Ember, S. W. J.; Zhu, J. Y.; Olesen, S. H.; Martin, M. P.; Becker, A. et al. *ACS Chem. Biol.* **2014**, *9*, 1160–1171.

239. Pardanani, A.; Hood, J.; Lasho, T.; Levine, R. L.; Martin, M. B. et al. *Leukemia* **2007**, *21*, 1658–1668.

240. Geron, I.; Abrahamsson, A. E.; Barroga, C. F.; Kavalerchik, E.; Gotlib, J. et al. *Cancer Cell* **2008**, *13*, 321–330.

241. Lénárt, P.; Petronczki, M.; Steegmaier, M.; Di Fiore, B.; Lipp, J. J. et al. *Curr. Biol.* **2007**, *17*, 304–315.

242. Rudolph, D.; Steegmaier, M.; Hoffmann, M.; Grauert, M.; Baum, A. et al. *Clin. Cancer Res.* **2009**, *15*, 3094–3102.

243. Yim, H. *Anticancer. Drugs* **2013**, *24*, 999–1006.

244. Chen, L.; Yap, J. L.; Yoshioka, M.; Lanning, M. E.; Fountain, R. N. et al. *ACS Med. Chem. Lett.* **2015**, *6*, 764–769.

245. Sharma, R. *PCT Int. Appl.* **2015**, WO 2015/049629 A1.

246. Sasmal, S. *PCT Int. Appl.* **2014**, WO 2014/128655 A1.

247. Smethurst, C. *PCT Int. Appl.* **2014**, WO 2014/154762 A1.

248. Zhou, C. *PCT Int. Appl.* **2014**, WO 2014/173241 A1.

249. Siegel, S. *PCT Int. Appl.* **2014**, WO 2014/128067 A1.

250. Engelhardt, H. *PCT Int. Appl.* **2015**, WO 2015/022332 A1.

251. Engelhardt, H. *PCT Int. Appl.* **2015**, WO 2015/06770 A1.

252. Schmees, N. *PCT Int. Appl.* **2014**, WO 2014/128111 A1.

253. Siegel, S. *PCT Int. Appl.* **2014**, WO 2014/026997 A1.

254. Engelhardt, H. *U.S. Pat. Appl. Publ.* **2014**, US 2014/0135336 A1.

255. Siegel, R. L.; Miller, K. D.; Jemal, A. *CA Cancer J Clin* **2015**, *65*, 5–29.

256. Mashalidis, E. H.; Śledź, P.; Lang, S.; Abell, C. *Nat. Protoc.* **2013**, *8*, 2309–24.

257. Viegas, A.; Manso, J.; Nobrega, F. L.; Cabrita, E. J. *J. Chem. Educ.* **2011**, *88*, 990–994.

258. Dalvit, C.; Fogliatto, G.; Stewart, A.; Veronesi, M.; Stockman, B. *J. Biomol. NMR* **2001**, *21*, 349–359.

259. Carr, H.; Purcell, E. *Phys. Rev.* **1954**, *94*, 630–638.

260. Meiboom, S.; Gill, D. *Rev. Sci. Instrum.* **1958**, *29*, 688–691.

261. Wlodarczyk, N.; Simenel, C.; Delepierre, M.; Barale, J. C.; Janin, Y. L. *Synthesis (Stuttg).* **2011**, *2*, 934–942.

262. Yin, J.; Buchwald, S. L. *J. Am. Chem. Soc.* **2002**, *124*, 6043–6048.

263. Buchanan, D. J.; Dixon, D. J.; Hernandez-Juan, F. A. *Org. Biomol. Chem.* **2004**, *2*, 2932–2934.

264. Bartberger, M. D. *PCT Int. Appl.* **2011**, WO 2011/153509 A1.

265. Davis, F. A.; Chen, B.-C. *Chem. Soc. Rev.* **1998**, *27*, 13.

266. Zhou, P.; Chen, B.-C.; Davis, F. A. *Tetrahedron* **2004**, *60*, 8003–8030.

267. Ruano, J. L. G.; Topp, M.; López-Cantarero, J.; Alemán, J.; Remuiñán, M. J. et al. *Org. Lett.* **2005**, *7*, 4407–4410.

268. Ruano, J. L. G.; de Haro, T.; Singh, R.; Cid, M. B. *J. Org. Chem.* **2008**, *73*, 1150–1153.

269. Stark, C. M.; Halper, M. *Phase-Transfer Catalysis: Fundamentals, Applications, and Industrial Perspectives*; Springer Science & Business Media, 2012.

270. Jin, Z.; Qiu, L. L.; Li, Y. Q.; Song, H. B.; Fang, J. X. *Organometallics* **2010**, *29*, 6578–6586.

271. Raders, S. M.; Moore, J. N.; Parks, J. K.; Miller, A. D.; Leissing, T. M. et al. *J. Org. Chem.* **2013**, *78*, 4649–4664.

272. Elford, T. G. Alpha-Exo-alkylidene gamma-lactones and gamma-lactams via 2-alkoxycarbonyl allylboronates: Mechanistic studies, diversity-oriented synthesis and target-oriented synthesis. Ph.D. thesis, University of Alberta, 2010.

273. Holzer, P. *PCT Int. Appl.* **2012**, WO 2012/175520 A1.

274. Clark, P. G. K.; Vieira, L. C. C.; Tallant, C.; Fedorov, O.; Singleton, D. C. et al. *Angew. Chem. Int. Ed.* **2015**, *54*, 6217–6221.

275. Sinha, S. C.; Keinan, E. *J. Org. Chem.* **1997**, *62*, 377–386.

276. Adamczyk, M.; Chen, Y.-Y.; Johnson, D. D.; Reddy, R. E. *Tetrahedron* **1997**, *53*, 12855–12866.

277. Sinha, S. C.; Keinan, E. *J. Org. Chem.* **1994**, *59*, 949–951.

278. Wang, Y.; Chen, A. M. *Org. Process Res. Dev.* **2008**, *12*, 282–290.

279. Ukeda, H.; Kawana, D.; Maeda, S.; Sawamura, M. *Biosci. Biotechnol. Biochem.* **1999**, *63*, 485–488.

280. Shoemaker, R. H.; Shoemaker, R. H. *Nat. Rev. Cancer* **2006**, *6*, 813–23.

281. Theodoulou, N. H.; Bamborough, P.; Bannister, A. J.; Becher, I.; Bit, R. a. et al. *J. Med. Chem.* **2015**, *ASAP*.

282. Chen, P.; Chaikuad, A.; Bamborough, P.; Bantscheff, M.; Bountra, C. et al. *J. Med. Chem.* **2015**, ASAP.

283. Hay, D.; Brennan, P.; Fedorov, O.; Tallant, C.; Monteiro, O. et al. *Med. Chem. Commun.* **2015**, *6*, 1381–1386.

284. Huang, D.; Rossini, E.; Steiner, S.; Caflisch, A. *ChemMedChem* **2014**, *9*, 573–579.

285. Anderson, J. C.; Horsfall, L. R.; Kalogirou, A. S.; Mills, M. R.; Stepney, G. J. et al. *J. Org. Chem.* **2012**, *77*, 6186–6198.

286. Perrin, L.; Werkema, E. L.; Eisenstein, O.; Andersen, R. A. *Inorg. Chem.* **2014**, *53*, 6361–6373.

287. Abboud, J. L. M.; Roussel, C.; Gentric, E.; Sraidi, K.; Lauransan, J. et al. *J. Org. Chem.* **1988**, *53*, 1545–1550.

288. Prasad, D. J. C.; Naidu, A. B.; Sekar, G. *Tetrahedron Lett.* **2009**, *50*, 1411–1415.

289. Boyd, E.; Chavda, S.; Coulbeck, E.; Coumbarides, G. S.; Dingjan, M. et al. *Tetrahedron Asymmetry* **2006**, *17*, 3406–3422.

290. Balalaie, S.; Soleiman-Beigi, M.; Rominger, F. *J. Iran. Chem. Soc.* **2005**, *2*, 319–329.

291. Cortes, S.; Krohn, H. *J. Org. Chem.* **1983**, *48*, 2246–2254.

292. Clements, A.; Rojas, J. R.; Trievel, R. C.; Wang, L.; Berger, S. L. et al. *EMBO J.* **1999**, *18*, 3521–3532.

293. Yu, D.; Perng, Y.-C. *PCT Int. Appl.* **2014**, WO 2014/134583 A2.

294. Aldrich, L. N.; Lebois, E. P.; Michelle Lewis, L.; Nalywajko, N. T.; Niswender, C. M. et al. *Tetrahedron Lett.* **2009**, *50*, 212–215.

295. Cui, J. J.; Shen, H.; Trandube, M.; Nambu, M.; Mctigue, M. et al. *J. Med. Chem.* **2013**, *56*, 6651–6665.

296. Zhang, Q.-R.; Xue, D.-Q.; He, P.; Shao, K.-P.; Chen, P.-J. et al. *Bioorg. Med. Chem. Lett.* **2014**, *24*, 1236–1238.

297. Kusakabe, K.-I. *PCT Int. Appl.* **2011**, WO 2011/013729 A1.

298. Jensen, L. H.; Wätjen, F.; Honoré, T.; Hansen, J. B.; Engelstoft, M. et al. *J. Med. Chem.* **1988**, *31*, 1115–1123.

299. Wipf, P.; Jung, J.-K. *J. Org. Chem.* **2000**, *65*, 6319–6337.

300. Storer, R. I.; Carrera, D. E.; Ni, Y.; MacMillan, D. W. C. *J. Am. Chem. Soc.* **2006**, *128*, 84–86.

301. Maruoka, K.; Itoh, T.; Araki, Y.; Shirasaka, T.; Yamamoto, H. *Bull. Chem. Soc. Jpn.* **1988**, *61*, 2975–2976.

302. Unsinn, A.; Wunderlich, S. H.; Knochel, P. *Adv. Synth. Catal.* **2013**, *355*, 989–995.

303. Zhou, J. Q.; Sheng, W. J.; Jia, J. H.; Ye, Q.; Gao, J. R. et al. *Tetrahedron Lett.* **2013**, *54*, 3082–3084.

304. Augner, D.; Gerbino, D. C.; Slavov, N.; Neudörfl, J. M.; Schmalz, H. G. *Org. Lett.* **2011**, *13*, 5374–5377.

305. Wang, X.; Gong, H.; Quan, Z.; Li, L.; Ye, H. *Synth. Commun.* **2011**, *41*, 3251–3258.

306. Edgar, K. J.; Bradsher, C. K. *J. Org. Chem.* **1982**, *47*, 1585–1587.

307. Yu, Q.; Zhang, N.; Huang, J.; Lu, S.; Zhu, Y. et al. *Chem. Eur. J.* **2013**, *19*, 11184–11188.

308. Abdel-Mohsen, H. T.; Conrad, J.; Beifuss, U. *Green Chem.* **2012**, *14*, 2686–2690.

309. Wang, G.-W.; Xia, J.-J.; Miao, C.-B.; Wu, X.-L. *Bull. Chem. Soc. Jpn.* **2006**, *79*, 454–459.

310. Donkor, I. O.; Zhou, X.; Agrawal, K. C.; Kishore, V. *Bioorg. Med. Chem.* **1998**, *6*, 1998–1998.

311. Hoffmann, S.; Nicoletti, M.; List, B. *J. Am. Chem. Soc.* **2006**, *128*, 13074–13075.

312. Haag, B. A.; Sämann, C.; Jana, A.; Knochel, P. *Angew. Chem. Int. Ed.* **2011**, *50*, 7290–7294.

313. Bailey, N.; Bamford, M. J.; Dean, D. K.; Pickering, P. L.; Wilson, D. M. et al. *PCT Int. Appl.* **2005**, WO2005/058837 A1.

314. Dawadi, P. B. S.; Schulten, E. A. M.; Lugtenburg, J. *J. Label. Compd. Radiopharm.* **2009**, *52*, 341–349.

315. Larsson, E. A.; Jansson, A.; Ng, F. M.; Then, S. W.; Panicker, R. et al. *J. Med. Chem.* **2013**, *56*, 4497–4508.

316. Kuszpit, M. R.; Giletto, M. B.; Jones, C. L.; Bethel, T. K.; Tepe, J. J. *J. Org. Chem.* **2015**, *80*, 1440–1445.

317. Murray, R. G.; Whitehead, D. M.; Le Strat, F.; Conway, S. J. *Org. Biomol. Chem.* **2008**, *6*, 988–991.

318. Guillon, J.; Lelong, V.; Renault, O.; Boulouard, M.; Dallemagne, P. et al. *Chem. Pharm. Bull.* **1998**, *46*, 711–714.

319. Lundina, I. B.; Frolova, N. N.; Postovskii, I. Y.; Bedrin, A. V.; Vereshchagina, N. N. *Khim. Farm. Z.* **1972**, *6*, 13–17.